GSB62

GEOLOGY OF THE DUNDAS – MT LINDSAY – MT YOUNGBUCK REGION

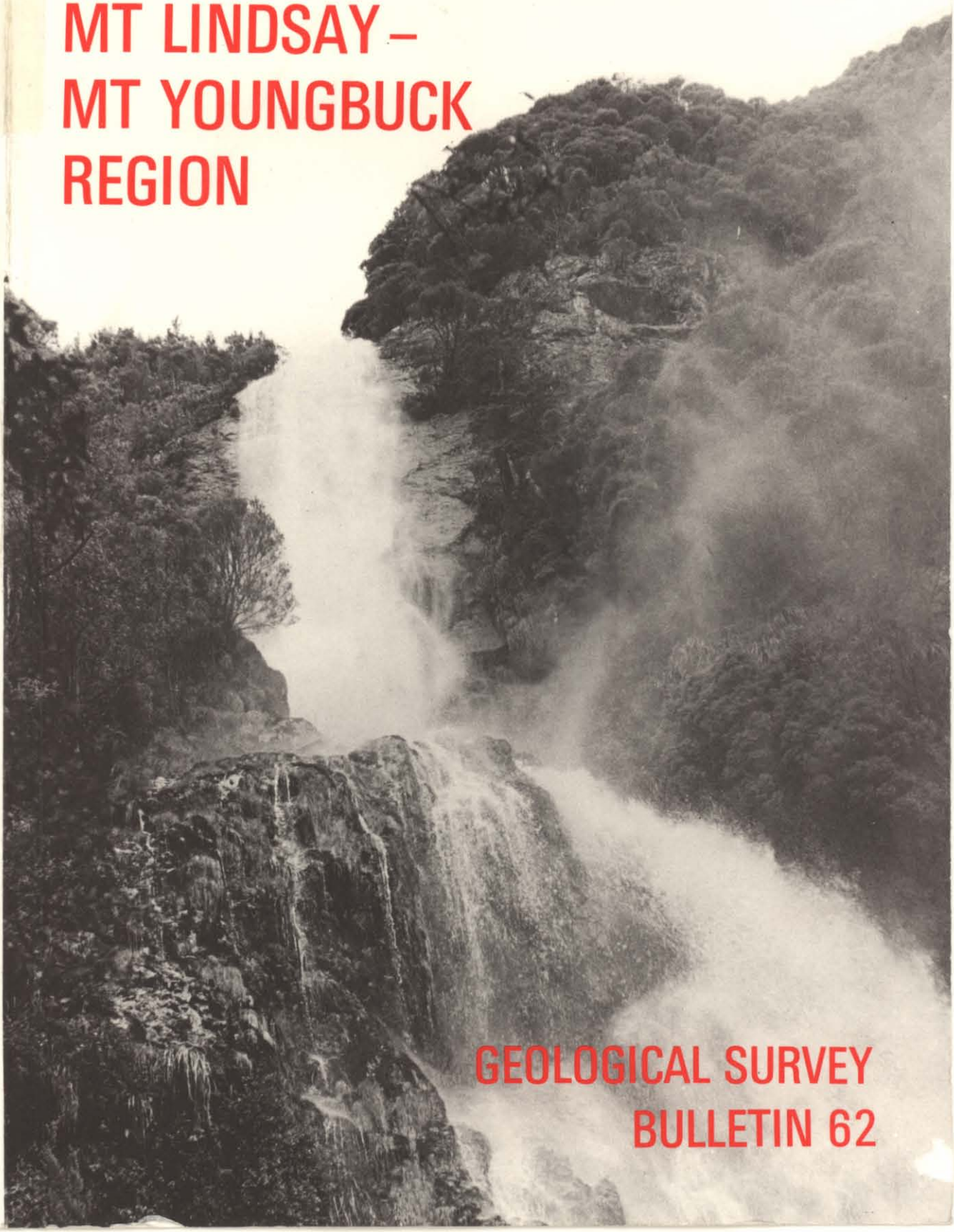

GEOLOGICAL SURVEY
BULLETIN 62

GEOLOGICAL SURVEY BULLETIN 62 GEOLOGY OF THE DUNDAS – MT LINDSAY – MT YOUNGBUCK REGION 1986 ISBN 0 7246 1931 3

GSB62

TASMANIA DEPARTMENT OF MINES

1986

GEOLOGICAL SURVEY
BULLETIN 62

Geology of the Dundas – Mt Lindsay – Mt Youngbuck region.

by A. V. Brown, B. Sc. (Hons).

DEPARTMENT OF MINES, P.O. BOX 56, ROSNY PARK, TASMANIA. 7018

ISSN 0082-2043
ISBN 0 7246 1931 3

BROWN, A. V. 1986. Geology of the Dundas - Mt Lindsay - Mt Youngbuck region. *Bull. geol. Surv. Tasm.* 62.

Accepted for publication November 1984.

ISBN 0 7246 1931 3 : ISSN 0082-2043

CONTENTS

	PAGE
INTRODUCTION	9
Ackowledgements	10
Previous literature	10
STRATIGRAPHY	12
Precambrian	12
Oonah Formation	12
Pieman River area	12
Introduction	12
'Lower' succession	13
'Upper' succession	13
Zeehan area	15
Dundas area	17
Ramsay River area	18
Structure	19
Summary	19
Eocambrian	23
Success Creek Group	23
Boundary relationship with the Oonah Formation	23
Introduction	23
Esc	24
Esd	24
Ess	25
Esru	25
Esr	25
Esrr	27
Esu	27
Palaeontology	28
Success Creek Group correlate (Esu)	28
Structure	29
Internal structures	29
Superimposed structures	29
Summary	33
Crimson Creek Formation	33
Introduction	33
Ecc	33
Structure	37
Summary	37
Cambrian	38
Dundas Group	38
Introduction	38
'Lower' Dundas Group successions (Ꞓmu)	38
Judith Formation (Ꞓdj)	39
Red Lead Conglomerate (Ꞓdre)	39
Hodge Formation (Ꞓdh)	40
Razorback Conglomerate (Ꞓdra)	41
Brewery Junction Formation (Ꞓdb)	42
Fault zone	43
'Upper' Dundas Group successions (Ꞓdl)	43
Misery Conglomerate (Ꞓdlm)	44
Denison Sub-Group correlate (Os)	44
Dundas Group correlate (Ꞓd)	45
Huskisson Group (Ꞓh)	45
Huskisson Group correlate (Ꞓh)	49
'Rosebery Group' correlate (Ꞓrg)	49
Correlate of Mount Read volcanic rocks (Ꞓmr)	50
Palaeontology	50
Dundas Group	50
Judith Formation	50
Hodge Formation	50
Brewery Junction Formation	51
Fernfields–Comet–Fernflow Formations	52
Climie Formation	52
Quartz sandstone sequence–Misery Hill	52
Huskisson Group	52

Comparison with Cambrian fossil faunas in other areas 53
Dial Range Trough 53
Beaconsfield area 53
Queenstown area 53
Smithton Basin and Adamsfield Trough 53
Summary 55
Structure 55
Ordovician 61
Gordon Limestone Sub-Group correlate (Ol) 61
Gordon Sub-Group–Eldon Group transition 61
Silurian-Devonian 61
Eldon Group correlate (S-Du) 61
Crotty Formation correlate (Sc) 63
Amber, Keel and Austral Creek Formation correlates (Sa,Sal,Sas) 63
Florence Formation correlate (Df) 64
Bell Formation correlate (Db) 65
Undifferentiated Eldon Group correlates (S-Du) 65
Structure 65
Quaternary 65
Glacial and related deposits (Qg) 65
Alluvium (Qra) 65
IGNEOUS ROCKS 66
Tertiary basalt (Tb) 66
Chemistry 66
Mineral chemistry 67
Devonian granitic rocks (Dg) 68
Massive quartz bodies (Dgq) 69
Eocambrian-Cambrian 69
Gabbro (Ꞓg) 69
Group 1 gabbro 69
Group 2 gabbro 70
Group 3 gabbro 70
Tonalite (Ꞓt) 70
Basalt successions 70
Introduction 70
Crimson Creek Formation tholeiites (Ecc and Eccb) 71
Mt Lindsay–Mt Ramsay area 71
Cleveland area 72
Arthur River–Wandle Road area 73
High-magnesian andesite suite (Ꞓba) 73
Low-titanium tholeiite basalts (Ꞓbm) 81
Black Hill Volcanics 81
Heazlewood River Volcanics 84
Mineral chemistry 85
Crimson Creek Formation tholeiite (Ecc and Eccb) 85
Plagioclase phenocrysts 85
Pyroxene phenocrysts 85
Accessory phases 85
High-magnesian andesite (Ꞓba and Ꞓbap) 85
Pyroxene phenocrysts 85
Chrome spinel grains 85
Low-titanium tholeiite basalt 89
Whole-rock chemistry 89
Ti ∿ Zr discriminant diagram 90
Ti ∿ Zr ∿ Y discriminant diagram 91
(Cr + Ni) ∿ Ti discriminant diagram 91
Rare Earth Element chemistry 91
Correlation–within Tasmania 98
Correlation–different tectonic settings 102
Precambrian basalt 104
Chemistry 105
Summary 105
Eocambrian–Cambrian basalt successions 105
Crimson Creek Formation tholeiite (Eccb) 105
High-magnesian andesite (Ꞓba) 105
Low-titanium tholeiite basalt (Ꞓbm) 106

Precambrian basalt 106
Classification 106
ULTRAMAFIC ROCK SUCCESSIONS 107
Introduction 107
Wilson River Ultramafic Complex 111
Harman River area 111
Serpentine Ridge area 115
Riley Knob area 115
Mt Stewart Ultramafic Complex 116
Huskisson River Ultramafic Complex 118
Colebrook Hill ultramafic body 118
Ring River–Kapi Creek area 118
Serpentine Hill Ultramafic Complex 119
Orthopyroxene-rich sequence 119
Olivine-rich sequence 121
Two-pyroxene gabbro 121
Dundas Ultramafic Complex 122
Major and trace element chemistry of ultramafic rocks 123
Introduction 123
Dunite samples 123
Pyroxenite samples 125
Mineral chemistry 126
Layered Dunite–Harzburgite succession 126
Harman River area 126
Mt Stewart and Adamsfield areas 127
Layered Pyroxenite-Dunite succession 127
Riley Knob area 127
Layered Pyroxenite-Peridotite and associated Gabbro succession 133
Serpentine Hill area 133
Summary of ultramafic successions 134
Amphibolite (Ɛsa) 135
PETROGENESIS OF ULTRAMAFIC-MAFIC SUCCESSIONS 136
Layered Dunite-Harzburgite succession 136
Layered Pyroxenite-Dunite succession 139
Layered Pyroxenite-Peridotite and associated Gabbro succession 141
MINERALISATION 142
SUMMARY 142
REFERENCES 144
APPENDIX 1: Late Cambrian agnostid faunas from the Huskisson River area (M. J. Clarke) 151
APPENDIX 2: Some Ordovician and Silurian rocks and fossils from the Huskisson River area, western Tasmania (M. R. Banks and C. F. Burrett) 151
APPENDIX 3: Fossil faunas in Eldon Group correlates within the Huskisson Syncline (M. J. Clarke and A. V. Brown) 161
APPENDIX 4: Tables of rock analyses 163

LIST OF PLATES

		PAGE
1.	Refolded isoclinal folds, 'upper' Oonah Formation	14
2.	Oolitic chert breccia with stromatolite clasts	28
3.	Soft-sediment deformation with slump zone, Success Creek Group	30
4.	Flow-banding in high-magnesian andesite	73
5.	Textural variations in weathered high-magnesian andesite	75
6.	Pillow lava flow in high-magnesian andesite	77
7.	Breccia flow in high-magnesian andesite	77
8.	Clinoenstatite and orthopyroxene phenocrysts in high-magnesian andesite	78
9.	Chrome spinel grains enclosed by amphibole pseudomorph of clinoenstatite	80
10.	'Cannon ball' structure in high-magnesian andesite	81
11.	Intermixed pillow lavas and breccia flow in low-titanium basalt	82
12.	Igneous layering in the LDH succession	112
13.	Mineral foliation defined by chrome spinel grains, LDH succession	113
14.	Boudinaged orthopyroxenite lenses, LDH succession	114
15.	Small lense of chrome spinel grains, LDH succession	116
16.	Igneous layering in LPD succession	117
17.	Thin sections of fossil-bearing rocks	152
18.	Sections of corals	155

LIST OF FIGURES

		PAGE
1.	Regional geology of the Dundas–Mt Lindsay–Mt Ramsay area (Parts 1 and 2)	in folder
2.	Regional geology of the Mt Youngbuck–Magnet area	in folder
3.	Geological compilation of the Zeehan–Waratah area, Dundas Trough	in folder
4.	Location map for Figures 1 to 3	8
5.	Structural traverse across the boundary of the Oonah Formation correlate and Concert Schist, Dundas area	16
6.	Location map for structural domains	20
7.	Stereographic plots, Oonah Formation	21
8.	Stereographic plots, Oonah Formation	22
9.	Cross-section: Success Creek Group, Pieman River	26
10.	Stereographic plots, Oonah Formation and Success Creek Group	31
11.	Cross-section: Success Creek Group, Renison Bell area	32
12.	Stereographic plots, Crimson Creek Formation	36
13.	Palaeontological correlation chart	in folder
14.	Stereographic plots: Dundas Group, Black Hill area	54
15.	Stereographic plots: Dundas Group, Dundas area	56
16.	Stereographic plots: Dundas Group, combined plot for Black Hill and Dundas areas	57
17.	Stereographic plots, Dundas Group	58
18.	Stereographic plots, Huskisson Group and 'Rosebery Group'	59
19.	Structural profile of Ringville area	60
20.	Eldon Group correlation, Huskisson–Zeehan areas	62
21.	Alkali-silica diagram, Tertiary basalt	67
22.	Part of pyroxene quadrilateral for sample from Crimson Creek tholeiitic basalts	72
23.	$Cr^* \sim Mg^*$ for chrome spinel from high-magnesian andesite samples	86
24.	Geochemical pattern for Crimson Creek Formation tholeiitic basalt	87
25.	Geochemical pattern for low-titanium tholeiite	88
26.	Geochemical pattern for high-magnesian andesite	89
27.	Comparison of geochemical patterns from Figures 24–26	90
28.	$Ti \sim Zr$ discriminant diagrams, Dundas Trough basaltic rocks	91
29.	$Ti \sim Zr \sim Y$ discriminant diagrams, Dundas Trough basaltic rocks	92
30.	$(Cr + Ni) \sim Ti$ discriminant diagrams, Dundas Trough basaltic rocks	94
31.	Chondrite-normalised REE patterns, Crimson Creek tholeiitic basalts	96
32.	Chondrite-normalised REE patterns for low-titanium tholeiite	96
33.	Chondrite-normalised REE patterns for high-magnesian andesite	97
34.	Comparison of chondrite-normalised REE patterns for Dundas Trough samples	97

35. Geochemical patterns for tholeiitic basalts from Smithton area 98
36. Ti ∿ Zr discriminant diagram for tholeiitic basalts from Smithton area..... 99
37. Ti ∿ Zr ∿ Y discriminant diagram for tholeiitic basalts from Smithton area 100
38. (Cr + Ni) ∿ Ti discriminant diagram for tholeiitic basalts from Smithton area .. 100
39. Chondrite-normalised REE patterns for tholeiitic basalts from Smithton area . 101
40. Zr/Y ∿ Zr discriminant diagram 102
41. Ti ∿ Y ∿ Zr discriminant diagram 103
42. Schematic geological map of Tasmania showing locations of ultramafic–mafic complexes 108
43. Distribution of areas of LDH and LPD succession ultramafic rocks in the Renison Bell–Mt Ramsay area 110
44. Geological map of the Serpentine Hill Ultramafic–Mafic Complex..... 120
45. Detailed geological map of part of the Serpentine Hill Ultramafic–Mafic Complex 122
46. AFM diagram with plot of analyses of ultramafic rocks from the LDH and LPD successions..... 124
47. LOI ∿ MgO/SiO_2 (wt%) diagram for samples from ultramafic rock successions 125
48. Cr* ∿ Mg* diagram for chrome spinel samples from the LDH and LPD successions 128
49. Chemical variation diagrams for orthopyroxene from the LDH and LPD successions 129
50. Part of the pyroxene quadrilateral with plot of Opx-Cpx pairs from the LDH and LPD sucessions 130
51. Variation in Al_2O_3 in coexisting orthopyroxene and chrome spinel 131
52. Distribution of Al and Cr in coexisting orthopyroxene and chrome spinel from Tasmanian ultramafic rocks and comparison with other ultramafic rock successions 132
53. Cr ∿ Fe^{3+} ∿ Al plot of chrome spinel grains from Tasmanian and other ultramafic rock successions 133
54. Cr* ∿ Mg* diagram for chrome spinel samples from the Serpentine Hill Ultramafic-Mafic Complex 134
55. Plot of ln K_D ∿ $Y^{\frac{2}{3}}$ for spinel samples from the LDH and LPD successions... 138
56. Camera lucida drawing of *Tentaculites* cf. *ornatus* 159
57. Camera lucida drawing of *?Cyrtograptus* 160

FIG 1 - PART 1

GEOLOGICAL SURVEY OF TASMANIA

REGIONAL GEOLOGY of the DUNDAS — MT. LINDSAY — MT. RAMSAY AREA

Geology by A.V. BROWN B.Sc. (Hons)

CARTOGRAPHY BY P. B. NANKIVELL

1 0.5 0 1 2 KILOMETRES

SCALE 1 : 25 000

1983

5 cm

CAINOZOIC — QUATERNARY

- Qra — Marsh and swamp deposits; alluvium; river gravels; talus.
- Qg — Glacial derived deposits : outwash conglomerate, gravel and sand.

Angular unconformity.

PALAEOZOIC — DEVONIAN

- Db — Sandstone, siltstone and mudstone (correlate of Bell Shale).
- Df — Quartz sandstone sequence (correlate of Florence Quartzite).
- Sas, Sa, Sal — Siltstone, mudstone and calcareous siltstone with limestone (Sal) and quartz sandstone (Sas) layers (correlate of Austral Creek Siltstone, Keel Quartzite, Amber Slate).
- Sc — Quartz sandstone with minor mudstone and granule conglomerate layers (correlate of Crotty Quartzite).

S – Du

PALAEOZOIC — SILURIAN

- Ol — Limestone and impure limestone with variable texture (correlate of Gordon Limestone).
- Os — Quartz sandstone and minor siltstone

PALAEOZOIC — ORDOVICIAN ?

- €dlm — Poorly sorted conglomerate, sandstone and siltstone (€dl) with indurated siltstone horizon (€dlc) indicated (upper part of Brewery Junction up to and including the Misery Conglomerate (€dlm),

Fault contact (Dundas Region).

PALAEOZOIC — CAMBRIAN

- €dl — Interbedded sandstone and siltstone (lower part of Brewery Junction Formation).
- €db — Poorly-sorted conglomerate, pebbly sandstone and sandstone, all dominantly chert derived, with minor acid tuff horizons ( ) indicated. (Razorback Conglomerate).
- €mu — €dra — Siltstone and mudstone with minor sandstone. (Hodge Slate).
- €dh — Poorly-sorted volcaniclastic polymic conglomerate. (Red Lead Conglomerate).
- €dre — Sandstone, siltstone and mudstone. (Judith Formation).
- €dj

DUNDAS GROUP

Erosional Break.

PROTEROZOIC — EDCAMBRIAN ?

- Ecc — Volcaniclastic lithicwacke siltstone and mudstone with minor carbonate and tholeiitic basalt. Areas of dominantly basalt indicated (Eccb)
- Esrr — Red chert and mudstone with minor conglomerate and carbonate layers.
- Esrc — Laminated siliceous siltstone with minor quartz sandstone and conglomerate horizons.

(Renison Bell Formation)

- Essu — Black mudstone, siltstone and minor sandstone (dominated by soft sediment and later tectonic deformation).
- Esd — Quartz sandstone with minor siltstone, pebbly sandstone and conglomerate (Dalcoath Formation).
- Esc — Poorly-sorted, immature, polymic conglomerate with sandstone lenses.

CRIMSON CREEK FORMATION

SUCCESS CREEK GROUP

Angular Landscape Unconformity.

PRECAMBRIAN ?

- Pu — Pom — Mudstone, siltstone, dolomite and conglomerate with minor lava and volcanic breccia.
- Pos — Indurated quartz sandstone, siltstone and mudstone. Metamorphic equivalents ( ) (Concert Schist) indicated.

OONAH FORMATION (and correlates)

HUSKISSON RIVER REGION

Equivalent units absent.

Contact relationship unknown.

- Ch — Laminated siltstone; graded sandstone and lithicwacke; pebbly sandstone and conglomerate ( ). acid-intermediate tuffaceous layers ( ); and silceous conglomerate units towards the top of the succession. Fossiliferous horizons indicated ( )

HUSKISSON GROUP

MOORES PIMPLE REGION

(Age relationship not known)

- €rg — Acid-intermediate volcaniclastic lithicwacks, tuff, siltstone and mudstone with dominantly conglomerate ( ) and quartz sandstone ( ) layers (correlates of Rosebery Group).
- €mv — Acid-intermediate tuff and minor siltstone and mudstone layers (correlate of Mount Read Volcanics).

IGNEOUS ROCKS

- TERTIARY — Tb — Alkali olivine basalt, with interbasalt sedimentary deposits indicated. ( ) Ts
- DEVONIAN — Dg — Granitic rocks with metamorphism of surrounding country - rocks indicated (small cross overprint) ; associated red/white massive quartz bodies (Dgq).
- CAMBRIAN (post-Middle Cambrian) — €g — Massive gabbro.
- MIDDLE CAMBRIAN — €b — Basalt, commonly with pillows and individual flows graded from coarse-grained base to fine-grained top; associated basalt intrusions indicated (€bi)

EOCAMBRIAN ? — CAMBRIAN ? (pre-Middle Cambrian) — €su

- €sg — Serpentinized layered peridotite with gabbro.
- €sp — Serpentinized layered peridotite and pyroxenite.
- €sd — Serpentinized dunite and interlayered pyroxene-bearing dunite (€sdp).
- €ss — Massive serpentinite.
- €sa — Amphibolite.

- Geological boundary — position approximate.
- Geological boundary — inferred.
- Geological boundary — transitional.
- Geological boundary — concealed.
- Fault — position approximate.
- Fault — inferred.
- Fault — concealed.
- Strike and dip of bedding — facing known; vertical, facing known; overturned; facing unknown; vertical, facing unknown.
- Strike and dip of compositional banding — in sedimentary rocks; in igneous rocks.
- Strike and dip of cleavage of unspecified type or relative age; vertical.
- Type of cleavage — slaty , crenulation.
- Fold hinge, with plunge and dip of axial surface; vertical axial surface.
- Early fold hinge, with plunge and dip of axial surface; vertical axial surface.
- Later fold hinge, with plunge and dip of axial surface; vertical and axial surface.
- Macrofossil locality in sparsely fossiliferous rocks.

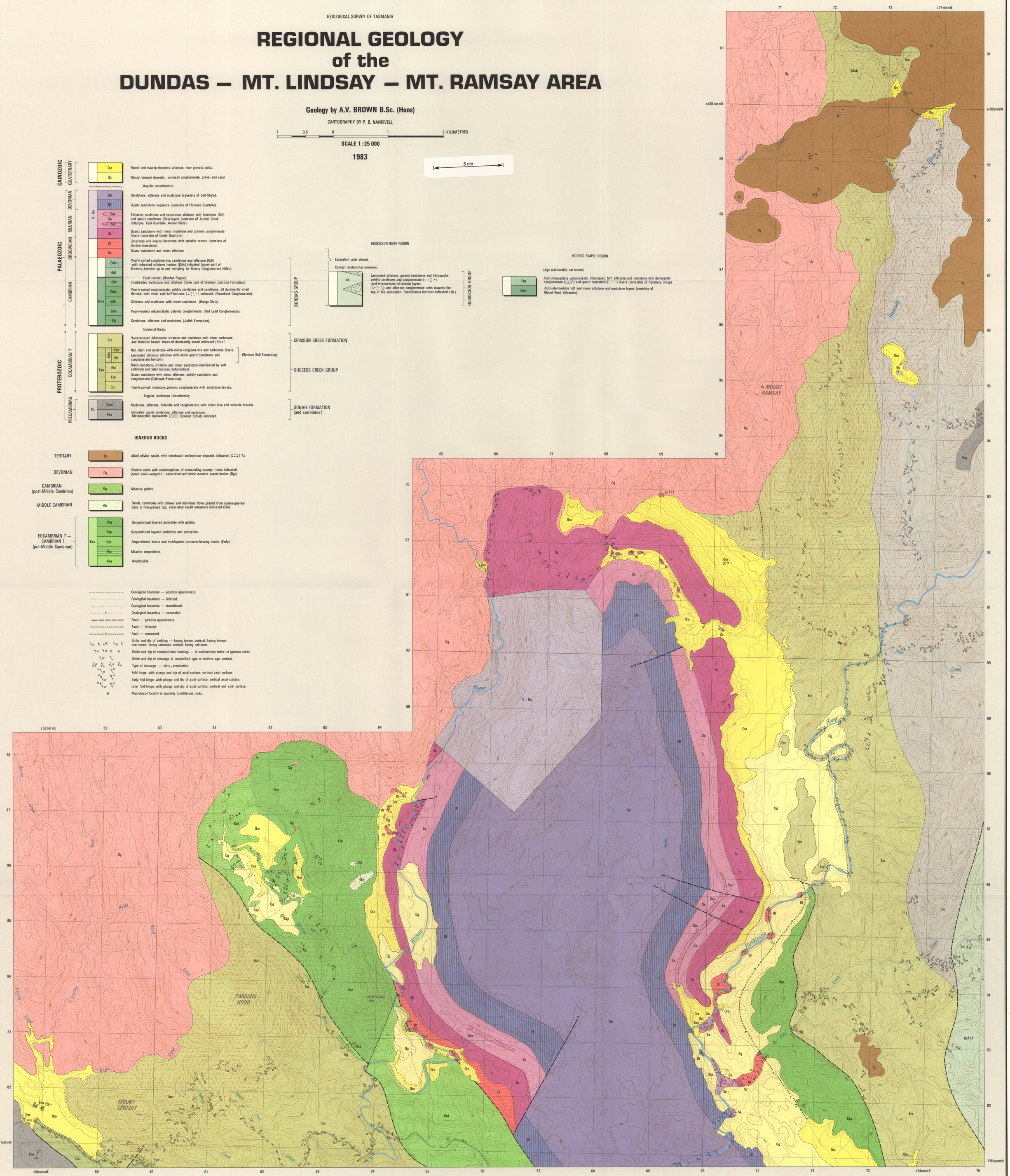

FIG 1 - PART 1

GSB62

GEOLOGICAL SURVEY OF TASMANIA

REGIONAL GEOLOGY OF THE DUNDAS — MT LINDSAY — MT RAMSAY AREA

Geology by A. V. BROWN B.Sc. (Hons.)

CARTOGRAPHY BY P. B. NANKIVELL

1 0.5 0 1 2 KILOMETRES

SCALE 1 : 25 000

5 cm

LOCALITY MAP SHOWING AREA COVERED ON CORINNA AND ZEEHAN 1 : 50 000 MAP SHEETS

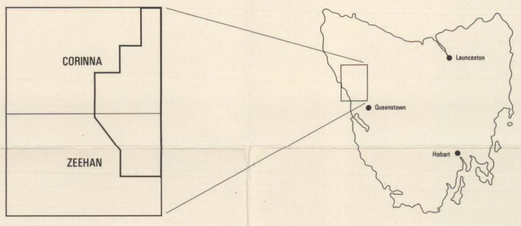

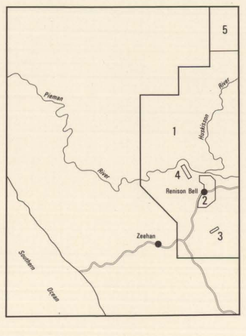

RESPONSIBILITY DIAGRAM

1. Mapped and compiled from detailed traverses on a scale of 1 : 10 000
2. Compiled on a scale of 1 : 10 000 (A.V.B.) from information supplied by Renison Ltd.
3. TURNER, N. J. 1979 : The boundary relationship of the Concert Schist and the Donah Quartzite and Slate correlate at Dundas. *Pap. Proc. R. Soc. Tasm.* 113 : 15-20
4. TAYLOR, B. L. 1954 : Bon Accord — Owen Meredith area. *Unpubl. Rep. Dep. Mines Tasm.* 1954 : 126-141
5. Compiled on a scale of 1 : 10 000 (A.V.B.) from information:-
   (a) supplied by Comstaff Pty. Ltd.; (b) obtained from detailed traverses (A.V.B.).

FIG. 1 PART 2 GSB62

GEOLOGICAL SURVEY OF TASMANIA

REGIONAL GEOLOGY OF THE MT YOUNGBUCK — MAGNET AREA

Geology and compilation by
A.V. BROWN B.Sc. (Hons)
1984

1 0 1 2 KILOMETRES

1:25 000

5 cm

REFERENCE

QUATERNARY — Qro — Marsh and swamp deposits; alluvium; river gravels.

TERTIARY — Erosional Break
Tsa– Sand, silt and volcanic breccia.
Tb– Tholeiitic and alkali olivine basalt.
Tsc– Sediments and conglomerate; silcrete indicated (Tscs).

Ts– Sediments

Angular Unconformity

DEVONIAN / SILURIAN — Siltstone; mudstone and calcareous siltstone(correlate of the Amber Formation).
Quartz sandstone with minor mudstone and granule conglomerate (correlate of the Crotty Formation).

ORDOVICIAN — Limestone and impure limestone with variable texture (correlate of the Gordon Limestone).
Quartzwacke and minor mudstone.

Erosional Break
EOCAMBRIAN — Volcaniclastic lithicwacke, siltstone, mudstone and tholeiitic basalt (correlate of the Crimson Creek Formation) Areas of dominantly basalt indicated Ecb.

Quartzwacke and minor mudstone (possible correlate of the Success Creek Group

Angular Landscape Unconformity

PRECAMBRIAN — Eo Indurated quartz sandstone , siltstone and mudstone (correlate of the Oonah Formation)
Ews Schistoze quartz sandstone, siltstone and mudstone (correlate of the "Whyte Schist")

Igneous Rocks

TERTIARY — Tholeiitic and alkali olivine basalt.

DEVONIAN — Porphyritic fine to coarse–grained biotite granite/adamellite

Fine to coarse–grained gabbro

Massive ultramafic cumulate.

CAMBRIAN — Massive and pillow aphyric basalt flows, commonly brecciated (low–titanium Tholeiitic) Individual flows graded from coarse–grained base to pillow tops./interbasalt sandstone and siltstone indicated Cbms.
Porphyritic (orthopyroxene , chromite), high –magnesium andesite, commonly with pillow and breccia flows. Associated coarse–grained pyroxenite ( ) Cbop

Tonalite and associated rocks.

Serpentinized, layered peridotite and pyroxenite . Serpentinitic melange indicated(.) Cum.

Serpentinized dunite with areas of interlayered pyroxene–bearing dunite.

- Geological boundary–position approximate
- Geological boundary–inferred.
- Geological boundary–transitional.
- Fault–position approximate
- Fault–inferred.
- Strike and dip of bedding–facing known; vertical, facing known; overturned; facing unknown; vertical, facing unknown.
- Strike and dip of compositional banding–in sedimentary rocks; in igneous rocks.
- Strike and dip of cleavage of unspecified type or relative age; vertical.
- Type of cleavage–slaty, crenulation.
- Fold hinge, with plunge and dip of axial surface; vertical axial surface.

RESPONSIBILITY DIAGRAM

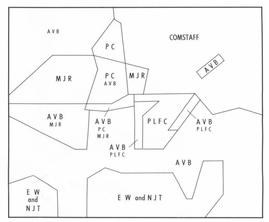

AVB 1:10 000 regional mapping

AVB Reconnaissance and or traverse mapping

PLFC Collins, P.L.F., 1983. Geology and Mineralization at the Cleveland Mine, Western Tasmania. *Unpubl. Ph.D. Thesis, Univ. of Tasm.*

PC Creenaune, P., 1980. The Volcanics of the Heazlewood River Complex. *Unpubl. B.Sc. Thesis, Univ. of Tasm.*

COMSTAFF Information supplied by Comstaff Pty Ltd on a scale of 1:50 000

MJR Rubenach, M.J., 1973. The Tasmanian Ultramafic–Gabbro and Ophiolite Complexes. *Unpubl. B.Sc. (Hons.) Thesis, Univ. of Tasm.*

E W and N J T Williams,E., and Turner,N., 1974. Geological Atlas 1:250 000 Series. Sheet SK–55/3 Burnie.

LOCALITY MAP

GS862

FIG 2.

CARTOGRAPHY BY P.B. NANKIVELL

GEOLOGICAL SURVEY OF TASMANIA

GEOLOGICAL COMPILATION OF THE ZEEHAN–WARATAH AREA, DUNDAS TROUGH

Compiled by A.V. BROWN B.Sc. (Hons.)

1984

0 2 4 6 8 10 KILOMETRES

SCALE 1:100 000

REFERENCE

PERMO–CARBONIFEROUS	Pt	Tillite
		Landscape unconformity
SILURO–DEVONIAN	S–Du	Eldon Group and correlates
		Disconformity
ORDOVICIAN	Ol	Gordon Limestone Sub–Group and correlates
	Os	Owen Formation and correlates, including Moina Sandstone
		Disconformity
CAMBRIAN	€d	Dundas Group and correlates, including Huskisson Group, €h (▨), and Rosebery Group, €r (▨),
		Erosional break
EOCAMBRIAN	Ecc	Crimson Creek Formation and correlates, areas of dominantly lava flows Eccb (⁘) indicated
	Esc	Success Creek Group and correlates
		Landscape unconformity
PRECAMBRIAN	Po	Oonah Formation and correlates
	Pws	Whyte Schist and correlates, including Concert Schist

Igneous Rocks

TERTIARY	Tb	Alkali Olivine and Tholeiitic Basalt, with associated sediment
JURASSIC	Jd	Dolerite
DEVONIAN	Dg	Granitoids
CAMBRIAN	€g	Gabbro
	€mrv	Pyroclastic and epiclastic acid to intermediate volcanic rocks (Mt Read Volcanics)
	€bp	Massive ultramafic cumulates
	€bm / €bu	Low –Titanium Tholeiite
EOCAMBRIAN	€ba	High–Magnesian Andesite, and associated coarse–grained pyroxenite
	€t	Tonalite and associated rocks
	€s	Serpentinized ultramafic–mafic rocks, tectonic melange €sm (▥) indicated

Geological boundary, including faulted and transitional — approximate

Geological boundary, including faulted and transitional — inferred

Dip and strike of bedding, facing known, facing unknown, overturned, vertical

Dip and strike of banding, sedimentary rocks vertical, igneous rocks, vertical

RESPONSIBILITY DIAGRAM

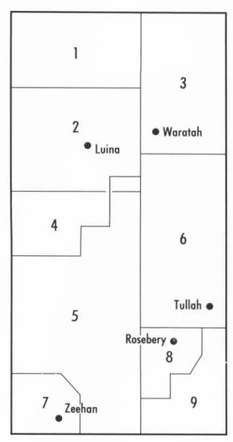

1 Air–photo interpretation

2 Brown, A. V. 1984 Regional Geology of the Mt Youngbuck–Magnet Area Fig.2 *Bull. Geol. Surv. Tasm. 62*

3 Baillie, P.W.; Williams, P.R.; Green, G.R.; Lennox, P.G.; Seymour, D.B.; In prep. Geological Atlas 1:50 000 Series. Sheet 36 (8015S). St Valentines

4 Williams, E.; and Turner, N.J. 1974. Geological Atlas 1:250 000 Series. Sheet SK–55/3. Burnie

5. Brown, A.V. 1983 Regional Geology of the Dundas–Mt Lindsay–Mt Ramsay Area Fig.1, *Bull. Geol. Surv. Tasm. 62*

6 After: Barton,C.M., et al. Geological Atlas 1 mile Series. Sheet 44 (8014N) Mackintosh.

7 Blissett, A.H., Gulline, A.B. , 1962. Geological Atlas 1 mile Series. Sheet 50 (7914S). Zeehan.

8 After: Green, G.R., 1983 The geological setting and formation of the Rosebery volcanic–hosted massive sulphide orebody ,Tasmania. *Unpubl. Ph.D. Thesis Univ. Tasm.*

9 Corbett, K.D.; Brown, A.V., 1976 Geological Atlas 1:250 000 Series Sheet SK–55/5. Queenstown.

5 cm

GS862

CARTOGRAPHY BY P.B. NANKIVELL

FIG. 3

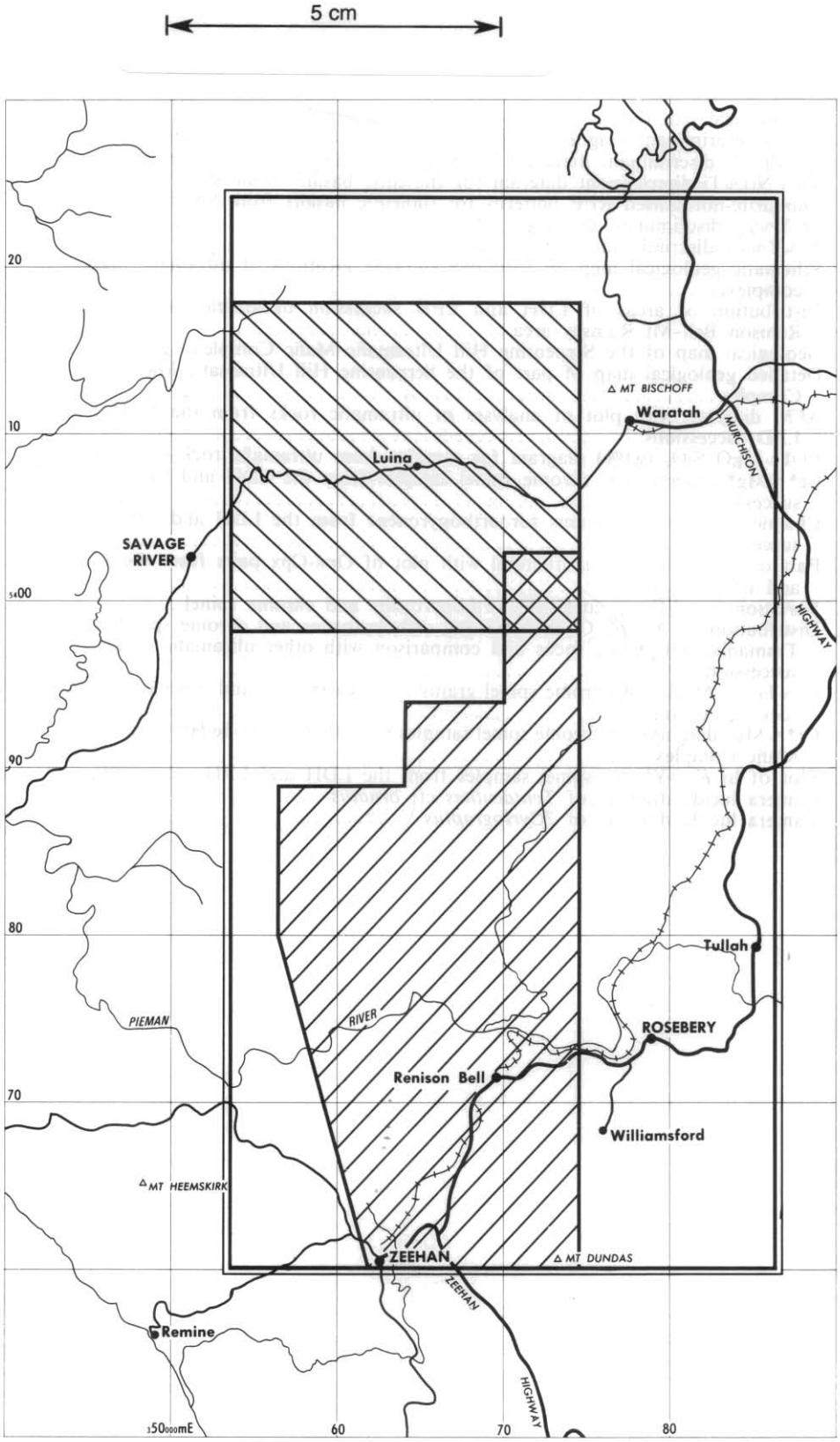

Figure 4. *Location map for Figures 1–3.*

INTRODUCTION

This report is based on information obtained whilst undertaking a mapping project over 1 000 km² of the Dundas Trough north of Dundas. The project necessitated the detailed mapping of the north-east quadrant of the Zeehan Quadrangle and the eastern half of the Corinna Quadrangle, as well as reconnaisance mapping of 250 km² of the south-east quadrant of the Magnet Quadrangle.

The project included the remapping of the type sections of the main sedimentary rock groups and formations of the Dundas Trough, and extending mapping to cover the areas of these successions to the north. It also involved delineating and defining the different mafic and ultramafic igneous phases between Dundas and the Heazlewood area, and investigating the petrography, chemistry and any associated mineralisation of these complexes.

During the project, mapping of approximately 600 km² was carried out on a scale of 1:5 000 and 1:10 000. Approximately 100 km of tape and compass traverses were plotted on a scale of 1:5 000, and then compiled on to 1:10 000 maps. The two 1:25 000 maps accompanying this report (fig. 1, 2) are compiled from these data, and the 1:100 000 interpretative solid geology map (fig. 3) is based on Figures 1 and 2, as well as other published and unpublished data.

Due to information obtained during this project, the writer disagrees with the four major conclusions of an earlier regional investigation by Blissett (1962, p. 17–20).

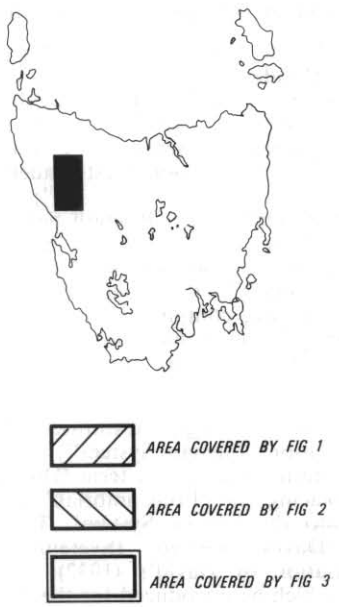

Figure 4. *Key to location map.*

These are:

> "1. The fossiliferous Middle to Upper (sic) Cambrian Dundas Group is conformable upon a sequence with similar lithology (the Crimson Creek Formation)". (p. 17)

So far no actual contact, undisturbed by faulting, of rocks belonging to the Dundas Group and the Crimson Creek Formation has been recognised in field mapping. The lithologies of the two groups are very different and from evidence so far obtained there is an erosional break between the deposition of these two groups during which some volcanic activity occurred. The depositional break probably spans, at least, the Early and early Middle Cambrian and possibly extends down into the Late Proterozoic.

> "2. The Upper (sic) Proterozoic or Lower (sic) Cambrian Oonah Quartzite and Slate passes up without a major hiatus into the Crimson Creek Formation, which may therefore extend from Lower (sic) to Middle Cambrian". (p. 17)

The Oonah Formation was subjected to an orogeny around 730 Ma, and a major landscape unconformity exists between the Oonah Formation and the stratigraphically succeeding Success Creek Group which, on the basis of fossil evidence (W. V. Preiss, pers. comm.) is probably Late Proterozoic in age. The Success Creek Group is conformably followed by the Crimson Creek Formation.

> "3. Rocks whose stratigraphical position was doubtful can now be placed within the Proterozoic–Cambrian succession. They include the highly disturbed sequence near Zeehan, between Trial Harbour and Zeehan, at Dundas, Renison Bell, and west of Rosebery". (p. 20)

Whereas the time span of the above-mentioned sequence of rocks is accepted, the correlation and distribution into specific groups by Blissett (1962) is not.

> "4. There may be a passage from the Dundas Group up into the Ordovician Junee Group on Misery Hill, McLean Creek and on the Huskisson River". (p. 20)

In the Huskisson River there is an implied disconformity between the top of the Dundas Group, which is middle Late Cambrian in age, and the Gordon Limestone correlate which is Middle to Late Ordovician in age. The siliceous clastic member of the Junee Group is missing. A similar situation may also occur at Misery Hill. The McLean Creek section may possibly represent a passage into the siliceous clastic rocks of the Junee Group but the relationship is obscured by faulted contacts.

5 cm

Acknowledgements

I am indebted to numerous people who produced or helped in the production of work necessary for the completion of this project. In particular I would like to acknowledge the assistance of: Ms H. M. Waldron for the Rare Earth Element determinations on basaltic samples; Dr J. B. Jago, for his constructive criticism of my compilation of Cambrian fossil data; Dr M. R. Banks, Dr C. F. Burrett, and Mr M. J. Clarke, for determination of numerous fossil finds; Dr J. A. Pearce, for many discussions about the dangers of the casual use of 'Pearce and Cann' diagrams; Dr N. J. Page and Dr G. K. Czamanske, for their encouragement and introduction to Alaskan-type ultramafic bodies; Professor D. H. Green, Dr S. Harley, and Dr G. A. Jenner for their guidance in experimental petrology; Dr P. L. F. Collins and Mr P. Creenaune for their permission to use analyses and sample material for REE determination; Mr L. A. Newnham, Goldfields Exploration, for assistance with logistical support during the mapping phase of the project; Aberfoyle Exploration, Amoco and C.R.A., for samples of basaltic lavas from diamond-drill hole cores; Mr M. J. Clarke and the late Dr N. Farmer for their review of the manuscript; Mr W. Jablonski, Central Science Laboratory, University of Tasmania for instruction on how to obtain good results from the electron microprobe; as well as numerous other people from the Department of Mines and many Universities and Mining and Exploration Companies with whom discussions relevant to this project were held.

Previous Literature

The following summary of previous literature only deals with the various uses of lithostratigraphic terminology. It is not intended to follow the time-related changes of attitudes of any specific writer, as their views in regard to age or correlation of different rock successions evolved or oscillated.

Historically, the geological literature of Tasmania has been plagued by confusion caused by the intermixing and synonymous use of lithostratigraphic and biostratigraphic terms. In this summary of the literature, only the development of lithostratigraphic terms will be considered.

The term 'Dundas Group' was originally used by Waller in 1905 (p. 624) to encompass a group of rocks that " . . . appears to have an extensive development on the west coast, though only in the North-east Dundas district has any attempt been made to define its limits. In this district the members of the group may be observed along the North-east Dundas Tramway from a point directly north of Leslie Junction to Williamsford . . . ".

Ward (1909*a*, p. 32) wrote "The greater part of the North Dundas tinfield (Renison Bell–Ringville area) consists of slate together with the coarser-grained sediments–sandstone, grit and conglomerate. The whole are to be considered as one series, and to them the term 'Dundas slates' has been applied, since the typical rock type is a slate". This general description is now known to include rocks now assigned to the Crimson Creek Formation (Taylor, 1954) (east of Renison Bell) and Success Creek Group (Taylor, 1954) (Renison Bell mine area), with the coarser-grained sediments in the Ringville–Dundas area belonging to the Dundas Group of Elliston (1954).

In 1910, Twelvetrees and Ward (p. 35–37) extended the term 'Dundas slates' into the Zeehan area after describing local sedimentary rock sequences. These sequences are now known to belong to the Crimson Creek and Oonah Formations. After working in the Stanley River tinfields, Waterhouse (1914, p. 33–34) differentiated an un-named group of " . . . schists, quartzites and slates of probable Pre-Cambrian age; . . . ", which have subsequently been incorporated into the Oonah Formation, from the 'Dundas slates' to the east in the Wilson River area (p. 41). The latter, he correctly stated, are continuous with the series of slate and sandstone developed at North Dundas (Renison Bell).

Conder (1918) remapped the area described by Ward (1909*a*), and although he continued with the concept and term 'Dundas slates' (p. 22), he recognised the 'red rock' horizon (p. 23) at Renison Bell, the top of which is now taken as the boundary between the Success Creek Group and the Crimson Creek Formation.

Reid (1925, p. 7–8) divided the rock sequences in the Dundas area into three series; the 'Proterozoic rocks', later to become the 'Concert Schist' (Blissett, 1962), being " . . . metamorphosed sediments . . . dipping at a high angle to the south-west underneath the Palaeozoic sediments, . . . "; and two Palaeozoic 'series', the 'Bischoff Series' and the 'Dundas Series'. The 'Bischoff Series', which later become Elliston's (1954) 'Carbine Group', is now included in the Oonah Formation. The 'Dundas Series', containing the 'younger rocks' of the area, is now included in either the Crimson Creek Formation or the Dundas Group (Elliston's).

Under the heading "Cambrian Cycle of Sedimentation: Pieman System", Carey (1947, p. 25) continued using the term 'Dundas Series' whilst placing the 'Pre-Cambrian' sedimentary rocks into the 'Davey System'. The common term 'Davey Group (System)' was a generalisation of David's (1932) 'Port Davey Series', which he introduced for the 'Port Davey and Ulverstone Schist Series'. Although never

defined, the term 'Davey Group' was widely used to encompass all the "Pre-Cambrian quartzite and schist sequences" in western Tasmania. Over the last twenty years this term has been found to be increasingly inappropriate, especially in the Port Davey area (Williams, 1979; 1982*a*).

In 1949, Hills and Carey (p. 21–22) proposed the 'Pieman Group' for all "Late Pre-Cambrian to Cambrian" rock systems of western Tasmania. In 1953, Carey (p. 1108) followed Elliston (1951) in using the terms 'Carbine Group', for the 'younger Pre-Cambrian', and 'Dundas Group' for the 'Cambrian' sequences. Carey (1953, p. 1108) pointed out that together, the Carbine and Dundas groups " . . . replaced the Pieman Group (System) used by Carey (1947) and Hills and Carey (1949) pending clearer definition of the old 'Dundas Series' of earlier workers".

Elliston (1951, 1954) used 'Davey Group' for the sequences of quartzite and schist exposed west of Dundas between Comet and Concert Creeks. Blissett and Gulline (1961*a*) followed Elliston in this usage, but Blissett (1962) and Blissett and Gulline (1962) introduced the term 'Concert Schist' for these rocks. All these writers considered that the quartzite and schist sequence was a window into underlying 'metamorphosed' or older 'Pre-Cambrian' rocks and that the 'younger' rocks in this area, the Carbine Group of Elliston (1951, 1954) were unconformably above. Williams (1978) suggested that this relationship is not valid. Turner (1979) has shown that the Concert Schist is a relatively higher metamorphic equivalent of, and gradational with, the surrounding rock successions [i.e. Carbine Group of Elliston (1951, 1954); Oonah Quartzite and Slate of Blissett (1962)].

Continuing the division of sequences in the Dundas area, Elliston (1951, 1954) defined the 'Carbine Group' ('younger Pre-Cambrian'), which was later incorporated into the Oonah Quartzite and Slate by Blissett (1962); and the Dundas Group, which is a fossiliferous Middle–Late Cambrian succession. Elliston (1954) also correlated the sandstone and mudstone sequence of the Renison Bell mine area with his 'Carbine Group'.

Taylor (1954) described four sequences of rocks which crop out along a 30 km section of the Pieman River west of Rosebery. He called the westernmost sequence 'Davey Group' (p. 20), but recognised (p. 21) that the degree of metamorphism of these rocks was not that of quartzite and schist of the Tyennan Block. This area was later included in the 'Oonah Quartzites and Slates' by Spry (1958) when he expanded the original definition of the 'Oonah Quartzite' of Hills and Carey (1949) ("A series of quartzites with slates which make up Oonah Hill, Zeehan") and greatly extended the area covered by this formation.

Taylor (1954, p. 21) also recognised the unconformable relationship between his 'Davey Group' and the overlying sequence which he defined as the Success Creek Group (p. 21). Continuing eastwards along the Pieman River, Taylor recognised another change near the mouth of the Wilson River and defined the sequence of rocks between this point and the ultramafic belt eight kilometres further east as the 'Crimson Creek Argillite Formation' (p. 23).

To the east of the ultramafic belt, Taylor (1954, p. 29) defined the Huskisson Group, and established a biostratigraphic and lithostratigraphic correlation with Elliston's Dundas Group. Taylor mistakenly considered the Success Creek Group to be a probable correlate of Elliston's 'Carbine Group' but stated (p. 27) " . . . [it is] . . . unwise at this stage to attach the name 'Carbine Group' to these rocks".

Campana *et al.* (1960) and Blissett and Gulline (1961*a*) combined Elliston's and Taylor's correlations and considered all the rock sequences defined as 'Carbine Group', 'Success Creek Group' and the sandstone and mudstone sequence in the Renison Bell mine area as 'Carbine Group'.

Blissett (1962, p. 23) used the term Oonah Quartzite and Slate after Spry (1958), but expanded it to include the Oonah Quartzites, Montana Melaphyre Volcanics and Nubeena Quartzites of Hills and Carey (1949), the Carbine Group of Elliston (1954) and the Success Creek Group of Taylor (1954), thus refuting the unconformable relationship reported by Taylor.

Solomon (1965) introduced the term 'Success Creek Phase' for a " . . . transgressive phase . . . " of sedimentation into which he included " . . . the Carbine Group at Dundas, the Smithton and Jane Dolomites, the Success Creek Group (Taylor, 1954), the sandstones and dolomite at Mt Bischoff, and the calcareous sequence below spilites on King Island and at Smithton". By doing this he correlated the Oonah Formation and correlates (Carbine Group, Bischoff Series) with rocks known to unconformably overlie the Precambrian successions (Success Creek Group, Smithton Dolomite). The term 'Success Creek Phase' is a confusion of chronostratigraphic and lithostratigraphic nomenclature and has been found inappropriate.

In summary, the following terms are inappropriate and are not used in this report:

> Davey Group; Carbine Group; Dundas Series; Dundas Slates; Davey System; Port Davey Series; Pieman Group; Oonah Quartzite; Oonah Quartzite and Slate; Crimson Creek Argillite Formation; Nubeena Quartzite; Montana Melaphyre Volcanics.

The following terms are considered to be adequate and have been used:

> Dundas Group; Huskisson Group; Crimson Creek Formation; Success Creek Group; Oonah Formation.

STRATIGRAPHY

Precambrian

OONAH FORMATION

PIEMAN RIVER AREA

Introduction

The Oonah Formation has never been strictly defined. The term Oonah Quartzite was originally used by Hills and Carey (1949) for "A series of quartzites with slates which makes up Oonah Hill at Zeehan". Spry (1958) extended this term to the Oonah Quartzite and Slate and increased the area covered by this formation to the north and west of Oonah Hill " . . . to the open country beyond the Pieman near Mt Livingstone". The area thought to have included rocks of the Oonah Formation was further extended by Blissett and Gulline (1962) and Blissett (1962) when, as well as following Spry's extension, they also included the 'Montana Melaphyre Volcanics' and 'Nubeena Quartzite' of Hills and Carey (1949), the 'Carbine Group' of Elliston (1954) and the Success Creek Group of Taylor (1954). The Success Creek Group was mistakenly incorporated into the Oonah Formation by Blissett and Gulline (1962) and Blissett (1962). Even though Taylor had mapped the unconformable relationship between the Oonah Formation and the Success Creek Group in the Pieman River, Blissett did not accept Taylor's findings and considered the term Oonah Quartzite of Hills and Carey (1949) had priority.

In this Bulletin, the Oonah Formation is used in its historical sense after Blissett (1962) with the exclusion of the Success Creek Group (Taylor, 1954), and the area covered by the formation is extended as far north as Mt Livingstone and west from Misty Valley to Whaleback Ridge on the basis of lithological and structural criteria. To the west of Whaleback Ridge, rocks of the Oonah Formation are gradational with rock sequences of the Whyte Schist. The above extension of the Oonah Formation is in physical continuity with the type section at Oonah Hill (Hills and Carey, 1949), and is a delineation of the northern continuation of the rocks included by Spry (1958) in his extension.

One of the characteristics of this sequence, as seen in the Pieman River " . . . is the presence of mica in small white to golden plates arranged parallel to bedding" (Taylor, 1954). The usual occurrence is that the white mica is associated with white indurated quartz sandstone, and the golden variety is associated with greyish indurated quartz sandstone and very-poorly sorted lithic sandstone and lithic wacke. Structurally, the presence of refolded mesoscopic and larger isoclinal folds is diagnostic of the Oonah Formation. In general, the Oonah Formation consists of interbedded white and grey indurated quartz sandstone and poorly-sorted wacke, with turbidite characteristics, interbedded with black, grey or green phyllitic mudstone and siltstone. Sedimentary rock nomenclature used in this report follows Williams, Turner and Gilbert (1954).

The age of the Oonah Formation has been considered by most writers to be Late Proterozoic to Early Cambrian. Radiometric dating over the last few years has dated the Penguin Orogeny, which deformed rocks of the Oonah Formation, at circa 725 Ma (Richards and Singleton, 1981; see Turner, 1982 for review of ages) making the formation of definite Proterozoic age and not as young as the Early Cambrian, as suggested by some writers (e.g. Campana *et al.*, 1960).

Correlation of rock sequences from different areas with the Oonah Formation is based on a combination of structural and lithological criteria. Lithologically the criteria included the recognition of turbiditic sequences of indurated quartz sandstone and quartz wacke, containing white or golden mica, interbedded with phyllitic siltstone and mudstone. Structurally, the presence of refolded isoclinal folds is diagnostic of the Oonah Formation in this area. The thickness, detailed stratigraphy and overall structure of the Oonah Formation is still unknown.

In the Pieman River at CP617744 (fig. 1), the Oonah Formation can be divided into two successions on the basis of lithology: a succession of siliceous indurated quartz sandstone and wacke interbedded with phyllitic mudstone and siltstone, typical of the sequences at Oonah Hill (Eos); and a succession of interbedded carbonate, mudstone and conglomerate with volcanic rock horizons and minor sandstone (Eom). On the basis of sedimentary structures, such as festoon current bedding and grading of beds, and structural evidence the carbonate-mudstone-volcanic succession is the uppermost of the two successions. Outcrop of the 'upper' succession continues north from the Pieman River in an arcuate zone along Misty Valley. Similar sequences of interbedded carbonate, calcareous sandstone, siltstone and mudstone with volcanic units occur in the Oonah, Queen and Montana Hill areas around Zeehan; in the Maestries-Comet areas at Dundas; and in the upper Huskisson-Ramsay River area. No volcanic rocks have so far been recorded in the sequence in the latter two areas.

The following use of the terms 'upper' and 'lower' successions is only applied to distinguish the dolomitic-mudstone-volcanic sequences from the sandstone-mudstone successions. Although an overall structural analysis of the Oonah Formation has not yet been done, the general structure in the mapped area (fig. 1) has been

ascertained along with a detailed sequence of structural events which have affected the Oonah Formation successions prior to deposition of the Success Creek Group.

'Lower' Succession

In the Pieman River section, the 'lower' succession of the Oonah Formation consists of monotonously interbedded sequences of indurated muscovitic quartz sandstone, quartz wacke and phyllitic mudstone. The sandstone beds are mainly very fine grained to fine grained, and range in thickness from less than 10 mm to greater than 500 mm. The thicker beds are commonly medium-grained to coarse-grained quartz wacke, and are more friable than the sandstone beds. Lithic components consist of indurated mudstone and chert fragments with minor zircon, green tourmaline, multiply twinned feldspar and magnetite grains. Rip-up mudstone fragments are common in the thicker turbidite beds. The matrix is usually mud-grade, can occupy up to 20% of the rock, and is now partly recrystallised as muscovitic beards around and between the clastic grains. Overgrowth between clastic quartz grains has occurred in some beds, but the clastic texture of sandstone predominates and the term quartzite cannot be applied.

In the area to the north of the Pieman River up to Mt Lindsay, and east of the Stanley River to Misty Valley, the 'lower' Oonah successions have features typical of a distal turbidite sequence, being dominantly Bouma B and C units with convolute laminations and minor graded sandstone units (Bouma A), at times with sole markings (Walker, 1967). Overall the succession is a monotonous repetition of dominantly laminar-bedded quartz and lithic sandstone, quartz wacke, siltstone and mudstone, alternating with zones dominated by mudstone and minor sandstone and siltstone. The sandstone beds are dominantly well-sorted quartz sandstone with some lithic fragments of indurated mudstone and chert, as well as clastic muscovite, green tourmaline and magnetite grains. No clasts of high-grade metamorphic terrain rocks have been observed.

Rocks exposed along Lone Spur [CP608782] are indurated quartz sandstone and wacke beds which range in grain size from very fine-grained to medium-grained, and are interbedded with siltstone and mudstone units. The sand-grade beds are up to 500 mm thick, with the interbedded siltstone and mudstone units ranging between one and five millimetres in thickness. The sandstone beds typically consist of 85–95% quartz grains, 0–10% rock fragments, and up to 15% matrix, and are well-sorted, the grains being angular to sub-rounded. Truncated cross-laminations are common. Quartzwacke beds are generally medium-grained, graded, and have angular to sub-angular grains of similar components to the sandstone beds, but in different proportions. Occasional horizons of very coarse-grained sandstone to granule conglomerate have 1–3 mm clasts of quartzite, phyllitic mudstone and rip-up mudstone clasts.

Sedimentary structures are common and include cross-bedding, grading, ripple and scour marks, flame structures, flute marks and up to 60 mm wide scour channels. Scour channels are usually filled by cross-laminated sandstone. Slump structures occur in siltstone units. Infilled festoon bedding has wavelengths up to 900 mm and amplitudes of 30 mm. Load casting accentuates sedimentary lensoids, flutes, flames, and interference ripples. Quartzwacke beds contain the greatest amount of sedimentary structures but contain very little metamorphic overprinting or recrystallisation.

In the dominantly laminated mudstone part of the sequence, the mudstone laminae are usually less than one millimetre thick, and are interbedded with 1–3 mm of siltstone and 1–5 mm of very fine-grained sandstone beds. Occasional 50–100 mm thick, medium-grained sandstone beds with cross-bedding occur. These sandstone units are usually boudinaged.

West of the Stanley River, along the Hydro-Electric Commission's Pieman Road, good exposures of the 'lower' successions exist in road cuttings and show typical variations through this part of the succession. The outcrops are commonly of muscovitic quartz sandstone and quartz wacke with subordinate black mudstone, the sandstone beds containing scour structures, rip-up mudstone clasts and cross-bedding. The cleaner part of the sequence has sandstone beds with thin mudstone partings or mudstone outlining cross laminations. Numerous sedimentary structures, as described above, are contained within the sand-grade units. In that part of the sequence dominated by mudstone, the sandstone units are usually fine-grained and boudinaged. Rip-up mudstone clasts can be up to 5 mm long and 0·5 mm thick, are tabular, and have ragged ends. Some sandstone beds are up to one metre thick with no apparent internal structures, whilst other beds contain cross-bedding outlined by green phyllitic mudstone. Most sand-grade beds have one good anastomosing cleavage, defined by secondary muscovite. The finer grained sandstone and siltstone units also contain a second cross-cutting crenulation cleavage, usually at a high angle to bedding. The interbedded mudstone units are indurated and have argillaceous to phyllitic characteristics. Where a crenulation cleavage is dominant the mudstone beds have a silky character with the dominant parting parallel to the compositional banding, formed during transposition, and not original bedding.

'Upper' Succession

An almost continuous outcrop of 'upper' succession sequences is exposed along a stretch of the Pieman River between CP617744 and CP621744. The overall succession is composed

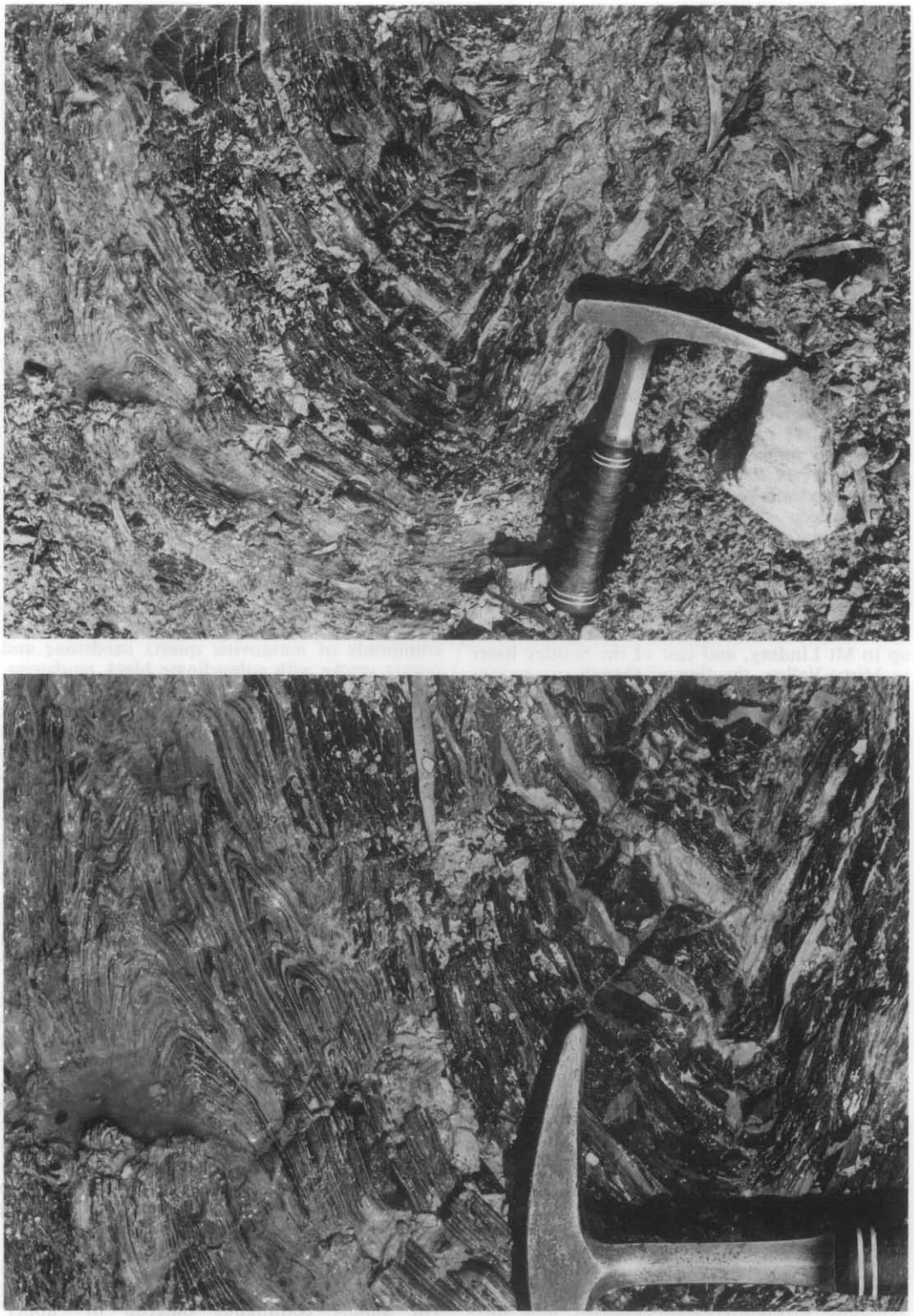

Plate 1. *Refolded isoclinal folds in the 'upper' Oonah Formation, Misty Valley area [fig. 1, CP634774]. Refolding fold* (top)*; Isoclinal folds on limb of refolding fold* (bottom).

of units of carbonate, sandstone, fine conglomerate, tuff and volcaniclastic lithic wacke interbedded with laminated siltstone and mudstone. Within the laminated part of the sequence the mudstone ranges from black to grey to purple with the siltstone being either purple or green. Both these rock types contain two easily recognisable cleavages, the morphologically dominant one being consistent with the north-westerly phase of Devonian deformation. In some of the thinner laminated units which also contain tuff horizons, intraformational soft-sediment disruption of bedding is evident.

The carbonate units are beds or lenses of recrystallised dolomite, and range in thickness from less than ten millimetres to greater than fifteen metres. The thicker units commonly have scoured tops which are infilled by siltstone. Some of the recrystallised carbonate units contain flow-aligned, elongate grains of quartz, chert and mudstone, in a cryptocrystalline carbonate matrix. The clasts range in size from fine-grained to medium-grained sand grade. Brecciated and foliated mudstone units are also interbedded with the carbonate units. Some carbonate beds have remnant bedding which is outlined by mudstone stringers and aligned grains of sand, both of which are parallel to the outer enveloping surfaces. Laminated mudstone units interbedded with carbonate horizons always carry two cleavages.

Sandstone beds range from fine-grained to coarse-grained, and often contain cross-bedding and ripple-marked bases. Some graded sandstone beds occur towards the top of the succession. Minor graded granule and fine-pebble conglomerate beds occur within the succession. The clasts in these units are up to four millimetres in diameter and the matrix is of coarse-grained sand grade.

Tuff horizons are interbedded with both laminated purple or grey mudstone and recrystallised carbonate-mudstone units. Thin, 0·25–5·0 mm vitric tuff horizons persist across two metres of outcrop without variation in thickness, implying that the water depth at the time of deposition was below wave base and above the carbonate compensation level. Soft-sediment disruption of bedding occured in parts of the sequence where thin tuff horizons are interbedded with laminated mudstone. The thicker tuff beds are 70–100 mm thick, are commonly reversely graded, and are usually overlain by siltstone.

Lithic tuff beds consist of clasts of vesicular lava, and clasts of feldspar microlites set in a matrix of black glass. In lithic vitric tuff horizons, the volcanic clasts are angular and flow-aligned. Crystal lithic tuff units contain a peperitic texture. One unusual five millimetre thick horizon consists of volcanic lava fragments of feldspar microlites in a black glass matrix, stacked one on top of another like mini-pillow lava. Associated volcaniclastic lithic wacke to granule conglomerate units are composed of angular to sub-rounded volcanic fragments, dominantly of feldspar laths in black glass, but some grains have chloritic pseudomorphs after ferromagnesian minerals in an indetermined matrix.

In Misty Valley, to the north-east of the Pieman River section, the 'upper' succession contains alternating sequences of laminated mudstone, indurated fine-grained lithic sandstone, carbonate lenses with mudstone laminae, foliated muscovitic siltstone and fine-grained crystal vitric tuff units. Throughout the sequence the mud component is recrystallised, sandstone units within laminated siltstone–mudstone sequences are boudinaged, and refolded isoclinal folds are common (plate 1). The foliated siltstone contains a good anastomosing cleavage, across which a crenulation cleavage is superimposed. In some lithic quartz sandstone beds the groundmass is pervaded by black iron oxide. Brecciated lithic vitric tuff units contain lava fragments with highly altered ferromagnesian minerals and lath-shaped feldspar in a quenched matrix of feldspar needles.

To the north of Misty Valley [around CP623785] occur further outcrops of alternating sequences of laminated black and grey mudstone and siltstone with up to 50 mm thick boudinaged layers of very fine-grained to fine-grained quartz sandstone and quartz wacke; and carbonate–mudstone horizons. The sandstone units contain ripple marks, scour and channel fill, and multiple-truncated cross-bedding. The quartz wacke units are commonly graded. Minor amounts of clastic muscovite, green tourmaline, zircon and iron oxide grains occur in sand grade units. Carbonate units range from 10–50 mm of recrystallised dolomite to silty and muddy dolomite with 1–3 mm of interbedded black mudstone horizons. Where mudstone is dominant the sequence is usually contorted and the interbedded sand-grade units show soft-sediment brecciation and/or boudinage structure.

Up to five cleavages can be measured in rocks of the Oonah Formation. The first surface is a slaty penetrative cleavage associated with isoclinal folding, the second is a cross-cutting crenulation cleavage associated with refolding of the isoclinal folds. The third surface is dominant in the closure zone of large scale folds which produce the regional anticlinorial–synclinorial folding. The fourth and fifth surfaces are consistent with Devonian deformation and appear as penetrative, crenulation or transposition cleavages, depending on composition and grain size of the affected beds.

ZEEHAN AREA

In the area south of the Pieman River towards Oonah Hill [around CP575685] (fig. 3), the 'lower' succession is dominated by thinly bedded sequences of fine-grained sandstone and medium-

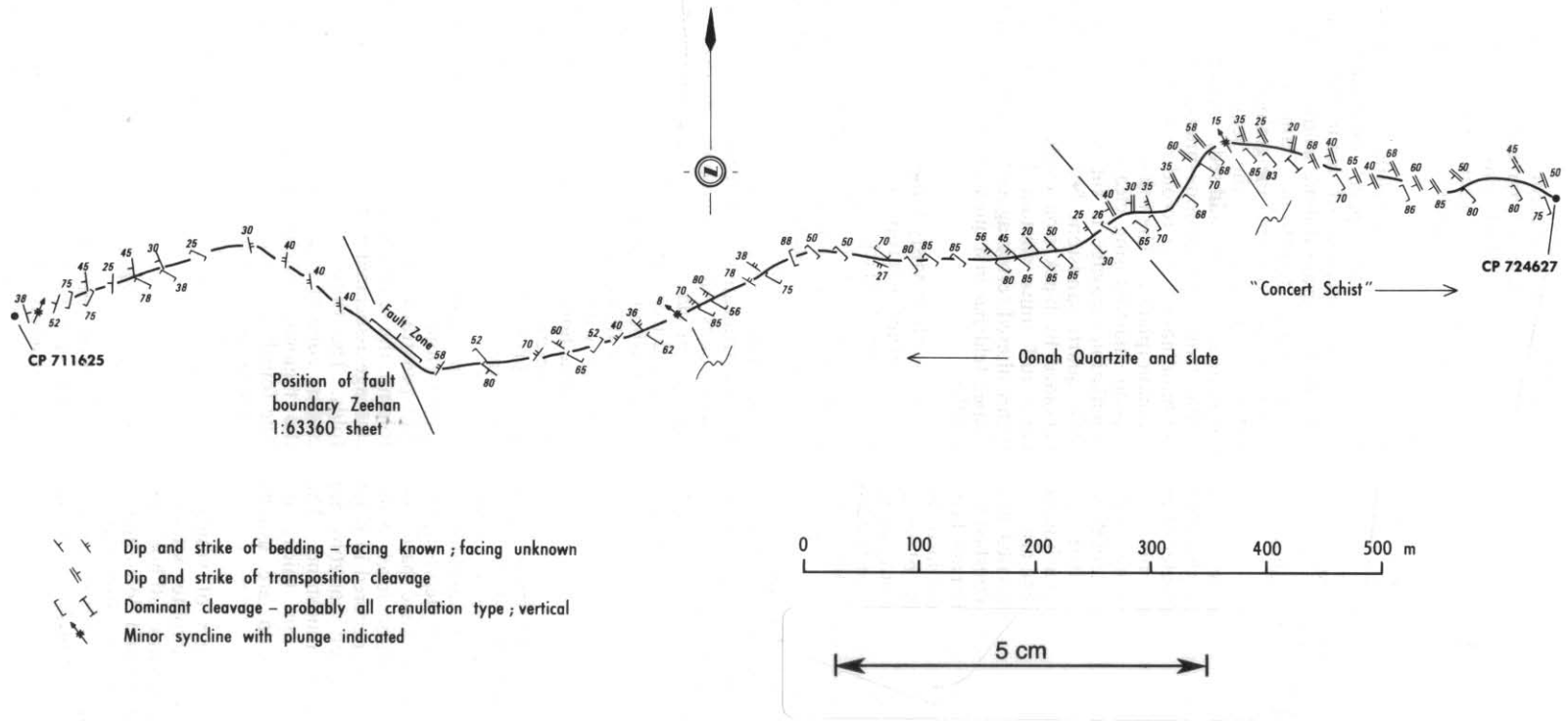

Figure 5. *Structural traverse across the boundary of the Oonah Formation correlate and Concert Schist, Dundas area.*

grained quartz wacke with interbedded siltstone and mudstone. In the thinly bedded parts of the sequence the sand-grade units form 60–80 mm thick sequences of 2–4 mm thick beds separated by one millimetre laminae of pale green or black mudstone. In that part of the sequence dominated by quartz wacke the sand-grade units range between 50 mm and 100 mm in thickness and are separated by 2–3 mm thick siltstone or mudstone beds. Cross bedding, ripple marks and festoon bedding occur in the sand-grade units in this area and some of the thicker units with cross-bedded tops contain numerous rip-up mudstone fragments up to 15 mm in length, in the lower part of the units. The white friable quartz sandstone beds commonly contain white mica whereas the grey quartz wacke units have golden micas.

The 'upper' succession of the Oonah Formation, as described in the Pieman River section and its north-easterly continuation into Misty Valley, can be correlated with the volcanic–mudstone–carbonate bearing sequences around Zeehan. These sequences were described by Montgomery (1893*a*, 1895, 1896) and the nature of the volcanic tuff and lava was first described as melaphyre (a term originally applied to any dark coloured porphyritic igneous rock but later restricted to altered basalt) by Thomae (1896) and Twelvetrees (1897). Hills and Carey (1949) used the term 'Montana Melaphyre Volcanics' for that part of the sequence around the Montana mine area, but with the far wider distribution of the 'upper' succession of the Oonah Formation, and the use of the non-definitive term melaphyre, the above formation name is only considered appropriate in an historical sense.

In the Zeehan area numerous references to dolomitic rocks interstratified with the siliceous and volcanic sequences of the Oonah Formation around the Oonah, Queen and Montana Hills can be found (Montgomery, 1893*a*, 1895, 1896; Thomae, 1896; Twelvetrees, 1901; Twelvetrees and Ward, 1910; etc.). Dark grey limestone and dolomitic limestone are developed locally to the north and west of Zeehan and also in the Dundas area (Blissett, 1962).

Petrographic and chemical data on the lavas associated with the 'upper' succession of the Oonah Formation is given on page 99.

DUNDAS AREA

In the Dundas area, correlates of the Oonah Formation occur on the north-western slopes of Mt Dundas. These sequences have previously been referred to by the now redundant terms of 'Bischoff Series' (Reid, 1925) and 'Carbine Group' (Elliston, 1954). To the east of the ultramafic rocks in the Dundas Rivulet (fig. 1), sequences of typical Oonah Hill-type indurated sandstone and mudstone occur. In the Maestries–Comet mine area, dolomitic conglomerate and carbonate mudstone successions were described by Blissett (1962), which are here correlated with the 'upper' succession of the Oonah Formation as described in the Pieman River.

The development of an extra cleavage and a higher grade of metamorphism within the succession becomes obvious along a spur track east of the Comet mine. The extra cleavage gives the rock assemblage a silky character, and the sequence is consistent with the description of Blissett (1962) for his 'Concert Schist'. The position of a sharp transitional boundary from normal Oonah Formation rocks into Concert Schist is considered to be 600 m east of the south-western fault margin of the Concert Schist as mapped by Blissett and Gulline (1962) at CP714625 on this spur track (fig. 5).

The Concert Schist of Blissett (1962) has its type section in Concert Creek between CP717639 and CP728641. Blissett considered that the Concert Schist was a basement high because of its higher degree of deformation compared to the surrounding Oonah Formation, but he was unable to find whether the boundary between the Concert Schist and Oonah Formation was unconformable or transitional. Turner (1979) has shown that the boundary between the Concert Schist and the Oonah Formation at CP715635 is a sharp but transitional contact in both degree of deformation and metamorphism. A similar relationship to that described by Turner (1979) has been observed on the western boundary of the Concert Schist at CP720626, and on the eastern margin at CP728620.

There are three observable cleavages in the Concert Schist whereas there are usually only two in rock sequences of the Oonah Formation in this area (Turner 1979; this study). The degree of mineral segregation and quartz recrystallisation in rocks of the Concert Schist is higher than in Oonah Formation sequences (Turner, 1979). Elliston (1954) used the now redundant term 'Davey Group' for this sequence of rocks. Rock samples from within the Concert Schist are indurated quartz sandstone and quartz wacke, interbedded with schistose black mudstone and green siltstone. In one area [CP728628], late large scale (up to two metres half angle) box folds are common.

In the Dundas area the sequences alternate between dominantly sandstone with minor siltstone and mudstone, and dominantly mudstone with minor sandstone and siltstone. Where sandstone is dominant the units are thick, greyish white and contain current bedding and ripple-marked bases. The associated siltstone and mudstone are thin units and have a well-developed fissile parting parallel to compositional layering. In that part of the sequence where mudstone is dominant it is dark grey to black in colour and highly fissile. The associated sandstone units are micaceous, graded and often contain flame structures and other sole markings.

The 'lower' succession correlates consist of interbedded, fine-grained micaceous quartz sandstone, thin-bedded micaceous quartz sandstone and siltstone, and laminated hard greyish black mudstone with a good bedding facility. Sedimentary structures within these units include grading, cross-laminations, ripple and sole marks. Isoclinal folds with a good axial plane cleavage parallel to bedding are quite prevalent throughout the sequence and these have been refolded by a later open style of folding.

The 'upper' succession is generally finer grained and consists of thinly interbedded quartz sandstone and black mudstone and includes interbedded dolomite and limestone and some horizons of lava flows and pyroclastic deposits. This sequence is considered to be a correlate of the upper part of the Oonah Formation, on structural and lithological grounds.

RAMSAY RIVER AREA

The large area correlated with the Oonah Formation in the upper Huskisson, Ramsay and Coldstream River area (fig. 1) [CP740930] consists of a central zone dominated by quartz sandstone and quartz wacke with minor laminated black mudstone which is correlated on structural and lithological criteria with the dominantly sandstone succession or 'lower' sequence of the Oonah Formation. The structural criterion used in all correlations with the Oonah Formation is the presence of refolded isoclinal folds within the succession. On either side of this zone, and in faulted contact with it, are sequences of dominantly calcareous siltstone and conglomerate with minor quartz wacke and mudstone. Although these sequences are correlated with the'upper' dominantly mudstone–siltstone succession of the Oonah Formation, no volcanic units have been found in this area and the lithology, in part, is different from that found in the Pieman River. This area of rocks is also considered to be a southern continuation of the Bischoff Series (Groves, 1968; Williams, 1982*b*) at Mt Bischoff, which is correlated with the Oonah Formation on both structural and lithological criteria.

The dominantly quartz sandstone and wacke sequence, correlated with Pos, continues to the south but as the boundaries cannot be accurately defined in the middle and southern part of the area the term Pu is used in Figure 1. In the solid geology compilation map (fig. 3) the area has been differentiated into Pom and Pos. The northern part of the correlate with Pos consists of clean quartz sandstone with laminated siltstone–mudstone and black mudstone. The sandstone units are from 10 mm to 20 mm thick and can be separated by 0·5 mm of black mudstone. In part of the sequence, well-bedded, indurated quartz sandstone and friable quartz wacke also occur with thinly bedded and laminated siltstone and mudstone. The thinner sand grade units contain sole markings whereas the thicker units contain rip-up mudstone platelets and other turbidite characteristics.

In the John Lynch Creek [CP742846] section to the south, the dominantly quartz-rich section consists of very fine-grained to medium-grained quartz sandstone and black mudstone. The quartz sandstone units are boudinaged within zones of dominantly mudstone.

The succession to the west of the Pos correlate, as exposed in the Ramsay River, varies in the proportion of different rock types but is dominated by thinly-bedded calcareous siltstone. The calcareous sequence of sedimentary rocks is in faulted contact with the Pos correlate on its eastern boundary [CP748945] and in faulted contact with an area of Crimson Creek Formation correlate along its western margin. In the northern part, the sequence is metamorphosed by the Meredith Granite [around CP734943] and the dominantly calcareous horizons consist of recrystallised carbonate with the mudstone and sandstone having been hornfelsed. Typical karst topography has developed in weathered calcareous units around CP736949. Calcareous pebble conglomerate, consisting dominantly of recrystallised carbonate clasts with minor indurated siltstone clasts and a groundmass totally pervaded by carbonate, occurs at CP736947 and CP736939. Along the southern part of the Ramsay River, sequences of recrystallised calcareous quartz-mica siltstone and sandstone with minor carbonate horizons contain numerous refolded isoclinal folds [CP734925].

To the east of the Pos correlate is another sequence dominated by calcareous siltstone and conglomerate with minor quartz wacke. This sequence is well exposed in the Coldstream River and the upper reaches of John Lynch Creek. It can be observed in faulted contact with Dundas Group correlates (Ɛh) at six different points between CP759935 and CP756912 in river and track sections. The western margin is in faulted contact with the Pos correlate at CP751944. This sequence also contains turbiditic quartz sandstone and quartz wacke. The turbiditic units show grading from sand to silt grade, and have laminated and cross-bedded siltstone horizons. The sand grade units are usually well bedded and clean, but some contain rip-up mudstone clasts. The sand grade units range in thickness from 50 mm to 300 mm and are interbedded with up to 50 mm of laminated siltstone horizons. Load enhanced sole marks and flame structures are common in the clean sandstone beds. Where mudstone units are dominant, the sandstone beds are boudinaged or are found as noses of rootless and isoclinal folds in the deformed mudstone. The quartz wacke units are muscovitic and contain angular fragments of quartzite, chert, indurated mudstone and quartzite, as well as brown tourmaline, hematite grains and clastic and secondary muscovite.

In the Mackintosh Quadrangle (Barton *et al.*, 1966) a sequence of mudstone and greywacke with bedded limestone was mapped in the Coldstream River (Ecm). This sequence is a probable correlate of Eom, being an easterly extension of the calcareous siltstone sequence (fig. 3). Re-examination of thin sections from rock samples described from this sequence (Collins *et al.*, 1981) shows that the siltstone, recrystallised limestone and calcareous conglomerate are similar to the rocks found in this study.

STRUCTURE

A detailed structural analysis of the whole of the Oonah Formation was not undertaken, but an area of approximately 30 km², from the Pieman River north to the foothills of Mt Livingstone, was mapped in detail to characterise the structure contained within the Oonah Formation, so as to be able to compare it with the structure contained in younger formations.

Rocks from within the Oonah Formation contain up to five different cleavages. Usually three are recognisable in any one outcrop, two of which are crenulation cleavages. The earliest recognised cleavage is associated with a phase of isoclinal folding which produced folds with an amplitude of from centimetres, in siltstone–mudstone horizons, to metres in quartz sandstone successions. The isoclinal folds are well exposed in quartz sandstone sequences within the Pieman River section between CP605741 and CP618744 and in the dominantly mudstone–siltstone successions around CP633773.

The second cleavage is associated with a phase of folding which refolded the isoclinal folds. This fold phase produced a random distribution of isoclinal fold axes, and crenulated the cleavage produced during isoclinal folding in the fold closures, but parallels this first cleavage in the fold limbs. Refolded isoclinal folds occur in the upper succession around CP633773 (plate 1).

The third folding phase produced large scale folds with an ENE-trending fold axis and is responsible for the anticlinorial–synclinorial structures which regionally dominate the Oonah Formation in the Zeehan–Pieman River–Mt Livingstone areas. Both of the earlier cleavages are crenulated in the fold hinge zones of these folds, but parallelism with one or other of the earlier cleavages can occur in the limbs. Good exposures of this phase of folding occur along Lone Ridge, especially between CP790590 and CP783600.

The fourth and fifth cleavages are steep surfaces with directions which are consistent with the earlier northerly and later north-westerly phase of Devonian deformation. No more than three cleavages were measured in any one outcrop, these usually being two of the first three cleavages and one of the Devonian directions, although where refolded folds are encountered in the fold zones of the third fold phase, it is possible that the five directions may be obtained.

The effects of the numerous fold phases on the Oonah Formation can be seen from stereographic plots of bedding and cleavage readings obtained from three different areas within the Oonah Formation succession. The first area (fig. 7*a* and *b*) is a 5 km by 3 km ellipsoid (area 1, fig. 6) to the west of the area covered by Figure 1, extending from the foothills of Mt Livingstone [at CP557830], five kilometres to the south along the ridge to the west of the Stanley River, to CP549780; and from the Stanley River bridge [CP576814] three kilometres along the HEC Lower Pieman Dam road to approximately CP543803. This information will be presented on the Corinna 1:50 000 series map sheet.

The data plotted on Figure 7 (*c* and *d*) is from an arcuate traverse along Lone Spur (area 2, fig. 6) from CP588802, south-east to the Pieman River around CP605741. Both of these areas show the dominance of the pre-Devonian ENE phase of folding within the dominantly quartz sandstone successions of the lower Oonah Formation.

Figure 8 (*a* and *b*) demonstrates the overprinting of Devonian deformation on the dominantly mudstone successions of the upper Oonah Formation in the Misty Valley area (area 3, fig. 6). Earlier phases of deformation are shown by the almost random spread of low level maxima.

Stereographic plots of bedding and cleavage (fig. 8*c* and *d*) from the Oonah Formation correlate in the Ramsay River area (area 4, fig. 6), show multi-phase deformation within this succession. This, plus the presence of refolded isoclinal folds and the lithology, were the basis of correlation with the Oonah Formation.

Data from holes drilled through the Tertiary basalt plateau south of Waratah have indicated that the Oonah Formation correlate in the Ramsay River area is continuous, under the basalt cover, with the previously correlated Bischoff Formation at Mt Bischoff.

Reconnaissance mapping to the west of the Stanley River, in the Whaleback Ridge area, has shown that the eastern edge of the Arthur Lineament is structurally and lithologically gradational with the Oonah Formation, similar to the situation which occurs between the Oonah Formation correlate and the Concert Schist to the east of Dundas (fig. 5).

SUMMARY

In the Zeehan–Pieman River–Mt Livingstone areas the Oonah Formation consists of a lower succession of quartz-rich distal turbidite sequences conformably overlain by an upper succession of mudstone, carbonate and extrusive volcanic rocks. Structurally the successions of the Oonah Formation contain refolded isoclinal folds which are folded on a regional scale by

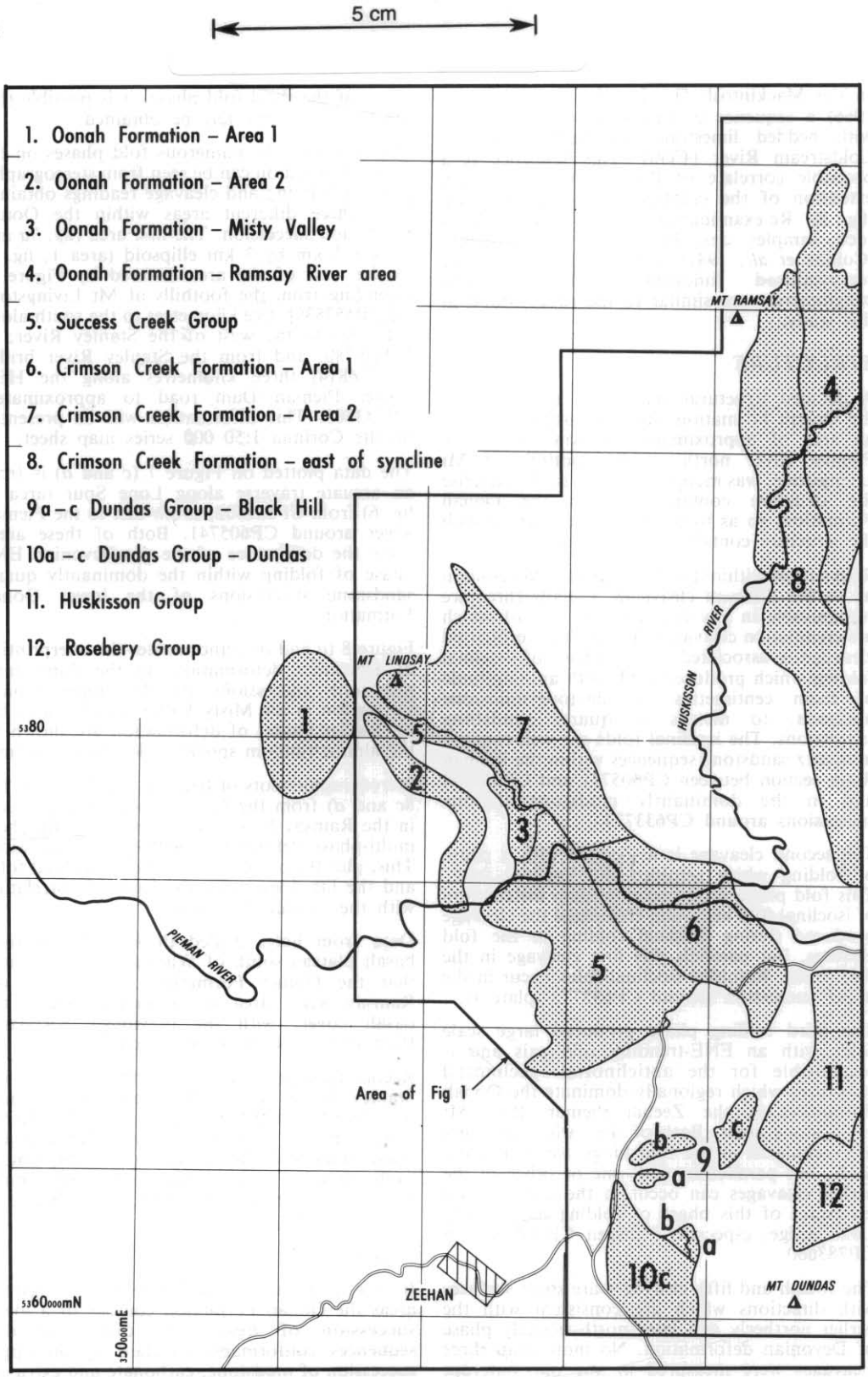

Figure 6. *Location map for structural domains.*

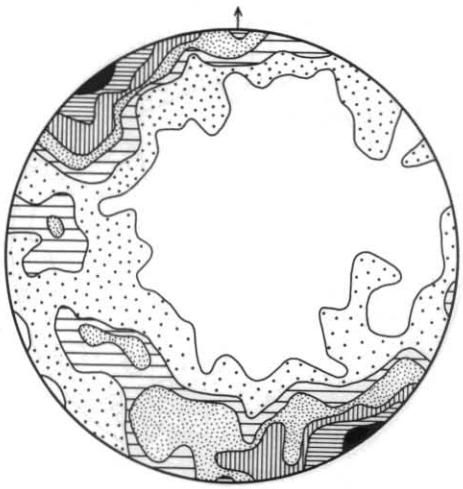

(a) Lambert Projection of 277 poles to bedding: Oonah Formation, Area 1 Figure 6. Contour intervals 0·25,1·25,2·5,4·5,6·5,8·5%.

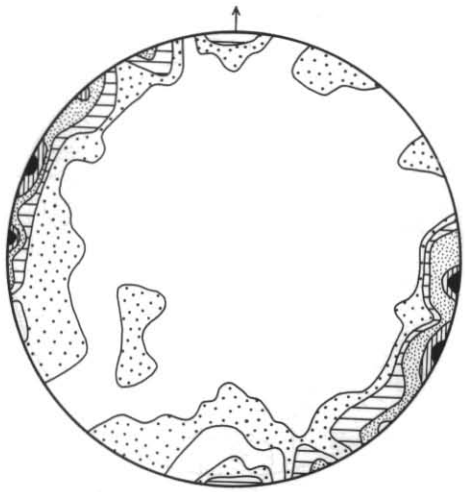

(b) Lambert Projection of 81 poles to undifferentiated cleavage: Oonah Formation, Area 1 Figure 6. Contour intervals 0·5,4·5,8,11·5,15·5%.

(c) Lambert Projection of 179 poles to bedding: Oonah Formation, Area 2 Figure 6. Contour intervals 0·25,2,3·5,5·5,7%.

(d) Lambert Projection of 106 poles to undifferentiated cleavage: Oonah Formation, Area 2 Figure 6. Contour intervals 0·5,3·5,6,9,12%.

Figure 7. *Stereographic plots, Oonah Formation (Areas 1 and 2, Figure 6).*

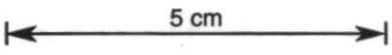

(a) Lambert Projection of 129 poles to bedding: Oonah Formation, Area 3 Figure 6. Contour intervals 0·5,2·5,5,7·5%.

(b) Lambert Projection of 77 poles to undifferentiated cleavage: Oonah Formation, Area 3 Figure 6. Contour intervals 0·5,3·5,6,11,13·5%.

(c) Lambert Projection of 245 poles to bedding: Oonah Formation, Area 4 Figure 6. Contour intervals 0·2,1,2,3,3·5,4·25%.

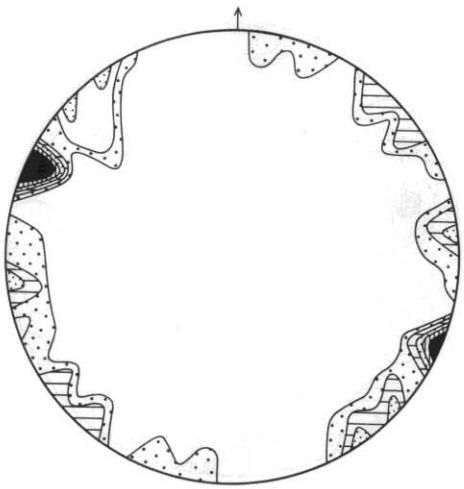

(d) Lambert Projection of 26 poles to undifferentiated cleavage: Oonah Formation, Area 4 Figure 6. Contour intervals 2,6,8,17,25%.

Figure 8. *Stereographic plots, Oonah Formation (Areas 3 and 4, Figure 6).*

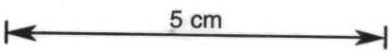

a third phase of folding. This deformation is considered to have occurred during the Penguin Orogeny, and to have been overprinted by both the early northerly and later north-westerly phases of Devonian deformation.

Eocambrian

SUCCESS CREEK GROUP

BOUNDARY RELATIONSHIP WITH THE OONAH FORMATION

In the Pieman River at CP621744, the 'upper' succession of the Oonah Formation is overlain by the basal formation of the Success Creek Group (Taylor, 1954). The boundary, being a landscape unconformity, represents a structural and low-grade metamorphic break as well as an hiatus in sedimentation. The transgressive onlap nature of the unconformity can be inferred from relationships observed in the Misty Valley area [CP634759-CP627788] and in creek sections south-west of the HEC's Lower Pieman Dam road between CP592801 and CP613795.

Taylor (1954) was the first to recognise the unconformable relationship between the rocks of the Oonah Formation downstream and the rock sequences upstream of CP621744 but he included, as the basal part of the Success Creek Group, what is now considered to be the uppermost outcrop of the mudstone-carbonate sequence of the Oonah Formation. Taylor (1954) also recognised the basal mixtite, which he described as " . . . a rather soft breccia containing angular fragments of purple sandstone and white tuff. The matrix is yellow to red fine grained material. The size of the fragments is extremely variable".

Blissett (1962) did not consider that the rocks described by Taylor as the Success Creek Group were different from the Oonah Formation. Blissett also considered that there was " . . . no evidence found for an unconformity between these beds and the coarser underlying series". By doing so, he incorrectly extended the area covered by the Oonah Formation up to a supposed conformable boundary with the Crimson Creek Formation at the confluence of the Wilson and Pieman Rivers [CP646765]. Field evidence obtained during this study validates the findings of Taylor (1954), regarding the existence of the Success Creek Group, and proves the unconformable relationship with the underlying Oonah Formation.

The difference in metamorphic grade on either side of the unconformity is slight. Within rocks of the Oonah Formation, the matrix fraction of the sandstone units is recrystallised and commonly occurs as muscovitic beards in the cleavage direction around and between the clastic grains. Overgrowth between clastic grains has occurred, but the basic clastic texture of the sandstone predominates. In the rock sequences above the unconformity, only partial recrystallisation of the matrix component has occurred and this is parallel to the dominant cleavage. Overgrowth between the clastic grains has not been observed in the Success Creek Group rocks outside the contact metamorphic aureole of the Meredith Granite.

INTRODUCTION

The Success Creek Group and correlates crop out over approximately 35 km^2 in an elongate NW-SW area between Mt Lindsay and Renison Bell (fig. 1). The boundary relationship with the Oonah Formation, along the south-west margin of this area, is dominated by faulted contacts developed during Devonian deformation. Along the north-east margin the sequences are either conformable, or in faulted contact with, the Creek Creek Formation. Between the Pieman River and the Dunkley Tram the lower formations are affected by a series of broad NE-SW trending folds, whereas between the Dunkley Tram and Renison Bell, parts of different formations are juxtaposed by a series of block faults. Along a line between CP638704 and CP678722, most of the Success Creek Group appears to be repeated by faulting, but neither the unconformity nor the basal mixtite are exposed.

Based on work carried out during this project, the Success Creek Group is here redefined, after Taylor (1954), to consist of four mappable formations, each having a variable thickness. All formations crop out in Taylor's type section along the Pieman River, where they have a total measured minimum thickness of 950 metres.

The basal formation is a mixtite (Esc; fig. 1), and consists of poorly sorted, immature, polymict conglomerate with sandstone lenses. This is gradationally followed by the second formation which is characterised by interbedded, clean, shallow-water quartz sandstone with minor siltstone, pebbly sandstone and conglomerate (Esd). In the Renison mine area this dominantly siliceous sandstone formation was originally called the 'Dalcoath Quartzite' (Gilfillan, 1965) but as the siliceous units of this member have a good clastic texture and, outside the mine area no quartzite textures were encountered, the term Dalcoath Formation is preferred.

The Dalcoath Formation grades rapidly into the third formation (Ess) which is dominated by laminated mudstone and siltstone with minor sandstone and conglomerate units. This formation is characterised by pervasive intraformational soft-sediment deformation which later reacted incompetently during localised large scale slump movements. The uppermost formation, part of which is exposed in the Pieman River, consists of thinly bedded siliceous siltstone with mudstone partings and minor sandstone and calcareous units (Esru). The lower member of this formation is a continuation of the 'Renison Bell Shale' (Gilfillan, 1965) from the Renison mine area

As the dominant units in this sequence are clastic siliceous siltstones with mudstone partings, the term shale is inappropriate and the term Renison Bell Formation is preferred.

In the Pieman River section the top member of the Renison Bell Formation (Esrr), as found to the north in the Mt Lindsay–Salmon Creek area, and to the south around and within the Renison mine area, is missing. In both the above areas the topmost carbonate units of the dominantly siltstone member are conformably followed by interbedded hematitic chert and mudstone with minor lithic wacke and conglomerate. The hematitic chert–mudstone sequence was first described by Conder (1918) as the 'red rock' sequence. In the Renison mine area the red rock sequence has been previously considered both as the basal unit of the Crimson Creek Formation (Blissett, 1962) and as a transitional formation separating the Success Creek Group and the Crimson Creek Formation (Newnham, 1975; Patterson *et al.*, 1981). Although the 'red rock' sequence is faulted out in Taylor's type section of the Success Creek Group–Crimson Creek Formation in the Pieman River, the essential difference between these two successions, the outgoing of the siliceous sandstone and siltstone and the incoming of basic volcaniclastic mudstone and lithic wacke, was recognised by Taylor. With this in mind, and the fact that the 'red rock' sequence represents a continuation of the shallow-water nature of the Success Creek Group, as against the turbiditic character of the Crimson Creek Formation, and that siliceous clastic units also occur within the 'red rock' sequence, it is considered that to be consistent with the original intent and definition of Taylor, the 'red rock' sequence should be included as a member of the Renison Bell Formation and be the uppermost member of the Success Creek Group.

Based on lithological character, sedimentary structures, and the presence of worm burrows and stromatolites, the Success Creek Group is considered to have been deposited in a shallow-water environment with the topmost member being a tidal flat–flood-plain environment. The presence of mudflow conglomerate, combining material from at least two different sources, plus intraformational soft-sediment structures and later large scale but short distance slumping in the finer units, suggests that deposition was within a relatively unstable rift environment which was deepening at the time.

Esc

The basal mixtite, as exposed along the Pieman River, is 50 m thick and consists dominantly of locally-derived material overlying the Oonah Formation rocks with landscape unconformity. The mixtite has an open framework, is immature, and of a polymict nature. The clasts range in size from pebble to coarse-cobble grade and the matrix is of silt, sand and carbonate. As well as angular to semi-rounded clasts of locally derived, recrystallised carbonate, dolomitic siltstone and mudstone, well-rounded cobbles of white, bluish-grey and pink quartzite, and red and grey chert are intermixed throughout the mixtite. Lenses of silt to coarse-sand grade material occur throughout the mixtite, having an orientation subparallel to bedding in the overlying sandstone sequence. The lenses consist of finer grained fragments of the same material as that within the conglomerate, in a matrix of partially recrystallised carbonate, mud and disseminated hematite.

Esd

Along the Pieman River the sandstone formation gradationally overlying the basal mixtite is approximately 550 m thick. Individual beds range in thickness from a few millimetres up to approximately 300 mm, are dominantly very fine-grained to fine-grained quartz sandstone, with minor medium-grained lithic sandstone, quartz wacke, granule to pebble conglomerate and siltstone.

The sandstone beds range from white and friable to bluish-grey and siliceous. They are usually very clean and well-sorted, with angular to subrounded grains of quartz, phyllitic mudstone, quartzite and chert with minor clastic muscovite and green tourmaline. The quartz grain to rock fragment content in different beds ranges from 95:5 to 70:30, the rock fragments being quartzite, chert and indurated mudstone. Minor clastic muscovite and green tourmaline also occur. Numerous sedimentary structures occur throughout the sandstone beds, including cross laminations, ripple marks, small scour channels, undulating and wispy bedding, and load-modified dish structures.

The wacke and conglomerate units are composed of the same components as the sandstone beds but also contain well-rounded quartz grains as well as clastic leucoxene and hematite. Interbedded laminated siltstone units are usually green and micaceous, 1–2 mm thick, and in places [around CP656690] are bioturbated in the plane of bedding.

In areas of Dalcoath Formation successions, between the Pieman River and Renison Bell, the rock units are uniform in character and little variation occurs from area to area. Towards the top of the formation, as exposed along the Argent Dam road [around CP685714], calcareous siltstone and laminated muscovitic mudstone appear within the dominantly sandstone succession, and the sequence rapidly grades into laminated siltstone and mudstone successions which contain fine-scale, soft-sediment deformation.

The Dalcoath Formation in the Renison mine area is 800 m thick and consists of thickly bedded quartz sandstone with interbedded siltstone and calcareous siltstone (Collins, 1972; Newnham, 1975; Patterson *et al.*, 1981). Orthoquartzite and protoquartzite have also been

recorded within this formation in the mine area (Patterson, 1979; Patterson *et al.*, 1981) and it is possible that the quartzite textures are a function of contact metamorphism due to granitic bodies within the mine area. Deep drilling in the mine area shows that a granitic body has intruded the area at depth and removed all trace of basement rock successions and the basal mixtite, and is in contact with the Dalcoath Formation (L. Newnham, pers. comm.).

Ess

Faulted against the eastern side of the sandstone formation in the Pieman River is what was originally a 75 m thick sequence of interbedded, laminated siltstone and mudstone with beds of friable and siliceous quartz sandstone up to 100 mm thick, and conglomerate. This formation now crops out as areas of highly disturbed sedimentary rocks which show all degrees of deformation from soft-sediment slumping to sliding, resulting in places in a highly deformed mélange (fig. 9). The mélange has an over and under zone of boudinaged sandstone and blocks of undisrupted laminated material in a schistose and brecciated siltstone–mudstone matrix.

In the area of Ess to the west of Renison Bell, the Dalcoath Formation grades rapidly into this third formation, which, like the river section, shows all degrees of deformation from soft-sediment slumping to large scale sliding, again resulting in localised, but highly deformed mélange.

Esru

The uppermost formation of the Success Creek Group consists of two very distinct members:

Esr; a sequence up to 100 m thick of thinly bedded siliceous siltstone with mudstone partings interbedded with minor, very fine-grained to fine-grained sandstone, calcareous siltstone, laminated mudstone, pebble conglomerate and calcareous units. This member is a continuation of the 'Renison Bell Shale' (Gilfillan, 1965) from the Renison mine sequence.

Esrr; a sequence up to 50 m thick of hematitic chert and mudstone with minor carbonate, lithic wacke and conglomerate units, the 'red rock' of Conder (1918).

The use of Esru on Figure 1 is restricted to areas which cannot be mapped successfully as either Esr or Esrr. Overall the Renison Bell Formation is fairly uniform but variations in thickness and rock type occur along strike from the Renison mine area to the Pieman River.

Esr

This dominantly siliceous siltstone member consists of thinly bedded (1–5 mm) siliceous siltstone with mudstone partings interbedded with minor, very fine-grained to fine-grained sandstone beds (10–200 mm thick), calcareous siltstone, laminated mudstone, carbonate and conglomerate units. The sequence as a whole contains a good planar fissility parallel to bedding due to the recrystallisation of mudstone laminae.

The sequence in the Pieman River is 75 m thick. The eastern margin is overturned and is in faulted contact with the Crimson Creek Formation. Mud-pellet bearing fine-grained sandstone and pebble conglomerate units occur towards the top of the sequence and the siltstone units range from siliceous to calcareous or muddy. Bedding thickness ranges from one millimetre to ten millimetres for the mudstone and siltstone units, and from 20 mm to 200 mm for the sandstone and conglomerate beds. Numerous sedimentary structures are found within the sandstone beds and the siltstone units are commonly cross-laminated. In the coarser grained beds the ratio of quartz grain to rock fragment ranges from 80:20 to 50:50, with the rock fragments being approximately one-third indurated mudstone and two-thirds quartzite, chert and clastic mica. Mudstone laths up to 0·5 mm thick and 5 mm long are common in the laminated siltstone and very fine-grained sandstone beds and are usually orientated parallel to bedding.

The lower part of this formation, as exposed along the overturned eastern side running from the Pieman River south-east to Success Creek, contains greenish-grey quartz sandstone beds in a sequence dominated by hematite-stained thinly interbedded siliceous siltstone and mudstone. The siltstone beds are often cross-laminated and the sandstone beds contain ripple marks and basal flame structures, as well as thin mudstone laminae partings.

From Crimson Creek, south-east towards Renison Bell, dolomitic siltstone horizons are found within this sequence and in some places soft-sediment deformation, similar to that found within Ess, is observed within horizons of laminated black mudstone towards the lower part of the formation.

In the Renison mine area (Gilfillan, 1965; Collins, 1972; Newnham, 1975; Patterson, 1979; Patterson *et al.*, 1981) the original 'Renison Bell Shale' is considered to conformably follow the Dalcoath Formation, the basal bed being the 'No. 3 carbonate/dolomite', a 4–8 m thick sequence of poorly laminated calcareous siltstone and dolomite. The siliceous siltstone member is reported to be 60 m thick and consists of laminated siltstone and mudstone with minor conglomerate and sandstone beds. Pebble conglomerate units within this sequence have erosional bases with the underlying siltstone beds. Soft-sediment deformation is reported from within the succession and could be a local equivalent of Ess, which is not reported as a separate mappable formation within the mine sequence. The top of the siltstone member in the mine area is taken as the 'No. 2 carbonate/dolomite horizon', a 5–15 m thick sequence of

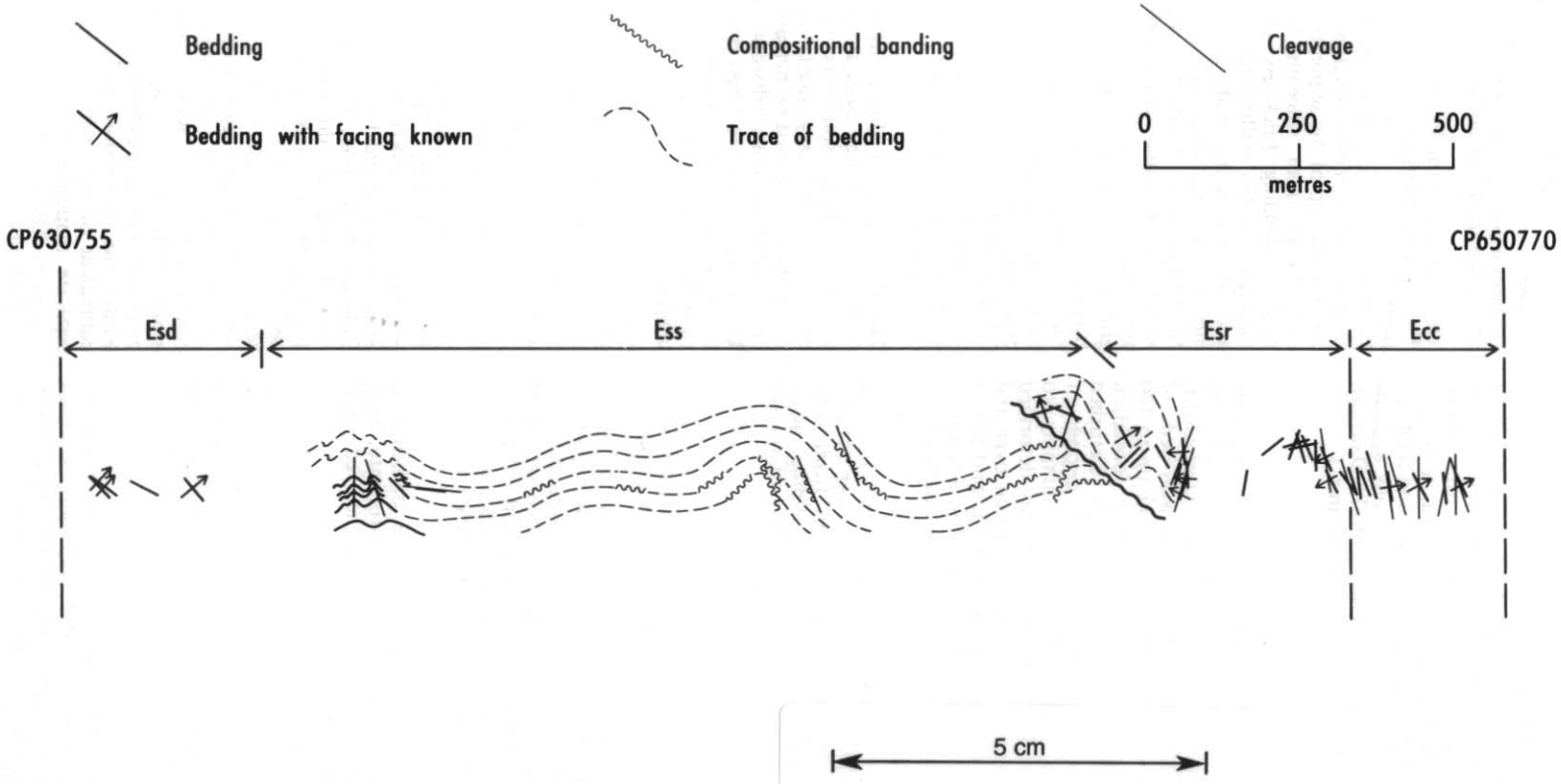

Figure 9. *Cross-section, Success Creek Group, Pieman River.*

calcareous siltstone, fine-grained sandstone and dolomite. As the carbonate horizons of the mine sequence cannot be followed with any certainty away from the mine area using only surface geology, correlation to any specific carbonate horizon or boundaries defined between different members as being specific carbonate horizons is speculative.

Esrr

In the Renison mine sequence, the 'red rock' member is here taken to include a 20–30 m thickness of hematitic chert and mudstone with interbedded coarse-grained sandstone, lithic wacke, conglomerate and siltstone, as well as the 15–20 m thick No. 1 carbonate/dolomite of the mine sequence. One kilometre to the north-west of the mine area, the surface outcrop of the 'red rock' member is restricted to red, pink and white chert with interbedded mudstone, lithic wacke and conglomerate beds. Carbonate units are rarely found in outcrop.

A correlate of the 'red rock' member occurs to the north of the Pieman River in the Misty Valley-Salmon Creek area. A good section through this correlate is exposed in cuttings along the Lower Pieman Dam road around CP615798. Regionally, this east-facing sequence underlies the Crimson Creek Formation with conformity, but in detail the contact zone contains many tectonic features. The sequence in this area is characterised by thinly interbedded hematitic red chert and mudstone, siltstone, lithic wacke and conglomerate with numerous thin carbonate beds, and is approximately 15 m thick.

Volcanic detritus in granule and conglomerate units found within the 'red rock' member during this study, and reported by earlier workers (Collins, 1972; Newnham, 1975; Hutchinson, 1979; Patterson, 1979; Djakic, 1980; Patterson *et al.*, 1981), is consistent with being derived from the volcanic units within the 'upper' succession in the Oonah Formation, and is dissimilar to the basic volcaniclastic detritus from the Crimson Creek Formation. It does not belong to the initial phase of the Crimson Creek Formation volcanics, nor represents a phase of volcanism which also produced the hematitic chert and mudstone by volcanic exhalative processes, as considered by Hutchinson (1979) and Djakic (1980).

Esu

A correlate of the Success Creek Group occurs between Lone Ridge and Salmon Creek (fig. 1). The basal contact with the Oonah Formation is a fault, the maximum measured thickness being 750 m. This succession has a similar lithology to that of the Success Creek Formation, being a dominantly quartz sandstone (Esd) sequence in the lower part, grading up through a sequence dominated by siliceous laminated siltstone (Esr) into a correlate of the 'red rock' member (Esrr). In detail, with the exception of the 'red rock' member correlate, it is not possible to map unambiguous boundaries between correlates of different formations, as defined along the Pieman River section. Numerous carbonate beds (0·5–5·0 m thick) and zones of laminated siltstone and mudstone, some containing soft-sediment deformation, are found within the lower, dominantly quartz sandstone part of the sequence and zones of well bedded clean sandstone occur in the upper, dominantly siliceous siltstone part of the sequence.

The sandstone beds are mainly very fine-grained to fine-grained, range in thickness from 5 mm to 50 mm and have 1–2 mm thick siltstone-mudstone interbeds. The coarser grained sandstone beds are up to 150 mm in thickness, have multiply truncated cross-bedding, basal ripple marks, flame structures and load modified basal bulges. In one part of the succession, a sequence of 50 mm thick quartz sandstone and carbonate beds alternates with 1–2 mm muddy siltstone interbeds. The laminated siltstone sequence also contains scour channels up to one metre wide which have been infilled with cross-bedded sandstone. Soft-sediment deformation features are also found within the mudstone members of this succession. Carbonate beds are usually laminated, with thin impersistent mudstone laminae parallel to bedding, recrystallised, and have laminated mudstone interbeds.

Above the dominantly laminated siliceous siltstone sequence is a 60 m thickness of interbedded black and hematitic mudstone, dolomitic carbonate, black oolitic chert, recrystallised brecciated chert units and laminated siliceous siltstone. The laminated siltstone units contain soft-sediment deformation and the brecciated chert units contain stromatolite clasts (plate 2). The sequence also contains sedimentary hematite, both as clastic grains in conglomerate units and as sand, silt and mud grade components in the finer grained units. Dolomitic horizons vary through the succession from thinly interbedded, with black chert, up to 15+ m thick beds to the north-west in the Stanley Reward area [CP580820]. This 60 m sequence grades into the 15 m of hematite dominated 'red rock' member correlate, which persists from the Stanley River area south-east until just to the east of the upper reaches of Misty Valley, where the 'red rock' member directly overlies the 'upper' Oonah Formation. All the other formations of the Success Creek Group are missing, indicating continual onlap of the basement succession by Success Creek Group sequences.

The rock units of the Success Creek Group indicate that the environment of deposition was one of localised basin infills, spreading out around hills of Oonah Formation successions. The shallow water to intertidal nature of the whole 1000 m of the succession is characterised

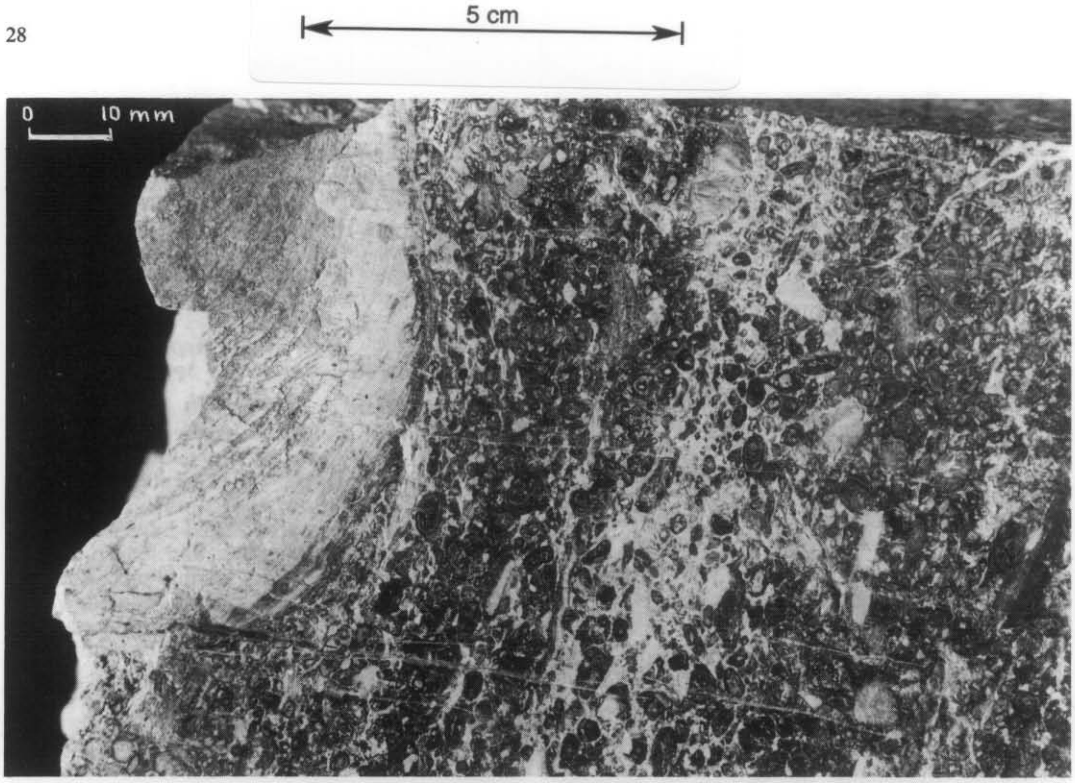

Plate 2. *Oolitic chert breccia with stromatolite clasts, from within a correlate of the 'red rock' member of the Success Creek Group in the Mt Lindsay area [fig. 1, CP609799].*

by clean sandstone units, multiply truncated cross-laminations, cross-bedded infillings of small scour channels, ripple marks, coarse sand lenses in mudstone, worm casts and stromatolite clasts, and brecciated and oolitic chert. The unstable nature of the basin is demonstrated by intraformational soft-sediment deformation and large scale structures which locally grade into a mélange zone contained within the overall succession.

PALAEONTOLOGY

The oldest fossil biota found during this study was one of stromatolite fragments. This was found within a recrystallised, brecciated and oolitic chert unit which occurs within a 60 m thick sequence of mudstone, carbonate, chert and siltstone which underlies the 'red rock' member correlate in the Mt Lindsay area [CP612798, fossil symbol missing from fig. 1]. The stromatolite fragments belong to *Baicalia* cf. *B. burra* (W. V. Preiss, pers. comm.) and are similar to those obtained from stromatolitic breccias associated with the 'Smithton' Dolomite in the Smithton Basin near Trowutta (Griffin and Preiss, 1976) and from core of a similar breccia from a drill hole near Forest (Brown, 1985).

Numerous carbonate horizons from the upper part of the Success Creek Group correlate in the Mt Lindsay area were treated for microfossils, but the samples obtained were barren.

SUCCESS CREEK GROUP CORRELATE (Esu)

A micaceous quartz wacke-mudstone sequence with minor interbedded siltstone, conglomerate and carbonate occurs in the Heazlewood River–Whyte River area to the north-west of the Meredith Granite and in an area to the south-east of Luina (fig. 2).

The basal relationship between the succession and the Oonah Formation/Whyte Schist correlate has not yet been established, but in the area mapped, along the Heazlewood River from CQ539031 north to the Corinna Road [CQ546075], it is considered to be a fault. Because of contact metamorphism by the Meredith Granite, exposure of cleavage is rare, but in thin section some of the siltstone samples carry one good primary cleavage.

The dominant rock type is a quartz wacke, commonly muscovitic, which is interbedded with varying amounts of mudstone, siltstone granule, and pebble conglomerate and carbonate units. The quartz wacke and granule conglomerate units are composed of similar material which was derived from a metasedimentary, and possibly granitic, terrain of a metamorphic grade equivalent to, or higher than, the Tyennan Block and the Arthur Lineament.

The quartz wacke contains elongate to rounded grains of quartz, secondary muscovite, plagioclase, microcline, biotite, hematite,

leucoxene, garnet, chlorite, amphibole, green tourmaline, zircon and clastic carbonate. Rock fragments include chert, phyllitic mudstone, meta-quartzite, quartz-mica schist and feldspar-phyric volcanic rocks. The volcanic clasts consist of microphenocrysts and acicular laths of plagioclase in a black glass groundmass.

This sequence is correlated with the Success Creek Group on the basis of stratigraphic position, dominantly siliceous clastic content, low level of structural deformation and lack of Crimson Creek Formation tholeiitic lavas and/or sedimentary rocks derived from such lavas.

STRUCTURE

Internal Structures

Within the Success Creek Group is a formation (Ess) dominated by black mudstone which is characterised by pervasive intraformational soft-sediment deformation. This sequence later reacted incompetently during localised large scale slump movements.

In a detailed investigation with Dr E. Williams of a section of this formation along the Argent Dam road from the turnoff with the Murchison Highway [CP683700] to a quarry at approximately CP681708, it was noted that this succession exhibited numerous structures developed during soft-sediment disruption, and that the rocks further behaved incompetently during later Devonian tectonic deformation. There is a convergence by Devonian tectonic flattening of soft-sediment and tectonic directions and attitudes in the structures developed, so that the origin of some structures is not readily apparent. However, there is sufficient evidence to show that the sedimentary sequence was developed on a very unstable shelf, probably indicating a rapid deepening of the depositional basin to the east.

Laminated siltstone beds commonly display both brittle discontinuous and continuous structures, and fragments resulting from the deformation are set in black mudstone, which initially behaved in a hydroplastic fashion. The black mudstone ranges from featureless in some specimens to commonly with soft-sediment transposition mudstone seams sweeping around a directional fabric of aligned siltstone fragments. Angular siltstone fragments are uncommon, the fragments being usually lenticular and aligned.

In the quarry at CP681708, the base of the deformed sequence (Ess) crops out and is gradational with the Dalcoath Formation (Esd). Within some outcrops, dismembered fold lenticles of the underlying laminated siltstone sequence are wrapped by black mudstone. The lenticles strike to 310° with a plunge of less than 20° and contain slickensiding, probably due to later movement.

Brittle deformation of another part of this succession (plate 3) is exposed in another quarry on the side of the Murchison Highway near CP683705. Outcrops of Ess are also well exposed along the Pieman River, between CP645762 and CP636752. Here the succession consists of deformed sequences of interbedded, finely laminated siltstone and transposed black mudstone, with horizons of 'pebbly' mudstone. The mudstone 'pebbles' are probably due to soft-sediment deformation. Lenses, ranging in thickness from 100 mm to tens of metres, of coherent blocks in a transposed black mudstone, probably indicating post depositional slumping, can also be seen.

Superimposed on the soft-sediment structures described above are two tectonic cleavages. Tectonic folds with hinges of strike 330° to 360° occur and do not appear to be associated with the cleavages.

Superimposed Structures

The regional structure of the Success Creek Group in the Renison Bell–Pieman River area is dominated by steep north-westerly trending faults with smaller north-easterly faults between. The basal contact with the Oonah Formation is now a décollement surface. This surface is considered to be continuous from the Western Hills to the Dunkley Tram area. In the Mt Lindsay area the contact between the Success Creek Group and the once unconformably overlain Oonah Formation is now also considered to be a décollement surface.

The structural hiatus between the Oonah Formation and the unconformably overlying Success Creek Group is amply demonstrated by Figure 10. The stereographic plots of total bedding and cleavage readings of the Oonah Formation (fig. 10*c* and *d*) have been affected by multiple phases of folding whilst the stereographic plots for bedding and cleavage within the Success Creek Group (fig. 10*a* and *b*; area 5, fig. 6) show a predominantly north-westerly phase of folding which is subject to a later minor phase of folding which caused a spreading of the bedding and cleavage.

The extra phases of deformation within the Oonah Formation are considered to be due to deformation during the Penguin Orogeny at approximately 730 Ma (see Turner, 1982 for review of ages). The deformation within the Success Creek Group, which is consistent with that measured within the Crimson Creek Formation (fig. 14) and the Dundas Group (fig. 20), is considered to be of Devonian age.

The earliest fold phase during Devonian deformation is considered to have had hinges of folds of a half wavelength of about 15 km (Williams, 1978). The folds strike at about 350° with deviations of ±15°. This trend has been

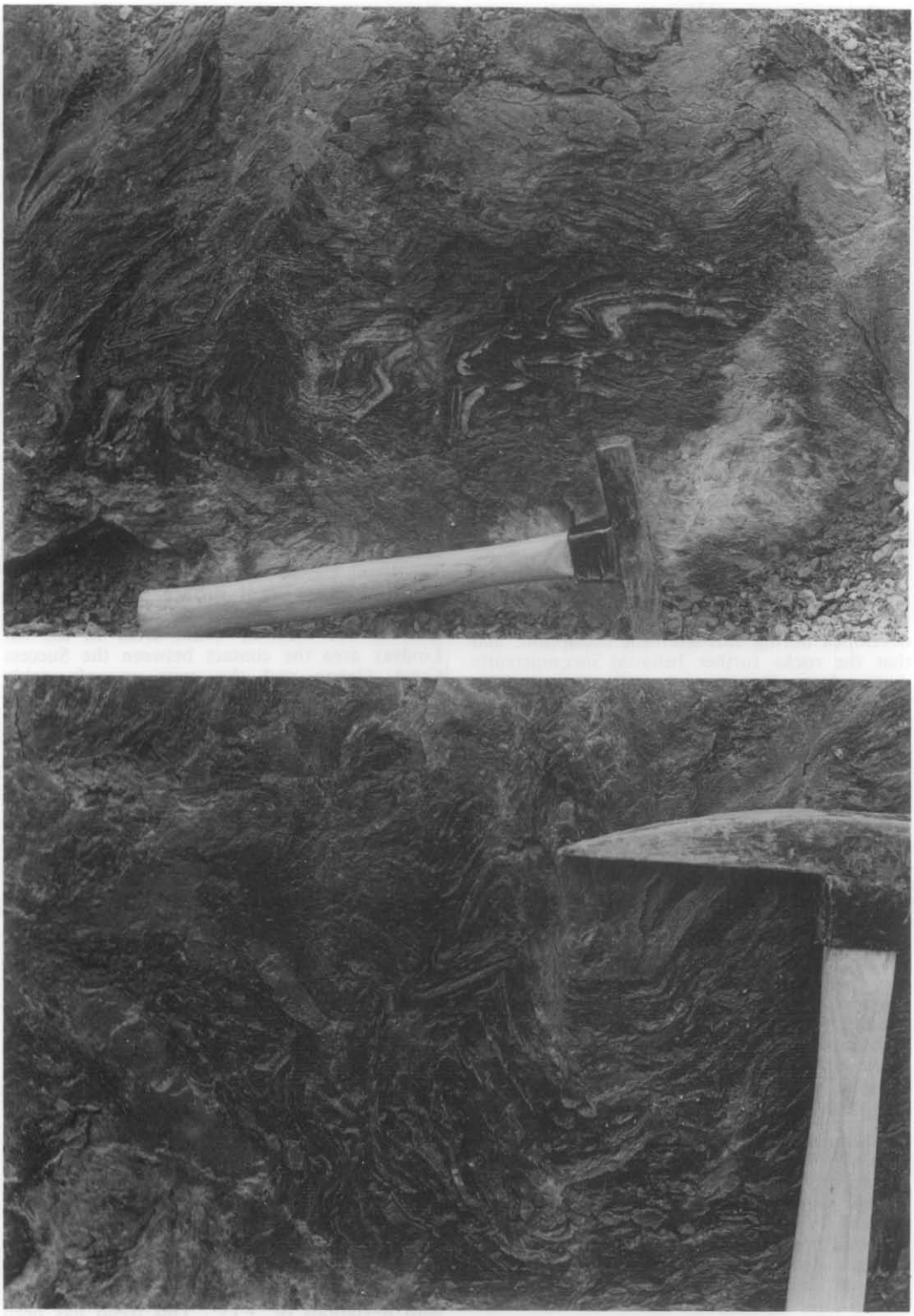

Plate 3. *Soft-sediment deformation with slump zone (Ess) in the Success Creek Group [fig. 1; CP683724].*

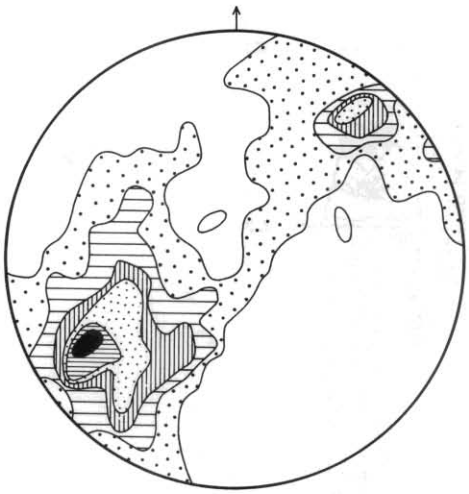

(a) Lambert Projection of 422 poles to bedding: Success Creek Group, Renison Bell–Dunkley Tram–Pieman River area, Area 5 Figure 6. Contour intervals 0·1,1·5,3,4,5,6%.

(b) Lambert Projection of 248 poles to undifferentiated cleavage: Success Creek Group, Renison Bell–Dunkley Tram–Pieman River area, Area 5 Figure 6. Contour intervals 0·5,2,3,4,5,6%.

(c) Lambert Projection of 586 poles to bedding: Oonah Formation, Areas 1–4 Figure 6. Contour intervals 0·1,1,2,2·75,3·5,4·5%.

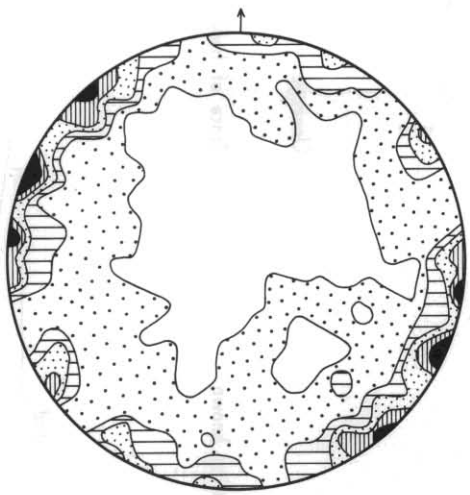

(d) Lambert Projection of 264 poles to undifferentiated cleavage: Oonah Formation, Areas 1–4 Figure 6. Contour intervals 0·2,2,4,6,8%.

Figure 10. *Stereographic plots, Success Creek Group (Area 5, Figure 6) and total Oonah Formation (Areas 1–4, Figure 6).*

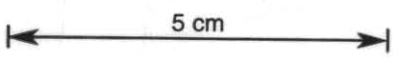

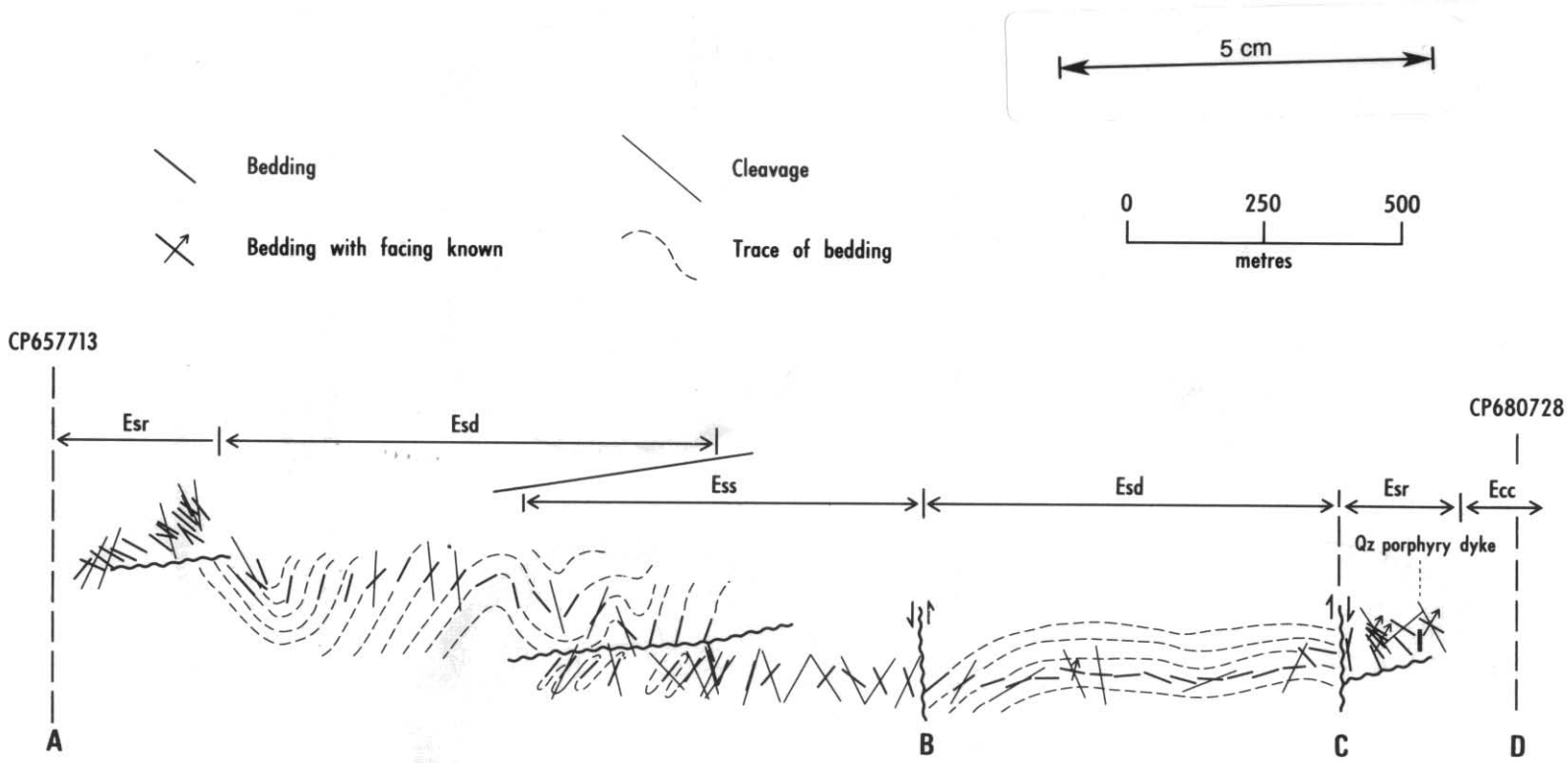

Figure 11. *Cross-section, Success Creek Group, Renison Bell area.*

called the West Coast Range/St Valentines Peak Trend (Williams, 1983). The later Devonian fold phase, the Zeehan/Gormanston Trend, produced folds containing fold hinges trending 325° with a deviation of ±10°, and deviation of the fold hinges due to interfering fold axes, conical folds, block anisotropy etc. (Williams, 1983). It is concluded that the first, dominantly northerly phase of Devonian folding tilted the whole of the Success Creek Group to the east, probably producing the basal décollement with the underlying Oonah Formation, and that the second, dominantly north-westerly phase, produced the folding and associated cleavage, which was followed by later faulting.

In the past, numerous geological maps have shown a south-easterly plunging anticline to the west of Renison Bell. A structural cross-section of this area (fig. 11(i), B-C) does not show such a structure. Another cross-section of the area, done independently by Dr. E. Williams along the Murchison Highway from opposite the Argent Dam to Renison Bell, confirms this finding.

SUMMARY

The Success Creek Group consists of approximately 1000 m of dominantly siliceous sediments deposited in a shallow water environment along the margin of a subsiding platform. The rock successions of the group fall into two main sequences; the basal mixtite and sandstone sequence and an overlying succession of laminated siltstone, mudstone and carbonate with varying amounts of interbedded conglomerate and sandstone. The upper part of this succession consists of carbonate units and coarse-grained sandstone lenses interbedded with mudstone and chert. The upper part probably represents a fluviatile environment.

These successions infilled a basin containing comparatively unmetamorphosed lithic sandstone, mudstone and carbonate with tuff units and lava flows of the Oonah Formation, with landscape unconformity. The unconformity also represents a structural hiatus.

Within the interbedded laminated siltstone and mudstone sequence is an horizon with numerous structures developed during soft-sediment disruption. This horizon behaved in an incompetent manner when later tectonic movement produced overprinting of soft-sediment structures by tectonic deformation. Evidence available from within this horizon indicates that the sedimentary sequence was developed on an unstable shelf.

The tectonic activity responsible for the rapid deepening of the basin probably coincided with the onset of vulcanism which is recorded as a turbidite sequence of immature volcaniclastic lithic wacke interbedded with laminated siltstone and mudstone of the overlying Crimson Creek Formation.

CRIMSON CREEK FORMATION

INTRODUCTION

Taylor (1954) defined the Crimson Creek Formation as that succession of rocks dominated by compact mudstone with volcaniclastic and lava horizons which occurs from near the Owen Meredith mine [CP670731], down Crimson Creek, along the Pieman River to the east, then along the Huskisson River to a contact with ultramafic rocks at CP706753. The section is approximately at right angles to the general strike of the formation and Taylor gives an average dip for the rocks within the formation of 72° to the north-east and a thickness of 12,000 feet (3656 m).

Both Taylor (1954) and Blissett (1962) considered that the top of the Success Creek Group cropped out to the north of the type section, and that the contact with the Crimson Creek Formation in the Pieman River at the site of the old suspension bridge [CP646763] was conformable. A structural cross-section of the area (fig. 11), constructed from information gathered during mapping at relatively low water level in the Pieman River, shows that the boundary of the two successions at this site is faulted and that the eastern margin of the siliceous siltstone member of the Renison Formation (Esr) is overturned. Continuing upstream, from this point to the confluence of Success Creek and the Pieman River, only rocks considered as belonging to Esr were observed. The last quartz sandstone bed was found on the western side of the mouth of Success Creek and the first volcaniclastic lithic wacke, typical of the Crimson Creek Formation, was found on the northern bank of the Pieman River a few metres downstream from opposite the mouth of Success Creek. Information used in the construction of the cross-section gives an average dip of 70° and a measured thickness of approximately 3950 m for Taylor's type section. To the north, in the Mt Lindsay–Parsons Hood area, a thickness of approximately 5000 m is indicated.

Ecc

Field work and thin section study of the sequence exposed within the original type area, as well as a northern extension along strike, and a southern extension of the Huskisson River section along the Pieman River to the contact with ultramafic rocks at CP716738, has shown that instead of a dominance of compact mudstone, the wacke-tuff:siltstone-mudstone ratio is at least 60:40. Colour variation in the sedimentary rocks of the Crimson Creek Formation represents iron oxidation-reduction colours, the mauve-purple to red-brown representing units with a high degree of volcaniclastic material, the buff-green representing sedimentary rocks with a low volcanic component. When fresh, sand grade units are blue-grey and the siltstone-mudstone beds dark grey to black.

The buff-green parts of the succession, being dominantly compact laminated siltstone and mudstone, are relatively resistant to weathering in comparison to the coarser sand grade units and therefore crop out more prominantly.

Regionally, the percentage of basaltic lava increases from south of the type area towards the Mt Lindsay area, on the western side of the Huskisson Syncline, and from south of the Pieman Road section on the eastern side of the syncline to the eastern slopes of Mt Ramsay, where the sequence is at least 25% lava flows. Continuing north beyond the Tertiary basalt, the sequence is dominated by basaltic lavas (Eccb) [around CQ745005] (fig. 1).

Correlates of the Crimson Creek Formation occur in the Cleveland area ('Luina Beds'; Rubenach, 1973: 'Deep Creek Volcanics–Halls Formation–Crescent Spur Sandstone'; Cox and Glasson, 1971; Collins, 1983: 'Arthur River Sequence'; Groves, 1968), and in the Waratah–Belmont road area (Williams and Brown, 1983), where the sequence ranges from dominantly pillow lava sequences (Eccb) to dominantly volcaniclastic wacke-siltstone or red mudstone-white chert successions (Eccs). Details of the regional geology of the Cleveland–Waratah area can be found in the references cited.

Throughout the whole of the Crimson Creek Formation the sedimentary units are fairly uniform, immature, turbidite flows of angular tholeiitic volcanic material, intermixed with a non-volcanic component which varies from place to place but is dominated overall by quartz-rich sedimentary rock grains derived from Precambrian sequences, interbedded with laminated and cross-bedded siltstone and mudstone.

Traversing across Taylor's type section from west to east, the first units consist of compact laminated siltstone and mudstone with minor thin sand-grade beds of intermixed quartz and volcaniclastic material. At 225 m above the base of the sequence, a 55 m thick volcaniclastic to tuffaceous wacke horizon is encountered [around CP637734]. This unit has been followed for 600 m along strike and is fairly uniform in thickness. It is well compacted and consists of poorly sorted, brecciated fragments of fine-grained basalt, angular fragments of clinopyroxene, feldspar and magnetite crystals, grains of chert, quartzite and indurated mudstone (plates of which reach 45 x 35 x 4 mm in size) in a matrix of volcanic-derived silt-grade and mud-grade material. The coarser grains are of a medium sand-grade and consist of the above material as well as fragments of quartz, hematite, chlorite, carbonate and fine-grained basalt.

Depending on the proximity to volcanic vents and the rate of volcanic activity, the sand-grade grains range in proportion throughout the whole succession and form a range of epiclastic rock types from hyaloclastite to tuffaceous wacke, volcanic, feldspathic and lithic greywacke to volcaniclastic lithic wacke. The main characteristics of the beds are rapid sedimentation by turbidity currents and fast burial of immature and poorly-sorted material derived from probable shallow water volcanic activity by quench spalling and mechanical disintegration of the lava flows.

Although the majority of tuffaceous wacke units are epiclastic and have turbidite characteristics, at least one unit is better described as a vitric crystal lithic tuff [CP678751] and was probably formed as a flow-head deposit in an ash turbidite similar to that found associated with the eruption of the Santorini Volcanoe, Greece (Sparks and Wilson, 1982).

The hyaloclastite units are epiclastic and are composed of grains of rounded but low sphericity vesicular glass, glass shards, which have irregular shapes but are usually drawn-out wisps, broken crystals of clinopyroxene and feldspar, and minor fine-grained basalt fragments composed of feldspar laths in devitrified glass in a matrix of silt and mud-grade volcaniclastic and calcareous material. The tuffaceous wacke beds contain glass shards, broken crystal grains and indurated mudstone grains in a matrix of volcanic-derived mud. As the percentage of volcaniclastic matrix decreases, the percentage of sedimentary rock grains and clastic carbonate components increases. The pyroxene content of the beds also decreases with decreasing volcaniclastic matrix, and the resultant rock type formed is a volcaniclastic lithic wacke.

The whole sequence is dominated by turbidite flows. The sand-grade units channel into the underlying laminated siltstone-mudstone beds and these channels are infilled by truncated, cross-bedded wacke units. The laminated beds range from 1–5 mm in thickness and contain cross-bedding. The wacke units range in thickness from 200 mm to 1·5 m, are usually graded, sometimes contain flow orientated rip-up mudstone clasts and are usually gradationally followed by laminated siltstone beds.

Traversing across the type section, the wacke units progressively become feldspathic. The basalt fragments are composed of clinopyroxene, plagioclase and magnetite in a chloritised groundmass of interlocking pyroxene and feldspar. Sedimentary rock fragments are dominated by undulose quartz, quartzite, chert, indurated mudstone clasts and clastic carbonate grains. In the dominantly volcaniclastic wacke units the broken crystal grains and basaltic components form a massive, well-compacted rock of poorly-sorted angular fragments in a volcanic-derived matrix. These rocks do not show any flow or preferred orientation of the grains and grading is not evident.

Numerous lava horizons and associated intrusive sills occur within the succession. The lavas are either aphyric or plagioclase and/or

clinopyroxene phyric tholeiitic lavas, have chilled margins and in places contain ripped-up sediment clasts in the basal parts. Sills have both chilled top and bottom margins and a gradation in grain size from fine-grained basalt through doleritic to granophyric, depending on the thickness of the sill. Detailed descriptions and information on the chemical variation of the lavas within the Crimson Creek Formation are given on page 69.

The Lower Pieman Dam road (LPDR) gives access to a 3000 m section through the Crimson Creek Formation. In the upper part of the succession, as exposed between the LPDR 27 km and LPDR 29 km marks, volcaniclastic wacke units are dominantly medium-grained and are derived from tholeiitic lavas. In the lower parts of the succession, as exposed between the LPDR 25 km and LPDR 27 km marks, the volcaniclastic lithic wacke units are fine-grained to medium-grained with minor tuffaceous horizons. Thin tholeiitic basalt flows occur in the lower part of the sequence. Overall the succession is a turbidite sequence but the presence of thin, interbedded, non-pillowed lava flows, vitric crystal lithic tuffaceous horizons and interbedded lava flows leave the question of water depth undetermined. Some sections only contain multiply graded wacke without laminated siltstone. In these sections the 100–200 mm thick units grade from medium-grained to very fine sand grade, whereas the thinner (20–100 mm thick) units grade from medium sand grade to mudstone. In other sections the wacke units are separated by laminated mudstone (< 1 mm). Thinly-bedded siltstone (1–5 mm) and mudstone occur as specific horizons up to 500 mm in thickness. These sequences contain multiply truncated cross-bedding and occasional intraformational soft-sediment slump structures in beds approximately 5 mm thick. Flame structures are common throughout the sequence.

The Crimson Creek Formation in the Mt Lindsay area is composed of volcaniclastic lithic wacke and minor tuffaceous wacke horizons, monotonous, interbedded, laminated siltstone and mudstone, tholeiitic basalt flows, and carbonate units. The clastic units show most of the characteristics of typical turbidite flows. The laminated siltstone and mudstone units may be calcareous, range in grain size from clay to silt grade, and commonly contain multiply truncated cross-laminations.

The carbonate horizons rarely crop out. One weathered bed, possibly a continuation of the No. 2 skarn-carbonate from the Mt Lindsay mine area, crops out in a road cutting on the LPD road at the 26·65 km mark [CP628811]. In the Mt Lindsay mine area three main carbonate horizons and a number of thinner horizons have been found in the succession by drilling programmes (Newnham and Schellekens, 1978; Schellekens, 1979). This part of the Crimson Creek Formation can be correlated with the 'Halls Formation' of the Cleveland mine sequence. Thin beds of calc-silicate hornfels were also found within the succession at the base of a waterfall on the Harman River [CP630834].

Lithic wacke beds range in thickness from 200 mm up to 1·5 m, are fine-grained to coarse-grained, usually graded, contain rip-up mudstone fragments up to 100 mm in length, basal scour and flame structures, and an occasional soft-sediment deformation zone in the upper part of a turbidite unit.

As the Crimson Creek Formation is unfossiliferous, the correlation of the rock successions along the eastern side of the Huskisson Syncline with the Crimson Creek Formation as found in the type area of Taylor (1954) is based on lithological criteria and the chemistry of the interbedded basalt flows. The southern extent of the Crimson Creek Formation on the eastern side of the syncline is considered to be in faulted contact with the south-eastern extension of the Huskisson Group (Ch). Along the Lower Pieman Dam road between the 43·5 and 41·2 km marks, road cuttings through the succession expose interbedded turbiditic sequences of highly weathered volcaniclastic lithic wacke, minor well-compacted lithic crystal tuffaceous wacke and tholeiitic lava flows, interbedded with laminated siltstone and mudstone. In numerous places this succession is intruded by gabbroic dykes, some associated with contemporaneous volcanism and some due to a later phase of gabbroic intrusions.

Wacke units range in thickness from approximately 100 mm up to one metre, are usually graded and often contain elongate mudstone fragments up to 50 mm in length. Some wacke units contain cross bedding with mudstone partings along the cross-laminations. The laminated siltstone and mudstone units contain planar and truncated cross-laminated units and range from 5 mm to 100 mm in thickness, the laminations being usually less than one millimetre. Lithologically the sequence consists of similar material to that on the western side of the Huskisson syncline, being derived from a mixed tholeiitic volcanic active source and Precambrian sedimentary rock sequences.

Traverses across the northern extension of this succession along John Lynch Creek, the upper reaches of the Pieman River, and tracks along the eastern face of Mt Ramsay, show that the succession is basically very uniform in composition along strike. However the proportion of lava flows in the succession increases to the north, until in the area around CQ725005, the succession is dominantly composed of lava flows with minor interbedded sedimentary clastic units (Eccb).

Brown (1980*a*, *b*) mentions that the tuffaceous wacke units within the Crimson Creek Formation could be either lithic crystal or crystal lithic, are well compacted, and derived from an acid

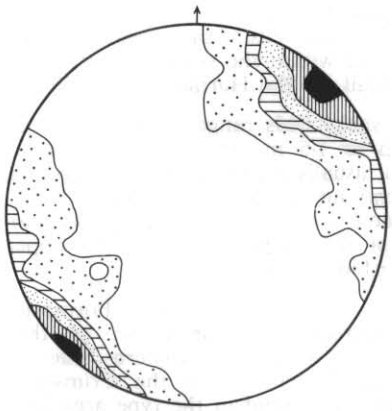

(a) Lambert Projection of 235 poles to bedding: Crimson Creek Formation, Mt Lindsay–Wilson River area, Area 7 Figure 6. Contour intervals 0·2, 2·5,4·5,8·5,17%.

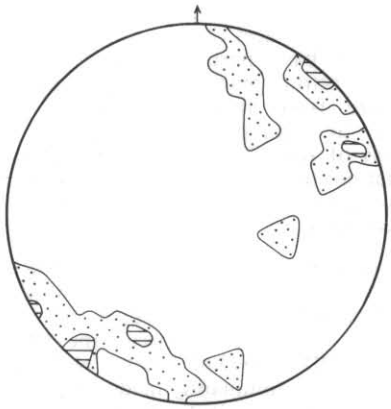

(b) Lambert Projection of 17 poles to undifferentiated cleavage: Crimson Creek Formation, Mt Lindsay–Wilson River area, Area 7 Figure 6. Contour intervals 3,9%.

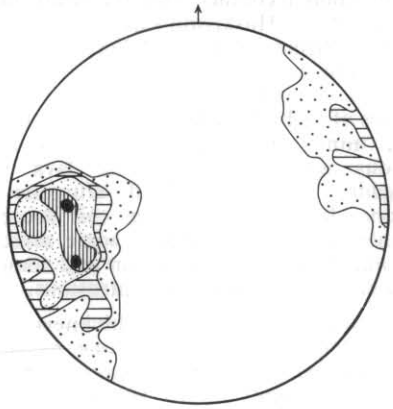

(c) Lambert Projection of 85 poles to bedding: Crimson Creek Formation, Renison Bell–Pieman River area, Area 6 Figure 6. Contour intervals 0·5,3,5·25,10,14·5%.

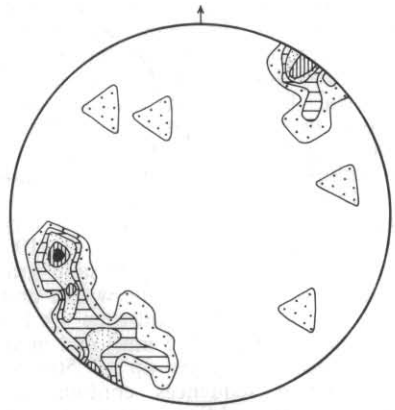

(d) Lambert Projection of 28 poles to undifferentiated cleavage: Crimson Creek Formation, Renison Bell–Pieman River area, Area 6 Figure 6. Contour intervals 1·5,5,9,12·5,16%.

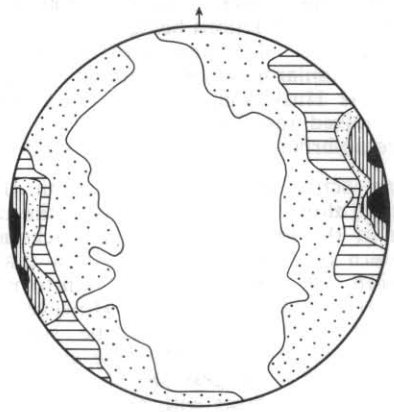

(e) Lambert Projection of 256 poles to bedding: Crimson Creek Formation, north-south area to east of Huskisson Syncline (fig. 1). Area 8 Figure 6. Contour intervals 0·2,2·5,5,7·25,9·5%.

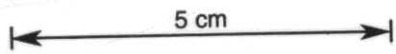

Figure 12. *Stereographic plots, Crimson Creek Formation (Areas 6–8, Figure 6).*

to basic volcanic source. The statement about material from an acid volcanic source is now known to be incorrect. The tuffaceous wacke units which contain acid volcanic-derived quartz occur to the west of the LPDR 44 km mark [CP759785] and are interbedded with carbonate and black mudstone. The preliminary correlation of this isolated outcrop on the LPD road with the Crimson Creek Formation was made prior to a traverse along the Pieman River from the Bastyan Dam site, downstream to CP759761. This river section shows that the outcrop in question is part of a northern extension of the 'Rosebery Group' and not part of the older Crimson Creek Formation. The assumption contained in Cooper and Grindley (1982), based on the two unpublished reports, that the presence of acid volcanic detritus within the Crimson Creek Formation suggests contemporaneity with early Mt Read-type volcanism, is incorrect.

Previous mapping (Blissett and Gulline, 1962) had the Crimson Creek Formation continuing south across the Pieman River into the Colebrook Hill area, but as the sequence in this area consists of metasedimentary and acid to intermediate volcanic detritus and not tholeiitic basalt with genetically related volcaniclastic lithic wacke and interbedded mudstone, this extension to the south [past CP750750] is no longer considered valid.

STRUCTURE

Over 300 bedding readings from a 50 km² strip of country between Renison Bell and Mt Lindsay were obtained from outcrops of rocks belonging to the Crimson Creek Formation. At over one half of these stations a sedimentary facing was obtained which, without exception, faces east. Cleavage readings were obtained mainly from the southern part of the area, as metamorphic diffusion associated with cooling of the Meredith Granite has obliterated the cleavage surface around Mt Lindsay.

Stereographic plots of bedding and cleavage readings (fig. 12; areas 6–8, fig. 6) show that folding of the Crimson Creek Formation successions in the extended type section area is consistent with having been formed during a single fold phase. The discrepancy of some 40° between the orientation of bedding readings in the Renison Bell–Pieman River and Mt Lindsay areas is considered to be due to basement irregularity effects during the north-westerly fold phase. The stereographic plots also show that a later spreading of bedding occurred around a very steep axis.

In both the Mt Lindsay and Renison Bell–Pieman River areas the cleavage (fig. 14) is consistent with having been formed as an axial surface cleavage to the folds indicated in the stereographic plots of bedding. From the above data and the fact that bedding is steeply dipping to overturned with all facings being to the east, it is concluded that the area of Crimson Creek Formation to the west of the Huskisson Syncline is the western arm of a large open synclinorial fold produced during a northerly fold phase and later reorientated by a north-westerly deformation. All outcrop-scale folds observed are consistent with being parasitic to the main fold.

The stereographic plot (fig. 12*e*; area 8, fig. 6) of 256 bedding readings from an approximately N-S, 20 x 2 km area of Crimson Creek Formation successions along the eastern side of the Huskisson Syncline is also consistent with the above interpretation. The bedding plot indicates a main fold axis to 345° with a later spreading about a very steep axis and a still later tilting to the south of the northern part of the area by the emplacement of the Meredith Granite. Along the eastern side of the syncline the bedding is again steeply dipping, dominantly to the west but also overturned to the east. All facings obtained within this 40 km² area were to the west, again suggesting that this area is one limb of a large open fold associated with the northerly phase of Devonian deformation. Within this eastern area, outcrop-scale folds with a vertical axial surface trending between 340° and 350° were observed. These folds are interpreted as belonging to the same phase of folding which produced the main fold and are parasitic on the eastern limb.

SUMMARY

The Crimson Creek Formation consists of a turbiditic sequence of volcaniclastic lithic wacke and laminated siltstone and mudstone interbedded with tholeiitic basalt. The formation overlies the Success Creek Group with transitional conformity. The proportion of volcaniclastic lithic wacke in the succession increases northwards from the type area on the western side of the syncline, towards Mt Lindsay.

A similar succession exists along the eastern side of the Huskisson Syncline with the basaltic content increasing to the north, until, to the south of Wombat Flat [CQ723028], areas of dominantly interbedded basalt flows with minor interbedded sediment occur.

Structurally, the Crimson Creek Formation contains the same deformation as the underlying Success Creek Group and the younger Dundas-Huskisson-'Rosebery' Group successions. This deformation is consistent with that known to have occurred during the mid-Devonian phase in western Tasmania.

Correlates of the Crimson Creek Formation occur in areas to the north of the Meredith Granite (fig. 2, 3) in the Cleveland/Waratah area. The formation then continues to the north-east, into the Waratah River–Wandle River area, where similar successions of tholeiitic basalt and turbiditic volcaniclastic sequences contain interbedded chert and mudstone units, with the dominantly basaltic parts of the succession consisting of piles of pillow lavas (Williams and Brown, 1983; Baillie *et al.*, in prep.).

Cambrian

DUNDAS GROUP

INTRODUCTION

All boundaries between rocks of the Crimson Creek Formation and Dundas Group successions, so far observed by the writer, are faulted. Remapping of Elliston's (1954) type area of the Dundas Group has shown that it consists basically of two distinct successions which are now fault juxtaposed (fig. 1), but may originally have been separated by a break in sedimentation or period of shallow water deposition. The lower part (€mu) is sparsely fossiliferous and consists, in some areas, of a basal sequence of laminated and thinly-bedded siliceous sandstone, siltstone and mudstone (€dj) which is gradationally overlain by a sequence dominated by mass-flow conglomerate (€dre). In the Ring River the laminated sequence (€dj) is missing and the mass-flow conglomerate sequence interdigitates with basaltic flows. The conglomeratic sequence (€dre) is conformably followed in all areas by a laminated and thinly-bedded sandstone, siltstone and mudstone sequence (€dh), which in turn is gradational upwards into a sequence of turbiditic chert conglomerate and sandstone (€dra). The top of the lower succession may have been a relatively shallow water sequence of sandstone and siltstone (€db), as there are numerous horizons of sand-starved ripple marks within the succession and the fossils are of a 'shallower' water fauna (Jago, 1973). The units within the lower succession vary rapidly in thickness and appear to have been localised basin infillings on eroded Crimson Creek Formation basement or on tectonically emplaced ultramafic-mafic bodies. Using the terminology of Elliston (1954), the lower succession consists of all rock units from the Judith Formation up to and including the lower part of the Brewery Junction Formation.

The upper succession of the Dundas Group (€dl) is a fossiliferous turbidite sequence, extending from the middle of Elliston's Brewery Junction Formation, as mapped by him in the type area, up to and including at least the Misery Conglomerate and possibly including a white friable sandstone sequence on the western slope of Misery Hill. The only known contact between these two successions is a fault which starts at approximately CP696620 and runs in a north-westerly direction, through the middle of the old township of Dundas, to approximately CP662650, cutting the Dundas Rivulet type section at CP686627 (fig. 1). It is only in the type area along the Dundas Rivulet that Elliston's formation names of Fernfield, Concert, Fernflow and Climie can be used, as outside a small area to the north and south of the Dundas Rivulet no biostratigraphic correlate of this part of the Dundas Group has the same lithology. This restricted area of the specific formations of Elliston's Dundas Group was also noted by Blissett (1962). A biostratigraphic correlate of the Dundas Group is the Huskisson Group (Taylor, 1954). This sedimentary succession has a different lithological character to the biostratigraphically equivalent units in the Dundas Group, as it is dominantly derived from material from an acid to intermediate volcanic terrain.

No formation of the original Dundas Group (Elliston, 1954) can be successfully walked very far outside the Dundas area, and any positive correlation with specific formations of the Dundas Group can only reliably be made on biostratigraphic evidence, as suggested by Banks (1956), Campana *et al.* (1960), and Solomon (1960). The only lithologies which are distinctive enough to be possibly correlated on lithological grounds are the Red Lead and Razorback Conglomerates.

Fossils so far found in the type area give an age range for the lower part of middle Middle Cambrian (*Ptychagnostus gibbus* zone) to late Middle Cambrian (*Lejopyge laevigata* II Zone), and the upper part from the *Lejopyge laevigata* III late Middle Cambrian passage zone up to the post Idamean (Banks, 1956; Jago, 1979).

Minor acid to intermediate detritus, presumably derived from the Mt Read Volcanics, enters the sedimentary cycle of the Dundas Group at the Razorback Conglomerate level in the late Middle Cambrian (*Ptychagnostus nathorsti* zone).

'LOWER' DUNDAS GROUP SUCCESSIONS (€mu)

The lower succession (€mu) has been divided into five formations following, wherever possible, the terminology of Elliston. Rock distribution patterns (fig. 1) of these formations do not follow Elliston's mapping, and while being somewhat similar to Blissett and Gulline (1962), major variations exist. €mu is used where boundaries between different conglomerate and finer grained formations could not be accurately followed because of lack of, or poor outcrop, and where lithological characteristics of a specific stratigraphic level are different from the type section.

Elliston (1954, p. 165) defined the Dundas Group as " . . . the group of formations exposed in the section along the Dundas Rivulet between the serpentine contact north of the Razorback and Mt Misery, together with those exposed on Spur Track II from a point 800 feet beyond its recrossing of the Dundas Rivulet to the tributary of White Spur Creek". The latter part of the defined area, between CP731636 and CP736632 on Spur Track II, is now known to be a southern extension of certain formations of the 'Rosebery Group' and lithologically dissimilar to the basal Judith Formation–Red Lead Conglomerate sequence as exposed in South Comet Creek.

A section down the north-eastern end of Mt Razorback shows that Elliston's stratigraphy of Razorback Conglomerate–Hodge Formation–Red Lead Conglomerate is correct. As the type section of the Judith Formation up to the Hodge Formation is not part of the Dundas Group, and as the fossiliferous part of the Judith Formation (as well as a continuation of the sequence up to the Red Lead Conglomerate) is exposed in South Comet Creek, this section was used in this study to represent the pre-Red Lead Conglomerate formations.

Judith Formation (€dj)

There are only two areas in which rocks belonging to this formation are known to exist in the general Dundas area. One is along South Comet Creek, the section from where a *Ptychagnostus gibbus* assemblage was obtained, and the second is along the eastern side of Kapi Creek, typically exposed along the North East Dundas Tram between CP705663 and CP711675. Elliston's 'South Comet Grit', as noted by Blissett (1962), is lithologically similar to the Red Lead Conglomerate, and as it appears to overlie the Judith Formation in the South Comet Creek section, is considered to belong in the Red Lead Conglomerate.

The 'Severn Slate', as defined on the Spur Track II, is part of the 'Rosebery Group' in the Moores Pimple area. Similarly an extension in the upper reaches of Judith Creek is considered to be a correlate of formations within the 'Rosebery Group'. Similar lithologies to those of the 'Severn Slate' could not be found in South Comet Creek, to the north of Mt Razorback, or anywhere else in the Dundas area. The existence of the 'Severn Slate' as part of the Dundas Group is thus in doubt, and following Blissett (1962), the Judith Formation is here taken as that sequence of rocks gradationally underlying the Red Lead Conglomerate, and having lithology typified by that section in South Comet Creek from where the fossil assemblage, described as belonging to the *Ptychagnostus gibbus* Zone (Öpik, 1951), was found.

In South Comet Creek, the Judith Formation consists of purple to greenish-grey micaceous sandstone, interbedded with red and white granule conglomerate, fine to medium-grained sandstone and minor conglomerate horizons. The conglomerate is dark purplish grey, siliceous, and contains rounded clasts of chert and quartzite which have an alignment parallel to bedding. The sandstone consists of angular fragments of quartz, chert and indurated mudstone with grains of magnetite-leucoxene set in a framework of granular fragments which are now chlorite. The siltstone units are unevenly bedded and usually overlie cross-bedded or graded sandstone beds. Overall the sequence is siliceous, well bedded and contains turbiditic characteristics. The reported fossil locality, " . . . 400 feet upstream from the junction of Stichtite Creek with the South Comet Creek" (Elliston, 1954; Blissett, 1962) did not yield any new specimens on re-examination.

To the east of Kapi Creek, a correlate of the Judith Formation consists dominantly of interbedded siltstone, sandstone and granule conglomerate with minor pebbly lithic wacke and cobble conglomerate. The succession has a minimum thicknes of 140 m. That part of the sequence dominated by siltstone also contains minor fine-grained sandstone laminations, thin, graded or pebbly granule conglomerate units and graded and cross-bedded sandstone beds and lenses. The upper part of the succession is dominated by sand-grade beds which also contain interbedded but disrupted granule conglomerate lenses, containing irregular and tabular siltstone fragments. The sandstone beds are often cross-bedded and at times have basal flame structures. The granule conglomerate units are occasionally graded and usually contain muddy siltstone stringers and irregular fragments of siltstone and chert. Pebbles within the granule-grade units are rounded quartzite. The fine-grained conglomerate beds contain pebbles of grey chert, black indurated mudstone, and carbonate within a lithic wacke matrix. Towards the top of this sequence the sandstone units become coarser and the amount of siltstone decreases. This sequence is transitional over approximately five metres with a correlate of the Red Lead Conglomerate. The transition starts with the incoming of rounded quartzite pebbles into the granule-grade units, then fine pebble conglomerate lenses within sandy granule units, passing upwards into thick siliceous granule conglomerate and finally poorly sorted mass-flow conglomerate.

The sequences to the east of Kapi Creek have previously been mapped as all formations from the Hodge up to the Fernflow by Elliston (1954), and as Hodge Formation and Razorback Conglomerate by Blissett and Gulline (1962). Rubenach (1967) considered that the conglomerate was possibly of Razorback type, but he later concluded (Rubenach, 1974) that the conglomerate sequences are so variable that Elliston's subdivisions could not be used. The whole sequence faces east and the lithology and mass-flow characteristics of the conglomerate succession are sufficiently unique in the Dundas sequence for the sequences in this area to be correlated with the Judith Formation and the Red Lead Conglomerate.

Red Lead Conglomerate (€dre)

In the South Comet Creek section, between Adelaide and Stichtite Creeks, the Red Lead Conglomerate is most appropriately described as a series of mass-flow conglomerate units which are typical mixtite. The mixtite has clasts of pebble to boulder grade, is poorly sorted, and has a silt to sand grade lithic wacke matrix. The largest clasts are rounded quartzite boulders. Pebbles and cobbles consist of angular to rounded jasper, red and grey banded chert,

indurated siltstone and carbonate. Elliston gave a thickness of 80 m for this section.

Based on lithological similarity and stratigraphic position, within a continuous sequence below both the Hodge Formation and the Razorback Conglomerate, correlates of the Red Lead Conglomerate occur on the north-eastern slope of Mt Razorback, where the conglomerate is approximately 120 m thick. The base is in faulted contact with tectonically emplaced ultramafic rocks on the northern face of Black Hill, and along the spur which runs NNE from Carbine Hill to the Ring River at CP720691. A maximum measured thickness of 300 m is obtained from the incoming of the first mixtite flow up to the last mixtite unit in this area. All of the above areas are windows into the lower Dundas Group sequences due to the uplift of the successions by ultramafic re-emplacement during Devonian deformation.

Along the north-eastern slope of Mt Razorback, the Red Lead Conglomerate is typical of the type section in clast and matrix size, variation and composition. An added component is the presence of serpentinite pebbles and detrital chromite grains in the conglomerate, specifically at the top of the Razorback open cut (Padmasiri, 1974). Numerous graded lithic wacke units occur within the conglomerate, and towards the top of the formation in this area the coarse clast component ceases. The last five metres of section before the basal Hodge Formation units are interbedded granule conglomerate and coarse sand-grade lithic wacke.

On the north face of Black Hill small areas of Red Lead Conglomerate interdigitate with massive and pillowed flows of low-titanium tholeiitic basalt (€bm). Clasts of the basalt are found within the conglomerate along this section and irregular blocks of conglomerate are found within the upper lava flows, suggesting contemporaneous formation and erosion.

To the east of Kapi Creek and across Confidence Saddle, the Red Lead Conglomerate correlate is typified by massive flows of poorly-sorted mixtite with clasts of dominantly sub-rounded to rounded, pebble to cobble grade, red and grey chert and minor, well-rounded cobbles and boulders of quartzite, and pebbles of red mudstone and of low-titanium tholeiitic basalt. Occasional cobbles of gabbro and carbonate also occur. The matrix is of silt to coarse sand grade and lithic wacke in character. Lenses and bedded units, some up to 500 mm thick, of siltstone, graded sandstone and granule conglomerate occur throughout the mixtite. One such unit is 150 mm thick and ranges from siltstone to sandstone with truncated convolute folds, overlain by well-bedded sandstone.

Approximately in the middle of the succession, as exposed on the ridge to the east of Kapi Creek and running south from Confidence Saddle, the conglomerate units fine in grain size and thin in unit thickness. A series of volcaniclastic wacke lenses occur within this zone, interbedded with thinly-bedded (10-20 mm) fine pebble-grade conglomerate, granule conglomerate and siltstone units. Above this zone is another phase of massive mixtite flows with horizons of pebbly granule conglomerate alternating with thinly interbedded siltstone and sandstone, and minor graded granule conglomerate to fine-grained sandstone units up to 50 mm thick.

The Confidence Saddle exposure can be followed in a north-easterly direction to the Ring River, where a basal section of 25 m consists of very irregular mixtures of red and grey chert, white quartzite cobbles and boulders, and brecciated gabbro in a basaltic matrix, grading to intermixed sedimentary clasts and fragmented basalt flows in a volcaniclastic wacke matrix. This section passes upwards into a thin zone of non-volcanic lithic wacke with interbedded mixtite and distorted laminated siltstone and sandstone units. The relative proportion of volcanic material decreases up through the sequence while the mixtite content increases. This zone of interdigitation with basalt flows grades upwards into a 50 m thick sequence of mixtite lithologically similar to the Red Lead Conglomerate.

Hodge Formation (€dh)

The fossiliferous Hodge Formation has been previously described as consisting of black micaceous slate (Elliston, 1954) and of grey to black micaceous shale, flaggy siltstone and silty mudstone with numerous partings of pale greywacke (Blissett, 1962). The type section is the area on the south-eastern slope of Mt Razorback from the Dundas Rivulet north to the Razorback mine, and west to the ultramafic body. The formation was considered by Elliston to be 180 m thick.

In the type area, the Hodge Formation consists of a thinly interbedded succession of very dark grey to black indurated siltstone with minor dark grey lithic sandstone units which contain siltstone laminae. Lenses and beds of coarse-grained lithic sandstone and sandy siltstone are common in the coarser grained parts of the succession. Sand-grade units from the Dundas Rivulet [CP694630] are composed of angular to subrounded grains of quartz, quartzite, chert, indurated to phyllitic mudstone, and clastic muscovite.

To the south, in the Red Lead mine area [CP695613], a fault block of Hodge Formation consists of finely laminated, grey indurated siltstone with minor graded units of coarse-grained grey to buff lithic sandstone and pink and buff granule conglomerate units up to 500 mm thick. The finer-grained units are composed dominantly of angular quartz, chlorite and opaque minerals, leucoxene and minor chromite.

The sand-grade and granule units also contain grains of quartzite, chert, indurated and pyritic mudstone, and quartz-mica schist.

A similar sequence of laminated and thinly interbedded siltstone and lithic wacke overlies the Red Lead Conglomerate with gradational conformity along the northern slopes of Mt Razorback. The uppermost few metres of this sequence have been channelled into and plastically deformed by the basal units of the overlying Razorback Conglomerate.

On the north slope of Black Hill, a fossiliferous correlate of the Hodge Formation (Jago, 1973) is fault juxtaposed with an extension of the basaltic lavas (€b) which interdigitate with the Red Lead Conglomerate in the Ring River. The succession in this area consists of laminated black and grey siltstone and mudstone with minor graded sand and granule-grade beds. The lower part is mainly composed of black and grey siltstone and mudstone with an occasional conglomerate unit containing pebbles of quartzite, chert and carbonate. The proportion of sand grade units increases up through the sequence. Towards the top, lenses of poorly-sorted chert-clast conglomerate occur within the laminated siltstone sequence. Sand and granule-grade beds vary in thickness from 2–3 mm up to 7–8 mm and are mainly composed of quartz and chert grains.

Overlying the Red Lead Conglomerate in the Ring River is a sequence of laminated and thinly-bedded fine-grained to medium-grained sandstone and minor indurated purplish-grey wispy siltstone lenses and granule conglomerate lenses of basic volcaniclastic material. This sequence grades into a succession dominated by grey siltstone and mudstone with minor boudinaged beds of dark green volcaniclastic coarse-grained lithic wacke and granule conglomerate. Occasional thin chert and quartz clast conglomerate units also occur. The upper part of the succession is a monotonous repetition of pale to dark grey mudstone, siltstone and sandstone, usually thinly-bedded and containing minor granule conglomerate units. Overall the sequence has similarities to the Hodge Formation, but it has an overall coarser grain size and a basic volcaniclastic component. As no fossils were found, the sequence has been designated by €mu. Without knowing their regional stratigraphic position, the sedimentary rock units exposed in the river section could not be correlated with the Hodge Formation on lithological similarities.

Razorback Conglomerate (€dra)

The Razorback Conglomerate is a well-bedded sequence of grey, green and greyish white, turbiditic, chert-clast conglomerate with interbedded siliceous sandstone and siltstone. This formation does not resemble the Red Lead Conglomerate, as suggested by Blissett (1962), nor is it similar to the conglomerate at Moores Pimple (Elliston, 1954). Both of these conglomerate sequences are poorly sorted, massive polymict mass-flow deposits, and the calcareous conglomerate at Moores Pimple is a stratigraphic and lithological correlate of the Salisbury Conglomerate of the 'Rosebery Group', as tentatively suggested by Blissett (1962).

The type section of the Razorback Conglomerate is considered by both Elliston (1954) and Blissett (1962) to be along the summit of Mt Razorback, and not in the Dundas Rivulet section. Elliston described the sequence as " . . . a coarse grey conglomerate containing cherty and jasperoidal siliceous pebbles up to six inches in diameter, but mainly less than one inch". The basal part of the succession along the top of Mt Razorback consists of interbedded granule conglomerate and sandstone beds cut by channel-filled chert conglomerate. The conglomerate units also contain blocks of plastically deformed Hodge Formation and rounded clasts of dolomite. The conglomerate is dominantly a chert clastic, fine-pebble conglomerate, with minor quartzite, siltstone and black mudstone clasts. The clasts have a good flow alignment parallel to a later foliation which permeates both clasts and groundmass. The interbedded sandstone and wacke units are composed of approximately 50:50 quartz:rock fragments. The rock fragments are dominantly chert, with grains of siltstone, mudstone, carbonate and minor lamella-twinned feldspar being present. The quartz wacke has a similar composition to the sandstone.

The conglomerate, sandstone and lithic wacke units contain different proportions of the same material, being dominantly grains of chert, sedimentary and volcanic quartz, feldspar, clastic muscovite and leucoxene. The fragments consist of quartzite, quartz sandstone, siltstone, and indurated and phyllitic mudstone. The metasedimentary rock fragments are well rounded and the grey and white chert clasts range from angular to subrounded. Normally the units have a low matrix component, are often graded and range in thickness around 150 mm.

In the Dundas Rivulet, to the south-east of Mt Razorback, where Elliston mapped a continuation of the Razorback Conglomerate, the typical chert clast conglomerate does not exist. Instead there is a sequence of well-bedded acid to intermediate crystal-vitric-lithic to vitric-crystal tuff horizons interbedded with siliceous granule chert conglomerate with up to 5 mm black mudstone fragments, feldspar-bearing lithic wacke, and sandstone and minor siltstone. The tuff units are composed of feldspar and quartz phenocrysts, glass shards and angular black mudstone fragments in a devitrified glass matrix. A south-eastern continuation of the sequence, exposed along the South Comet Tram at CP693625, was described by Banks (1956), and a small area to the north-west of Dundas Rivulet [around CP693630], was mapped by Blissett and

Gulline (1961). Sandstone and wacke units within the Dundas Rivulet section are composed of feldspar crystals, angular to semi-rounded sedimentary and embayed volcanic quartz grains, rare pumice pieces, mudstone and basaltic rock fragments, clastic muscovite, and rounded grains of quartzite, in a groundmass of similar but far finer-grained material.

The succession on the northern end of Mt Razorback contains beds of graded, coarse-grained dark green sandstone, purple siltstone and coarse granule conglomerate with large blocks of angular buff siltstone, interbedded with green sandy siltstone, buff siliceous sandstone and minor coarse-grained pebble conglomerate.

The thickest exposed section through the Razorback Conglomerate is on the upper northern slopes of Black Hill around CP694661, where approximately 150 m of section is exposed. At the base of the sequence, gradationally up from the Hodge Formation, grey and khaki-green, fine to medium pebble-grade chert conglomerate is interbedded with lenses and beds of granule conglomerate and coarse-grained sandstone. The pebble conglomerate is composed of angular clasts of white, grey and red chert and minor carbonate, with an occasional well-rounded quartzite boulder in the thicker units. The matrix in the conglomerate units is sand grade, and similar in composition to the clast material. Towards the base of the sequence, the granule conglomerate units contain wispy sandstone bands and siltstone flakes. Granule conglomerate horizons also show disrupted bedding.

Progressing up the section, the conglomerate beds thicken considerably and are interbedded with sequences of graded sandstone and siltstone. The clasts within the conglomerate average 5–10 mm in long axis with a smaller proportion of 50–60 mm clasts.

The sequence towards the top is dominated by coarse granule-clast sandstone with minor pebble conglomerate. The granule clasts are of red and purple mudstone as well as chert, being tabular in shape and 10–20 mm in size. Quartzite pebble clasts (50 mm long axis) and occasional carbonate cobbles (150 mm long axis) also occur in the thicker units, which also contain sandstone lenses up to 50 mm thick. Well-bedded sandstone and siltstone alternate with the conglomeratic units. The sandstone units are usually grey to greenish-grey and up to 200 mm thick, with the lower 80 mm containing cross-bedding.

The Black Hill section is truncated on the eastern end by a fault which places the Razorback Conglomerate against an area of low-titanium basalt (Ꞓbm) around CP695662, but to the west an extension of the sequence is cut by the Murchison Highway [CP670651] and a small ridge continues to the west until outcrop ceases at the junction of numerous large faults around CP660651 (fig. 1, 3). The westernmost extent of the conglomerate sequence consists of interbedded chert clast pebble conglomerate with medium-grained to coarse-grained sandstone and siltstone units. Numerous cross-bedded units occur within this sequence.

In the Ring River, upstream from Ringville [CP731683], the lower pebble conglomerate units contain clasts of chert, siltstone, quartzite, indurated quartz sandstone, and quartz-mica schist. A few metres up the sequence the first acid to intermediate crystal vitric tuff unit is encountered, the phenocrysts being feldspar and quartz. Above this horizon the granule conglomerate units contain clasts of crystal tuff and quartz feldspar porphyry, as well as volcanic quartz and feldspar grains mixed with clasts from sedimentary rocks. The continuation of the Ring River sequence upstream from this point is dominated by material from an acid to intermediate volcanic source and it has been correlated with the Huskisson Group. The gradation from a dominantly sedimentary rock source to a volcanic one can also be observed along the North East Dundas Tram around CP718662, and along the Wallace Tram around CP720653.

The reason for correlating the sequence in the Ring River–Colebrook Hill area with the Huskisson Group is the change of dominant source to acid to intermediate volcanic rather than a continuation of the metasedimentary rock source for the successions which overlie the Razorback Conglomerate in the Dundas Group type area.

Brewery Junction Formation (Ꞓdb)

The Brewery Junction Formation, as defined by Elliston (1954) in the Dundas Rivulet, is here considered to consist of two sequences separated by a fault. This fault trends in a north-westerly direction through the middle of the old township of Dundas, crossing the Dundas Rivulet at CP686627.

The sequence upstream from the fault gradationally overlies the Razorback Conglomerate correlate, and comprises unfossiliferous, thinly-bedded (5–10 mm) and laminated (0·5–1 mm) grey and greyish-green siltstone and sandstone with minor granule conglomerate lenses. The siltstone units are usually less than 10 mm in thickness and can either be laminated or contain truncated cross-bedding. Sandstone units form both beds and lenses, are usually graded, and some beds contain sole markings. The graded units range in thickness between 20 mm and 30 mm and contain grains of quartz, feldspar and clastic muscovite and biotite. The granule conglomerate lenses contain chert, black mudstone and feldspar grains, as well as quartz. Overall the grade of sedimentation fines upwards from the basal part of the sequence which contains granule conglomerate, sandstone with sedimentary structures, and minor siltstone, through a zone

of alternating siltstone and graded sandstone, into thinly-bedded and laminated siltstone with minor 20–30 mm thick graded sandstone units. The granule conglomerate units contain volcanic and sedimentary quartz, feldspar, chert, indurated mudstone, clastic mica and quartzite grains.

In the Grand Prize area and along the northern face of Mt Razorback, the sequence overlying the Razorback Conglomerate is one of light grey, irregularly laminated and thinly-bedded sandy siltstone and minor, graded coarse-grained to fine-grained sandstone. Most sandstone beds grade from coarse sand to silt and are up to 20 mm thick. Overlying the Razorback Conglomerate on the top of Black Hill is a sequence of blue-grey to khaki-green siltstone with granule conglomerate lenses and graded sandstone beds. The sandstone beds range in thickness between two and twenty millimetres and the siltstone between one and ten millimetres.

All of the above areas have a transition from the Razorback Conglomerate and contain some sedimentary features that could suggest a shallowing upwards sequence. The whole succession from the Judith Formation to the lower part of the Brewery Junction Formation is sparsely fossiliferous, dominantly thinly-bedded and laminated siltstone and sandstone with a zone of mass-flow conglomerate, the Red Lead Conglomerate. A later zone of chert-clast turbiditic pebble conglomerate, the Razorback Conglomerate, is restricted to the Mt Razorback–Black Hill–Ring River area, where it originally appears to have been an irregular basin fill.

FAULT ZONE

The fault separating the two parts of the Brewery Junction Formation is marked on its western end [CP696621] by a thin zone of sheared sedimentary and crystal-vitric tuff rocks. The fault trends in a north-westerly direction through CP692624, where it cuts through an outcrop, and the bedding between the lower grey-black and upper purple-green successions is at right angles. Although colour of a sedimentary sequence is a poor indicator for division, the unfossiliferous sequence to the north-east is grey to black whereas the sequence to the south-west is purple to green in silt, sand and conglomerate-grade units.

At CP691625 is a shaft driven down into a zone of quartz veins, while another shaft is in a similar position at CP684628. Where the fault crosses the Dundas Rivulet is a zone of fractured and disorientated blocks of both sequences and an adit has been driven to the north-west along the fault. On the hillside overlying the adit [around CP685627] are costeans cut at right angles across a large outcrop of vein quartz. There is another small knoll of massive vein quartz (Dgq) around CP672641, and this is considered to be on the line of the fault to where it terminates around CP655652 (fig. 3).

'UPPER' DUNDAS GROUP SUCCESSIONS (€dl)

The upper part of the Dundas Group consists of sequences of randomly varying lenses and bedded units of coarse to fine-pebble conglomerate, grading to coarse-grained to fine-grained sandstone or lithic wacke with siltstone and mudstone interbeds. The alternation of coarse-grained and fine-grained material is a striking feature of the whole sequence. The coarser units are usually graded and at times have scoured tops infilled by fine-grained material. Cross-bedding, grading and sole marks are common throughout the sequence.

The upper part of the Brewery Junction Formation is a fossiliferous turbidite sequence which appears to be the lowest part of a continuous succession that goes up to and includes at least the Misery Conglomerate and possibly the siliceous white sandstone sequence along the western side of Misery Hill.

Elliston mapped six formations within this succession of changing lithologies. The succession in the rivulet corresponds to Elliston's map (but not to Blissett and Gulline, 1962), but no specific sequence could be traced very far from the rivulet section.

Downstream from the fault, the upper part of the Brewery Junction Formation is dominated by interbedded purple sandy siltstone and minor graded green sandstone lenses. In the lower part of the sequence, as exposed on the western bank of the Dundas Rivulet north of the road bridge at Dundas [CP686626], a 10 m thick lens or slide block of acid to intermediate volcanic tuff occurs within the sequence. Minor granule conglomerate and fine pebble conglomerate horizons and lenses with clasts of purple and green mudstone fragments occur within the sequence downstream from the road bridge. The granule conglomerate units are commonly graded through to siltstone which contains cross-bedding. The number of granule conglomerate units increases up through the sequence. The conglomerate units range in thickness over a short distance and in places contain angular blocks of brecciated sandstone and siltstone beds up to 100–150 mm and clasts of red and green mudstone in a purple sand grade matrix. Towards the top of the Brewery Junction Formation, the purple siltstone beds decrease in frequency and the green sandstone units become coarser and muscovitic and green granule conglomerate units appear, interbedded with purple medium-grained lithic wacke. The top 50 m is dominantly siltstone and sandstone with approximately ten metres of the sequence being grey calcareous siltstone and silty limestone [around CP685624]. This is the only calcareous horizon known in the Dundas area, and is highly fossiliferous.

The incoming, over two to three metres, of well-sorted and at times graded, fine pebble conglomerate and granule conglomerate around CP684624 signifies the start of a 600 m thick sequence dominated by conglomerate. This sequence was called the 'Fernfields Conglomerate' by Elliston. The sequence consists of irregularly alternating successions of coarse (up to three metres thick) and fine (up to 1·5 m) pebble conglomerate grading to granule conglomerate and sandstone (up to 75 mm thick) with interbeds of siltstone containing sandstone laminae up to 3 mm thick. The thicker conglomerate units have scoured tops infilled by coarse-grained sandstone. The conglomerate beds become thinner and fewer up through the sequence but the grain size of the clasts increases. Clasts within the conglomerate are of white quartzite and red and green mudstone. The mudstone clasts are up to 50 mm long axis within 200 mm thick graded units with a siltstone top. The quartzite boulders are up to 250 mm long axis.

All conglomerate developments cease around CP681617 and there begins a sequence of approximately 250 m of thinly-bedded and laminated siltstone and mudstone with minor sandstone, which Elliston (1954) called the 'Comet Slate'. This sequence consists mainly of thinly interbedded grey siltstone and mudstone with minor green sandstone. Towards the top of the sequence the sand-grade units increase in thickness, grain size and frequency.

The incoming of a 300 mm thick poorly-sorted conglomerate [CP680614] begins a 200 m thick sequence, the 'Fernflow Conglomerate' of Elliston. The conglomerate units are pebble grade but have subrounded pink and white quartzite boulders up to 250 mm long axis, as well as red and green mudstone clasts (19–20 mm) in a greyish-green sand-grade matrix. The interbedded siltstone is usually purple. Some of the conglomerate units have internal deformation of bedding, which in places is boudinaged and streaked out with intermixed siltstone.

With the outgoing of conglomeratic units [around CP679617] the sequence is dominated by laminated purple and green siltstone with thinly-bedded grey and greyish-green sandstone. An occasional conglomerate unit occurs towards the top of this sequence (Elliston's 'Climie Slate and Tuff') which continues down the rivulet to the Murchison Highway. The top part of the Climie Formation consists of interbedded lithic wacke, sandstone, siltstone and mudstone which passes gradationally into pebbly sandstone and micaceous siltstone, then rapidly into coarse conglomerate interbedded with lithic wacke, pebbly sandstone and siltstone of the Misery Conglomerate.

Misery Conglomerate (Cdlm)

Although speculation about the nature of the boundary between the 'Climie Slate and Tuff' and Misery Conglomerate has occurred in the past, all workers who have actually mapped the area (Elliston, 1954; Blissett, 1962; Williams, 1975; this study) agree that the two sequences are conformable and part of a continuous sedimentary sequence. The coarse conglomerate is of cobble to boulder grade and is composed of rounded and elongate clasts, dominantly of quartzite but with subsidiary amounts of siltstone, chert, quartz and minor volcanic material in a poorly-sorted quartz and chert sand-grade matrix which is stained by hematite, giving the sequence a red-brown colour. The upper part of the Misery Conglomerate includes conglomerate units interbedded with coarse-grained sandstone and pebbly sandstone. Overall the conglomerate units have a closed framework and contain a strong alignment of clasts. Within the whole sequence, irregular boundaries due to load casting occur between siltstone and coarser grained units. Grading occurs in siltstone, sandstone and conglomeratic units.

Interbedded green siltstone and white siliceous sandstone with minor conglomerate lenses appear to gradationally overlie a sequence of red-brown sandstone and coarse conglomerate on the southern flank of Misery Hill to the north of the Murchison Highway and Dundas Rivulet. The contact is considered to be gradational rather than unconformable or disconformable, as in continuous outcrop the massive conglomerate grades into pink sandstone by the outgoing of clasts. The junction between white and pink sandstone is sharp and parallel with bedding and occurs purely as a colour change without a major change of grain size or texture. Similarly a sharp transition occurs between the white and pink sandstone and the overlying white sandstone–green siltstone sequence. Conglomerate lenses, similar to the Misery Conglomerate but in a white sand rather than hematite-stained matrix, occur in the sequence of white and pink sandstone, suggesting continuous sedimentation rather than a disconformity with the later finer grained sequence. Although the transition from typical Misery Conglomerate to the white sandstone sequence appears to be conformable, on fossil evidence (see page 52) there must be a break in sedimentation within the sequence due to the varying lithological units.

Denison Sub-Group correlate(?) (Os)

A sequence of white siliceous sandstone and green siltstone occurs on the western flank of Misery Hill. This sequence is a different facies to the Misery Formation. The sandstone is siliceous, friable and bioturbated. The actual contact relationship with the Misery Formation is not exposed and the probability of a faulted contact is as high as a gradational one. On the lower slopes of Misery Hill the sequence is overturned and dips to the east, and although small areas of box folding exist, the Misery Conglomerate and the sandstone sequence are structurally comparable.

The sequence, as exposed on the north-western face of Misery Hill, consists of dominantly coarse-grained sandstone and granule conglomerate with minor medium-grained bioturbated sandstone and thin green siltstone beds. On the lower western slopes [around CP668610] the green siltstone becomes dominant and only minor white sand-grade units occur. This sequence is depicted as being a correlate of the sandstone member of the Owen Conglomerate due to historical precedence, as no evidence to the contrary was found. Nowhere else within the area mapped are there any rocks that could be assigned to the Denison Sub-Group, and the sequences in the Huskisson River mapped as 'Zeehan Conglomerate' and conformably underlying 'Gordon Limestone' (Blissett and Gulline, 1962; Blissett, 1962) are, in fact, part of a continuous phase of sedimentation belonging to the Huskisson Group.

DUNDAS GROUP CORRELATE (Ꞓd, fig. 3)

An area of Ꞓd (fig. 3) in the Hatfield River–Hatfield–Coldstream interfluve, originally mapped as Ꞓgs; greywacke conglomerate, sandstone and mudstone sequences (Barton *et al.*, 1966) and described in Collins *et al.* (1981), is correlated with the lower Dundas Group successions (Ꞓmu) on the basis of the overall lithology and the presence of ultramafic and mafic detritus. The succession has a faulted contact along its western margin with Oonah Formation correlates.

The succession is well exposed along a forestry track, 'Huskisson Drive', and consists of calcareous conglomerate interbedded with calcareous lithic wacke, siltstone and mudstone. No fossil faunas have been recovered from the sequence to date. Around CP777944, the conglomerate units range between granule and cobble grade and contain clasts of recrystallised carbonate, chert, tholeiitic and feldspar-rich basalt, pyroxenite, peridotite, quartzite, indurated mudstone and quartz wacke. Some of the clasts have been completely replaced by carbonate, whilst other clasts have only been replaced around their outer rims. The matrix is of sand-grade material, similar to the clast material, with grains of quartz, chlorite and muscovite, and pervaded by carbonate. The interbedded lithic wacke and siltstone beds are finer grained versions of the conglomerate units. The succession is consistent with having been formed by erosion of pre-Dundas Group rock formations in the Waratah–Heazlewood River area.

HUSKISSON GROUP (Ꞓh)

The Huskisson Group, defined by Taylor (1954) along the Huskisson River between CP714751 and CP707771, is a biostratigraphic correlate of part of the Dundas Group. Taylor divided the group into nineteen unnamed formations based on lithological variations, namely the incoming and outgoing of conglomerate horizons within a laminated siltstone and mudstone succession. Due to the lensoidal nature of the conglomeratic units, Taylor's formations are not valid mapping units and further mention in the text is for reference purposes only.

In the type section, the group is bounded both at the base and top by faults. No sequences were found which could be correlated with Denison Sub-Group successions, as considered by Blissett (1962), nor is the sequence continuous with the Gordon Sub-Group Limestone (Ol) [at CP723764], as thought by both Taylor (1954) and Blissett (1962). A minimum thickness of 1300 m was measured in the type area. In general, the group is composed of a succession of clastic sedimentary rocks whose background sedimentation consisted of laminated and thinly-bedded siltstone and mudstone with minor sandstone and lithic wacke, into which numerous horizons of mass-flow conglomerate units were deposited. The conglomeratic units in the lower 1000 m of the sequence were derived from a mixed metasedimentary and active acid to intermediate volcanic terrain, whereas those in the upper 200 m are from a dominantly metasedimentary source, with minor reworked volcanic material. The dominance in most of the sequence of acid to intermediate volcanic detritus is the main difference between the Huskisson and the Dundas Group sequences and, as such, is the main reason that the Huskisson Group is considered as a viable group in lithostratigraphic mapping.

On biostratigraphic, lithological and structural criteria the Huskisson Group can be followed to the north-west of the type area to the southern slope of Merton Hill [CP677795]. To the south-east, the group can be followed in an arcuate zone across the Pieman River, along Colebrook Hill, to faulted contacts with Oonah Formation or 'Rosebery Group' successions in the Frazer Creek–Ring River area. In the Ring River area (fig. 1), the Huskisson Group has a transitional boundary with the lower Dundas Group sequences and is defined by the incoming of felsic volcaniclastic detritus. This transition occurs at the stratigraphic level of the Razorback Conglomerate. The upper boundary in the Ring River area is a faulted contact against 'Rosebery Group' formations. This fault runs in a north–south direction to the west of Wescott Hill (fig. 3). An area around CP752662 (fig. 1, part 2) listed as Ꞓrg? is now considered part of the Huskisson Group (fig. 3).

The lower part of the succession in the Huskisson River (Formation 1 of Taylor, 1954) consists of light to dark grey laminated and thinly bedded siliceous siltstone (1–2 mm thick), mudstone (0·5 mm thick) and minor siliceous sandstone beds (1–2 mm thick). A thick chert clast conglomerate horizon occurs 80 m up the succession and is lithologically similar to units within the

Razorback Conglomerate. Due to re-emplacement of the ultramafic body during Devonian deformation, the basal 70 m of the section is overturned and slivers of sheared serpentinite have been tectonically emplaced throughout the lowermost 50 m of the sequence.

The first units to contain a mixture of metasedimentary and volcaniclastic material occur approximately 150 m up section, but still within Formation 1 of Taylor. Volcanic detritus, from andesitic to dacitic lavas and tuff, continues to occur within the succession to approximately CP727756, being 1050 m up section. The intervening 900 m, corresponding to Taylor's Formations 2–13, consist of a background sedimentation of siltstone and mudstone with interbedded sandstone and lithic wacke which hosts numerous units of granule to coarse cobble conglomerate from a mixed metasedimentary and volcaniclastic terrain. Some units consist completely of epiclastic volcanic material. The combination of metasedimentary detritus, dominated by chert, and acid to intermediate volcanic detritus indicates a lithological correlation with the Razorback Conglomerate. Fossil faunas obtained from localities within the dominantly volcaniclastic part of the succession (page 52) give a Late Middle Cambrian age which is consistent with the lithological correlation.

Within this 900 m section the resultant rock types of sand grade and coarser beds vary according to the proportion and grain size of the volcaniclastic component. Volcaniclastic sandstone is usually very fine-grained to medium-grained and composed of quartz fragments and crystals with devitrified glass and broken shards. The volcaniclastic wacke is poorly sorted and consists mainly of medium to very coarse-grained equant to elongate feldspar crystals with an average grain size of 2–3 mm, and volcanic quartz grains (0·5–1·0 mm but occasionally up to 5 mm) in a silt grade matrix of devitrified glass and carbonate grains. Some of the very coarse-grained volcanic wacke units are composed of closely packed angular feldspar and fragmented quartz crystals in a matrix of broken shards and fragmented pumice and glass. These are more aptly described as volcaniclastic crystal wacke. Other units are epiclastic equivalents of vitric crystal tuff, being composed of devitrified shards, volcanic glass and fractured quartz crystals. These units contain angular fragments, are poorly sorted, immature, and usually have an open framework. Some beds are well compacted and contain flow orientated elongate grains. The majority of the feldspar again contains either simple or multiple twins and has undergone alteration. The quartz grains are clear, contain resorption embayments, have usually been broken and contain sharp edges but curved sides.

The granule conglomerate units range in thickness from 1–5 mm up to one metre. They are poorly sorted, contain well-rounded chert and carbonate clasts as well as subrounded to angular embayed quartz crystals, volcanic feldspar crystals, clasts of andesitic lava, porphyritic and non-porphyritic pumice, and leucoxene grains.

Pebble conglomerate units are usually poorly sorted and have an open framework. The beds can be up to 10 m thick, with varying clast sizes, but average 10–20 mm in 1–2 m thick beds. The clasts range from well-rounded metasedimentary to angular volcaniclasts. The metasedimentary clasts include chert, carbonate, quartzite, indurated mudstone, quartz wacke, and mica schist. The volcaniclastic material is dominated by feldspar crystals, with embayed and fractured quartz crystals, leucoxene grains, feldspar phyric pumice, and andesitic lava clasts in a groundmass of granulated glass, shards, quartz and carbonate grains.

The background sedimentation of laminated and thinly interbedded siltstone and mudstone contains muscovitic sandstone beds up to 50 mm thick where interbedded with siltstone; or where interbedded with laminated siltstone and mudstone, the sandstone units are 10–50 mm thick and contain ripple marks. Some units show intraformational soft-sediment disruption and other units have basal flame structures.

In one area, towards the top of the sequence [CP727756], a lense of poorly-sorted medium-grained volcaniclastic crystal-vitric wacke, composed of angular fragments of feldspar and quartz crystals with devitrified glass shards, infills an irregular five metre deep tongue-shaped scour within underlying thinly-bedded medium-grained to coarse-grained muscovitic sandstone and laminated siltstone. The infilled channel and finer sediments on either side of the channel were then covered by a three metre thick unit of the same composition as the channel fill.

Along the section of the Huskisson River from the fault contact with an area of Gordon Sub-Group limestone (Ol) [CP727757] up to the fault near CP724761, is an area of dominantly laminated and thinly-bedded, fine-grained muscovitic sandstone and siltstone with minor granule and pebble conglomerate units of mixed volcaniclastic and metasedimentary material. This zone is considered to have been deposited during the waning stages of a felsic volcanic phase. The sequence now contains open folds forming a basin and dome fold pattern. Due to folding, the thickness of this section is not known and no estimate was included in the minimum thickness estimates for the group as a whole.

Upstream from the fault [near CP724761] is an approximately 200 m thick sequence dominated by turbiditic chert and quartzite clast conglomerate (Formations 15–17 of Taylor, 1954). Underlying this conglomeratic sequence is a 45 m thick succession of richly fossiliferous (*Glyptagnostus reticulatus*) black pyritic

mudstone and siltstone with minor sandstone (Formation 14 of Taylor). An unknown thickness (but in excess of 55 m) of interbedded fine-grained pebble conglomerate and sandstone underlies the *Glyptagnostus* horizon. This lower turbiditic conglomeratic phase was not recognised by either Taylor (1954) or Blissett (1962). The succession is dominated by 20–30 mm chert clasts with up to 80 mm well-rounded quartzite cobbles within some units. The conglomerate units are lensoidal, between 200 mm and 500 mm thick, and are usually graded from pebble conglomerate to coarse-grained sandstone. The sandstone and lithic wacke units contain angular grains of quartz, chert, mudstone and chlorite which are normally flow orientated. Overall the sand grade units are greenish-brown and muscovitic.

The change from a mixed volcaniclastic and metasedimentary source with mass-flow conglomerate, to siliceous turbiditic conglomerate flows derived from a dominantly metasedimentary source, may indicate a break in sedimentation which would correspond to the implied shallow water period, or disconformity, at the end of the acid to intermediate volcanic phase (*Lejopyge laevigata* III Zone) recorded in the Dundas area succession.

Overlying the *Glyptagnostus* horizon is a sequence of turbiditic conglomerate and sandstone approximately 200 m thick. This represents Formations 15–17 and the lateral equivalent Formation 19 of Taylor (1954) and was considered a correlate of the Mt Zeehan Conglomerate by Blissett and Gulline (1962) and Blissett (1962). The conglomerate units increase in clast size and unit thickness over the first 100 m of section and gradually fine over the next 100 metres. Interbedded with the conglomerate units are medium-grained to coarse-grained muscovitic sandstone and lithic wacke, pebbly sandstone and granule conglomerate. The clasts are well rounded, in places flow aligned, and vary in size. The chert clasts average between 10–30 mm, 50–70 mm, or 100–120 mm in different horizons. Quartzite cobbles up to 200 mm occur in the coarser section of the sequence.

The granule conglomerate beds contain chert, quartzite, quartz-mica schist, indurated mudstone and andesitic lava clasts with clastic muscovite and quartz grains, in a matrix of medium-grained sand composed of similar material to the clasts. Pebble conglomerate units consist of rounded clasts of chert, quartzite, mudstone, carbonate and andesitic lava in a groundmass of medium-grained sand of a metasedimentary origin with minor acid to intermediate volcaniclastic feldspar crystals and carbonate grains. All volcanic-derived detritus is sub-angular to sub-rounded.

The thickest conglomeratic sequence is in the second 50 m of section, and is part of Formation 16 of Taylor. In this section, pebble to cobble conglomerate flows with lenses of granule conglomerate and coarse-grained sandstone occur. The clasts are dominantly chert with minor quartzite, mudstone and carbonate. Clast size varies, but falls within one of three ranges: 10–30 mm; 50–70 mm; or 100–120 mm. Cobble conglomerate units are very lensoidal, impersistent along strike, and usually contain quartzite clasts up to 150 mm in a background of 10–30 mm chert clasts.

Above the thick conglomerate zone the conglomerate units fine in grain size and thin in unit thickness. This part of the sequence contains laminated siltstone and siliceous sandstone, laminated and thinly bedded sandstone and siltstone, and green-brown muscovitic sandstone with cross-bedded granule sandstone and pebbly sandstone lenses. Towards the top, the sequence fines upwards and units become friable with clasts of less than 10 mm.

Taylor considered that the upper limit of the Huskisson Group was the base to the 'Gordon River Limestone', and that 'in general aspects' the conglomerate sequence overlying the *Glyptagnostus* horizon was similar to the 'West Coast Range (Owen) Conglomerate'. Blissett and Gulline (1962) and Blissett (1962) took the coarse conglomerate (part of Formation 16) and the overlying turbiditic sandstone and conglomerate sequences (Formation 17) to be a correlate of the Mt Zeehan Conglomerate and the Moina Sandstone. This, they considered, then graded upwards into the 'Gordon River Limestone' correlate. The above correlation is now considered to be erroneous, as the succession, including the *Glyptagnostus* horizon, consists of turbiditic conglomerate flows probably deposited on a prograding fan. The lowermost outcrop of the Gordon Sub-Group limestone in the Huskisson River [near CP723765] is 30 m upstream from the last Huskisson Group sequence outcrop (at low water level), and contains macro-fossils and conodonts which are also found in the lower limestone member of the Gordon Sub-Group in the Florentine Valley, indicating a Middle–Late Ordovician age (Appendix 2).

This fossil evidence indicates a hiatus in sedimentation between the middle Late Cambrian and middle Middle Ordovician in this area. Regional mapping indicates a faulted relationship between the uppermost outcrop of the Huskisson Group and the lowermost limestone outcrop in the Huskisson River.

To the north-west of the type area (in the Merton Hill area) are outcrops of both the dominantly volcaniclastic part and the siliceous conglomerate part of the Huskisson Group. These outcrops occur in road cuttings along the Lower Pieman Dam road, between CP680789 and CP685788; along the HEC transmission line maintenance track, between CP681789 and CP688780; and in Merton Creek around CP679793. The dominantly volcaniclastic part of the succession

is fossiliferous with a late Middle Cambrian fauna (page 52). This fauna occurs 50 m down sequence from the siliceous conglomerate–sandstone units which form part of the turbidite sequence underneath the *Glyptagnostus* horizon.

The lower fossil fauna occurs in a sequence of laminated siltstone and mudstone with interbedded volcaniclastic wacke, sandstone and granule conglomerate, with rip-up mudstone clasts. The volcaniclastic wacke units are epiclastic equivalents of crystal vitric tuff, being dominantly feldspar crystals with minor quartz crystals and devitrified glass. The crystal grains are very angular. The finer grained units are composed of glass shards, feldspar and quartz grains, and glass fragments, being an epiclastic equivalent of vitric crystal tuff.

Overlying the volcaniclastic sequence is a succession of laminated and thinly-bedded siltstone, sandstone and fine-pebble conglomerate. The sandstone and conglomerate units are usually graded and the conglomerate beds are lensoidal along strike. Some sandstone beds contain ripple marks.

As the faunas in the volcaniclastic part of the succession are of late Middle Cambrian age, and only 50 m separates these horizons from the siliceous turbiditic sequence with the *Glyptagnostus* horizon in the lower part, the possibility of a disconformity around the *Lejopyge laevigata* III Zone, as suggested by evidence from the Dundas type area, is further supported.

To the south-east of the type area, the Pieman River [between CP722737 and CP756732] gives a section through a lateral variant of the Huskisson Group (fig. 1, 3). Overall, the sequence is finer in grain size, not having the quantity of conglomerate units found in the type section, and is dominantly well-bedded siltstone and medium-grained to coarse-grained volcaniclastic wacke with minor mudstone and mixed-source conglomerate.

The volcaniclastic wacke units are typically poorly sorted, immature, dominated by volcanic-derived feldspar crystals and containing volcanic quartz, devitrified glass and chert as well as quartzite grains and minor andesitic lava clasts. The volcanic detritus is angular and the metasedimentary grains are rounded. Some beds contain elongate mudstone fragments up to 10 mm long.

In the middle of the river section [around CP735731], numerous pebbly granule conglomerate units derived from a mixed metasedimentary felsic volcanic component occur within the sequence. The conglomerate units are interbedded with fine-grained to medium-grained volcaniclastic silty sandstone beds, again of a mixed source origin.

To the south of the river section, along Colebrook Hill, the sequence contains medium-grained volcaniclastic wacke units in a laminated siltstone and mudstone succession. The volcanic component is slightly less than in the river section and clastic muscovite grains are prevalent. These beds are poorly sorted, contain angular volcaniclastic grains of pumice with feldspar phenocrysts, feldspar and quartz crystals, devitrified glass, and felsic lava fragments consisting of feldspar laths, magnetite and leucoxene in a black glass groundmass. Thin andesitic lava units are also found within the sequence. On the southern end of the spur south of Colebrook Hill [around CP748683] a sequence of well-bedded friable quartz sandstone and quartz wacke occurs. These units are fine-grained to medium-grained and contain minor feldspar, mudstone and clastic muscovite grains as well as quartz and quartzite. The majority of grains are of a metasedimentary origin and are angular. Further along strike [around CP750677], the sequence changes to sandy siltstone with the sand grade grains being of indurated mudstone, quartzite and chert, as well as quartz. It is possible that this sandstone unit may be a correlate of the Stitt Quartzite of the 'Rosebery Group' as described by Green (1983).

The transition between the lower Dundas Group succession and the Huskisson Group can be seen in the Ring River near Ringville [CP731682]; on the North East Dundas Tram near Great Northern Creek [CP718662]; and along Wallace's Tram near CP720653. The incoming of felsic volcanic detritus coincided with the start of chert conglomerate sedimentation of the Razorback Conglomerate. In the Ring River [around CP731682], granule and pebble conglomerate units containing rounded chert clasts and angular volcaniclastic feldspar, quartz and fragmented glass, are interbedded with crystal-vitric granule conglomerate and volcaniclastic wacke. Minor pebble conglomerate, derived from a metasedimentary origin only, also exists within the sequence.

Along the North East Dundas Tram between CP719663 and CP722668, volcaniclastic sandstone and wacke units, derived from an acid to intermediate volcanic source, contain volcanic glass, shards and pumice fragments, angular feldspar and broken quartz crystal grains in a fragmented glass matrix. Where the North East Dundas Tram crossed Frazer Creek [CP726665], approximately 150 m up section, numerous beds of mixed metasedimentary and volcanic pebble conglomerate occur. The metasedimentary clasts are well rounded and consist of chert, indurated mudstone, quartzite, quartz wacke and carbonate. The volcanic material includes felsic lava clasts and broken crystal grains in a matrix of granulated glass and carbonate. In some of the dominantly volcaniclastic beds the glass shards still retain their original shape.

In the North East Dundas Tram–Montezuma Falls area [CP734669], approximately 300 m up sequence, the grain size of the volcaniclastic

units is finer, the coarser units being poorly-sorted, granule-bearing volcaniclastic wacke. The granule-grade material is rounded and consists of quartz-mica schist, chert, quartzite and mudstone in a medium-grained sand of fragmented glass, feldspar and quartz grains and minor felsic lava grains.

The succession in the Ring River between CP747673 and CP747669 is dominated by fine-grained muscovitic sandstone with pebbly quartz wacke units. The pebbles are of a metasedimentary origin. To the east, along the North East Dundas Tram towards Williamsford, the sequence is dominated by thinly-bedded siltstone and carbonate, fine-grained to medium-grained volcaniclastic sandstone and wacke. In the lower reaches of Conliffe Creek, volcaniclastic wacke with angular quartz and feldspar crystals, rounded grains of quartzite, quartz-mica schist and clastic carbonate grains, are interbedded with siltstone and mudstone.

The area in the upper reaches of the Ring River has a regional monoclinal structure trending to 020°, with a variable but dominantly flat plunge, and facing east. In the hinge zone of this synclinal structure, as exposed in the Ring River around the Fahl mine [CP742676] numerous mesoscopic folds can be observed, and the sequence in the next 500 m section of the Ring River, to the east, contains a zone of intraformational soft-sediment slumping which includes rootless folds, boudinage structures and disrupted bedding.

HUSKISSON GROUP CORRELATE (Ch, fig. 3)

To the west of the Burns Peak [CP780845]–Bulgobac [CP825905] area and east of the Dundas Group correlate in the Hatfield River area, is an area of mixed sedimentary and volcaniclastic units correlated with the Huskisson Group on the basis of mixed felsic volcanic and metasedimentary lithology; stratigraphic position, overlying a Dundas Group correlate; and having a structural discontinuity with the 'Rosebery Group' successions to the south of the Marionoak River. An inferred fault between the northern extension of the 'Rosebery Group' and the Huskisson Group correlate is postulated along the present course of the Marionoak River on the basis of the structural evidence. The units within the 'Rosebery Group' north of the Pieman River section, as exposed along the HEC Lower Pieman Dam road, strike north–south and are, in places, overturned to the west. The southernmost 2·5 km of the Huskisson Group correlate, between CP759840 and CP756816, has a continuous north-easterly dip and strikes NW–SE (fig. 3). The sequence, consisting of lithic sandstone and mudstone with interbedded siliceous pebble to boulder conglomerate lenses, has a consistent structural trend to be a southern continuation of an open synclinal fold structure to the north (Collins *et al.*, 1981). The conglomerate contains elongate quartzite cobbles and 10–20 mm pebbles of red mudstone and grey and white chert in a siliceous sand-grade matrix. Further north, the succession contains mudstone, quartzite, greywacke and tuffaceous greywacke-mudstone with conglomerate and crystal-vitric tuff units (Collins *et al.*, 1981).

'ROSEBERY GROUP' CORRELATE (Crg)

The term 'Rosebery Series' was introduced by Finucane (1932) and changed to 'Rosebery Group' by Taylor (1954). Taylor's definition of the 'Rosebery Group' included all rock successions in the Pieman River east of the ultramafic rocks at CP743733 to CP774784. Blissett and Gulline (1962) considered the area along the Pieman River between CP743733 and CP757732 to be a southern continuation of the Crimson Creek Group. This correlation with the Crimson Creek Group is here considered erroneous, as the presence of felsic volcanic detritus and not mafic tholeiitic detritus, as is typical of the Crimson Creek Formation, and the structural continuity of the section with the Huskisson Group type area, both rule out such a correlation. This part of the area, included by Taylor in his definition of the 'Rosebery Group', is here considered a southern continuation of the Huskisson Group.

Campana and King (1963) subdivided the 'Rosebery Group' into five formations; the Primrose Pyroclastics and Slate, Stitt Quartzite, Natone Volcanics, Wescott Dolomitic Beds, and Munro Creek Slates and Quartzite. These formations were retained by Brathwaite (1969) in his revision of the Group, when he also added the Chamberlain Shale. Likewise Green (1983), in his remapping and revision of the 'Rosebery Group', retained the existing formation names. The writer agrees with Green (1983) in respect to the fact that the 'Rosebery Group' in the area mapped consists of a series of fault slices, whose original relationships with each other are still uncertain. It is considered most probable that the 'Rosebery Group' formed contemporaneously with the Mt Read Volcanics and is a correlate of part of the Dundas Group as was earlier considered by Hills (1915) and Taylor (1954), and is not a correlate of the Success Creek Group (Campana and King, 1963; Solomon, 1965; Loftus-Hills *et al.*, 1967), nor of the Oonah Formation (Blissett, 1962).

The correlation of different sedimentary sequences in the vicinity of Moores Pimple [CP742641] with formations of the 'Rosebery Group' is based on lithological similarities with those developed in the Rosebery area. The area to the north of Moores Pimple, designated as Crg (with quartz sandstone overprint; fig. 1) consists of interbedded quartz sandstone and quartz wacke, micaceous siltstone and black mudstone. This area is correlated with the Stitt Formation.

The lensoidal area north of Moores Pimple (Crg) (with conglomerate overprint; fig. 1), contains conglomerate flows of a mixed metasedimentary and felsic volcanic origin. The conglomerate units are poorly sorted, range from fine pebble to cobble in grade, have an open framework and flow-orientated clasts. The metasedimentary clasts are usually rounded and consist of black, grey and white chert, red and black indurated mudstone and carbonate with angular feldspar-phyric felsic lava and volcaniclastic quartz grains. Some apple-green clasts, X-ray diffractograms of which show a combination of carbonate, quartz and mica (the mica probably being fuchsite), occur throughout the conglomerate units. The matrix of the conglomeratic units comprises medium-grained sand grains of the same composition as the clasts, and is pervaded by carbonate. Clast sizes range from less than 10 mm up to 100 mm, with an occasional 140 mm clast. This conglomerate sequence is correlated with the Salisbury Formation of the 'Rosebery Group'.

To the west of Moores Pimple occurs an undistinguished succession of interbedded calcareous siltstone, dolomite, grey and red mudstone, chert and carbonate conglomerate, volcaniclastic crystal wacke and lithic wacke. The lithic wacke units contain angular fragments of clastic carbonate, siltstone, quartzite and chert with volcaniclastic quartz in a fine sand-grade matrix which is permeated by carbonate.

To the east of Moores Pimple, laminated mudstone and siltstone is interbedded with sandstone, volcaniclastic wacke and possible crystal tuff units. Numerous beds around CP747640 contain sedimentary facings which give an original west facing to the sequence. This is the only west-facing sequence found in the area and the relationship between this sequence and the rest of the successions is unknown.

The main difference between the areas designated as 'Rosebery Group' correlates (Crg) and Huskisson Group (Ch) in the Ring River–Moores Pimple area is the predominance of carbonate, both as interbedded units and secondary permeation of other beds in the sequence. Overall the 'Rosebery' Group successions are considered to have formed in a proximal position to the Mt Read volcanic belt with the Huskisson Group being a distal facies to both the Mt Read volcanic belt and the 'Rosebery Group'. The Huskisson Group also received mass-flow conglomerate-grade units from a probable western sedimentary source as part of prograding fans within elongate rift troughs whose background sedimentation was open marine, and of a siltstone and mudstone grade.

CORRELATE OF THE MT READ VOLCANIC ROCKS (Cmr)

The small area to the east of the 'Rosebery Group' correlate [around CP753642] consists of massive crystal tuff horizons with elongate fiami clasts, interbedded with minor siltstone units. The area has been tentatively designated Cmv, due to the preponderence of pyroclastic units as compared with the epiclastic-dominant sequences which were correlated with 'Rosebery Group' formations, but may equally belong to a pyroclastic formation within the 'Rosebery Group'.

PALAEONTOLOGY

DUNDAS GROUP

Of the numerous fossil locations found within rock successions of the Dundas Group and correlates, very few faunas have a good degree of age certainty, most having either a fair or poor degree only. Another problem with the majority of the faunas found during the late 1940s and early 1950s is that most of them were never described, and most of the material was destroyed in a fire at the Bureau of Mineral Resources in 1953. A summary of the more relevant faunas which can be reasonably reliably dated is given in Figure 13.

Judith Formation

The oldest Cambrian fauna so far found in the Dundas area came from a boulder (M. R. Banks, pers. comm.) found in that part of South Comet Creek which is considered to contain rocks of the Judith Formation. Öpik (1951) recorded *Lorenzella, Pachyaspis, Pagetia, Peronopsis, Ptychagnostus*, and *Triplagnostus*, and suggested a correlation with the *Ptychagnostus gibbus* Zone. The original fauna was destroyed in the BMR fire and attempts to relocate the fauna " . . . four hundred feet upstream from the junction of Stichtite Creek with the South Comet Creek" (Elliston, 1954) have proved unsuccessful.

Hodge Formation

From what was later to become the type area of the Hodge Formation, Thomas and Henderson (1945) collected dendroids, cystoids and a trilobite fragment. They described the dendroids, which included *Archaeocryptolaria* and *Archaeolafoaea* and, by comparison with very similar dendroids from Victoria (Chapman and Thomas, 1936), which also co-existed with two trilobite-bearing units having a probable age of low in the Middle Cambrian, considered that the age of the sedimentary succession that was to become the Hodge Formation was similar. The dendroids and hydroids from the original location of Thomas and Henderson (1945) were redescribed by Quilty (1971), who followed Banks (1956) and gave the fauna a *Ptychagnostus atavus* or *P. nathorsti* Zone age.

Rubenach (1967) obtained a fauna (RB1, Jago, 1973) from a correlate of the Hodge Formation on the northern face of Black Hill [CP681661] approximately 2·5 km NNW of the Hodge

5 cm

AGE	STAGE	ZONE
EARLY ORDOVICIAN	DATSONIAN	*Cordylodus proavus* / *Mictosaukia perplexa*
	PAYNTONIAN	*Neoagnostus quasibilobus* with *Tsinania nomas*
LATE CAMBRIAN	pre-PAYNTONIAN	*Sinosaukia impages* *R. clarki maximus* with *R. papilio* *R. bifax* with *N. denticulatus* *R. clarki prolatus* with *Caznaia sectatrix* *R. clarki patulus* with *Caznaia squamosa* *H. lilyensis* *Peichiashania tertia* with *P. quarta*
	post-IDAMEAN	*P. secunda* with *P. glabella* *Wentsuia iota* with *Rhaptagnostus apsis* *post-Irvingella* *Irvingella tropica*
	IDAMEAN	*Stigmatoa diloma* *Erixanum sentum* *Proceratopyge cryptica* *Glyptagnostus reticulatus*
LATE / MIDDLE (Boundary preferred by Jago (1979))		*Glyptagnostus stolidotus*
	MINDYALLAN	*Acmarhachis quasivespa* *Erediaspis eretes* ZONE OF PASSAGE
MIDDLE CAMBRIAN	BOOMERANGIAN	*Lejopyge laevigata* — *III (H. arepo)*, *II (Pr. agra)*, *I (Pt. cassis)*
	UNDILLAN	*Ptychagnostus nathorsti* *Doryagnostus notalibrae* *Ptychagnostus punctuosus*
	FLORAN	*Evagnostus opimus* *Ptychagnostus atavus*
	TEMPLETONIAN	*Ptychagnostus gibbus* *Peronopsis longinqua*

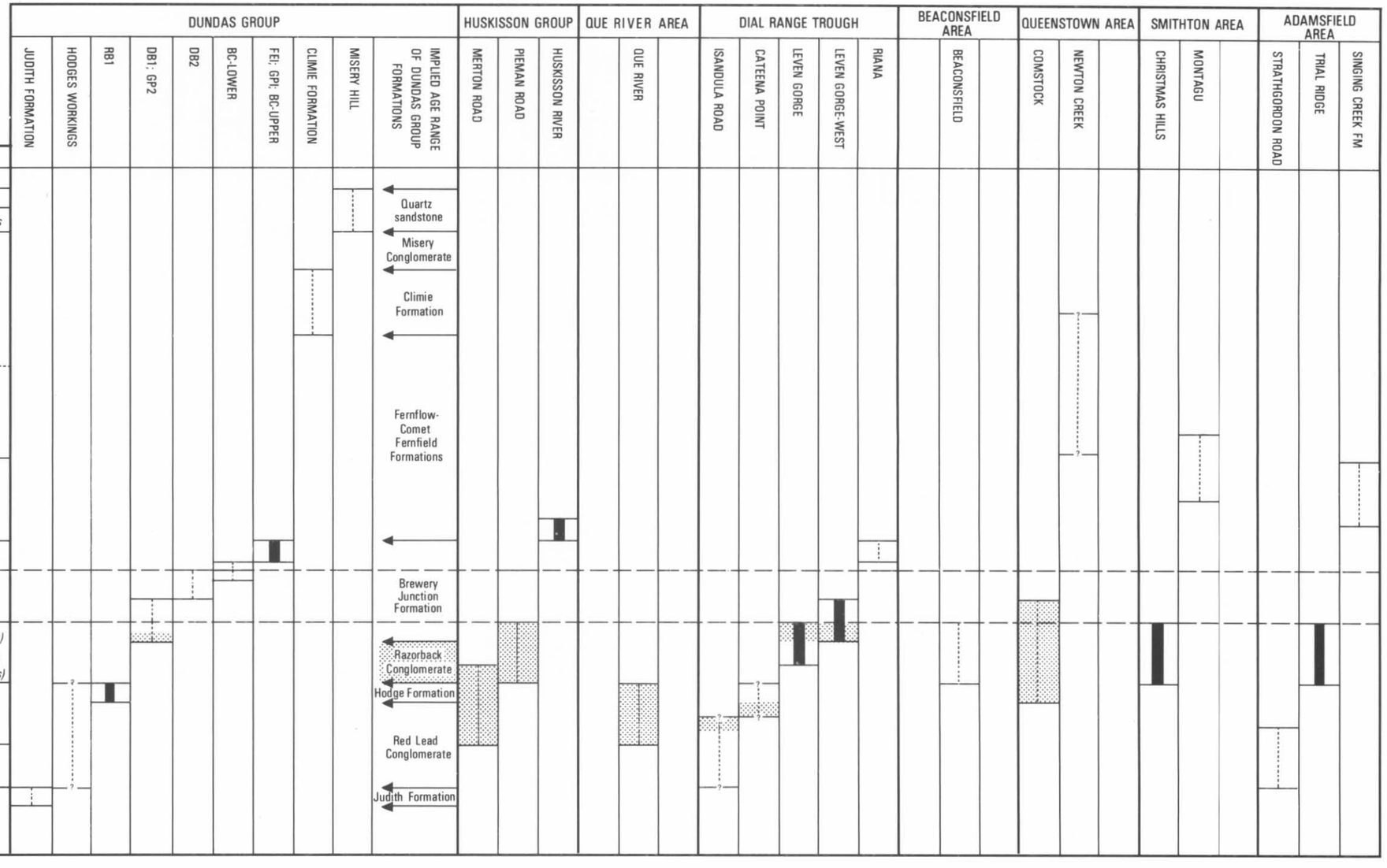

Figure 13. *Palaeontological correlation chart.*

DEGREE OF CERTAINTY OF AGE DETERMINATION — GOOD — FAIR — POOR

SUCCESSIONS CONTAINING ACID TO INTERMEDIATE VOLCANIC PYROCLASTIC AND/OR EPICLASTIC UNITS.

GSB62

workings. Included in this fauna are both polymerid and agnostid trilobites, inarticulate brachiopods, gastropods, numerous hydroids and dendroids (described by Quilty, 1971), as well as hyolithids and sponge spicules. The agnostid trilobites include *Ptychagnostus (Ptychagnostus)* sp., and indicate the *Ptychagnostus nathorsti* Zone (Jago, 1973; 1979).

Öpik (1951) listed a fauna collected by Elliston from the Bonnie Point area on the North East Dundas Tram and considered it to be of late Middle Cambrian age. The area from where the fauna was collected was subsequently incorrectly correlated with the Hodge Formation by Elliston (1954) and Blissett and Gulline (1962). Mapping during this project has shown that the succession in this area does not belong to the Hodge Formation, but is a correlate of the felsic volcanic epiclastic sequence of the Huskisson Group, and it overlies the local equivalent of the Razorback Conglomerate which crops out in the Ring River near Ringville, indicating a correlation with the Brewery Junction Formation. The original fauna from the Bonnie Point area was poorly preserved, never described, and later destroyed by fire (M. R. Banks, pers. comm.). Jago (1972) has recollected from this area and lately K. D. Corbett (pers. comm.) has also collected a fauna from 300 m east of Bonnie Point. Both of these collections include *Clavagnostus*, indicating that the sequence is a biostratigraphic correlate of the Brewery Junction Formation.

Brewery Junction Formation

Numerous fossil localities from within the sequence mapped as Brewery Junction Formation and correlates are known in the Dundas area. In the type area of the Brewery Junction Formation, all fossil locations are within the 'upper Brewery', no faunas having so far been recovered from the laminated succession of the 'lower Brewery'.

The stratigraphically lowest fauna (DB1, fig. 13) is possibly as old as the *Lejopyge laevigata* III Zone, but probably belongs in the Passage Zone (J. B. Jago, pers. comm., 1977). This fauna contains agnostids and pagetiid trilobites. The stratigraphic postion of the DB1 fauna is just above the highest lens of epiclastic felsic volcanic material found in the Dundas Group type area. The DB1 fauna is considered to be an equivalent of the GP2 fauna from the Black Hill area (Blissett and Gulline, 1962; Jago, 1973); the St Valentines Peak fauna (Jago, 1973; Jago *et al.*, 1975); and the fauna from the west side of the Leven Gorge in the Dial Range Trough (Burns, 1965; Jago, 1973).

Continuing up-sequence, downstream along the Dundas Rivulet from DB1, a consistent younging of fossil faunas is recorded. The most diagnostic fauna is DB2, which contains *Tasagnostus*, a damesellid trilobite, plus other fragmentary material, indicating a middle Mindyallan age (J. B. Jago, pers. comm., 1977) and is considered to be probably equivalent to the BJ1 and BJ2 faunas of Jago (1973) (J. B. Jago, pers. comm., 1977).

The third main fossil location within the Brewery Junction Formation occurs in the Dundas Rivulet section and is the FE1 fauna of Jago (1972). The outcrop containing this fauna occurs about 50 m below the top of the formation. The fauna contains *Rhyssometopus (Rhyssometopus)* sp., *R. (Rostrifinis)* sp., *Aulacodigma* sp., *Palaeodotes* sp., and a nepeid as well as numerous agnostids including *Idolagnostus* sp., *Aspidagnostus* sp. 1, *Ammagnostus(?)* sp. and *Pseudagnostus* sp. 2. Jago (1972) considers that this fauna probably belongs to the *Glyptagnostus stolidotus* Zone of the Mindyallan Stage.

In the Grand Prize mine–Barkers Creek area (to the west of Black Hill, fig. 1, part 2), four fossiliferous units correlated with parts of the Brewery Junction Formation are known (Elliston, 1951; Blissett and Gulline, 1962). These locations were resampled by Jago (1973). The area is one with complex block faulting of various lithologies, which have very little lateral extent, and in the past they have been interpreted as belonging to many different formations within the Dundas Group. This area has been included within an area of undifferentiated 'lower' Dundas Group successions (fig. 1, part 2), as the succession along the spur to the west of Black Hill is a correlate of the 'lower' Brewery Junction Formation.

Two fossil localities in Barkers Creek (Elliston, 1954) were resampled by Jago (1973). The older fauna, BC lower (fig. 13), belongs to the *Cyclagnostus quasivespa* Zone and contains *Agnostus(?)* sp., cf. *Cyclagnostus* sp., *Aspidagnostus* sp. 3 and *Oedorhachis(?)* sp. (Jago, 1973). This confirms the age obtained by Gatehouse (1961) with *Rhyssometopus (Rostrifinis)* cf. *rostrifinis* for a fauna collected by him from this locality.

The upper BC fauna is considered to belong to the *Glyptagnostus stolidotus* Zone (Jago, 1973) as suggested by Öpik (1967) and contains *Aulacodigma* sp., *Agnostus(?)* sp., *Acmarhachis* sp., and *Agnostardis* sp. 1. (Jago, 1973). From this locality Öpik (1967) noted the presence of *Palaeodotes*.

The two faunas in the Grand Prize area (Blissett and Gulline, 1962) (fig. 13) were resampled by Jago. The oldest fauna (GP2) contains agnostid trilobites as well as a pagetiid trilobite, which Jago (1973) considered correlated with the St Valentines Peak fauna and the DB1 fauna (J. B. Jago, pers. comm.) (fig. 13). The original collection from the GP1 site of Jago (1973), collected by Blissett and Gulline (1962), was described by Gatehouse (1961). This fauna is a correlate of the FE1 fauna from the type section along the Dundas Rivulet (Jago, 1973).

Fernfields–Comet–Fernflow Formations

That part of the upper Dundas Group succession hitherto referred to as the Fernfields, Comet and Fernflow Formations (Elliston, 1954; Banks, 1956; Blissett and Gulline, 1962; Blissett, 1962; and others) has only yielded poorly preserved non-diagnostic fossils (Banks, 1962*a*; Blissett, 1962; Jago, 1979). An age of early Late Cambrian is attributed to these formations because of their stratigraphic position in the Dundas Rivulet succession overlying the Brewery Junction Formation (above the FE1 fauna) and underlying the Climie Formation.

Climie Formation

The Climie Formation contains two poorly-preserved fossil horizons (Jago, 1978). The lower fauna contains the trilobites *Olenus* sp., *Neoagnostus* sp., and *Agnostus* sp. as well as inarticulate brachiopods. The upper fauna also contains inarticulate brachiopods as well as the trilobites *Agnostus* sp., *Lotagnostus(?)* sp., *Peltura(?)* sp., and unassigned Olenidae. Jago (1978) suggested that the lower fauna is probably of early post-Idamean age, with the higher fauna being slightly younger, rather than Late Idamean. However, Jago (pers. comm., 1984) now considers that the faunas are pre-Payntonian (fig. 13).

Quartz sandstone sequence–Misery Hill

K.D. Corbett has recently discovered a very Late Cambrian saukiid trilobite and a gastropod from a quartz sandstone and siltstone sequence on the western side of Misery Hill (Jago, in prep.). This sequence is shown on Figure 1 (part 2) as 'Os'; quartz sandstone and minor siltstone; but it was considered to have probably conformably followed the Misery Conglomerate.

It is possible, due to the occurrence of the trilobites of Late Cambrian age, that the sandstone sequence was deposited as part of a continuing sedimentation cycle at the top of the Dundas Group successions and that a disconformity, similar to that indicated in the Huskisson River, occurs between the top of the sandstone succession and the overlying limestone units of the Gordon Sub-Group (Ol) which occur to the west of this sequence on the western slopes of Misery Hill.

HUSKISSON GROUP

Four new locations of the *Glyptagnostus reticulatus* fauna have been found from rock sequences belonging to the Huskisson Group, in addition to a resampling of the original location of Taylor (1954) from his unit 18. Three of the new locations are upstream from Taylor's original location and within his unit 18, but unlike Taylor's collection the fauna contains abundant *Pseudagnostus idalis* with only subordinate *G. reticulatus*. The preservation of the fauna is very good and a considerable number of the *Pseudagnostus* specimens are complete. A list of the faunas is given in Appendix 1. The fourth location is within unit 14 of Taylor and contains abundant *G. reticulatus* and spicules of *Protospongia* sp., as well as rare fragments of another small agnostid (Appendix 1). The preservation of this fauna is also very good. The occurrence of the above fauna substantiates the suggestion of Blissett (1962) that unit 14 and unit 18 of Taylor (1954) represent the same stratigraphic unit.

From approximately 100 m downstream from the above location, and on the opposite side of a fault, Öpik (1951) described poorly preserved hydroids and the brachiopods(?) *Otusia* sp. and (?)*Protorthis* sp., from a collection made by Taylor, and dated them as middle Middle Cambrian. Quilty (1971) re-examined the fauna collected from this locality and the fauna obtained approximately three kilometres downstream (the locations of the faunas from these two localities were reversed by Quilty, 1971). The lower fauna obtained by Taylor upstream of the faulted contact with the ultramafic rocks contains *Protospongia*, dendroids, hydroids and the brachiopods *Protorthis* and (?)*Otusia*. Öpik (1951) regarded the fauna as having a probable Middle Cambrian age. This fauna underlies the incoming of detritus from an acid to intermediate volcanic source which is now dated by the discovery of two fossil localities approximately five kilometres north-west of the river section. The older fauna, MR1 (Merton Road, CP679793; there is no fossil symbol on Figure 1 part 2, as the location was found after publication of the map), is from a laminated siltstone unit between felsic volcaniclastic lithic wacke units and probably of Undillan to Boomerangian age (J. B. Jago, pers. comm., 1984) (fig. 13). The younger of the two (PR1, CP682788) contains two faunas, one in a mudstone unit, which represents the background sedimentation, and the other in interbedded sand-grade volcaniclastic units which contain characteristics of turbidity currents. Jago (pers. comm., 1984) recorded at least two species of *Ptychagnostus, Diplagnostus, Grandagnostus* and one other agnostid genus as well as dendroid fragments and acrotretid brachiopods from within the mudstone unit. In the sandstone unit, Jago (pers. comm., 1983) recorded *Peronopsis*, dolichmetopid pygidia, dorypygid(?) cranidia and numerous other fragments of trilobites, as well as echinodermata and articulate brachiopod fragments, and suggested a possible *Lejopyge laevigata* I–III Zone for this fauna.

The two new faunas (MR1 and PR1) agree with Öpik's determination and give a late Middle to early Late Cambrian age for one phase of dominantly feldspar phyric acid to intermediate volcanism within the Mt Read volcanic belt.

In the Huskisson River [near CP723761] there is a faulted contact relationship between the fossiliferous, dominantly felsic volcanic-derived succession and the dominantly continental-derived mass flow and turbiditic conglomerate

succession. With the presence of *G. reticulatus* in the non-volcaniclastic sequence, an upper limit of the lowermost Late Cambrian can be given for the cessation of the phase of felsic volcanism which was the main source of approximately 1000 m of succession in the Huskisson River. The dominantly feldspar phyric epiclastic acid to intermediate succession within the Huskisson River is correlated with the Razorback Conglomerate and lower part of the Brewery Junction Formation of the Dundas Group type area, which also contains felsic volcaniclastic units. The non-volcaniclastic units in the Huskisson River are correlated with the 'upper' Brewery Junction Formation–Fernfield Formation. These give a good age control on one phase of dominantly feldspar phyric acid to intermediate volcanism within the Mt Read volcanic belt. This volcaniclastic part of the Huskisson Group continues in an arcuate direction to the south-east, through Colebrook Hill, to the upper Ring River.

Similar aged felsic volcanism is found within the Mt Read volcanic belt at Comstock near Queenstown, at Que River, and in the Dial Range Trough and at Beaconsfield (fig. 13). It is interesting to note, however, that the fossiliferous late Middle Cambrian sedimentary sequences at Christmas Hills in the Smithton Basin (Jago, 1979), and at Trial Ridge in the Adamsfield Trough (Jago, 1979) (fig. 13), do not contain any evidence of felsic volcaniclastic detritus or associated lava or tuff.

The *Glyptagnostus reticulatus* horizon (Taylor's unit 14 and unit 18) is 45 m thick and is overlain by approximately 100 m of mass-flow conglomerate units, which is probably a relatively short time span for deposition. This indicates that the suggestion of both Taylor (1954) and Blissett (1962), that the conglomerate of unit 19 can be correlated with the Zeehan Conglomerate, is incorrect, and that a correlation with the basal part of the Fernfields Formation is more logical.

COMPARISON WITH CAMBRIAN FOSSILIFEROUS FAUNAS IN OTHER AREAS

Dial Range Trough

In the Dial Range Trough, the Cateena Group and the Radfords Creek Group (Burns, 1965) contain fossiliferous sequences which have minor amounts of acid to intermediate pyroclastic and epiclastic rock units (fig. 13). The Cateena Group contains two known fossil horizons. The lowermost, on Isandula Road, contains inarticulate brachiopods, echinodermata, polymerid trilobites including nepeids, the agnostid trilobite *Peronopsis* and a pagetiid (Jago, 1972). Jago suggests a probable age of *Ptychagnostus atavus* or *P. punctuosus* Zone. The younger fauna at Cateena Point is probably of *P. nathorsti* Zone age (Jago, 1972) and contains a fauna with hydroids and dendroids (Quilty, 1971), brachiopods and trilobites including *Peronopsis*. The Cateena Group is a probable biostratigraphic correlate of the Que River Beds and the basal parts of the Huskisson and Dundas Groups.

The Radfords Creek Group (Burns, 1965) contains three fossil locations. The oldest, several hundred metres above the base in the Leven Gorge, contains a fauna which probably belongs to the *L. laevigata* II or III Zone (Öpik *in* Banks, 1956; Jago, 1979). On the western side of the Leven Gorge a fauna of probably *L. laevigata* III or Passage Zone (Jago and Daily, 1974) has been collected. The youngest fauna, from Riana, is probably of late Mindyallan age (Jago, 1973; 1979).

The felsic volcaniclastic parts of the above two groups are probable correlates of that phase of felsic volcanism recorded in the Dundas Trough successions during the Undillan and Boomerangian Stages.

Beaconsfield area

Within the Beaconsfield area (Green, 1959; Gee and Legge, 1974) a fossiliferous succession of probable Boomerangian age (J. B. Jago, pers. comm., 1984) (fig. 13) contains a 70 m thick lens of altered pyroxene andesite (Green, 1959). This again correlates with the coeval phase of felsic volcanism during the late Middle Cambrian.

Queenstown area

A fossiliferous limestone at the base of the Comstock Tuff in the Queenstown area contains a fauna of probable late Middle Cambrian age (Jago *et al.*, 1972) (fig. 13). In the Tyndall Range a poorly preserved middle Late Cambrian (Jago, 1979; pers. comm., 1984) fauna of trilobites, brachiopods and cystoids was obtained from the Newton Creek Sandstone (Corbett, 1975) which overlies the felsic volcanic succession. This fauna, although younger than the *G. reticulatus* fauna from the Huskisson River, also places an upper limit, in the Queenstown area, to the felsic volcanism during the early part of the Late Cambrian. Jago (1979) notes that in both the Que River and Queenstown areas the bulk of the Mt Read volcanic rocks lies beneath the fossiliferous units.

Smithton Basin and Adamsfield Trough

Well preserved and diagnostic Boomerangian Stage faunas have been obtained from non-felsic volcanic-derived sequences in both the Smithton Basin and Adamsfield Trough (fig. 13). This indicates that the felsic volcanic phase of the Mt Read volcanic belt, recorded from Elliott Bay through Queenstown, along the eastern margin of the Dundas Trough, up along the Fossey Mountains–Dial Range Trough and at Beaconsfield, was a spatially limited event around the western and northern margins of the Tyennan Block. Late Cambrian faunas from both the Smithton and Adamsfield areas also occur in sedimentary rocks of a non-felsic volcanic origin.

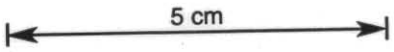

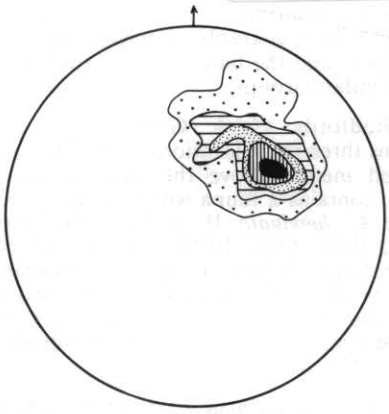

(a) Lambert Projection of 55 poles to bedding: Dundas Group, Nevada Creek–Grand Prize area, Area 9a Figure 6. Contour intervals 1,6, 12,17,23%.

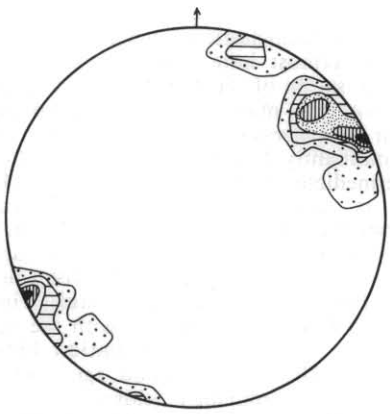

(b) Lambert Projection of 21 poles to undifferentiated cleavage: Dundas Group, Nevada Creek–Grand Prize area, Area 9a Figure 6. Contour intervals 2,7,12,17,21%.

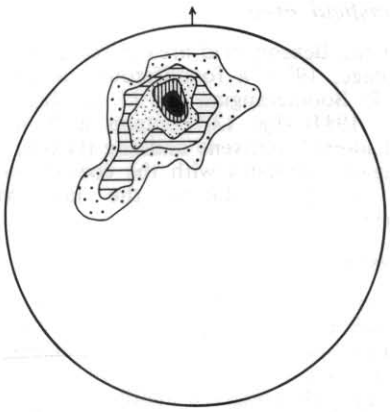

(c) Lambert Projection of 40 poles to bedding: Dundas Group, Black Hill area, Area 9b Figure 6. Contour intervals 1,6,11,21,26%.

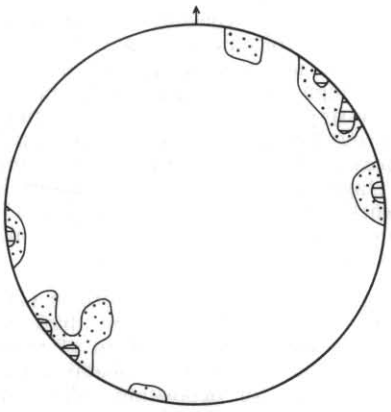

(d) Lambert Projection of 9 poles to undifferentiated cleavage: Dundas Group, Black Hill area, Area 9b Figure 6. Contour intervals 5,15%.

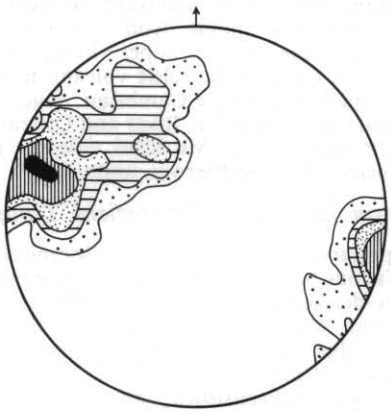

(e) Lambert Projection of 110 poles to bedding: Dundas Group, Kapi Creek area, Area 9c Figure 6. Contour intervals 0·5,2·25,4,7·75, 15%.

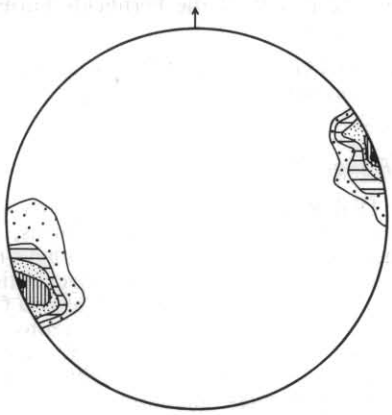

(f) Lambert Projection of 23 poles to undifferentiated cleavage: Dundas Group, Kapi Creek area, Area 9c Figure 6. Contour intervals 2,10,24,35, 50%.

Figure 14. *Stereographic plots, Dundas Group, Black Hill area (Area 9, Figure 6)..*

SUMMARY

The fossil faunas of the Dundas Trough show intermittent to possibly continuous deposition from the middle Middle Cambrian (*P. gibbus* Zone) up to near the Cambro-Ordovician boundary. The term Dundas Group (Elliston, 1954) has precedence for dominantly sedimentary-derived successions, whereas the Huskisson Group, being at least Undillan to Idamean in age, has precedence for successions derived from a mixed felsic volcanic and sedimentary rock environment. Fossil horizons found within the Huskisson Group indicate a phase of dominant feldspar phyric volcanism in the late Middle Cambrian. This phase is also recorded in the Dundas Group, at Que River, and in the Queenstown, Dial Range and Beaconsfield areas. Huskisson Group correlates may, in the future, replace the enigmatic 'Rosebery Group'.

The presence of conodonts (Appendix 2) within the overlying Gordon Sub-Group limestone, which indicates a Blackriverian age (Darriwilian Stage), implies a disconformity between the early Late Cambrian and the middle Middle Ordovician in the Huskisson River area. Along with the evidence from the Misery Hill area, this suggests that there is no example known of a transition between the Dundas and Junee Groups in the Huskisson River area, and that the lithological equivalent of the Owen Conglomerate and overlying sandstone, as found elsewhere in Tasmania, is missing from the stratigraphic succession in the Dundas–Huskisson River area.

STRUCTURE

To obtain the main structural characteristics of the Dundas Group, stereographic plots of bedding and cleavage readings, obtained from known fossiliferous Dundas Group sequences in the Dundas township (area 10, fig. 6) and Black Hill (area 9, fig. 6) areas were plotted as six separate sub-areas, three from Black Hill and three from Dundas, each based on a major fault-bounded area (fig. 14, 15). Each set of three sub-areas was then combined (fig. 16) so that the effects of faulting and tilting of the folds during solid-state re-emplacement of the ultramafic rocks could be analysed.

The stereographic plots of bedding in the Black Hill area (fig. 14) show that the three sub-areas belong to the same open anticlinal structure, which was modified by block rotation along steep normal faults during ultramafic rock replacement. The combined bedding plot (fig. 16*a*) of the three sub-areas forms a southerly plunging anticlinorium. The stereographic plots of cleavage readings show that the cleavage probably formed after faulting and re-emplacement of the ultramafic rocks had occurred, and that a little spreading of the cleavage occurred by later rotation about a very steep axis (fig. 16*b*).

Stereographic plots of bedding from the Dundas area show single maxima, with spread, for each sub-area (fig. 15) which, when combined (fig. 16*c*), suggest that the three sub-areas are part of a western limb of a southerly plunging anticline. Again, the cleavage formed after fault modification of the folding and the imposed cleavage trend is the same as that in the Black Hill area (fig. 16*d*).

When bedding readings from both the Dundas and Black Hill areas are combined into a single stereographic plot, one main phase of folding is recognised which produced a single southerly-plunging anticlinal structure running through both areas (fig. 17). From the associated stereographic plots of cleavage it is seen that the main cleavage forming event was superimposed upon the probable fault-modified folds.

Stereographic plots of data obtained from the rock units to the east of the Dundas–Black Hill area, and correlated on lithological criteria with those of the Huskisson (area 11, fig. 6) and 'Rosebery' (area 12, fig. 6) Groups (fig. 18), show one main fold phase of northerly trend with a later spread of bedding and cleavage poles about a steep axis. Even though numerous major faults occur in the area (fig. 1), these do not appear to affect the fold orientation, again implying block rotation between steep normal faults and, by implication, suggesting that the only modification to the simple open type folding which formed in the Dundas–Moores Pimple area was by fault block rotation during simultaneous re-emplacement of ultramafic rocks.

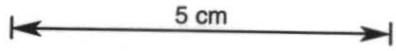

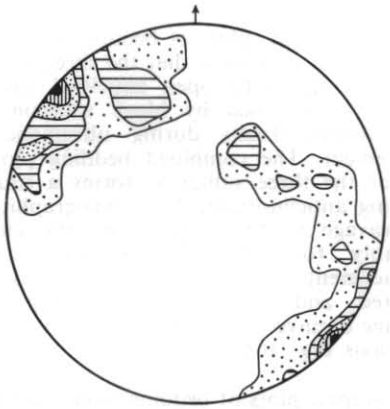

(a) Lambert Projection of 63 poles to bedding: Dundas Group, area to east of Dundas township, Area 10a Figure 6. Contour intervals 1,6,10,15,20%.

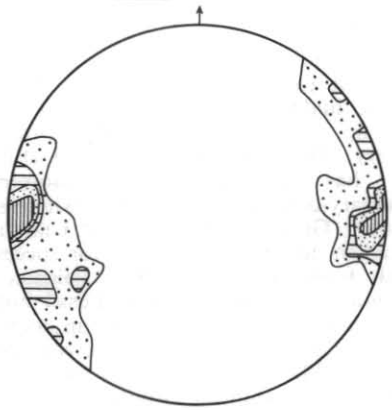

(b) Lambert Projection of 21 poles to undifferentiated cleavage: Dundas Group, area to east of Dundas township, Area 10a Figure 6. Contour intervals 2,7,12,21%.

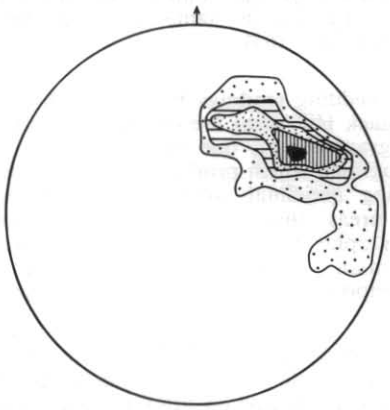

(c) Lambert Projection of 43 poles to bedding: Dundas Group, Dundas township area, Area 10b Figure 6. Contour intervals 1,6,10,15, 20%.

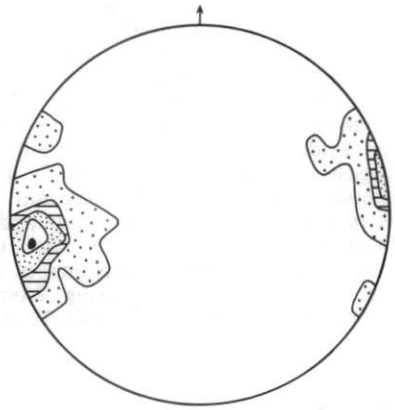

(d) Lambert Projection of 42 poles to undifferentiated cleavage: Dundas Group, Dundas township area, Area 10b Figure 6. Contour intervals 1,8, 15,23,30,37%.

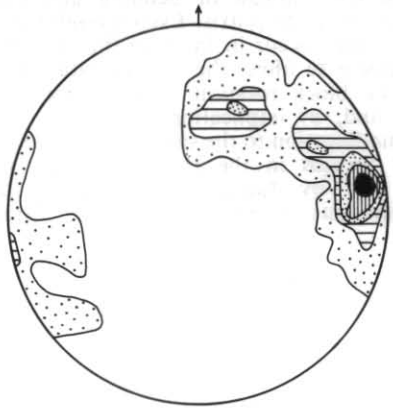

(e) Lambert Projection of 118 poles to bedding: Dundas Group, Dundas Rivulet area to south-west of Dundas township, Area 10c Figure 6. Contour intervals 0·5,4·5,9,13,17%.

(f) Lambert Projection of 62 poles to undifferentiated cleavage: Dundas Group, Dundas Rivulet area to south-west of Dundas township, Area 10c Figure 6. Contour intervals 1,10,20,30,40%.

Figure 15. *Stereographic plots, Dundas Group, Dundas area (Area 10, Figure 6).*

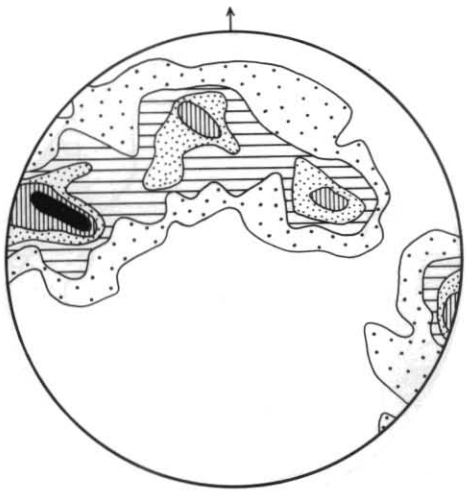

(a) Lambert Projection of 208 poles to bedding: Dundas Group. Combination of readings from Figure 14, Kapi Creek–Black Hill–Nevada Creek area, Area 9 Figure 6. Contour intervals 0·2,2,4,6, 8%.

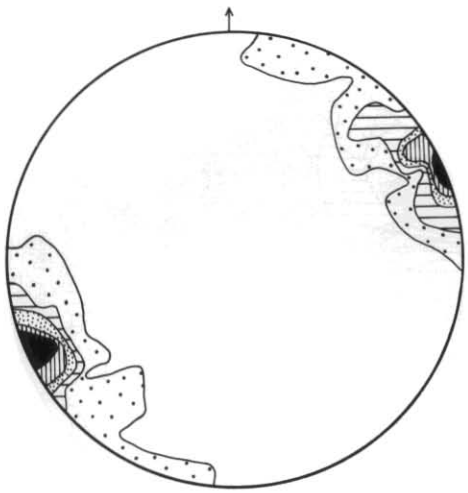

(b) Lambert Projection of 63 poles to undifferentiated cleavage: Dundas Group. Combination of readings from Figure 14, Kapi Creek–Black Hill–Nevada Creek area, Area 9 Figure 6. Contour intervals 1,5,10,15, 20%.

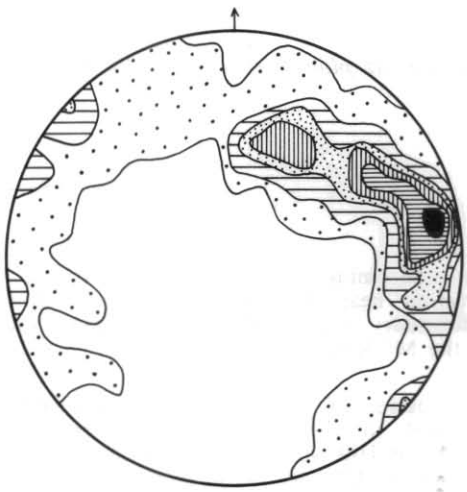

(c) Lambert Projection of 224 poles to bedding: Dundas Group. Combination of readings from Figure 15, Dundas township–Dundas Rivulet areas, Area 10 Figure 6. Contour intervals 0·2,2,4,6,8,10%.

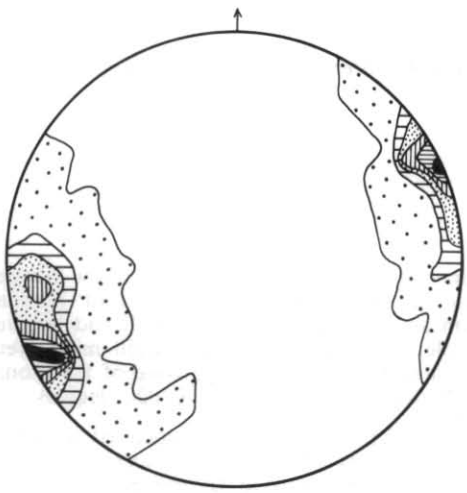

(d) Lambert Projection of 125 poles to undifferentiated cleavage: Dundas Group. Combination of readings from Figure 16, Dundas township–Dundas Rivulet areas, Area 10 Figure 6. Contour intervals 0·5,5,10,15,20,25%.

Figure 16. *Stereographic plots, Dundas Group. Total readings for each of Areas 9 and 10 (Figure 6).*

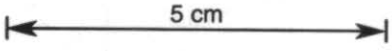

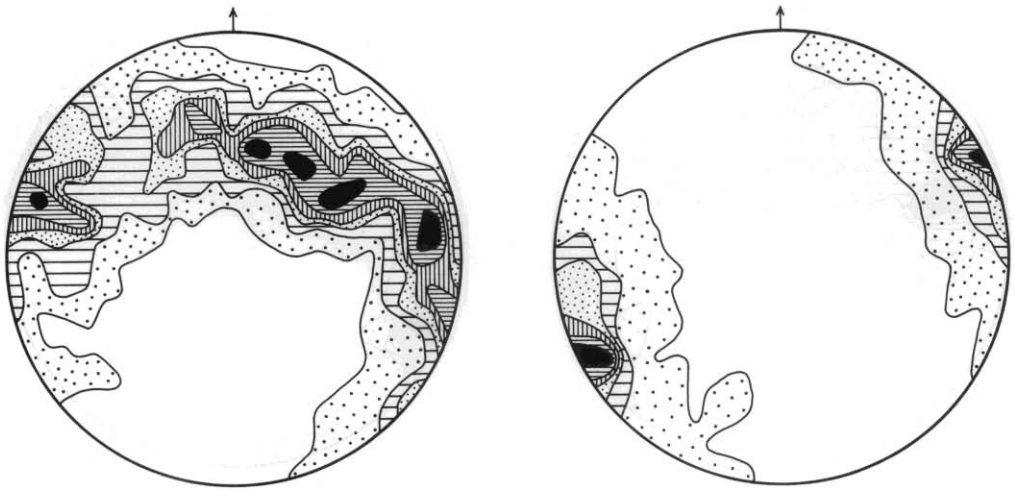

(a) Lambert Projection of 432 poles to bedding: Dundas Group. Combination of readings from Figure 16. Contour intervals 0·1,1,2,3,4,5%.

(b) Lambert Projection of 188 poles to undifferentiated cleavage: Dundas Group. Combination of readings from Figure 16. Contour intervals 0·25,4·5,9,13,17,21%.

Figure 17. *Stereographic plots, Dundas Group. Total reading plots (Areas 9 and 10, Figure 6).*

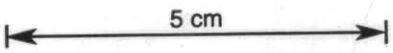

Numerous small-scale folds with shallow plunges occur in the Ring River–North East Dundas Tram area between Colebrook Hill and Moores Pimple, especially around the Fahl mine area. This area contains the hinge zone of a regional synclinorium, which trends to 020 degrees.

Another exposure of folds associated with this area of Huskisson Group sequences is along an exploration access road to the Ring River at Ringville. A profile (fig. 19) shows the style of folding and the deviation in strike of the fold axis and cleavage direction that occurs within this area. This section demonstrates that, at least locally, a dominant cleavage has been superimposed upon earlier folds, which in a number of localities range from isoclinal to box folds, as they neither conform in strike nor dip to the axial surface due to rotation about steep axes of the earlier folds. Cleavage also varies in direction along strike, indicating a later imposed strain.

Regionally, the folds in the Dundas area are relatively open, but they become tighter to the east, becoming very tight and variable in direction near the eastern boundary of the sedimentary sequences with the volcanic rocks of the Mt Read volcanic belt.

Examination of thin sections from all samples collected in the Dundas, Black Hill, and Colebrook Hill–Moores Pimple areas shows only a primary cleavage. As all cleavages observed are primary and are vertical (fig. 14–18), but the strike varies regionally across the area mapped, this implies that a varying stress field occurred over the Dundas–Black Hill area, after tilting of the folds, and produced a regionally fanned cleavage.

Overall the folding found in the Dundas Group and correlates is consistent with being the same as that found in the Crimson Creek Formation and Success Creek Group, suggesting that the only regional deformation which affected these post-Penguin Orogeny successions was the Devonian deformation.

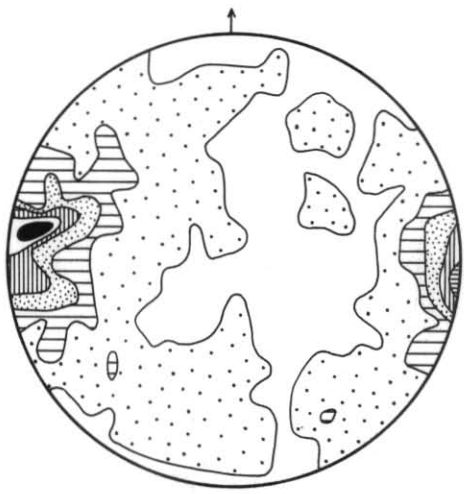

(a) Lambert Projection of 251 poles to bedding: Huskisson Group. Colebrook Hill–Ring River area, Area 11 Figure 6. Contour intervals 0·2, 2,4,6,8,10%.

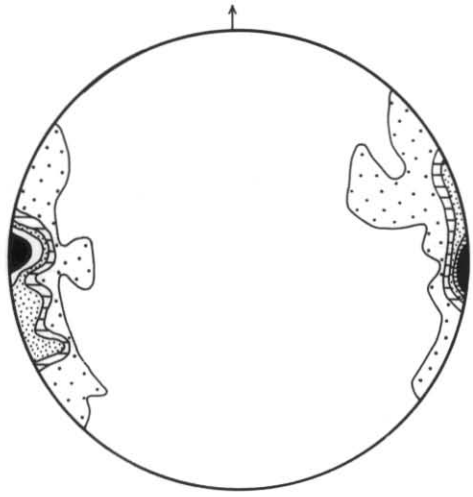

(b) Lambert Projection of 76 poles to undifferentiated cleavage: Huskisson Group. Colebrook Hill–Ring River area, Area 12 Figure 6. Contour intervals 0·5,8,16,24,32%.

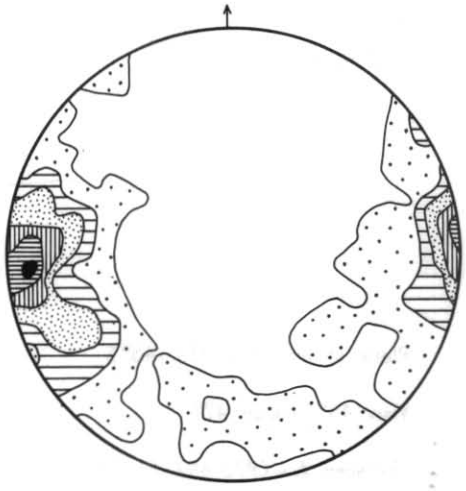

(c) Lambert Projection of 156 poles to bedding: 'Rosebery Group'. Montezuma Creek–Moores Pimple–Bather Creek area, Area 12 Figure 6. Contour intervals 0·25,3,5·5,8,10·5,13%.

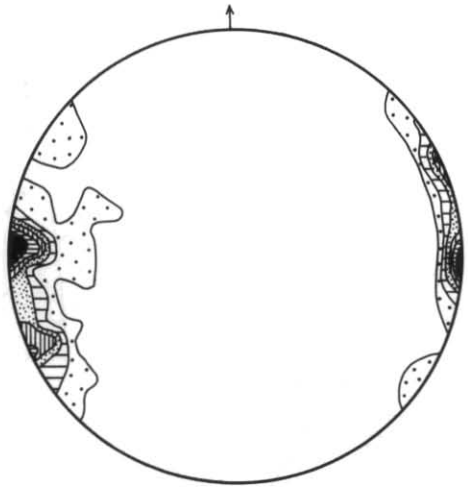

(d) Lambert Projection of 92 poles to undifferentiated cleavage: 'Rosebery Group'. Montezuma Creek–Moores Pimple–Bather Creek area, Area 12 Figure 6. Contour intervals 0·5,7,13·5,20,26·5,33%.

Figure 18. *Stereographic plots, Huskisson Group and 'Rosebery Group' (Areas 11 and 12, Figure 6).*

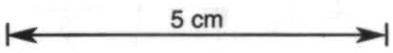

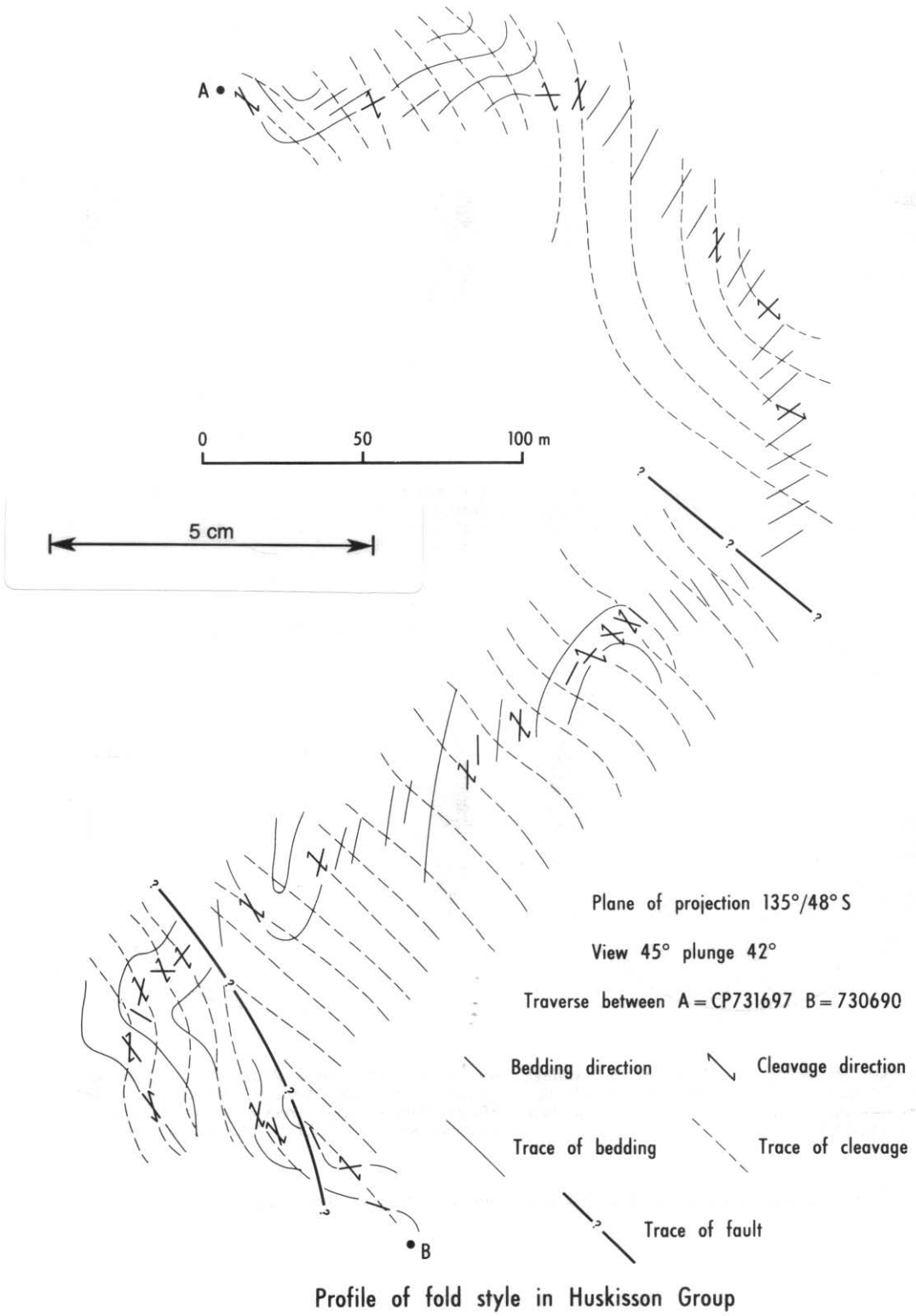

Figure 19. *Structural profile, Ringville area.*

Ordovician

GORDON LIMESTONE SUB-GROUP CORRELATE (Ol)

The main areas of outcrop of a litho- and biostratigraphic correlate of part of the Gordon Sub-Group Limestone succession (Corbett and Banks, 1975; Baillie, 1979; as used in Cooper and Grindley, 1982; and Webby *et al.*, 1981) are around the outer edges of the Huskisson Syncline (fig. 1), and to the north-east and south-west of an area of Eldon Group correlates to the north of the Meredith Granite (fig. 2). Four small areas of highly weathered limestone also occur in association with basal Eldon Group correlate successions in the vicinity of Misery Hill (fig. 1 part 2, CP671612).

On the southern nose of the Huskisson syncline, the limestone sequence crops out in the Huskisson River [near CP723764] to the north of an implied fault with Huskisson Group rocks. In this area the successions consist of blue-grey, highly fossiliferous, well-bedded and cross-laminated or stylolitic limestone with interbedded black mudstone laminae. Both macro and micro faunas have been collected from this area. The macro fauna includes calcareous algae, corals, bryozoa, brachiopods, rostroconchs, gastropods, trilobites and conodonts, which are *Belodina compressa* (Branson and Mehl) of Middle to Late Ordovician age (Appendix 2). In the creek section to the north of CP723764, outcrops of the limestone succession consist of interbedded limestone (50–150 mm thick) and black mudstone units (2–4 mm thick).

On the eastern side of the Huskisson Syncline, the Huskisson River exposes a section through the limestone succession between CP702837 and CP718858. Along this stretch of the river the rock units range between well-bedded limestone (up to 200 mm thick) with some units containing chert nodules, separated by 5 mm thick black mudstone horizons; and thinly-bedded and laminated limestone beds (15 mm thick, some with ripple marks), which are separated by 1–2 mm thick black mudstone horizons.

In John Lynch Creek [around CP709825], the limestone beds are up to 500 mm thick and are separated by 2–3 mm thick mudstone units. Muddy limestone and calcareous mudstone beds up to 100 mm thick also occur within this section.

In the Little Wilson River [near CP643867] the limestone beds are up to 200 mm thick and contain interbedded 1–2 mm thick mudstone units. Some of the limestone beds contain thin (less than 1 mm) wispy and discontinuous mudstone laminae, whilst other beds consist of massive or foliated limestone.

The original maximum thickness of the limestone succession in the area of the Huskisson Syncline is unknown because of Devonian faulting, but a minimum thickness of 550 m is exposed in John Lynch Creek, and 150 m in the Little Wilson River. This compares with between 300 m and 600 m in the Zeehan area (Blissett, 1962) and 2350 m in the Florentine Valley (Baillie, 1979).

Gordon Sub-Group–Eldon Group transition

On the western side of the syncline, in the Little Wilson River [near CP643867], an apparently conformable transition between the limestone and overlying quartz sandstone sequence is exposed. The latter is the basal Eldon Group correlate in this area. Between the last limestone bed, which contains conodonts of Blackriverian age (Appendix 2), and the first quartz sandstone unit, is a 600 mm thick unit of pale grey pug. Bedding on either side of this pug unit is conformable, and no tectonic features were discernable within this weathered limestone bed.

Although the transition between the limestone succession and the Eldon Group correlate in the Huskisson Syncline area is structurally conformable, the biostratigraphy implies a disconformity in sedimentation between the Middle Ordovician (Blackriverian/Darriwilian) (Appendix 2) and Early Silurian (Llandoverian), which is the probable age of the base of the Eldon Group correlate in this area.

The transition between the Gordon Sub-Group Limestone succession (Gordon Limestone) and the basal Eldon Group succession (Crotty Formation) was originally considered as conformable in the Zeehan area (Gill and Banks, 1950) but the possibility of the existence of a disconformity in the type section was noted by Bradley (1954) and Blissett (1962), due to the presence of 'rolled limestone' and 'rolled fragments of *Tetradium* from the Gordon Limestone' in the lower part of the Crotty Formation.

Silurian-Devonian

ELDON GROUP CORRELATE (S-Du)

In 1866 Gould described fossiliferous Silurian rocks from the West Coast which he called the Eldon Beds. Thomas (1947) introduced the term Eldon Group and the formations were formally defined by Gill and Banks (1950), with the type area being to the south of Zeehan. Within the core of the Huskisson Syncline (fig. 1 and 2) exists a litho- and biostratigraphic correlate of the Eldon Group. In general, the stratigraphic succession of the Eldon Group in the type area is similar to that in the Huskisson Syncline, but the thicknesses of the different formations vary markedly and a previously unrecognised limestone sequence within one of the formations has been delineated. To the north of the Meredith Granite, in the upper reaches of the Whyte River, a synclinal area containing lithostratigraphic and biostratigraphic correlates of at least the lower two formations of the Eldon Group exists (fig. 2)

HUSKISSON RIVER AREA (This Study)		ZEEHAN AREA	
		Blissett, 1962 Banks, 1962	Gill and Banks, 1950
Florence Formation		Florence Formation	Florence Formation
Calcareous and laminated siltstone member 150-180m	Sa	Austral Creek Formation	Keel Quartzite
Dominantly friable and siliceous quartz sandstone member 50-150m (thickest where Sal missing)	Sas	Keel Formation	
Calcareous and laminated siltstone 0-25m	Sa	Amber Formation	Amber Slate
Limestone and calcareous siltstone member 60-80m	Sal		
Laminated siltstone and mudstone 180-240m	Sa		
Crotty Formation		Crotty Formation	Crotty Formation

Figure 20. *Eldon Group correlation, Huskisson–Zeehan areas.*

Crotty Formation correlate (Sc)

A bio-lithostratigraphic correlate of the basal Crotty Formation crops out around most of the outer rim of the Huskisson Syncline (fig. 1, parts 1 and 2). The original thickness of the succession in this area is unknown, because of Devonian faulting and granite emplacement, but a minimum thickness of 400 m is exposed in a creek section at the northern end of the syncline [around CP681920], and 250 m in the Huskisson River section on the southern end of the syncline. This compares with approximately 500 m in the type area (Gill and Banks, 1950). Unlike the Crotty Formation in the type area, the correlate in the Huskisson Syncline appears to be reasonably fossiliferous.

Lithologically the succession is dominated by white and pink quartz sandstone with minor granule and pebble conglomerate, siltstone and mudstone units. Truncated cross-bedding is common in sandstone units. Around the syncline, the succession contains interbedded siliceous and friable sandstone with interbeds of thinly bedded and laminated siltstone and mudstone. The sandstone units generally range in thickness from 20–300 mm, but beds up to 600 mm thick were measured. The thicker units commonly contain cross-bedding. The friable sandstone units are commonly fossiliferous and have formed by the leaching of calcareous sandstone beds. In places (e.g. Merton Hill [CP675797], fig. 1; and at the northern end of the syncline, around CP681921 and CP703891) the lowermost sandstone beds contain disseminated, black, semi-rounded chromite grains. The conglomerate interbeds are well exposed in a roadside quarry [CP695785] and range in grain size up to fine pebble grade.

A number of fossil locations were found within the area mapped as Crotty Formation. The two thickest localities are in a quarry at the 35·9 km mark on the LPD road [CP696785] where abundant, very large and coarse-ribbed *Rostricellula synchoneua* (Gill) and up to 30 mm diameter crinoid ossicles were found (location 5, Appendix 3); and at CP703891, on the north-eastern flank of the syncline (fig. 1, part 1) where *R. synchoneua* and crinoid ossicles were also abundant.

An Early Silurian (Llandoverian) age is probable for this fauna (Appendix 3) and the fauna is a correlate of the one within the Crotty Formation in the Zeehan area (Gill and Banks, 1950) and probably equivalent to the Gell Formation in the Tiger Range area of the Florentine Valley (Baillie, 1979).

Amber, Keel and Austral Creek Formation correlates (Sa, Sal, Sas)

From a combination of three sections around the Huskisson Syncline, one across the nose of the syncline along the LPD road, and two on the eastern side of the syncline in the Huskisson River [around CP700834] and in John Lynch Creek [around CP703824], an average thickness of the different sequences within the Amber Formation correlate (Sa) was obtained. This correlate is 100 m thick, followed by 75–100 m of a limestone sequence (Sal), then 25 m of Sa, 75–100 m of a dominantly quartz sandstone (Sas), and then another 100–150 m of Sa.

Lithologically, the areas of Sa are usually well-bedded and laminated, grey-green siltstone and mudstone with minor, 50–300 mm thick, cross-bedded sandstone units with siltstone partings. The limestone sequence (Sal) contains highly fossiliferous, well-bedded blue-grey carbonate with laminated black mudstone, as well as units of clastic limestone. In some areas this sequence has an alternating lithology of highly calcareous siltstone with limestone lenses. The lithostratigraphic correlate of the Keel Formation (Sas) consists of well-bedded friable (leached) and siliceous sandstone. Flaggy bedding is common, as well as multiple cross-bedding. Thinly-bedded siliceous sandstone units, up to five millimetres thick, with green micaceous mudstone partings are commonly bioturbated.

Along the LPD road's transect of the southern nose of the Huskisson Syncline, faunas were obtained from four locations within a succession of siltstone, calcareous siltstone and minor sandstone. The faunas are biostratigraphic correlates of the Amber Formation in the Zeehan area. Lithologically, locations 1 and 4 (Appendix 3) correlate with the Amber Formation , whereas locations 2 and 3 occur in a calcareous siltstone–impure limestone sequence which overlies a 50–150 m thick dominantly siliceous sandstone sequence (Sas). The sandstone sequence would, on lithological criteria and stratigraphic position, be correlated with the Keel Formation, making the overlying sequence a stratigraphic correlate of the Austral Creek Formation. On the available biostratigraphic evidence, no age difference can be determined between the faunas from locations 1 and 4 and those from locations 2 and 3.

The correlate successions within the Huskisson Syncline are highly fossiliferous when compared with the Zeehan type area of the Amber–Keel–Austral Creek Formations (Gill and Banks, 1950; Blissett, 1962) (fig. 20). Assemblage 1 (Appendix 3) was obtained from a road cutting at the 40·5 km mark on the LPD road [CP729792] and contains: *Leptostrophia* sp., parvicostellate form, very common; the rhynchonellid? *Ancillotoechia* sp., common; *Tentaculites* sp., very common; *Cornulites* sp.; smooth ostracods, and trilobite fragments. Location 4 (LPD 37·4 km, CP702784) contained: *Ancillotoechia* sp. or *Stegerhynchus* sp., very common; *Leptostrophia* sp., very common; *Tentaculites* sp., very common; *Actinopteria* sp., and rare loxonemids. Both of these localities have a stratigraphic position within Sa, below Sal (location 4), and below Sas with Sal being represented in this area by calcareous siltstone.

Locations 2 and 3 are both above Sas in what stratigraphically is a correlate of the Austral Creek Formation. At location 2 (LPD 38·5 km, CP714784) are: *?Ancillotoechia* sp. or *Stegerhynchus* sp., very common; cf. *Delthyris* sp.; *Leptostrophia* sp., common; *Nucleospira* sp.; *Encrinurus* sp., very common; *Trimerus (Trimerus)* sp.; *Tentaculites* sp., very common; smooth ostracods; *Actinopteria* sp.; cf. *Grammysia* sp.; crinoid debris and fragments of colonies of favositids and heliotids. From location 3 (LPD 37·9 km, CP708783): *Atrypa* sp., a very large species; *?Ancillotoechia* sp. or *Stegerhynchus* sp.; *Leptostrophia* sp. (a parvicostellate form), very common; *Encrinurus* sp.; *Tentaculites* sp., very common; *Gillatia* sp.; and other ostracods, and rare michelinoceratids and loxonemids.

The Keel Formation in the Zeehan area is poorly fossiliferous, but Banks (1962*a*) considered that it was possibly of Upper Wenlock or Lower Ludlow Stage. Clarke (Appendix 3) considers that the faunas above and below the Keel Formation correlate are of Middle Silurian (Wenlock) age, making the Keel Formation correlate in the Huskisson Formation the same age.

The limestone member of the Amber Formation (Sal) is also considered as Middle Wenlock due to the same faunal control. This succession also contains the first recorded occurrence of *Geisonocerous* sp. described from Tasmania (Brown and Stait, 1983). Within the limestone member on the eastern side of the syncline in the Huskisson River [around CP700833], a highly fossiliferous part of the succession contains a fauna which included dasyclad algae, tabulate and rugose corals, bryozoa, brachiopods, bivalves, gastropods and echinoderms (Appendix 2). The rugose corals may include *Tryplasma lonsdalei* Etheridge and *Stereoxylodes* sp. close to *S. multicarinatus* McLean. Tabulate corals include a favositid, probably *Pachypora*, and *Syringopora* sp.. Banks and Burrett (Appendix 2) consider that the corals are consistent with a Middle Silurian age.

Banks (1957) recorded a thin lenticular limestone sequence at the same stratigraphic level in the Queenstown area. It contains numerous fossils including crinoid columnals, colonial corals including favositids, syringoporids and staureaceans; brachiopods including rhynchonellids, and *Tentaculites*. The limestone (Sal) in the Huskisson River is between 60 m and 80 m thick and occurs over at least four kilometres along the southern and south-western part of the Huskisson Syncline, and probably continues underneath the syncline to the eastern side where it crops out in the Huskisson River around CP700834. The succession may consist of separate lenses, but due to the thickness and strike length along the southern edge of the syncline, it is highly probable that the original area covered was at least twenty square kilometres.

Along the Huskisson River, around CP703786 and to the north around CP703822, Taylor (1954) mapped a " . . . band of shale occurring between the Keel and Florence Formations" and considered that " . . . this band is a persistent formation of the Eldon Group and for it the name Hill Shale is proposed". Blissett (1962), although recognising that Taylor had defined a formation between the Keel and Florence Formations, proceeded to define the same stratigraphic succession in the Zeehan type section of Gill and Banks (1950), which he called the Austral Creek Formation. Although Taylor's 'Hill Formation' has historical precedence, it is relatively unknown within geological literature whereas the term Austral Creek Formation is now well entrenched.

Along the LPD road section, within the section from which Taylor defined the 'Hill Shale', occur fossil locations 2 and 3 of Clarke and Brown (1980). Due to the similarity of faunas at locations 1 and 4 and those at locations 2 and 3, the Austral Creek Formation correlate in the Huskisson area must be considered to be the same age as the Amber Formation correlate, which is Wenlock, and not Early Ludlovian (Banks, 1962*a*) or Late Ludlovian or Devonian (Blissett, 1962). Another implication of the biostratigraphy of the successions between the Crotty and Florence Formation correlates in the Huskisson River section is that the limestone (Sal) and dominantly quartz sandstone (Sas, Keel Formation lithostratigraphic correlate) are also of a similar age and are in fact only members of the Amber Formation and not really formations in their own right.

Florence Formation correlate (Df)

The correlate of the Florence Formation within the Huskisson area consists of well-bedded, fossiliferous, siliceous and friable quartz sandstone interbedded with minor laminated siltstone. The friable units are leached and highly fossiliferous. Both the siliceous and friable beds can contain cross-bedding. Throughout the succession occur zones of interbedded and bioturbated, laminated siltstone (up to 100 mm thick) and interbedded muddy sandstone beds between 100 mm and 300 mm thick. Platy bedding, scour marks and multiple ripple-marked horizons are common through the succession. The maximum thickness found around the Huskisson Syncline is 373 m [CP704817], with the average thickness being between 300 m and 350 m. This thickness compares with approximately 500 m in the type area (Gill and Banks, 1950).

Two typical sections through the Florence Formation correlate occur in the Huskisson River between CP750818 and CP702815, and to the east of Merton Hill around CP681797. They contain a succession of white to grey siliceous and friable (leached) sandstone with abundant fossils. The fauna includes the coarse-ribbed

brachiopod *Notoconchidium florencensis* (Gill, 1950), as well as smaller brachiopods and crinoid columns. The faunas obtained from the above two areas, and the lithological character and stratigraphic position of the succession, allows it to be correlated with the Florence Formation in the Zeehan area (Gill and Banks, 1950) and for it to be considered as having the same Lower Devonian age.

Blissett and Gulline (1962) mapped a small pinnacle as 'Permian tillite' at CP750685. On re-mapping this area the only material found was a white friable sandstone with the brachiopod *Notoconchidium*. Based on the lithology and fauna, the only material found belongs with the Florence Formation. Due to the nature of the outcrop and the thick vegetation, the contact relationship with the underlying Huskisson Group rocks could not be established. This outcrop may represent a large, glacial erratic (Qg), or may possibly be a remnant of Florence Formation sandstone which unconformably overlies the Huskisson Group succession.

Bell Formation correlate (Db)

With a fairly sharp but gradational contact, the lithology changes from the white sandstone of the Florence Formation into 950+ m of interbedded dark grey siliceous siltstone with mudstone lamellae, bioturbated muddy sandstone and siltstone, and minor sandstone.

The succession also contains multiple ripple-marked horizons, scours and bulbous bases in the sandstone units, cross-laminated and thinly bedded, often micaceous sandstone with platy partings, and siltstone units 2–5 mm thick with convolute slumping. Overall the sequence is similar to that described by Gill and Banks (1950) from the Zeehan area and Baillie and Williams (1975) from the Strahan area. A good section through the gradation from the Florence to the Bell Formation correlates is exposed in the Huskisson River around CP705818.

Numerous fossil localities occur along the Huskisson River section through the syncline, but two representative faunas were collected from highly fossiliferous units on either side of the syncline axis at CP701800 and CP695798. Although slightly different lithologies occur at the two locations, the fauna collected from each site was almost identical. The faunas include numerous *Pleurodictyum megastomum* and favositiids, numerous trilobite fragments which include *Dalmanites* and *Gravicalymene*, the brachiopods *Isorthis* and *Eospirifer parahentius*, bryozoan and crinoid debris, and ostracods (M.J.Clarke, pers. comm., 1984).

Undifferentiated Eldon Group correlates (S-Du)

The area designated as S-Du on the north-western side of the Huskisson Syncline (fig. 1) is due to this area not being mapped. Photo-interpretation of the formations from the south does not correspond to a similar interpretation from the north. The preferred interpretation is a continuation of the Florence Formation from the south with the SSE plunging syncline–anticline system in the Crotty Formation to the north continuing into the centre of the Huskisson Syncline. The ridge between CP665875 and CP675895 would then be of Bell Formation, with the ridge possibly being formed due to an anticlinal structure produced by high level granitic intrusion.

STRUCTURE

Devonian deformation of the Silurian-Devonian rocks which form the Huskisson Syncline is ambiguous due to the lack of cleavage relationship around the syncline. Two possible explanations are possible given the available data. The deformation is either the result of the interference of the earlier northerly fold phase, or the deformed syncline was formed during one fold phase with the irregularities being due to the underlying rock formations. The preferred explanation is the interference of the effects of two fold phases, as this is consistent with the cleavages obtained from the only outcrop with both northerly and north-westerly cleavage, and is also consistent with evidence obtained from the Eocambrian–Cambrian rock succession in the surrounding area.

Quaternary

GLACIAL AND RELATED DEPOSITS (Qg)

Quaternary glacial outwash deposits of conglomerate, sand and silt are common throughout the mapped area. The deposits are usally covered with one to two metres of well-washed gravel dominated by quartzite and Owen Conglomerate pebbles and boulders. Within the outwash conglomerate units are pebble to boulder grade clasts of pink and white quartzite, vein quartz, Owen Conglomerate, and volcanic rocks from the Mt Read volcanic belt. Clasts of gabbro are found in the deposits in the area around CP725705. Pebbly sandstone and cross-bedded sandstone beds are common in the sand and silt units. Areas of varves, some with intraformation slumps, crop out along the LPD road near the 39·3 km mark.

ALLUVIUM (Qra)

All post-glacial deposits, including river gravel, reworked glacial deposits, talus and scree, swamps, and man-made tailing dumps have been mapped under Qra.

IGNEOUS ROCKS

Tertiary basalt (Tb)

Remnant areas of what was most probably once a continuous plateau of Tertiary basalt occur across an area from north-west of Nineteen Mile Creek (fig. 2), east to the Magnet Range (fig. 2) and the south-west margin of the Burnie–Waratah basalt field (fig. 1 and 2), and south to Lynch Hill (fig. 1) [CP731826].

The thickness of individual flows ranges from less than one metre, usually of highly vesicular basalt, to greater than ten metres, usually with columnar jointing. A well-exposed section through the basaltic sequence showing flow thickness variations, textural variations and interbedded sediments occurs along the Ramsay River between CQ732003 and CP736999 (fig. 1). Similar variations and thicknesses were also recorded in sections of bore holes drilled through the Burnie–Waratah Tertiary basalt field to the east of Waratah in the St Valentines Quadrangle (Brown and Forsyth, 1984).

The pre-basalt topography varied across the mapped area, but was not as varied as present day topography. On the western side (fig. 2) the pre-basalt surface was in the order of ±100 m around 400 m (above present sea level), while on the eastern side the surface was approximately ±100 m around 500 m (apsl). Areas of Precambrian successions had a more rugged topographic expression than areas of Cambrian successions. The height of the pre-basalt surface to the east of Waratah is fairly consistent with that in the mapped area, being approximately 350–450 m (apsl) in the bore holes.

Information from bore hole samples suggests that there is a general gradation from basal alkali-olivine basalt up into olivine-bearing tholeiitic basalt (Brown and Forsyth, 1984). The alkali-olivine basalt flows occur between a lower zone of pre-basalt sediment containing a microflora of late Eocene to early Oligocene age, and a zone, up to 50 m thick, of lacustrine sediments and basalt interflows which contains a microflora of early Oligocene age, indicating an age for the alkali-olivine basalt flows of 35–40 Ma. The lower basalts in the bore hole sequences are petrographically and chemically similar to those found in the remnant areas shown on Figures 1 and 2.

The southernmost residual area of Tertiary basalt caps Lynch Hill [CP731826]. This outlier is an olivine-phyric basalt which overlies successions belonging to the Crimson Creek Formation at a height of 370 metres. Basal flows of the basalt field north of Mt Ramsay (fig. 1, around CP723999) and on the Waratah–Savage River road (fig. 2, CQ739061) are also alkali-olivine basalt. In thin section, some of these samples (85-0041, 85-0042) contain large olivine phenocrysts (2·0–2·5 mm) which have reacted with the magma producing embayed and skeletal crystals. All the samples (85-0040, 85-0041, 85-0042 and 78-440) also contain smaller olivine phenocrysts (1–2 mm) which have not reacted with the enclosing magma and contain numerous euhedral black opaque grains (approximately 0·02 mm diameter) disseminated throughout. One of the samples (85-0040) from this area also contains microphenocrysts of plagioclase (0·7–1·0 mm in length). The groundmass is usually partially flow-orientated interlocking feldspar laths, the interstices of which are filled with anhedral titaniferous-augite, black skeletal opaque grains (Fe-Ti oxide) and black glass.

Samples from the area covered by the western side of Figure 2 (85-0043, 85-0044, 85-0047) are alkali-olivine basalt, but with a far wider range of textures. This range appears to be gradational, with the groundmass to the olivine phenocrysts being either flow orientated, intergranular, or sub-ophitic. A similar range in texture is also found in the bore hole samples obtained from the succession of flows to the east in the St Valentines Quadrangle.

The size and proportion of the olivine phenocrysts within flow-orientated groundmass differs between samples, but ranges from 0·9 to 3·3 mm with a mean around 1·8 mm. The larger phenocrysts (2·5–3·3 mm) have usually reacted with the magma, producing embayed and skeletal crystals. Most of the olivine phenocrysts contain disseminated small (0·005–0·02 mm) euhedral black opaque mineral grains. The groundmass consists of flow-orientated plagioclase laths (0·25–0·75 mm), having symmetric twin extinction suggesting a composition of labradorite, skeletal to elongate subhedral black opaque grains up to 2·0 mm in length, and pale purple titaniferous grains (0·05–0·15 mm).

In samples with an intergranular groundmass, plagioclase (labradorite) crystals and laths form an interlocking texture, the interstices of which are filled with titaniferous augite and black opaque mineral grains. The samples with sub-ophitic texture contain a groundmass dominated by large (up to 2·5 mm long) titansalite grains partially enclosing plagioclase laths and euhedral opaque grains. Euhedral olivine grains are between 0·5 mm and 0·75 mm long but an occasional large (3 mm) skeletal grain occurs. Plagioclase laths range between 0·5 mm and 0·8 mm in length with euhedral opaque grains being approximately 0·1 mm across and acicular opaque grains up to 0·5 mm long.

CHEMISTRY

Analyses of five basalt samples selected from remnant areas covered by Figure 2, with their CIPW and Rittmann norm values, are presented in Table 1 (analyses 1–5). All tables of chemical analyses and electron microprobe analyses are placed in Appendix 4. Also presented (table 1, analyses 6–8) are the analyses of three alkali-olivine basalt samples from the drill hole successions to the east of Waratah.

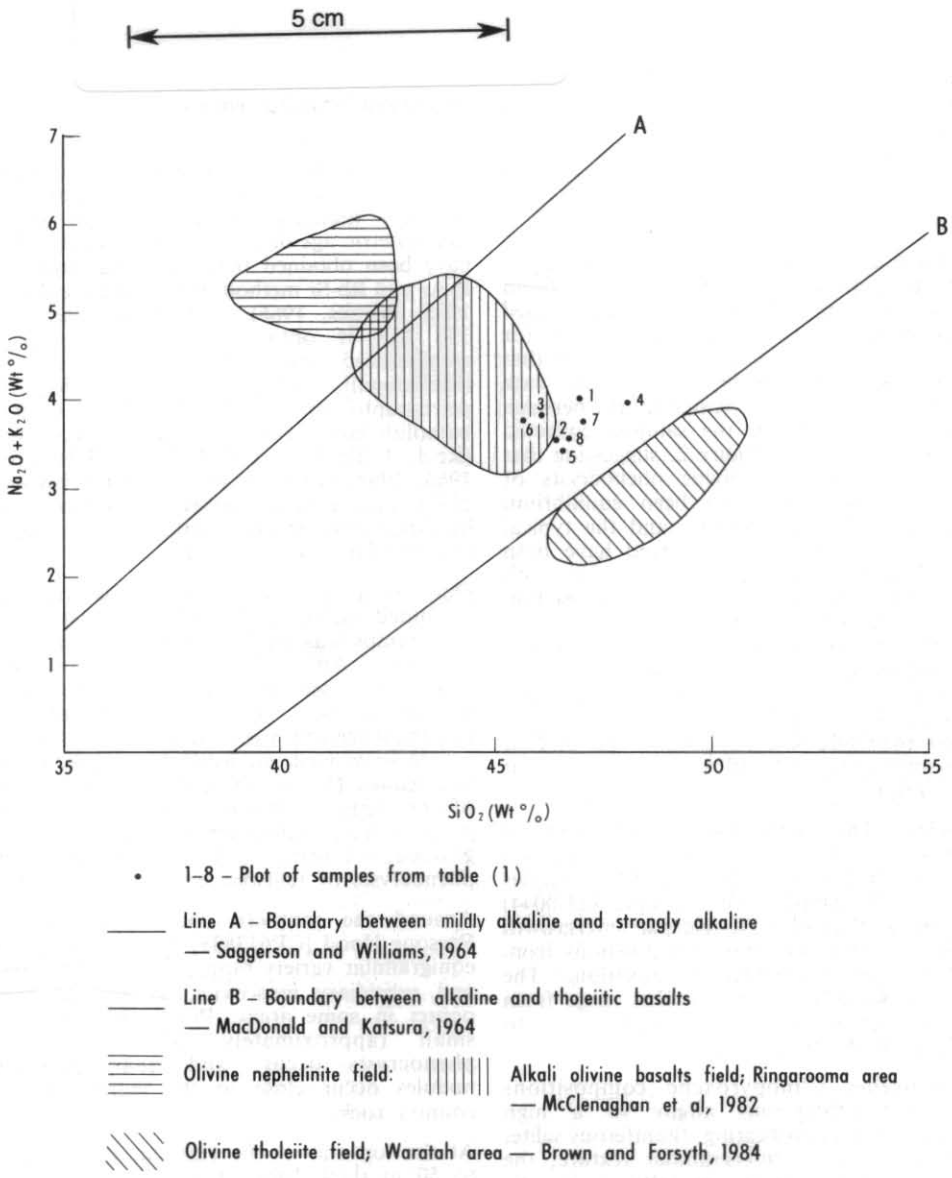

Figure 21. *Alkali-silica diagram, Tertiary basalt.*

Using the MacDonald and Katsura (1964) dividing line for alkali and tholeiitic basalt, Figure 21 shows that all samples obtained from the remnant areas have alkaline affinities, and that the three basalts analysed from the lowermost flows of the bore hole intersections east of Waratah have a similar chemistry. Included in Figure 21 is the field containing the other sixteen samples analysed from the bore hole successions; all of these samples have a tholeiitic nature.

Figure 21 also shows that the most alkaline of the alkali-olivine basalts from the mapped area correspond with the least alkaline of the alkali-olivine basalts from the younger basalt field of the Ringarooma-Derby area of north-east Tasmania.

MINERAL CHEMISTRY

Analyses of the mineral constituents from the three main textural types which occur across Figure 2, as well as all other mineral analyses, were obtained using the JEOL JX50A electron microprobe scanning electron microscope fitted with an energy dispersive analysing system consisting of a PGT energy dispersive detector with an Ortec EEDS II analysing system (MRC), at the Central Science Laboratory, University of Tasmania. Results for Tertiary basalt are given in Table 2.

Olivine: The olivine phenocrysts which do not show a reaction relationship with the enclosing basalt range between Fo_{81} and Fo_{77} (table 2, analyses 3–7) in all samples, and the groundmass

olivine ranges between Fo_{72} and Fo_{66} (table 2, analyses 8–11). One sample (85-0047) has an olivine phenocryst of Fo_{85} (table 2, analysis 1) and another (85-0045) has a skeletal grain of Fo_{90} (table 2, analysis 2) with evidence of resorption.

Calculation of theoretical olivine compositions, and the temperature at which olivine will begin to crystallise at one atmosphere pressure (based on Roeder and Emslie, 1970) were made for the samples analysed, with the assumption that all Fe_2O_3 and FeO was liquid FeO. The data gives olivine of Fo_{84-85} at temperatures between 1230°C and 1290°C for the samples collected from areas covered by Figure 2, suggesting that the minor amount of olivine phenocrysts of Fo_{84-85} were likely to have been equilibrium olivine rather than xenocrysts, and the typical olivine phenocryst of Fo_{81-77} would have been produced under conditions of equilibrium with the magma. The olivine grains with reaction characteristics and a composition of Fo_{89-90} were xenocrysts which probably crystallised in the source region, and were out of equilibrium with the magma at the time of crystallisation under surface conditions. Samples from the bore hole sequence (85-0049, 85-0050) gave olivine of Fo_{84} at a temperature of 1250°C, and of Fo_{85} at 1285°C respectively.

Plagioclase: The composition of the unaltered plagioclase is typically labradorite (Ca:Na:K = 60:37:3 to 58:39:3) (table 2, analyses 15–17) in all samples. One sample (85-0044) contained a plagioclase/K-feldspar intergrowth as well as various alteration compositions from labradorite to an albite composition. The plagioclase/K-feldspar compositions range from (Ca:Na:K = 28:64:8) through to (Ca:Na:K = 8:56:37).

Clinopyroxene: Clinopyroxene compositions range from titaniferous augite to a high aluminous, chromium-bearing, titaniferous salite. In samples with an intergranular texture, the anhedral clinopyroxene crystallised in the interstices is a titaniferous augite (Ca:Mg:Fe = 42:40:18) (table 2, analysis 14) with approximately 1·5 wt% TiO_2. Large purple groundmass clinopyroxenes in the sub-ophitic textured rocks are high aluminous, chromium-bearing, titaniferous salite (Ca:Mg:Fe = 47:38:15) (table 2, analysis 12). These crystals have an average of 4·85 wt% Al_2O_3; 2·27 wt% TiO_2; and 0·48 wt% Cr_2O_3. Clinopyroxene glomeroporphs with a similar composition to these (Ca:Mg:Fe = 50:33:17) and approximately 6 wt% Al_2O_3, 2 wt% TiO_2, and 0·5 wt% Cr_2O_3, occur in some of the alkali-olivine basalt flows from the Ringarooma–Derby area (McClenaghan *et al.*, 1982).

Opaque mineral: The opaque mineral grains differ in the relative amount of titanium to iron content, but are usually titaniferous magnetite, with an average composition of $(Fe^{2+}_{1\cdot6611}, Mn_{0\cdot02}, Mg_{0\cdot0804}, Fe^{3+}_{0\cdot4141}, Al_{0\cdot0627}, Ti_{0\cdot7617})_3O_4$.

Devonian granitic rocks (Dg)

The area shown as Dg on the northern margin of Figure 1 and along the southern margin of Figure 2 represents the southern, eastern and northern margins of the Meredith Granite. Radiometric age dates of approximately 350 Ma have been obtained from this body using both K-Ar and Rb-Sr methods (McDougall and Leggo, 1965; Brooks, 1966). A K-Ar (biotite) age of 356 Ma is obtained when the data are recalculated using the revised standards (McDougall, pers. comm., 1983) The petrography and chemistry of parts of the batholith have been described by many writers (Reid, 1923; Jack and Groves, 1965; Groves, 1966, 1968; Stockley, 1972; and Groves *et al.*, 1973), and a recent review of previous work, including new chemical data, can be found in Collins (1983; p. 107–115).

Only the outer margins of the batholith were examined during mapping for this study, and no attempt was made to map out the internal structures. Although many textural variations exist, two dominant rock types were observed. In the southern part of the batholith, the dominant textural variation is a medium-grained to coarse-grained, equigranular, biotite granite/adamellite. In the northern and eastern parts of the batholith the dominant rock type is a porphyritic, medium-grained to very coarse-grained, biotite granite/adamellite with phenocrysts of feldspar up to 25 mm long.

Around the southern and eastern edges of Parsons Hood [CP613838] the grain size of the equigranular variety ranges from fine to coarse, and subsidiary muscovite, as well as biotite, occurs in some areas. Porphyritic zones with small (approximately 10 mm) feldspar phenocrysts occur, and quartz-tourmaline nodules occur close to the margin with the country rock.

At the top end of the Harman River, a 30 m to 50 m thick zone of cryptocrystalline chert with chromite grains represents the replacement of serpentinised ultramafic rocks. This replacement zone is then separated from a coarse-grained equigranular granite/adamellite by a 20 m to 30 m wide zone of massive quartz-tourmaline.

The main textural variety in the upper reaches of the Wilson River is a medium-grained to coarse-grained equigranular biotite granite adamellite with porphyritic zones. The phenocrysts are small feldspar crystals (up to 10 mm in length). Numerous late-stage dykes and veins of aplite and quartz-tourmaline cut the granitoids in this area.

At the northern end of the Huskisson Syncline, along a creek section between CP681922 and CP681925, a large textural variation occurs over a short distance. The grain size ranges from fine to very coarse, and the rock type ranges between equigranular and porphyritic with

phenocrysts of either feldspar (10–20 mm) or both feldspar and rounded or square quartz grains (up to 5 mm). Pegmatitic patches of quartz, feldspar, or biotite and quartz-tourmaline also occur. Near the contact of the granitoid with quartzite of the Crotty Formation [CP681922], numerous xenoliths (up to 100 mm long) of biotite-rich material, as well as pegmatitic patches and stringers of biotite, can be observed.

Along the margin of the batholith to the north and west of Mt Ramsay [CP708949], the dominant textural variation is porphyritic biotite granite/adamellite, with quartz and feldspar phenocrysts. The grain size ranges from medium-grained to coarse-grained and late stage quartz-tourmaline veins are common. Although textural variations exist, they are not as rapid, nor as common as in the southern part of the batholith.

An area of fine-grained to medium-grained equigranular biotite granite/adamellite is exposed along the Waratah–Savage River road [around CQ727058]. Five hundred metres to the west of this equigranular patch, quartz porphyry and quartz tourmaline dykes cut porphyritic biotite granite/adamellite along the old South Bischoff track. The phenocrysts are both feldspar and quartz.

In the Mt Stewart area, a marginal zone of quartz-feldspar porphyry occurs near the ultramafic rocks in the Castray River, but the dominant variation in this area is a medium-grained to coarse-grained porphyritic biotite granite/adamellite with feldspar phenocrysts. One unusual textural variety, a 'schistose' granitoid with a strong biotite foliation, is exposed along the Mt Youngbuck track around CQ587012. Numerous late-stage quartz tourmaline and quartz phyric aplitic dykes cut the granitoid in this area. Veins of quartz tourmaline also intrude the ultramafic rocks in the southern part of the Mt Stewart body.

Two small bodies of highly weathered granitic rocks were mapped along the northern side of Mt Bell around CQ625061 and CQ629056. Small dykes of fine-grained to medium-grained equigranular, biotite granite adamellite intrude the area of dominantly high-magnesian andesite around CQ670035.

MASSIVE QUARTZ BODIES (Dgq)

Numerous knolls of massive red, white and milky quartz, veined with later white quartz, occur to the south and west of Melba Flats (fig. 1) [CP672666]. These knolls appear to be associated with major fault lines and are possibly associated 'with the Devonian granitoid intrusions. Similar bodies were also found along fault boundaries in the McLean Creek area [CP585579] to the south-west of Zeehan.

Eocambrian–Cambrian

GABBRO (€g)

Gabbroic rocks intrude many different rock sequences as dykes, sills and stocks within the entire mapped area. The term gabbro has been used for any igneous rock with a grain size greater than 0·5 mm and consisting of plagioclase and pyroxene with or without an opaque mineral phase. Two distinctive groups of gabbro have been recognised and samples from at least one other, and possibly more groups, have been obtained. The two distinctive groups can be recognised by field and petrographic or chemical characteristics.

The oldest recognised phase of gabbroic rock formation in the study area was probably associated with the tholeiitic volcanism of the Crimson Creek Formation. Samples of this phase are only found within areas of the Crimson Creek Formation. The second group of gabbroic rocks is associated with the Serpentine Hill Ultramafic Complex and examples occur across a zone from Serpentine Hill *via* Confidence Saddle and the Ring River area to Colebrook Hill. This phase of gabbroic activity is also considered to have formed the McIvor Hill Gabbro (fig. 42, area 9). The third general group of gabbroic rocks include types which are relatively enriched in plagioclase with respect to ferromagnesian minerals, and which intrude the fossiliferous Cambrian sequences (Dundas Group and correlates). The source of this group of gabbroic rocks is not known and the chemistry of samples collected overlaps that of the earlier two phases. A number of gabbroic samples could not be assigned to any specific phase.

GROUP 1 GABBRO

These gabbroic rocks intrude the Crimson Creek Formation. Chemical analyses of twelve samples from various areas are given in Table 3 (analyses 1–12). In general they contain >0·2 wt% TiO_2; >2·0 wt% alkalis ($Na_2O = K_2O$); and have Zr and Y contents >10 ppm. In thin section, the samples are characterised by clinopyroxene and an opaque mineral phase which forms a graphic intergrowth with the clinopyroxene. Fine-grained samples have mineral grains between 0·5 mm and 1·0 mm, medium-grained samples between 1·0 mm and 2·0 mm, coarse-grained samples 2 mm and 4 mm, and very coarse to pegmatitic samples >5 mm. Most of the bodies have chilled margins and the texture and chemistry of samples changes rapidly across any specific body. Samples are usually altered such that the plagioclase is now albite, with the most calcic plagioclase obtained by electron probe analyses being andesine ($An_{36·7}$) (table 4, analyses 9–10). The clinopyroxene grains were originally calcic augite (table 4, analyses 1–3), and their analyses fall on the trend defined by pyroxene grains from basaltic samples from within the Crimson Creek Formation (fig. 24). In the majority of samples

the ferromagnesian minerals have been altered to amphibole group minerals, and plagioclase ranges from andesine to labradorite (table 4, analyses 9–10).

GROUP 2 GABBRO

Gabbroic rocks in group 2 are predominantly intrusive within ultramafic rocks in the Serpentine Hill–Ring River area, and are considered to constitute the gabbroic body on the western side of Colebrook Hill (fig. 1), and the McIvor Hill Gabbro (fig. 42, area 9). This group (table 3, analyses 13–23) has a relatively depleted chemistry in comparison with group 1 gabbro. The rocks contain < 0·2 wt% TiO_2; < 2·0 wt% $Na_2O + K_2O$, and their Zr and Y contents are usually below detection limit (4 ppm), but can be up to 10 ppm.

The main hand specimen characteristic of this group is that it is a two-pyroxene gabbro and does not contain an opaque mineral phase. In thin section, the texture ranges from a fine-grained granular mosaic, through medium-grained and coarse-grained granular mosaics, to pegmatitic. Some of the coarser-grained samples (3–4 mm) have stubby plagioclase grains in an interlocking texture with anhedral clinopyroxene.

The coexisting pyroxene phases are a low-calcic magnesian pigeonite and a magnesian salite (table 5, analyses 1–6). The plagioclase is anorthositic bytownite (table 5, analyses 7–10).

GROUP 3 GABBRO

Analyses of samples of gabbroic rocks which cannot be placed in either of the first two groups are given in Table 3 (analyses 24–33), together with analyses of two basaltic samples intruded by one of the gabbroic bodies (analyses 34–35). Analyses 24–27 are of samples which intrude the ultramafic rocks of the upper Harman River area and are probably associated with the Middle Cambrian low-titanium basaltic phase (Ꞓbm), bodies of which intrude the ultramafic rocks of this area and form elongate bodies (dykes?) with a general strike to 060 degrees.

Samples of these gabbroic rocks are plagioclase-rich and have a graphic intergrowth of the opaque mineral phase with the ferromagnesian minerals, similar to coarse-grained parts of thick flows of Ꞓbm in both the Black Hill and Heazlewood River areas. In comparison with samples from Group 1 with a similar texture, these samples have a depleted chemistry.

Similarly textured but chemically varied samples to those which intrude the ultramafic rocks in the Harman River area also intrude rocks of the Huskisson Group in the Pieman River (table 3, analyses 29–32) and the Colebrook Hill ultramafic body (table 3, analysis 28). The pyroxene phase is now altered to amphibole (table 4, analyses 7–8). The stratigraphic setting of these samples makes them younger than Ꞓbm and they must represent another phase of gabbroic formation.

Another source of gabbroic rocks would be intrusive magmas associated with basaltic phases within the Mt Read volcanic belt. In the south-eastern corner of the Zeehan Quadrangle, a gabbroic body (table 3, analysis 33) intrudes a basaltic sequence which is interbedded with fossiliferous Cambrian sedimentary rocks containing detritus from an acid to intermediate volcanic source. A sample of a pyroxene basalt (table 3, analysis 34) and a feldspathic andesite (table 3, analysis 35) were collected, together with a sample of the gabbro. Neither the texture nor the chemical analysis of the gabbro are characteristic enough to correlate this sample with other samples from group 3. The clinopyroxene phase (table 4, analysis 5) is chrome-bearing diopside. An analysis of the pyroxene phenocryst phase in the pyroxene basalt is given in Table 4 (analysis 6) and plotted on Figure 22. A description of the regional geology of this area can be found in Corbett (1984).

TONALITE (Ꞓt)

A large area of tonalitic rocks in faulted contact with the north-eastern margin of the Heazlewood River Ultramafic Complex (fig. 2) has been mapped by Rubenach (1973) and Creenaune (1980). Rocks belonging to the tonalitic suite intrude the high-magnesian andesite in the area around CQ580060, the ultramafic rocks (the body at CQ560069 having a chilled western margin against the ultramafic rocks), and the low-titanium tholeiite. Of the three bodies of tonalitic rocks associated with the low-titanium lavas, one is faulted [CQ620107], one has an ambiguous contact (eastern margin of the body at CQ560069), and one, by the physical shape of the body, probably indicates an intrusive relationship [CQ621076]. A zircon age of 520 Ma for the tonalitic body around CQ581056 has been obtained (Kimbrough and Brown, in prep.). This is in agreement with all field evidence, and agrees with the age, based on fossiliferous evidence, of the low-titanium lavas. On the above evidence, an Early Cambrian age for the extrusion of the high-magnesian andesite is highly probable, suggesting that the Crimson Creek Formation is latest Precambrian (i.e. Eocambrian) which is consistent with it conformably overlying the Success Creek Group, the upper part of which contains brecciated samples of *Baicalia* cf. *B. burra*-like stromatolites.

BASALT SUCCESSIONS

INTRODUCTION

Three chemically and petrographically distinct basaltic sequences have been recognised within the mapped area. The three types can be recognised in the field by hand specimen characteristics and in the laboratory by chemical and petrographic criteria.

The oldest basaltic phase is part of the Eocambrian Crimson Creek Formation and correlates (Ecc), within which it forms discrete

lava fields (Eccb) as well as individual flows within the sedimentary sequence. The lavas were also the source of the majority of the material for the sand-grade sedimentary rocks within this formation. The second oldest succession belongs to a phase of high-magnesian andesite volcanism (Ꞓba). This succession consists of interlayered pillow lavas, hyaloclastite, breccia and thin tabular flows. The largest bodies of this succession occur in areas covered by Figure 2, but a small area of this very distinct rock type has also been mapped in the Stonehenge area to the west of Zeehan [around CP567594]. The youngest of the three basaltic events is a low-titanium tholeiite succession (Ꞓbm), which in the Black Hill area (fig. 1) interdigitates with a lower Dundas Group conglomerate sequence, the Red Lead Conglomerate (Ꞓdre). In an area to the west of Mt Cleveland (fig. 2) occurs a large fault-bounded block of this phase and in the area to the south of the Heazlewood Ultramafic Complex, the low-titanium tholeiite lavas have intruded and overlie an area of high-magnesian andesite.

The three basalt types can be distinguished by the use of many different chemical discriminant diagrams, but for simplicity, a geochemical pattern of trace elements was plotted for each type, and from these the elements with the greatest variation between types were picked as discriminants. In the following section, the field distribution and petrographic characteristics will be discussed for each type and then the chemistry of all three types will be compared and contrasted.

CRIMSON CREEK FORMATION THOLEIITES (Ecc and Eccb)

Basaltic rocks within the Crimson Creek Formation are usually pale to medium grey when fresh but have a purple to green tinge when altered. They are predominantly porphyritic, having black clinopyroxene and/or white plagioclase phenocrysts. A minor number of flows or parts of flows are aphyric. Thin flows (less than two metres thick) are usually tabular and occur interbedded with a dominance of sedimentary rocks. Thicker flows are found within areas which are mainly interbedded basalt flows (Eccb). The volcanic pile within areas of Eccb consists of tabular and pillow-structured flows interbedded with lapilli and crystal tuff units, volcanic breccia, and conglomerate flows and minor sedimentary rocks.

The proportion of basaltic to sedimentary rocks within the Crimson Creek Formation differs across the mapped area, but overall it increases from south to north. In the type area, only minor basaltic flows occur within a dominantly sedimentary rock succession, the predominant rock type being a volcaniclastic lithic wacke or greywacke, in the traditional German sense. Progressing north-west, towards Mt Lindsay, the proportion of basalt to sedimentary rock increases. To the south of Mt Lindsay the lowest basalt flow in this part of the succession is 50 m above the transitional base of the formation with the 'red rock' member of the Success Creek Group.

A similar situation exists along the eastern side of the Huskisson Syncline, the percentage of basaltic rock in the succession increasing to the north, until in the area around CQ725005 (fig. 1) the sequence is dominated by basalt (Eccb). Similar areas of Eccb occur to the south of Cleveland; to the north of the Heazlewood ultramafic body (fig. 2); and in the Arthur River area (fig. 3). The largest concentration of basalt occurs in the Cleveland area where, in the mine sequence, it is known as the 'Deep Creek Volcanics' (Collins, 1983).

Correlates of the Crimson Creek Formation to the north of the Meredith Granite (fig. 2 and 3) have in the past been referred to as the 'Arthur River Sequence' (Groves and Solomon, 1964; Groves, 1968); the 'Luina Beds' (Rubenach, 1973); or 'Deep Creek Volcanics–Hall Formation–Crescent Spur Sandstone' (Collins, 1983 *after* Cox, 1968; Cox and Glasson, 1971). These formations have also previously been correlated with the Crimson Creek Formation (Groves *et al.*, 1973; Williams, 1979).

The areas to the north of the Meredith Granite, depicted as Ecc and Eccb on Figures 2 and 3, are considered to have been a northern extension of a once continuous elongate band of active volcanism and associated sedimentation which conformably succeeded and overlaid the terrigenous successions of the Success Creek Group correlate. The Crimson Creek Formation and correlates can now confidently be followed from west of Melba Flats (fig. 1), south of the type area, along both sides of the Huskisson Syncline, north past Waratah, to an area dissected by the Hellyer River around CQ750750 (fig. 3; St Valentines Quadrangle).

It is recommended that the terms 'Arthur River Sequence' and 'Luina Beds' be discontinued and that 'Deep Creek Volcanics–Halls Formation–Crescent Spur Sandstone' be restricted in use to those sequences within the Cleveland mine area.

Mt Lindsay–Mt Ramsay area

The basalt flows in the Mt Lindsay and Mt Ramsay areas are characterised by plagioclase and/or black clinopyroxene phenocrysts and/or glomerocrysts. These occur in an intersertal groundmass which contains a relatively high percentage of iron-titanium oxide mineral. The groundmass clinopyroxene is typically altered to chlorite and/or actinolite, giving the rock a greenish tinge, with the purplish tinge of some samples being due to alteration of the iron-titanium minerals.

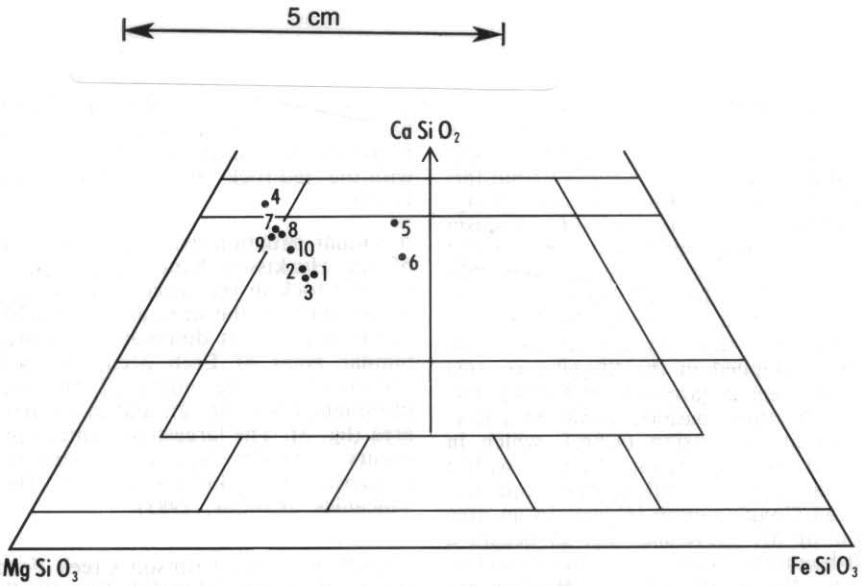

Figure 22. *Part of the pyroxene quadrilateral showing the composition of clinopyroxene from tholeiitic basalt within the Crimson Creek Formation. Plot numbers refer to analyses in Table 6 (Appendix 4).*

Petrographic variations between basalt samples from different areas within the Crimson Creek Formation are fairly small, the main variation being grain size and groundmass texture. Plagioclase and clinopyroxene phenocryst compositions have been determined by electron probe analysis, and representative analyses of clinopyroxene grains from within samples from the Mt Lindsay and Mt Ramsay areas are listed in Table 6. The compositions of the clinopyroxene phenocrysts are very similar within different flows from the same area (fig. 22), but differ in different areas according to the tholeiitic differentiation trend, with an indication that the samples from the Mt Ramsay area contain more primitive compositions than those from the Mt Lindsay area. Overall the clinopyroxene grains are a chromium-bearing augite. Electron probe analyses of plagioclase crystals ranged from labradorite to albite, the majority being albite.

Fine-grained samples contain plagioclase microphenocrysts (1 mm) in a groundmass of skeletal and acicular plagioclase and 0·1–0·2 mm anhedral clinopyroxene grains. Microglomeroporphyritic patches of 0·2 mm anhedral clinopyroxene and 0·5 mm subhedral plagioclase occur in some samples. In medium-grained samples, the plagioclase phenocrysts range between two and three millimetres in length, with microphenocrysts between 0·9 mm and 1·0 mm. The groundmass texture ranges from subophitic to ophitic with anhedral clinopyroxene being 0·5 mm in length, and plagioclase laths up to one millimetre. Magnetite is ubiquitous and chlorite the main alteration mineral of clinopyroxene. Actinolite replaces clinopyroxene in some samples.

In coarse-grained varieties, plagioclase phenocrysts up to four millimetres in length coexist with stubby one millimetre chromian augite microphenocrysts. The groundmass plagioclase formed as stubby subhedral grains up to 1·5 mm, which often form clusters with the grains parallel to each other along their C axis. The associated clinopyroxene ranges from subhedral to anhedral and from 0·4–0·7 mm in length, with 0·2–0·3 mm iron-titanium oxide grains as intersertal grains.

Some of the samples which contain large (3–4 mm) plagioclase phenocrysts have a groundmass consisting of grains between 0·15 mm and 0·35 mm of interlocking subhedral clinopyroxene, plagioclase laths and acicular magnetite. Numerous quench-textured flows occur within the succession. These usually consist of radiating acicular feldspar grains with the interstices filled with brown glass and 0·005 mm to 0·01 mm magnetite grains. Occasional plagioclase microphenocrysts occur in some samples.

Cleveland area

The 'Deep Creek Volcanics' are exposed over approximately 10 km² and are estimated to be between 400 m and 600 m thick (Collins, 1983). Due to the range of chemistry, it is considered that this volcanic pile represents the site of an eruption centre, possibly the major site within the Crimson Creek Formation. These volcanic rocks are described by Collins (1983) as being " . . . characterised by a predominance of mafic green, spilitic tholeiitic basalt with intercalated green to green-grey lithovitric and lapilli tuff, red-brown argillite and minor chert, mafic green volcaniclastic greywacke and red-brown volcaniclastic conglomerate."

Volcanic breccia and agglomerate have been described as being interbedded with the basaltic lava flows (Cox, 1968), but the true nature of these units is questioned by Collins (1983). Numerous pillow structures are also recorded.

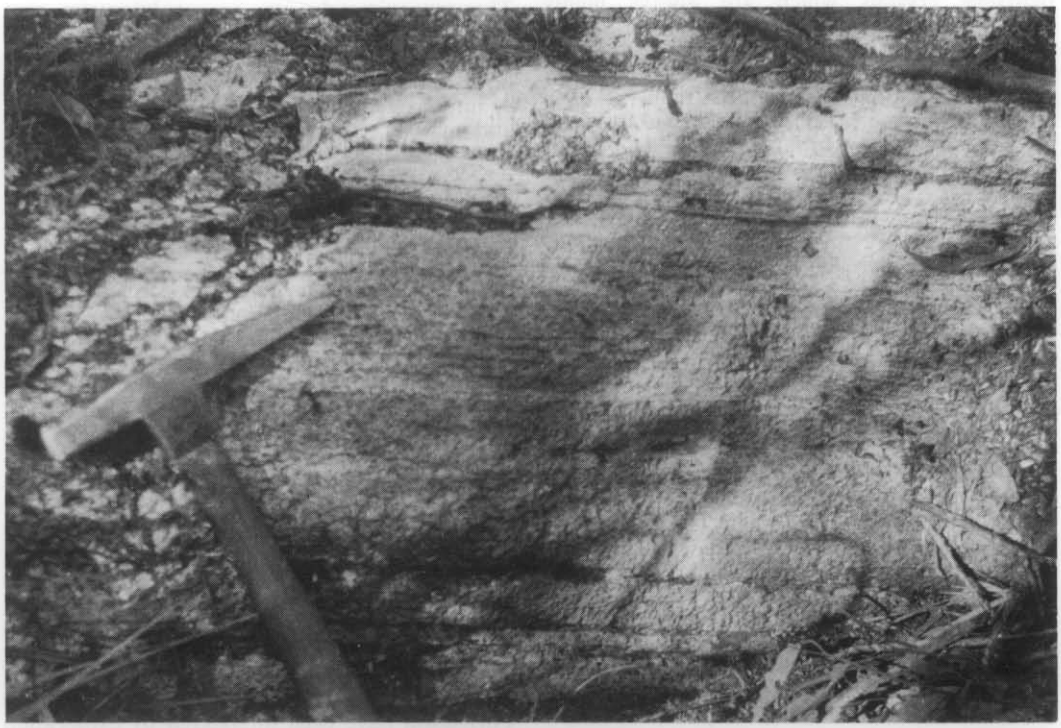

Plate 4. *Flow-banding in high-magnesian andesite [fig. 2; CQ672033].*

Collins (1983) records similar textures, grain size variations and mineral compositions, both primary and secondary, as are found in the samples from south of the Meredith Granite. Thin section descriptions of flows from other areas in the Cleveland district are also found in Creenaune (1980), Foden (1973), and Rubenach (1973). Foden (1973) recorded coexisting sub-calcic augite in some samples.

Arthur River–Wandle Road area

In the Arthur River–Wandle Road area (fig. 3) [CQ760210] (Williams and Brown, 1983), the basalt forms pillow-structured flows and contains intercalations of basaltic lapilli tuff, some of which contain abundant pyroxene crystals. The basalt sequence contains both aphyric and porphyritic rocks, the phenocrysts being plagioclase and/or clinopyroxene, with a matrix consisting of feldspar laths, clinopyroxene crystals and opaque mineral grains with an intersertal texture. Chlorite, actinolite and sericite are typical alteration minerals, with secondary calcite and quartz being present in some samples. A detailed textural and mineralogical description of basalt samples from this area can be found in Groves and Solomon (1964).

HIGH-MAGNESIAN ANDESITE SUITE (€ba)

The largest body of high-magnesian andesite mapped is approximately 15 km² in area, extending from north of the Meredith Granite, in a north-east direction, to north of the Corinna Road around CQ700080 (fig. 2). Although the outcrop ranges from totally metamorphosed and replaced by silica, along the southern part of this area, to highly weathered in the northern part, a wide range of textural varieties are exposed in the area accessible by Betts Track. The textures range between; orbicular or spherical ball structures, usually 10–30 mm in diameter [around CQ688052], but occasionally up to 200 mm [CQ653038] and which are probably equivalent to the 'spheroidal websterite' described from the Magnet area (Twelvetrees and Petterd, 1898; Twelvetrees, 1900; Nye, 1923); to interbedded breccia and agglomerate flows with flow-banding [CQ673035], vesicular and fine-grained lava with flow-banding (plate 4), which coarsens up to 10–30 mm crystal flows with minor basaltic material in the interstices, the main areas of which are mapped as basaltic pyroxenite (€bap) on Figure 2. All flows contain ubiquitous chrome spinel grains, and most flows are porphyritic with euhedral pyroxene phenocrysts [e.g. CQ685049].

In the area to the west of Heazlewood Hill and south of the Heazlewood River, numerous textural varieties are exposed along another track section between CQ583069 and CQ573060. Here the lava flows range from vesicular, through fine to medium and coarse-grained porphyritic to basaltic pyroxenite. The basaltic pyroxenite consists of a coarse-grained aggregate of

pyroxene crystals which are always highly weathered, but in contrast to similar grain sized pyroxenite from the adjacent ultramafic body, are never serpentinised. It is within this area that field relationships indicate that the high magnesian andesite (€ba) is intruded by, and overlain by, the low titanium tholeiite (€bm). Of the numerous areas of basaltic pyroxenite mapped, the area which shows the best textural variation is that traversed by the Corinna Road, around CQ591072. In this area a textural range from basaltic pyroxenite to flow-banded lava with 'ball' structures occurs. In the past, all outcrops of the basaltic pyroxenite have been mapped as part of the ultramafic body. Due to the high degree of weathering of the rocks in this area, thin section work was not possible, but the numerous textural variations are easily seen in weathered hand specimens (plate 5).

Small areas of €ba occur in the vicinity of the Magnet mine in the zone commonly known as the 'Magnet Dyke'. This zone is between 100 m and 300 m wide, approximately six kilometres long, and lies between the Magnet and Persic mines. The zone is mainly composed of low-titanium basalt (€bm) but areas of €ba have been mapped at the southern end around the Magnet mine (fig. 2) and have been reported from the north-east end around the Persic mine (Nye, 1923). The first description of high-magnesian andesite from Tasmania was of a sample from the western side of the Magnet mine (Twelvetrees, 1900). The field description is by Twelvetrees, with a thin section description by Rosenbusch, who wrote "If we follow the rock back to its original and unaltered state, we shall find phenocrysts of bronzite or enstatite (now bastite) in a groundmass of rhombic and monoclinic pyroxenes (now a mixture of serpentine and chlorite mineral). It is therefore a porphyritic form of websterite-a websterite-porphyry."

An area of mixed volcanic rocks (€bu) in the valley of the Whyte River to the west of the Magnet Range, often termed the 'Whyte River Complex' (e.g. Rubenach, 1973; Collins, 1983), is known to contain a mixture of various igneous rock suites including €ba and €bm. This area also contains at least two feeder pipes for picritic lavas of an unknown age (€bp). Picrite flows have so far not been recognised in this area, but they are known to exist below the Tertiary basalt cover to the east in the St Valentines Quadrangle.

The first 'modern' recognition of high-magnesian andesite in Tasmania was made by Rubenach (1973) who mapped the northern end of the body of €ba to the south of Thirteen Mile Creek. Outcrops within the road cuttings around CQ634080 consist of highly weathered vesicular and porphyritic flows, some with pillow structures. The well-exposed section along the road cutting is typical of the whole body in this area. Outcrops to the south are also highly weathered.

The approximately one square kilometre area of €ba cut by the Little Castray and Whyte Rivers to the north of the Mt Stewart ultramafic body (fig. 2) consists of a continuous succession of interlayered breccia, agglomerate, pillow lava, and pyroxene and spinel phyric laminar flows. Contact relationships with the surrounding rock types were not determinable due to lack of continuous outcrop.

Outside the area covered by Figure 2, high-magnesian andesite lavas have also been found in an area approximately four kilometres west of Zeehan. Here, interbedded pillow, breccia and massive flows infill structurally-controlled depressions within the Precambrian Oonah Formation, and in turn appear to be overlain by a sedimentary rock succession with lithological characteristics similar to the Razorback Conglomerate of the Dundas Group. A fault-bounded block of €ba occurs a further kilometre to the west of the above location. The dominant flows are pillow lavas (plate 6), with subsidiary breccia (plate 7) and porphyritic flows with minor intercalations of sedimentary rock units consisting of epiclastic material spalled from the surrounding flows and composed of broken phenocrysts and groundmass material. In the area around the old Nubeena mine, dykes of HMA material intruding the Precambrian Oonah Formation have been intersected by exploration company drill holes.

In thin section, the lavas are very similar, irrespective of which area they come from. The main difference is in the amount of alteration and degree of replacement by secondary minerals which the rocks have undergone.

The samples in the Magnet area are highly altered, the groundmass is permeated by secondary quartz and carbonate, and the phenocrysts are dominantly altered to chlorite, amphibole or serpentine group minerals. The chrome spinels are the only chemically recognisable primary mineral grains. Although a high degree of alteration and replacement has occurred in the samples from this area, the original texture is preserved in hand specimen and can be recognised in thin section. The pyroxene phenocrysts were orthopyroxene and clinoenstatite (plates 8 and 9) and are up to 5 mm long, but average approximately 1–5 mm by 0·5 mm in size. Ubiquitous chrome spinel grains are from 0·3 mm to 1 mm diameter. The large pyroxene phenocrysts are euhedral and do not usually show twinning, whereas the smaller (1·0–1·5 mm) stubby phenocrysts are subhedral, exhibit multiple twinning, and are consistent with having originally been clinoenstatite. The groundmass of the lavas contains elongate pyroxene grains between 0·07 mm and 0·15 mm long.

Samples from the road cutting near Thirteen Mile Creek (Rubenach, 1973; Creenaune, 1980) contain phenocrysts of pleochroic green to light brown amphibole pseudomorphs after 1–2 mm

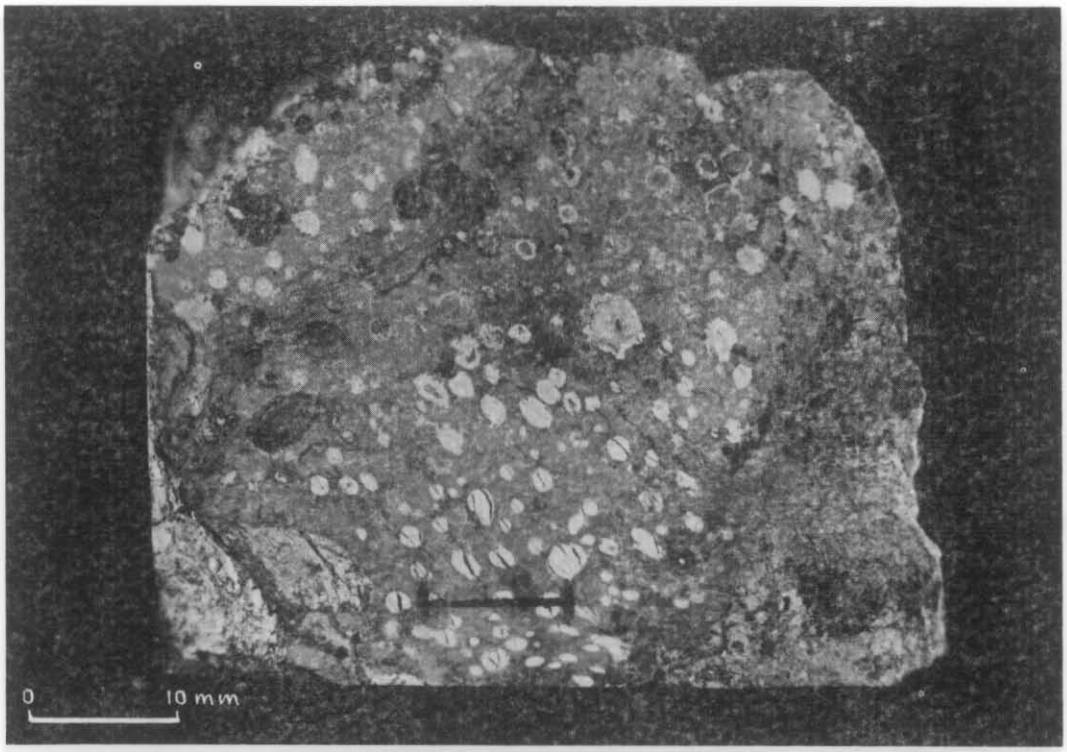

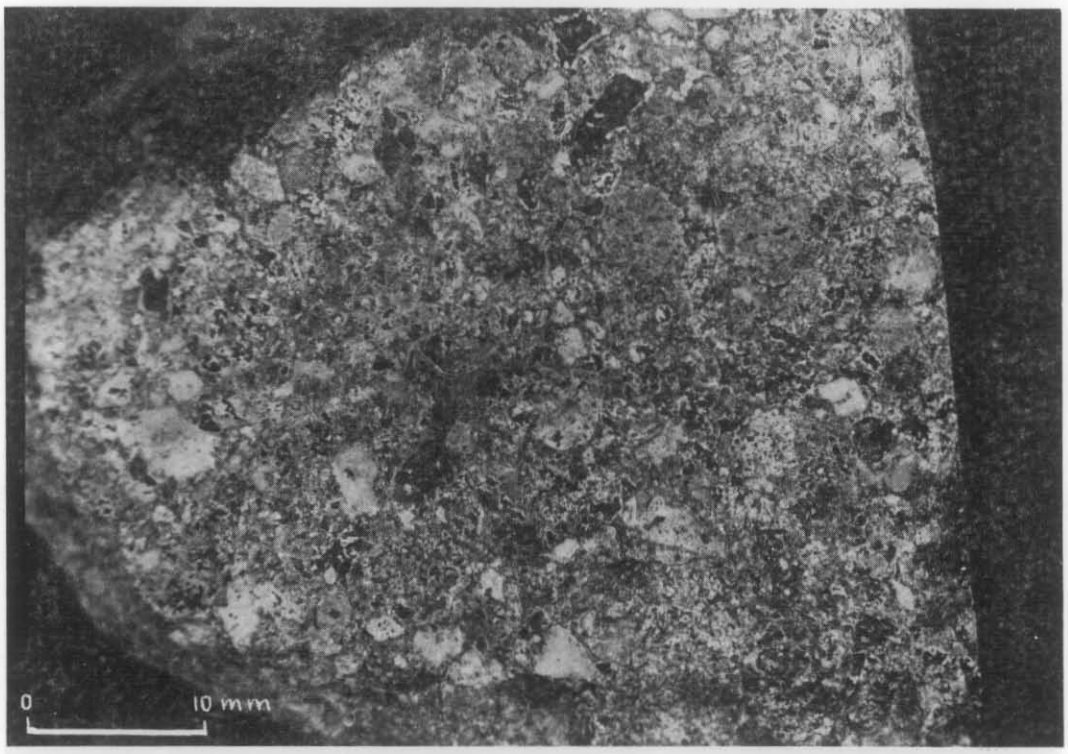

Plate 5. *Textural variations in weathered high-magnesian andesite (variations from along the track between CQ573060 and CQ583069, fig. 2). Vesicular* (top)*; Brecciated* (bottom).

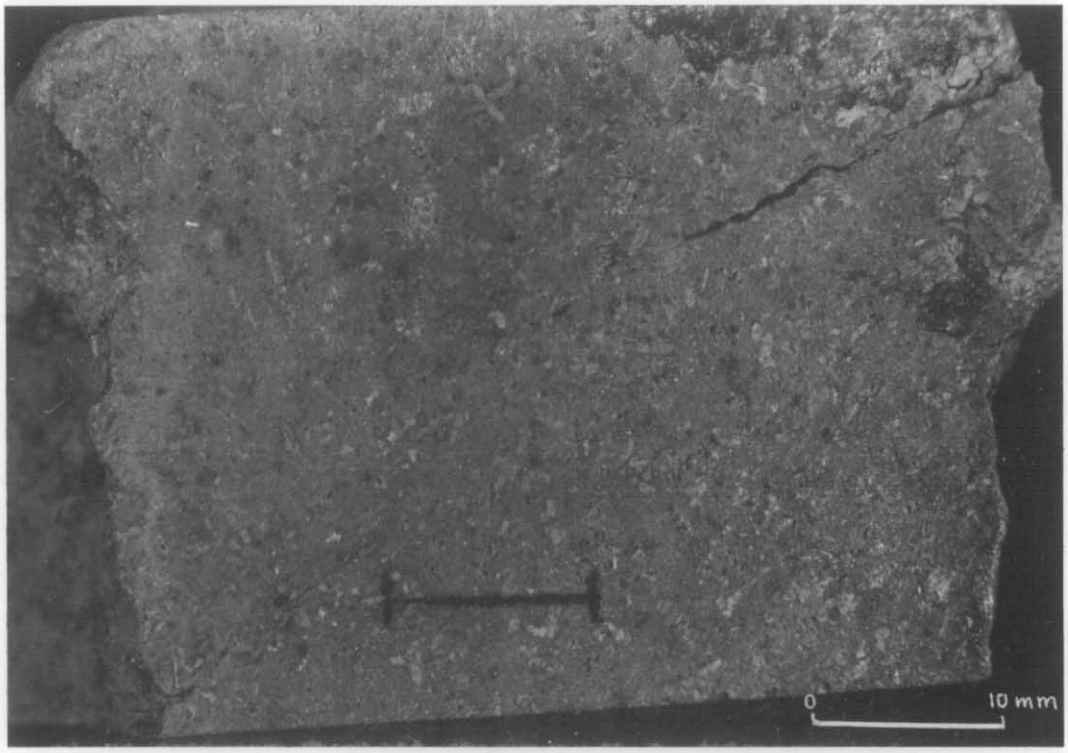

Plate 5. *Textural variations in weathered high magnesian andesite. Fine-grained with small phenocrysts* (top)*; Coarse-grained with large phenocrysts* (bottom).

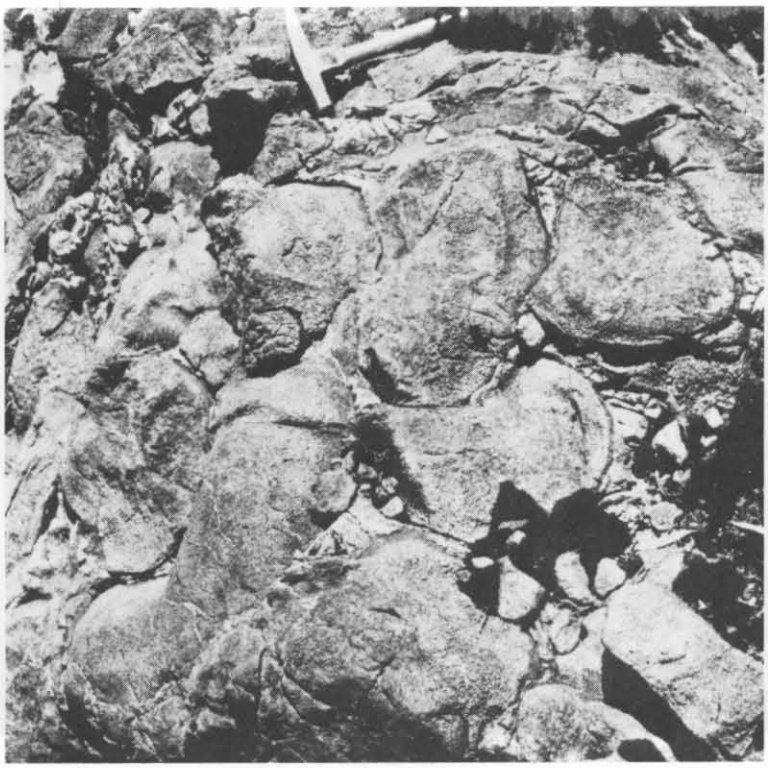

Plate 6. *Pillow lava flow in high-magnesian andesite, Comstock Creek area [CP566585].*

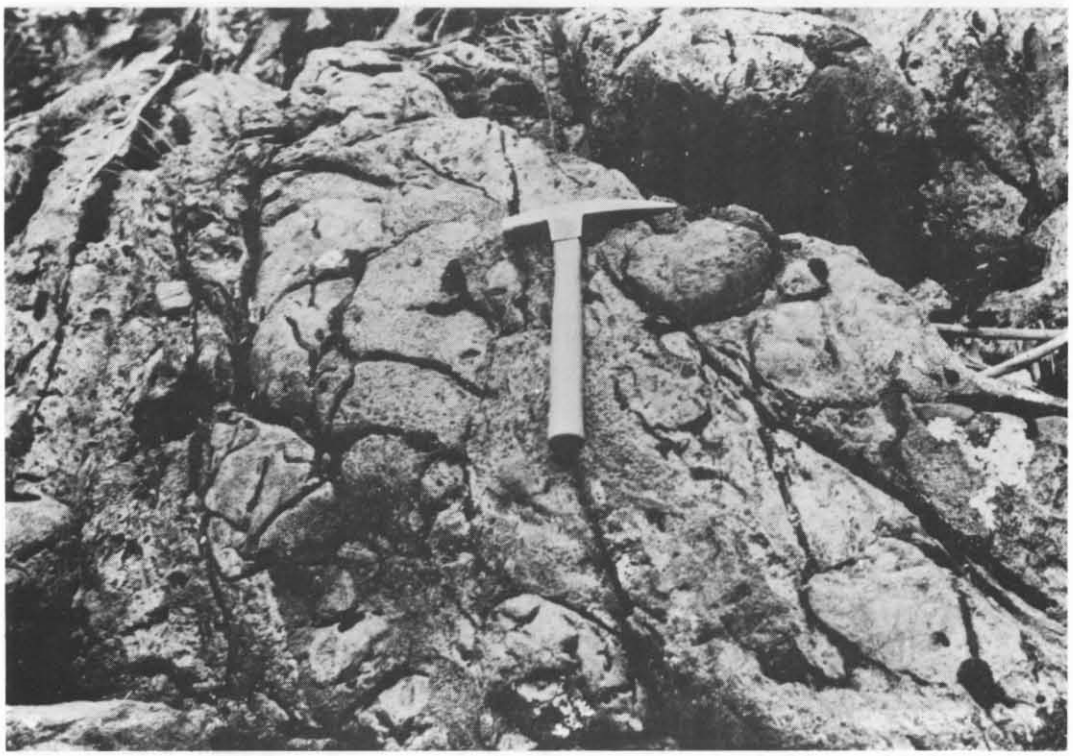

Plate 7. *Breccia flow in high-magnesian andesite, Comstock Creek area [CP566585].*

5 cm

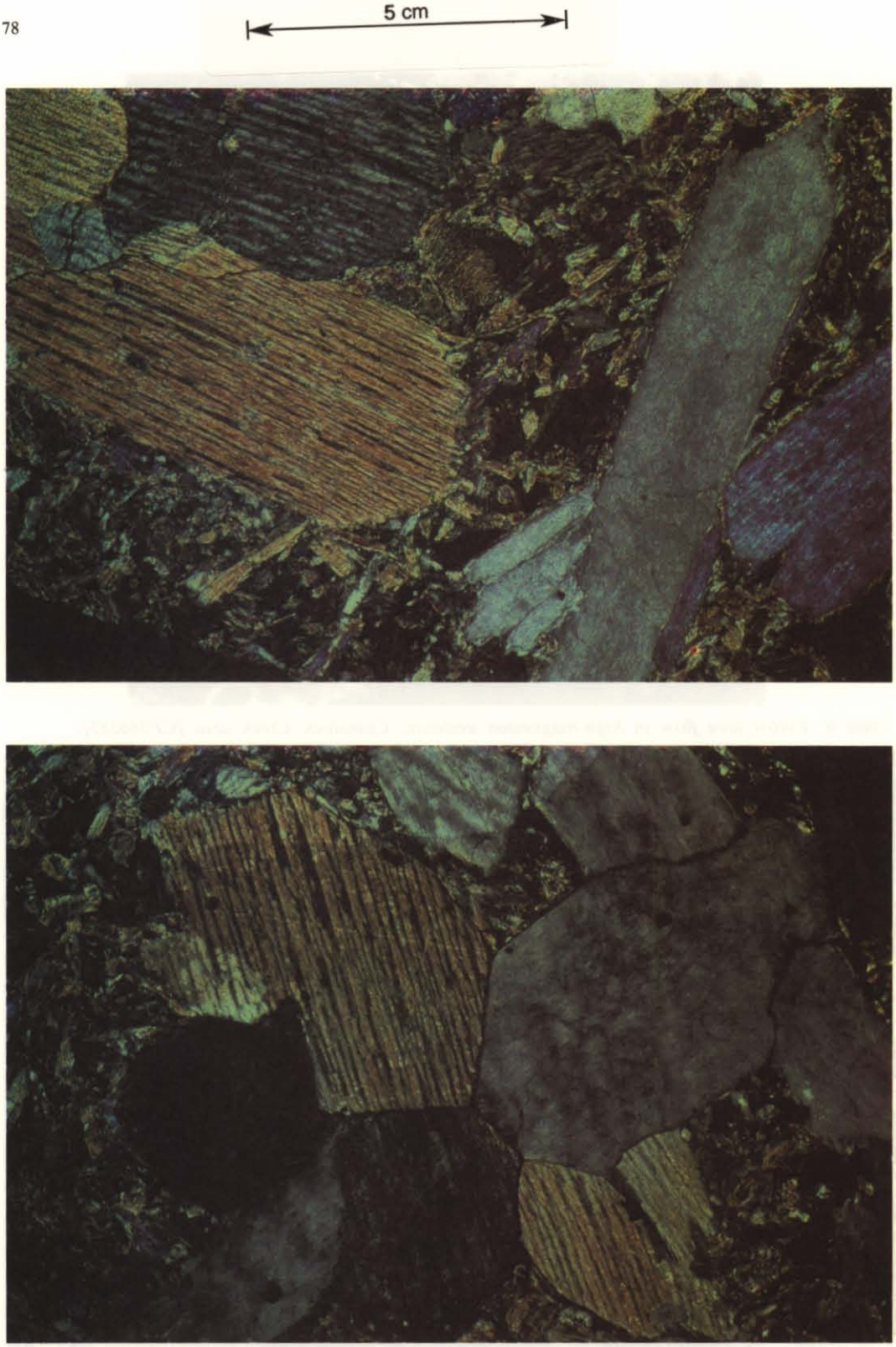

Plate 8. *Clinoenstatite and orthopyroxene phenocrysts in high-magnesian andesite, now pseudomorphed by amphibole-group minerals. Polarised light, specimen 85-0031 [CP569597]. Field of view 2·5 × 3·5 mm.*

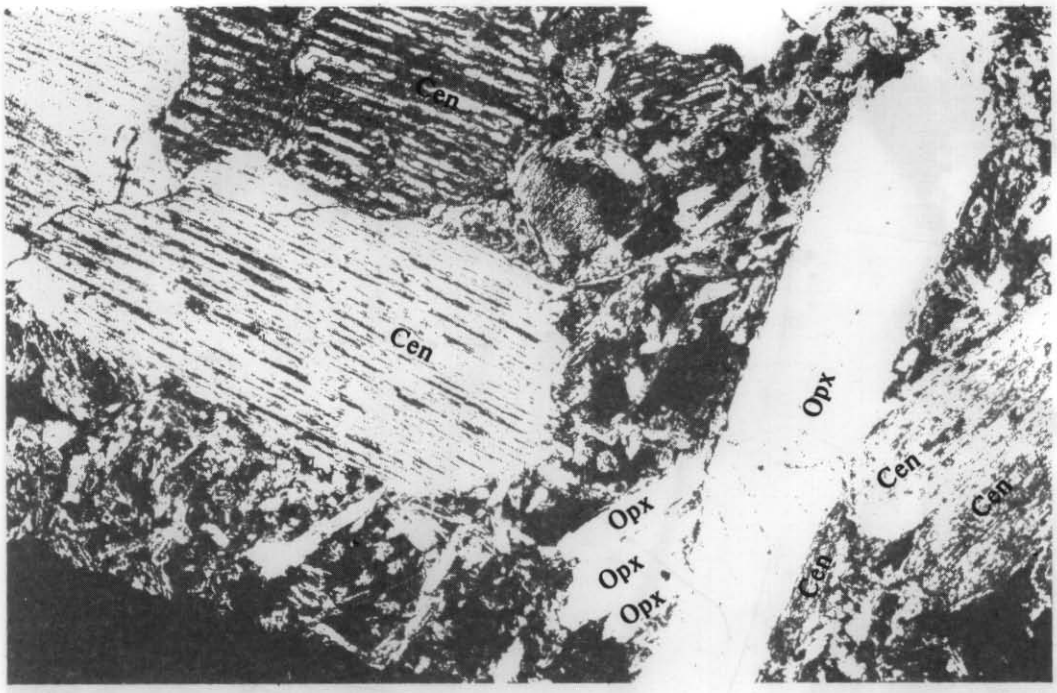

euhedral to subhedral orthopyroxene, multiple-twinned clinoenstatite crystals, and 0·1–0·25 mm euhedral chrome spinel grains set in a groundmass which originally had a felty texture of pyroxene crystals and intersertal glass, but which is now replaced by a uniform composition of chromian actinolite and chlorite. In some of the amygdaloidal and breccia flows the phenocrysts are partially deformed and altered to chlorite with the groundmass being replaced by quartz and calcite. The pyroxene phenocrysts occur as single crystals, crusiform twins, or in glomeroporphyritic patches.

In the Stonehenge area to the west of Zeehan, lavas differ in texture depending on which type of flow the samples came from. The flows range from vesicular and porphyritic, pillowed, tabular and porphyritic, or brecciated but always contain the same components. In the coarser grained parts of a tabular flow (e.g. C1461) the amphibole pseudomorphed phenocrysts are four to six millimetres long and enclose chrome spinel grains up to 0·5 mm diameter. The phenocrysts are set in a groundmass with original pyroxene crystals up to 0·5 mm in length, and euhedral chrome spinel grains (0·1–0·27 mm diameter) which have a similar chemical composition to those enclosed by the phenocrysts. Flows with vesicular tops have chlorite pseudomorphs of 0·5 mm long pyroxene crystals set in a groundmass of less than 0·25 mm grains.

In the more weathered areas of high-magnesian andesite, as in the area traversed by Betts Track and to the south of the Heazlewood and Little Castray Rivers, the flows are vesicular to porphyritic and contain distinctive flow banding. Vesicles are 1·0–2·5 mm in diameter and pyroxene phenocrysts are up to three millimetres in length, with chrome spinel grains being 0·05–0·1 mm diameter. The groundmass consists of pyroxene crystals and glass. Coarse-grained samples contain the same mineralogy as the finer-grained lavas but the very coarse-grained parts of flows consist dominantly of an original pyroxene crystal mush with interstices filled by a basaltic groundmass. As the Meredith Granite is approached, the flows progressively become replaced by cryptocrystalline silica.

A sample from a 200 mm diameter 'cannon ball' (plate 10) contains a flow-orientated quench groundmass with altered pyroxene microphenocrysts (1–2 mm long) and chrome spinel grains (0·05–0·1 mm) in a groundmass of skeletal pyroxene and sheaves of acicular pyroxene crystals up to 0·7 mm diameter. The interstices of the flow-aligned sheaves and skeletal grains are filled by glass. The groundmass is now dominantly replaced by quartz. The same texture exists in the surrounding part of the flow. Twelvetrees (1900) observed that the ball structures, irrespective of size " . . . drop out of their cavities readily upon being tapped with the hammer. The spheres split easily in halves,

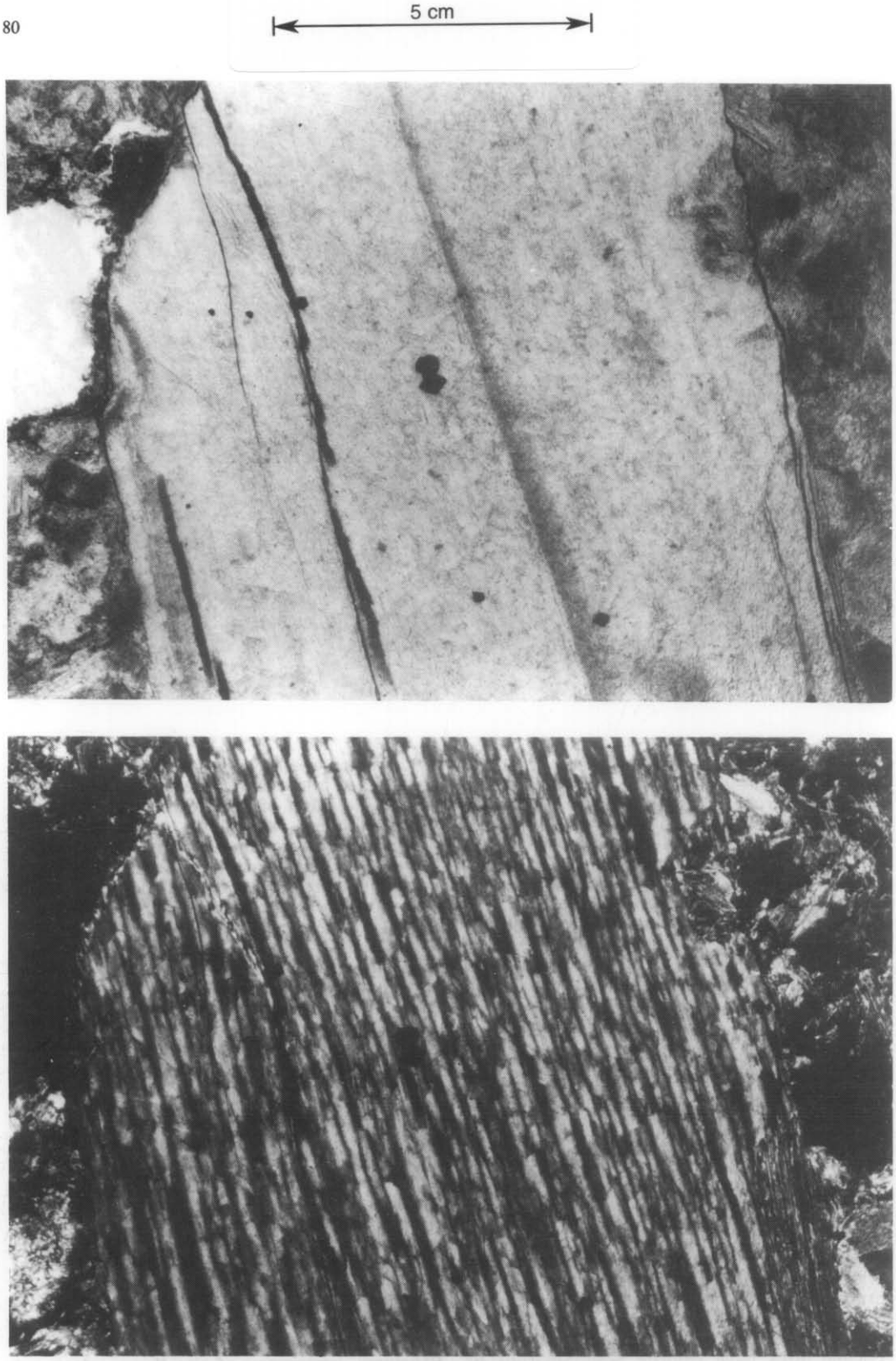

Plate 9. *Chrome spinel grains enclosed by amphibole pseudomorph of clinoenstatite. Plane light* (top)*; Polarised light* (bottom). *Specimen 85-0031 [CP569597]. Field of view 2·5×3·5 mm.*

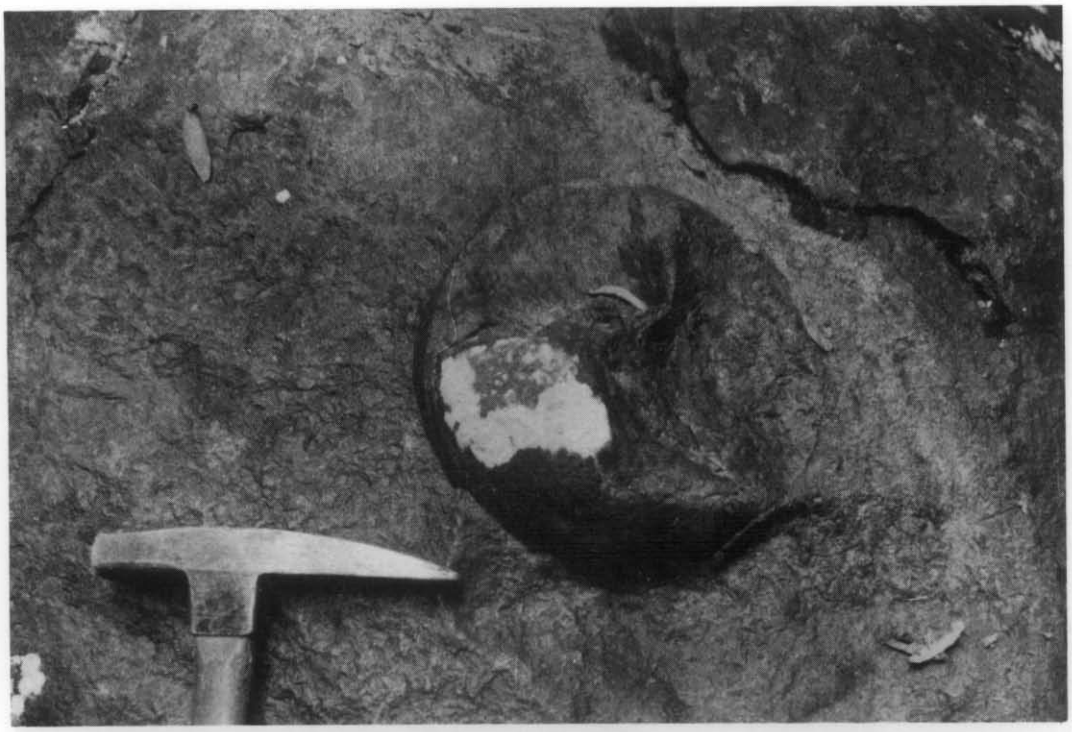

Plate 10. *'Cannon ball' structure in high-magnesian andesite [fig. 2, CQ653037].*

and to the naked eye appear to consist of the same substance as their matrix, and without any sign of a radiating or concentric structure''. This field observation of Twelvetree's has now been substantiated by thin section examination.

Throughout all the areas of high-magnesian andesite mapped, the samples are remarkably uniform in mineralogy. The only primary mineral phases recognised were orthopyroxene, clinoenstatite and chrome spinel. In neither hand specimen nor thin section was there any evidence that olivine, clinopyroxene or plagioclase had been present in any of the samples studied from western Tasmania.

LOW-TITANIUM THOLEIITE BASALT (€bm)

Volcanic rocks belonging to a phase of volcanism which produced low-titanium, dominantly quartz normative, tholeiitic lavas have been recognised in two main areas. The first is in the Black Hill–Ring River area (Black Hill Volcanics) (fig. 1 and 3), and the second is in the Mt Youngbuck–Mt Cleveland area (fig. 2 and 3) (Heazlewood River Volcanics; Creenanune, 1980; Rubenach, 1974). The exact areal distribution of rocks from this volcanic phase is still unknown, but basaltic rocks belonging to this phase of volcanism are also found in the so-called 'Whyte River Complex' and 'Magnet Dyke'; in the Arthur River–Wandle Road area in the St Valentines Quadrangle (Williams and Brown, 1983); and intruding correlates of the Success Creek Group in the Mt Youngbuck area; the Crimson Creek Formation in the Colebrook Creek area (fig. 1); and the ultramafic rocks in the Harman River area (fig. 1).

Black Hill area

Along the northern face of Black Hill and in the Ring River–Colebrook Creek area (fig. 1), subaqueous flows of pillowed and massive lavas with intercalated volcanic agglomerate and thin sedimentary rock units interdigitate with mass-flow conglomerate units belonging to the middle Middle Cambrian Red Lead Conglomerate (€dre) of the Dundas Group. The best exposure of the interdigitating relationship is along the Ring River around CP720691. The interdigitating nature of the contact can also be seen along Colebrook Creek [near CP723708] and remnant blocks of conglomerate are also associated with lava flows which crop out along the northern face of Black Hill (fig. 1).

The basalt was originally mapped as a separate entity to the ultramafic rocks by Rubenach (1967) who included it as part of the ultramafic-mafic rocks of the Serpentine Hill Complex, and considered that the Dundas Group was unconformably superimposed. Although Rubenach recognised the extrusive nature of the rocks, he considered that pillow lavas were rare, and he recorded the coarse-grained subophitic to ophitic parts of the flows as dolerite and interpreted these as being intrusive in the lavas and not part of the flows.

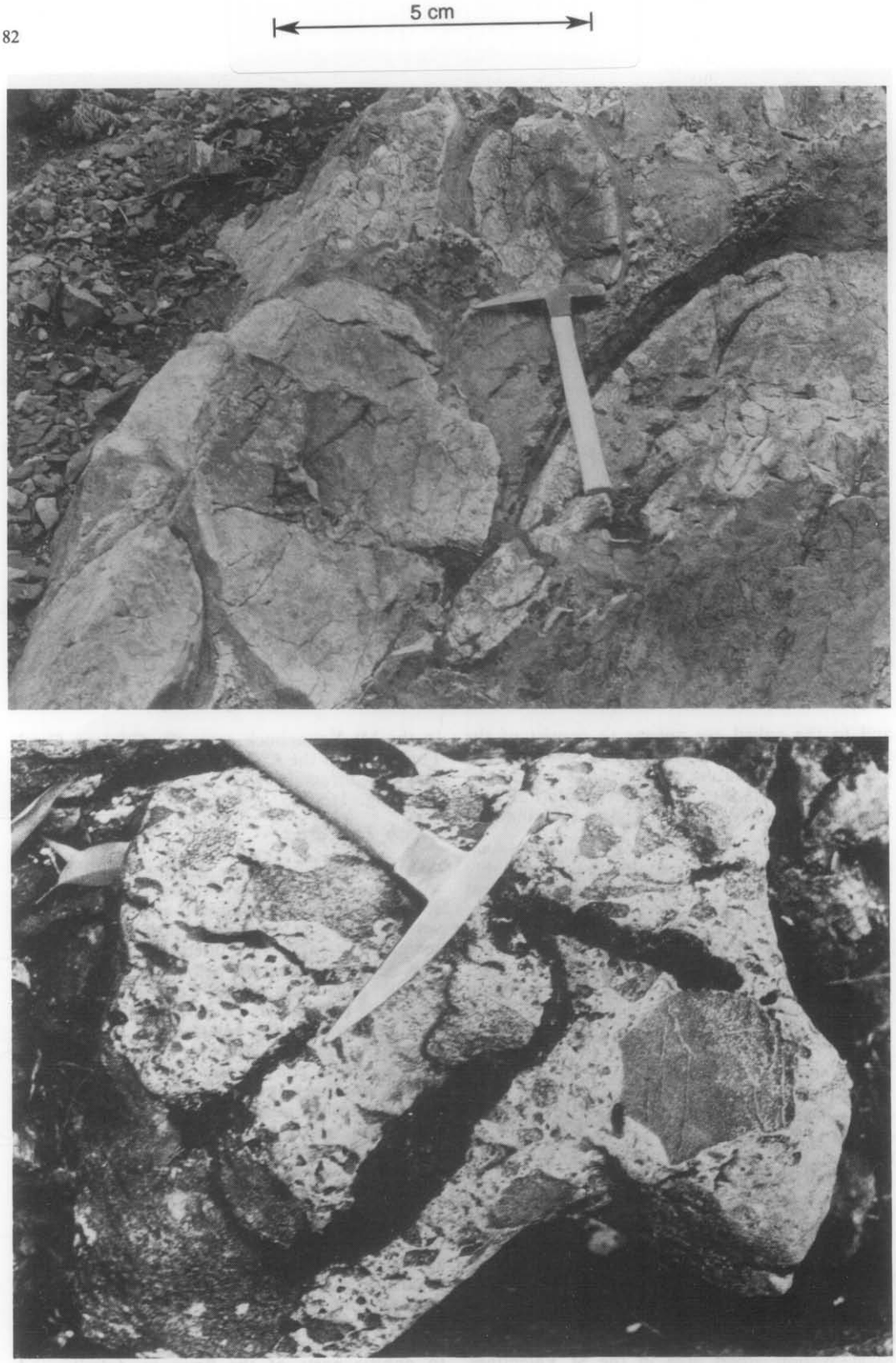

Plate 11. *Intermixed pillow lavas and breccia flow in low-titanium basalt, Black Hill area [fig. 1, CP697665].*

Most of the contact relationships between the volcanic sequence and the surrounding country rocks are faulted (fig. 1), the faults being associated with the Devonian deformation. In Kapi Creek [CP704666] lava has extruded through a stratigraphic correlate of the Judith Formation (€dj) causing contact metamorphic effects in the siltstone-mudstone succession and producing a chilled margin to the feeder channels.

The contact exposed in the Ring River between the western edge of the volcanic rocks and serpentinised pyroxenite (€sp) is faulted (fig. 1). The fault zone is marked by a highly sheared and weathered serpentinite. In the Ring River and Colebrook Creek sections, the eastern contact between the lava sequence and rocks of the Dundas Group is interdigitating, with evidence that flows of conglomerate and flows of basalt collided, resulting in an intermixing of lava and sedimentary flows, and fragments of each of the two rock types being incorporated in the other [CP720691].

Further upstream, within the overlying sedimentary rock succession [around CP723693], interbedded mudstone and siltstone with an occasional siliceous conglomerate lense (€mu) are interbedded with irregular lenses of pyritic volcaniclastic wacke, indicating that not all of the volcanic pile was covered at the one time by sediment and that the phase which produced the pyritisation probably occurred almost directly after eruption of the lava.

A fault block of this lava succession is intersected by the Ring River around CP730687, and an exploration access track to the east. Numerous grain size variations are exposed within this fault block. The variations range from vesicular through medium-grained quartz-bearing basalt to very coarse-grained zones with quartz-feldspar graphic intergrowths. An unusual lava with a banded texture exists in one area [CP731681]. The banding is green and white in hand specimen, the white bands being 0·5 mm wide and consisting, in thin section, of dominantly quartz with accessory stubby and anhedral altered pyroxene (actinolite) grains. The green bands are 1–3 mm thick, are dominated by acicular sheaves of actinolite after pyroxene, and contain subordinate albitised plagioclase and quartz. The texture in these bands is subophitic, and an occasional microphenocryst of plagioclase occurs.

The southern contact with lower Dundas Group successions (€dra and €dh) along the northern slopes of Black Hill is faulted, but evidence from along the upper hillslopes and in creek sections indicates an original interdigitating relationship between the dominantly faulted-out Red Lead Conglomerate and the volcanic succession.

The best exposure of the basaltic sequence is along a spur ridge running north-east from Black Hill towards Confidence Saddle. In this area, massive flows of pillow lava with red chert interstices are abundant and are interbedded with pillow breccia and agglomerate (plate 11). The main volume of the volcanic pile comprises massive, bottle-green flows which weather to a pale yellow-green. The rocks usually carry a good penetrative cleavage, consistent with the main phase of Devonian cleavage formation, are highly altered and have been affected by a phase of fluids which produced a high secondary pyrite content.

Texturally, the lavas range from vesicular and amygdaloidal to aphyric and ophitic, and in grain size from quenched, through fine-grained and medium-grained basaltic with subophitic textures, to very coarse-grained with granophyric textures. The medium-grained parts of the lava flows have previously been described as dolerite and the very coarse-grained parts as gabbro, causing confusion as to the exact nature of the body. Thick flows range from pillowed tops down into fine-grained basalt with variolitic texture, to subophitic medium-grained basalt through a coarse-grained zone into a chilled base. The very coarse-grained ophitic-textured parts of the flows contain areas of graphic intergrowths of quartz and feldspar set in an ophitic texture of plagioclase (up to 4 mm long) and pyroxene intergrown with skeletal iron-titanium oxide grains.

In thin section, quenched and fine-grained basalt samples contain variolitic sheaves of actinolite, chlorite and albitised plagioclase in a groundmass replaced dominantly by calcite. In some samples elongate skeletal pyroxene crystals occur between the variolites and have interstitial quartzo-feldspathic mesostasis. In the quenched and fine-grained basalt samples the iron-titanium oxide mineral content is usually less than one percent.

The fine-grained to medium-grained basalt consisted originally of pyroxene grains (0·5 mm) subophitically intergrown with 0·2 mm long plagioclase crystals, but now consists of dark blue-green to brownish-green, elongate and fibrous actinolite, epidote, secondary quartz, altered skeletal iron-titanium oxide mineral grains and secondary pyrite. In some samples, the original mineralogy is totally replaced by an intergrowth of quartz and amphibole but the subophitic texture is still preserved.

Amygdaloidal fine-grained samples have rounded to irregular-shaped amygdales surrounded by flow-aligned feldspar laths from 0·15–0·2 mm long, within a groundmass of quartz and carbonate. The amygdales are filled by chlorite, quartz and zeolites, with ubiquitous euhedral pyrite (85-0033, 85-0034, 85-0035).

The coarser-grained lavas have subophitic to ophitic textures and are composed of actinolite, chlorite, albite and interlocking skeletal opaque mineral grains with chlorite after pyroxene.

Volcanic breccia and agglomerate samples are composed of pillow lava fragments, microphenocrystic lava and fine-grained to medium-grained basalt with a rock flour matrix. The present mineralogy is actinolite, chlorite, albite, quartz and secondary euhedral pyrite.

Heazlewood River area

The largest single body of the low-titanium tholeiite (Cbm) in the study area occurs to the west of Mt Cleveland. This body is composed of north-south striking, easterly dipping, subaqueous flow units and associated breccias, agglomerate and sedimentary rocks. It is in faulted contact with a rock succession correlated with the Crimson Creek Formation to the east; an area of high-magnesian andesite lava (Cba) and Silurian-Devonian sedimentary successions to the south; ultramafic rocks to the west; and a tonalitic complex and an ultramafic mélange to the north (fig. 2). This area was originally mapped by Rubenach (1973) and restudied by Creenaune (1980).

Creenaune established that the whole area was a sequence of differentiated basalt flows with interbedded hyaloclastite, fine-grained volcaniclastic sedimentary rock and mudstone, and not two discrete areas, one basaltic flows and the other dolerite dyke swarms, as was concluded by Rubenach (1973). Numerous pillow lava flows were mapped by Creenaune around CQ609075, in the area previously mapped as dolerite dyke swarms by Rubenach. Field observations made during this study substantially agree with those of Creenaune (1980).

The degree of alteration of the lavas is medium to high, but not as high as in the Black Hill area. The thin section observations of Creenaune (1980) from the volcanic rocks in the Heazlewood River area are similar to those obtained from samples from the Black Hill area, and from basaltic rocks with similar field relationships and chemistry from the Wandle River area (Williams and Brown, 1983) and from the Mt Youngbuck and Whyte River area.

The present mineralogy of the rocks is dominantly actinolite, albite, epidote, chlorite and a small amount of quartz and magnetite. Creenaune (1980) records some fresh plagioclase grains with a composition of An_{51-62} and relict augite crystals preserved in the coarser parts of thicker flows. Some lavas are replaced by quartz in varying degrees, usually starting from variolitic centres and progressively replacing larger areas until, in some samples from the Jasper Hill area, they are totally replaced by quartz in thin section, whereas in hand specimen the original texture of the basaltic rock is still evident. Another characteristic of these lavas is that in the coarser part of the flows, skeletal magnetite occurs intergrown with actinolite, usually replacing pyroxene, and graphic intergrowths of quartz and feldspar are common, indicating primary quartz crystallisation.

A considerable range in grain size occurs within the coarser flows, and the grouping of grain sizes observed by Creenaune (1980) is considered a practical division for field mapping purposes. The thicker flows range from pillow lava to quenched amygdaloidal basalt tops, through fine-grained basalt with a grain size of less than 0·7 mm, to a fine-grained to medium-grained basalt (1–3 mm) (which in the past has been called dolerite) to a coarse-grained (3–5 mm) zone which quickly grades into a chilled basal zone. The coarse zone has previously been called gabbro.

Texturally, the basalts range from variolitic amygdaloidal or fine-grained ophitic within the finer-grained parts of flows, to subophitic and ophitic in the coarser zones, with rare granophyric textures in the very coarse-grained parts of flows (Creenaune, 1980).

Similar graphic intergrowths of quartz and feldspar to those observed in samples from the Black Hill area, as well as skeletal magnetite with intergrown actinolite after pyroxene, are present. This texture, associated with the coarser parts of the thicker flows, is found within numerous dykes (which have chilled margins and a gabbroic centre) which cut successions belonging to the Crimson Creek Formation in the Pieman River–Mt Ramsay area and in the Harman River area to the west of the ultramafic rocks [around CP626840].

Pillow lavas in the Cleveland area are usually tightly packed, of an irregular shape, have vesicular fringes and only contain a small amount of hyaloclastite material between separate pillows (Creenaune, 1980). In contrast, the pillow fields in the Black Hill area have a high amount of interpillow material and contain numerous interbedded breccia and agglomerate flows. The brecciated nature of the flows was also observed in the Persic mine area to the north-east of the 'Magnet Dyke'. Flows with a range of textures from variolitic to granophyric exist around the Magnet mine area.

Pillow and breccia flows dominate around Jasper Hill and to the west, to the south-west of this main area. In a one kilometre radius around CQ577064 (fig. 2), field relationships indicate that dykes of Cbm cut the high-magnesian andesite lavas (Cba), providing a relative age relationship between the two. Along the contact where the lavas overlie the southern extent of the Heazlewood River ultramafic rocks [e.g. around CQ589067] (fig. 2), the basalt consists of brecciated flows. Areas of dominantly vesicular flows overlie basaltic pyroxenite (Cbap) around CQ586059 and breccia flows dominate around CQ589059. Near CQ593058 reddish laminated siltstone with interbedded sandstone overlies basaltic pyroxenite (Cbap). Lavas overlying these sediments show all textural ranges from vesicular to very coarse-grained. Another thin sedimentary intercalation occurs near CQ595060.

The macroscopic textures of the volcanic rock are preserved in the Jasper Hill area, although alteration has occurred on a mineralogical scale which resulted in the rock being partially to completely replaced by quartz with subordinate amounts of actinolite, chlorite and epidote. This alteration could explain the anomalous chemistry of some of the lavas obtained from this area (Rubenach, 1973; Creenaune, 1980), as there is no field evidence that more than one phase of lavas exist.

Field relationships indicate that both the high-magnesian andesite and low-titanium tholeiite basalt successions were extruded through the Eocambrian Success Creek Group (Esc) and Crimson Creek Formation (Ecc) correlates. The high-magnesian andesite (€ba) is older than the low-titanium tholeiite (€bm) which, in the Black Hill–Ring River area, is known to have an extrusion age of about 530 Ma (*Ptychagnostus atavus* Zone).

MINERAL CHEMISTRY

Crimson Creek Formation tholeiite (Ecc and Eccb)

Plagioclase phenocrysts

Because of the degree of alteration of most samples, electron probe analysis of the majority of plagioclase phenocrysts gave a composition of albite. Of three samples probed from the Mt Lindsay area, fourteen out of fifteen grains gave an albite composition, with the remaining grain (from 85-0004) being oligoclase (An_{22}). Samples from the Pieman River area gave analyses ranging from albite (An_0) to labradorite (An_{52}). The two samples from the eastern side of the Huskisson Syncline (85-0010 and 85-0051) ranged from oligoclase to labradorite (An_{16}–An_{65} and An_{29}–An_{64} respectively). Of the three samples analysed from the Mt Ramsay area, only one (85-0011) contained albite, another contained oligoclase (An_{22}), andesine (An_{37}) and labradorite (An_{62}), while the third ranged from albite (An_4) to labradorite (An_{62}). The evidence strongly suggests that the original plagioclase composition was labradorite, the typical tholeiitic plagioclase species, which had a high calcium content (approximately An_{65}–An_{70}).

Pyroxene phenocrysts

Ten of the twelve samples probed to obtain pyroxene compositions contained fresh clinopyroxene, the other samples containing ferro-actinolite to ferro-actinolitic hornblende pseudomorphs of the clinopyroxene grains. The amphibole terminology used follows the International Mineralogical Association Commission on New Minerals and Mineral Names (Leake, 1978). Typical electron probe analyses are listed in Table 6 (analyses 1–10) and the average for each sample is plotted on Figure 22. The compositions and plot show that the clinopyroxene grains range from one sample of chrome diopside to chromium-bearing augite, along an apparent iron-enrichment trend, but one which also appears to be depleted in calcium at a greater rate than the normal tholeiitic trend. Regionally, the three samples from the Mt Ramsay area (plot numbers 7–9) are enriched in calcium and chromium and depleted in titanium, iron and manganese with respect to the grains found in the samples from the Mt Lindsay area (plot numbers 1–3). The reason for the compositions of grains from two of the samples from the Pieman River region (plot numbers 5 and 6) is not known, but it may have something to do with cooling history, as these two samples are from what were thought in the field to be sills rather than flows.

Accessory phases

Iron-titanium oxides: The larger opaque grains are ilmenite, having an average composition of $(Fe^{2+}_{0.8256}, Mn_{0.1578}, Mg_{0.0038}, Fe^{3+}_{0.0111}, Al_{0.0147}, Ti_{0.9870})_2O_3$. Smaller opaque grains have differing proportions of iron to titanium.

Amphibole: As well as ferroactinolite in sample 85-0010, numerous clinopyroxene grains from samples in the Mt Ramsay area are altered to amphibole minerals. The alteration in this area has produced tremolitic hornblende to magnesio-hornblende.

Other secondary mineral phases include chlorite, calcite, epidote and quartz.

High-magnesian andesite (€ba and €bap)

Pyroxene phenocrysts

Although two texturally different pyroxene species occur as phenocrysts in high-magnesian andesite flows, none of the fifty phenocrysts from ten samples analysed gave a pyroxene analysis. The analyses were consistently of a chromium-bearing calcic amphibole to a more magnesium amphibole-serpentine group mineral mixture (table 7*b*). Broad beam analysis of the groundmass of any specific sample gave similar compositions to those obtained from phenocrysts within the sample. The phenocrysts in the Stonehenge samples are actinolite, and those from the Magnet samples anthophyllite/serpentine to cummingtonite.

Chrome spinel grains

The only relatively chemically unaltered component of the high-magnesian andesite samples are the chrome spinel grains. To test the reliability of using spinel grains as an indicator mineral for the recognition of highly weathered samples as either high-magnesian andesite or basaltic pyroxenite, concentrates of spinel grains were made from five highly altered lava samples from the Magnet area, so that the resultant analyses could be compared with those obtained from the three least altered samples from this area which were used for whole rock analyses. Five grains from each concentrate were

randomly selected in each sample and analysed by electron probe. The analyses from each sample were then averaged to give a single representative composition for each sample. A range in the Cr/Cr + Al ratio of the average compositions of 0·89 to 0·92 was obtained (fig. 23, table 7*a*, analyses 1–5), with an overall average for the 25 analyses of 0·90. Mg/Mg + Fe ratios for the samples ranged between 0·62 and 0·72, with an overall average of 0·69. The three freshest samples from the Magnet area (85-0025 to 85-0027, table 7*a*, analyses 6–8), have spinel grains which gave an average Cr/Cr + Al ratio of 0·93, 0·92 and 0·91 respectively and a Mg/Mg + Fe ratio of between 0·67 and 0·70 (fig. 23). As the grains from the highly altered samples gave results consistent with those from the least altered samples, and as the chrome spinel grains appear to remain relatively unaltered with respect to their chromium to aluminium ratio (but not to their magnesium to iron ratio), the presence of chrome spinel grains with their characteristic high Cr/Cr + Al ratios has been used in the recognition of highly weathered lava and basaltic pyroxenite samples and to differentiate basaltic pyroxenite from layered ultramafic pyroxenite where the Cr/Cr + Al ratio is between 0·60 and 0·74.

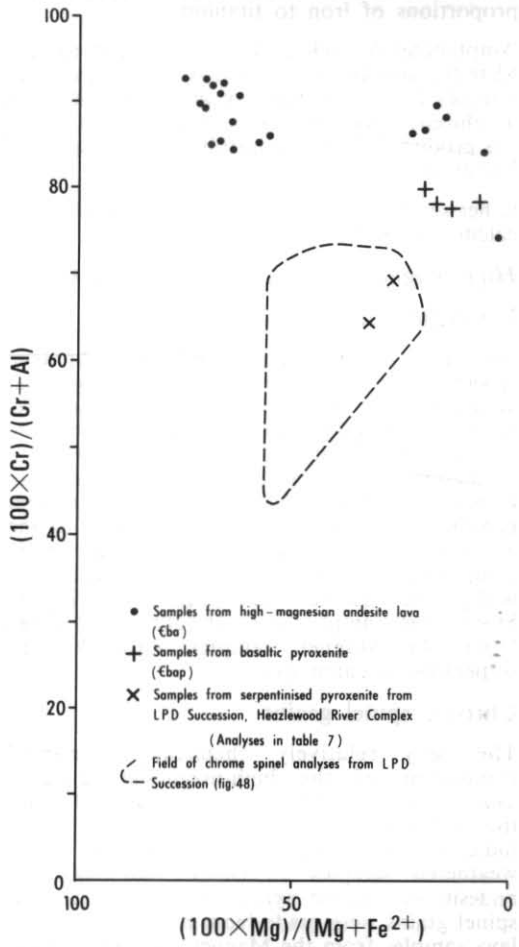

Figure 23. *Plot of analyses of chrome spinel grains from high-magnesian andesite samples. Analyses Table 7a, Appendix 4.*

The analysed sample from the Thirteen Mile Creek area (85-0023, table 7) has a slightly lower Cr/Cr + Al ratio than the samples from the Magnet area, being 0·85 with a Mg/Mg + Fe ratio of 0·58 (fig. 24). This ratio is in a similar range to both the well-exposed flows in the Stonehenge area (around CP571598, 85-0028 to 85-0030), and two samples from a bore hole to the east (at CP575601; 85-0055, 85-0056; table 7), which have Cr/Cr + Al ratios between 0·84 and 0·86 (fig. 23), with a variation in the Mg/Mg + Fe ratio of 0·55 and 0·70. The lowest Cr/Cr + Al ratio (85-0090, table 7) was obtained for spinel from the lava sample with 'cannon ball' texture.

Samples obtained from the Betts Track area are within the metamorphic aureole of the Meredith Granite. Two samples of silicified lavas were chosen from close to the contact with the granite (85-0057–450 m; and 85-0058–250 m). Both of these samples have an extremely low Mg/Mg + Fe ratio, the lowest being closest to the granite, but both samples retain their high Cr/Cr + Al ratio of approximately 0·90 (fig. 24). Three samples of highly altered basaltic pyroxenite from close to the granite in the Mt Stewart area (table 7, analyses 18–20) were also obtained. Again, an extremely low Mg/Mg + Fe ratio (0·062) was obtained from one sample, the other two having 0·20 and 0·24, with the Cr/Cr + Al ratio remaining between 0·84 and 0·87.

Four samples of highly weathered basaltic pyroxenite and another lava sample (85-0061) were chosen from the body of €ba–€bap to the south of the Heazlewood River and west of Heazlewood Hill. Mg/Mg + Fe ratios of 0·15 to 0·20 were given by the spinel in the basaltic pyroxenite samples which have Cr/Cr + Al ratios of between 0·78 and 0·81. The lava contained spinel grains with an average Cr/Cr + Al ratio of 0·80 and Mg/Mg + Fe ratio of 0·06.

To compare the basaltic pyroxenite spinel compositions with the serpentinised ultramafic pyroxenite, two samples of ultramafic pyroxenite (85-0076, 85-0077) in a relatively weathered condition and as close as possible to the body containing the three basaltic pyroxenite samples were selected. These samples contained chrome spinel grains with an average composition such that Cr/Cr + Al ratios were 0·65–0·70 and Mg/Mg + Fe ratios were 0·27–0·32 (table 7). This range in the ratio of chromium to aluminium is consistent with that found in the majority of pyroxenite samples from the Layered Pyroxenite-Dunite successions (LPD) of the Dundas Trough (fig. 48). The only ultramafic pyroxenite units which are known to have chromium to

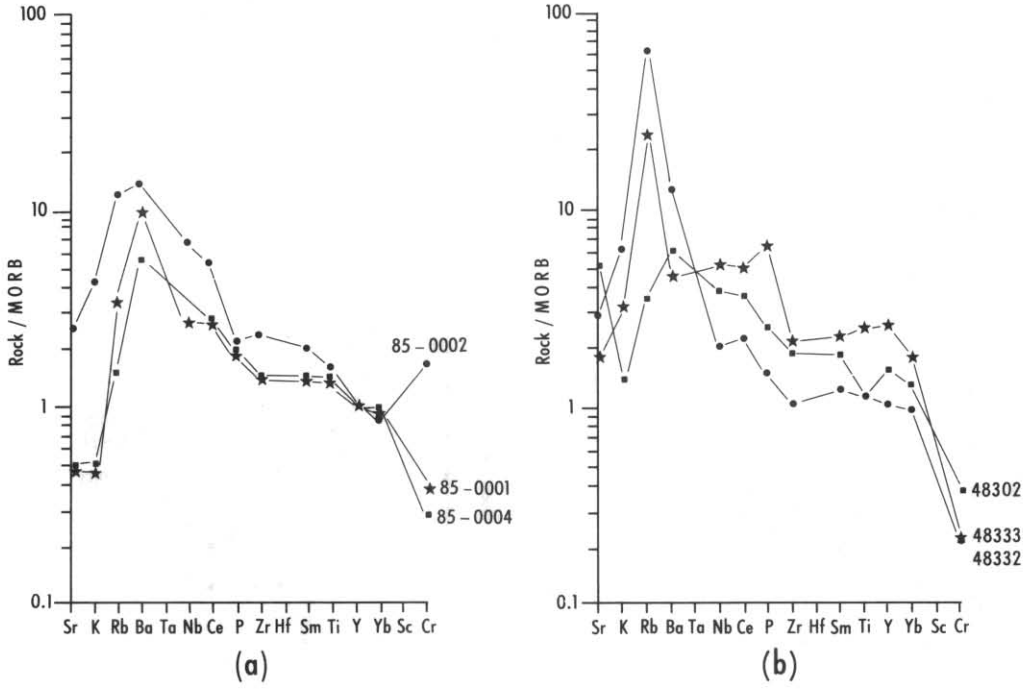

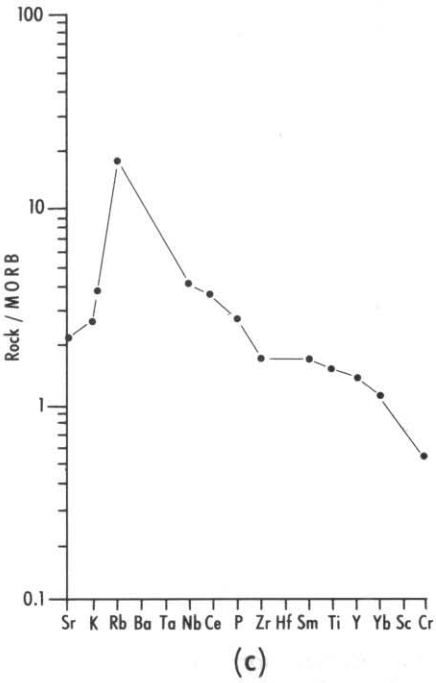

Figure 24. *MORB normalised geochemical patterns for Crimson Creek tholeiitic basalts. (a) Samples from type area; (b) Samples from Cleveland area (Collins, 1983); (c) Average pattern. Normalising values from Pearce (1980). Sr = 120 ppm; $K_2O = 0.15\%$; Rb = 2.0 ppm; Ba = 20 ppm; Ta = 0.18 ppm; Nb = 4 ppm; Ce = 10.0 ppm; $P_2O_5 = 0.12\%$; Zr = 90 ppm; Hf = 2.4 ppm; Sm = 3.3 ppm; $TiO_2 = 1.5\%$; Y = 30 ppm; Yb = 3.4 ppm; Sc = 40 ppm; Cr = 250 ppm.*

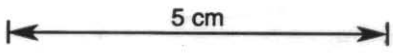

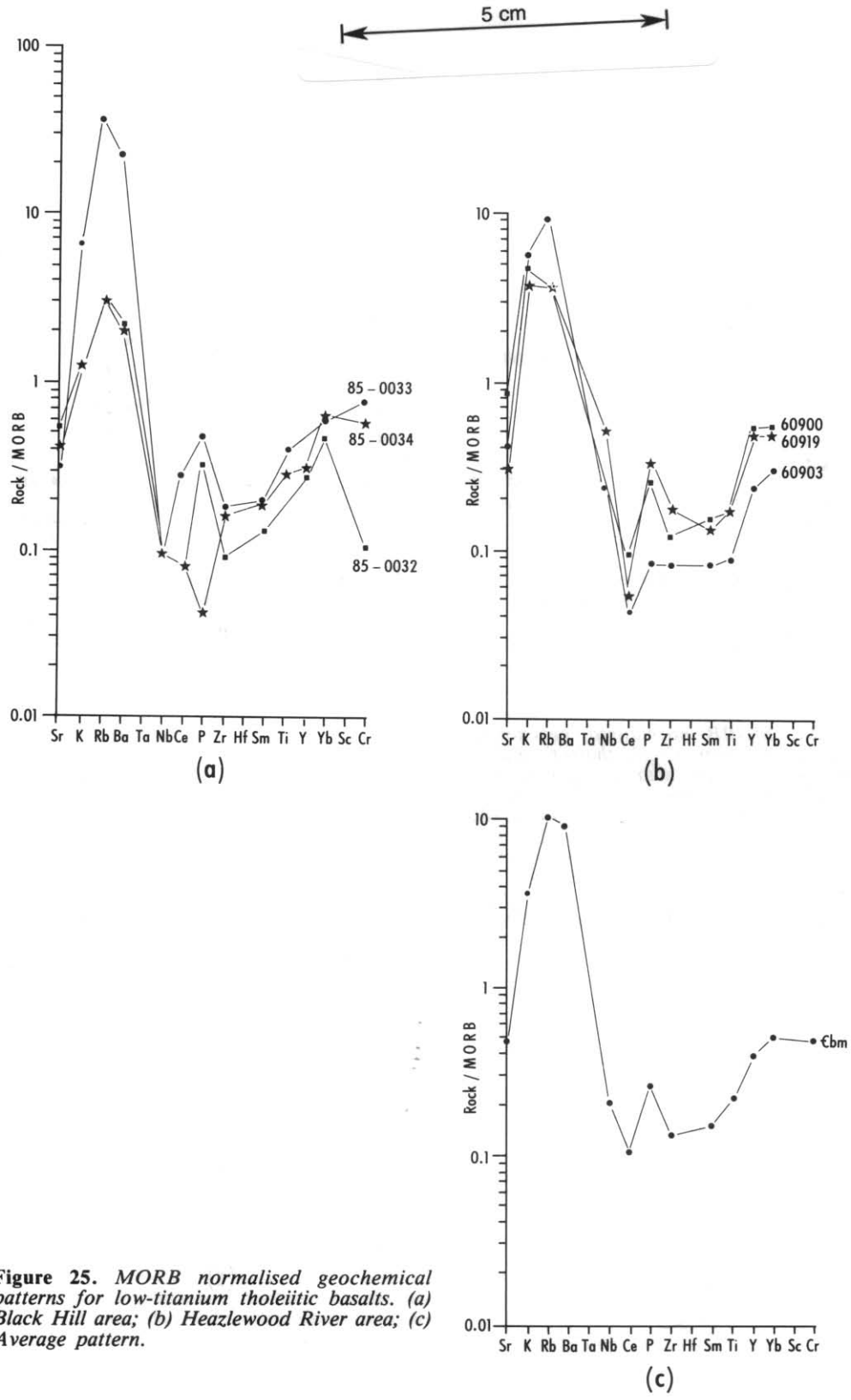

Figure 25. *MORB normalised geochemical patterns for low-titanium tholeiitic basalts. (a) Black Hill area; (b) Heazlewood River area; (c) Average pattern.*

aluminium ratios of approximately 0·9 are from pods and lenses of a massive coarse-grained orthopyroxenite (En_{92}) which occurs in the Layered Dunite-Harzburgite Succession (LDH) (p. 125). The field relationship of these bodies and the close association of the dunite with chrome spinel grains with chromium to aluminium ratios in the 0·89 to 0·93 range is very distinctive, and these pyroxenite bodies cannot be confused, in the field, with areas of basaltic pyroxenite.

Low-titanium tholeiite basalts

All the samples of low-titanium basalt which were collected were aphyric, and in thin section the alteration to the groundmass was sufficient to deter study by electron probe.

WHOLE-ROCK CHEMISTRY

Major and trace element chemistry was obtained for thirty-two whole-rock samples collected from different areas of the three major Eocambrian to Cambrian basalt types. Of these, fifteen were from areas within the Crimson Creek Formation (Ecc, Eccb) (table 8); eleven from areas of high-magnesian andesite and basaltic pyroxenite (Ebа, Ebap) (table 9); five were of low-titanium basalt (Ebm) from the Black Hill area, and one from the Magnet area (table 10). The samples from the Crimson Creek Formation were supplemented by a further twenty-eight analyses from areas of Crimson Creek Formation correlates to the north of the Meredith Granite, twenty-four of which were from the 'Deep Creek Volcanics' at Cleveland (Collins, 1983), and four from the Arthur River–Wandle Road area (table 8) (Williams and Brown, 1983). Two additional analyses of high-magnesian andesite samples from the Thirteen Mile Creek area are also included in Table 9 (Rubenach, 1973; Creenaune, 1980), as well as ten analyses of low-titanium basalt from the Heazlewood River area (table 11) (Creenaune, 1980).

It is obvious from field and petrographic observations, and mineral chemistry studies, that the three basalt suites have undergone varying degrees of alteration and that the present major and trace element chemical analyses do not represent the pristine eruptive chemistry. Because of this, the purpose of analysing the major and trace element whole-rock chemistry was to obtain chemical criteria to correlate any specific area of basaltic rocks in the Dundas Trough with one of the three phases, and to be able to correlate these phases with other areas of similar lithostratigraphic successions within Tasmania.

Figures 24 to 27 contain geochemical pattern diagrams plotted from the data obtained from the three basaltic types and normalised with a typical Mid-Ocean Ridge Basalt (MORB). The values for the typical MORB are those from Pearce (1980) and are included in the caption of Figure 24. The following trace element chemistry grouping is used: High Field Strength (HFS) elements (Ti, Zr, P and Nb–these elements tend to be immobile under sea water alteration

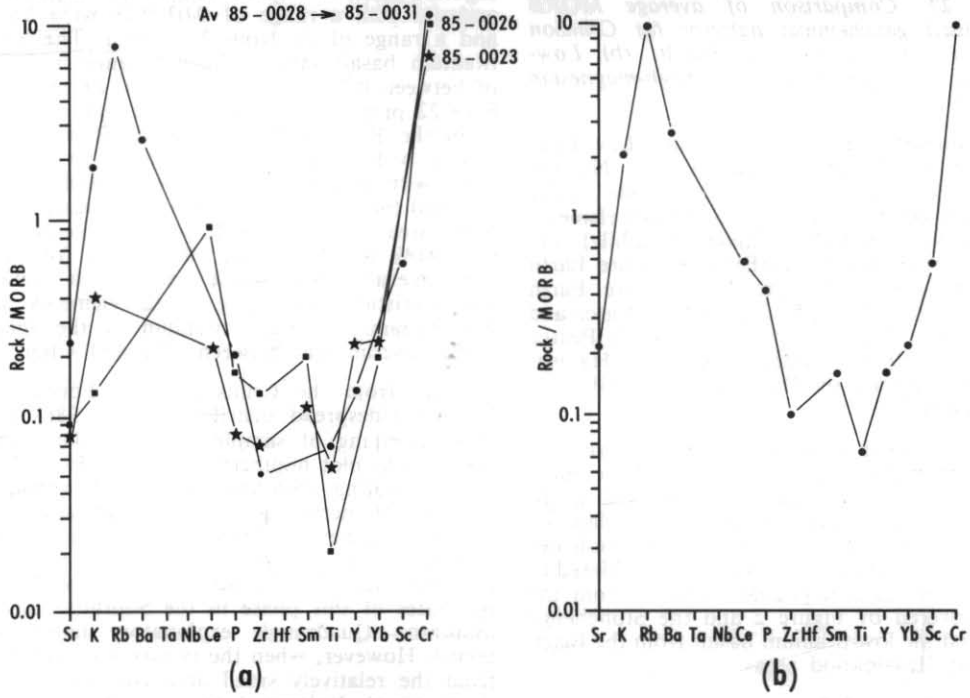

Figure 26. *MORB normalised geochemical patterns for high-magnesian andesite samples. (a) Various patterns (see text); (b) Average pattern.*

5 cm

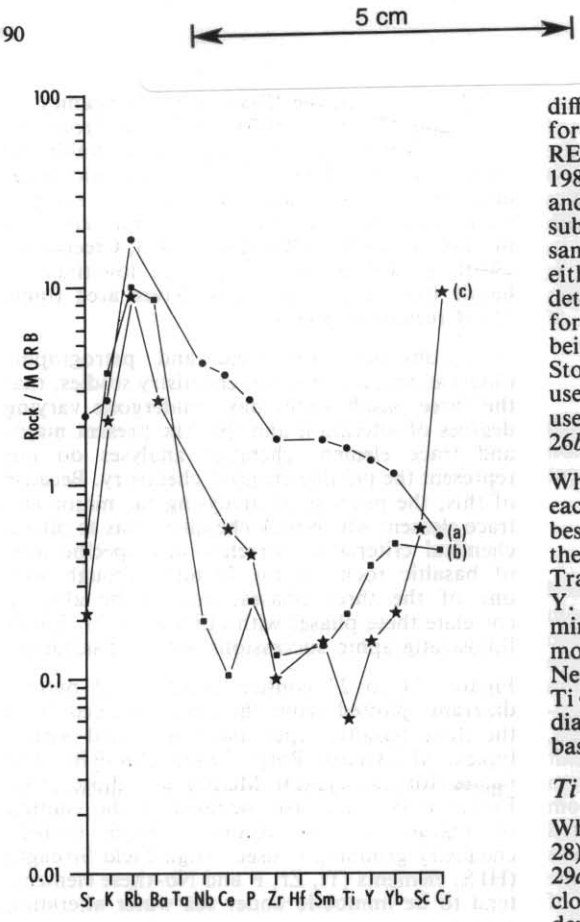

Figure 27. *Comparison of average MORB normalised geochemical pattern: (a) Crimson Creek Formation tholeiitic basalt; (b) Low-titanium tholeiitic basalt; (c) High-magnesian andesite.*

or greenschist facies metamorphism); Low Field Strength (LFS) elements (Rb, Sr, Ba, Na and K–these elements tend to be mobile under alteration conditions); Transition (TE) elements (Cr, Ni, V, Sc and Co–relatively immobile); and Rare Earth Elements (REE): Light Rare Earth Elements (LREE) La-Sm; Heavy Rare Earth Elements (HREE) Eu-Lu and Y (see Pearce and Cann, 1973; Pearce, 1975; Coish, 1977; Pearce and Norry, 1979; Saunders *et al.*, 1980; Hajash, 1984 for reviews on the use and mobility of these elements).

The geochemical patterns (fig. 25–28) were used to decide which elements would be the most use for discriminant diagrams, as well as to check on the field and petrographic correlations: e.g. the Crimson Creek Formation tholeiites from the north and south of the Meredith Granite; the high-magnesian andesite from the areas covered by Figure 2 and the Stonehenge area; and the low-titanium basalt from the Black Hill and Heazlewood areas.

The samples used to obtain the characteristic pattern for each basalt type from each of the different areas, and finally an overall pattern for each type, were those samples for which REE data were available (Waldron and Brown, 1985). Only two samples of high-magnesian andesite were available when the samples were submitted for REE determination and in these samples the values of Rb, Ba and Nb were either lower than detection limit or not determined. In order to obtain a typical pattern for the high-magnesian andesite, a third pattern, being the average of the four samples from the Stonehenge area (85-0028 to 85-0031) has been used in Figure 26*a*, and all nine analyses were used to obtain the type pattern used in Figure 26*b*.

When a comparison of the typical pattern for each of the three phases is made (fig. 27), the best elements to be used as discriminants are the HFS elements (Ti and Zr) as well as the Transition Element Cr, and the REE Ce and Y. As cerium was only determined for a minimum number of samples and is considered mobile under sea water interaction (Sun and Nesbitt, 1978), it was decided to use Ti∿Zr, Ti∿Y∿Zr, and (Cr + Ni)∿Ti discriminant diagrams to correlate and separate the different basaltic types.

Ti∿Zr discriminant diagram

When using Ti and Zr as discriminants (fig. 28), the samples of high magnesian andesite (fig. 29*a*) and low-titanium basalt (fig. 28*b*) define close, but small exclusive fields. The most depleted phase in titanium is the high-magnesian andesite with a range of 0·03–0·18 wt% TiO_2 and a range of Zr from 3–20 ppm. The low-titanium basalt samples have a range in TiO_2 of between 0·20 and 0·57 wt% and Zr of from 8 to 22 ppm. It is noticeable that the samples from the Black Hill and Wandle Road areas have a wider range of TiO_2 content (0·28–0·57 wt%, with an average of 0·38 wt%) and Zr (8–22 ppm) than the samples from the Heazlewood River area (0·20–0·31 wt%, with an average of 0·24 wt% for TiO_2; and 10–17 ppm for Zr), but overall this phase defines a small characteristic field using these elements as discriminants. Overall, titanium is the most useful discriminant between €ba and €bm.

Samples from the Crimson Creek Formation have a widespread distribution (fig. 28*c*) but some grouping of samples from similar areas occurs (e.g. plot numbers 1, 4 and 5; 6–8; 11–14), indicating different phases of volcanic activity with increasing Ti and Zr (and variations in other elements). From field evidence, the increase in Ti, Zr, Nb, etc. occurs up through the sequence. The same trend is found in correlates of this phase in the Smithton Basin (Smithton Quadrangle explanatory notes, in prep.). However, when the twenty-four samples from the relatively small area covered by the 'Deep Creek Volcanics' are plotted (fig. 28*c*), they spread across the whole field defined by

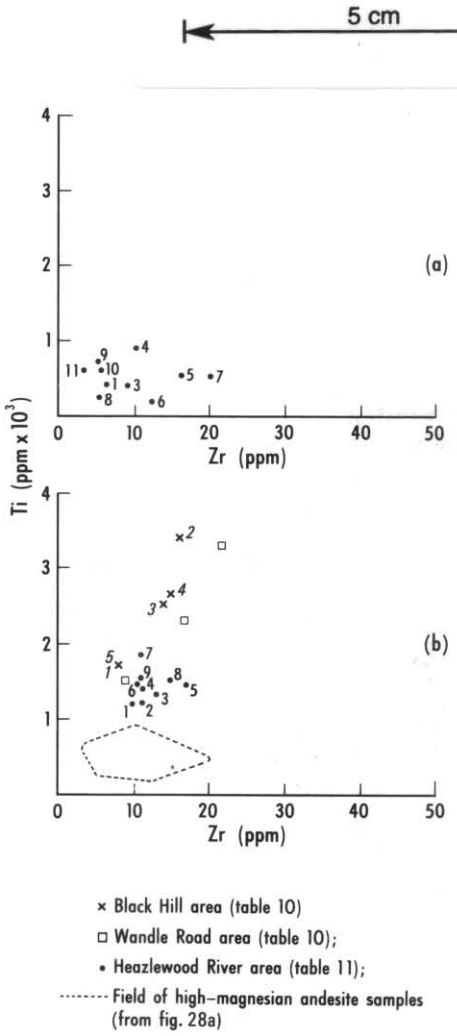

Figure 28. *Ti∿Zr discriminant diagram for: (a) high-magnesian andesite samples (table 9); (b) low-titanium basalts.*

the samples from south of the Meredith Granite, indicating a zone of multiple extrusion. A similar spread occurs with the three basalt samples from a relatively small area along the Wandle Road (Williams and Brown, 1983). Although the samples occupy a large area on this discriminant diagram they form a totally separate field from those defined by €ba and €bm samples, indicating that these elements are useful as discriminants for basalt samples from within the Eocambrian–Cambrian sequences of the Dundas Trough, without any other constraints.

The samples from the Crimson Creek Formation define a narrow band around a uniform relationship between Ti and Zr from 1·00 to 4·74 wt% and 60 to 270 ppm, with the higher values having a greater spread from a linear relationship.

Ti∿Zr∿Y discriminant diagram

Samples from the Crimson Creek Formation form a relatively well-defined cluster on a Ti∿Zr∿Y discriminant diagram (fig. 29*a*), which is often used as a discriminant diagram after Pearce and Cann (1973). When the samples from the Cleveland–Arthur River areas are plotted (fig. 29*b*) an extremely good correlation with the Crimson Creek Formation lavas is obtained and the field defined is only marginally expanded. The samples of €bm (fig. 29*c*) define a broad elongate field with the samples from the Heazlewood River and Black Hill areas occupying two separate parts of the field, but being overlapped by the sample from the Wandle River area. The €ba samples show an almost random distribution (fig. 29*d*), and some of the samples overlap the field defined by the €bm samples. As the values for the high-magnesian andesite samples are near detection limit and a change of a few ppm will drastically change the ratios of the elements, this diagram is not considered useful for discriminating between €ba and €bm phases.

(Cr+Ni)∿Ti discriminant diagram

The use of chromium, nickel and titanium as discriminants again shows the tendency for samples from the Crimson Creek Formation (fig. 30*a*) and correlates in the Cleveland–Arthur River area (fig. 30*b*) to cluster in a well-defined field. The grouping into three separate tight parts of the overall field of samples from the 'Deep Creek Volcanics' probably indicates three different batches of magma. This clustering can also be observed when only Ti and Zr are used as discriminants (fig. 28*c*). The low-titanium basalt (€bm) (fig. 30*c*) and high-magnesian andesite samples (fig. 30*d*) also form two distinctive fields, giving a second definitive discriminant diagram on which to distinguish different basaltic areas from within the Dundas Trough.

Although Cr content is affected by clinopyroxene fractionation and Ni by olivine fractionation, these elements are added in this case to accentuate the high chrome and nickel content of €ba with respect to Eccb and €bm, and to differentiate between €ba and €bm when their Ti contents are very close.

Rare Earth Element chemistry

REE analyses by Radiochemical Neutron-Activation (RNAA) were obtained for eleven of the fourteen samples from the Crimson Creek Formation correlate at Cleveland (Waldron and Brown, 1985). Instrumental Neutron Activation Analyses (INAA) were obtained for three samples. Of the fourteen samples, three were selected from the extended type area of the Crimson Creek Formation (85-0001, 85-0002, and 85-0004; fig. 31*a*), three from the Cleveland area (48302, 48332, and 48333; fig. 31*b*); three

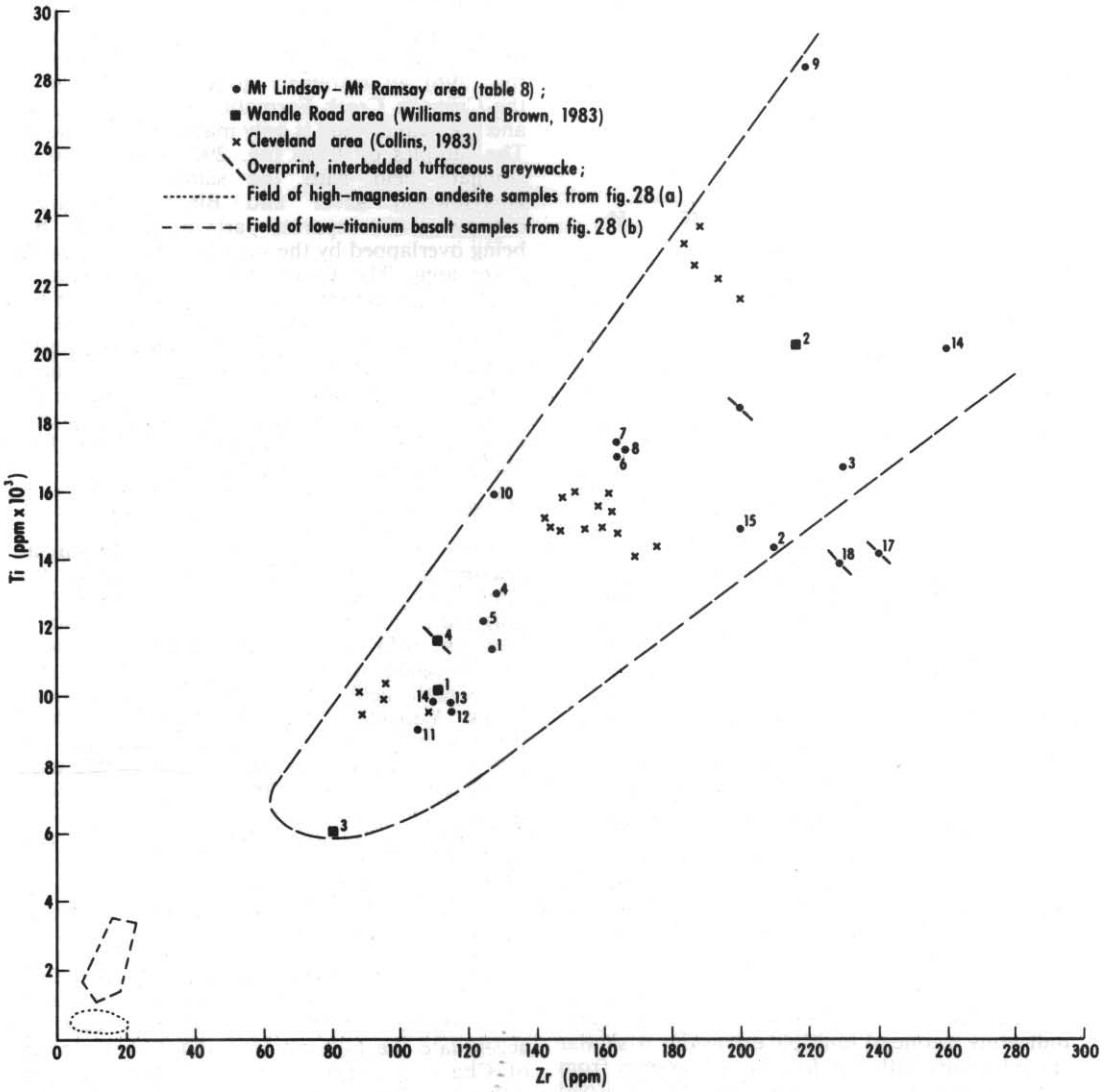

Figure 28c. *Ti∿Zr discriminant diagram for basalt samples from the Crimson Creek Formation and correlates in the Dundas–Waratah region.*

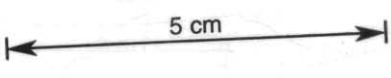

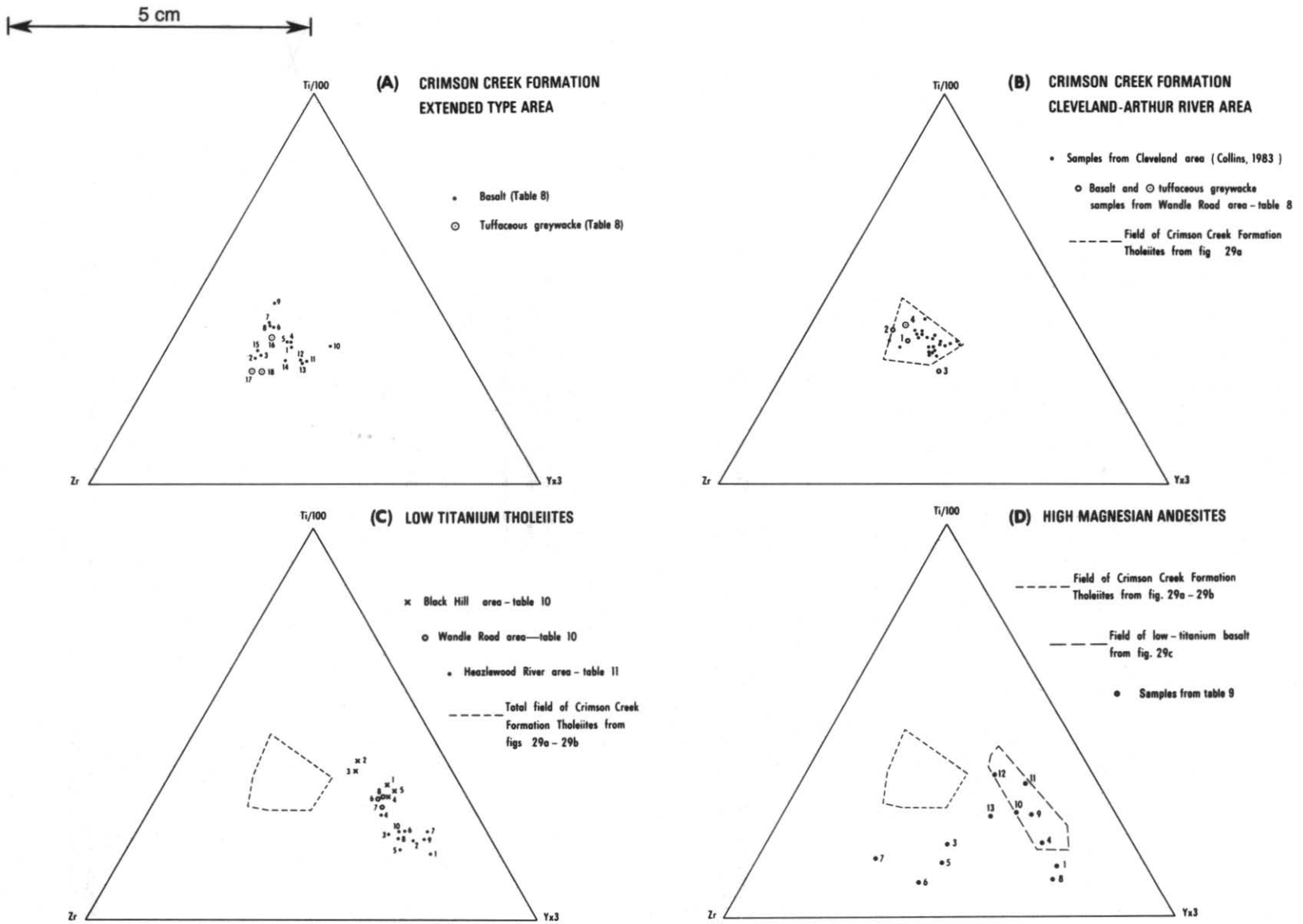

Figure 29. *Ti∿Zr∿Y discriminant diagrams, Dundas Trough basaltic rocks.*

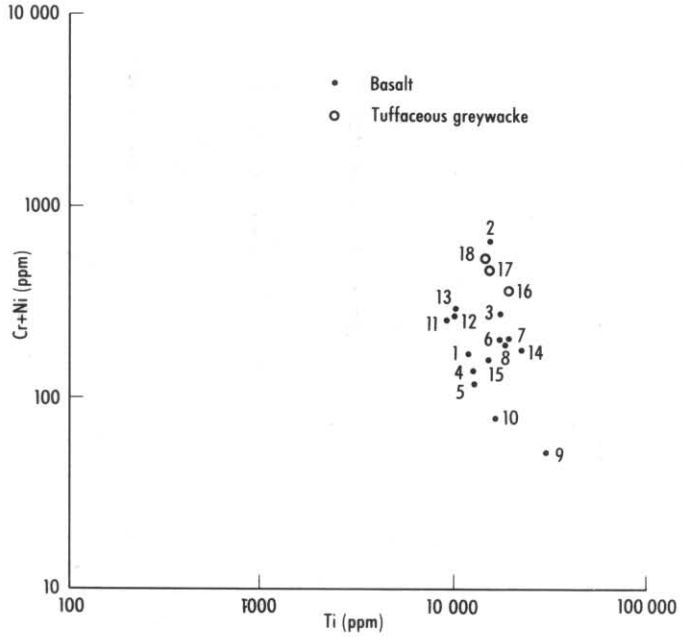

Figure 30*a*. *(Cr + Ni)∿Ti discriminant diagram of Crimson Creek Formation tholeiite samples from the extended type area. Analyses Table 8.*

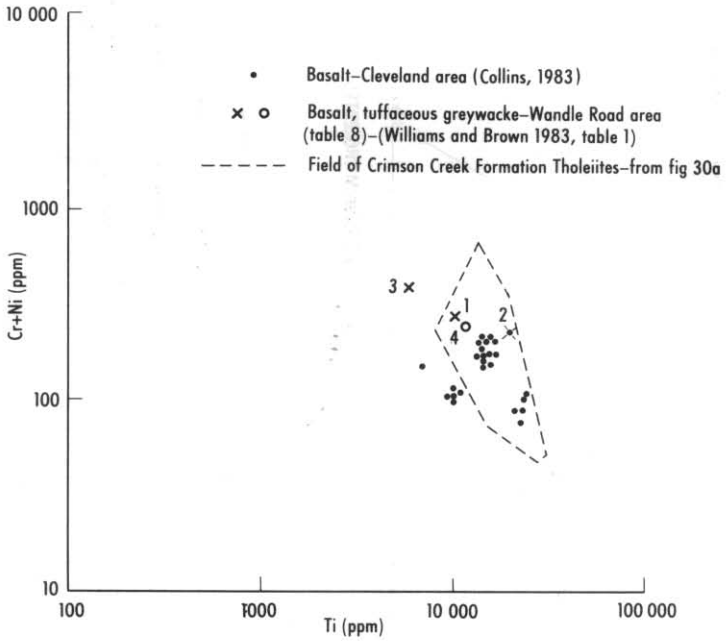

Figure 30*b*. *(Cr + Ni)∿Ti diagrams for samples from Crimson Creek Formation correlates in the Cleveland–Arthur River area.*

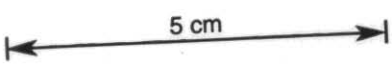

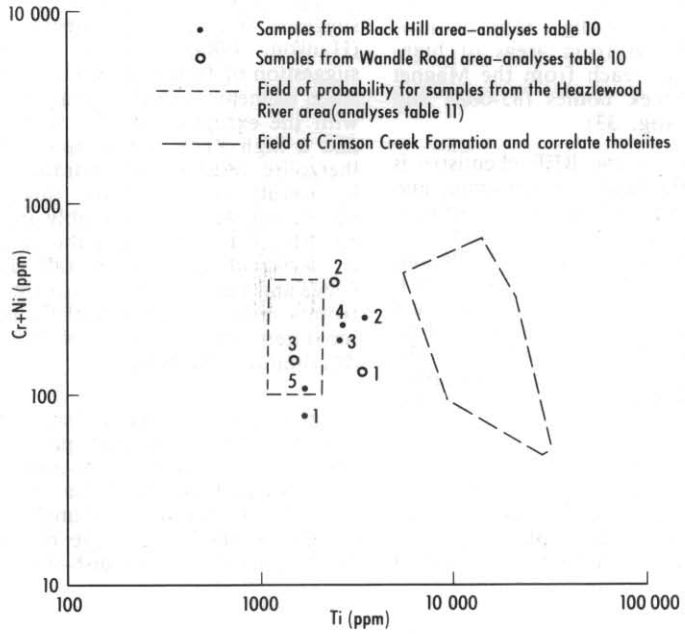

Figure 30*c. (Cr + Ni)∿Ti discriminant diagram for low-titanium basalt samples.*

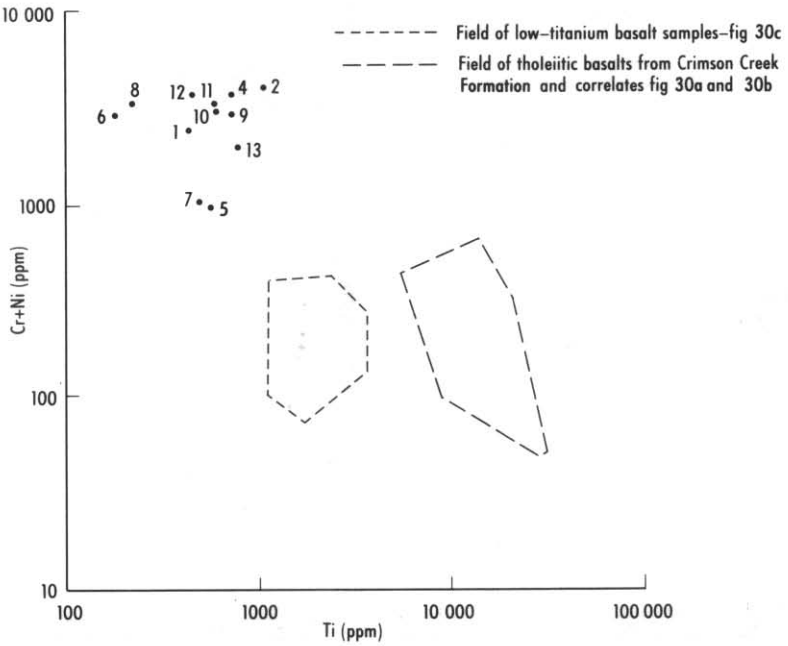

Figure 30*d. (Cr + Ni)∿Ti discriminant diagram for high-magnesian andesite samples (analyses table 9).*

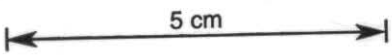

each from the Black Hill (85-0032, 85-0033, 85-0034; fig. 32*a*) and Heazlewood River areas (60900, 60903, and 60919; fig. 32*b*) of low-titanium basalt; and two from areas of high-magnesian andesite, one each from the Magnet and Thirteen Mile Creek bodies (85-0025 and 85-0023) respectively (fig. 33).

The dominant feature of the REE chemistry is that it supplements the field, petrographic, and major and trace element chemistry in defining three distinctive basaltic phases within the Eocambrian–Cambrian successions in the Dundas Trough. As the chondrite-normalised REE patterns from the different areas of each phase are so similar, the patterns are considered to represent the original magmatic character of the different phases, with minor secondary alteration characteristics, and not an imposed pattern due to later alteration.

The oldest of the three phases, the Crimson Creek Formation tholeiite, has parallel chondrite-normalised REE patterns and a high overall abundance of REE indicating, along with the HFS element contents, derivation from a relatively enriched fertile mantle source. The HREE depleted character of these samples suggests retention of garnet in the residue (Hanson, 1980). This is consistent with the suggestion of Pearce (1980) that lavas with higher trace element contents, relative to MORB, but with the exception of Yb, Sc and Cr (fig. 28), and a high Zr/Y are compatible with a garnet lherzolite residue. The parallelism, yet change in overall content of the three samples from the Cleveland area, probably indicates different batches of melting from the same source. This is consistent with the overall chemistry of the Cleveland samples, as each of the patterns comes from a sample from each of the different clusters separated on the $(Cr+Ni)\sim Ti$ and $Ti\sim Zr$ discriminant diagrams.

Of the two high-magnesian andesite samples, the chondrite-normalised pattern for 85-0023, having a concave or dish-shaped REE pattern, is considered to be closer to the magmatic pattern than the more strongly LREE enriched sample (85-0025) from the mineralised zone in the Magnet mine. The dish-shaped REE pattern

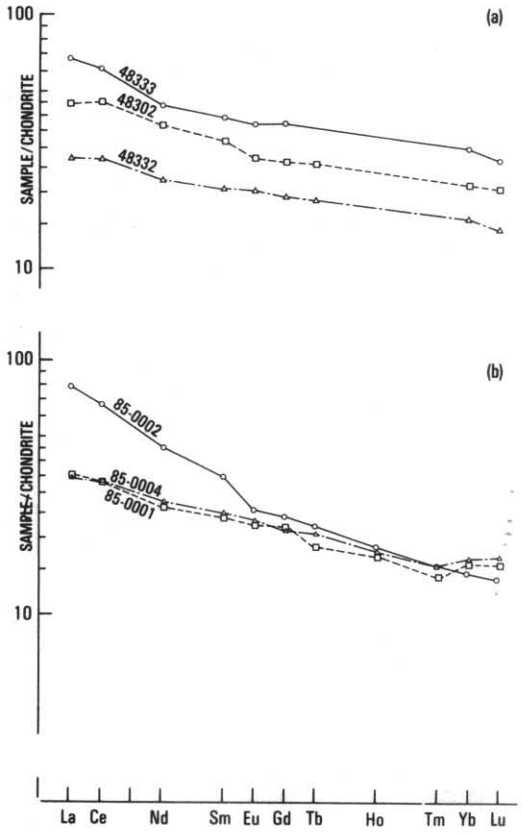

Figure 31. *Chondrite-normalised REE patterns for Crimson Creek Formation tholeiitic basalts. (a) Cleveland area; (b) Mt Lindsay area.*

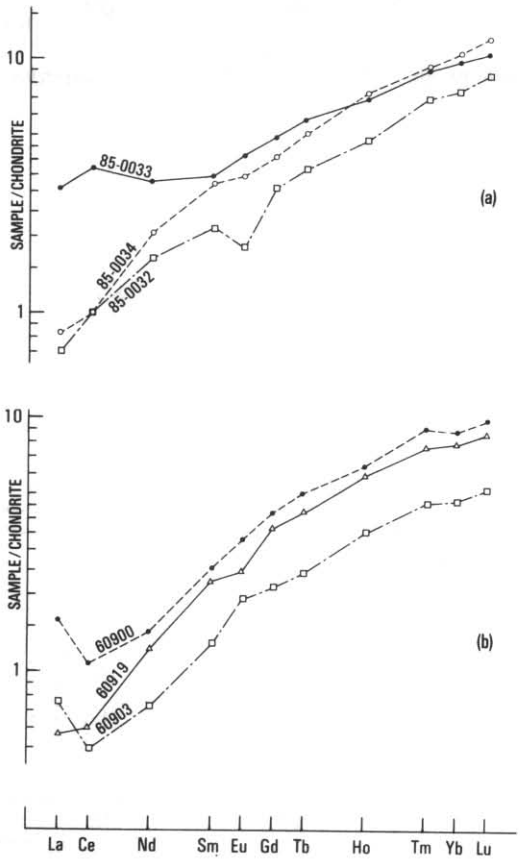

Figure 32. *Chondrite-normalised REE patterns for low-titanium tholeiite. (a) Black Hill area; (b) Heazlewood River area.*

5 cm

is characteristic of high magnesian andesite samples from other areas (e.g. Cape Vogel; Jenner, 1981), and combined with a low CaO/Al_2O_3 ratio (0·55), low TiO_2 and highly refractory chrome spinel grains, indicates that these lavas were probably derived from a depleted mantle source by a second-stage melt (Duncan and Green, 1980; Jenner, 1982).

The chondrite-normalised REE patterns for the low-titanium basalt samples from the Black Hill and Heazlewood River areas are all LREE depleted, which, along with their overall low HFS element content, suggests derivation by partial melting from an extremely depleted source, possibly one which had already produced the Crimson Creek Formation tholeiites and high-magnesian andesite phases. The La enrichment of the samples from the Heazlewood River area is considered to be due to secondary reactions, probably with sea water, and not a reflection of the original magmatic character. Negative Eu anomalies, as shown by 85-0032, are usually associated with shallow crustal fractionation of plagioclase. If this is the case for this sample, it indicates that any crustal cumulate derived from 85-0032, in the Black Hill area, would have plagioclase as well as pyroxene and olivine(?) as a phase. Sun and Nesbitt (1978) have also recorded Eu as being mobile under certain conditions and giving both negative and positive anomalies. The higher LREE content in sample 85-0033 is also considered to be due to secondary alteration, as the overall consistency and near parallelism of the samples from both areas indicates a common parent which produced a basaltic phase with a chondrite-normalised REE pattern typified by sample 85-0034. All three samples from the Black Hill area are of fine-grained basalt and demonstrate the range of REE content of this basaltic phase. The samples from the Heazlewood River area were chosen such that a range of patterns would be obtained if the patterns varied with the range of grain size of the flows in this area. Due to the freshest samples available being used for REE determination, the three samples analysed came from different flows, but sample 60919 is a pillow basalt; 60900 a medium-grained basalt ('dolerite' of Creenaune, 1980) and 60903 a very coarse-grained basalt ('coarse dolerite' of Creenaune, 1980). The first two samples (60919 and 60900) are very similar in overall REE abundances to the fine-grained

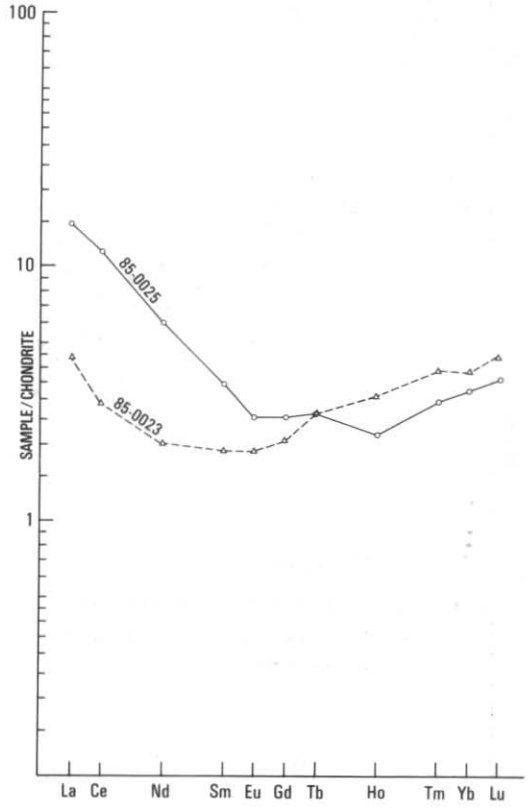

Figure 33. *Chondrite-normalised REE patterns for high-magnesian andesite.*

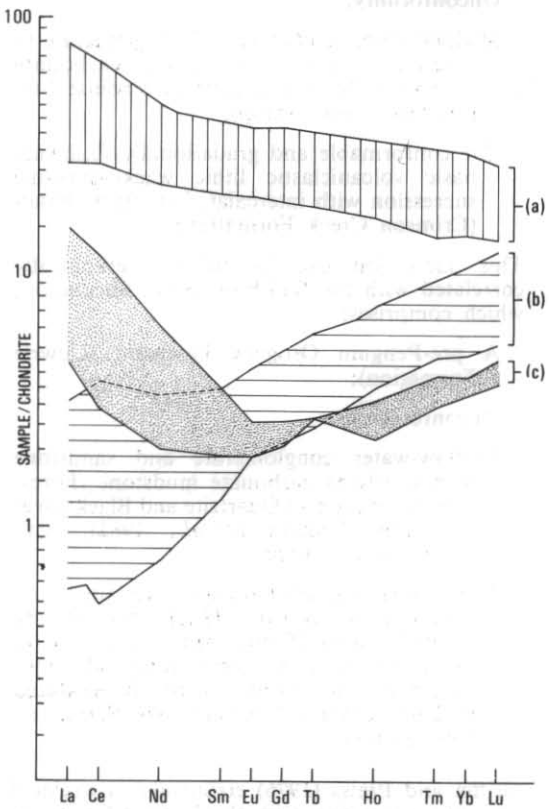

Figure 34. *Comparison of chondrite-normalised REE patterns for Dundas Trough samples: (a) Crimson Creek Formation tholeiite; (b) Low-titanium tholeiite; (c) High-magnesian andesite.*

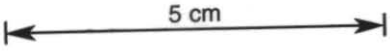

basalt samples from the Black Hill area, whereas the coarser-grained sample (60903) represents a more slowly cooled and more differentiated part of a flow.

CORRELATION–WITHIN TASMANIA

No evidence has so far been obtained to suggest that the middle Middle Cambrian low-titanium basalt (Ꞓbm) occurs anywhere else in Tasmania other than in the Dundas Trough. Similarly, lavas of high-magnesian andesite are so far only known from the Dundas Trough. The only volcanic phase which is known to have a lithostratigraphic correlate outside the Dundas Trough is the Crimson Creek Formation tholeiite (Eccb).

Numerous authors have commented on the lithological similarity of the Crimson Creek Formation and the volcano-sedimentary succession in the Smithton Basin.

The Dundas Trough succession consists of:

A pre-Penguin Orogeny basement, the Oonah Formation;

Unconformity;

Shallow-water sandstone and conglomerate to siliceous siltstone mudstone carbonate succession with Eocambrian stromatolites (Success Creek Group);

The conformable and gradationally following basic volcaniclastic lithic wacke–siltstone succession with intercalated tholeiitic basalt (Crimson Creek Formation);

This succession can be lithostratigraphically correlated with the Smithton Basin Succession, which comprises:

A pre-Penguin Orogeny basement (Cowrie Formation);

Unconformity;

Shallow-water conglomerate and sandstone with overlying carbonate mudstone (Forest Conglomerate and Quartzite and Black River Dolomite; Lennox *et al.*, 1982), with stromatolitic breccia.

This sequence is gradationally overlain in the Forest area (Brown, 1985), and in the Trowutta area (Griffin and Preiss, 1976), by a volcaniclastic lithic wacke–siltstone–mudstone succession with intercalated tholeiitic basalt (Crimson Creek Formation correlate).

Griffin and Preiss (1976) erroneously correlated the latter succession with the Dundas Group on the basis of a late Middle Cambrian fauna (Gulline, 1959; Jago and Buckley, 1971) which occurs in " . . . sedimentologically similar sequences . . . ten kilometres to the west at Christmas Hills".

The tholeiitic basalts within the correlate of the Crimson Creek Formation in the Smithton Basin (Smithton Explanatory Report, in prep; Griffin, 1974) are petrographic and chemical correlates of the tholeiitic basalt from the Crimson Creek Formation and correlates, as described in this study and by Collins (1983). Olivine phyric tholeiite lavas occur in the lower part of the volcanic sequence in the Smithton area, with a range of TiO_2 from 0·60 to 0·70 wt%, and with higher Mg, Cr and Ni contents than those obtained from samples in the pyroxene/plagioclase phyric lavas (Brown, 1985; Smithton Explanatory Report, in prep.). Similar low TiO_2 aphyric lavas were described from the lower part of the sequence in the Trowutta area by Griffin (1974).

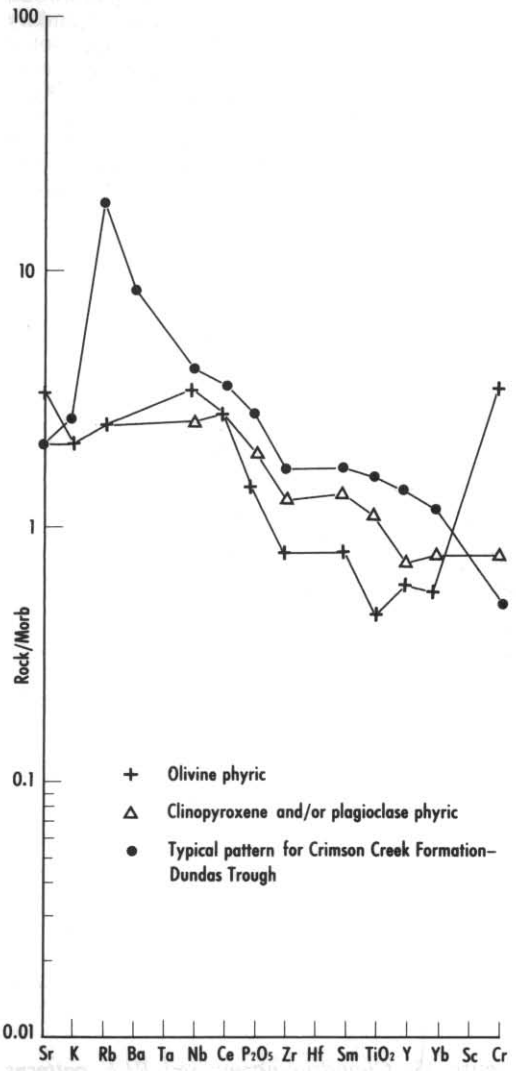

Figure 35. *Geochemical pattern of Crimson Creek Formation correlate basalt in the Smithton Basin.*

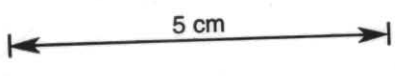

The geochemical patterns for the olivine and pyroxene/plagioclase lavas from the Smithton area are very similar to the typical pattern obtained from the samples of the Crimson Creek Formation and correlates (fig. 35), with the exception of the Rb and Ba peak, which pervades all lavas in the Dundas Trough irrespective of basalt type (fig. 24–27), and which is considered to be an alteration feature. The pattern for the olivine phyric lavas (fig. 35) also shows a high chromium content. The more primitive nature of these lavas in comparison to the pyroxene/plagioclase phyric lavas is shown by the higher Cr and Ni contents and the lower overall content of HFS elements (Ti, Y, Zr, Nb, P).

On a Ti∿Zr discriminant diagram (fig. 36) the pyroxene/plagioclase phyric and associated aphyric samples fall within the field defined by the samples from the correlates in the Dundas Trough, with the olivine phyric samples from the Smithton area, and the low TiO_2 aphyric samples from Trowutta, forming a smaller separate field. The samples with the lower Ti, Zr and Nb contents are towards the base of the succession and these elements increase in lava flows up through the pile.

Similarly, when the samples are plotted on a Ti∿Y∿Zr discriminant diagram, all samples, with the exception of two from Trowutta which only just fall outside, fall within the field defined by the Dundas Trough samples (fig. 37).

On the (Cr + Ni)∿Ti discriminant diagram (fig. 38), the pyroxene/plagioclase and associated aphyric samples occupy the same field as the Dundas Trough samples, with the olivine phyric samples from the Smithton area and two of the 'aphyric' lavas from the Trowutta area defining a separate field. Four of the aphyric lavas from the Trowutta area, with TiO_2 contents similar to the olivine-bearing lavas, have significantly lower Cr and Ni values, probably reflecting both olivine and pyroxene fractionation, and extend the field defined by the Dundas Trough samples, but not to the extent where they overlap with one of the other phases.

The patterns obtained from chondrite-normalised REE data (Waldron and Brown, 1985) for the pyroxene/plagioclase lavas are very similar to the patterns formed by the samples from the Crimson Creek Formation tholeiite and correlate samples (fig. 39*a*). Patterns for the olivine phyric

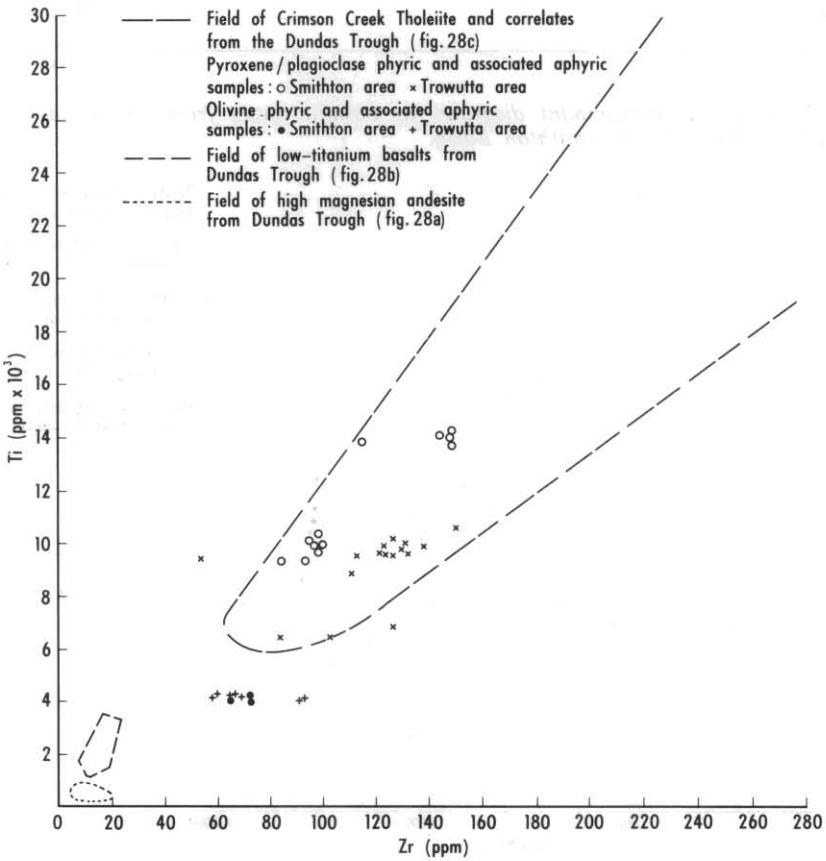

Figure 36. *Ti∿Zr discriminant diagram for basaltic rocks from within Crimson Creek Formation correlates in the Smithton Basin.*

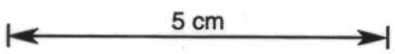

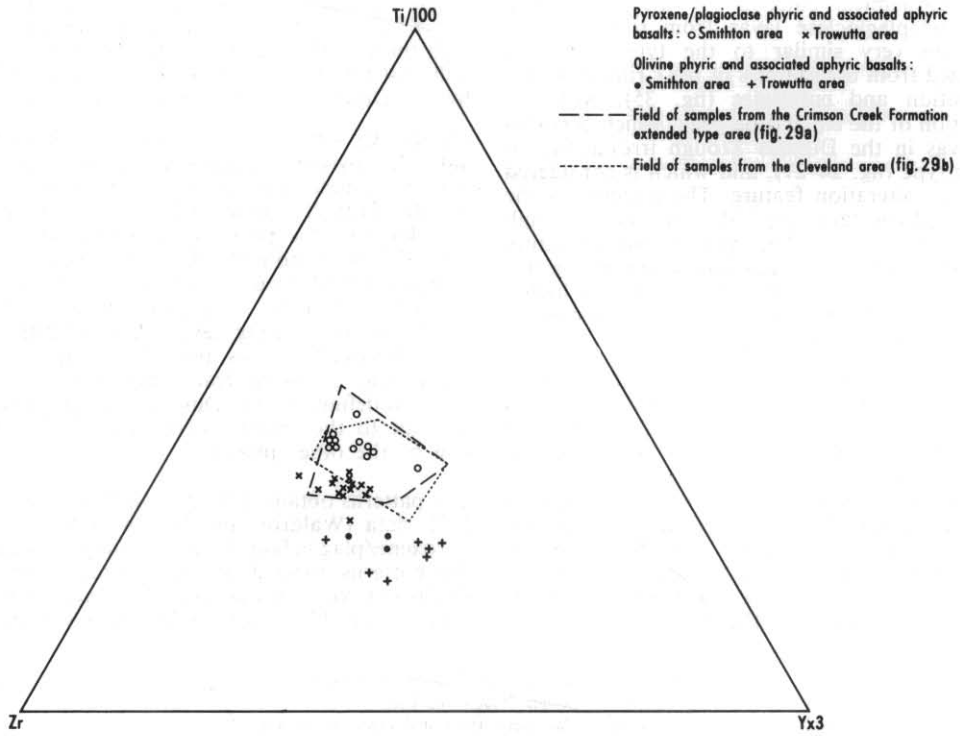

Figure 37. *Ti∿Y∿Zr discriminant diagram for basaltic rocks from within the Crimson Creek Formation correlates in the Smithton Basin.*

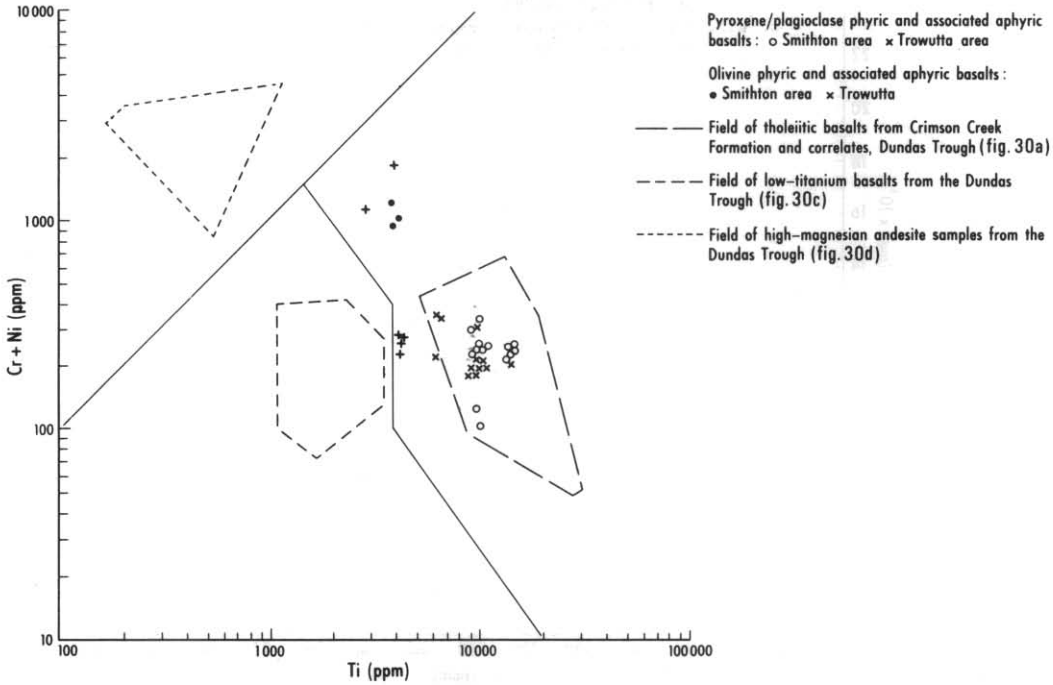

Figure 38. *(Cr+Ni)∿Ti discriminant diagram for basaltic rocks from within the Crimson Creek Formation correlates in the Smithton Basin.*

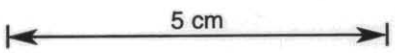

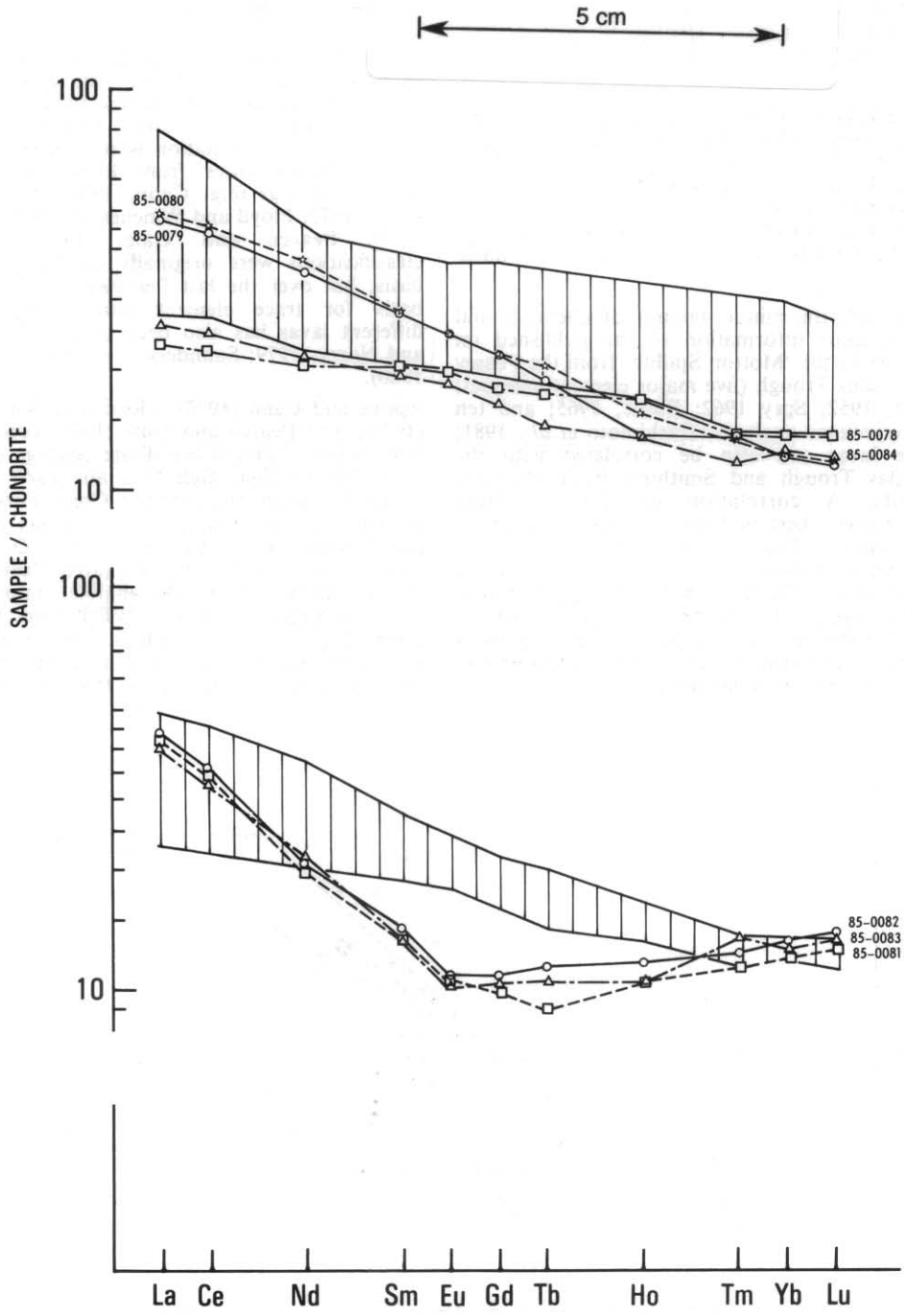

Figure 39. *Chondrite-normalised REE patterns for tholeiitic basalts from Smithton area. (a) Patterns for plagioclase/pyroxene phyric samples, with field defined by Crimson Creek Formation tholeiitic basalts; (b) Patterns for olivine phyric samples, with field defined by plagioclase/pyroxene phyric samples.*

lavas are concave, but have a similar abundance of light and heavy end-member rare earth elements with a lower abundance of mid-range REE than the pyroxene/plagioclase lavas (fig. 39*b*).

The chemical correlation of the tholeiitic basalts from within the lithostratigraphically similar sequences in the Dundas Trough and Smithton Basin increases the probability of the overall correlation to such an extent that a one to one relationship between the Eocambrian successions of the Dundas Trough and Smithton Basin exists.

Even with the minor amount of chemical and petrographic information so far published on samples of the 'Motton Spillite' from the Fossey Mountains Trough (five major element analyses; Scott, 1952; Spry 1962; Burns, 1965; and ten clinopyroxene analyses, Hashimoto *et al.*, 1981) these lavas can also be correlated with the Dundas Trough and Smithton Basin tholeiitic basalts. A correlation of the associated Barrington Chert and the calcareous phases of the Success Creek Group and Black River Dolomite, which underlie the volcaniclastic successions in the Dundas Trough and Smithton Basin respectively, further elucidates a pattern of Eocambrian sedimentation and volcanism during Eocambrian times in the north-west and western parts of Tasmania.

CORRELATION–DIFFERENT TECTONIC SETTINGS

Immobile trace elements (particularly HFS) have been used over the last fifteen years in an attempt to discriminate between basaltic rock suites and to correlate those suites whose tectonic environment of formation were unknown, with similar basalt suites from known Cainozoic tectonic settings (e.g. Cann, 1970; Pearce and Cann, 1973; Floyd and Winchester, 1975; Coish, 1977; Pearce and Gale, 1977). These classifications were originally on an empirical basis, but over the last few years a theoretical basis for trace element partitioning within different lavas has also been used (e.g. Pearce and Norry, 1979; Saunders *et al.*, 1980; Pearce, 1980).

Pearce and Cann (1973), Floyd and Winchester (1975), and Pearce and Gale (1977) considered that basalts from Within-Plate settings can be recognised by their high Ti/Y and Zr/Y ratios. When data from the Crimson Creek Formation tholeiites and correlates in the Dundas Trough and Smithton Basin are plotted on a Zr/Y∿Zr discriminant diagram (fig. 40) (after Pearce and Norry, 1979), 65% of the eligible samples fall in the Within-Plate Basalt (WPB) field. Of the remaining 35%, two-thirds are from the Cleveland area and these fall in the mixed WPB and Mid-Ocean Ridge Basalt (MORB) field.

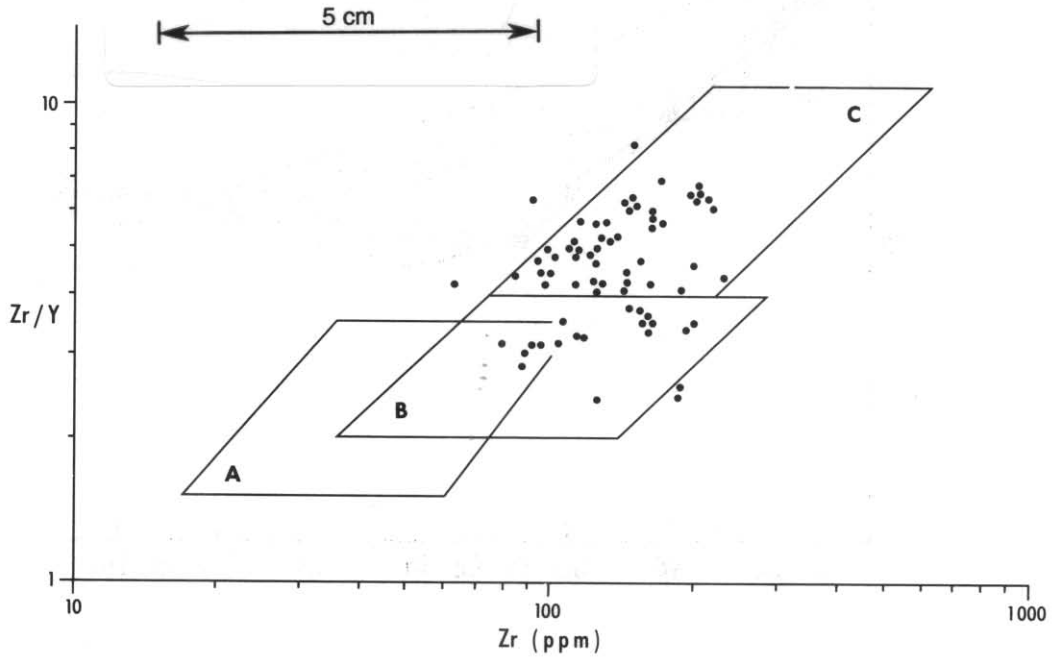

Figure 40. *Zr/Y∿Zr discrimination diagram (after Pearce and Norry, 1979) showing plot of Crimson Creek Formation and correlates tholeiitic basalt samples. Field A = Island arc tholeiite; Field B = Mid-ocean ridge basalt; Field C = Within Plate basalt.*

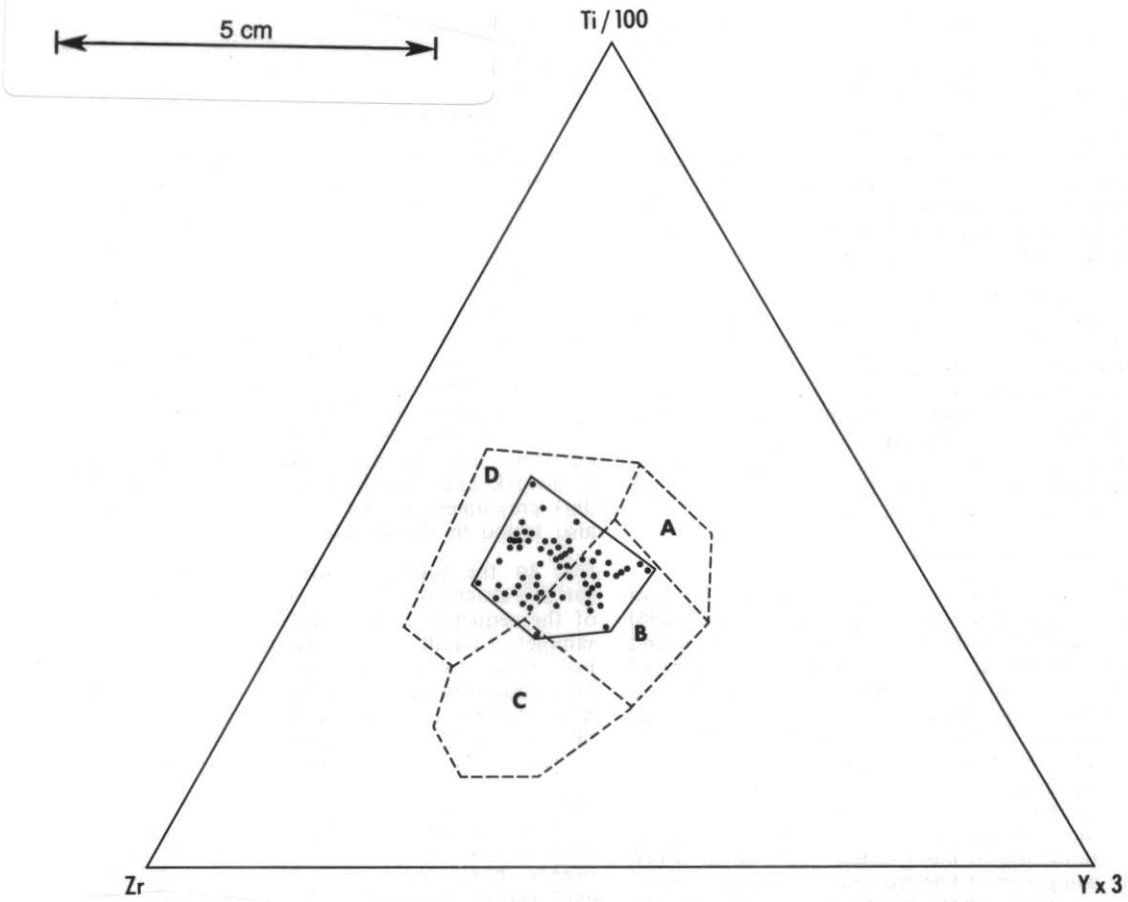

Figure 41. *Ti∿Y∿Zr discrimination diagram with tholeiitic basalt samples from within the Crimson Creek Formation and correlates in the Dundas Trough and Smithton Basin. Field A–D after Pearce and Cann (1973).*

A and B = Low potassium tholeiite

B and C = Calc-alkali basalt

B = Ocean Floor basalt

D = Within Plate basalt

On a Ti∿Y∿Zr discriminant diagram (fig. 41), following the procedure of Pearce and Cann (1973), the field defined by the Crimson Creek Formation tholeiites corresponds almost equally to areas of WPB and Ocean-Floor Basalts, but when individual samples are considered, 62% of the sixty-nine samples fall in the WPB field. This 62% is made up of 67% of the fifteen samples from the extended type area; 38% of the twenty-four Cleveland samples; 67% of the three samples from Wandle Road; 92% of twelve samples from Smithton, and 73% of fifteen samples from Trowutta. This overlap into the Ocean-Floor Basalt field could be due to an inherent weakness in the Ti∿Y∿Zr diagram (Holm, 1982), which tends to place some tholeiites from initial spreading/rifting centres in the Ocean-Floor field irrespective of whether they possess continental or oceanic characteristics.

When the MORB-normalised geochemical patterns are considered, the pattern for the Crimson Creek Formation tholeiite has higher overall trace element contents, relative to MORB, with the exception of Yb, Sc, and Cr. This type of pattern, according to Pearce (1980), indicates a Within-Plate setting with garnet lherzolite residium. The garnet lherzolite residium is consistent with the depleted HREE chondrite-normalised patterns which these lavas contain.

With the use of purely chemical data, correlation of the Crimson Creek Formation tholeiite suite with different tectonic environments has an overall probability of 60-70% for a Within-Plate setting. The samples from the Smithton Basin are proven to have extruded through Precambrian basement and deposited on top of shallow water terrigenous successions. In the Dundas Trough a similar environment existed

with the added presence of an unstable tectonic environment before extrusion of the first volcanic phase, probably indicating intracontinental rifting. It is suggested that the tectonic setting of the Dundas Trough and Smithton Basin during the Eocambrian–Cambrian mafic volcanic phases was a Within-Plate continental setting and that the use of a purely chemical correlation without lithostratigraphic control for the Tasmanian Eocambrian–Cambrian basaltic phases could be misleading.

This suggestion is strengthened by data presented in another recent study (Withnall, 1985) where lavas similar to the Crimson Creek Formation tholeiites are recorded. When plotted on some geochemical discrimination diagrams, the lavas are similar to modern mid-ocean ridge basalts (MORB) but in the field they are conformably underlain and overlain by shallow-water sediments interpreted to have been deposited on a shelf or in an epicontinental sea.

Precambrian basalt

Numerous bodies of glassy amygdaloidal lava and breccia [the 'melaphyre' of Thomae (1896) and others; or the 'spilite' of Twelvetrees and Ward (1910) and later workers] are associated with the siliceous siltstone, mudstone and dolomite successions of the 'upper' Oonah Formation in the areas around the Western, Oonah, Montana and Queen mines, and underground in the Spray and Grubb mines, in the Zeehan area. The breccia members of this volcanic phase are reported to range from coarse conglomerate to fine-grained 'tuff', all of which are composed of basaltic material (Montgomery, 1893*b*; 1895; 1896; Twelvetrees, 1901). In the Queen, Oonah and Western mines, the volcanic units are conformably enclosed within the sedimentary strata. The lavas are usually highly altered and carry a tectonic fabric.

Thomae (1896) recognised rocks of a volcanic origin within the strata of the Zeehan area, and he described these rocks as being " . . . a greenish-grey, or in some places dark green, hard amygdaloidal rock, weathering to a soft red or yellow earth, the cavities being filled with delessite (a chlorite mineral), siderite, calcite, and rarely with quartz. It gets very hard at a depth of a few hundred feet, where it is less decomposed. Here it apparently consists chiefly of altered plagioclase and augite with its characteristic decomposition products, and both physical and chemical characteristics point to its being a melaphyre."

Waller (1902) reported that in the Western mine "The prevailing rocks . . . consist of . . . slates, limestone and sandstone interbedded with tuff and flows of vesicular melaphyre". Numerous horizons of " . . . tuff and melaphyre . . . were intersected in the mine workings, the largest unit of which was up to 400 feet [120 m] thick in the centre and lensed out on either side".

Hills and Carey (1949) described a part of this sequence in the Montana area and called the succession the 'Montana Melaphyre Volcanics' after the term applied to the volcanic rocks by Thomae (1896) and Twelvetrees (1897).

King (1961) records " . . . amygdaloidal spilite enclosing large fragments of slate". The lava was described by King as consisting of vesicular glass and scoriaceous material with the cavities being filled with calcite, chlorite and cryptocrystalline silica.

Blissett (1962) noted that the upper part of the Oonah Formation was of a finer grain than the lower part and that 'spilitic' lava flows and 'pyroclastic' bands occur within the upper part of the formation near Zeehan. He reported that these lava units are associated with bedded limestone and dolomitic limestone around the Comstock and Oonah mines, and that similar dark grey limestone and dolomitic limestone was also found in the Dundas area.

Due to the highly weathered nature of the surface outcrops of the lava flows and reports of the sequence being 'harder' at depth, seven samples of basaltic rocks from the 'upper' Oonah Formation were obtained from drill-hole intersections in the Oonah Hill area [CP595625]; three samples (table 12, analyses 1–3) are from the western end and the other four (table 12, analyses 4–7) are from the eastern end.

The seven samples selected for analysis were the freshest available, based on hand-specimen examination, being core material selected from twenty bore holes available from different exploration companies. Petrographically the samples are very similar in both areas. They have a similar range in grain size and the samples from the western end of Oonah Hill are highly vesicular. In thin section, the grain size ranges from 0·1–0·25 mm for fine-grained samples, 0·25–0·50 mm in medium-grained samples and 0·45–1·35 mm in the coarse-grained samples. The grain size measurements were made on the length of the plagioclase laths in both the vesicular and non-vesicular lavas. The samples consist of an irregular latticework of interlocking plagioclase laths, the interstices of which are filled with glass and acicular magnetite grains. Vesicles and fractures are filled with carbonate, quartz, cryptocrystalline silica, and a pale-green isotropic mineral. The plagioclase laths are replaced by sericite and quartz. Areas of glass are now replaced by chlorite, and the magnetite by leucoxene. Carbonate, which from the bulk rock analysis is probably dolomite, pervades all samples to varying degrees. One sample (analysis 7) contains remnant outlines of stubby subhedral to broken skeletal euhedral microphenocrysts (0·22–0·45 mm diameter) which, on remnant grain outlines, were probably olivine.

On petrographic evidence, the samples found in the Pieman River and Misty Valley areas (p. 13), as well as detritus found within the coarser

clastic rocks of the Success Creek Group (p. 25–29) are consistent with having been derived from this phase of volcanic activity.

CHEMISTRY

The three samples from the western side of Oonah Hill and one sample from the eastern side (table 12, analyses 1–4) are highly altered but still contain the characteristics defined by the less altered samples from the eastern end (table 12, analyses 5–7). The latter are characterised by high Al_2O_3, TiO_2, Zr and Nb contents and low CaO. The low CaO content is most probably due to leaching of Ca from the rocks, and indicates that the carbonate present is dolomite. All samples, irrespective of their state of alteration, are high in Al_2O_3, possibly reflecting the original nature of the lavas, but may also reflect metosomatic changes.

Although the number of samples is small and the lavas are altered, the chemical analyses obtained are distinctive enough, and differ from any of the Eocambrian–Cambrian basaltic phases, to enable classification on their chemical characteristics. Using the MacDonald and Katsura (1964) dividing line for alkali and tholeiitic basalts, the least altered lavas are mildly alkaline. An average analysis (table 12, analysis 8) obtained from the recalculated anhydrous values of the least altered analyses (table 12, analyses 5–7) has quartz, corundum, orthoclase, anorthite, albite, hypersthene, ilmenite and apatite as normative minerals, defining the analysis as a quartz tholeiite on the criteria of Green (1970). This classification is considered misleading due to the low calcium and possibly high alumina content. A recalculated analysis with an equal amount of CaO and MgO, as is approximately the case with most mildly alkaline basalts, gives an olivine-hypersthene normative compostion indicating an olivine basalt (Green, 1970), which is consistent with petrographic evidence. The most probable composition of the original lavas in the 'upper' Oonah Formation is of a high-alumina, mildly alkaline olivine basalt with high Ti, Zr and Nb.

Summary

EOCAMBRIAN–CAMBRIAN BASALT SUCCESSIONS

CRIMSON CREEK FORMATION THOLEIITE (Eccb)

Basaltic rocks from within the Crimson Creek Formation and correlates in the Dundas Trough are clinopyroxene (chromium-bearing augite) and/or plagioclase (labradorite) phyric lavas which are both qtz-hy (25 of 42 samples) and ol-hy (16 of 42 samples) normative. One sample from the Cleveland area is ol-ne normative. The number of qtz-hy to hy-ol normative samples from the extended type area is 10:5; in the Cleveland area 13:10; and 2:1 in the Wandle Road area.

Chemically the lavas are characterised by SiO_2 contents of between 44 and 51 wt%; TiO_2 >1·0 wt%; MgO between 3·5 and 8·5 wt%; Zr >60 ppm; Y > 20 ppm and Nb > 5 ppm. The 100Mg/Mg + Fe^{2+} ratio (Mg* number) has a range of 33 to 61 and an average of 49. The Mg* number differs between areas, ranging from 33 to 61 with an average of 49 for fifteen samples from the extended type area; 37 to 52 and an average of 47 for twenty-three samples from the Cleveland area; and 52 to 65 and an average of 59 for three samples from Wandle Road.

The tholeiites have a high total REE content and chondrite-normalised patterns show LREE enrichment, with (La/Yb)N = 1·3–3·5. In both the Dundas Trough and the Smithton Basin, lavas of this phase of volcanism have a progressive enrichment in the concentration of Ti, Zr and Y up through the sequence.

HIGH-MAGNESIAN ANDESITE (€ba)

High-magnesian andesite lavas and breccias are characterised by pyroxene and chrome spinel phenocrysts and have anhydrous SiO_2 contents of 53 to 59 wt% with an average of 56 wt%. TiO_2 is less than 0·2 wt%; MgO is between 18 and 24 wt%; with Zr 3–12 ppm and an average of 6 ppm; Y 3–10 ppm and average of 6 ppm; Nb < 3 ppm and concave chondrite-normalised REE patterns with (La/Yb)n $\cong$ 1.

With the exception of the two carbonated samples from the Magnet area, which have Mg* values of 69, the Mg* number ranges from 76–79 and has an average of 77. The pyroxene phenocrysts in these lavas are altered and consist of chlorite/amphibole/serpentine group mineral pseudomorphs after clinoenstatite and orthopyroxene. Chrome spinel grains within the lava phase are euhedral, indicating that they were in equilibrium with the melt at the time of eruption and as they are unzoned, had been in equilibrium with the melt phase since formation. They are highly refractory and have Cr/Cr + Al ratios of between 0·89 and 0·94.

Although the rocks described contain chemical and petrographic similarities to some of the rocks now loosely included in the term *boninite*, the mineralogy and chemistry of *boninites* (Kuroda and Shiraki, 1975; Shiraki and Kuroda, 1977; Komatsu, 1980) have a far larger variation in mineralogy and texture than the high-magnesian andesite described.

Komatsu (1980) indicates that *boninites* were originally described by Kikuchi (1890) and named by Petersen (1891). Johannsen (1937) defined *boninite* as a glass-rich, nearly feldspar-free olivine bronzite andesite which carries phenocrysts of olivine, bronzite and augite. The HMA lavas from western Tasmania only contain orthopyroxene, clinoenstatite and spinel phenocrysts.

Following Green (*in* Sun and Nesbitt, 1978) and Jenner (1982) the use of the term *boninite* should

be avoided when discussing high-magnesian andesite, and the chemically descriptive term high-magnesian andesite (after Green *in* Sun and Nesbitt, 1978) should be used to describe an orthopyroxene and/or clinoenstatite and chrome spinel phyric lava with SiO_2 contents of approximately 56–59 wt%, MgO > 9·0 wt%, Mg* number > 66, Cr contents between 600 and 3000 ppm, and Ni 200–700 ppm with Cr/Ni > 3.

The age of extrusion of the high-magnesian andesite lavas is still unknown, but an early Cambrian age (circa 570–600 Ma) appears most likely. Lavas of this phase are younger than the Crimson Creek Formation tholeiite basalts, as they intrude rock sequences of the Success Creek Group and Crimson Creek Formation correlates in the area covered by Figure 2. On field evidence, the high-magnesium lavas are considered to predate the low-titanium tholeiite phase of volcanism which has a biostratigraphically controlled age of *P. gibbus* (circa 530 Ma). The HMA lavas are also older than the tonalitic bodies (Ct, fig. 2) which occur in the Heazlewood area. A plug of tonalite which intrudes HMA lavas around CP580060 (fig. 2) gave a zircon age of 520 Ma (Kimbrough and Brown, in prep.).

The other important feature of the HMA lavas in western Tasmania is that in the Stonehenge area [CP575601] to the west of Zeehan they overly the Precambrian Oonah Formation, and in the area around the old Nubeena mine [CP608588] they have been intersected by drill holes intruding the Oonah Formation, indicating that the presence of high-magnesian lavas does not automatically indicate an island-arc setting (Cameron *et al.*, 1979; Beccaluva *et al.*, 1980; Crawford *et al.*, 1981).

LOW-TITANIUM THOLEIITE BASALTS (Cbm)

The low-titanium basalts are aphyric but any flow can have a large grain size variation from pillow-structured tops, down through fine, medium, and coarse, to very coarse-grained basalt (which resembles fine-grained gabbro in hand specimen), to a chilled base overlying another pillow-structured top of a previous lava flow or occasionally intercalated sedimentary rocks.

The lavas from the two main areas of outcrop, the Black Hill–Ring River and Heazlwood areas, were originally correlated on physical and petrographic criteria. Chemical data, including REE data, now confirm this correlation.

There are some differences in the major and trace element contents of the samples from the two main areas. It is considered that whereas the trace element variation is probably magmatic, the major element variations are more probably due to crustal contamination and/or secondary alteration. When a range of trace elements are used for a geochemical pattern (fig. 25), and chondrite-normalised REE patterns are compared for samples obtained from the two areas, the results indicate that the lavas from both these areas, as well as the 'intrusive' basalt from the Wandle Road area (Williams and Brown, 1983), belong to the same phase of volcanic activity.

The TiO_2 content of the basalts range between 0·20 and 0·60 wt%, with the samples from the Black Hill area having a wider range of values (0·28–0·57 wt% and an average of 0·4 wt%) compared to those from the Heazlewood area (0·20–0·31 wt%, with an average of 0·24 wt%). On the Ti∿Y∿Zr discriminant diagram (fig. 29) it appears as if the Heazlewood samples have a much higher Y content than those from the Black Hill area, but the average for the Black Hill samples is 10·2 ppm; for the Heazlewood samples 11·3 ppm; and the Wandle Road samples 13·3 ppm. Zirconium averages 15 ppm and niobium is less than 4 ppm. The Mg* numbers of samples from the Black Hill area range from 40 to 65 with an average of 50, and the samples from the Heazlewood area range from 56 to 67 with an average of 64. Chondrite-normalised REE patterns for these lavas are severely LREE depleted, (La/Yb)N < 0·5 and the overall contents of REE are low.

This, the youngest basaltic phase of the Eocambrian–Cambrian Dundas Trough successions, can be dated as middle Middle Cambrian (*Ptychagnostus atavus* Zone) on biostratigraphic evidence, indicating an age of approximately 525 Ma.

PRECAMBRIAN BASALT

The lava flows found within the 'upper' succession of the Oonah Formation are mildly alkali and are characterised by their high TiO_2, Zr and Nb contents. They may be a correlate of the pillow lava sequences within the Burnie Formation (Gee, 1977) as exposed on the foreshore at Sulphur Creek, and possibly to other lava units within the Burnie Formation near Burnie. They are not considered to be part of the Cooee Dolerite phase of magma as the lavas are interbedded with the sedimentary rocks of the Oonah Formation and are deformed by the Penguin Orogeny, and not intruded along structurally-controlled tectonic surfaces produced during the Penguin Orogeny, as is the Cooee Dolerite (Gee, 1977).

Classification

The first attempt at an overall classification of the Eocambrian–Cambrian volcanic rocks of western Tasmania was made by Varne (1978) and Varne and Foden (referred to in Brown *et al.*, 1980). This classification is mainly based on chemical data obtained from unpublished theses (e.g. Foden, 1973; Griffin, 1974; White, 1975). The proposed classification has five volcanic associations, three of which occur in the Dundas Trough and two within the Mt Read volcanic belt.

The first group of lavas, the 'Low-titania Ophiolite Association', included the high-magnesian andesite (€ba) and low-titanium tholeiite (€bm) of this study. The second group, 'olivine tholeiites' or 'Tholeiitic Basalt Association', are here described as the Crimson Creek Formation and correlate tholeiitic lavas. The third subdivision was of an 'Alkaline Basalt Association' which corresponds to the Precambrian basaltic rocks in the 'upper' succession of the Oonah Formation.

Varne and Foden (referred to in Brown *et al.*, 1980) suggested that the 'Alkaline Basalt Association' may have been part of an alkalic volcanic phase at the onset of continental rifting during the early Cambrian. Due to the occurrence of the Penguin Orogeny (circa 730 Ma) between the extrusion of these lavas, and the probable Eocambrian age of the unconformably overlying shallow-water Success Creek Group and conformably following Crimson Creek Formation tholeiitic lavas, it is considered that this suggestion is no longer viable. This phase of mildly alkaline lavas belongs to a phase of Precambrian lavas and is not a precursor to the tholeiitic volcanic rocks within the Crimson Creek Formation.

The chemical range of the Crimson Creek Formation tholeiitic lavas has been extended by this study and that of Collins (1983), but the range is still consistent with that reported by Varne in being olivine or quartz normative tholeiites whose chemical affinities are more like those of continental 'Within Plate Basalt' rather than of 'Ocean Floor Basalts'.

The 'Low-titania Ophiolite Association' includes both the high-magnesian andesite and low-titanium tholeiite basalt (€bm). Field evidence exists to show that these two basaltic phases belong to two different sequences and that a time gap of possibly fifty million years may separate these lava sequences.

Following the suggestion of Varne and Foden (referred to in Brown *et al.*, 1980) that the mafic lava suites within the Dundas Trough were possibly the product of progressive melting within part of an upwelling mantle diapir beneath an intracontinental rift system, Brown and Waldron (1982), using preliminary results of this study and REE patterns for the Eocambrian–Cambrian basaltic suites, produced a clarification of this phase of volcanic activity in the Dundas Trough and Smithton Basin, and identified the high-magnesian andesite and low-titanium tholeiite as separate volcanic phases.

ULTRAMAFIC ROCK SUCCESSIONS

INTRODUCTION

Three different ultramafic rock successions have been recognised within the study area. The successions can be recognised either by field characteristics and/or mineral chemistry. The three groups are a high-magnesium layered dunite-harzburgite succession, which contains a tectonic fabric formed by plastic deformation of cumulate layers; a layered pyroxenite-dunite succession, which is dominated by orthopyroxene; and a multiply intrusive ultramafic-gabbro succession. Other areas of ultramafic rocks in Tasmania can be successfully correlated with this grouping.

Five of the fifteen well-known areas of ultramafic-mafic rocks within Tasmania are included in the area mapped; these are the Mt Stewart, Wilson River, Huskisson River, Serpentine Hill and Dundas complexes (areas 4–8, fig. 42). A sixth area, the Heazlewood River complex (area 3, fig. 42), occurs in the area covered by reconnaissance mapping to the north of the Corinna Road.

The largest volume of ultramafic rocks consists of well-layered dunite, orthopyroxene-bearing dunite and harzburgite. This is termed the Layered Dunite-Harzburgite (LDH) succession. This succession is relatively uniform in composition, and contains a foliation parallel to layering defined by primary mineral alignment of orthopyroxene and chrome spinel grains, as well as later flattening and elongation of olivine grains. The second succession is also well layered, but is dominated by orthopyroxene. The main rock types are orthopyroxenite, olivine orthopyroxenite, and dunite. No harzburgite is found in this succession. This sequence is called the Layered Pyroxenite-Dunite (LPD) succession. As well as the uniform layering, another significant feature of both of the above successions is the apparent lack of feldspar as a mineral constituent. Plagioclase or hydrogarnet after plagioclase were not observed in any rocks from the LDH or LPD successions or correlates in either the study area or at Adamsfield. The only location at which plagioclase is known to occur within the ultramafic successions is in the Serpentine Hill and Heazlewood River complexes.

The third subdivision is characterised by multiple intrusions of various ultramafic and mafic rock types. The first part of this third group is similar to the LPD succession in that it is a well-layered sequence dominated by orthopyroxenite with subsidiary olivine pyroxenite and dunite, but differs from the LPD succession in that the sequence contains numerous sedimentary-like structural features and delayed mineral grading in the upper part of the dunite layers. The second phase is dominated by plagioclase-bearing dunite which contains zones enriched in chrome spinel. The third phase consists of multiple intrusions of two-pyroxene gabbro. The plagioclase dunite magma intruded and brecciated the dominantly pyroxenite sequence and the gabbro intrudes both of the ultramafic phases. This succession is termed the Layered Pyroxenite-Peridotite and associated Gabbro (LPG) succession.

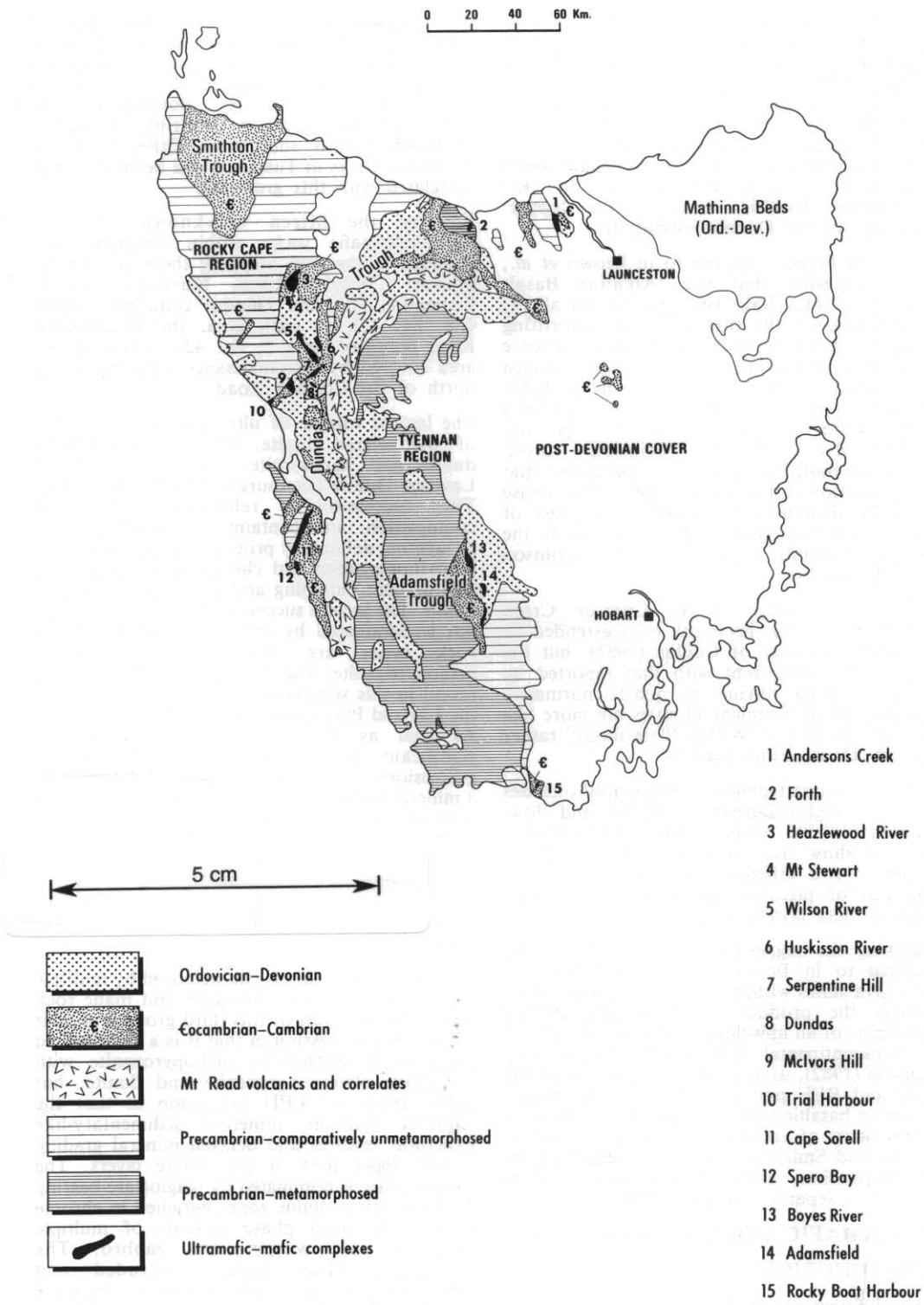

Figure 42. *Schematic geological map of Tasmania showing location of ultramafic–mafic complexes. Rock distribution after Williams (1976).*

The LDH succession and correlates form the western side of the Heazlewood River Ultramafic Complex, the 'Nineteen Mile Creek Dunite' of Rubenach (1973); occupy the whole of the Mt Stewart complex; and occur as the major part of the Wilson River and Huskisson River Ultramafic Complexes. They are also known to form a large part of the Adamsfield and Boyes River Ultramafic Complexes (area 13–14, fig. 42).

The LPD succession is found as fault-bounded blocks intermixed or juxtaposed with areas of the LDH succession in the northern (Harman River) and southern (Riley Knob) parts of the Wilson River Ultramafic Complex; near Lynch Hill in the Huskisson River complex (fig. 43); and forms the Colebrook Hill and Dundas bodies. Another area of LPD succession occurs at Adamsfield, where rafts within sheared serpentinite sheaths are fault juxtaposed with areas of LDH succession (Brown, 1972; Varne and Brown, 1978). The multiply intrusive LPG succession has so far only been observed at Serpentine Hill and to the east in the Kapi Creek–Ring River area, but is thought to also occur as part of the Heazlewood River Complex.

The only part of the Heazlewood River Ultramafic Complex (Rubenach, 1973) examined in detail during this study was the southernmost tail of the complex to the south of Corinna Road and to the west of the areas of €ba and €bm (fig. 2). This area contains a sequence of layered orthopyroxenite and olivine orthopyroxenite which has chemical and petrographic characteristics similar to rocks of the LPD succession. The area was examined to facilitate the mapping and chemical separation of basaltic pyroxenite (€bap) from ultramafic pyroxenite (€sp) (fig. 2). Rubenach (1973) subdivided the Heazlewood River Ultramafic Complex into the 'Nineteen Mile Creek Dunite', which is a correlate of the LDH succession; and the 'Caudrys Hill Pyroxenite' and 'Brassey Hill Harzburgite', both of which consist of interlayered peridotite and pyroxenite with plagioclase. The following descriptions of the different successions, especially the relationships exposed in the Serpentine Hill area, show that remapping of the Heazlewood River Complex is required before any correlation is made for these plagioclase-bearing sequences.

Interpretation of the ultramafic rocks of Tasmania has been much debated in the past. Their importance in tectonic models at times has been over-emphasised, and often misinterpreted, due to lack of factual information as to the nature of the different complexes. One of the most important features of the ultramafic bodies of western Tasmania is their size, or lack thereof. The ultramafic rocks of the Heazlewood River complex crop out over an area of approximately 32 km²; those of the Mt Stewart complex over approximately 7·5 km²; the Wilson River complex 27 km²; at Huskisson River 6·5 km²; Colebrook Hill less than one km²; at Dundas three km²; the Kapi Creek–Ring River area 2·5 km²; and at Serpentine Hill two square kilometres.

The Adamsfield complex covers five square kilometres and the Boyes River body crops out over 15 km². In total, ultramafic rocks only occupy approximately 80 km² of nearly 1000 km² of the Dundas Trough studied. The term 'complex' is used for an area of any size which contains ultramafic rocks belonging to one or more of the three recognised successions which occur on the West Coast of Tasmania, and not in the sense of a large area of genetically related ultramafic-mafic rocks, as for example those found in the classical ophiolite complexes of eastern Europe.

Chemical analyses of bulk rock samples and electron probe analyses of mineral constituents of the different rock types in the various successions were obtained to allow chemical classification of the three successions. The results are included in tables in Appendix 4. The area chosen to chemically characterise the LDH succession was the Harman River area at the northern end of the Wilson River complex; that for the LPD succession as the Riley Knob area at the southern end of the Wilson River complex; and the Serpentine Hill area was used for the multiply intrusive LPG succession.

The physical and petrographic features of the different areas of ultramafic rocks will be discussed under their geographic associations and then the chemical characteristics of the three different successions will be considered.

Figures 1 to 3 show that the ultramafic rocks lie along a general north-south trending elongate 'S' shaped area. Their present position and relationships with surrounding rocks are the result of Devonian deformation, as can be seen by the position of the Wilson and Huskisson River complexes. Although the whole of the western margin of the Wilson River complex is in contact with the Eocambrian Crimson Creek Formation, the eastern margin is in contact with rock types which differ from those belonging to the fossiliferous Cambrian Huskisson Group, the Ordovician Gordon Limestone correlate, and the Silurian Crotty and Amber Formation correlates (fig. 1). The intrusion of the Meredith Granite (circa 350 Ma) replaced an eleven kilometre long section which would once have formed a continuous belt of ultramafic material from south-west of Serpentine Hill to north-west of Bronzite Hill (fig. 3). The Meredith Granite also metamorphosed the ultramafic rocks around the contact margins, as well as around high level intrusions in the Harman River and Mt Stewart areas, indicating that the ultramafic rocks had been re-emplaced into their present position before the Devonian granitic event.

Evidence exists in the basal conglomerate units of the Dundas Group that some ultramafic rocks

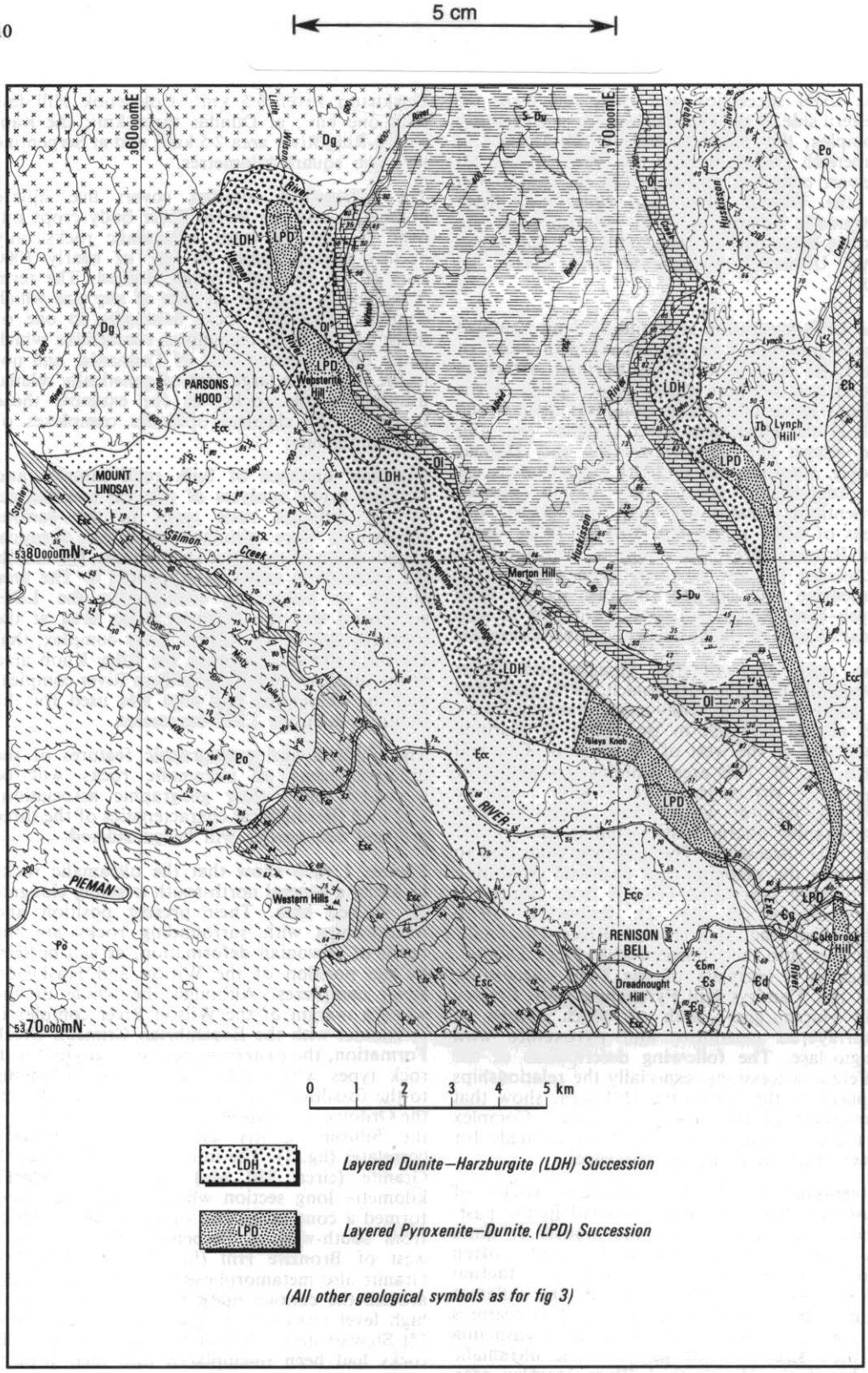

Figure 43. *Distribution of areas of LDH and LPD succession ultramafic rocks in the Renison Bell–Mt Ramsay area.*

had been emplaced into the basin of deposition of the Dundas Group, as detritus from these ultramafic rocks is included in the Red Lead Conglomerate at the Razorback mine workings (Padmasiri, 1974) and at Confidence Saddle (Rubenach, 1974; this study). Similar evidence of a Cambrian emplacement age for the ultramafic successions into basins of active deposition also occurs at Adamsfield (Carey and Banks, 1954; Banks, 1962*b*).

In the following descriptions, the terminology used to describe the ultramafic rocks follows Irvine's (1982) modification of Jackson (1967) and Wager, Brown and Wadsworth (1960).

WILSON RIVER ULTRAMAFIC COMPLEX

The Wilson River Ultramafic Complex lies on the western side of the Huskisson Syncline. The northern extent of this 17 km long body is in contact with the Meredith Granite in the upper Harman River area, where it is approximately three kilometres wide. The southern extent crops out in the Pieman River around CP718739, where it is approximately 500 m wide. The northern six kilometres along strike of this complex is dominantly composed of LDH succession rocks but also includes two small areas occupied by infaulted blocks of LPD succession (fig. 43). The middle zone of seven kilometres (Serpentine Ridge) consists entirely of LDH succession rocks, whereas the southern four kilometres, between Riley Knob and the Pieman River, is dominantly of LPD succession with minor blocks of LDH succession material surrounded by sheared serpentinite. Earlier studies of this area are found in Waterhouse (1914), Reid (1921) and Taylor (1954, 1955).

HARMAN RIVER AREA

At the northern end of the Wilson River complex, in a three kilometre diameter area around CP625865, the layered nature of the LDH succession is well exposed. Rocks belonging to the LDH succession are now known to occupy the majority of this area (fig. 43) and not just the western side, as shown in Figure 1. The interlayered dunite, orthopyroxene-bearing dunite and harzburgite, depending on the content of orthopyroxene in any specific layer, range in thickness between 25 mm and 400 mm with an average of approximately 150 mm (plate 12). The rocks are composed of three mineral types, namely olivine, enstatite and chrome spinel.

The dunite layers are considered to have been cumulates with sharp phase contacts with adjacent layers. Chrome spinel occurs as a subsidiary mineral phase in varying proportions from one to five percent, and in some places is present in a higher concentration and forms a mineral foliation (plate 13). The harzburgite and pyroxene-dunite layers have both olivine and orthopyroxene as cumulus phases, with the orthopyroxene crystals being fairly uniform in size. Chrome spinel is an accessory phase in both pyroxene-dunite and harzburgite but is less common than in dunite layers (being approximately 1%) and does not form mineral foliations.

Across a two kilometre traverse from the granitic rocks on the western margin [CP608868] eastwards to the northernmost area of LPD succession [CP627863] (fig. 1), the percentage of harzburgite increases to the east. The western part of the area consists of interlayered dunite with thin, subordinate pyroxene-bearing dunite. After 100–150 m, harzburgite layers enter the succession, the formation of pyroxene-dunite or harzburgite only depending on the amount of orthopyroxene present in any specific layer. By half-way, the succession consists mainly of harzburgite, in layers between 100 mm and 400 mm thick, with dunite in 10 mm to 50 mm layers. Over the eastern 750 m of the traverse, the succession is dominantly harzburgite with thin interlayers of dunite.

Occasional boudinaged lenses and irregularly shaped veins or dykes of late stage coarse-grained orthopyroxenite occur throughout the succession. The lenses range from 500–600 mm in length and up to 75 mm thick, to three to five metres in length and 100–150 mm thick (plate 14). The lateral extent of the lenses is unknown, and the orientation of the lenses and dykes is subparallel to layering.

The enstatite crystals are tabular and elongate in the plane of bedding in both the pyroxene-dunite and harzburgite layers but are not aligned in any specific direction within this plane. Where the percentage of pyroxene crystals in any specific layer is low, the crystals form a mineral foliation rather than a specific continuous layer.

In thin section, the degree of serpentinisation is such that in dunite and pyroxene-bearing dunite samples the original texture cannot be unambiguously interpreted, and in harzburgite samples no relict silicate mineral cores remain. In the dunite and pyroxene dunite samples, olivine grains are now remnant cores (ranging in size from 0·20–0·65 mm but usually between 0·35–0·45 mm) of fresh olivine surrounded by a mesh of serpentine group minerals (lizardite with minor chrysotile). If adjacent cores with uniform extinction are taken as an original olivine crystal, then many grains have straight crystal boundaries parallel to extinction. Optical deformation lamellae parallel to (100) occur in many cores. Kink bands parallel to (001), as observed in similar rocks from the Adamsfield area (Varne and Brown, 1978), were not found in any samples from the Harman River area.

The closely associated aggregates of remnant cores with uniform extinction indicate that the majority of crystals in these rocks were between two and four millimetres in length, with some crystals being up to five millimetres. Some of the larger grains are now wedge-shaped and

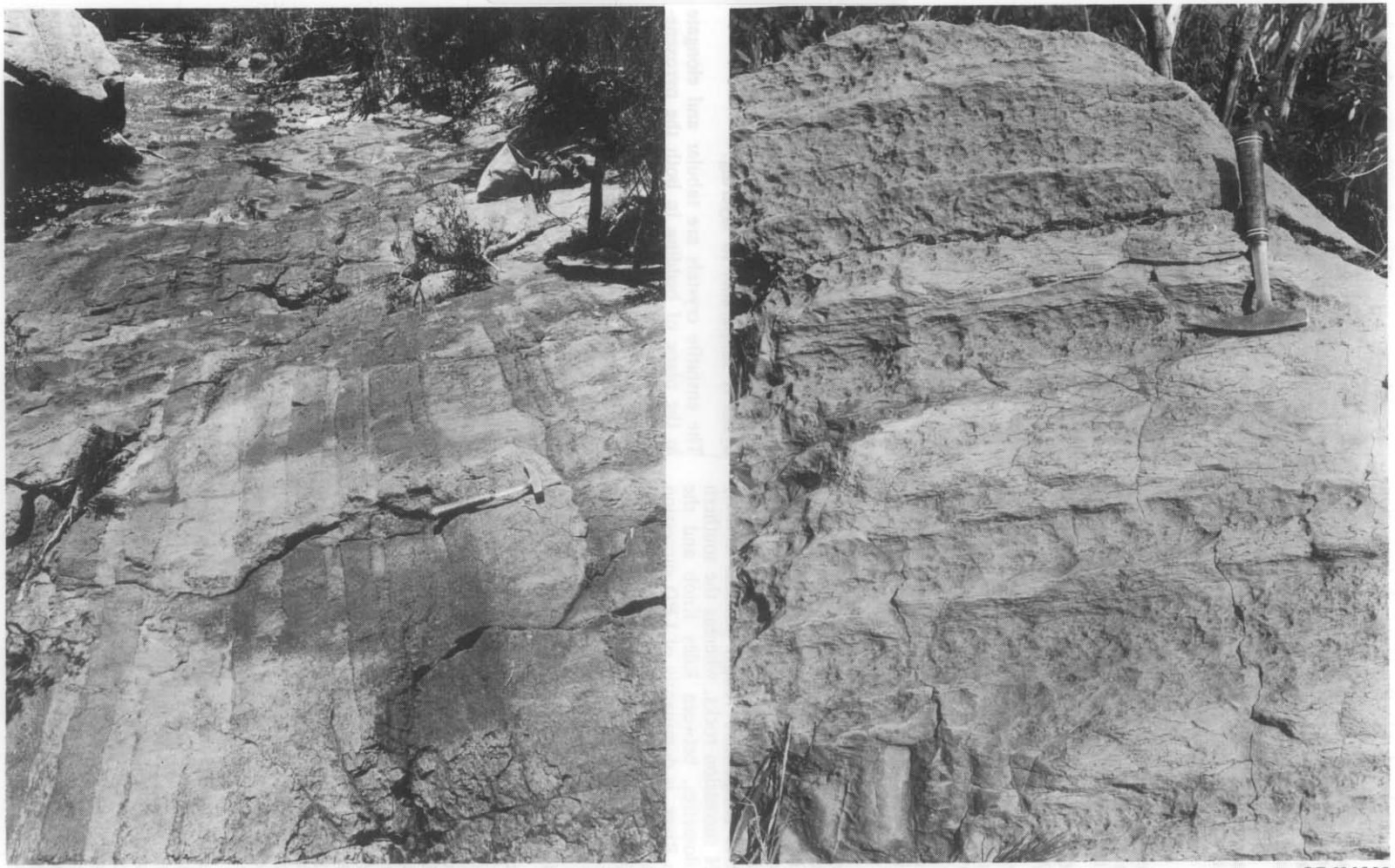

CP612870

CP621859

Plate 12. *Igneous layering in the LDH succession, Upper Harman River area [fig. 1].*

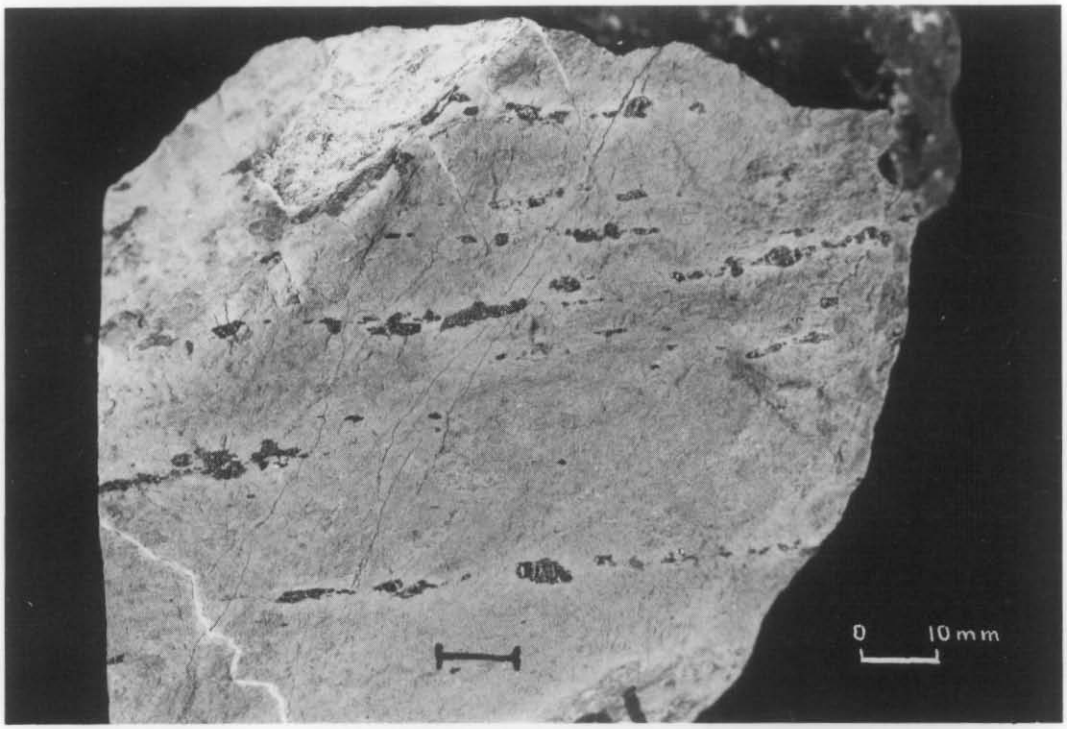

Plate 13. *Mineral foliation defined by chrome spinel grains in LDH succession [fig. 1, CP679792].*

elongate in the direction of layering. The strong, probable Devonian tectonic foliation found in the surrounding serpentinite sheath is also seen in samples from within the rafts of layered material. In thin section, the foliation produces a spaced fracture 0·3–0·45 mm apart at an angle of 10° to 25° to the mineral foliation (layering). In some samples, this later foliation produces a crenulation cleavage or kink-band effect which persists across all grains cut by the foliation.

Where orthopyroxene grains are present they define a mineral foliation parallel to layering. Some grains contain kink bands. In some dunite samples, trains of fractured euhedral chrome spinel grains (0·25–0·75 mm) form a mineral foliation which is also parallel to layering. The coarse-grained pyroxenite lenses and dykes are boudinaged and consist of interlocking grains of orthopyroxene, ranging in size from 0·5–5 mm, and which contain undulose extinction. Zones of fracturing and brecciation occur through these grains, but no recrystallisation has occurred.

No evidence of a protogranular or porphyroclastic texture (Mercier and Nicolas, 1975) was found in any sample collected from this succession. The overall evidence is consistent with a well-layered cumulate succession which has undergone plastic to solid state deformation (Raleigh, 1967; Carter and Ave'Lallement, 1970) without distortion of the layering during tectonic dismembering and emplacement of the succession into basins of deposition prior to the middle Middle Cambrian.

The western margin of the northernmost block of LPD succession with the LDH succession [between CP629861 and CP630870] is a zone of cataclasis, indicating a faulted contact and not a continuous sequence. This block contains thin layered orthopyroxenite, of varying grain size, interlayered with serpentinised orthopyroxenite and minor dunite. The area to the north of this block, around CP635874, consists of serpentinised and contact metamorphosed LDH succession.

Along the fault zone between the two successions [around CP629863], samples from the zone of cataclasis have undergone recrystallisation to amphibole minerals, probably due to this area being within the aureole of a high-level granitic intrusion. In the layered part of the LPD succession raft, both pyroxenite and olivine pyroxenite layers contain relict primary minerals but the dunite samples are totally serpentinised. The pyroxenite samples have either an even-grained or interlocking adcumulate texture, with grains ranging in size from 0·5–5 mm. The larger grains contain sweeping extinction and fracture zones. No recrystallisation of the fracture material has occurred. Olivine pyroxenite samples contain 0·5–0·75 mm olivine grains which are poikilitically enclosed by one to three millimetre

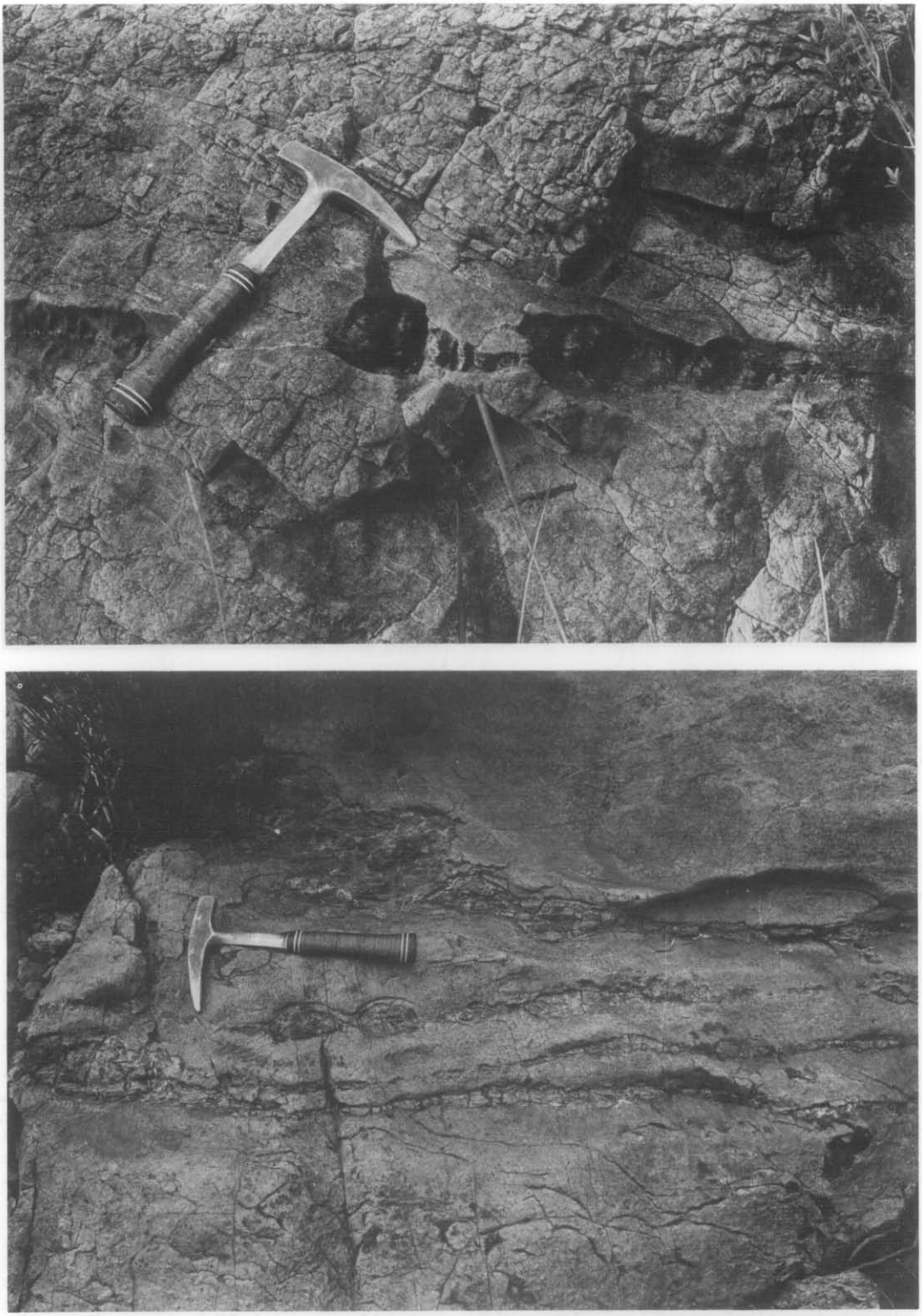

Plate 14. *Boudinaged orthopyroxenite lenses in LDH succession [fig. 1, CP622859* (top)*; CP623855* (bottom)*].*

orthopyroxene grains, most of which contain undulose extinction.

In the areas around CP625867 and CP630850 (fig. 1), high level granitic intrusions have metamorphosed the serpentinite into an equigranular metadunite which resembles a slightly metamorphosed coarse-grained sandstone in both hand-specimen texture and colour. Another block of LPD succession occurs to the east and south of the latter area of metadunite, the highest point of which is Websterite Hill (fig. 43).

In thin section, metadunite samples have an equigranular mosaic texture. The average grain size ranges between 0·45 mm and 0·7 mm with coarser-grained samples having grains up to 1·35 mm across, and finer-grained samples down to 0·25 mm. Many olivine grains, in lower-grade samples, have a pleochroic light to dark orange-brown colour and enclose dusty magnetite throughout the whole grain. In higher-grade samples, the orange-brown colouration disappears and the dusty magnetite has coagulated to form small (0·01 mm) magnetite grains. In some samples, areas up to 4·5 mm by 2·75 mm containing a mosaic of 0·35–0·45 mm grains have a common extinction.

Sheaves of a colourless acicular mineral with very high relief occur between and around isolated olivine grains and probably represent amphibole minerals after serpentinised orthopyroxene. Primary chrome spinel grains usually show alteration around their edges and are ubiquitously subhedral. Minor post-Devonian serpentinisation has occurred along cracks and fractures within these samples.

SERPENTINE RIDGE AREA

The seven kilometre long Serpentine Ridge is a strike ridge of interlayered dunite, pyroxene-bearing dunite and harzburgite belonging to the LDH succession. The proportion of harzburgite in the succession increases from west to east. Most of this ridge consists of serpentinite after the respective rock types, but layering, euhedral to subhedral chrome spinel stringers and foliations, and the variation in percentage of pyroxene in different layers, is easily observed in outcrop.

In the southern part of this zone, to the south of the Lower Pieman Dam Road and between Sweeney and Riley Creeks (fig. 1), an area of outcrop exists where some samples contain relict cores of olivine. The samples have a similar texture to those from the Harman River area, and contain flattened and elongated olivine grains up to five millimetres in length (based on mutual extinction of adjacent cores) with both disseminated euhedral (0·15–1·0 mm) and two to three millimetre trains of fractured anhedral spinel grains.

Along the eastern margin of the body, in Sweeney Creek, the sheared serpentinite sheath contains small blocks of LPD succession pyroxenite (identified by mineral chemistry), which in thin section contains an even-grained adcumulate texture and consists of 1·7–7·0 mm grains of orthopyroxene with minor 0·2–0·25 mm euhedral chrome spinel which is both enclosed by and occurs along the grain boundaries between the pyroxene grains. Concentrations of chrome spinel also occur in the dunite along the southern part of the ridge, which was once an alluvial osmiridium working area. One chrome spinel nodule ($75 \times 50 \times 50$ mm) was recovered, and analysis revealed a high concentration of Platinum Group Elements in comparison to whole rock samples, rich in disseminated spinel, from this succession (Brown *et al.*, in prep.). Further north [around CP670791] occur small lenses (200 mm long by 5 mm thick; plate 15) and zones enriched in disseminated chrome spinel forming a mineral foliation.

RILEY KNOB AREA

To the south of Serpentine Ridge, the four kilometre section between Riley Knob [CP689764] and the Pieman River contains dominantly LPD succession material, with large blocks of coarse-grained orthopyroxenite in sheared serpentinite from the LDH succession, cropping out in the Huskisson River along the eastern margin of the ultramafic body.

An excellent section of LPD succession crops out in the vicinity of Riley Knob (plate 16). The outcrop consists of thin, uniform layers of orthopyroxenite, olivine orthopyroxenite and dunite. Harzburgite has not been found in this succession. The layered ridges in this area are surrounded by sheared serpentinite and each of the layered rafts is orientated so that its strike is in the direction of the dominant regional foliation and the layering is either vertical or dips steeply to the east, as is also the case with the regional foliation.

Orthopyroxene layers dominantly range in thickness between one to two millimetres and 150 mm, the majority being less than 20 mm thick with occasional layers between 20 mm and 150 mm in thickness. Olivine orthopyroxenite layers mainly range between one to two millimetres and 20 mm in thickness, the majority being less than or equal to five millimetres. An occasional layer is found between 20 mm and 100 mm thick. The majority of dunite layers are also between one to two millimetres and 20 mm in thickness, with layer thickness being evenly divided between very thin (less than 5 mm) and thin (6–20 mm). The number of dunite layers between 20 mm and 200 mm in thickness is small, but exceeds the number of orthopyroxenite layers of this thickness.

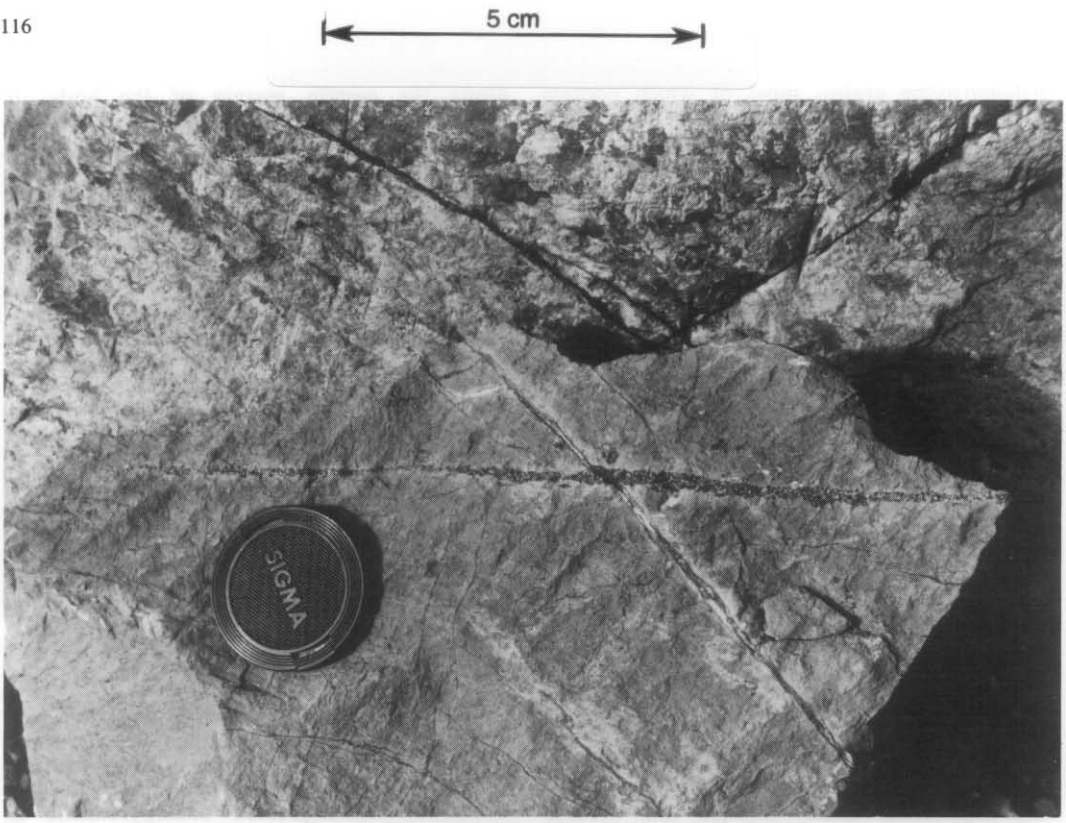

Plate 15. *Small lense of chrome spinel grains in the LDH succession [fig. 1, CP690791].*

As in other areas of LPD succession sampled, the dunite layers are now completely serpentinised, but these layers always carry a higher percentage of chrome spinel grains (0·14–0·36 mm) than the dominantly pyroxenite layers. Olivine pyroxenite samples have either an even-grained granular or interlocking texture and consist of approximately 85–90% orthopyroxene, 1–2% clinopyroxene, 1–2% chrome spinel, and up to 10% olivine. The olivine grains, ranging in size from 0·45 to 1·35 mm, normally occur between orthopyroxene grains, but some are partially enclosed by postcumulus overgrowths on orthopyroxene with an occasional sample having olivine grains poikolitically enclosed by orthopyroxene. Orthopyroxene grains range in size from 0·45 to 2·25 mm, the larger grains containing kink bands and/or fine exsolution lamellae of clinopyroxene. Diopside occurs as individual anhedral grains (0·14–0·23 mm across) and occupies areas between orthopyroxene grains. In some samples, clinopyroxene also occurs as stringers of exsolution blebs along cleavage planes within orthopyroxene grains.

The orthopyroxenite layers are dominantly of an even-grained adcumulate texture but some interlocking textured samples exist. The grain size ranges from 0·45 to 4·5 mm in most samples. Minor intergranular diopside and accessory chrome spinel (0·2–0·4 mm) occur along boundaries between orthopyroxene grains within these samples. An occasional spinel grain is enclosed by orthopyroxene. Some of the larger orthopyroxene grains contain stringers of clinopyroxene blebs or thin exsolution lamellae along the cleavage planes.

Due to lack of continuous outcrop, the presence or absence of cyclic layering could not be ascertained. One section of 259 layers was measured (table 13) and shows that the layered sequence contains rhythmic layering. The dominant rhythm is dunite to orthopyroxenite to dunite to orthopyroxenite (45% of layers), followed by dunite to orthopyroxenite to olivine orthopyroxenite to orthopyroxenite (24% of layers). All contacts are sharp phase contacts, and no size or mineral grading was observed in any layer. The classical three-state rhythm, dunite to olivine orthopyroxenite to orthopyroxenite, found in many stratiform complexes, only occurs on four occasions in this sequence.

MT STEWART ULTRAMAFIC COMPLEX

The Mt Stewart Ultramafic Complex (area 4, fig. 42; fig. 2) is composed of thick dunite layers with thin interlayered pyroxene-dunite of the LDH succession. Harzburgite layers are rare in this area. The southern half of the complex is underlain and surrounded by intrusions of the Devonian Meredith granitic body. The northern half is in faulted contact with a sedimentary

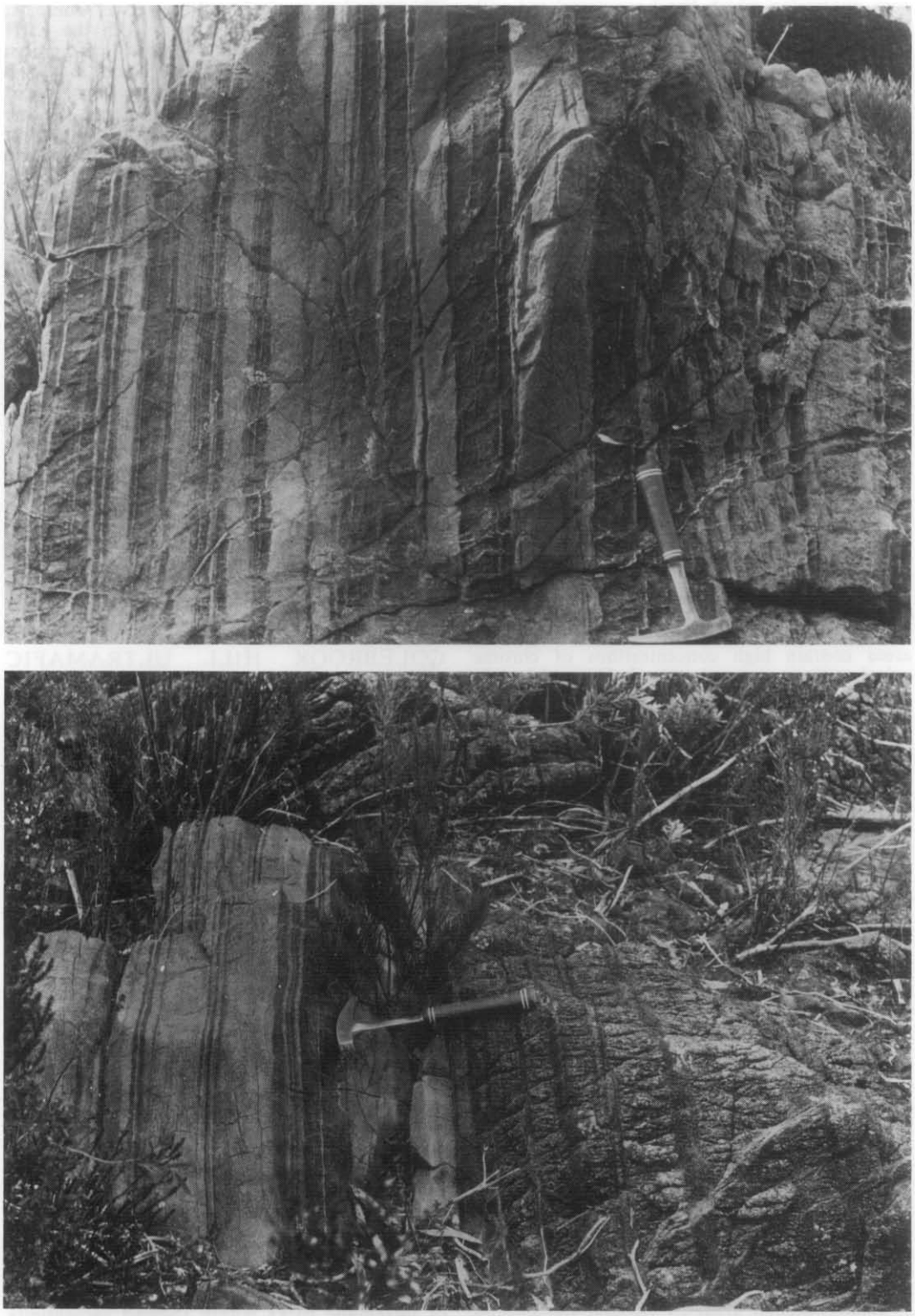

Plate 16. *Igneous layering in the LPD succession at Riley Knob [fig. 1, CP699765* (top)*; CP700764* (bottom)*].*

rock succession which has been correlated with the Success Creek Group (€sq, fig. 2). To the north-east of the complex is a small area of high-magnesian andesite flows (€ba, fig. 2), and bodies of basaltic pyroxenite occur further along the north-eastern margin. Some of these bodies are highly metamorphosed by the underlying granitic rocks [around CQ585027] and now consist of mainly amphibole minerals, whereas other areas [around CQ608025] are highly weathered.

Numerous late stage coarse-grained and very coarse-grained orthopyroxenite dykes and veins cut the succession throughout the area. In thin section, samples of these dykes consist of large (3–5 mm) grains with an interlocking texture but which contain a high strain, undulose extinction and kink bands. Chrome spinel grains one to two millimetres in size are enclosed by the orthopyroxene grains and these spinel grains in turn enclosed original silicate grains which are now serpentine group minerals.

Dunite and pyroxene-dunite samples contain the same texture, grain size and deformation characteristics as similar samples from the Harman River area. The enclosed chrome spinel grains are generally larger, and a greater percentage of grains enclosed or partially enclosed earlier silicate minerals which are now replaced by serpentine group minerals. Numerous areas contain high concentrations of chrome spinel grains, one such area being enriched in disseminated pods up to five millimetres across [around CP590998] (fig. 2).

Metadunite samples, as well as partially metamorphosed residual serpentinite, have similar textures to similar samples from the Harman River area. One feature which persists throughout many samples of metadunite is the four to five millimetre areas of 0·2–0·35 mm recrystallised olivine grains which have a common extinction.

Earlier literature on this area can be found in Reid (1921) and Rubenach (1973).

HUSKISSON RIVER ULTRAMAFIC COMPLEX

The Huskisson River Ultramafic Complex is an irregularly shaped area of ultramafic rocks on the eastern side of the Huskisson Syncline. Rocks of the Crimson Creek Formation occur along its eastern margin and the Ordovician Gordon Limestone correlate occurs along the south-western margin from north of the Lower Pieman Dam Road to the south where outcrop ceases beneath glacial outwash sediments (fig. 1). The northern extent is traversed by the Huskisson River around CP719759 (fig. 1), where the rocks consist of sheared serpentinite and blocks of LDH succession. The southern extent crops out as small, isolated areas of sheared serpentinite with blocks of LPD succession, from south of CP710830 (fig. 1) to the Pieman River.

This complex, as with the Wilson River Complex, is a mixture of material from both the LDH and LPD successions. The majority of the area north and south of John Lynch Creek is known to be serpentinite after LDH succession (based on the mineral chemistry of remnant chrome spinel grains). One area of LDH succession occurs around CP728817, approximately one kilometre south-west of Lynch Hill [CP731826]. This area contains interlayered orthopyroxenite, olivine orthopyroxenite and subordinate dunite. Layers are between 5 mm and 10 mm in thickness. The texture and mineralogy of the layers are similar to the material at Riley Knob, having both even-grained and interlocking adcumulate textures. Orthopyroxene grains are between 1 mm and 5 mm across, clinopyroxene between 0·2 mm and 0·4 mm, and chrome spinel grains 0·1 mm and 0·15 mm. The only sample which contained exsolution lamellae of clinopyroxene in orthopyroxene and kink bands in the larger grains was a very coarse-grained (8–30 mm) orthopyroxenite.

The Wilson River and Huskisson River complexes are most probably joined beneath the Huskisson Syncline. This high probability of connection is based on information contained in a detailed aeromagnetic survey carried out in 1981 (R. G. Richardson, pers. comm.; Corbett *et al.*, 1982).

COLEBROOK HILL ULTRAMAFIC BODY

The small area of ultramafic rocks cropping out along the western side of Colebrook Hill is composed of sheared serpentinite enclosing irregular pods of remnant LPD succession material. From the knoll at CP747721 (fig. 1), north to the main road, the dominantly serpentinite body has been subjected to contact metamorphic effects. Remnant layering can be observed in some areas and pods of orthopyroxenite with chemical affinities to the LPD succession occur around CP746728 (fig. 1).

RING RIVER–KAPI CREEK AREA

The zone of ultramafic and gabbroic rocks in the Kapi Creek–Ring River area contains a high degree of shearing. The zone is composed of sheared serpentinite with blocks of remnant layered ultramafic material intruded by gabbroic rocks. The gabbroic rocks are the result of multiple intrusions, as there are chilled margins in the gabbro, both against areas of ultramafic rocks and other areas of gabbro where one dyke has intruded another. This area has been metamorphosed by the underlying and cross-cutting granitic rocks, and most of the rocks of this zone are highly altered. To the north-west of the main gabbroic area (fig. 1), blocks of ultramafic rocks within sheared serpentinite contain remnant textures suggesting that some of the ultramafic rocks originally contained post-

cumulus plagioclase, and that the parent rock was probably a plagioclase dunite, as found in the Serpentine Hill complex. Other areas of blocky serpentinite indicate that the original rock types were layered. Some of the layers, on the basis of the disseminated chrome spinel content, were dunite, while other layers, on the basis of bastite pseudomorphs, were pyroxenite.

The northern extent of this zone, in Colebrook Creek [CP721708] (fig. 1), contains kink-banded pyroxenite pods in a sheared serpentinite. This area has also been intruded by later gabbroic rocks. Textural features found within the rocks throughout this zone suggest that they are an extension of the Serpentine Hill complex.

SERPENTINE HILL ULTRAMAFIC COMPLEX

The Serpentine Hill Ultramafic Complex (fig. 2, 44) consists of fault-disrupted blocks of multi-phase ultramafic-gabbroic sequences, and is exposed through a fault window between an area of the Eocambrian basic volcaniclastic succession, to the north and west, and fossiliferous middle Middle to Late Cambrian sequences to the south and east. The basaltic rocks immediately to the south-west of the complex belong to the low-titanium tholeiitic phase and interdigitate with basal conglomerate units of the fossiliferous Cambrian succession.

The first ultramafic unit to form was an orthopyroxene-rich layered sequence which was later intruded and dismembered by a magma which produced an olivine-rich sequence. Both of these sequences were in turn intruded by a two-pyroxene gabbro (see fig. 45).

ORTHOPYROXENE-RICH SEQUENCE

The layering in the orthopyroxene-rich sequence consists of a variety of alternating rock types. Because of the brecciated nature of this sequence, no data on cyclicity in layering variation could be obtained. The layers are formed from varying proportions of olivine and orthopyroxene cumulates, which in places have feldspar as a post-cumulus phase. There are four main variations within the layering which are defined by mineralogy and grain size. In the first variation, the lower 5–10 mm of a layer consists of olivine and minor chrome spinel followed by a sharp but discontinuous boundary into a 25–50 mm thick zone where orthopyroxene joins olivine as the cumulus phase. The orthopyroxene crystals can be up to 1–2 mm across. A sharp boundary separates this upper zone from the overlying layer where orthopyroxene alone is the cumulus phase. The orthopyroxenite layers are between 50 mm and 100 mm thick.

The second variation consists of very thin layers (from less than 5 mm up to 20 mm, with an occasional 50–60 mm layer), which are marked by sharp contacts and are composed of olivine, olivine and orthopyroxene in different proportions, and orthopyroxene cumulates. In any section an orthopyroxenite layer separated two, three or four combinations of the other layer types.

A third variation occurs as 100–200 mm thick layers of harzburgite containing stubby orthopyroxene crystals with a uniform 8–10 mm cross-section and minor feldspar as a post-cumulus phase, followed by a 20–50 mm thick layer of feldspathic orthopyroxenite. The orthopyroxene grains are usually 4–5 mm across and the feldspar makes up between 30% and 50% of the layer. It is within this layer variation that unconformities and scours are common.

The final variation occurs within orthopyroxenite, with layers being defined by grain size differences. Contacts are sharp and within any specific layer the grain size is consistent. All the above layers also contain 1–2% disseminated chrome spinel grains.

Numerous primary features are found within the orthopyroxene-rich sequence and include unconformities, troughs, modal layering, slump structures, and syndepositional faults. Some angular discordance between layers appears to have been formed by scouring, as the infilling layers contain cross-bedding and reverse grading. The cross-bedding is defined by thin, flow-aligned crystal layers and lamination. Where olivine-rich lenses are observed cross-cutting underlying layers, they usually contain a thin (1–2 mm) basal zone with a very high concentration of chrome spinel grains, again indicating flow of crystal mushes.

Syndepositional soft-sediment faults are shown by the sharp basal steps in the overlying layer, and the intraformational disruption of some zones within an otherwise well-layered succession indicates probable slumping. Channels up to 200 mm deep occur in some orthopyroxene layers. These channels are infilled by alternating laminae, between 10 mm and 25 mm thick, of olivine and orthopyroxene grains.

Very few of the primary minerals remain, because of the serpentinisation of the sequence. In thin section, olivine cumulate layers now contain serpentine minerals (dominantly lizardite), magnetite and spinel. The olivine-orthopyroxene layers have only minor remnant orthopyroxene grains within a serpentinitic matrix. The majority of orthopyroxene samples display some cataclastic deformation and have undergone partial recrystallisation, resulting in a serpentinised protoclastic texture. The large orthopyroxene grains are 7–8 mm in length and the surrounding recrystallised grains 0·5 mm across. Other samples have a mosaic adcumulate texture, with the orthopyroxene grains ranging in size from one to ten millimetres. Minor intergranular anhedral clinopyroxene occurs in these samples as well as clinopyroxene exsolution lamellae and blebs within the large orthopyroxene grains.

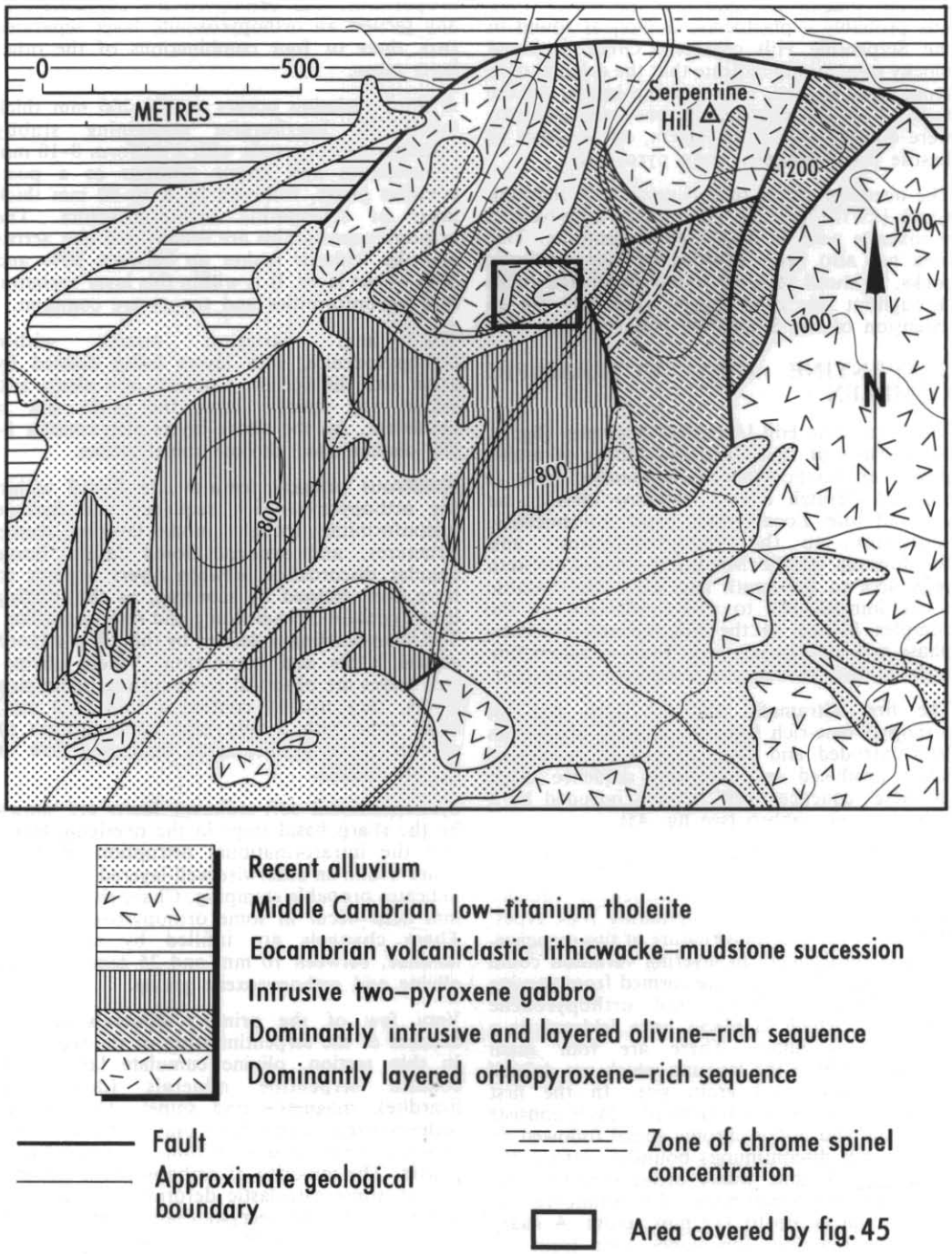

Figure 44. *Geological map of the Serpentine Hill Ultramafic–Mafic Complex.*

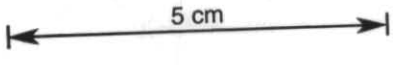

Websterite samples contain 7–8 mm long grains of orthopyroxene which enclose euhedral chrome spinel grains (0·01–0·15 mm). Clinopyroxene grains are between three and five millimetres across, some contain simple twins, and other grains have orthopyroxene exsolution lamellae. The texture ranges between mosaic adcumulate and protoclastic. In feldspar-bearing orthopyroxene samples, the pyroxene grains are usually stubby and three to five millimetres across. The feldspar has been altered to hydrogarnet.

OLIVINE-RICH SEQUENCE

The olivine-rich sequence is dominated by chrome spinel-rich olivine cumulates with zones which contain either orthopyroxene or feldspar as a post cumulus phase. The magma from which the olivine-rich sequence formed appears to have intruded the earlier layered orthopyroxene-rich sequence as sills, thus breaking this earlier sequence into irregularly shaped rafts, blocks and xenoliths. Layers of olivine with chrome spinel, and at times with post-cumulus feldspar or orthopyroxene, formed within these sills. Where the sills were only a few metres thick the resultant layering was plastically deformed by sinking rafts and blocks of the layered orthopyroxene-rich sequence, forming zones in which the olivine-rich crystal mush has been squeezed between the accumulating blocks. Layering in undisturbed parts of this sequence is thin (less than 5 mm to 50 mm), at times discontinuous and lensoidal over a few metres.

Isolated blocks of the orthopyroxene-rich sequence have smooth scalloped edges where enclosed by the olivine-rich material, probably representing a reaction zone between the intruding and the earlier formed sequence. The only sharp irregular margins observed between the two sequences are in the disruption zones.

In some parts of the olivine-rich sequences occur 50–100 mm thick layers with cumulus orthopyroxene, 10–15 mm in length. These grains define a mineral foliation parallel to layering.

The olivine-rich sequence contains zones with a high chrome spinel content, either as a high concentration of disseminated grains or as irregular pods and lenses. In the area to the east of the road (fig. 44), a five metre thick zone in this sequence contains irregular pods and lenses (50–70 mm thick) of chrome spinel grains. The pods occur a few metres apart from each other along the zone. The enclosing rock type ranges from an olivine cumulate with post-cumulus feldspar, to olivine cumulate with poikilitic orthopyroxene. This area does not contain blocks of the orthopyroxene-rich sequence but it is cut by late stage, thin, orthopyroxenite dykes which intrude the area at a high angle to layering within the olivine-rich sequence. Similar thin orthopyroxene dykes also cut the ultramafic sequences in other parts of the complex. Within the area of the five metre thick zone of chrome spinel pods, numerous gabbro dykes intrude the sequence in a consistent direction, nearly parallel to layering.

Although samples of dunite now consist of serpentine group minerals, magnetite and spinel, the majority of samples still show a remnant cumulate texture in thin section, as the olivine grain boundaries are outlined by dusty magnetite. Abundant euhedral chrome spinel grains are enclosed by the olivine grains and range in size between 0·5 mm and two millimetres. Some spinel grains enclose 0·05–0·15 mm silicate grains. In samples with post-cumulus feldspar, the olivine grains range in size from one to five millimetres, spinel grains are 0·25–0·35 mm, and the feldspar is now hydrogarnet. Orthopyroxene grains, which form a mineral foliation in some olivine cumulate layers, are usually between eight and ten millimetres in length.

Pods and lenses of chrome spinel concentrations consist of euhedral to subhedral grains, ranging in size from 0·1–1·0 mm, with a mosaic texture. Some of the grains originally enclosed early silicate grains, which are now altered to amphibole-group minerals. In samples with lower concentrations, the spinel grains occur as strings around cumulus olivine grains and are enclosed by post-cumulus orthopyroxene, or are between 0·7–1·15 mm euhedral to subhedral grains and cluster around stubby orthopyroxene grains in dominantly olivine cumulate layers. Because of the degree of serpentinisation, the only residual primary mineral phase is chrome spinel.

TWO-PYROXENE GABBRO

In the area covered by Figure 45, gabbro intrudes both the orthopyroxene and olivine-rich sequences as irregular dykes, stringers and pegmatitic patches. In the area of gabbroic rocks to the south of the area covered by Figure 45 (fig. 44) evidence of the multiply intrusive nature of the gabbroic phase is found in the form of sharp contacts between areas of differing grain size. Irregularly cross-cutting the gabbroic and ultramafic sequences are late stage, thin and uniform diopside-plagioclase dykes (2–5 mm thick) and irregular pegmatitic patches, from which clinopyroxene crystals up to 100 mm in length have been recorded.

In thin section, the gabbro samples have a range in texture from fine-grained granular mosaic through medium-grained and coarse-grained granular to pegmatitic. The coarse-grained samples contain three to four millimetre stubby plagioclase grains in a matrix of anhedral orthopyroxene and clinopyroxene. The mineral chemistry of the gabbro is given in Table 5.

Rubenach (1974) considered that the layered ultramafic succession graded into a transition zone of ultramafic material and hypersthene gabbro. His transition zone, mapped as Csg on Figure 1 [around CP682673], is here considered

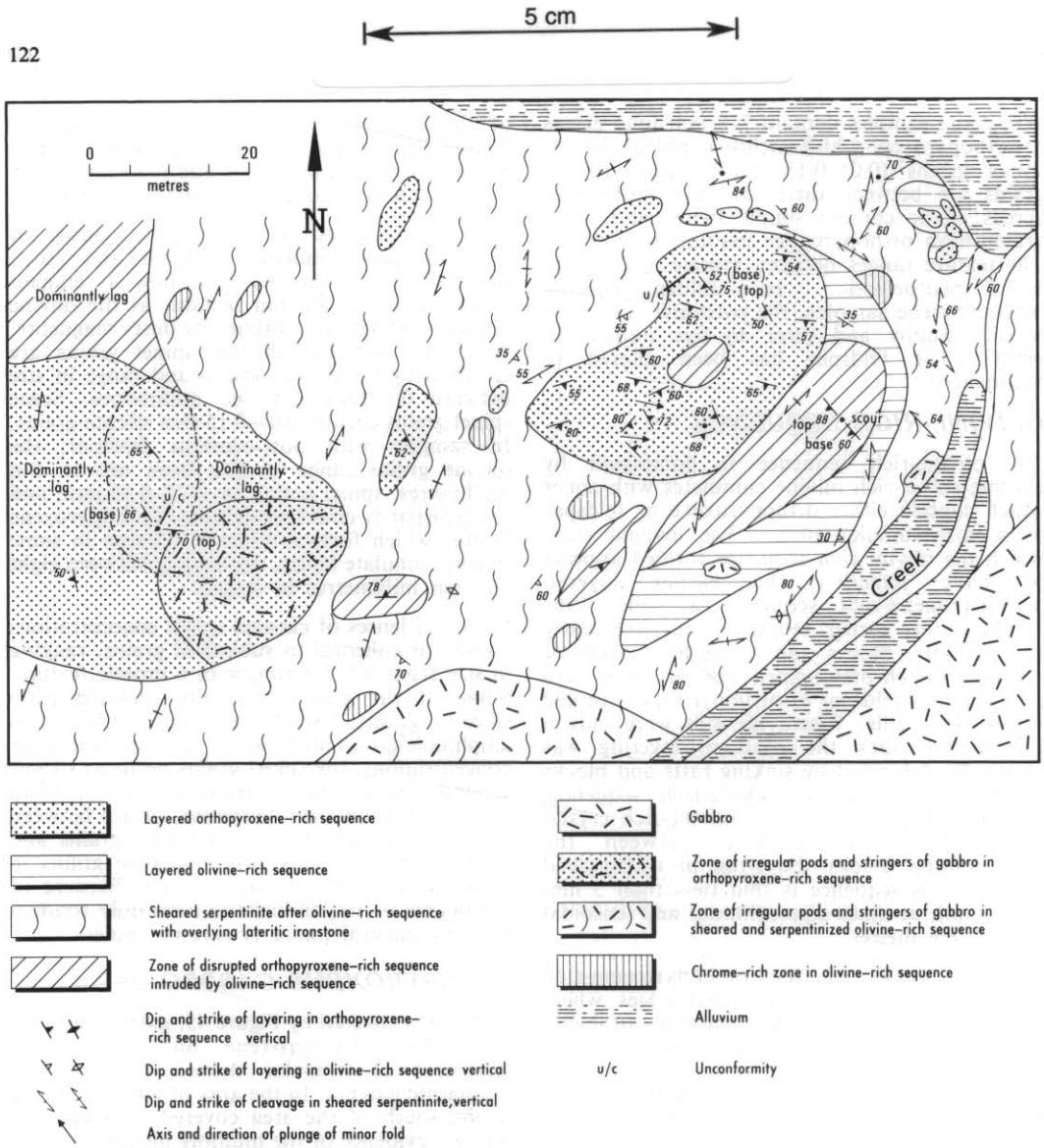

Figure 45. *Detailed geological map of part of the Serpentine Hill Ultramafic–Mafic Complex.*

to have been formed by the two-pyroxene gabbro intruding the olivine-rich sequence, which now forms this area, as sills are parallel to subparallel to layering. The strike difference between the sills and layering in the ultramafic sequence in the area around CP683674 is from ten to fifteen degrees.

DUNDAS ULTRAMAFIC COMPLEX

The Dundas Ultramafic Complex is now mainly massive serpentinite, with a small residual block of LPD succession at the north-western end [around CP680647]. The complex is exposed through a fault window within Dundas Group successions, which were originally deposited on top of the ultramafic body. The ultramafic detritus found within the Red Lead Conglomerate in the Razorback mine workings is considered to have come from this body and not from the younger Serpentine Hill Complex. The Serpentine Hill Complex is considered to have formed as a crustal chamber associated with the low-titanium tholeiitic lavas which interdigitate with the Red Lead Conglomerate in the Ring River area.

The remnant area, in the north-west corner of this complex, contains partially serpentinised ultramafic rocks with recognisable layering similar in dimension and rock type to that described from the Riley Knob area. Layers of serpentinite after dunite are between 10 mm and 50 mm thick, with olivine pyroxenite layers 10–20 mm thick. Orthopyroxenite layers are generally relatively fresh and occur as layers between 10 mm and 50 mm thick with an occasional layer between 150 mm and 200 mm. Disseminated chrome spinel is euhedral and ubiquitous on the weathered surface.

In thin section, some samples of the pyroxenite layers have an even-grained granular texture, the orthopyroxene grains being between 0·25 and 2·75 mm with minor clinopyroxene grains between 0·1 and 0·15 mm. The clinopyroxene grains occur in areas between numerous orthopyroxene grains and were most probably post-cumulus phase. Chrome spinel grains in these samples are between 0·2 and 0·25 mm across. The majority of pyroxenite samples collected are highly deformed and consist of large (4–7 mm) anhedral orthopyroxene grains with thin clinopyroxene exsolution lamellae and kink bands, surrounded by a recrystallised mosaic of 0·1–0·5 mm orthopyroxene and minor clinopyroxene grains. Although the pyroxenite samples have a high degree of internal deformation, the layering is still easily recognisable.

Primary grains in olivine orthopyroxene samples have two grain size ranges. One has orthopyroxene between 1·25 mm and 2·25 mm and olivine grains between 0·75 mm and 1·75 mm. In the second range, the orthopyroxene grains are between 0·65 mm and 1·75 mm, the olivine being 1·35–2·75 mm and minor chrome spinel between 0·2 mm and 0·45 mm across. Numerous zones of brecciation through these samples now contain recrystallised mosaics of 0·1–0·25 mm grains.

Serpentinite after dunite layers has fine-grained magnetite outlining the original olivine grains which were 0·4–0·5 mm across with 0·2–0·35 mm chrome spinel grains.

The smaller body of sheared serpentinite to the south of the main body [around CP700615] contains a higher degree of deformation than the main Dundas body. Along the northern side of this body the serpentinite is massive, bottle green, and contains a high concentration of disseminated chrome spinel. Stichtite is common within the serpentinite area and individual areas of purple have a chrome spinel grain as a nucleus.

Small blocks of fractured, serpentinised and altered pyroxenite occur in the serpentine. In thin section, these areas consist of large (10–30 mm), broken remnant orthopyroxene grains with clinopyroxene exsolution lamellae surrounded by zones of highly birefringent amphibole.

Earlier studies of this area are found in Taylor (1955) and Blissett (1962).

MAJOR AND TRACE ELEMENT CHEMISTRY OF ULTRAMAFIC ROCKS

INTRODUCTION

Because of the high degree of serpentinisation of whole rock dunite samples in all successions, only representative samples were analysed: Pyroxenite and olivine pyroxenite samples from the LPD succession and pyroxenite samples from the LDH succession are relatively fresh, and samples from each of the main areas of LPD succession rocks were analysed. Whole rock analyses of ultramafic rocks from the Serpentine Hill Complex were not obtained due to the degree of serpentinisation. Analyses of gabbroic samples from this complex are discussed on page 69.

Major and trace element analyses (tables 14, 15, Appendix 4) were made in an attempt to define any variation in the bulk rock chemistry within, or between, different areas of ultramafic rocks in the mapped area. Overall the results indicate that there are two chemically distinct groups. These correspond to samples from the LDH succession and samples from the LPD succession respectively, and the minor variations in each group exist in most areas of the respective successions.

When the analyses are plotted on a weight percent AFM diagram (fig. 46) a small iron-enrichment trend is indicated by the samples from the LPD succession, being between M(=MgO)=80·0 and 84·0. However in the Riley Knob area, variation in the AFM ratio of samples from along a 250 m strike section is similar to that obtained across the 120 m of section and both encompass the whole range defined by all samples. Each area consists of rafts of layered material surrounded by sheared serpentinite, and not a continuous physical section, and because of the results of the samples from the Riley Knob area, no overall reconstruction of a classical upward-iron succession can be made.

DUNITE SAMPLES

Whole rock and trace element data are given for six partially serpentinised samples, four metadunite samples, and five samples of serpentinite after dunite, three from the LDH succession and two from the LPD succession (table 14). The results are plotted on a weight per cent AFM diagram. Recalculated anhydrous compositions for the dunite reveal higher silica and lower magnesium values for the whole rock when compared with the composite olivine grains. This is most probably a result of both the small amount of low calcic, low alumina enstatite grains contained within these samples, and the non-isochemical serpentinisation which they have undergone.

The non-isochemical serpentinisation of the samples is reflected by the MgO/SiO_2 ratio changing with the increase in the degree of serpentinisation, which is measured by an increase in loss on ignition value (fig. 47). The whole rock samples have an MgO/SiO_2 average ratio of 1·12, compared with an average ratio of 1·24 for the olivine grains which constitute greater than ninety-five percent of the samples. Similarly the metadunite whole rock samples reflect the MgO loss during serpentinisation before contact metamorphism occurred, because

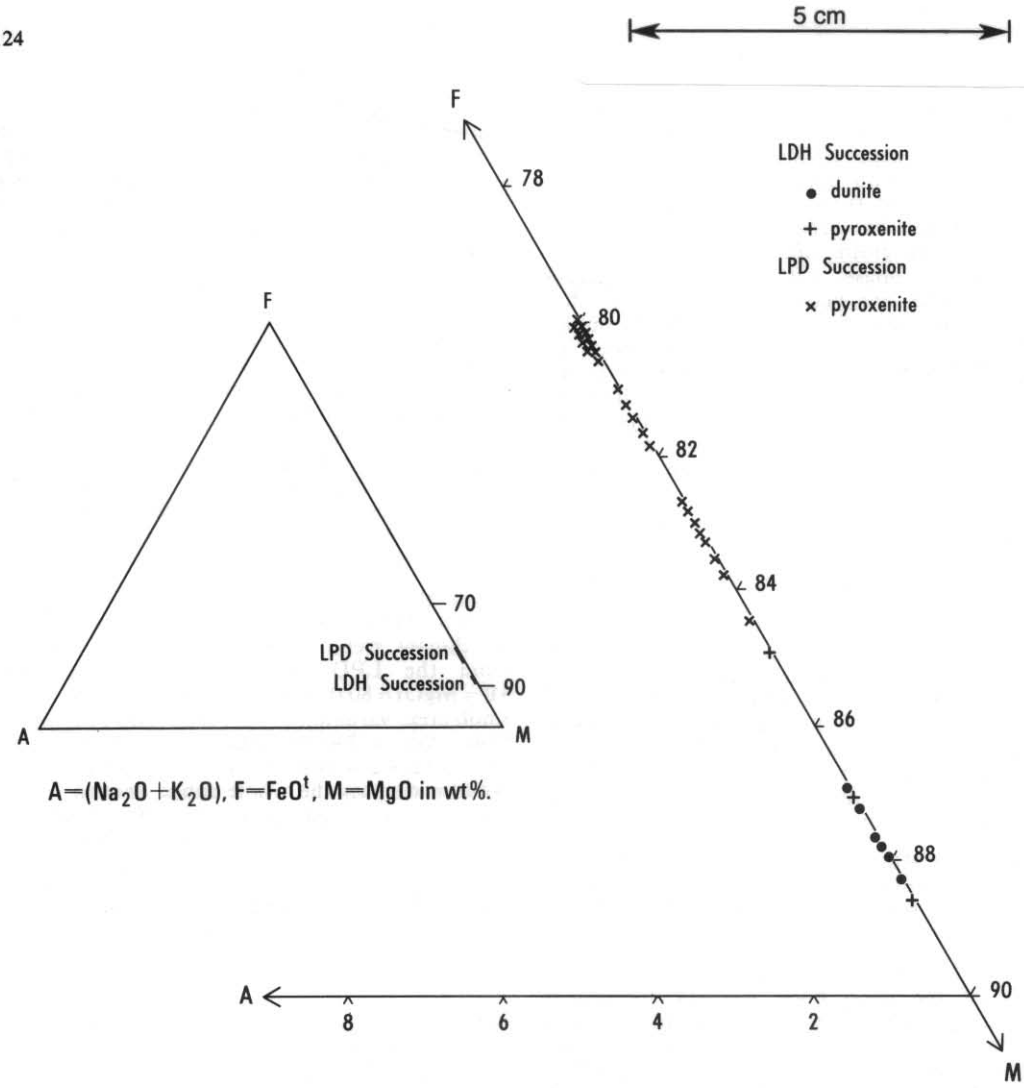

Figure 46. *AFM diagram with plot of analyses of ultramafic rocks from the LDH and LPD successions.*

even though the Mg value of the constituent olivine grains increases from an average forsterite content of 93·36 for unmetamorphosed samples to 94·84 in the metadunite samples, the MgO/SiO_2 ratio of the whole rock samples averages 1·17 in comparison to 1·28 for the constituent grains.

In metadunite samples, the higher forsterite content of the recrystallised olivine grains (table 19) is partly due to iron loss during serpentinisation and partly due to subsolidus re-equilibration at elevated temperatures over a period of time, possibly equivalent to the time taken for the metamorphosing granitic mass to cool. During serpentinisation, iron in excess of that which can be accommodated into the serpentine group minerals (usually lizardite) forms very fine-grained (dusty) magnetite. On metamorphism (> 500°C, probably 600–700°C), the magnetite is not reincorporated into the recrystallised olivine lattice but stays as specific dusty grains scattered throughout the recrystallised olivine.

The second mechanism by which the forsterite content of olivine can be increased slightly is by subsolidus re-equilibration between olivine and coexisting chrome spinel at elevated temperatures over a period of time. Experimental work (Roeder *et al.*, 1979) has indicated that the Mg* of spinel grains increases instead of decreasing with temperatures above 1200°C over very short time periods (two weeks). Field evidence from areas of high-magnesian andesite lavas near granitic masses indicates that the Mg* of the enclosed spinel grains decreases as the granitic body is approached (p. 85). This change must be time related as well as temperature dependent. Evidence from coexisting olivine and chrome spinel grains within the metadunite zones of the LDH succession (table 20) also indicates a lowering of the Mg* of the spinel and an increase of the forsterite value of the olivine in

comparison to the values obtained from samples in the surrounding unmetamorphosed areas (average spinel Mg* of 37 in the metadunite compared with an average of 49 in the surrounding dunite), again indicating the reverse to the experimental work.

Serpentinite samples after dunite from the LDH succession have an MgO/SiO_2 ratio of 1·06 and those from the LPD succession a ratio of 0·92, again indicating the non-isochemical nature of the serpentinisation process for dunite samples, and reflecting the overall lower magnesian content of the LPD succession.

On the AFM diagram (fig. 46), the dunite and associated orthopyroxenite samples from the LDH succession fall into a distinctive field between M = 87·0 and 88·5. The metadunite samples from this succession have a similar average M ratio (88·13), as do serpentinite samples (M av. = 87·45).

Dunite samples from the LPD succession at Colebrook Hill (analyses 14–15, table 14) have an average M value of 82·93, which falls within the field defined by the pyroxenite and olivine pyroxenite samples for this sequence (M = 80·0 to 84·5).

The chromium content of dunite samples ranges between 1750 ppm and 2200 ppm with an average of 1950 ppm. One sample (analysis 3, table 14) with an anomalously high chromium value (6860 ppm) was not used in the average. Nickel contents range between 2250 and 2700 ppm, with an average of 2486 ppm, but the mineral chemistry of these samples (table 15) shows that nickel is not evenly distributed throughout the samples or grains. Electron probe analyses of constituent grains only occasionally record nickel contents higher than detection limit (0·1889 wt% NiO, equivalent to 1485 ppm; the average whole rock value of 2486 ppm represents a NiO content of 0·3163 wt% if uniformly distributed).

PYROXENITE SAMPLES

The majority of pyroxenite samples analysed were orthopyroxenite (table 15) with subsidiary olivine and/or minor chrome diopside content. One sample of websterite was also analysed (analysis 19, table 15). The main difference between pyroxenite samples from within the LDH and LPD successions is that those from the LDH succession have lower Al_2O_3 (average 0·28 wt% cf. 1·55 wt%), CaO (average 1·24 wt% cf. 2·03 wt%), and total iron contents (average 5·1 wt% cf. 7·15 wt%); and higher MgO contents (average 34·01 wt% cf. 30·80 wt%) for samples with less than 4·0 wt% CaO.

Chromium contents of the samples from both successions overlap and have a range of 2600 to 5800 ppm (average 4530 ppm). Nickel contents of samples from the LDH succession have slightly higher but overlapping values to those of the LPD succession, being 770 to 900 ppm (average 840 ppm) cf. 400 to 859 ppm (average 586 ppm). When considering the total range of

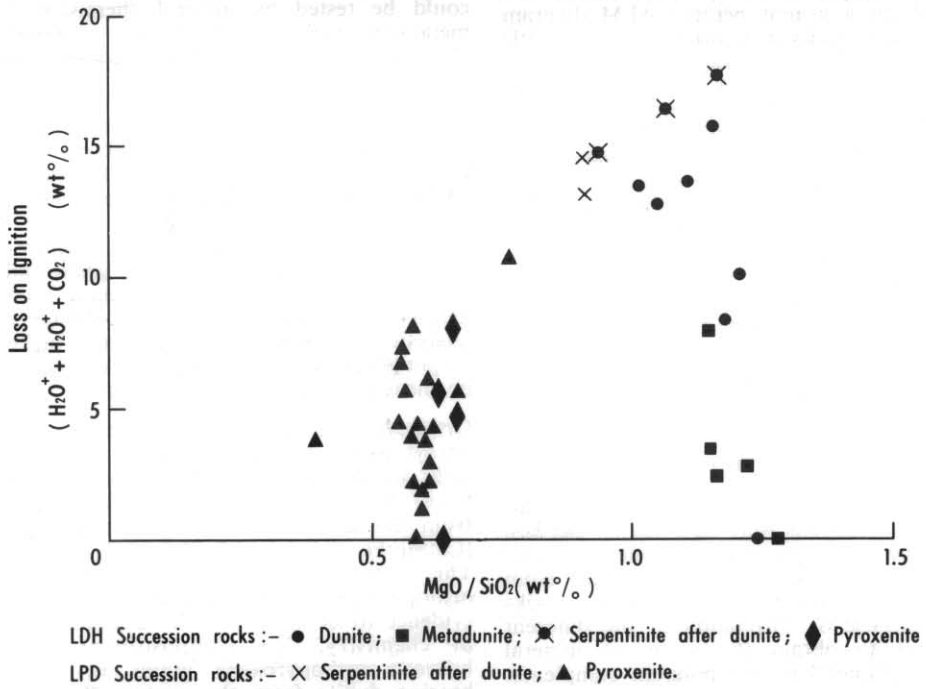

Figure 47. *Loss on ignition∿MgO/SiO₂ (wt%). Degree of isochemical serpentinisation. Samples on base line represent parental compositions based on mineral chemistry.*

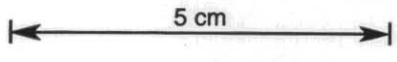

chemistry, the variations are most probably due to a different parental magma composition for the two successions.

Overall, the chromium content of pyroxenite samples is double that of the dunite samples, even though the dunite contains a higher percentage of chrome spinel grains. This makes chromium a useful element in identifying the original rock type of serpentinite samples when other evidence is lacking. The high chromium content of pyroxenite samples also reflects the ability of chromium to enter the pyroxene mineral lattice in comparison to olivine, when the composition and the pressure and temperature conditions of crystallisation are similar.

The average MgO/SiO_2 ratios between component minerals and bulk rock from the same pyroxenite samples from the LPD succession indicate that serpentinisation of the majority of pyroxenite samples was an isochemical process, as both the constituent minerals and whole rock have MgO/SiO_2 ratios of 0·59, although one sample (analysis 17, table 15) has obviously gained MgO.

In pyroxenite samples from the LDH succession the average MgO/SiO_2 ratio for the whole rock and the mineral components is 0·65 and 0·63 respectively, indicating a slight enrichment in MgO during serpentinisation, probably at the expense of the associated dunite layers.

When the samples from the area studied are compared on a weight percent AFM diagram with ultramafic rocks from other areas, the LPD succession samples are always more magnesian than rocks from the large layered complexes (e.g. Bushveld and Stillwater Complexes, which have M values of less than 0·79). However, they are similar to the most magnesian samples found in 'alpine' and 'ophiolitic' complexes in New Zealand (Coleman, 1966), Newfoundland (Church, 1977), Vourinos (Jackson, Green and Moores, 1975; Harkins, Moores and Green, 1980); Troodos (Moores and Vine, 1971) etc. This indicates that the Tasmanian samples probably originated from a more magnesian magma than these other complexes. The other main feature of the Tasmanian complexes is that they are orthopyroxene-rich and not clinopyroxene-rich.

MINERAL CHEMISTRY

Samples from each of the three different ultramafic successions were analysed by electron micro-probe to obtain the component mineral characteristics. Similar data was collected from samples from other areas of ultramafic rocks for the purpose of correlation of the different areas, and to obtain the range of mineral chemistry exhibited by the different complexes.

The mineral grains in most samples were tested by a five-point traverse for chemical zoning and then five to eleven grains of each remnant mineral species were analysed from each sample. The analyses were then averaged to obtain a representative analysis for each mineral species in each sample. Overall, no mineral grain showed significant or consistent zoning. Nickel was randomly distributed throughout olivine grains, as was calcium and aluminium in orthopyroxene grains from the LDH succession. Studies on exsolution in pyroxene grains in samples from the LPD succession were not undertaken and the grains analysed from samples of this succession were as homogeneous as could be obtained. Due to serpentinisation, chrome spinel grains usually had a thin magnetite rim but inside this rim the grains were fairly homogeneous. Tables of the average mineral compositions are included as Appendix 4.

LAYERED DUNITE-HARZBURGITE SUCCESSION

Harman River area

Analyses of coexisting mineral phases of fourteen samples of serpentinised dunite and two of orthopyroxenite were obtained from samples collected from across a 1500 m section between CP608867 and CP628863 of the LDH succession in the Harman River area of the Wilson River Ultramafic Complex. Seven samples of serpentinised dunite from the Mt Stewart area and three from the Adamsfield area were also analysed so that the correlation of the LDH succession on field and petrographic evidence could be tested by mineral chemistry. Eight metadunite samples were probed to obtain the characteristics of this group of rocks.

Olivine grains from within serpentinised dunite samples have a very uniform composition of $Fo_{93\text{-}94}$ (average 93·36, table 16) across the 1500 m section. The olivine grains from this succession consist only of SiO_2, MgO and FeO, with some samples also registering a nickel content (0·35 wt%). If NiO was detected in a specific grain the majority of analyses of that grain and the majority of grains from the sample recorded nickel in the analysis. When a diffuse beam analysis of a grain which registered nickel on a spot analysis was obtained, nickel would not be measured above detection level.

Orthopyroxene grains within the dunite samples always had a calcium content of less than 0·5 wt%, with the majority of grains having contents below detection limit. The orthopyroxene grains from this area have a compositional range of (Ca:Mg:Fe = 0·0–0·5:93·3–93·7:6·5–9·1) (table 17). The lenses and veins of coarse-grained orthopyroxenite, which are considered on field evidence to be late stage, have a similar range of chemistry. The compositional variation between orthopyroxene grains in pyroxene-bearing dunite from the western (basal?) side of the complex in this area ($En_{93\cdot5\text{-}93\cdot7}$), and those from coarse-grained orthopyroxenite lenses one

kilometre up section ($En_{93\cdot3-93\cdot5}$) is so small that it is insignificant and implies a very uniform parental composition and pressure and temperature regime during formation. Chemical evidence for the coarse-grained pyroxenite lenses and dykes being later than the layered dunite-harzburgite in which they occur is shown by composition of the minor olivine component of these rocks. In two areas of LDH succession, at Mt Stewart and Adamsfield, the olivines from the coarse-grained orthopyroxenite lenses are $Fo_{86\cdot4}$ and Fo_{89} respectively. This is in comparison to Fo_{93-94} and Fo_{93} respectively for olivine from within the layered sequence in which the orthopyroxenite samples occurred.

Within orthopyroxene grains from this succession, and correlates in the Mt Stewart and Adamsfield areas, whenever Al_2O_3, CaO, or Cr_2O_3 are recorded above detection limit the values are less than 0·5 wt%, 0·5 wt% and 0·3 wt% respectively. These three elements are unevenly distributed within grains, and not all spot analyses on a specific grain registered the presence of the element, and not all grains within a sample registered amounts of the elements above detection limit. The orthopyroxene grains in the LDH succession have a composition similar to that predicted for protoenstatite.

As with olivine and orthopyroxene, chrome spinel grains in samples of the LDH succession (table 18) have a very small range of composition and are usually composed of Al_2O_3, Cr_2O_3, FeO and MgO. An occasional grain registered MnO or TiO in its composition, with Mn being more frequently present. When present, Mn is always less than 0·5 wt% and Ti less than 0·25 wt%. Only rarely does Mn occur in more than half of the analyses taken in any one sample.

Overall, dunite from the LDH succession has olivine grains of Fo_{93-94}, orthopyroxene grains of En_{93-94} and chrome spinel with a $100\times Cr/(Cr+Al)$ ratio (Cr*) of 87–93 with a variable $100\times Mg/(Mg+Fe^{2+})$ ratio (Mg*) but an average of 49 (fig. 48). Orthopyroxene crystals in the associated coarse-grained pyroxenite lenses and dykes are En_{93-94} with the associated chrome spinel grains having a Cr* of 92–94, and Mg* of 47 (average).

Mt Stewart and Adamsfield areas

Olivine from serpentinised dunite in the Mt Stewart area has a compositional range of Fo_{92-93}. The associated chrome spinel grains have Cr* of 89–94. The Mg* is lower than in the Harman River area, with an average of 41·90. This lower Mg* is considered to result from metamorphism by the underlying granitic mass, as chrome spinel from serpentinite or high-magnesian andesite and associated basaltic pyroxenite samples in close proximity to granitic masses always has a lower Mg* than in similar samples at a distance from the granitic rocks.

Coarse-grained orthopyroxenite, associated with the dunite, has orthopyroxene grains with En_{92} and chrome spinel of Cr* of 89 with the Mg* being 36. Enclosed olivine grains are Fo_{86}. Considering that the samples from this area are fifteen kilometres away from the Harman River body, the analyses of this succession are extremely uniform. Although re-equilibration of the succession is a possible method of obtaining such consistent mineral chemistry over a large area, it will be seen (p. 135) that the mineral chemistry of this succession is consistent with having been a primary precipitate from the spatially associated high-magnesian andesite.

Correlates of the LDH succession at Adamsfield contain olivine of Fo_{92-93} and orthopyroxene of En_{93-94}. Neither calcium nor aluminium were detected in quantities above detection limit. Chrome spinel has a Cr* of 90–94 and a range of Mg*, the average of which is 48. Further mineral chemistry analyses of samples from this area, other than those used in this study, can be found in Varne and Brown (1978).

An extra unit exists in the LDH succession in the Adamsfield area which has so far not been found in other areas of the succession. This unit is a massive coarse-grained orthopyroxenite (Brown, 1972; Varne and Brown, 1978). Samples from this unit contain orthopyroxene of En_{89}, olivine of Fo_{89}, and chrome spinel having a Cr* of 90. This massive orthopyroxenite is considered to be a correlate of the late-stage orthopyroxenite veins and dykes of the Harman River and Mt Stewart areas. Field relationships in the Adamsfield area indicate that the orthopyroxenite overlies the interlayered dunite-pyroxene dunite-harzburgite sequence. The present outcrop relationship is an irregular boundary with evidence of interdigitation, possibly due to later plastic and/or solid flow.

Overall, the LDH succession is a highly depleted succession of well-layered dunite, pyroxene-bearing dunite, harzburgite, and massive orthopyroxenite which has a characteristic high magnesian, high chrome chemical signature allowing correlates of this succession to be unambiguously identified. The chemical composition of the orthopyroxene is consistent with the grains originally having been protoenstatite. There is no evidence of exsolution lamellae of a calcic pyroxene nature in any grain studied from within samples of this succession. The overall chemical data suggests that this succession is likely to have formed from a liquid in the forsterite + protoenstatite + chrome spinel + liquid field.

LAYERED PYROXENITE-DUNITE SUCCESSION

Riley Knob area

Only partially serpentinised olivine pyroxenite and pyroxenite layers were able to be analysed from the LPD succession as no sample of serpentinised dunite contained remnant olivine cores. The orthopyroxene minerals range between En_{85} and En_{89} and have an average composition

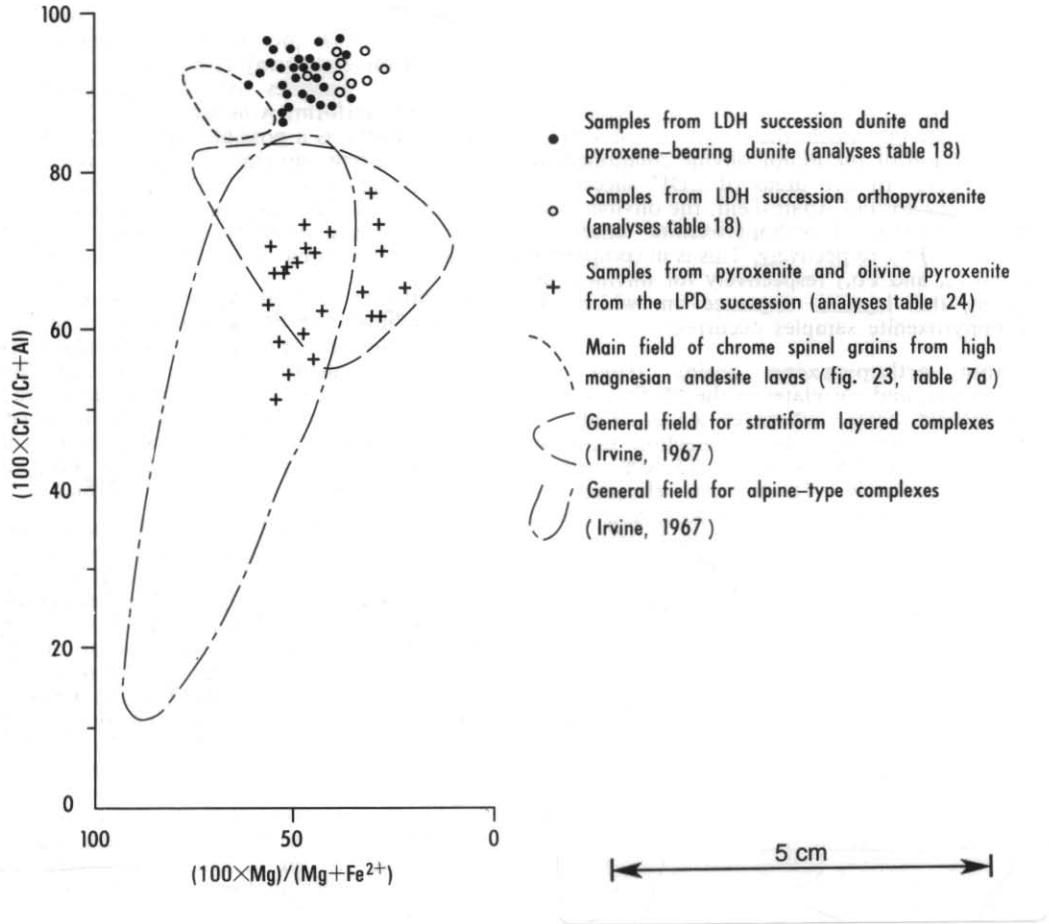

Figure 48. *$(Cr \times 100)/(Cr + Al) \sim (Mg \times 100)/(Mg + Fe^{2+})$ diagram for chrome spinel samples from the LDH and LPD successions.*

of (Ca:Mg:Fe = 1·87:87·82:10·33), with the calcium content ranging between 0·6 wt% < CaO < 2·0 wt% and the aluminium content between 0·75 wt% < Al_2O_3 < 2·0 wt% (table 22, Appendix 4). Olivine grains range between Fo_{87} and Fo_{90} (table 21), and usually have a similar Mg* to the coexisting orthopyroxene mineral. Minor chrome diopside grains average (Ca:Mg:Fe = 47·26:48·94:3·78) and chrome spinel has a Cr* of 63·86 with a Mg* of 48·93. The range of Cr* in spinel grains from the succession is far larger than that from the LDH succession, and grains from the two successions define totally separate fields on a Cr* ∿ Mg* diagram (fig. 48).

The range in chemistry of coexisting mineral phases in samples from this area indicates a well-defined hiatus between the chemistry of the coexisting phases from within the LPD and LDH successions. This hiatus is reflected by the higher FeO, Al_2O_3 and CaO contents of the orthopyroxene grains, higher FeO of the olivine grains, and significantly lower Cr_2O_3 and higher Al_2O_3 contents of the chrome spinel grains. The presence of chrome diopside as a coexisting mineral phase also indicates a bulk compositional difference between the magmas from which the two successions formed.

A similar range of chemistry in the coexisting mineral phases is found in samples from all other areas of LPD succession (tables 21–24), giving an average olivine composition of $Fo_{87\cdot48}$; orthopyroxene composition of (Ca:Mg:Fe = 1·94:86·41:11·65); clinopyroxene of (Ca:Mg:Fe = 46·86:48·66:4·49) and chrome spinel with Cr* of 65·49 and Mg* of 42·97, indicating a consistent parental magma composition for the now spatially separated areas of this succession. As with the LDH succession correlates at Adamsfield, the LPD succession samples from this area have compositions corresponding very closely to the overall average values of the whole LPD succession (tables 21–24).

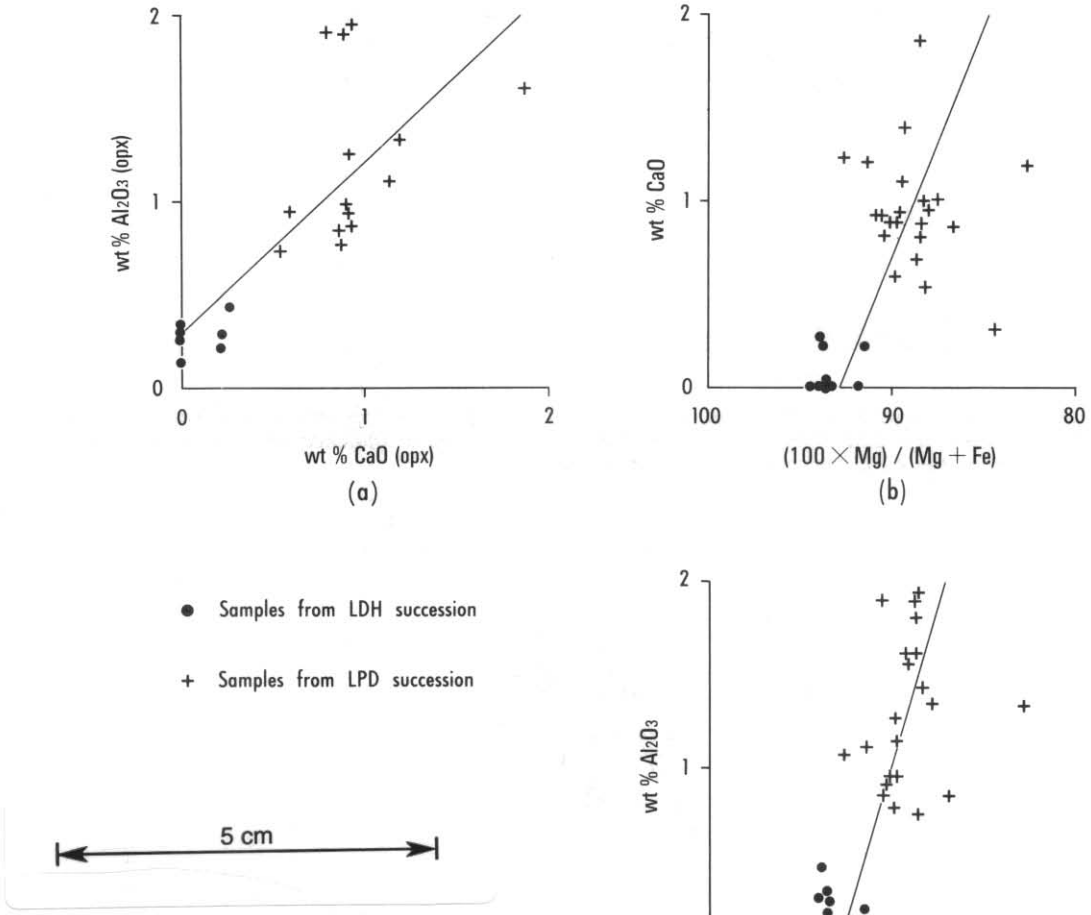

Figure 49. *Chemical variation diagrams for orthopyroxene from the LDH and LPD successions. (a) Al_2O_3∿CaO; (b) CaO∿Mg*; (c) Al_2O_3∿Mg*.*

When chemical composition variation diagrams (fig. 49) are plotted for orthopyroxene analyses from all samples from both the LDH and LPD successions, CaO, Al_2O_3, MgO and FeO all have good, scattered, linear relationships with each other, indicating a compositional control on crystallisation as well as temperature, pressure and oxygen fugacity control.

The compositions of coexisting orthopyroxene and clinopyroxene grains from samples of the LPD succession (fig. 50), irrespective of which area the samples came from, have an overlapping compositional field with parallel tie lines and a restricted range in chemistry but with a small iron-enrichment trend, again suggesting a dominant bulk chemical control. The coexisting pyroxene species in the LPD succession lie at the magnesian end of any compositional trend defined by coexisting pyroxene from peridotite samples from both the large layered ultramafic complexes (Bushveld, Stillwater etc.) and 'alpine' or 'ophiolitic' complexes.

Although there is a small range in the composition of the coexisting pyroxenes and their tie lines are parallel, samples from different areas overlap the range defined by the samples from Riley Knob, and there is not a discernible trend from which a theoretical body may be reassembled along the lines of an upward iron-enrichment trend.

When analyses of coexisting orthopyroxene and chrome spinel are plotted (fig. 51*a*), Al_2O_3 defined a scattered linear relationship between coexisting pairs, again indicating a compositional control. In terms of weight percent content, the LDH succession samples are extremely depleted in Al_2O_3 in comparison to samples from any other

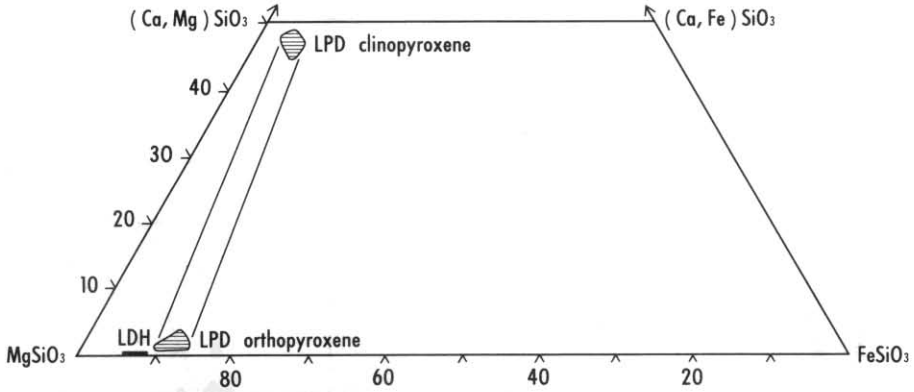

(a) Part of the pyroxene quadrilateral, showing area of plot of orthopyroxene analyses from the LDH succession (c), and orthopyroxene + coexisting clinopyroxene (hatched areas with boundary tie lines) from the LPD succession (b and c).

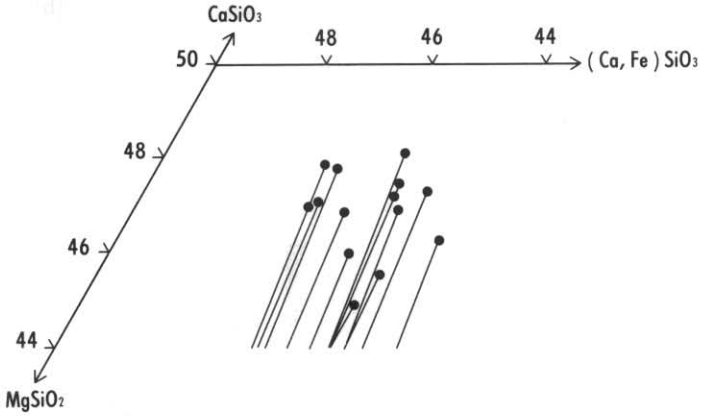

(b) Part of the pyroxene quadrilateral, showing compositions and direction of tie lines for clinopyroxene from the LPD succession (compositions table 23).

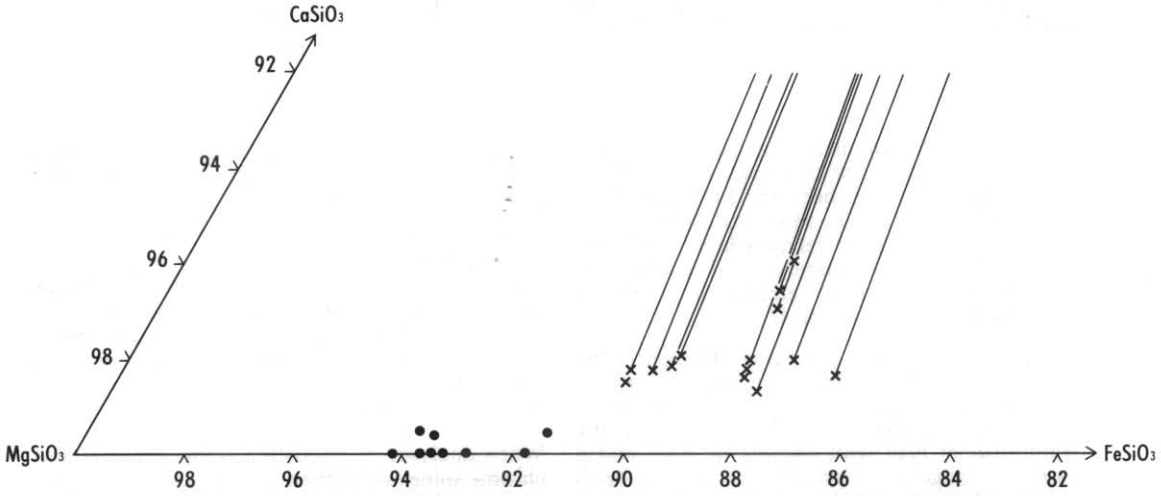

(c) Part of the pyroxene quadrilateral, showing compositions and direction of tie lines for orthopyroxene from the LPD succession (crosses), and compositions of orthopyroxene from the LDH succession (dots) (compositions tables 17 and 22).

Figure 50.

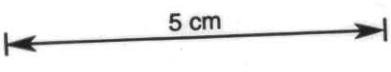

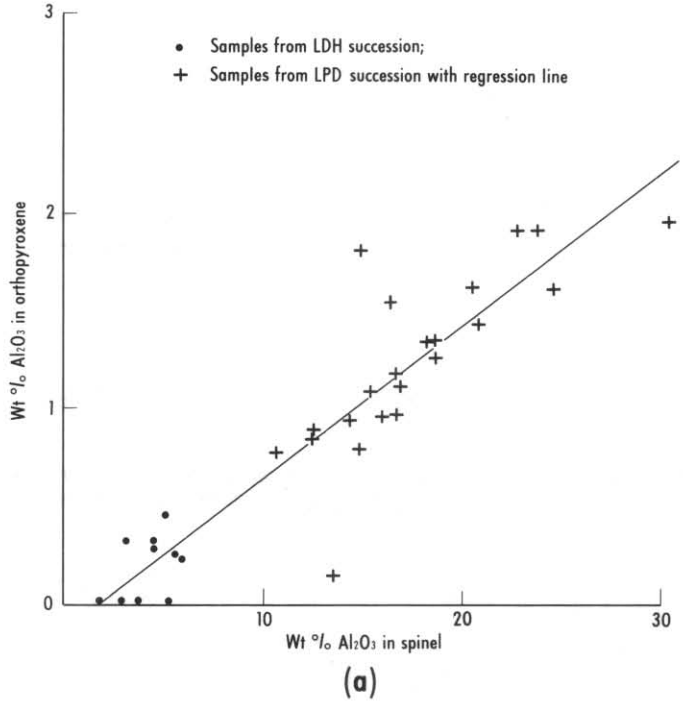

(a)

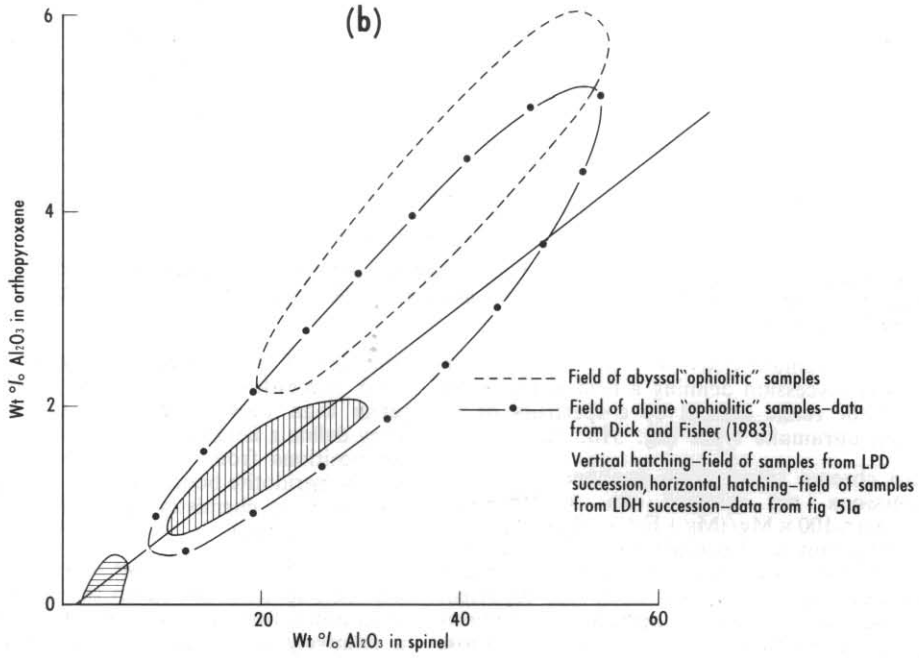

Figure 51. *Variation in Al_2O_3 in coexisting orthopyroxene and chrome spinel.*

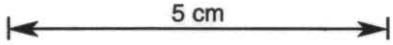

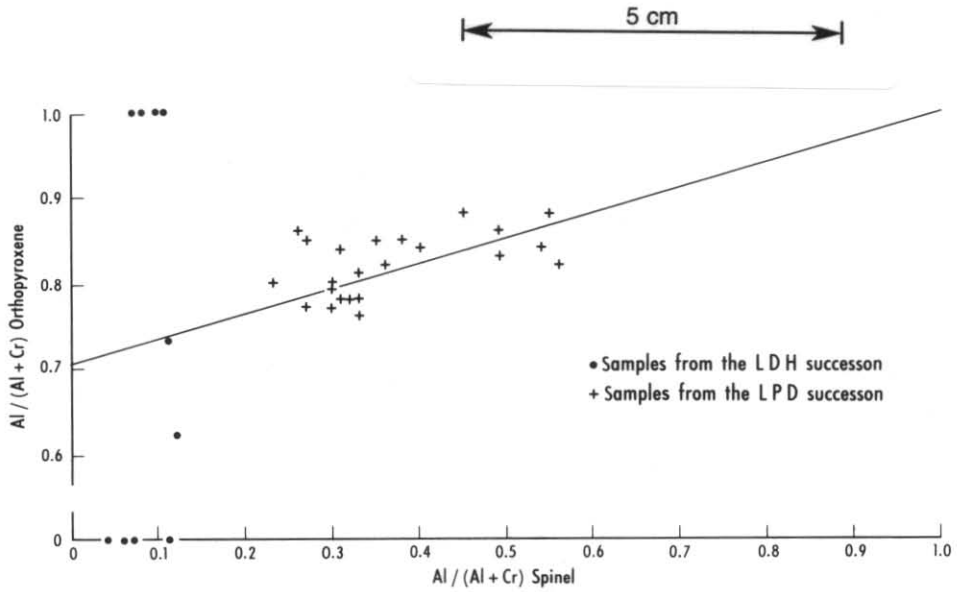

Figure 52*a*. *Distribution of Al and Cr in coexisting orthopyroxenite and spinel for samples from the LDH succession and LPD succession, with regression line defined by all samples.*

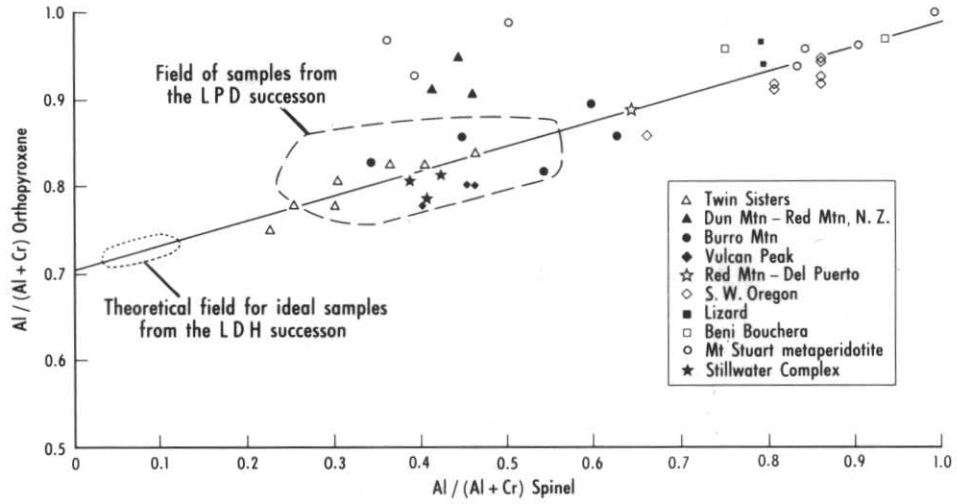

Figure 52*b*. *Distribution of Al and Cr in coexisting orthopyroxene and spinel from alpine-type peridotite, after Dick (1977) with regression line and fields defined by samples from the Tasmanian ultramafic samples (fig. 52a).*

recorded ultramafic body, with the samples from the LPD succession defining a field at the lower end of the range defined by a spectrum of all existing ultramafic types (fig. 51*b*, 52).

When chrome spinel grain analyses from both successions are plotted on a $100 \times Cr/(Cr + Al) \sim 100 \times Mg/(Mg + Fe^{2+})$ diagram (fig. 48), the grains from samples of LDH succession rocks define a field more enriched in chromium than any other ultramafic body yet reported. The spinel grains from the orthopyroxenite veins and lenses are slightly more iron rich than those in dunite and pyroxene-bearing dunite samples, again suggesting a later stage formation of the massive, coarse-grained orthopyroxene phase, as is indicated by both field and olivine composition data.

Analyses of the chrome spinel grains from the LPD succession have a larger compositional range than those from the LDH succession. They define a field which overlaps chrome spinel compositions from both alpine-type and large layered peridotite bodies (fig. 48) and again show the hiatus in chemistry between the LDH and LPD successions.

When plotted on a $Cr\text{-}Fe^{3+}\text{-}Al$ triangular plot (fig. 53), spinel grains from the LDH and LPD successions form two separate fields, both with a relatively small range in Fe^{3+}, the majority of which have an exceedingly low Fe^{3+} component. The samples do not define an Fe^{3+} enrichment trend, indicating a fairly consistent and low oxygen fugacity environment of formation for both of the successions.

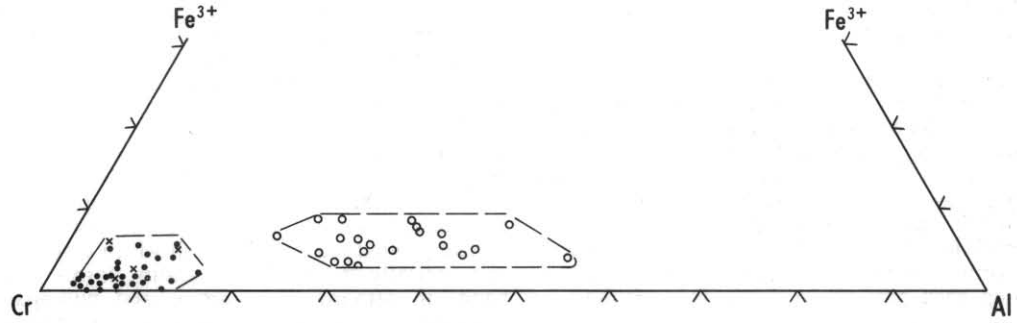

Figure 53*a*. *Cr∿Al∿Fe³⁺ plot of chrome spinel analyses from the LDH and LPD successions.*

- ● *dunite, pyroxene-bearing dunite, and harzburgite*
- × *massive orthopyroxenite*
- o *samples from LPD succession*

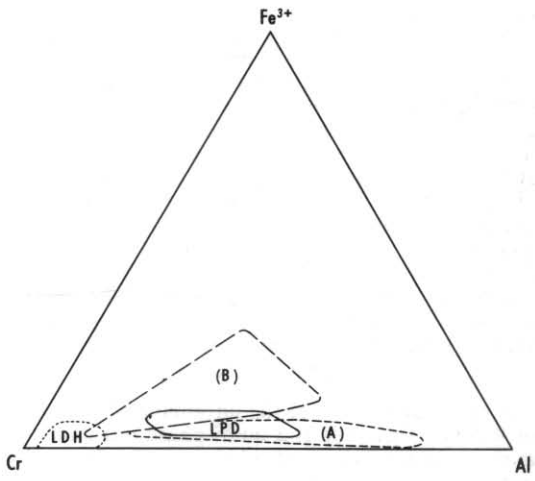

Figure 53*b*. *Cr∿Al∿Fe³⁺ diagram with field of spinel compositions from the LDH and LPD successions (fig. 53a) compared with fields of spinel composition from a non-Fe³⁺ increasing body (A; Josephine Peridotite, Dick, 1977); and an Fe³⁺ increasing body (B; Marum Peridotite, Jaques, 1981).*

LAYERED PYROXENITE-PERIDOTITE AND ASSOCIATED GABBRO SUCCESSION

Serpentine Hill area

The degree of serpentinisation of the LPG succession frustrated an attempt to gain a full range of silicate mineral chemistry. Only pyroxenite samples within the orthopyroxene-rich sequence contained primary silicate minerals. Orthopyroxene grains from this sequence (table 25) have an average of (Ca:Mg:Fe = 2·1:87·0:10·9), with coexisting clinopyroxene being (Ca:Mg:Fe = 47·6:48·4:4·0). Associated chrome spinel grains (table 26) have an average Cr* of 62·05 and Mg* of 46·75 (fig. 54). Silicate grains enclosed by the spinel are now tremolite or tremolitic hornblende (table 25).

The only residual primary phase in the olivine-rich sequence is chrome spinel. Analyses of spinel grains from samples within the general olivine-rich sequence have a slightly lower average Cr* than those within samples from the orthopyroxene-rich sequence (59·15 compared to 62·05), whereas samples from the five metre thick zone of chrome spinel pods and lenses have a much higher average ratio of 68·85 (table 26). All spinel analyses from the LPG succession plot within the field defined by samples from the LPD succession, but the presence of plagioclase as a mineral phase, the evidence of multiple magma phases, the presence of associated gabbro and the very different Platinum Group Element contents (Brown *et al.*, in prep.), all suggest that the LPG succession is derived from a different parental magma to those which formed the LPD and LDH successions.

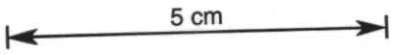

SUMMARY OF ULTRAMAFIC SUCCESSIONS

In the past, the ultramafic complexes of western Tasmania have been described as both disrupted ophiolites (Rubenach 1973, 1974) and 'ophiolitic' (Varne, 1978; Varne and Brown, 1978; Brown *et al.*, 1980). With the evidence obtained in this study, no ultramafic rock complex within Tasmania can be described as an ophiolite or 'ophiolitic', nor can the tectonic environment of formation of these bodies be suggested as having been part of an ocean-floor setting.

The ultramafic rocks of western Tasmania are orthopyroxene-rich and this feature alone separates the ultramafic rocks of this area from the world-wide, dominantly clinopyroxene-rich sequences, which are usually associated, by the describing authors, with spreading ridge, ocean-floor, island-arc or back-arc environments.

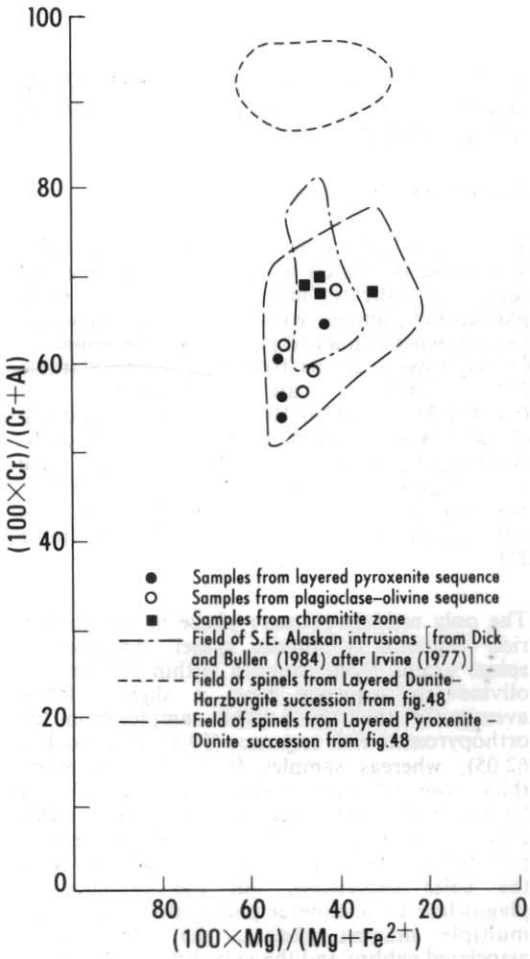

Figure 54. *$(Cr\times 100)/(Cr+Al)$ ∿ $(Mg\times 100)/Mg+Fe^{2+}$) diagram with the analyses of chrome spinel samples from the Serpentine Hill Ultramafic-Mafic Complex.*

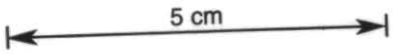

The Layered Dunite-Harzburgite Succession is a well-layered sequence dominated by dunite and pyroxene-bearing dunite in comparison to the harzburgite content. Late stage, massive, coarse-grained orthopyroxenite units, and/or dykes and veins, overlie or cut the layered sequence. As well as distinct layering, this succession also contains primary mineral foliations, parallel to layering, of orthopyroxene and chrome spinel. The whole succession has an overprinted tectonic foliation which elongates and optically strains olivine grains, forms kink bands in orthopyroxene grains and pull-apart structures in large (2 mm) euhedral chrome spinel grains. No evidence consistent with protogranular or porphyroblastic textures has been observed but the interpretation of original textures is ambiguous due to the masking effect of serpentinisation. Chrome spinel grains are euhedral and a co-precipitating phase with olivine. No rounded or holly-leaf shaped spinel grains were observed, again indicating that only primary mineral phases are present.

The Layered Pyroxenite-Dunite Succession is again orthopyroxene-rich but also contains minor chromian diopside grains in most pyroxenite layers. This succession is also characterised by very thin to thin layering and unambiguous cumulate and adcumulate textures, being either granular or interlocking. There is a chemical hiatus between mineral constituents of the LDH and LPD successions, possibly suggesting two different source magmas. Samples from the LPD succession define a small iron-enrichment trend and plot at the magnesian end of any trend defined by other ultramafic bodies. The succession was dismembered in the solid state and rafts of layered material with serpentinitic sheaths were emplaced into basins of deposition before the middle Middle Cambrian.

The third subdivision of the ultramafic complexes of western Tasmania is a multi-phase ultramafic-mafic succession, consisting of layered pyroxenite-peridotite and associated gabbro (LPG succession). This succession consists of an original layered, orthopyroxenite-rich sequence, with numerous sedimentary-style structures. An olivine-rich sequence intrudes and disrupts the first sequence, forming a layered succession incorporating blocks of the orthopyroxenite-rich sequence and containing zones which are rich in chrome spinel. Both of these ultramafic sequences were then intruded by a phase of massive two-pyroxene gabbro. Although the mineral chemistry of the constituent mineral phases of the orthopyroxene-rich sequence is similar to that of the LPD succession, it contains plagioclase as a major post-cumulus phase and layer types (e.g. deferred graded dunite) not found in the LPD succession. The olivine-rich sequence does not exist in the LPD succession and also contains plagioclase as a post-cumulus phase. Some of the gabbro samples appear to contain cumulus plagioclase. This third subdivision of the ultramafic rocks

also contains a higher overall PGE content than either the LDH or LPD succession.

The obvious relationships between different chemical elements in different mineral phases of these successions indicate a compositional control. Low TiO_2, Al_2O_3, CaO, Na_2O and K_2O contents of the coexisting mineral phases in the LDH succession probably indicate a low abundance of these elements in the parental magma for this succession. As spinel is the only mineral which takes large amounts of Fe^{3+} into its lattice, the amount of ferric iron within spinel grains is considered to be a measure of the Fe^{3+} in the melt, which is in turn a direct function of the prevailing oxygen fugacity. Thus both the LDH and LPD successions formed under conditions of low (LPD) to very low (LDH) oxygen fugacity.

The coexisting mineral chemistry of the LDH succession indicates formation under bulk chemical control in the forsterite (Ol) + protoenstatite (Pen) + spinel (Sp) + liquid stability field under conditions of low oxygen fugacity, high temperature and low pressure, and regularly fluctuating between Ol + Sp; Ol + Pen + Sp, and Pen + Sp, with the degree of incongruent melting of protoenstatite possibly dictating whether pyroxene-bearing dunite or harzburgite was formed.

Because of the sharp layer boundaries and thin to very thin layering in both the LDH and LPG successions, and the similar densities of olivine and enstatite, gravitational settling of the cumulus mineral phases could not have produced these successions.

AMPHIBOLITE (€sa)

Amphibolite and amphibolitised pyroxenite have been mapped in four different settings within and associated with the ultramafic rock successions. These include areas along the western margin of the ultramafic bodies with the country rocks; within the contact metamorphic aureoles of granitic bodies intruding ultramafic rocks; in fault zones and zones of cataclasis within and between different bodies of ultramafic rocks; and within areas of layered pyroxenite which has undergone *in situ* amphibolitisation.

All amphibolite found as lenses along the western margin of the Wilson River Ultramafic Complex (area 5, fig. 42; fig. 1), as well as the Heazlewood River and Serpentine Hill Ultramafic Complexes (areas 3 and 7, fig. 42; figs 1 to 3) (Rubenach, 1973), has a well-developed mineral foliation indicating conditions of formation which included tectonic stress as well as metasomatism. Amphibolites within layered pyroxenite bodies retain their external layering and textural features and probably result from a combination of metasomatic and serpentinisation processes as described by Coleman (1966). Similar primary textural appearances are retained within those samples from within the metamorphic aureoles of granitic intrusions. Many of the samples retain sufficient residual primary mineral grains for the original rock type to be recognised.

Analyses of amphibolite samples from different settings are given in Table 27. These include foliated amphibolite (analyses 1, 2); amphibolite from within granitic aureoles (analyses 3, 4); amphibolised cataclastic pyroxenite from within a faulted contact between areas of LDH and LPD succession rocks (analysis 5); and amphibolite derived by *in situ* alteration of pyroxenite and gabbro (analyses 6–10).

Foliated amphibolite crops out in at least four places along the western margin of the Wilson River body, occurring as lenses between the country rocks and the sheared serpentinite sheath of the ultramafic body, or within the serpentinite sheaf. One good example of this type is exposed in the Harman River [near CP635839] and consists of a well-foliated amphibolite which crops out as a prominant bar across the river and has sharp contacts against sheared serpentinite to the east and Crimson Creek Formation rocks to the west. This amphibolite contains 0·25–1·0 mm grains of colourless to light green pleochroic magnesio-hornblende (table 28, analysis 6) with a strong mineral foliation, along which broken chrome spinel grains are spread out as stringers up to four millimetres in length. Thin zones (0·5 mm wide) of non-aligned amphibole grains, magnetite and chrome spinel fragments, all between 0·2 mm and 0·35 mm across, also occur throughout the sample. The zones are parallel to the mineral foliation. The eastern edge of this lens, against the sheared serpentinite, consists of cataclastic amphibolite with light green to light brown pleochroic anhedral grains (magnesio-hornblende) up to one millimetre in length, and disseminated magnetite. The tectonic fabric within the lens is not aligned with the foliation within the surrounding serpentinite, nor with the tectonic foliation superimposed on the amphibolite which causes the cataclasis along the eastern margin. This suggests that this body formed prior to emplacement into its present position.

A lens of amphibolite has been described from the Ahearne Creek area [CP697794], four kilometres to the south-east of the Harman River lens (Rubenach, 1973). This lens crops out along the contact of the serpentinite and country rock and samples are described as having a protoclastic texture with porphyroblasts of magnesio-hornblende (table 28, analysis 8) up to three millimetres in length surrounded by grains with an average size of 0·3 mm. Some specimens from this lens are reported (Rubenach, 1973) to contain relict olivine grains and porphyroblasts, which is consistent with the lens having been formed from olivine-rich rocks of LDH succession. Rubenach also noted a discordance between the internal mineral foliation and the foliation in the surrounding

serpentinite, again suggesting formation of the amphibolite prior to re-emplacement of the ultramafic rocks during Devonian deformation events, which produced the present juxtaposition with the country rocks.

On the western margin of the ultramafic mass in the Huskisson River [CP706753], blocks of amphibolite with a strong mineral foliation occur within the serpentinite sheath. The mineral grains in these samples are between 0·5 mm and 1·0 mm in length and have light to pale green pleochroism and optical properties typical of magnesio-hornblende.

In the Pieman River [around CP714738], a sequence of originally layered pyroxenite and olivine pyroxenite has undergone cataclasis with the resultant rock-flour recrystallised to interlocking grains (up to 2·5 mm) of mid-green to light brown pleochroic magnesio-hornblende (table 28, analysis 7). Remnant orthopyroxene grains (0·3 mm across) and euhedral chrome spinel grains (0·15–0·25 mm) remain in most samples.

Amphibolite from the metamorphic aureole around the northern edge of the Wilson River body (table 27, analyses 3, 4) consists of closely-packed acicular to bladed grains, with a mean grain size of 0·7 mm. Numerous blade-like and columnar aggregates show simple twins, the twin plane being parallel to elongation of the crystal. The grains are colourless and have optical properties consistent with actinolite. The samples do not have an internal mineral foliation. The samples were originally obtained as pyroxenite samples from part of the LDH succession which, in this area, is dominated by thick harzburgite layers with thin interlayered dunite and medium to coarse-grained orthopyroxenite lenses. The remnant layering contains a good foliation parallel to layering.

A sample of amphibolite from the margin of an area of LPD succession which has a faulted contact with LDH succession rocks (table 27, analysis 5) consists of fibrous anthophyllite and columnar aggregates of actinolite and minor tremolite (table 28, analyses 1–3) aligned with both an early mineral foliation as well as the later tectonic foliation. Annealing of fibres has occurred in some areas, but the resultant anhedral grains (up to 1 mm in length) are not aligned with the tectonic foliation.

To the east of the Huskisson Syncline, in the tail of the Huskisson River Ultramafic Complex (area 6, fig. 42; fig. 1, 3), blocks of 'pyroxenite' crop out in areas dominated by sheared and blocky serpentinite. Two samples of such 'pyroxenite' (table 27, analyses 8, 9) turned out to be further samples of *in situ* alteration of pyroxenite to amphibolite. The original texture of the rock is preserved in both hand specimen and thin section and appears to have consisted of cumulus orthopyroxene and possibly minor post-cumulus feldspar(?) poikilitically enclosed by clinopyroxene (pyroxene analyses, table 28*b*). The samples now consist dominantly of fibrous, acicular and columnar tremolite (table 28*c*, analyses 4, 5) with minor remnant areas of primary pyroxene minerals.

Intruding the ultramafic rocks in the Colebrook Hill area (fig. 1) [CP767728] are gabbroic dykes belonging to Group 2 Gabbro (p. 70), the ferromagnesian minerals of which have been metasomatised to amphibole group minerals. The primary texture in hand specimen and thin section is still interlocking granular, with grains between 0·25 mm and 0·65 mm across. The plagioclase has been altered to a dark brown hydrogarnet, the original pyroxene grains are now remnant cores in a pervading mass of acicular sheaves, and columnar crystals of light to mid-brown pleochroic hornblende. Thin cross-cutting fractures are filled by fibrous anthophyllite.

From the above evidence there are at least two different sets of conditions for the formation of amphibolite associated with ultramafic bodies. One set of conditions includes the presence of tectonic forces as well as metasomatic processes, resulting in the lenses of amphibolite found along the margin of the ultramafic bodies and the country rock. All samples of this type from the extended study area are along the western margin of the ultramafic bodies on the western side of the Huskisson Syncline, and the amphibolite is characterised by the composition of the amphibole mineral, magnesio-hornblende, and an internal mineral foliation.

Amphibolite formed by *in situ* metasomatic processes associated with cataclasis, serpentinisation and/or contact metamorphic effects, results in the primary texture of the original rock being preserved but the constituent mineral grains being replaced by tremolite-actinolite and minor anthophyllite. The alteration of the bulk chemistry of the rocks occurred under conditions such that the mobility of many elements, especially SiO_2, Al_2O_3, FeO, MgO and CaO was possible.

PETROGENESIS OF ULTRAMAFIC-MAFIC SUCCESSIONS

LAYERED DUNITE-HARZBURGITE SUCCESSION

Data obtained from the layering and mineral chemistry of the coexisting phases of the LDH succession gave an indication of the composition of the parent magma, as well as the temperature and pressure conditions under which the LDH succession crystallised. Layering indicates that the conditions of formation included an oscillating supply of: olivine (Ol) + chrome spinel (Sp) (dunite); Ol + orthopyroxene (Opx) + Sp (pyroxene-bearing dunite or harzburgite); progressing to a late stage Opx + Sp ± minor Ol (massive coarse-grained orthopyroxenite). As the

layers have sharp boundaries, primary chrome spinel and orthopyroxene foliations within dunite layers, and the density of olivine and orthopyroxene is similar, then simple gravitational settling of crystallised mineral phases does not explain the formation of layers within this succession. Such layers and mineral foliations would need virtual *in situ*, laminar nucleation of the different mineral phases, probably at the crystal mush–liquid interface, as well as repeatable and reversible temperature fluctuations, or cyclic PH_2O changes assuming crystallisation from a liquid of gradually changing composition. A mechanism such as undercooling, with small temperature fluctuations due to crystallisation in the undercooled state (Hawkes, 1967), as well as possible variation in the activity of silica (Keith, 1954) as was suggested for the formation of layering of the ultramafic rocks at Adamsfield (Brown, 1972), may account for the layering found within the LDH succession.

An estimate of temperature of formation may be obtained using a geothermometer based on coexisting olivine and chrome spinel. Although there has been a lot of discussion as to the reliability of this geothermometer and the most realistic values of free energies of the spinel end members (Irvine, 1965; Evans and Frost, 1975; Jackson, 1969; Fabries, 1979; Roeder *et al.*, 1979; Engi and Evans, 1980; etc.), Varne and Brown (1978), using Jackson's (1969) equation, showed that the mineral components of rocks from the ultramafic sequence at Adamsfield, now correlated with the LDH succession, probably offered a good guide to the temperature of formation of these rocks.

Using Jackson's (1969) equation, seventeen samples of the LDH succession from the Harman River, Mt Stewart and Adamsfield areas (table 29) gave a mean nominal equilibration temperature of 1290 ± 73°C. A temperature of 1292°C is obtained for an average olivine-spinel pair for this succession. Roeder *et al.* (1979) disagree with the values of free energy used by Jackson (1969), as the latter's equation gave unrealistic values when used for basaltic rocks rather than ultramafic rocks. The merits of this disagreement are outside the framework of this study, but using the equation of Roeder *et al.* (1979), a mean nominal temperature of equilibration for the LDH succession samples of 661 ± 34°C is obtained, with a temperature of 662°C for the average pair. If the equation of Roeder *et al.* (1979) is correct, then the temperature represents a re-equilibration temperature and not crystallisation temperature. This is not considered to be the case, as Irvine (1965) showed that if coexisting olivine and spinel grains equilibrated at a given temperature and pressure, then a linear relationship would be expected from a plot of: $\ln X^{ol}_{Mg}(1-X^{sp}_{Mg})/(1-X^{ol}_{Mg})X^{sp}_{Mg}$ against Y^{sp}_{Cr} at low $Y^{sp}_{Fe_3+}$ where X^{α}_{i} is the mole fraction of component i in phase α and Y^{T}_{i} is the mole fraction of trivalent ions in the octahedral sites of the spinel structure, with $Y^{sp}_{Cr} + Y^{sp}_{Al} + Y^{sp}_{Fe_3+} = 1$. The $Y^{sp}_{Fe_3+}$ value of the spinel grains from the LDH succession is low and falls within a small range (fig. 53). A plot of the above relationship (fig. 55) shows that samples from the LDH succession cluster around a linear relationship and define a regression line subparallel to, and higher than, the calculated 1200°C isotherm [taken from Varne and Brown (1978) and calculated for $Y^{sp}_{Fe_3+} = 0$ using data of Jackson (1969)], suggesting that the olivine and spinel grains are very close to their equilibrium compositions, and indicating a temperature of crystallisation of 1300 ± 50°C.

Estimates of pressure conditions existing during crystallisation are harder to establish. Chrome spinel grains from the LDH succession are very uniform in composition, have an average weight percent content of Cr_2O_3 of $68{\cdot}25 \pm 7{\cdot}53$, low Al_2O_3 contents (average of $4{\cdot}04 \pm 1{\cdot}48$ wt%), very low TiO_2 (< detection limit of the electron probe, ~0·2 wt%) and Fe_2O_3 contents, indicating crystallisation from a Cr-rich, Ti-poor liquid at low oxygen fugacity.

Hill and Roeder (1974) indicated that for basaltic magmas, the weight percent of Cr_2O_3 in chrome spinel increases with temperature at low pressure and low oxygen fugacity. Jaques (1980, 1981) showed that chrome spinel becomes increasingly Cr-rich at low pressure and that liquids capable of crystallising high chrome-rich spinel (62–64 wt% Cr_2O_3) require a liquid with 1500–2000 ppm Cr and crystallisation at very low (2–5 kb) pressure.

Jaques and Green (1980) indicate that the weight percent of Al_2O_3 in spinel and coexisting orthopyroxene crystallising from liquids of basaltic to picritic composition has values of < 0·5 wt% Al_2O_3 in Opx at temperatures of approximately 1350°C and pressures of 2 kb to 5 kb. The $Cr/(Cr+Al)$ ratio of spinel and Opx increases and the weight percent of Al_2O_3 and CaO decreases in Opx with increasing temperature at these very low pressures. Spinel grains in their study only reached a $Cr/(Cr+Al)$ ratio (Cr*) of 80, indicating that the parent liquid for the LDH succession required, as a minimum, higher Cr* values than the liquid compositions obtained in that study. They also showed, for both the peridotites used in the study, that chrome spinel near the solidus at very low pressure (2–5 kb) was more chrome-rich than that formed at higher pressures (10–15 kb).

The above experimental work suggests that chrome spinel with compositions similar to those found in the LDH succession, and coexisting with olivine of Fo_{92-94} and low Al_2O_3 and CaO orthopyroxene of En_{93-94}, may be obtained at temperatures around 1350°C and very low pressure (2–5 kb) from an anhydrous melt of basaltic composition.

Studies of the chemistry of the coexisting mineral phases in the ultramafic successions indicate that a bulk liquid composition control played an important part in the production of the LDH succession. These studies also indicate that the liquid was low in TiO_2, CaO, Na_2O and K_2O, rich in SiO_2, MgO and Cr, and probably had a 'basaltic' Al_2O_3 content. The experimental studies of Jaques and Green (1980) suggest that at the high temperatures and low pressures predicted above, Al_2O_3 remains in the liquid during crystallisation of Ol + Opx + Sp with compositions similar to those found in the LDH succession, suggesting that low contents of Al_2O_3 found in the coexisting Opx and spinel does not indicate a low liquid Al_2O_3 content. If the deduction of pressures of 2–5 kb is correct, then the liquid in equilibrium with both olivine and orthopyroxene would be quartz normative (Jaques and Green, 1980).

The $Mg/(Mg + Fe^{2+})$ ratio of the liquid can be estimated using studies on equilibrium between olivine and basaltic liquids (Green and Ringwood, 1967; Roeder and Emslie, 1970). These studies indicate that the composition of olivine precipitated from a basaltic liquid is virtually independent of temperature, and that it depends almost totally on the magnesium to ferrous iron ratio of the liquid. Using distribution coefficients of 0·27–0·30 (Roeder and Emslie, 1970) the liquid in equilibrium with olivine of $Fo_{92\text{-}94}$ would have a $Mg/(Mg + Fe^{2+})$ ratio of 76–78 for a K_D of 0·27 and 80–82 for a K_D of 0·3. In a plot of ln K_D for magnesium to ferrous iron of coexisting olivine-spinel pairs, against mole proportion of chromium in the coexisting spinel (after Irvine, 1965), samples from the LDH succession lie in a spread around a linear trend (fig. 55). This indicates some re-equilibration in the subsolid state, possibly occurring over a time interval at elevated temperatures and resulting in a slight increase of the $Mg/(Mg + Fe^{2+})$ ratio of olivine at the expense of the coexisting chrome spinel (Roeder *et al.*, 1979). This, along with evidence of some re-equilibrium between olivine and spinel from a comparison of spinel grains in the LDH succession with those in the HMA, indicates that a more realistic value of primary olivine for this succession was Fo_{92} and that the $Mg/(Mg + Fe^{2+})$ ratio of the parental liquid was 76–78.

The composition of orthopyroxene within the LDH succession is similar to that of clinoenstatite from within high-magnesian andesite lavas (Dallwitz *et al.*, 1966; Jenner, 1981), indicating that the original field of crystallisation may have been one where Ol + Pen + Sp co-precipitated. Keith (1954), working in the $MgO\text{-}SiO_2\text{-}Cr_2O_3$ system at low pressure, showed that chrome spinel would precipitate with either forsterite or protoenstatite along cotectic liquidus boundaries and that protoenstatite melts incongruently to forsterite plus liquid. This could partly explain the varying percentages of orthopyroxene in the different pyroxene-bearing dunite and harzburgite layers. The study of Keith (1954) also showed that with decreasing temperature, the system moved from: Ol + Sp: to Ol + Pen + Sp: to Pen + Sp, which is consistent with the mineral variation up through the LDH succession.

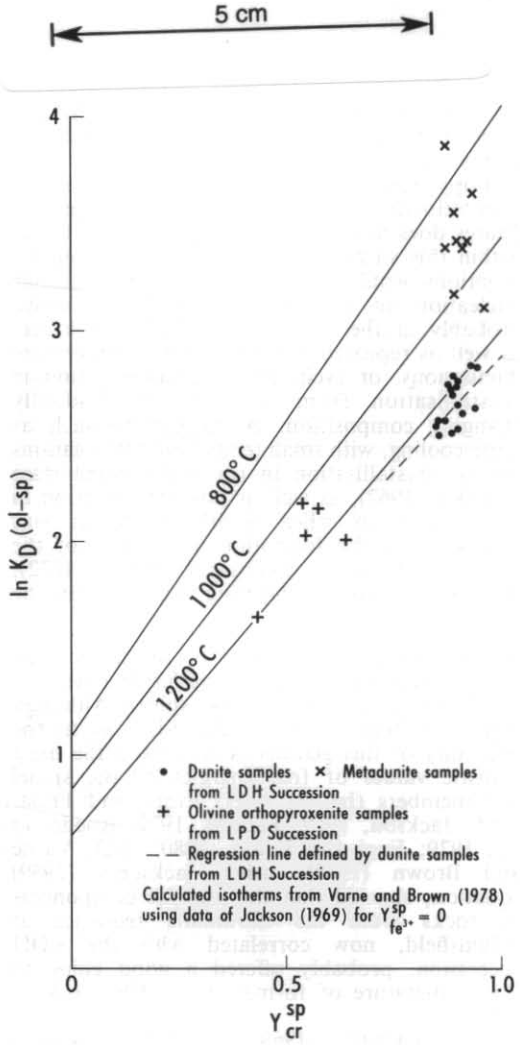

Figure 55. *ln K_D (ol-sp)∿Y^{sp}_{cr} for spinel samples from LDH and LPD successions.*

In summary, data from the LDH succession and experimental work suggest that the succession was formed by crystallisation at temperatures of 1300 ± 50°C and very low pressure (2–5 kb) in the forsterite + protoenstatite + spinel + liquid stability field from a quartz normative liquid, rich in magnesium and chromium and low in titanium, calcium, sodium and potassium. If the liquid contained a small water content, then the temperature would have been slightly lower (> 1200°C) and the pressure slightly higher (< 5–10 kb) than those indicated for anhydrous conditions (Jenner, 1982).

A basaltic rock which exists in the Dundas Trough and is consistent with the above criteria is the high-magnesian andesite (HMA) (€ba). This phase has previously been suggested as the possible source of the orthopyroxene-rich ultramafic sequences in Tasmania (Rubenach, 1973; Varne and Brown, 1978). Duncan and Green (1980) predicted the formation of lavas such as the high-magnesian andesite from an original fertile mantle diapir source as a second stage melt. The first stage melt would have produced a picritic liquid which would be capable of producing the Crimson Creek Formation tholeiitic basalts by crystal fractionation. Field evidence shows that the Crimson Creek Formation tholeiitic lavas were extruded as the first phase of an Eocambrian–Cambrian volcanic event and that they were followed by the high-magnesian andesite, as a second stage melt, and finally in the middle Middle Cambrian by the low-titanium tholeiite basaltic phase.

The Tasmanian HMA's have pseudomorphed clinoenstatite and orthopyroxene phenocrysts with chrome-rich (Cr* = 89–92) spinel grains, set either in a groundmass of replaced microlites or devitrified glass. Although the textures are porphyritic to glomeroporphyritic, no relict or pseudomorphed olivine, clinopyroxene or plagioclase grains were recognised in any sample from the three main areas from which the HMA's were collected and studied. The sample most likely to reflect the original composition of the Tasmanian HMA's comes from the Heazlewood area (13 Mile Creek; table 9, analysis 1). This sample is considered to have undergone weathering changes but not to have been exposed to possible metasomatic alteration by granitic fluids as in those from the Stonehenge area, or alteration by later volcanic activity and even later ore-bearing fluid phases, as those in the Magnet area. The similarity of the composition of chrome spinel grains from the HMA and LDH succession, as recognised in many other areas of genetically related basaltic and peridotitic rocks (Dick and Bullen, 1984), is also indicative of a genetic relationship, especially in view of the unusually high Cr*.

On an anhydrous basis, this lava has a SiO_2 content of 56·18 wt%, low TiO_2 (0·08 wt%), CaO (5·05 wt%), total alkalis ($Na_2O + K_2O = 0{\cdot}46$ wt%) high MgO (18·76 wt%), a Cr content of 1860 ppm, a 'U'-shaped chondrite-normalised REE pattern, and a Mg number of 77. These characteristics are consistent with the requirements of the data obtained from the LDH succession and experimental work (Jaques and Green, 1980; Green, 1981; Jenner, 1982), suggesting that the HMA and LDH successions originated from the same source. Using a $K_D = 0{\cdot}27$ (Roeder and Emslie, 1970), olivine in equilibrium with this HMA would have been $Fo_{92{\cdot}7}$. Using an extrapolation of Roeder and Emslie's (1970) data for the olivine saturation surface, a temperature of 1395°C is indicated. The occurrence of chrome-rich spinel grains of similar composition to those within the LDH succession, and clinoenstatite in the HMA and orthopyroxene of protoenstatite composition in the LDH succession, also indicates a common parent liquid.

Experimental work on chemically and mineralogically similar lavas from Cape Vogel, Papua New Guinea (Jenner, 1981; 1982) has shown that the lavas are in equilibrium with olivine of Fo_{92}, protoenstatite and chrome-rich spinel of (Cr*90) at temperatures >1200°C and pressures of < 5–10 kb. Green (1981) suggested that lavas of a composition close to that required (but with SiO_2 of 53–54 wt%) probably formed under conditions with temperatures of 1300–1350°C and pressures of 7–8 kb.

The tectonic environment of formation of HMA lavas has been much discussed (Sun and Nesbitt, 1978; Cameron *et al.*, 1979, 1980; Crawford *et al.*, 1981; Duncan and Green, 1980; Jenner, 1981; 1982). Formation by anhydrous or slightly hydrous melting in a continuously melting and rising mantle diapir, within a continental setting at high temperature and low pressure, appears to be a more likely source for these magmas when associated with olivine + orthopyroxene + chrome-rich spinel cumulate successions, than formation by subduction-related processes in an island-arc setting (Crawford *et al.*, 1981; 1984) by water-saturated melting of peridotite at around 10 kb pressure and temperatures of 1100°C, as was predicted by earlier experimental work (Green, 1973; 1976).

LAYERED PYROXENITE-DUNITE SUCCESSION

Using a similar approach to that above, data relating to the composition of the parent liquid from which the LPD succession crystallised, and the conditions under which such crystallisation occurred, can be obtained. Layering in the LPD succession is very thin to thin (majority of layers < 200 mm) with sharp boundaries between succeeding layers. Rhythmic layering indicates that crystallisation occurred under conditions such that the fields of crystallisation oscillated between: Ol + Sp to Opx + Sp ± minor Cpx to Ol + Sp; Ol + Sp to Opx + Sp ± minor Ol and Cpx to Ol + Sp; and Ol + Sp to Opx + Cpx + Sp to Opx + Ol + Cpx + Sp to Ol + Sp. This indicates that whatever processes were involved during crystallisation, they would have required more than temperature fluctuations at constant pressure and liquid composition, as the experimental work of Jaques and Green (1980) on the melting characteristics and mineral stability fields in equilibrium with basaltic liquids shows a minimum temperature fluctuation of 100°C (1260–1360°C at 5 kb) would be needed to obtain the: Ol + Sp to Opx + Cpx + Ol + Sp to Ol + Sp sequence. Obviously many more factors are involved to obtain a change in crystallisation which results in layering as found within the LPD succession.

One major feature of the LPD succession is the apparent lack of plagioclase as a constituent mineral phase, especially when plagioclase occurs in the LPG succession (which has a similar range of silicate and spinel chemistry to the LPD succession) as a post-cumulus phase in both the orthopyroxene-rich and olivine-rich sequences.

An estimate of the nominal temperature of crystallisation can be obtained using a geothermometer based on coexisting Opx and Cpx pairs after Wood and Banno (1973) and Wells (1977). The range of temperatures obtained (table 30) is 950–1127°C (average 1042 ± 33°C) for Wood and Banno, and 851–1064°C (average 954 ± 40°C) for Wells, giving a temperature difference between the two geothermometers of 60–100°C. Temperature differences of this order were also found within a single sample (85-0154, table 30) when analyses from numerous touching Opx-Cpx pairs were obtained from within the same 10 mm diameter sample used for probe work. The range of temperature from different areas of the LPD succession are also similar, and again overlap the range which can be obtained from a single sample.

Using Jackson's (1969) olivine-spinel geothermometer for samples which contained relict olivine grains, a range of 1190–1327°C (1215 ± 97°C) was obtained. As the results of the two pyroxene and olivine-spinel geothermometers for the same sample can range from an agreement of 2°C (85-0205, tables 29, 30) to a variation of 200–300°C (85-0204, tables 29, 30), it is obvious that most temperatures represent the results of subsolidus re-equilibration, but nevertheless they indicate temperatures of crystallisation of >1200°C.

Using the data of Roeder and Emslie (1970), a Mg number of 0·65–0·68 is indicated for the liquid in equilibrium with the LPD succession olivine (Fo_{87-88}). This is considerably lower than that considered to be the characteristic of primary liquids (76–78, Green, 1971; etc.) but is in the range of one of the basaltic rocks which was possibly derived from the same liquid as the LPD succession, the olivine tholeiite basalt from the Smithton Basin.

Chrome spinel grains from this succession have an average Cr* of 66 and contain an average of 17·7 wt% Al_2O_3, indicating a lower Cr* of the LPD parental liquid than that for the LDH succession (Hill and Roeder, 1974; Jaques, 1980; 1981). The chrome spinel grains in this succession have a wider range of Cr-Al substitution than grains from within the LDH succession, and some grains contain up to 0·78 wt% TiO_2. The coexisting Opx has an average Al_2O_3 content of 0·5 wt% and the Cpx 1·65 wt%, indicating a liquid with higher TiO_2 and CaO contents and different conditions of crystallisation than those of the LDH succession. Probable lower temperatures and/or higher pressures allowed Al_2O_3 to enter crystal structures rather than stay in the liquid (Jaques and Green, 1980).

Coexisting olivine and orthopyroxene have a similar Mg* (87–89), with olivine having a slightly higher value than the orthopyroxene in any specific sample. When considering the Mg* of olivine and orthopyroxene and the Cr* of coexisting spinel grains in relation to the anhydrous melting data on peridotitic compositions (Jaques and Green, 1980), minerals from the LPD succession are in equilibrium with 'pyrolite' at 1200–1300°C and 5 kb, and between 1250°C and 1300°C and 5 kb are in equilibrium with the 'Tinaquillo lherzolite' liquid, indicating a temperature-pressure regime if the succession crystallised from liquids of similar composition. Al_2O_3 in coexisting Opx and spinel falls on the regression line defined by data from the 'Tinaquillo lherzolite' liquid, and the Al_2O_3 content of orthopyroxene in this system indicates a pressure of 4–5 kb at 1250–1300°C.

In summary, data from the LPD succession and experimental work suggests that the LPD succession crystallised at temperatures of 1200–1300°C and pressures of 5 kb or greater, depending on the parent liquid composition, in the Ol + Sp + liquid to Opx + Cpx + Ol + Sp + liquid stability fields.

It has previously been suggested that all the orthopyroxene-rich ultramafic rocks in Tasmania formed from the same source and were associated with the HMA lavas (Rubenach, 1973; Varne, 1978; Varne and Brown, 1978; Brown *et al.*, 1980). Information gathered during this study indicates that this suggestion is no longer valid. The main points against the original suggestion are the hiatus in chemical composition between the two successions, the implication of a higher pressure of formation for the LPD succession than for the LDH succession, and the lack of a pervasive tectonic foliation within the LPD succession.

Field evidence shows that pieces of both successions occur together along the same tectonic line in the Dundas Trough as well as at Adamsfield. They are always in faulted contact with each other and evidence contained within the LPD succession suggests that it was dismembered in a 'cold' state compared to a plastic to cold state for the LDH succession in both the area covered by this study and at Adamsfield (Brown, 1972). Nowhere do the two successions display an original spatial relationship, mainly due to at least two phases of tectonic emplacement through overlying sedimentary rock successions.

If the LPD succession was formed prior to the LDH succession, there is the possibility that it was a magma chamber product of the first phase of Eocambrian–Cambrian volcanic activity. This is consistent with a first stage melting event from a lherzolitic source producing an olivine

tholeiite basalt and the LDH succession as the cumulate phase. The lowest basalts in the Crimson Creek Formation found in the Dundas Trough have clinopyroxene and plagioclase phenocryst phases and a Mg number of 55–56. These lavas would not have been in equilibrium with the liquid from which the LPD succession crystallised. At the base of the Crimson Creek Formation correlate in the Smithton Basin exists an olivine tholeiite basalt with a Mg number of 67, indicating equilibrium with olivine of Fo_{86-88} at a temperature of 1275°C (at 1 kb) using the data of Roeder and Emslie (1970). The Cr content of these basalts is 800–850 ppm, suggesting spinel grains with a Cr* between 40 and 50 being present (Hill and Roeder, 1974; Jaques, 1980; 1981). Although the LPD succession would not have been in equilibrium with a liquid of this composition, it is probable that this whole phase of volcanic activity had a picritic parental liquid, possibly similar to that on King Island (Waldron *et al.*, in press), from which the LPD succession could have crystallised. Further detailed chemical study may solve the problem of the chemical hiatus between the two successions and detailed field work in other areas, for example the Heazlewood River Ultramafic Complex, may give a clearer picture of the relationships between the different successions, but evidence obtained during this study cannot unambiguously define the parent liquid of the LPD succession.

LAYERED PYROXENITE-PERIDOTITE AND ASSOCIATED GABBRO SUCCESSION

Physical characteristics of the LPG succession indicate an overall size difference (far smaller) and continuous magma movements, dissimilar to those occurring during crystallisation of both the LDH and LPD successions. The presence of plagioclase as a mineral phase in both the orthopyroxene-rich and olivine-rich sequences, which otherwise have a similar range of mineral chemistry to the LPD succession, indicates a different parental composition and/or lower temperatures and pressures of crystallisation than for those of the LDH and LPD successions. Layer characteristics indicate multiple intrusion of liquids during the formation of both of the ultramafic sequences. Scouring and infilling of scour channels with cross-bedded crystal-mush lenses indicates crystal-mush density flows, and unconformities indicate tilting of earlier formed layers, probably by later liquid influx. These are all characteristics of a small active magma chamber.

The two-pyroxene geothermometer of Wood and Banno (1973) gave a range of temperature of 957–1013°C (average 990 ± 19°C) and that of Well's (1977) a range of 877–922°C (average 895 ± 22°C). As exsolution phenomena are evident in many samples (the samples used for geothermometry were selected on the basis that no exsolution could be distinguished in thin section), these temperatures obviously indicate re-equilibration temperatures. Samples of the associated two-pyroxene gabbro gave a range of 893–938°C (average 912 ± 22°C) using Wood and Banno (1973) and 903–953°C (average 926 ± 26°C) using Wells (1977).

When comparing mineral chemistry from this succession with data obtained from the anhydrous melting of peridotitic composition (Jaques and Green, 1980), the Al_2O_3 content of coexisting Opx (average 1·6 wt%) and spinel (average 18·1 wt%) lies near the regression line defined by the 'Tinaquillo lherzolite' liquid. The Al_2O_3 content in Opx indicates a temperature of 1100°C. To obtain the Mg* of Opx and Cr* of the spinel in equilibrium with this liquid, an extrapolation to 1100°C of the 2 kb data is necessary. This is the right temperature-pressure region for melting of the 'Tinaquillo lherzolite' liquid to obtain the Ol + Opx + Cpx + plagioclase (Pl) + Cr + liquids stability field.

Tectonic juxtaposition of the plagioclase-bearing ultramafic sequences and areas of the middle Middle Cambrian low-titanium tholeiite basalt (Cbm) occurs in the Serpentine Hill and Heazlewood River areas. As the only phase of deformation which middle Middle Cambrian sequences are known to have suffered is the open folding of the Devonian deformation, this juxtaposition of similar sequences in two spatially separated regions suggests a possible genetic link between the rock sequences.

The lavas are altered in both areas, especially in the Serpentine Hill area, where samples have anomalously low MgO values. An anhydrous recalculation of the average low-titanium tholeiite basalt composition from the Heazlewood area is similar in composition to that calculated to be the equilibrium melt composition from the 'Tinaquillo lherzolite' at 2 kb and 1250°C with approximately 25% melting (Jaques and Green, 1980). Although this temperature is higher than the data from mineral chemistry and experimental work indicate, a tenuous link between the basalt and ultramafic sequences is possible. This link is strengthened by preliminary REE data which indicate that a two-pyroxene gabbro sample from the Serpentine Hill area, which is part of the LPG succession, has a chondrite-normalised LREE depleted pattern with a slope parallel to the low-titanium tholeiite patterns, but with slightly lower chondrite-normalised values.

In summary, low-titanium, magnesium-rich, quartz normative tholeiitic to andesitic lavas found along the Dundas Trough of western Tasmania were liquids which had the characteristic of crystallising orthopyroxene, rather than clinopyroxene, as the dominant pyroxene phase at low pressures and high temperatures. The composition of these liquids is also consistent with having been in equilibrium with the LDH succession found in the Eocambrian–Cambrian troughs of western

Tasmania. The bulk or source peridotites were probably originally more refractory than the 'Tinaquillo lherzolite' used by Jaques and Green (1980). These liquids are considered to have been produced by multiple anhydrous or mildly hydrous melting, of a 'second stage' melt from an upwelling mantle diapir. The constraints of liquid petrogenesis do not define the tectonic environment but are consistent with a continental rift environment. The first melting event produced a picritic liquid from which the olivine and quartz tholeiite magmas were obtained by batch melting and varying amounts of crystal fractionation of different mineral phases.

MINERALISATION

No new areas of sulphide mineralisation within areas of ultramafic-mafic rocks were observed during this study. Investigations into nickel mineralisation associated with ultramafic-mafic bodies in western Tasmania were carried out by Williams (1958), and a summary produced by Hughes (1965). Noldart (1976) summarised the lateritiitic nickel deposits at Beaconsfield and the chromite potential of this area was investigated by Summons *et al.* (1981). Asbestos deposits in the Andersons Creek area (Twelvetrees, 1917; Reid, 1919), as well as throughout Tasmania (Taylor, 1955), have also been studied in the past.

PGE minerals associated with the LDH succession have been studied by Twelvetrees (1914), Reid (1921), and Nye (1929), with a summary by Elliston (1965). Studies of the specific PGE mineralogy of these areas have been done by Cabri and Harris (1975) and Ford (1981). A study of the PGE mineral potential of the Serpentine Hill Complex (LPG succession) was undertaken, as a separate study, during this project and the results will appear in Brown *et al.* (in prep).

It is usually considered that Os and Ir are concentrated in the residuum of a first-stage melting phase and are then precipitated as an alloy phase in the second stage melt. This consideration is consistent with observations in western Tasmania where Os-Ir-Ru mineral grains are associated with areas of the LDH succession. Platinum, palladium and ruthenium are thought to be susceptible to the degree of sulphur saturation of a liquid and when this is high enough sulphide minerals of Pt-Pd-Ru are formed. These minerals are usually associated with a fresh influx of late stage olivine-rich liquid associated with trocolite and anorthosite units in large stratiform complexes. This is partially consistent with observations in the Serpentine Hill Complex, which is considered to be the youngest of the ultramafic-mafic complexes and associated with the middle Middle Cambrian low-titanium tholeiite basalt.

The Serpentine Hill Ultramafic-mafic Complex is enriched in Pt, Pd, Ru, Rh, and Ir with respect to samples so far analysed from all other Tasmanian ultramafic-mafic bodies, indicating that the simplistic sulphide saturation model is not the only control of PGE mineral formation. There are uncertainties in the behaviour and distribution of PGE in undepleted mantle rocks, during partial melting and in different environments of magma crystallisation, as well as an apparent original heterogeneous distribution of PGE in the mantle material (Page, Cassard and Haffty, 1982). It is possible that when the Heazlewood River Ultramafic Complex is studied in detail, zones of PGE-rich chromitite, similar to those defined at Serpentine Hill (Brown *et al.*, in prep.), will be found.

SUMMARY

Although numerous major and minor features of the Eocambrian-Cambrian geology of western Tasmania have been resolved or simplified during this study, the key to modelling the tectonic environment of western Tasmania lies in further detailed surface and deep crustal structural analyses of the area. Information obtained during this study, added to previous data, reinforces the implication that the Dundas Trough represents part of a failed continental rift zone.

In the past, some plate tectonic models have been proposed which either ignored or mistakenly interpreted detailed regional geological data, especially structural and geochemical data. This study has produced several constraints which any future attempt at tectonic modelling must consider. These constraints include the character of the Success Creek Group sedimentation; the chemical nature of the Eocambrian to Cambrian tholeiitic to andesitic volcanic rocks; the regional setting of the high-magnesian andesite; as well as the true nature of the ultramafic rocks of western Tasmania.

The presence of Precambrian correlates in the Ramsay River area as well as the Dundas area puts further constraints on the position of any plate margin which may be drawn along western Tasmania.

The Success Creek Group represents 1000 m of shallow-water sedimentation, the dominant source for which was the Oonah Formation. The boundary between the Precambrian rocks and the Success Creek Group is an onlap angular unconformity. This unconformity represents an hiatus in sedimentation, during which the Penguin Orogeny occurred, producing a structural and low-grade metamorphic difference.

The basal formation of the Success Creek Group is a mixtite which was derived from a mixture of local and exotic material. The second

formation, the Dalcoath Formation, is a sequence of interbedded, clean, shallow-water quartz sandstone with minor siltstone, pebbly sandstone, and conglomerate. The Dalcoath Formation grades into the third formation which is dominated by laminated mudstone and siltstone with minor sandstone and conglomerate. This formation is characterised by pervasive intraformational soft-sediment deformation which later reacted incompetently during large scale slump movements and probably represents the results of an unstable basin of deposition. The top formation is the Renison Formation, the dominant units of which are clastic siliceous siltstone with mudstone partings. The upper member of this formation is the 'red rock' of Condor (1920).

The conformable transition from the top of the Success Creek Group, the fluviatile 'red rock' member, into the Crimson Creek Formation, which consists of basic volcaniclastic sedimentary rocks with turbidite characteristics interbedded with tholeiitic volcanic rocks, also indicates basin instability with deepening occurring to allow a change from shallow-water sedimentation to one of turbiditic character.

The tectonic emplacement of parts of the Layered Pyroxenite Dunite Succession (LPD), which are consistent with having been formed as crustal cumulates from the primary magma of the Crimson Creek Formation tholeiitic basalts, into a basin of deposition at the beginning of Dundas Group sedimentation, indicates both a time break between deposition of the two successions and a change of tectonic stress from tensional to compressional. This implied break and change in tectonic stress is consistent with the findings of Williams (1978).

Interdigitating with basal conglomerate units of the Dundas Group is a suite of low-titanium tholeiitic basalts. This lava suite is considered to have been comagmatic with the parental magma from which the Serpentine Hill ultramafic body, the Layered Pyroxenite-Gabbro succession (LPG), formed. Later tectonic emplacement of this ultramafic body into its present juxtaposition with Crimson Creek Formation succession rocks and the lower Dundas Group sedimentary rocks and low-titanium tholeiitic lavas is considered to have occurred due to deformation during Devonian times. This assumption is based on the fact that the only structural evidence found in the rock successions surrounding the ultramafic body is consistent with proven Devonian directions.

The third ultramafic association found on the West Coast is the Layered Dunite-Harzburgite Succession(LDH). This is a layered cumulate succession formed from a basaltic to andesitic magma, considered to be the high-magnesian andesite (HMA), and consists of a well-layered succession of dunite, orthopyroxene-bearing dunite, and harzburgite. The pervasive tectonic fabric within the LDH succession is considered to be an expression of plastic flow at high temperature during tectonic dismembering and emplacement of the succession higher into the crust. The deformation of the LDH succession consisted of flattening and elongation of olivine and orthopyroxene grains and brittle pull-apart of chrome spinel grains whilst leaving the layering and mineral foliation intact. The less competent, late stage, orthopyroxenite veins and dykes were boudinaged. The LDH succession is not a tectonised mass of dominantly harzburgite with dunite pods and lenses which is commonly taken as 'residual tectonite' or 'tectonised harzburgite', and is traditionally taken as representing the lower part of an ophiolite and indicative of a 'sea-floor environment'.

All three of the ultramafic successions are consistent with being high temperature, low pressure, cumulate bodies formed as crustal magma chamber products, each from one of the three different magma events found within the Eocambrian-Cambrian successions within the Dundas Trough.

Many papers over the last few years have shown that chrome spinel in peridotite and spatially associated lavas is effectively a petrologic fingerprint to host rock petrogenesis. The high Cr* of the spinel, associated with high Mg*, olivine and enstatite, and the low Al_2O_3 and CaO of the enstatite in the ultramafic rocks of the LDH succession indicate associated lavas which are normally only found in island-arc or continental settings. Peridotite from ocean ridge settings contains enstatite saturated with diopside, indicating melting around the Ol + En + Di + Sp pseudoinvariant point (Dick and Fisher, 1983) whereas the LDH succession contains enstatite understaturated with respect to diopside, which is consistent with melting in the Ol + En + Sp field at low pressure (Keith, 1954; Jaques and Green, 1980; Jenner,1982).

Because of the high temperature and low oxygen fugacity of the melt implied by the residual mineralogy and experimental work, a melt with a low water content would be expected. These conditions have been experimentally duplicated (Jaques and Green, 1980; Jenner, 1982), and are consistent with melting of a mantle diapir beneath a failed continental rift, which is a more favourable setting for the production of the associated terrigenous sedimentary rocks than an island-arc system. Under such conditions the tholeiitic basalts within the Crimson Creek Formation would represent the first stage of melting and the HMA would be the second melt stage along the lines postulated by Duncan and Green (1980). As these lavas conformably overly shallow water terrigenous sedimentary rocks in the Dundas Trough, Smithton Basin, and probably in the Dial Range Trough, a continental setting for the extrusion of these lavas is indicated rather than an island-arc setting.

The ultramafic rocks of western Tasmania are tectonically dismembered and multiple re-emplaced crustal cumulate bodies. Due to the evidence presented in this study, the terms alpine peridotite, ophiolite, or residual harzburgite, with their applied tectonic connotations, are inappropriate terms for the western Tasmanian ultramafic rocks, and should be avoided.

In summary, the following sequence of geological events, all occuring before the middle Middle Cambrian, are consistent with an intracontinental rift environment for western Tasmania at that time:

(a) the shallow water nature of the original sediments which infilled the proto-Dundas Trough;

(b) the gradual deepening of an elongate basin, probably less than 70 km wide (Williams, 1980), into which tholeiitic lavas and associated turbiditic sedimentary rocks formed;

(c) the low-pressure melting required to form the ultramafic rocks;

(d) formation of lavas resulting from a second stage melting of the depleted mantle source.

Sedimentation of the Dundas Group and correlates occurred in restricted basins which were accessible to both metasedimentary and acid to intermediate volcanic detritus, at similar times but in different places, indicating an environment of sediment source to both the east and west of the trough. The acid to intermediate volcanism, although widespread on the small scale of western Tasmania, was short lived, and could easily have been the result of melting of lower crustal units by the residual heat of the diapir.

The continuation, conformably in places, of the Dundas Group successions by terrestrial and shallow marine siliceous clastic sediments, then limestone, sandstone and siltstone successions, and finally mudstone of the Denison, Gordon and Eldon Groups, indicates a continental setting for western Tasmania from Late Precambrian to Devonian times.

REFERENCES

BAILLIE, P. W. 1979. Stratigraphic relationships of Late Ordovician to Early Devonian rocks in the Huntley Quadrangle, south-western Tasmania. *Pap. Proc. R. Soc. Tasm.* 113:5–13.

BAILLIE, P. W.; WILLIAMS, P. R. 1975. Sedimentary and structural features of the Bell Shale correlate (Early Devonian), Strahan Quadrangle, western Tasmania. *Pap. Proc. R. Soc. Tasm.* 109:1–15.

BAILLIE, P. W.; *et al.* In prep. Geological atlas 1:50 000 series. Sheet 36 (8015S). St Valentines. *Department of Mines, Tasmania.*

BANKS, M. R. 1956. The Middle and Upper Cambrian series (Dundas Group and its correlates) in Tasmania, *in* RODGERS, J. (ed.). *El Sistema Cambrico.* 2:165–212. 20th International Geological Congress, Mexico.

BANKS, M. R. 1957. The stratigraphy of Tasmanian limestones, *in* HUGHES, T. D. The limestones of Tasmania. *Miner. Resour. geol. Surv. Tasm.* 10:39–85.

BANKS, M. R. 1962*a*. Silurian and Devonian systems, *in* SPRY, A. H.; BANKS, M. R. (ed.). The geology of Tasmania. *J. geol. Soc. Aust.* 9(2):177–187.

BANKS, M. R. 1962*b*. Cambrian system, *in* BANKS, M. R.; SPRY, A. H. (ed.). The geology of Tasmania. *J. geol. Soc. Aust.* 9(2):127–145.

BARTON, C. M.; *et al.* 1966. Geological atlas 1 mile series. Zone 7 sheet 44 (8014N). Mackintosh. *Department of Mines, Tasmania.*

BECCALUVA, L.; PICCARDO, G. B.; SERRI, G. 1980. Petrology of northern Apennine ophiolites and comparison with other Tethyan ophiolites, *in* PANAYIOTOU, A. (ed.). *Ophiolites. Proceedings International Ophiolite Symposium, Cyprus, 1979.* 314–331. Ministry of Agriculture and Natural Resources : Cyprus.

BLISSETT, A. H. 1962. One mile geological map series. K/55–5–50. Zeehan. *Explan. Rep. geol. Surv. Tasm.*

BLISSETT, A. H.; GULLINE, A. B. 1961*a*. The Proterozoic–Upper Cambrian succession in West Tasmania. *Aust. J. Sci.* 23:337–339.

BLISSETT, A. H.; GULLINE, A. B. 1961*b*. Tin mineralisation near Mt Razorback. *Tech. Rep. Dep. Mines Tasm.* 5:136–161.

BLISSETT, A. H.; GULLINE, A. B. 1962. Geological atlas 1 mile series. Zone 7 sheet 50. Zeehan. *Department of Mines, Tasmania.*

BRADLEY, J. 1954. The geology of the West Coast Range of Tasmania. Part 1: Stratigraphy and metasomatism. *Pap. Proc. R. Soc. Tasm.* 88:193–243.

BRATHWAITE, R. L. 1969. *The geology of the Rosebery ore deposit.* Ph.D. thesis, University of Tasmania : Hobart.

BROOKS, C. 1966. The rubidium-strontium ages of some Tasmanian igneous rocks. *J. geol. Soc. Aust.* 13:457–469.

BROWN, A. V. 1972. *Petrology and structure of the Adamsfield ultramafic mass.* B.Sc. (Hons) thesis, University of Tasmania : Hobart.

BROWN, A. V. 1980*a*. Geological traverse along the Hydro-electric Commission's Pieman Road, from LPD 45.5 km to the Stanley River (LPD 20.2 km). *Unpubl. Rep. Dep. Mines Tasm.* 1980/33.

BROWN, A. V. 1980*b*. Some aspects of the geology of the Mt Lindsay–Dundas area, western Tasmania. *Unpubl. Rep. Dep. Mines Tasm.* 1980/42.

BROWN, A. V. 1985. Preliminary report on the Forest No. 1 diamond-drill hole and chemical analyses of associated tholeiitic basalts in the Smithton and Woolnorth Quadrangles. *Unpubl. Rep. Dep. Mines Tasm.* 1985/62.

BROWN, A. V.; FORSYTH, S. M. 1984. Chemistry of Tertiary basalt and palynology of interbedded sediments from B.H.P. drill holes, E. L. 33/79. *Unpubl. Rep. Dep. Mines Tasm.* 1984/39.

BROWN, A. V.; STAIT, B. A. 1983. The first recorded occurrence of *Geisonoceras* sp. in Tasmania. *Unpubl. Rep. Dep. Mines Tasm.* 1983/16.

BROWN, A. V.; WALDRON, H. 1982. Preliminary review of the Eocambrian–Cambrian basaltic association and tectonic setting within western and north-western Tasmania. *Unpubl. Rep. Dep. Mines Tasm.* 1982/10.

BROWN, A. V.; RUBENACH, M. J.; VARNE, R. 1980. Geological environment, petrology and tectonic significance of the Tasmanian Cambrian ophiolitic and ultramafic complexes, *in* PANAYIOTOU, A. (ed.). *Ophiolites. Proceedings International Ophiolite Symposium, Cyprus, 1979.* 649–659. Ministry of Agriculture and Natural Resources : Cyprus.

BROWN, A. V.; PAGE, N. J.; LOVE, A. H. in prep. Geology and platinum-group element (PGE) geochemistry of the Serpentine Hill Complex, Dundas Trough, western Tasmania.

BURNS, K. L. 1965. One mile geological map series. K/55–6–29. Devonport. *Explan. Rep. geol. Surv. Tasm.*

CABRI, L. J.; HARRIS, D. C. 1975. Zoning in Os-Ir alloys and the relation of the geological and tectonic environment of the source rocks to the bulk Pt:Pt + Ir + Os ratio for placers. *Can. Mineral.* 13:266–274.

CAMERON, W. E.; NISBET, E. G.; DIETRICH, V. J. 1979. Boninites, komatites and ophiolitic basalts. *Nature* 280:550–553.

CAMERON, W. E.; NISBET, E. G.; DIETRICH, V. J. 1980. Petrographic dissimilarities between ophiolitic and ocean-floor basalts, *in* PANAYIOTOU, A. (ed.). *Ophiolites. Proceedings International Ophiolite Symposium, Cyprus, 1979.* 182–192. Ministry of Agriculture and Natural Resources : Cyprus.

CAMERON, W. E.; MCCULLOCH, M. T.; WALKER, D. A. 1983. Boninite petrogenesis: chemical and Nd-Sr isotopic constraints. *Earth planet. Sci. Lett.* 65:75–89.

CAMPANA, B.; KING, D. 1963. Palaeozoic tectonism, sedimentation and mineralization in west Tasmania. *J. geol. Soc. Aust.* 10:1–54.

CAMPANA, B.; KING, D.; MCKENNA, D. 1960. Unconformable units of the Cambrian succession of West Tasmania. *Aust. J. Sci.* 22:352–353.

CANN, J. R. 1970. Rb, Sr, Y, Zr and Nb in some ocean floor basaltic rocks. *Earth planet. Sci. Lett.* 10:7–11.

CAREY, S. W. 1947. Report of the Government Geologist for 1945. *Rep. Dir. Mines Tasm.* 1945:21–29.

CAREY, S. W. 1953. The geological structure of Tasmania in relation to mineralization. *Publs 5th emp. min. metall. Congr.* 1:1108–1128.

CAREY, S. W.; BANKS, M. R. 1954. Lower Palaeozoic unconformities in Tasmania. *Pap. Proc. R. Soc. Tasm.* 88:245–269.

CARTER, N. L.; AVE'LALLEMANT, H. G. 1970. High temperature flow of dunite and peridotite. *Bull. geol. Soc. Am.* 81:2181–2202.

CHAPMAN, F.; THOMAS, D. E. 1936. The Cambrian hydroida of the Heathcote and Monegeeta districts. *Proc. R. Soc. Vict.* 48:193–212.

CHURCH, W. R. 1977. The ophiolites of southern Quebec: oceanic crust of Betts Cove type. *Can. J. Earth Sci.* 14:1668–1673.

CHURCH, W. R.; RICCIO, L. 1977. Fractionation trends in the Bay of Islands ophiolite of Newfoundland: polycyclic cumulate sequences in ophiolites and their classification. *Can. J. Earth Sci.* 14:1156–1165.

CLARKE, M. J. 1984. Late Cambrian agnostid faunas from the Huskisson River area. *Unpubl. Rep. Dep. Mines Tasm.* 1984/19.

CLARKE, M. J.; BROWN, A. V. 1980. Fossil faunas in Eldon Group correlates within the Huskisson Syncline. *Unpubl. Rep. Dep. Mines Tasm.* 1980/47.

COISH, R. A. 1977. Ocean floor metamorphism in the Betts Cove ophiolite, Newfoundland. *Contrib. Mineral. Petrology* 60:255–270.

COLEMAN, R. G. 1966. New Zealand serpentinites and associated metasomatic rocks. *Bull. geol. Surv. New Zealand.* NS76.

COLLINS, P. L. F. 1972. *The geology and mineralization at Renison Bell, Tasmania.* B.Sc. (Hons) thesis, University of Tasmania : Hobart.

COLLINS, P. L. F. 1981. The geology and genesis of the Cleveland tin deposit, western Tasmania : fluid inclusions and stable isotope studies. *Econ. Geol.* 76:365–392.

COLLINS, P. L. F. 1983. *Geology and mineralisation at the Cleveland mine, western Tasmania.* Ph.D. thesis, University of Tasmania : Hobart.

COLLINS, P. L. F.; GULLINE, A. B.; WILLIAMS, E. (comp.). 1981. Geological atlas 1 mile series. Sheet 44 (8014N). Mackintosh. *Explan. Rep. geol. Surv. Tasm.*

CONDER, H. 1918. The tinfield of North Dundas. *Bull. geol. Surv. Tasm.* 26.

COOPER, R. A.; GRINDLEY, G. W. (ed.). 1982. Late Proterozoic to Devonian sequences of southeastern Australia, Antarctica and New Zealand and their correlation. *Spec. Publ. geol. Soc. Aust.* 9.

CORBETT, K. D. 1975. Preliminary report on the geology of The Red Hills–Newton Creek area, West Coast Range, Tasmania. *Tech. Rep. Dep. Mines Tasm.* 19:11–25.

CORBETT, K. D. 1984. Geological maps and summary of the Cambrian stratigraphic units and relationships in the Henty River–Williamsford area. *Unpubl. Rep. Dep. Mines Tasm.* 1984/84.

CORBETT, K. D.; BANKS, M. R. 1975. Revised terminology of the Late Cambrian–Ordovician sequence of the Florentine–Denison Range area, and the significance of the 'Junee Group'. *Pap. Proc. R. Soc. Tasm.* 109:121–126.

CORBETT, K. D.; RICHARDSON, R. G.; COLLINS, P. L. F.; GREEN, G. R.; BROWN, A. V. 1982. The 1981 West Coast aeromagnetic survey: summary of information and results. *Unpubl. Rep. Dep. Mines Tasm.* 1982/39.

CORREY, J. J. 1983. *The geology of the rocks of the Gordon and Eldon Group correlates and the Parmeener Super-Group in the Mt Bobs–Boomerang area, southeastern Tasmania.* B.Sc. (Hons) thesis, University of Tasmania : Hobart.

COX, R. 1968. *The economic geology of the Cleveland and Magnet mines, Tasmania.* Ph.D. thesis, University of Sydney.

COX, R.; GLASSON, K. R. 1971. Economic geology of the Cleveland mine, Tasmania. *Econ. Geol.* 66:861–878.

CRAWFORD, A. J.; BECCALUVA, L.; SERRI, G. 1981. Tectono-magmatic evolution of the West Philippine–Mariana region and the origin of boninites. *Earth planet. Sci. Lett.* 54:346–356.

CRAWFORD, A. J.; CAMERON, W. E.; KEAYS, R. R. 1984. The association boninite low-Ti andesite–tholeiite in the Heathcote Greenstone Belt, Victoria; ensimatic setting for the early Lachlan Fold Belt. *Aust. J. Earth Sci.* 31:161–175.

CREENAUNE, P. J. 1980. *The volcanics of the Heazlewood River complex.* B.Sc.(Hons) thesis, University of Tasmania : Hobart.

DALLWITZ, W. B.; GREEN, D. H.; THOMPSON, J. E. 1966. Clinoenstatite in a volcanic rock from the Capwe Vogel area, Papua. *J. Petrology* 7:375–403.

DAVID, T. W. E. 1932. *Explanatory notes to accompany a new geological map of the Commonwealth of Australia.* Commonwealth Council for Scientific and Industrial Research : Sydney.

DICK, H. J. B. 1977. Partial melting in the Josephine Peridotite I, The effect on mineral composition and its consequence for geobarometry and geothermometry. *Am. J. Sci.* 277:801–832.

DICK, H. J. B.; BULLEN, T. 1984. Chromian spinel as a petrogenetic indicator in abyssal and alpine-type peridotites and spatially associated lavas. *Contrib. Mineral. Petrology* 86:54–76.

DICK, H. J. B.; FISHER, R. L. 1983. Mineralogic studies of the residues of mantle melting: abyssal and alpine-type peridotites, *in* KORNPROBST, J. (ed.). *Kimberlites II: The mantle and crust–mantle relationships.* 295–308. Elsevier : Amsterdam.

DJAKIC, A. W. 1980. *Geology and formation of the Red Rock (Lower Cambrian chert bearing horizon–West Tasmania).* B.Sc. (Hons) thesis, University of Tasmania : Hobart.

DUNCAN, R. A.; GREEN, D. H. 1980. Role of multistage melting in the formation of oceanic crust. *Geology* 8:22–26.

ELLISTON, J. N. 1951. *Dundas mineral field.* B.Sc. (Hons) thesis, University of Tasmania : Hobart.

ELLISTON, J. N. 1954. Geology of the Dundas district, Tasmania. *Pap. Proc. R. Soc. Tasm.* 88:161–183.

ELLISTON, J. N. 1965. Platinoid deposits of Tasmania. *Publs. 8th Commonw. min. metall. Congr.* 1:522.

ENGI, M.; EVANS, B. W. 1980. A re-evaluation of the olivine-spinel geothermometer: Discussion. *Contrib. Mineral. Petrology* 73:201–203.

EVANS, B. W.; FROST, B. R. 1975. Chrome-spinel in progressive metamorphism; a preliminary analysis. *Geochim. Cosmochim. Acta.*. 39:959–972.

FABRIES, J. 1979. Spinel-olivine geothermometry in peridotites from ultramafic complexes. *Contrib. Mineral. Petrology* 69:329–336.

FINUCANE, K. J. 1932. The geology and ore deposits of the Rosebery district. *Mining Chem. Eng. Rev.* 25:43–46.

FLOYD, P. A.; WINCHESTER, J. A. 1975. Magma type and tectonic setting discrimination using immobile elements. *Earth. planet. Sci. Lett.* 27:211–218.

FODEN, J. 1973. *The geochemistry of spilites from the Cambrian of western Tasmania.* B.Sc. (Hons) thesis, University of Tasmania : Hobart.

FORD, R. J. 1981. Platinum-group minerals in Tasmania. *Econ. Geol.* 76:498–504.

GATEHOUSE, C. G. 1961. Cambrian fossils from the Zeehan Quadrangle. *Unpubl. Rep. Dep. Mines Tasm.*

GEE, R. D. 1977. Geological atlas 1 mile series. Zone 7 Sheet 28 (8015N). Burnie. *Explan. Rep. geol. Surv. Tasm.*

GEE, R. D.; LEGGE, P. J. 1974. Geological atlas 1 mile series. Zone 7 sheet 30 (8215N). Beaconsfield. *Explan. Rep. geol. Surv. Tasm.*

GILFILLAN, J. F. 1965. Tin ore deposits at Renison Bell. *Publs 8th commonw. min. metall. Congr.* 1:495–496.

GILL, E. D. 1950. Preliminary account of the palaeontology and palaeoecology of the Eldon Group formations in the Zeehan area, Tasmania. *Pap. Proc. R. Soc. Tasm.* 1949:231–258.

GILL, E. D.; BANKS, M. R. 1950. Silurian and Devonian stratigraphy of the Zeehan area, Tasmania. *Pap. Proc. R. Soc. Tasm.* 1949:259–272.

GREEN, D. H. 1959. Geology of the Beaconsfield district, including the Andersons Creek ultramafic complex. *Rec. Qn Vict. Mus.* N.S. 10.

GREEN, D. H. 1970. A review of experimental evidence on the origin of basaltic and nephelinitic magmas. *Phys. Earth planet. Interiors* 3:221–235.

GREEN, D. H. 1971. Composition of basaltic magmas as indicators of conditions of origin: application to oceanic volcanism. *Phil. Trans. R. Soc. Lond.* 268:707–725.

GREEN, D. H. 1973. Experimental melting studies on a model upper mantle composition at high pressure under water-saturated and water-undersaturated conditions. *Earth planet. Sci. Lett.* 19:37–53.

GREEN, D. H. 1976. Experimental petrology in Australia–A review. *Earth Science Rev.* 12:99–138.

GREEN, D. H. 1981. Petrogenesis of Archaean ultramafic magmas and implications for Archaean tectonics, *in* KRONER, A. (ed.). *Precambrian plate tectonics.* 469–489. Elsevier : Amsterdam.

GREEN, D. H.; RINGWOOD, A. E. 1967. The genesis of basaltic magmas. *Contrib. Mineral. Petrology* 15:103–190.

GREEN, G. R. 1983. *The geological setting and formation of the Rosebery volcanic-hosted massive sulphide orebody, Tasmania.* Ph.D. thesis, University of Tasmania : Hobart.

GRIFFIN, B. J. 1974. *Cambrian tectonism and vulcanism in the Smithton Basin.* B.Sc. (Hons) thesis, University of Tasmania : Hobart.

GRIFFIN, B. J.; PREISS, W. V. 1976. The significance and provenance of stromatolitic clasts in a probable late Precambrian diamictite in northwestern Tasmania. *Pap. Proc. R. Soc. Tasm.* 110:111–127.

GROVES, D. I. 1966. The geology of the Heazlewood–Godkin area. *Tech. Rep. Dep. Mines Tasm.* 10:26–40.

GROVES, D. I. 1968. *The cassiterite-sulphide deposits of western Tasmania.* Ph.D. thesis, University of Tasmania : Hobart.

GROVES, D. I.; MARTIN, E. L.; MURCHIE, H.; WELLINGTON, H. K. W. 1973. A century of tin mining at Mount Bischoff. *Bull. geol. surv. Tasm.* 54.

GROVES, D. I.; SOLOMON, M. 1964. The geology of the Mt Bischoff district. *Pap. Proc. R. Soc. Tasm.* 98:1–22.

GULLINE, A. B. 1959. The underground water resources of the Smithton district. *Undergr. Wat. Supply Pap. Tasm.* 5.

HAJASH, A. 1984. Rare earth element abundances and distribution patterns in hydrothermally altered basalts: experimental results. *Contrib. Mineral. Petrology* 85:409–412.

HANSON, G. N. 1980. Rare earth elements in petrogenetic studies of igneous systems. *Ann. Rev. Earth planet. Sci.* 8:371–406.

HARKINS, M. E.; GREEN, H. W.; MOORES, E. H. 1980. Multiple intrusive events documented from the Vourinos Ophiolite Complex, northern Greece. *Am. J. Sci.* 280A:284–295.

HASHIMOTO, M.; SAITO, Y.; KASHIMA, N. 1981. Relic clinopyroxenes and metamorphism of the Motton Spilite of the Leven Hills district, Tasmania. *Pap. Proc. R. Soc. Tasm.* 115:173–179.

HAWKES, D. D. 1967. Order of abundant crystal nucleation in a natural magma. *Geol. Mag.* 104:473–486.

HILL, R.; ROEDER, P. L. 1974. The crystallization of spinel from basaltic liquid as a function of oxygen fugacity. *J. Geol.* 82:709–729.

HILLS, C. L. 1915. The zinc-lead sulphide deposits of the Read–Rosebery district, Part II. Rosebery Group. *Bull. geol. Surv. Tasm.* 23.

HILLS, C. L.; CAREY, S. W. 1949. Geology and mineral industry, *in* CERUTTY, L. (ed.). *Handbook for Tasmania.* Australian and New Zealand Association for the Advancement of Science : Hobart.

HOLM, P. E. 1982. Non-recognition of continental tholeiites using the Ti-Y-Zr diagram. *Contrib. Mineral. Petrology* 79:308–310.

HUGHES, T. D. 1965. Nickel mineralization in Tasmania. *Publs. 8th Commonw. min. metall. Congr.* 1:523–524.

HUTCHINSON, R. W. 1979. Evidence of exhalative origin for Tasmanian tin deposits. *CIM Bull.* 72(808):91–104.

IRVINE, T. N. 1965. Chromian spinel as a petrogenetic indicator. *Can. J. Earth Sci.* 2:648–672.

IRVINE, T. N. 1982. Terminology for layered intrusions. *J. Petrology* 23:127–162.

JACK, R.; GROVES, D. I. 1965. Geology of the Mt Meredith–Yellowband Creek area. *Tech. Rep. Dep. Mines Tasm.* 9:26–36.

JACKSON, E. D. 1967. Ultramafic cumulates in the Stillwater, Great Dyke, and Bushveld intrusions, *in* WYLLIE, P. J. (ed.). *Ultramafic and related rocks.* 20–38. Wylie : New York.

JACKSON, E. D. 1969. Chemical variation in coexisting chromite and olivine in chromitite zones of the Stillwater Complex, *in* WILSON, H. D. B. (ed.). Magmatic ore deposits, a symposium. *Econ. Geol. Monogr.* 4:41–71.

JACKSON, E. D.; GREEN, H. W.; MOORES, E. M. 1975. The Vourinos ophiolite, Greece: cyclic units of lineated cumulates overlying harzburgite tectonite. *Bull. geol. Soc. Am.* 86:390–398.

JAGO, J. B. 1972. *Biostratigraphic and taxonomic studies of some Tasmanian Cambrian trilobites.* Ph.D. thesis, University of Adelaide.

JAGO, J. B. 1973. Cambrian agnostid communities in Tasmania. *Lethaia* 6:405–421.

JAGO, J. B. 1978. Late Cambrian fossils from the Climie Formation, western Tasmania. *Pap. Proc. R. Soc. Tasm.* 112:137–153.

JAGO, J. B. 1979. Tasmanian Cambrian biostratigraphy–a preliminary report. *J. geol. Soc. Aust.* 26:223–230.

JAGO, J. B.; BUCKLEY, J. H. 1971. An abrupt upper Middle Cambrian faunal change, Christmas Hills, Tasmania, Australia. *Pap. Proc. R. Soc. Tasm.* 105:83–85.

JAGO, J. B.; DAILY, B. 1974. The trilobite *Clavagnostus* Howell from the Cambrian of Tasmania. *Palaeontology* 17:95–109.

JAGO, J. B.; PIKE, G. A.; MILLS, D. 1975. Cambrian stratigraphy of the St Valentines Peak area, north-western Tasmania. *Pap. Proc. R. Soc. Tasm.* 109:85–90.

JAGO, J. B.; REID, K. O.; QUILTY, P. G.; GREEN, G. R.; DAILY, B. 1972. Fossiliferous Cambrian limestone from within the Mt Read Volcanics, Mt Lyell mine area, Tasmania. *J. geol. Soc. Aust.* 19:379–382.

JAQUES, A. L. 1980. *Petrologic and experimental studies on the petrogenesis of Papua New Guinea ophiolites.* Ph.D. thesis, University of Tasmania : Hobart.

JAQUES, A. L. 1981. Petrology and petrogenesis of cumulate peridotites and gabbros from the Marum Ophiolite Complex, northern Papua New Guinea. *J. Petrology* 22:1–40.

JAQUES, A. L.; GREEN, D. H. 1980. Anhydrous melting of peridotite at 0–15 kb pressure and the genesis of tholeiitic basalts. *Contrib. Mineral. Petrology* 73:287–310.

JENNER, G. A. 1981. Geochemistry of high-Mg andesites from Cape Vogel, Papua New Guinea. *Chemical Geology* 33:307–332.

JENNER, G. A. 1982. *Petrogenesis of high-Mg andesites.* Ph.D. thesis, University of Tasmania : Hobart.

JOHANSSEN, A. 1937. *A descriptive petrography of the igneous rocks. Volume 3. The intermediate rocks.* University of Chicago Press : Chicago.

KEITH, M. L. 1954. Phase equilibria in the system MgO-Cr_2O_3-SiO_2. *J. Am. Ceram. Soc.* 37:490–496.

KIKUCHI, Y. 1890. On pyroxenic components in certain volcanic rocks from Bonin Island. *J. Coll. Sci. Imp. Univ. Japan* 3:67–89.

KING, D. 1961. *A statistical and geological review of the Zeehan silver-lead mines, west Tasmania.* Rio Tinto Southern Pty Ltd (Open file report 61–335).

KOMATSU, M. 1980. Clinoenstatite in volcanic rocks from the Bonin Islands. *Contrib. Mineral. Petrology* 74:329–338.

KURODA, N.; SHIRAKI, K. 1975. Boninite and related rocks of Chichi-jima, Bonin Islands, Japan. *Rep. Faculty Sci. Shizucka University* 10:145–155.

LAJOIE, J. (ed.). 1970. Flysch sedimentology in North America. *Spec. Pap. geol. Assn. Canada.* 7.

LARDEUX, H. 1969. *Les tentaculites d'Europe occidentale et d'Afrique du nord.* Centre Natl. de la Recherche Scientifique : Paris.

LEAKE, B. E. 1978. Nomenclature of amphiboles. *Am. Mineralogist* 63:1023–1052.

LENNOX, P. G.; CORBETT, K. D.; BAILLIE, P. W.; CORBETT, E. B.; BROWN, A. V. 1982. Geological atlas 1:50 000 series. Sheet 21 (7916S). Smithton. *Department of Mines, Tasmania.*

LINK, A. G. 1970. Age and correlations of the Siluro-Devonian strata in the Yass Basin, New South Wales. *J. geol. Soc. Aust.* 16:711–722.

LOFTUS-HILLS, G.; SOLOMON, M.; HALL, R. J. 1967. The structure of the bedded rocks west of Rosebery, Tasmania. *J. geol. Soc. Aust.* 14:333–337.

MACDONALD, G. A.; KATSURA, T. 1964. Chemical composition of Hawaiian lavas. *J. Petrology* 5:82–133.

MCCLEAN, R. A. 1975. Lower Silurian rugose corals from central New South Wales. *J. Proc. R. Soc. N.S.W.* 108:54–69.

MCCLENAGHAN, M. P.; TURNER, N. J.; BAILLIE, P. W.; *et al.* 1982. Geology of the Ringarooma-Boobyalla area. *Bull. geol. Surv. Tasm.* 61.

MCDOUGALL, I.; LEGGO, P. J. 1965. Isotopic age determinations on granitic rocks from Tasmania. *J. geol. Soc. Aust.* 12:295–332.

MEIJER, A.; ANTHONY, E.; REAGAN, M. 1982. Petrology of volcanic rocks from the fore-arc sites, *in* LEE, M.; *et al.* (ed.). *Initial reports of the Deep Sea Drilling Project.* 60:709–729.

MERCIER, J-C. C.; NICOLAS, A. 1975. Textures and fabrics of upper-mantle peridotites as illustrated by xenoliths from basalts. *J. Petrology* 16:454–487.

MONTGOMERY, A. 1893*a*. Report on the country between Mole Creek and the Mount Dundas silver field, and on the discovery of coal at Barn Bluff. *Rep. Secr. Mines Tasm.* 1892–93.

MONTGOMERY, A. 1893*b*. Report on the progress of the mineral fields of the County of Montagu. *Rep. Secr. Mines Tasm.* 1892–93.

MONTGOMERY, A. 1895. Report on the progress of the mineral fields in the neighbourhood of Zeehan; Viz.:-Mackintosh River, Mount Black, Mount Read, Mount Dundas, Mount Zeehan, Stanley River, and Mount Heemskirk. *Rep. Secr. Mines Tasm.* 1894–95:vii–xxxviii.

MONTGOMERY, A. 1896. Report on the Zeehan-Dundas mineral fields in February 1896. *Rep. Secr. Mines Tasm.* 1895–96:xxi–xxxviii.

MOORES, E. M.; VINE, F. J. 1971. The Troodos Massif, Cyprus and other ophiolites as oceanic crust: evaluation and implications. *Phil. Trans. R. Soc. London.* A268:443–466.

NEWNHAM, L. A. 1975. Renison Bell tinfield. *Monogr. Ser. australas. Inst. Min. Metall.* 5:581–583.

NEWNHAM, L. A.; SCHELLEKENS, R. R. 1978. *Annual report, 1977–78. Mt Lindsay (E.L. 2/63) and Stanley River (E.L. 18/73) areas.* Renison Limited (open file report 78–1280).

NOLDART, A. J. 1976. Beaconsfield lateritic nickel deposits, T. *Monogr. Ser. australas. Inst. Min. Metall.* 1:1006–1008.

NYE, P. B. 1923. The silver-lead deposits of the Waratah district. *Bull. geol. Surv. Tasm.* 33.

NYE, P. B. 1929. The osmiridium deposits of the Adamsfield district. *Bull. geol. Surv. Tasm.* 39.

ÖPIK, A. A. 1951. Notes on the stratigraphy and palaeontology of Cambrian, Ordovician, and Silurian rocks in Tasmania. *Rec. Bur. miner. Resour. Geol. Geophys. Aust.* 1951/5.

ÖPIK, A. A. 1967. The Mindyallan Fauna of north-western Queensland. *Bull. Bur. Min. Resour. Geol. Geophys. Aust.* 74.

PADMASIRI, S. 1974. *The geology of the Razorback Mine.* B.Sc. (Hons) thesis, University of Tasmania : Hobart.

PAGE, N. J.; CASSARD, D.; HAFFTY, J. 1982. Palladium, platinum, rhodium, ruthenium, and iridium in chromitites from the Massif du Sud and Tiebaghi Massif, New Caledonia. *Econ. Geol.* 77:1571–1577.

PATTERSON, D. J. 1979. *Geology and mineralization at Renison Bell, western Tasmania.* Ph.D. thesis, University of Tasmania : Hobart.

PATTERSON, D. J.; OHMOTO, H.; SOLOMON, M. 1981. Geologic setting and genesis of cassiterite-sulfide mineralization at Renison Bell, western Tasmania. *Econ. Geol.* 76:393–438.

PEARCE, J. A. 1975. Basalt geochemistry used to investigate past tectonic environments on Cyprus. *Tectonophysics* 25:41–67.

PEARCE, J. A. 1980. Geochemical evidence for the genesis and eruptive setting of lavas from Tethyan ophiolites, *in* PANAYIOTOU, A. (ed.). *Ophiolites. Proceedings International Ophiolite Symposium, Cyprus, 1979.* 261–272. Ministry of Agriculture and Natural Resources : Cyprus.

PEARCE, J. A.; CANN, J. R. 1973. Tectonic setting of basic volcanic rocks determined using trace element analyses. *Earth planet. Sci. Lett.* 19:290–300.

PEARCE, J. A.; GALE, G. H. 1977. Identification of ore deposition environment from trace-element geochemistry of associated igneous host rocks, *in Volcanic processes in ore genesis.* 14–24. Institute of Mining and Metallurgy : London.

PEARCE, J. A.; NORRY, M. J. 1979. Petrogenetic implications of Ti, Zr, Y, and Nb variations in volcanic rocks. *Contrib. Mineral. Petrology* 69:33–47.

PETERSEN, J. 1891. Beitrage zur Petrographie von Sulphur Island, Hachijo und Mijakeshima. *Jahrb. Hamburg Wiss. Anst.* 8:1–59.

QUILTY, P. G. 1971. Cambrian and Ordovician dendroids and hydroids of Tasmania. *J. geol. Soc. Aust.* 17:171–189.

RALEIGH, C. B. 1967. Experimental deformation of ultramafic rocks and minerals, *in* WYLLIE, P. J. (ed.). *Ultramafic and related rocks.* 191–199. Wylie : New York.

REID, A. M. 1919. Asbestos in the Beaconsfield district. *Rep. geol. Surv. Tasm.* 8.

REID, A. M. 1921. Osmiridium in Tasmania. *Bull. geol. Surv. Tasm.* 32.

REID, A. M. 1923. The Mount Bischoff tin field. *Bull. geol. Surv. Tasm.* 34.

REID, A. M. 1925. The Dundas mineral field. *Bull. geol. Surv. Tasm.* 36.

RICHARDS, J. R.; SINGLETON, O. P. 1981. Palaeozoic Victoria, Australia: igneous rocks, ages and their interpretation. *J. geol. Soc. Aust.* 28:395–421.

ROEDER, P. L.; EMSLIE, R. F. 1970. Olivine-liquid equilibrium. *Contrib. Mineral. Petrology* 29:275–289.

ROEDER, P. L.; CAMPBELL, I. H.; JAMIESON, H. E. 1979. A re-evaluation of the olivine-spinel geothermometer. *Contrib. Mineral. Petrology* 68:325–334.

RUBENACH, M. J. 1967. *The Serpentine Hill complex.* B.Sc. (Hons) thesis, University of Tasmania : Hobart.

RUBENACH, M. J. 1973. *The Tasmanian ultramafic-gabbro and ophiolite complexes.* Ph.D. thesis, University of Tasmania : Hobart.

RUBENACH, M. J. 1974. The origin and emplacement of the Serpentine Hill complex, western Tasmania. *J. geol. Soc. Aust.* 21:91–106.

SAGGERSON, E. P.; WILLIAMS, L. A. J. 1964. Ngurumanite from southern Kenya and its bearing on the origin of rocks in the northern Tanganyika alkaline district. *J. Petrology* 5:40–81.

SAUNDERS, A. D.; TARNEY, J.; MARSH, N. G.; WOOD, D. A. 1980. Ophiolites as ocean crust or marginal basin crust : A geochemical approach, *in* PANAYIOTOU, A. (ed.). *Ophiolites. Proceedings International Ophiolite Symposium, Cyprus, 1979.* 193–204. Ministry of Agriculture and Natural Resources : Cyprus.

SCHELLEKENS, R. R. 1979. *Annual report, 1978–79. Mt Lindsay (E.L. 2/63) and Stanley River (E.L. 18/73) areas, western Tasmania.* Renison Limited (Open file report 79–1381).

SCOTT, B. 1952. The occurence of pillow lavas near Penguin, Tasmania. *Pap. Proc. R. Soc. Tasm.* 86:123–125.

SHEEHAN, P. M.; BAILLIE, P. W. 1981. A new species of *Eospirifer* from Tasmania. *J. Palaeont.* 55:248–256.

SHERRARD, K. M. 1954. The assemblages of graptolites in New South Wales. *J. Proc. R. Soc. N.S.W.* 87:73–101.

SHERRARD, K. M. 1967. Tentaculitids from New South Wales, Australia. *Proc. R. Soc. Vict.* N.S. 80:229–246.

SHIRAKI, K.; KURODA, N. 1977. The boninite revisited. *J. Geogr. (Tokyo)* 86(3):34–50.

SOLOMON, M. 1960. The Dundas Group in the Queenstown area. *Pap. Proc. R. Soc. Tasm.* 94:33–50.

SOLOMON, M. 1965. Geology and mineralization of Tasmania. *Publs 8th commonw. min. metall. Congr.* 1:464–477.

SPARKS, R. S. J.; WILSON, C. J. N. 1982. Flow head deposits in ash turbidites. *Ann. Rep. Research School of Earth Sciences Aust. National University.*

SPRY, A. H. 1958. Some observations of the Jurassic dolerite of the Eureka cone sheet near Zeehan, *in Dolerite: a symposium.* 95–129. Department of Geology, University of Tasmania : Hobart.

SPRY, A. H. 1962. Igneous activity, *in* SPRY, A. H.; BANKS, M. R. (ed.). The geology of Tasmania. *J. geol. Soc. Aust.* 9(2):255–284.

STEVENS, N. C.; PACKHAM, G. H. 1953. Graptolite zones and associated stratigraphy at Four-Mile Creek, south-west of Orange, N.S.W. *J. Proc. R. Soc. N.S.W.* 86:94–99.

STOCKLEY, J. L. 1972. *The Meredith Granite.* B.Sc. (Hons) thesis, University of Tasmania : Hobart.

STRUSZ, D. L. 1961. Lower Palaeozoic corals from New South Wales. *Palaeontology* 4:334–361.

SUMMONS, T. G.; GREEN, D. C.; EVERARD, J. L. 1981. The occurrence of chromite in the Andersons Creek area, Beaconsfield, Tasmania. *Econ. Geol.* 76:505–518.

SUN, S. -S.; NESBITT, R. W. 1978. Geochemical regularities and genetic significance of ophiolitic basalts. *Geology* 6:689–693.

TAYLOR, B. L. 1954. Progress report on the North Pieman mineral area. *Unpubl. Rep. Dep. Mines Tasm.* 1954:149–203.

TAYLOR, B. L. 1955. Asbestos in Tasmania. *Miner. Resour. geol. Surv. Tasm.* 9.

THOMAE, W. F. A. 1896. The Zeehan and Dundas silver field, Tasmania. *Trans. Inst. Min. Metall.* iv:50–67.

THOMAS, D. E. 1947. A critical review of the Lower Palaeozoic succession of Tasmania. *Proc. R. Soc. Vict.* 59:23–52.

THOMAS, D. E. 1960. The zonal distribution of Australian graptolites. *J. Proc. R. Soc. N.S.W.* 94:1–58.

THOMAS, D. E.; HENDERSON, Q. J. 1945. Some fossils from the Dundas Series, Dundas. *Pap. Proc. R. Soc. Tasm.* 1944:1–8.

TURNER, N. J. 1979. The boundary relationship of the Concert Schist and the Oonah Quartzite and Slate correlate at Dundas. *Pap. Proc. R. Soc. Tasm.* 113:15–20.

TURNER, N. J. 1982. Tasmanian Proterozoic rocks. *Unpubl. Rep. Dep. Mines Tasm.* 1982/45.

TWELVETREES, W. H. 1897. Microscopical studies of Tasmanian rocks. *Pap. Proc. R. Soc. Tasm.* 1896:89–97.

TWELVETREES, W. H. 1900. Report on the mineral fields between Waratah and Corinna. *Rep. Secr. Mines Tasm.* 1899–1900:cxl–ccviii.

TWELVETREES, W. H. 1901. Report on the mineral districts of Zeehan and neighbourhood. *Rep. Secr. Mines Tasm.* 1900–01:3–108.

TWELVETREES, W. H. 1914. The Bald Hill osmiridium field. *Bull. geol. Surv. Tasm.* 17.

TWELVETREES, W. H. 1917. Asbestos at Andersons Creek. *Miner. Resour. geol. Surv. Tasm.* 4.

TWELVETREES, W. H.; PETTERD, W. F. 1898. On some igneous rocks from the Heazlewood district. *Pap. Proc. R. Soc. Tasm.* 1897:24–38.

TWELVETREES, W. H.; WARD, L. K. 1910. The ore-bodies of the Zeehan field. *Bull. geol. Surv. Tasm.* 8.

VARNE, R. 1978. The Cambrian volcanic associations of Tasmania and their tectonic setting, *in* GREEN, D. C.; WILLIAMS, P. R. (ed.). *Geology and mineralization of N. W. Tasmania. Abstracts of symposium.* Geological Society of Tasmania (Tasmanian Division) : Hobart.

VARNE, R.; BROWN, A. V. 1978. The geology and petrology of the Adamsfield Ultramafic Complex, Tasmania. *Contrib. Mineral. Petrology* 67:195–207.

WAGER, L. R.; BROWN, G. M.; WADSWORTH, W. J. 1960. Types of igneous cumulates. *J. Petrology* 1:73–85.

WALDRON, H. M.; BROWN, A. V. 1985. Rare Earth Element patterns of Eocambrian–Cambrian basaltic suites, western Tasmania. *Unpubl. Rep. Dep. Mines Tasm.* 1985/37.

WALDRON, H. M.; BROWN, A. V.; KEAYS, R. R. in press. Geological setting and petrochemistry of Eocambrian–Cambrian volcano-sedimentary rock sequences from south east King Island. *Aust. J. Earth Sci.*

WALKER, R. G. 1967. Turbidite sedimentary structures and their relationship to proximal and distal depositional environments. *J. Sed. Petrology* 37:25–43.

WALLER, G. A. 1902. Report on the Western Silver mine, Zeehan. *Department of Mines, Tasmania.*

WALLER, G. A. 1905. Notes on the geological structure of the West Coast of Tasmania. *Report of Tenth Meeting, Australasian Association for the Advancement of Science, Dunedin, 1904.* 622–630.

WARD, L. K. 1909*a*. The tinfield of North Dundas. *Bull. geol. Surv. Tasm.* 6.

WARD, L. K. 1909*b*. [Report by Assistant Government Geologist on West Coast exploration]. *Rep. Dep. Lands and Surveys Tasm.* 1908–09:31–35.

WATERHOUSE, L. L. 1914. The Stanley River tinfield. *Bull. geol. Surv. Tasm.* 15.

WATERHOUSE, L. L. 1916. The South Heemskirk Tin Field. *Bull. geol. Surv. Tasm.* 21.

WEBBY, B. D.; VANDENBERG, A. H. M.; COOPER, R. A.; *et al.* 1981. The Ordovician System in Australia, New Zealand and Antarctica. *Sci. Publ. Int. Union Geol.* 6.

WELLS, P. R. A. 1977. Pyroxene thermometry in simple and complex systems. *Contrib. Mineral. Petrology* 62:129–139.

WHITE, N. 1975. *Cambrian volcanism and mineralization–south-west Tasmania.* Ph.D. thesis, University of Tasmania : Hobart.

WILLIAMS, E. 1976. Structural map of pre-Carboniferous rocks of Tasmania. *Department of Mines, Tasmania.*

WILLIAMS, E. 1978. Tasman Fold Belt System in Tasmania. *Tectonophysics* 48:159–206.

WILLIAMS, E. 1983. The areal distribution of rock units during Early Palaeozoic times. *Unpubl. Rep. Dep. Mines Tasm.* 1983/61.

WILLIAMS, H.; TURNER, F. J.; GILBERT, C. M. 1954. *Petrography. An introduction to the study of rocks in thin sections.* W. H. Freeman and Company : San Fransisco.

WILLIAMS, K. L. 1958. Nickel mineralization in western Tasmania, *in F. L. Stilwell memorial volume.* 263–302. Australasian Institute of Mining and Metallurgy : Melbourne.

WILLIAMS, P. R. 1975. The relationship between the Cambrian rocks and the correlate of the Junee Group at Misery Hill, near Zeehan. *Tech. Rep. Dep. Mines Tasm.* 18:36–39.

WILLIAMS, P. R. 1979. *Basin development, environment of deposition and deformation of a Precambrian(?) conglomeratic flysch sequence at Bathurst Harbour, S. W. Tasmania.* Ph.D. thesis, University of Tasmania : Hobart.

WILLIAMS, P. R. 1982*a*. Geological atlas 1:50 000 series. Sheet 91 (8011S). Davey. *Explan. Rep. geol. Surv. Tasm.*

WILLIAMS, P. R. 1982*b*. Structural geology of the Mt Bischoff Precambrian rocks. *Unpubl. Rep. Dep. Mines Tasm.* 1982/11.

WILLIAMS, P. R.; BROWN, A. V. 1983. An unusal occurrence of ultramafic and mafic rocks north of Mt Bischoff, NW Tasmania. *Pap. Proc. R. Soc. Tasm.* 117:53–58.

WITHNALL, I. W. 1984. Geochemistry and tectonic significance of Proterozoic mafic rocks from the Georgetown Inlier, north Queensland. *BMR J. Aust. Geol. Geophys.* 9:339–352.

WOOD, B. J.; BANNO, S. 1973. Garnet-orthopyroxene and orthopyroxene-clinopyroxene relationships in simple and complex systems. *Contrib. Mineral. Petrology* 42:109–124.

APPENDIX 1

Late Cambrian agnostid faunas from the Huskisson River area

M. J. Clarke

Abstract

Three rich agnostid faunas have been located in the Dundas Group in the Huskisson River area. All locations can be assigned to the *Glyptagnostus reticulatus* zone.

INTRODUCTION

Geologist A. V. Brown has located three rich agnostid faunas in black graphitic slate in the Dundas Group sequence exposed in the Huskisson River. The localities and faunas are given below.

LOCALITIES AND FAUNAS

Location 1079 [CP723762] (Unit 14 of Taylor, 1954)

Glyptagnostus reticulatus (Angelin) and spicules of the sponge *Protospongia* sp. occur in great profusion. Rare fragments of another small (?immature) agnostid also occur. Preservation is good to very good.

Location 1143 [CP715766] (Unit 18 of Taylor, 1954)

Pseudagnostus idalis Öpik occurs in profusion with rare specimens of *Glyptagnostus reticulatus* (Angelin). A considerable number of the *Pseudagnostus* specimens are complete and articulated. Preservation is excellent.

Location 1197 [CP712770] (Unit 18 of Taylor, 1954)

Pseudagnostus idalis Öpik occurs in moderate abundance with rare fragments of *Glyptagnostus reticulatus* (Angelin). Most of the *Pseudagnostus* specimens are complete. Preservation is only moderate.

All three localities can be unequivocally assigned to the earliest Idamean *Glyptagnostus reticulatus* Zone (early Late Cambrian). This conclusion agrees in part with Öpik (1951), as location 1143 is close to that from which Öpik recorded a *Glyptagnostus reticulatus* fauna. However, location 1079 is close to the locality from which Öpik recorded poorly-preserved hydroids and the brachiopods *?Otusia* sp. and *?Protorthis* sp., and dated as middle Middle Cambrian. The suggestion of Blissett (1962) that Units 14 and 18 of Taylor (1954) represent the same stratigraphic interval is substantiated. Both Taylor (1954) and Blissett (1962) correlated the overlying Unit 19 with the Zeehan Conglomerate (= Misery Hill Conglomerate). Thus the youngest rocks in the Huskisson River Dundas Group section are significantly older than those from the Climie Slate of the Zeehan area.

APPENDIX 2

Some Ordovician and Silurian rocks and fossils from the Huskisson River area, western Tasmania

M. R. Banks
C. F. Burrett

Abstract

Specimens (C1130) from the base of the Gordon Subgroup in the Huskisson River area are biomicrites containing calcareous algae, corals, bryozoa, brachiopods, rostroconchs, gastropods, trilobites and conodonts. The conodonts are *Belodina compressa* (Branson and Mehl) of Middle–Late Ordovician age. An oolitic echinodermal microsparite (C1140) occurs slightly higher stratigraphically and contains *Tasmanognathus careyi* Burrett which indicates a correlation with the microfauna of the Lower Limestone Member of the Benjamin Limestone in the Florentine Valley.

A sandstone replete with external moulds of large diameter crinoid-columnals(?) demonstrates the presence of a correlate of the Crotty Quartzite. Despite the unusual shape of the columnals(?), no taxonomic assignment can be made.

A pale grey biomicrite (C981) contains dasyclad algae, tabulate and rugose corals, bryozoa, brachiopods, bivalves, gastropods and echinoderms. The rugose corals may include *Tryplasma lonsdalei* Etheridge and *Stereoxylodes* sp. close to *S. multicarinatus* McLean. Tabulates include a favositid, probably *Pachypora*, and *Syringopora* sp. These corals are consistent with a Middle Silurian age.

Tentaculites cf. *ornatus* Sowerby occurs in siltstone correlated with the Amber Formation and is consistent with a Wenlockian age.

A specimen of *?Cyrtograptus* may also be present. If correctly identified this would indicate a Wenlockian age for the limestone in the Amber Formation.

INTRODUCTION

Several specimens of limestone and one of sandstone from the Huskisson River area were made available by A. V. Brown, Tasmania Department of Mines, for determination of age and/or of the fossils present. M. J. Clarke made available siltstones with abundant *Tentaculites*.

The specimens bore the field numbers C631, C981, C1130-I, C1130-II and C1140. Details of these specimens are:

C631: AMG reference CP64318672; limestone of Gordon Subgroup, five metres below contact with overlying sandstone; Little Wilson River.

C981: AMG reference CP70038335; limestone member within Amber Formation.

C1130: AMG reference CP72597639; limestone of Gordon Subgroup;

Micro I–base of Subgroup.

Micro II–approximately 160 m above base of Subgroup.

Macro I–approximately 120 m above base of Subgroup.

Macro II–approximately 220 m above base of Subgroup.

C1140: AMG reference CP72597639; limestone of Gordon Subgroup.

Crinoid specimen UTGD 122483: AMG reference CP696785; fossiliferous sandstone, Crotty Formation; former Department of Main Roads quarry at about 38·85 km mark on the Lower Pieman Dam Road.

Siltstone: AMG reference CP729792; correlate of Amber Formation.

The opportunity was also taken to determine the petrology of the limestones submitted.

PETROLOGY

LIMESTONE

Specimen C981

This rock is a pale grey micrite with 'dolomitic' patches, poorly developed stylolites, and many fossil fragments up to 34 mm long. The fossils include polyzoa, tabulate corals and echinoderm elements. In thin section (Plate 17*a*), the rock has fossil fragments forming 60% to 90% of the rock in a micritic matrix. The fossil fragments include those of dasyclad algae, tabulate and rugose corals, bryozoa, inarticulate brachiopods, bivalves, gastropods and echinoderms. These fragments are unsorted and show few signs of abrasion. Several of them do, however, show signs of boring. The rock also contains a small proportion (1–2%) of angular and subangular quartz grains of silt to coarse sand grade.

The clasts are in a micrite matrix which shows development of small calcite and dolomite rhombs and mosaic patches of calcite and siderite microspar. The matrix also has irregular, laminar, sharp-sided bodies of large carbonate grains, representing fillings of 'fenestrate' birdseyes. The carbonate grains lining these cavities and cavities in the fossils are calcite, then dolomite in places, ferroan dolomite and abundant siderite. Irregular poorly-defined zones of fine-grained calcitic and sideritic mosaic traverse the rock and probably represent incipient stylolites. At least one of these has been split by a fracture and the cavity filled with the ferroan dolomite and siderite. Well-formed pyrite crystals form about one percent of the rocks and seem to be concentrated at the junction between the micrite matrix and later sideritic mosaic zones or in those zones, but are not restricted thereto.

The rock is a partially sideritised biomicrite clearly of marine origin, having accumulated in shallow, probably clear water on a surface which included very little extraneous detrital material. There was an abundant attached benthos but there was very little movement of bottom waters, although conditions were not reducing. It seems that some more-or-less laminar cavities as well as intra-skeletal cavities were present in the newly deposited rock. Subsequent to deposition, recrystallisation of the matrix began and led to the development of small calcite and dolomite rhombs in the micrite and to patches of mosaics of calcite and siderite microspar. Later fractures were filled with ferroan dolomite and/or siderite. At some stage the laminar cavities, and other cavities including the intra-skeletal, were lined with calcite, a thin layer of dolomite in places, then ferroan dolomite and predominant siderite. Stylolitisation began at a late stage in the history recorded in the rock, the stylolites being represented by zones with fine calcite and siderite mosaics and marginal pyrite. The pyrite probably represents a late introduction of sulphide or sulphate-bearing solutions with local reduction.

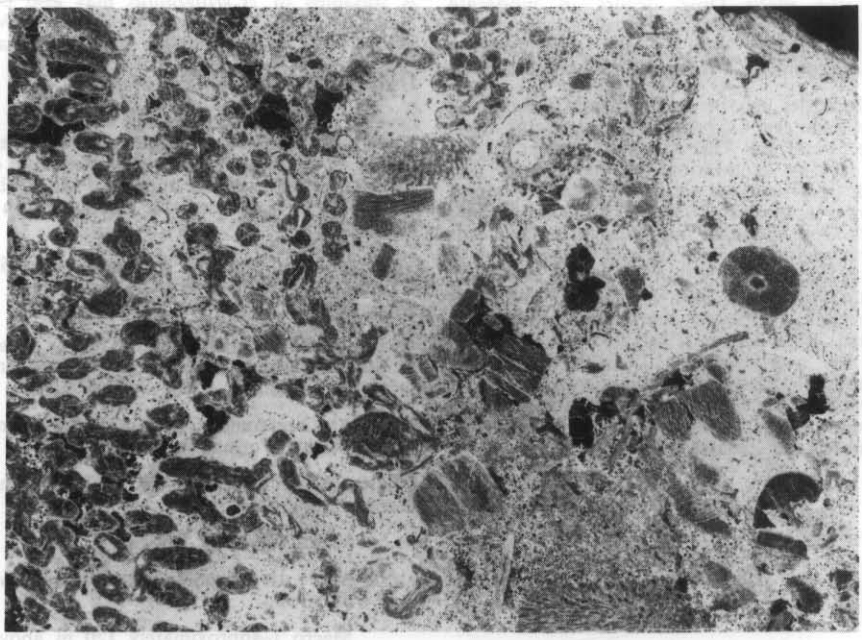

Plate 17*a*. Biomicrite–mainly syringoporid, pachyporid and echinoderm fragments in a micritic matrix; TDM C981-B7, ×5.

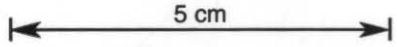

Specimen C1130-I

In hand specimen, this rock is a 'crinoidal' biomicrite with small patches (?burrows) of dolomite. Shell fragments are very abundant in some specimens and reach 13·5 mm long. Shells recognisable in hand specimen include algae, corals, bryozoa, brachiopods, trilobites and echinoderms. The dolomitic patches are up to 11·5 mm long and 2·5 mm wide. In thin section (Plate 17*b*), the rock is composed of fossil fragments, minor pellets and intraclasts, sparse oolites and rare, very angular quartz grains, both free and as nuclei of oolites. The fossil fragments have a marked parallel orientation leading in some places to a strong primary fabric. Some of the fossils are outlined by a thin corona of carbonaceous matter. The matrix is micrite in places, microspar in others, and rarely sparite. There are patches of dolomitic(?) sparite, commonly with individual grains and the whole body outlined by 'limonitic' material. In places there are small oval or circular bodies filled with one to a few crystals of sparite with some micrite between the spar. These may be borings filled with micrite which has later undergone recrystallisation. The rock has numerous stylolites. Pyrite occurs as a rim around some fossil fragments, associated with the stylolites, and possibly in places as a replacement.

The rock is an echinodermal biomicrite deposited in shallow, marine conditions with some agitation of the bottom waters but little introduction of extraneous detrital material. After deposition, and possibly boring, ?dolomitisation occurred, followed by stylolitisation and then the introduction of pyrite.

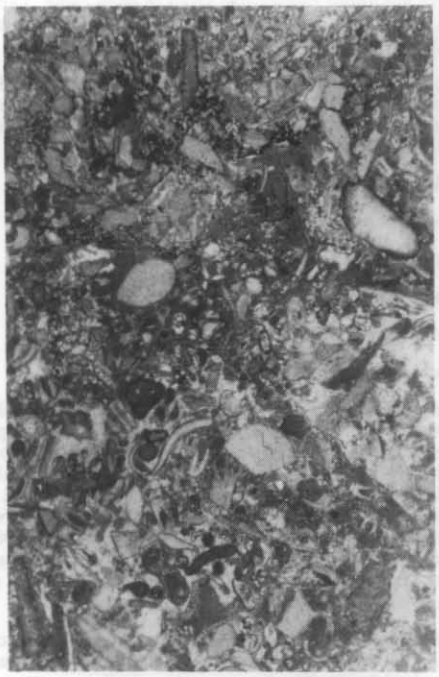

Plate 17*b*. Echinodermal bimicrite–algal, echinoderm and arthropod fragments in a micritic matrix; TDM C1130-I, ×4.

Specimen C1130-II

This rock (Plate 17*c*) is very similar to 1130-I but the micrite is almost completely converted to microspar in places. There are fossil fragments up to 13·5 mm long. On weathered surfaces the (?)ferroan dolomite appears to occupy burrows up to 11·5 mm long and 2·5 mm wide. Fossils present include algae, corals, trepostome bryozoa, impunctate brachiopods, bivalves, trilobites and crinoids.

Depositional conditions and a post-depositional history similar to those inferred for 1130-I appear likely.

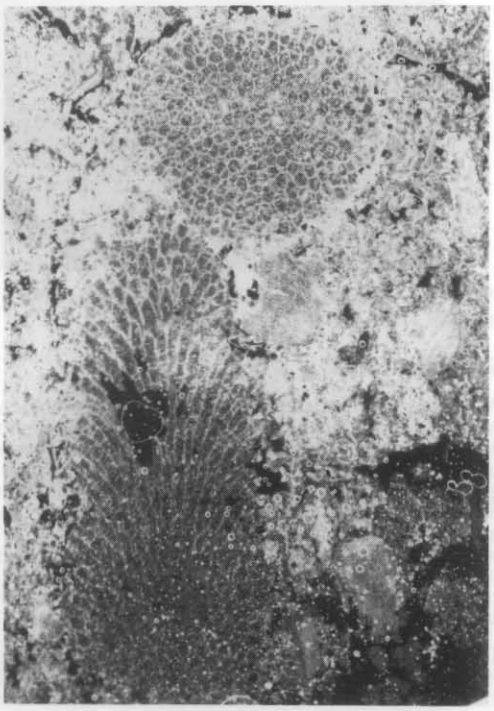

Plate 17*c*. Echinodermal biomicrite–bryozoal and echinodermal fragments in a sparse micritic matrix; TDM C1130-II, ×5.

Specimen C1140

This rock is a medium-grey to light-grey micrite, the weathered surface of which is marked by numerous, randomly distributed small projections (less than one millimetre high and round). On broken surfaces, numerous small cleavage surfaces of calcite can be seen, showing the presence of echinoderm elements. The rock is cut by calcite veins and later stylolites with amplitudes of more than 25 mm.

In thin section (Plate 17*d*), the rock is a well-sorted, oolitic, echinodermal microsparite with some angular quartz grains, both free and as nuclei for oolites. There are a few clasts of micrite with dolomite rhombs and also of mudstone. The rock is grain-supported, or almost so.

This rock was deposited on a sea floor swept by active currents or waves, probably a shallow sea floor. Fracturing took place subsequent to deposition, the fractures subsequently being healed by calcite. Stylolitisation later occurred.

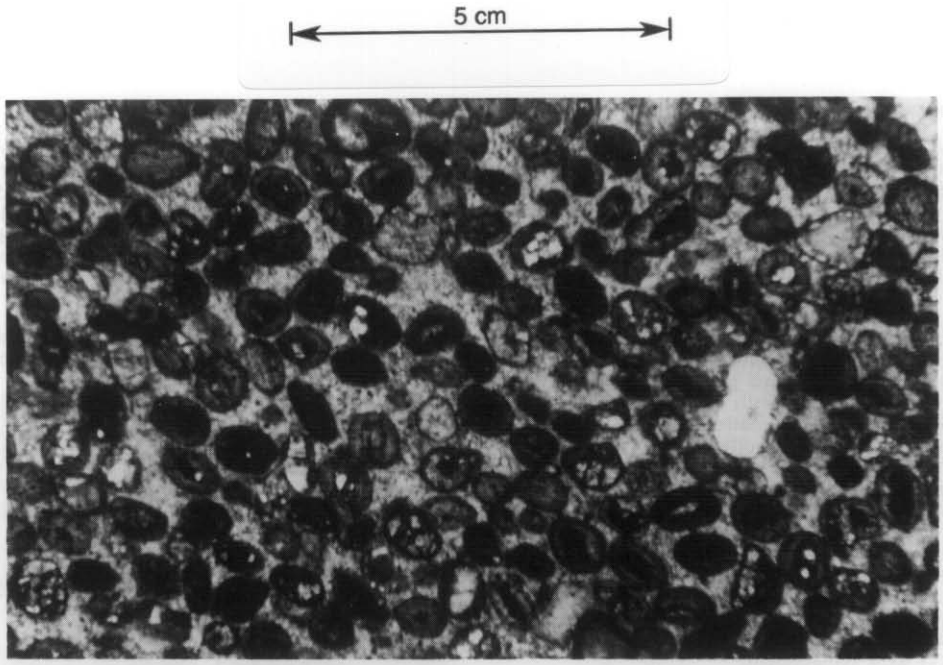

Plate 17*d*. Oolitic echinodermal microsparite–oolites, echinoderm fragments and quartz grains in a microspar matrix; TDM C1140, ×20.

Specimen UTGD 122483

A quartz-rich sandstone with very abundant impressions of discoidal plates with large, central biconical depressions was also submitted. The discoidal plates range up to 29 mm in diameter and have generally been referred to in Tasmanian geological literature (e.g. Gill, 1950) as crinoid columnals. The quartz grains are of medium sand-grade and the rock is well sorted. The rock is now somewhat porous and, in places, friable suggesting the initial presence of a carbonate cement. In other places the grains are cemented by silica.

The lithological characters suggest a strongly wave-swept environment of deposition, possibly with crinoids growing on or close to a bed of coarse sand. The current strength was adequate to produce a well-sorted, grain-supported sand with grains up to medium sand grade but not to sort the crinoid columnals.

The lithology and the presence of the crinoid columnals suggest correlation with the Crotty Quartzite.

COELENTERATA

RUGOSA

Five thin sections show obliquely transverse and obliquely longitudinal sections of a coral which is either solitary or fasciculate, and another section contains a transverse section of a smaller solitary coral.

Order CYSTIPHYLLIDA

Family TRYPLASMATIDAE

Genus *TRYPLASMA* Lonsdale, 1854

?Tryplasma lonsdalei Etheridge

(Plate 18*a*)

The section is of an apparently simple coral with circular or slightly elliptical cross-section, 9 mm long diameter by 7·8 mm short diameter.

The corallum has numerous low, rounded interseptal external ridges. The wall is thick (0·4 mm) and septothecal. Two cycles of short, thick septa occur, the longer reaching one-third of the way to the axis, the shorter half or slightly more of the length of the longer. Both cycles may be spinose but in the absence of a longitudinal section this cannot be determined. There are about twenty-five septa in each cycle. Tabulae are present but probably sparse. Lack of longitudinal section precludes comments on tabular spacing.

The specimen is assigned to *T. lonsdalei* on the basis of size, septal character and number but the assignment cannot be regarded as positive because of lack of material.

Order STAURIIDA

Suborder ARACHNOPHYLLINA

Family ENTELOPHYLLIDAE

Genus *STEREOXYLODES* Wang, 1944

Stereoxylodes sp.

(Plate 18*b–e*)

Five sections thought to be conspecific are available of this coral. Unfortunately none could be properly oriented. The largest section (C981A) is probably obliquely transverse. Another section (C981B) is about half of a transverse section. Two sections (C981E and C981F) are partial longitudinal and partial transverse sections of a curved corallum. One section (C981C) is an oblique longitudinal section from the axial portion at a small diameter to the peripheral portion at a larger diameter.

The corallite is a curved or irregular, almost circular cone with some angulations suggesting a partial phaceloid habit. The largest section indicates a corallite at least 18 mm in diameter. The wall appears externally smooth in some places or furnished with very low, rounded interseptal ridges in others. It is about 0·2 mm thick and septothecal. Very marked rugosities are revealed by the longitudinal section.

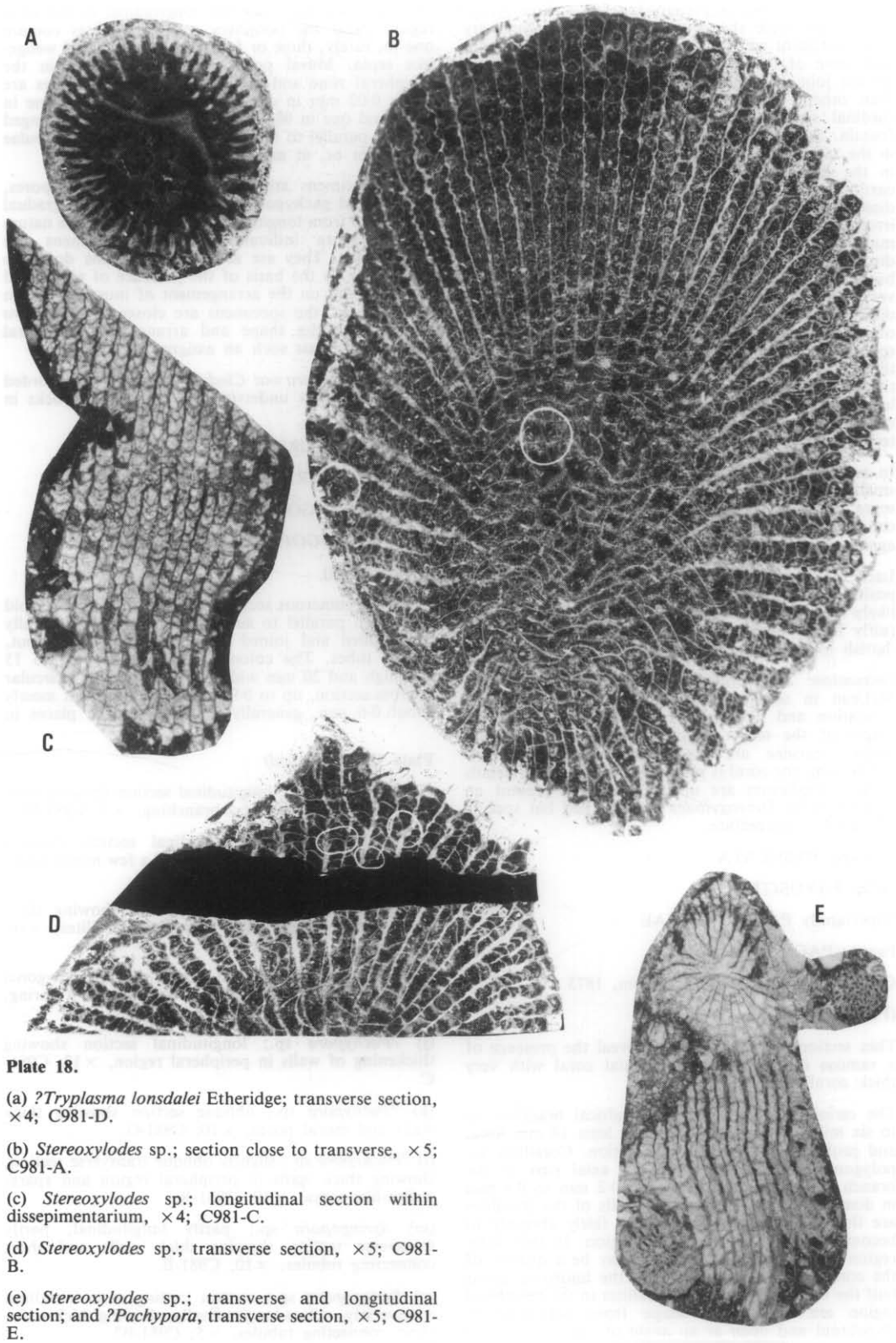

Plate 18.

(a) *?Tryplasma lonsdalei* Etheridge; transverse section, ×4; C981-D.

(b) *Stereoxylodes* sp.; section close to transverse, ×5; C981-A.

(c) *Stereoxylodes* sp.; longitudinal section within dissepimentarium, ×4; C981-C.

(d) *Stereoxylodes* sp.; transverse section, ×5; C981-B.

(e) *Stereoxylodes* sp.; transverse and longitudinal section; and *?Pachypora*, transverse section, ×5; C981-E.

Septa occur in two, or perhaps locally, in three cycles. The longer cycle shows a crude bilateral symmetry (not coincident with the long axis of the thin section) and some of the septa almost reach the centre but do not join there. One of the septa is much shorter than others adjacent to it and is presumably the cardinal septum, withdrawal of which produces a fossula. Several of the longer septa curve cardinally in the tabularium. The longer septa tend to be wavy in the dissepimentarium and those in the counter-cardinal quadrants to be dilated in the dissepimentarium producing fusiform septa. A few irregularly developed carinae occur on the longer septa, mainly in the dissepimentarium. A very few discontinuities occur in septa, especially peripherally, but may not be of biogenic origin. Because of the very oblique nature of the transverse section it is difficult to provide an accurate statement on the number of primary septa. Thirty-two can be counted but the spacing in the more distal part of the section suggests there may be as many as sixty-six major septa near the calyx. Minor septa are half to two-thirds of the length of the primary ones and tend to be thin, straight and without carinae. One or two very short tertiary septa may be present.

In an ill-defined peripheral zone the dissepiments are small and inosculating between the major and minor septa. Adaxially the dissepiments form a single series concave to the axis with a few lateral dissepiments against major septa.

Lack of a suitable longitudinal section precludes positive statements about the tabulae but it seems likely from transverse sections that there is a zone of fairly highly convex tabellae and an axial series of flattish to gently concave tabulae.

Discussion: The coral is close to *S. multicarinatus* McLean in size, septal number and arrangement, carination and peripheral breakdown. However the length of the minor septa is greater than in that species, carinae are much less abundant in the tabularium, the coral is probably phaceloid and details of the tabularium are unclear. For the present an assignment to *Stereoxylodes* is warranted but specific allocation is premature.

Subclass TABULATA

Order FAVOSITIDA

Superfamily PACHYPORICAE

Family PACHYPORIDAE

Genus *?PACHYPORA* Lindstrom, 1873

(Plate 18*e–l*)

Thin sections of specimen 981 reveal the presence of a ramose (or frondescent) colonial coral with very thick corallite walls.

The cerioid colonies include cylindrical branches up to six millimetres across, up to at least 18 mm long, and probably of circular cross-section. Corallites are polygonal in cross-section in the axial part of the branch and range from less than 0·2 mm to 0·4 mm in diameter. In this region, the walls of the corallites are thin but increase gradually to fairly abruptly to become thick in the peripheral region. In this latter region the thickness of the wall may be a quarter of the corallite diameter, restricting the lumen to about half the total diameter. The corallites in the peripheral region are variable in shape from polygonal to alveolitoid and open at an angle of 100° to 110° to the outer surface. They are longitudinal in the axial region. Near the periphery a few corallites contain one to, rarely, three or four short, wide-based wedge-like septa. Mural pores can be seen only in the peripheral zone and then only rarely. The pores are about 0·02 mm in diameter. In two colonies (one in 981B and one in 981G) the mural pores are arranged in rows parallel to the margin of the colony. Tabulae are absent or, at most, rare.

These specimens are clearly favositid (mural pores, cerioid) and pachyporicean (thick walls). The gradual divergence from longitudinal to oblique and the nature of the septa indicate that the specimens are pachyporids. They are assigned with some doubt to *Pachypora* on the basis of the presence of alveolitoid corallites and on the arrangement of mural pores. In colony form, the specimens are closer to *Cladopora* but the corallite shape and arrangement of mural pores are against such an assignment.

Neither *Pachypora* nor *Cladopora* have been recorded in what are now understood to be Silurian rocks in Australia.

Order AULOPORIDA

Superfamily SYRINGOPORICAE

Family SYRINGOPORIDAE

Genus *SYRINGOPORA* Goldfuss, 1826

(Plate 18*m–n*)

There are numerous sections of a fasciculate phaceloid coral with parallel to subparallel corallites, generally thick-walled and joined by numerous, short, stout, hollow tubes. The colonies sectioned are up to 15 mm high and 20 mm wide. The corallites are circular in cross-section, up to 0·9 mm in diameter but mostly about 0·6 mm, generally separated but in places in

Plate 18 *(Continued)*

(f) *?Pachypora* sp.; longitudinal section showing thin-walls in axial region and branching, ×5; C981-B8.

(g) *?Pachypora* sp.; longitudinal section showing branching, alveolitoid corallites and a few mural pores, ×5; C981-D.

(h) *?Pachypora* sp.; oblique section showing thick walls and alveolitoid and polygonal corallites, ×10; C981-B.

(i) *?Pachypora* sp.; oblique section showing polygonal corallites, sparse mural pores, a septum and a boring, ×10; C981-D.

(j) *?Pachypora* sp.; longitudinal section showing thickening of walls in peripheral region, ×12; C981-C.

(k) *?Pachypora* sp.; oblique section showing thick walls and mural pores, ×10; C981-G.

(l) *?Pachypora* sp.; slightly oblique transverse section, showing thick walls in peripheral region and sparse wedge-like septa, ×10; C981-B.

(m) *Syringopora* sp.; partly longitudinal, partly transverse section showing thick walls and short connecting tubules, ×10; C981-B.

(n) *Syringopora* sp.; section cutting some corallites transversely, others longitudinally, showing thick walls, short connecting tubules, ×5; C981-B7.

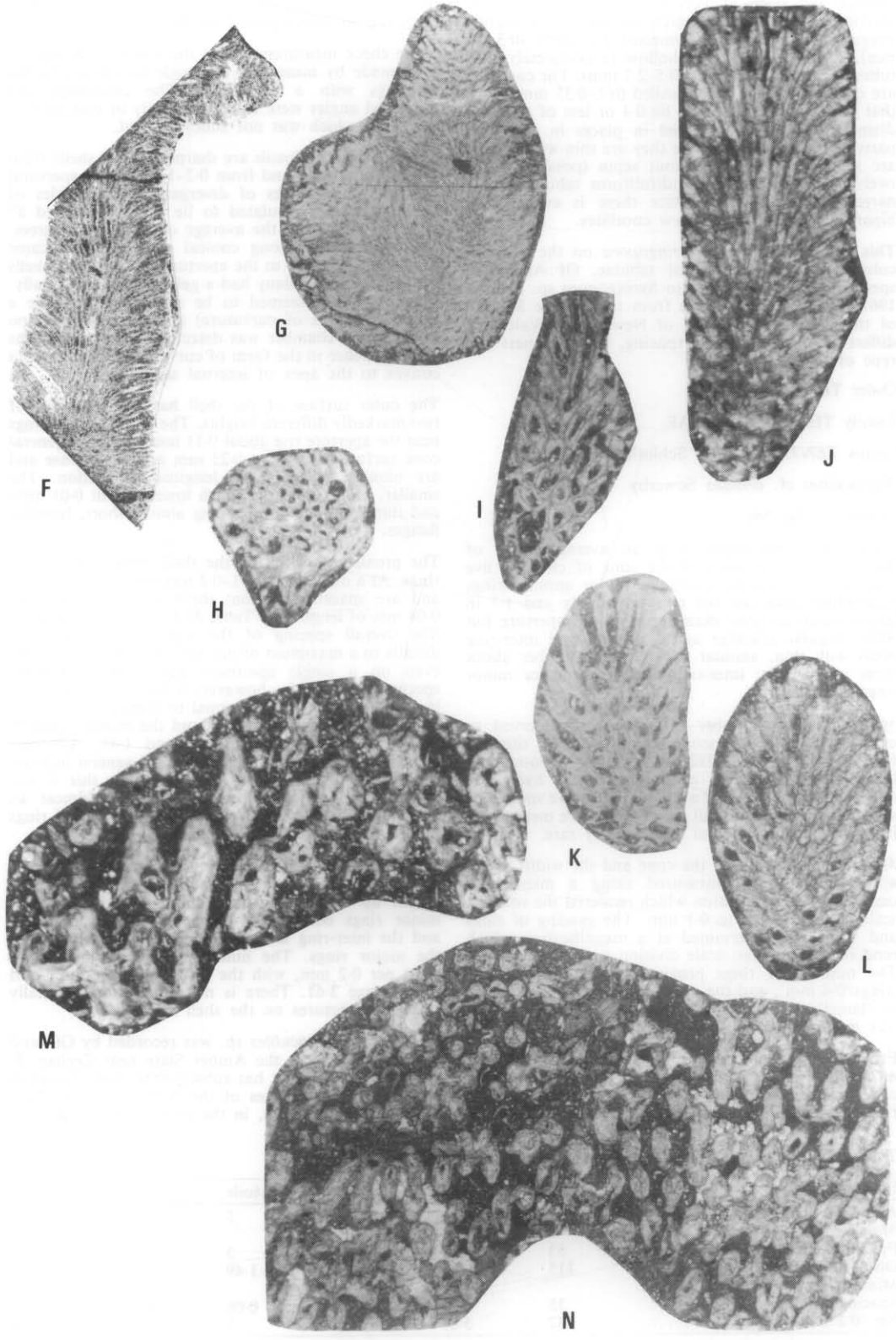
F
G
H
I
J
K
L
M
N
5 cm

contact and open at between 60° and 90° to the exterior. The corallites, which are gently but slightly irregularly curved, are connected by short (0·3–0·7 mm), stout (0·4–0·5 mm), hollow to completely-filled tubes at irregular intervals (0·5–2·7 mm). The corallites are characteristically thick-walled (0·1–0·35 mm), such that the central lumen may be 0·4 or less of the total diameter but are thin-walled in places in the inner parts of the colonies. Where they are thin-walled there are signs of very short, stout septa (possibly about twelve, C981-B7), of infundifuliform tabulae and a narrow syrinx. In one place there is evidence of bipartite fission to form new corallites.

This coral is placed in *Syringopora* on the basis of colony form and shape of tabulae. Of Australian species it is closest in size to *Syringopora* sp. (Strusz, 1961, plate 45, fig. 10–11) from the Middle Silurian of the Wellington District of New South Wales but differs from it in corallite spacing, wall thickness and type of septa.

Order TENTACULITIDA

Family TENTACULITIDAE

Genus *TENTACULITES* Schlotheim, 1820

Tentaculites cf. *ornatus* Sowerby

(Table 31, fig. 56)

Diagnosis: Tentaculites, with an average angle of divergence of the sides of the cone of close to five degrees, with bluntly triangular major annular rings numbering three per 0·4 mm proximally and 1·7 in length equal to cone diameter near the aperture but with irregular spacing; apical portion and inter-ring areas with thin, annular minor rings, number about three in 0·2 mm; inter-ring areas (except for minor rings) rectilinear.

Material: Large number of specimens preserved as external moulds of uncompressed cones in siltstone from locality 1 [CP729792]; the moulds are commonly lined with a powdery coating of ferric hydroxide minerals; of the material available, sixty-five specimens were measured but not all parameters were measurable in all specimens; internal moulds very rare.

Method: The length of the cone and the width at the apertural end were measured using a micrometer ocular, at a magnification which rendered the smallest scale division equal to 0·1 mm. The spacing of rings and striae was determined at a magnification which rendered the smallest scale division equal to 0·02 mm. The number of rings proximally was measured as 'rings/0·4 mm', and the number of inter-ring lamellae as 'lamellae/0·2 mm'. The spacing of rings distally was measured to the nearest 0·02 mm.

From the length and apertural diameter measurements, an average angle of divergence of the sides was calculated [$=2\ \tan^{-1}(AD/2L)$]. The ratio 'number of rings/apertural diameter' was calculated by dividing the apertural diameter by the distal ring spacings of rings (up to three) closest to the aperture.

Some check measurements of the angle of divergence were made by measuring the angle on camera lucida drawings with a protractor. The calculated and measured angles were close, especially in that part of the shells which was not subcylindrical.

Description: The fossils are sharply conical shells from 1·4–14·4 mm long and from 0·2–1·25 mm in apertural diameter. The angles of divergence of the sides of the cones were calculated to lie between 4° and 8° with the mode and the average close to five degrees. The shells had a long conical portion but became subcylindrical close to the aperture. Most of the shells were straight but many had a gentle curve proximally. The apex itself seemed to be sharp (i.e. to have a very low radius of curvature) and no differentiation of an initial chamber was detected. A few specimens show evidence in the form of curved ferruginous septa convex to the apex of internal septation.

The outer surface of the shell has annular rings of two markedly different heights. The larger, major rings near the aperture rise about 0·15 mm above the general cone surface, are about 0·25 mm across the base and are bluntly triangular in longitudinal section. The smaller, minor rings are much lower (about 0·01 mm) and thinner (0·005 mm), being almost short, lamellar flanges.

The proximal portion of the shell shows only minor rings. At a diameter of 0·1–0·2 mm major rings appear and are spaced such that there are about three in 0·04 mm of length (see Table 31 for statistical details). The overall spacing of the major ridges increases distally to a maximum of one millimetre but is variable even on a single specimen and broadly between specimens. There is, however, a fairly narrow range in the ratio 'rings/length equal to diameter', i.e. 0·58 to 4, with an average of 1·7 and the modal value of the ratio falling between 1·25 and 1·49. Although there is, on all specimens examined, a general increase in spacing of the higher rings distally, this is not regular and in some specimens there is almost an alternation between narrowly and widely-spaced rings proximally or distally.

The spaces between major rings are rectilinear except for the minor rings. The inter-ring areas range in length up to several times major ring length. The minor rings occupy the proximal part of the shell and the inter-ring areas with little impingment on to the major rings. The number ranges from 1·14 to eight per 0·2 mm, with the modal number three and the average 3·61. There is no sign of longitudinally oriented structures on the shell surface.

Comments: Tentaculites sp. was recorded by Gill and Banks (1950) from the Amber Slate near Zeehan. It was not described. It has subsequently been found in abundance in correlates of the Amber Slate at Trial Harbour, Queenstown, in the Princess River area on

Table 31. STATISTICS OF Tentaculites *cf.* ornatus *SOWERBY*

Parameter	Number	Average	Range	Mode	o	o^2
Angle of divergence	52	5·4	4–8	5	1·08	1·16
Major rings						
Proximal (no./0·4 mm)	53	3·5	1–10	3	1·68	2·81
Distal (no./shell diam.)	115	1·7	0·58–4	1·25–1·49	0·56	0·31
Minor rings						
Spacing (mm)	35	0·07	0·025–0·175	0·06	0·032	0·10
No./0·2 mm	37	3·61	1·14–8	3	1·73	3·01

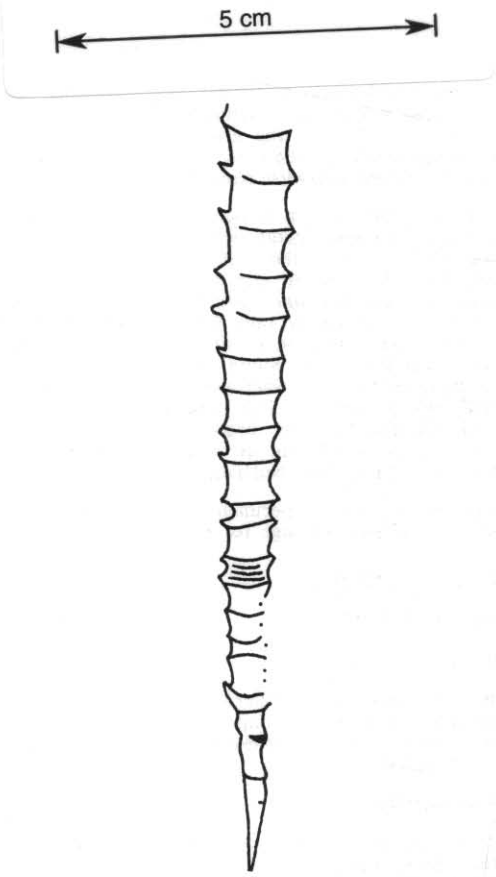

Figure 56. *Tentaculites* cf. *ornatus* Sowerby; *camera lucida drawing of external mould (×10) showing irregular spacing and longitudinal section of major rings, also minor rings; TDM H1 (iii). Correlate of Amber Formation, Huskisson Syncline.*

the Gordon River, and *Tentaculites* sp. has been noted in the Keel Quartzite, the Florence Quartzite, and the transitional unit at the base of the Bell Shale.

Clarke and Brown (Appendix 3) correlated the *Tentaculites*-bearing siltstone from the Huskisson Basin with the Amber Formation at Zeehan and deduced a Wenlockian age for siltstone from the Huskisson.

The closest species to the Huskisson *Tentaculites* recorded from other parts of Australia is *T. ornatus* Sowerby described by Sherrard (1967) from the Hume Limestone at Yass, N.S.W., subsequently placed as a member of the Silverdale Formation (Link, 1970) and assigned a Ludlovian age on conodont evidence.

The Tasmanian specimens are somewhat larger, have lower and narrower major rings, apparently a less regular ring spacing than the Yass specimens, but about the same number of rings in a length equivalent to the diameter. Detailed comparisons cannot be made because of lack of relevant information concerning the Yass material.

Tentaculites ornatus Sowerby from its type area in the Wenlock Limestone at Dudley was redescribed and figured by Lardeux (1969, p. 42–44, plate 14, fig. 103; text figures 25–26). The Tasmanian specimens are close to those figured by Lardeux in major ring section shape, in the overall arrangement of minor and major rings, including the occasional appearance of paired major rings, but the spacing of major rings in the Tasmanian material is much more variable. Lardeux did not quote the ratio of ring spacing to diameter in the apertural region. From his figures, the ratio would appear to be between 1·1 and 1·7. Also from his figures there appear to be between two and three minor rings per 0·2 mm proximally. In view of the few, probably minor, differences between the Tasmanian material and *T. ornatus* from Dudley, it is probably best for the time being to assign the Tasmanian material as *T.* cf. *ornatus* Sowerby. The Tasmanian collection is closer to *T. ornatus* Sowerby than it is to the material from Yass and closer than the Yass material is to *T. ornatus* from Dudley.

ECHINODERMATA

?CRINOIDEA

External moulds of a discoidal element have been reported to be present in the Crotty Quartzite by Gill (1950, p. 240; as "Crinoid Columnal 1") at Zeehan and are also known from the Calder Pass [DP108148] (Ward, 1909*b*), Trial Harbour (Waterhouse, 1916), and The Sand Hill, Queenstown.

The specimens from the Huskisson River area range from 12–29 mm in diameter (most common about 22 mm) and are up to six millimetres high. The elements range from about four to about eight times as wide as they are high. One side of the circular elements is almost flat, the other gently convex. The moulds contain a central column which decreases regularly in diameter from both external surfaces to an approximately central position, i.e. it appears to be almost biconical. The central column at its narrowest point has a diameter about one-fifth of that of the element but in small specimens may be as much as one-third. The external surface and that of the columns is smooth, whether due to an original condition or to smoothing by abrasion is not clear. It must be recalled in this connection that the enclosing sediment is of medium sand grade so that a fine original ornament may not have been preserved.

The only previous description of this form is by Gill (1950, p. 24). His specimen was 16 mm in diameter, four millimetres thick, and had a central canal described as being 'biconvex in outline' in longitudinal section, and 5·5 mm in diameter. The cross-section along a diameter was described as having a planate-oval outline.

These elements have been referred to as crinoid columnals (Gill, 1950) and this is still the preferred identification. However, it is not clear how they may have been stacked in a column, whether as a series of plates with flat surface up or a series with flat surface down, or a series with pairs of plates succeeding one another, each pair with plane surfaces apposed. Whatever the arrangement, there may have been regularly occurring points in the column with very small areas of apposition to one or both neighbours, a situation which would produce great flexibility but marked weakness. The biconical nature of the lumen in each element is also a puzzle.

Another possibility is that they are centro-dorsal plates of a stalked echinoderm but there is no evidence on either surface or around the margin as would be expected where the adjacent calical plates impinged. The great number of the one type of plate is also difficult to explain if they are centro-dorsals.

It has always been assumed that the impressions are those of calcitic elements. This is the most likely

explanation, particularly as limestone with large echinoderm elements occurs at about the same stratigraphic level elsewhere in Tasmania, e.g. Mt Bobs (Correy, 1983) and on the Gordon River. However, no such calcitic bodies have been found in the Crotty Quartzite.

Phylum HEMICHORDATA

Class GRAPTOLITHINA

Family CYRTOGRAPTIDAE

?CYRTOGRAPTUS sp.

Material: In thin section 'E' cut from limestone C981, there are seven fragments of brown material embedded in the limestone within an area of 36 mm². Four of these are aligned in a way that suggests original continuity.

Description: The main fragment, and the three other fragments which may have been originally continuous with it, are curved in a gentle sigmoid from a convexity of which arises a long uniformly curved branch. The sigmoidally curved segment is about 0·075 mm thick where it is continuous. One of the isolated fragments of this segment has two wedge-shaped extensions on the convex side, the wedges being 0·5 mm and 0·75 mm long and about 0·15 mm thick at the larger end. Both wedges widen in the same direction. The uniformly curved branch is about 4·5 mm long, more-or-less smooth on its concave side and with thirteen projections on its convex side. Most of the projections curve out and back towards the origin of the branch and terminate sharply (i.e. they are hook-shaped). The hook closest to the origin is about 0·5 mm long and the other hooks become progressively shorter away from the branch origin.

The three 'isolated' fragments include a distinctly U-shaped one and two others in close proximity.

Interpretation: The brown, translucent nature of the fragments suggests that they are composed of carbonaceous matter and the regularity in spacing and shaping of the 'hooks' suggests a biological origin.

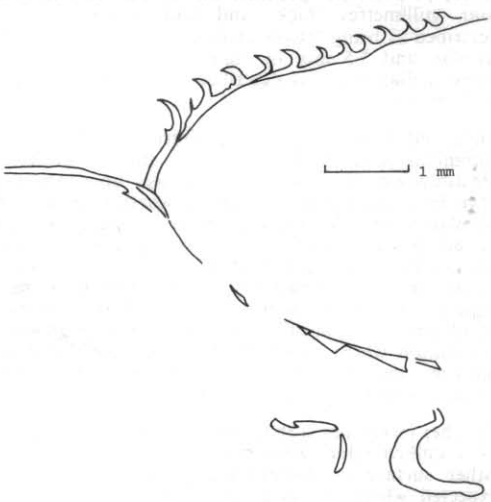

Figure 57. *?Cyrtograptus; camera lucida drawing of thin section, showing conical thecae on stipe and hooked thecae on cladia; C981 E; limestone in correlate of Amber Formation, Wenlockian; Huskisson Syncline.*

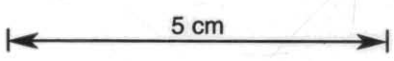

If a biological origin is correct, the fragments may be those of a hydroid, a ctenostome, or a graptolite. Of these possibilities, the graptolite origin is most likely, especially as there is a faint suggestion of regularly spaced transverse bands (?fusellar half rings).

If the graptolite origin is accepted, the most likely possibility is *Cyrtograptus*, with a thecal spacing of about 11·5/10 mm on the main stipe and about thirty-three hooked thecae/10 mm on the cladia. Another possibility is *Diversograptus* and insufficient is preserved to rule this possibility out. *Cyrtograptus* has been reported from Australia. *C.* aff. *insectus* Boucek has been noted from New South Wales by Stevens and Packham (1953), and Sherrard (1954) and Thomas (1960, p. 43, and fig. 200) figured a *Cyrtograptus* from Tasmania. The present specimen, if a *Cyrtograptus*, is different in thecal spacing from the forms previously described from Australia.

Implications: If this specimen is a *Cyrtograptus*, it implies a Wenlockian age for the limestone.

OTHER FOSSILS

ORDOVICIAN

Bryozoa

The specimens (C1130 Micro II) from close to the base of the Gordon Subgroup contain abundant ramose trepostomes and rare fenestrate bryozoa (probably cryptostomes).

Brachiopoda

These specimens also contain abundant small brachiopods including dalmanellids, strophomenids and rhynchonellids.

Gastropoda

Several species of gastropods are present but not abundant.

Rostroconcha

Rare specimens of a rostroconch occur.

Trilobita

The most abundant trilobite present is a species of *Pliomerina* similar to that in the Lords Siltstone and its correlates. It is common. Also present is a small species of *Bumastoides* similar to one in the Lower Limestone Member of the Benjamin Limestone.

SILURIAN

Bryozoa

A ramose trepostome is very abundant in available thin-sections of C981.

Cephalopoda

Nautiloids, identified by Dr B. A. Stait as *Geisonoceras* sp., are present.

SUMMARY

Specimens from near the base of the Gordon Subgroup in the Huskisson River area contain *Belodina compressa* (Branson and Mehl) indicative of a Middle–Late Ordovician age. From an horizon 160 m further up in the section, *Tasmanognathus careyi* Burrett has been obtained and indicates correlation with the Lower Limestone Member of the Benjamin Limestone. A

specimen from 160 m above the base contains trepostome and fenestrate bryozoa, brachiopods, gastropods, rostroconchs, trilobites such as *Pliomerina* and *Bumastoides*. The trilobites suggest correlation with the Lower Limestone Member or Lords Siltstone Member of the Benjamin Limestone. A sandstone above the Gordon Subgroup contains abundant, large echinoderm, probably crinoidal columnals characteristic of the uppermost member in the Crotty Quartzite at Zeehan.

A limestone in the Amber Formation contains rugosan corals close to *Tryplasma lonsdalei* Etheridge, and *Stereoxylodes* sp., tabulates *Syringopora* sp. close to a species from the Middle Silurian of New South Wales and ?*Pachypora*, as well as other fossils. The coral content is consistent with but not compulsive evidence for a Late Llandoverian or Wenlockian age.

A siltstone correlated with the Amber Formation contains *Tentaculites* cf. *ornatus* Sowerby which is consistent with a Wenlockian age.

Cyrtograptus sp. may be present in the limestone in the correlate of the Amber Formation. If the identification is correct, the limestone is Wenlockian.

Addendum

M. R. Banks

I should report for the record that the possible *Cyrtograptus* from the Huskisson Basin (see page 160) has been seen by Dr R. B. Rickards and others at the University of Cambridge, England. They do not regard it as *Cyrtograptus*, and they think it unlikely to be a graptolite but are unable to make any suggestions as to its biological affinities. I dissolved what little I had left of the enclosing limestone and detected no remains of graptolites in the residue.

APPENDIX 3

Fossil faunus in Eldon Group correlates within the Huskisson Syncline

M. J. Clarke
A. V. Brown

Abstract

Lists of the faunas present at five localities within shallow-water sequences of sandstone and mudstone formed during the Silurian Period are presented. Correlations with similar sequences elsewhere in Tasmania are suggested.

INTRODUCTION

Road cuttings along the Hydro-Electric Commission's Lower Pieman Dam road between the 40·5 km [CP729792] and 35·9 km [CP696785] marks give access to approximately 350 m of highly fossiliferous, interbedded laminated siltstone-mudstone, calcareous mudstone and friable and siliceous sandstone successions. These successions are correlates of the Eldon Group. Fossil collections were made from five localities.

LOCALITY 1–LPD 40·5 km [CP729792]

Leptostrophia sp. (parvicostellate form) very common

Rhynchonellid *?Ancillotoechia* sp. or *?Stegerhynchus* sp. very common

Cornulites sp. common

Tentaculites sp. very common

Smooth ostracods

Trilobite fragments

LOCALITY 2–LPD 38·5 km [CP714784]

?Ancillotoechia sp. or *Stegerhynchus* sp. very common

cf. *Delthyris* sp.

Leptostrophia sp. common

Nucleospira sp.

Encrinurus sp. very common

Trimerus (Trimerus) sp.

Tentaculites sp. very common

Smooth ostracods

Actinopteria sp.

cf. *Grammysia* sp.

Crinoid debris and fragments of colonies of favositids and heliolitids

LOCALITY 3–LPD 37·9 km [CP708783]

Atrypa sp. a very large species

?Ancillotoechia sp. or *Stegerhynchus* sp.

Leptostrophia sp. (a parvicostellate form) very common

Encrinurus sp.

Tentaculites sp. very common

Gillatia sp. and other ostracods

Michelinoceratids and loxonemids rare

LOCALITY 4–LPD 37·4 km [CP702784]

?Ancillotoechia sp. or *Stegerhynchus* sp. very common

Leptostrophia sp. very common

Tentaculites sp. very common

Actinopteria sp.

Loxonemids rare

LOCALITY 5–LPD 35·9 km [CP696785]

Rostricellula synchoneua (Gill)

Crinoid ossicles (very large, up to 30 mm in diameter)

CONCLUSIONS

The sequence of predominately siltstone and calcareous siltstone with subordinate sandstone (localities 1–4) which occupies the core of the syncline may be correlated with the Amber Formation of the Zeehan area. A Middle Silurian (Wenlockian) age is probable. *Gillatia* and *Atrypa* are unknown below the Late Llandoverian, and *Nucleospira, Trimerus, ?Ancillotoechia* or ?*Stegerhynchus* and *Delthyris* are unknown below the Wenlockian. These faunas are dissimilar to those from the proven Late Llandoverian faunas from the Richea Formation in the Tiger Range (Sheehan and Baillie, 1981) despite the overall similarity in facies. This further supports the younger age assignment.

The underlying sequence of sandstone and quartzite exposed in the Department of Main Roads quarry immediately west of the Huskisson River (locality 5) can be correlated both lithologically and faunally (abundant very large and coarsely-ribbed *Rostricellula*) with the Crotty Formation of the Zeehan area. An essentially Early Silurian (Llandoverian) age is probable.

In all probability, the facies change from sandstone to siltstone and shale (Crotty Formation to Amber Formation and Gell Formation to Richea Formation) is diachronous, occuring first in the Tiger Range and later in the Huskisson River area. This does not necessarily imply that sedimentation was laterally continuous between the two areas.

APPENDIX 4

Whole-rock major and trace element and electron microprobe analyses

LIST OF TABLES

PAGE

1. Whole-rock major and trace element analyses with CIPW and Rittman Norms for Tertiary Basalt samples 164
2. Chemical analyses and structural formulae of olivine, clinopyroxene and plagioclase from Tertiary basalt 166
3. Whole-rock major and trace element analyses of gabbro samples 168
4. Chemical analyses and structural formulae of clinopyroxene and plagioclase for group 1 and 3 gabbro samples 174
5. Chemical analyses and structural formulae of pyroxene and plagioclase for group 2 gabbro samples 176
6. Chemical analyses and structural formulae of pyroxene from Crimson Creek Formation tholeiite basalt samples 178

7*a*. Chemical analyses and structural formulae of chrome spinel from high-magnesian andesite samples 180

7*b*. Chemical analyses and structural formulae of amphibole replacement of high-magnesian andesite phenocrysts and groundmass 182

8. Whole-rock chemical analyses of basalt and greywacke samples from within the Crimson Creek Formation 183
9. Whole-rock chemical analyses of high-magnesian andesite samples 186
10. Whole-rock chemical analyses of samples of low-titanium basalt, Black Hill area 188
11. Whole-rock chemical analyses of samples of low-titanium basalt, Heazlewood River area 189
12. Whole-rock chemical analyses of Precambrian alkali basalt samples 190
13. Layer rhythms in LPD succession at Riley Knob 193
14. Whole-rock chemical analyses of dunite, metadunite and serpentinite samples from LDH and LPD successions 194
15. Whole-rock chemical analyses of pyroxenite samples from the LDH and LPD successions 196
16. Chemical analyses and structural formulae of olivine from the LDH succession 198
17. Chemical analyses and structural formulae of orthopyroxene from the LDH succession . 200
18. Chemical analyses and structural formulae of chrome spinel from the LDH succession . 201
19. Chemical analyses and structural formulae of olivine from metadunite samples from the LDH succession 204
20. Chemical analyses and structural formulae of chrome spinel from metadunite samples from the LDH succession 205
21. Chemical analyses and structural formulae of olivine from the LPD succession 207
22. Chemical analyses and structural formulae of orthopyroxene from the LPD succession . 208
23. Chemical analyses and structural formulae of clinopyroxene from the LPD succession .. 210
24. Chemical analyses and structural formulae of chrome spinel from the LPD succession . 212
25. Chemical analyses and structural formulae of pyroxene and amphibole from the LPG succession 214
26. Chemical analyses and structural formulae of chrome spinel from the LPG succession . 215
27. Whole-rock chemistry of amphibolite and amphibolitised pyroxenite samples 217
28. Chemical analyses and structural formulae for amphibole, pyroxene, and chrome spinel from amphibolite and amphibolitised pyroxenite samples 218
29. Mean nominal equilibration temperatures for olivine-spinel pairs using the geothermometers of Jackson, and Roeder *et al.* 220
30. Equilibration temperatures for coexisting OPX-CPX pairs for samples from the LPD and LPG successions using the geothermometers of Wood and Banno, and Wells 221

Table 1. WHOLE ROCK MAJOR AND TRACE ELEMENT ANALYSES WITH CIPW AND RITTMAN NORMS FOR TERTIARY BASALT SAMPLES

Plot No.	1	2	3	4	5	6	7	8
Reg. No.	85-0043	85-0044	85-0046	85-0047	78-440	85-0048	85-0049	85-0050
SiO_2	46.94	46.46	46.06	48.11	46.6	45.72	47.08	46.63
TiO_2	1.67	1.85	2.06	1.59	1.6	1.73	1.91	1.79
Al_2O_3	13.81	12.91	13.11	14.14	13.9	13.36	13.11	12.62
Fe_2O_3	2.88	1.89	2.07	1.97	1.2	1.09	1.65	3.05
FeO	8.52	9.59	9.49	9.20	10.5	10.21	8.87	7.84
MnO	0.20	0.17	0.16	0.14	0.17	0.16	0.16	0.15
MgO	8.46	10.74	10.53	9.21	9.8	7.47	10.84	8.86
CaO	8.50	8.75	8.63	7.69	8.9	9.07	8.41	9.04
Na_2O	2.80	2.40	2.32	2.93	2.8	2.96	2.44	2.49
K_2O	1.20	1.14	1.55	1.06	0.64	0.83	1.29	1.06
P_2O_5	0.35	0.46	0.43	0.34	0.38	0.38	0.44	0.38
CO_2	2.60	0.30	0.09	0.09)		5.32	0.21	1.05
H_2O^-	0.84	0.79	0.60	0.89)	2.91	0.23	0.78	1.17
H_2O^+	1.32	2.15	2.57	1.65)		1.11	2.36	3.03
Total	100.09	99.60	99.67	99.01	99.40	99.41	99.55	99.16
Cr	280	290	290	270	294	210	270	270
Ni	180	240	230	150	226	175	210	230
Zr	130	155	130	125	114	105	145	120
Y	20	19	21	21	18	19	20	19
Nb	17	27	27	14	11	13	29	25
Rb	24	28	22	22	8	13	26	25
Sr	370	460	580	320	312	420	470	470
Ba	160	240	230	140	210	180	220	280
V	175	200	190	160	198	140	160	155
Sc	21	17	19	17	n.d.	18	18	15
Co	65	48	54	44	69	46	49	42

Table 1. (continued)

Plot No.	1	2	3	4	5	6	7	8
Reg. No.	85-0043	85-0044	85-0046	85-0047	78-440	85-0048	85-0049	85-0050
CIPW norms								
Q	-	-	-	-	-	-	-	-
Or	7.09	6.74	9.16	6.27	3.78	4.91	7.62	6.27
Ab	23.69	20.31	19.63	24.79	23.69	25.04	20.64	21.07
An	21.57	21.09	20.78	22.30	23.47	20.72	21.01	20.13
Lc	-	-	-	-	-	-	-	-
Ne	-	-	-	-	-	-	-	-
Di	14.84	15.64	15.55	11.07	14.85	17.92	14.40	17.92
Hy	7.37	6.29	2.56	11.55	3.28	0.99	8.18	12.55
Cl	12.60	18.98	20.82	13.74	21.75	17.65	17.30	7.28
Mt	4.18	2.74	3.00	2.86	1.74	1.58	2.39	4.42
Il	3.17	3.51	3.91	3.02	3.04	3.29	3.63	3.34
Ap	0.83	1.09	1.01	0.80	0.90	0.90	1.04	0.90
Rittman norms								
Quartz	-	-	-	-	-	0.8	-	-
Sanidine	5.5	6.0	11.0	4.1	-	1.6	7.8	5.1
Anortho-clase	-	-	-	-	-	-	-	-
Plagio-clase	53.7	48.5	45.2	56.6	57.5	41.9	48.1	49.7
Nepheline	-	-	-	-	-	-	-	-
Leucite	-	-	-	-	-	-	-	-
Clinopy-roxene	24.9	26.2	22.5	24.6	23.5	-	26.5	32.8
Olivine	4.9	14.1	16.6	10.4	14.8	-	12.8	5.4
Orthopy-roxene	-	-	-	-	-	24.7	-	-
Magnetite	1.6	1.6	1.6	1.7	1.7	1.3	1.4	1.5
Ilmenite	1.9	1.8	2.0	1.7	1.6	13.5	1.9	1.8
Apatite	0.8	1.0	1.0	0.8	0.9	0.8	1.0	0.9
Cord-ierite	-	-	-	-	-	15.4	-	-
Calcite	6.6	0.8	0.2	0.2		13.5	0.6	2.8

Analyses by Department of Mines Analytical Laboratory - Analysts J. Furst, M. Frith, M. Pickering and R. Roby

Table 2. CHEMICAL ANALYSES (OXIDE WEIGHT %) AND STRUCTURAL FORMULAE OF OLIVINE (O=4), CLINOPYROXENE (O=6) AND PLAGIOCLASE (O=8) FROM TERTIARY BASALT SAMPLES

Plot No.	1	2	3	4	5	6	7	8	9
Reg. No.	85-0044	85-0045	85-0043	85-0043	85-0045	85-0046	85-0047	85-0044	85-0045
Mineral	olivine-skeletal	olivine-skeletal	olivine-phenocryst	olivine-phenocryst	olivine-phenocryst	olivine-phenocryst	olivine-phenocryst	olivine-groundmass	olivine-groundmass
SiO_2	39.39	40.55	38.56	38.12	38.01	38.57	38.49	37.15	37.37
TiO_2									
Al_2O_3									
Cr_2O_3									
FeO	14.70	10.08	18.56	20.12	21.18	18.13	18.86	25.29	23.69
MnO									
MgO	45.78	49.10	42.88	41.04	40.15	42.96	42.33	37.16	38.39
CaO			0.16	0.23	0.29	0.22	0.13	0.30	0.24
Na_2O									
K_2O									
Total	99.87	99.73	100.16	99.73	99.63	99.88	99.81	99.90	99.69
Si	0.9891	0.9969	0.9842	0.9871	0.9880	0.9854	0.9871	0.9831	0.9833
Ti									
Al									
Cr									
Fe	0.3087	0.2072	0.3962	0.4357	0.4604	0.3874	0.4045	0.5597	0.5213
Mn									
Mg	1.7132	1.7990	1.6311	1.5838	1.5554	1.6358	1.6178	1.4656	1.5054
Ca			0.0044	0.0064	0.0081	0.0060	0.0036	0.0085	0.0068
Na									
K									
Total	3.0109	3.0031	3.0158	3.0129	3.0120	3.0146	3.0129	3.0169	3.0167
Mg*	84.7	89.7	80.5	78.4	77.2	80.9	80.0	72.4	74.3

Table 2. (continued)

Plot No.	10	11	12	13	14		15	16	17
Reg. No.	85-0046	85-0047	85-0045	85-0046	85-0047		85-0043	85-0046	85-0047
Mineral	olivine-groundmass	olivine-groundmass	clinopyroxene	clinopyroxene	clinopyroxene		plagioclase	plagioclase	plagioclase
SiO_2	36.26	35.97	48.08	47.02	50.94		53.74	51.93	53.93
TiO_2			2.27	2.92	1.41		-	-	-
Al_2O_3			4.85	5.45	1.98		28.75	29.58	28.26
Cr_2O_3			0.48	0.25			-	-	-
FeO	29.01	29.88	8.65	8.84	10.89		0.62	0.85	1.02
MnO	0.34	0.27	-	-	-		-	-	-
MgO	33.77	33.31	13.10	12.45	13.84		0.24	0.78	0.52
CaO	0.41	0.23	21.81	22.33	20.45		12.18	12.76	11.38
Na_2O			0.39	0.35	0.36		4.12	3.42	4.24
K_2O							0.48	0.34	0.40
Total	99.79	99.66	99.63	99.61	99.87		100.13	99.66	99.75
Si	0.9811	0.9785	1.8118	1.7790	1.9163		2.4351	2.3706	2.4511
Ti			0.0643	0.0831	0.0399		-		
Al			0.2155	0.2431	0.0878		1.5359	1.5919	1.5142
Cr			0.0143	0.0075	-		-	-	-
Fe	0.6564	0.6798	0.2726	0.2797	0.3427		0.0235	0.0325	0.0388
Mn	0.0078	0.0062	0.7357	0.7020			-	-	-
Mg	1.3617	1.3504	0.8806	0.9053	0.7759		0.0162	0.0531	0.0352
Ca	0.0119	0.0067	0.0285	0.0257	0.8243		0.5914	0.6241	0.5542
Na					0.0263		0.3620	0.3027	0.3736
K							0.0277	0.0198	0.0232
Total	3.0189	3.0215	4.0233	4.0254	4.0131		4.9918	4.9947	4.9903
Mg*	67.5	66.5	73.0	71.5	69.4				
Ca			46.6	48.0	42.4	Ca	60.3	65.9	58.3
Mg			38.9	37.2	39.9	Na	36.9	32.0	39.3
Fe			14.4	14.8	17.6	K	2.8	2.1	2.4

Table 3. WHOLE ROCK MAJOR AND TRACE ELEMENT ANALYSES OF GABBRO SAMPLES. ANALYSES 1-12 GROUP 1 GABBRO, 13-23 GROUP 2 GABBRO, 24-35 GROUP 3 GABBRO

Plot No.	1	2	3	4	5	6	7
Reg. No.	85-0091	85-0092	85-0093	85-0094	85-0095	85-0096	85-0097
SiO_2	49.50	45.80	42.80	48.30	47.80	49.30	45.50
TiO_2	0.28	0.70	1.80	0.86	0.40	0.86	0.75
Al_2O_3	13.80	16.20	16.30	15.00	16.00	14.40	14.83
Fe_2O_3	1.60	2.90	3.00	2.50	1.70	1.20	7.64
FeO	7.70	8.00	9.90	7.90	5.40	10.10	14.10
MnO	0.22	0.18	0.16	0.21	0.18	0.19	0.38
MgO	9.50	7.70	7.40	7.10	9.30	7.20	6.46
CaO	11.00	10.20	11.20	10.30	10.20	10.70	0.06
Na_2O	1.20	1.60	1.50	2.30	1.60	1.80	0.03
K_2O	0.92	1.20	0.90	0.57	2.10	1.20	0.46
P_2O_5	0.03	0.07	0.08	0.08	0.03	0.07	0.04
CO_2	0.13	0.15	0.25	0.30	0.02	0.12	0.31
H_2O^+	2.90	4.40	4.10	4.00	4.10	2.50	8.21
H_2O^-	0.31	0.65	0.69	0.47	0.54	0.38	0.85
Total	99.09	99.75	100.08	99.89	99.43	100.02	99.62
Cr	719	384	337	182	1050	143	143
Ni	162	99	88	97	196	70	84
Zr	7	33	43	40	15	39	20
Y	10	36	19	15	15	28	27
Nb	<4	<4	<4	5	<4	4	<4
Rb	175	36	25	18	83	52	85
Sr	122	245	226	190	305	332	4
Ba	-	-	-	-	-	-	157
V	-	-	-	-	-	-	-
Sc	-	-	-	-	-	-	-
Co	-	-	-	-	-	-	49

Analyses by Department of Mines Analytical Laboratory -
Analysts J. Furst, M. Frith, M. Pickering and R. Roby.

Table 3. (continued)

Plot No.	8	9	10	11	12	13	14
Reg. No.	85-0098	85-0099	85-0100	85-0101	85-0102	85-0103	85-0104
SiO_2	47.02	48.49	49.80	48.62	47.90	46.77	50.10
TiO_2	0.46	2.07	1.63	0.90	0.87	0.02	0.07
Al_2O_3	17.07	21.03	16.06	14.64	14.90	16.96	12.20
Fe_2O_3	1.87	0.61	4.17	1.90	1.92	1.10	1.40
FeO	6.20	1.33	6.04	8.39	8.55	5.89	6.70
MnO	0.16	0.14	0.17	0.20	0.20	0.14	0.22
MgO	8.59	4.21	4.61	8.20	8.51	9.74	14.70
CaO	11.15	13.76	9.55	9.44	10.52	13.75	7.60
Na_2O	1.73	3.22	4.45	2.46	1.79	0.79	0.90
K_2O	1.10	0.89	0.09	0.78	1.01	0.54	0.45
P_2O_5	0.07	0.35	0.20	0.11	0.10	0.04	0.02
CO_2	0.16	0.16	0.22	0.33	0.19	0.18	0.16
H_2O^+	3.51	3.92	2.50	3.32	3.33	3.02	4.90
H_2O^-	0.30	0.24	0.45	0.50	0.31	0.19	0.62
Total	99.39	100.42	99.94	100.33	99.39	99.13	100.04
Cr	675	25	86	395	459	534	1540
Ni	166	107	63	131	139	181	334
Zr	23	15	112	44	42	<4	<4
Y	15	9	38	16	13	<4	<4
Nb	<4	5	5	5	<4	<4	<4
Rb	51	26	<4	27	34	153	71
Sr	163	299	94	206	204	99	103
Ba	269	568	174	640	664	-	-
V	-	-	-	-	-	-	-
Sc	-	-	-	-	-	-	-
Co	45	20	34	51	49	-	-

Table 3. (continued)

Plot No.	15	16	17	18	19	20	21
Reg. No.	85-0105	85-0106	85-0107	85-0108	85-0109	85-0110	85-0111
SiO_2	48.67	46.77	48.09	47.92	47.32	48.89	48.50
TiO_2	0.05	0.02	0.04	0.15	0.11	0.11	0.08
Al_2O_3	17.16	16.96	13.35	15.11	15.24	15.10	17.47
Fe_2O_3	1.20	1.10	1.81	2.03	0.88	1.01	1.08
FeO	4.14	5.89	8.14	5.22	5.06	6.43	4.98
MnO	0.12	0.14	0.20	0.18	0.24	0.20	0.18
MgO	9.80	9.74	12.42	11.28	10.68	10.48	9.57
CaO	11.31	13.75	11.68	10.20	15.86	13.70	13.27
Na_2O	1.80	0.79	0.70	2.17	0.72	0.84	1.31
K_2O	0.93	0.54	0.11	0.72	0.58	0.44	0.42
P_2O_5	0.04	0.04	0.14	0.12	0.02	0.02	0.03
CO_2	0.22	0.18	0.00	0.00	0.12	0.12	0.10
H_2O^+	3.57	3.02	2.89	4.17	2.27	2.53	2.79
H_2O^-	0.26	0.19	0.00	0.00	0.13	0.14	0.14
Total	99.47	99.13	99.57	99.27	99.23	100.01	99.92
Cr	432	534	670	430	650	400	170
Ni	130	181	165	570	170	165	155
Zr	11	<4	<2	6	<2	<2	<2
Y	<4	<4	4	8	3	2	2
Nb	<4	<4	<3	<3	<3	<3	<3
Rb	56	153	10	55	200	120	115
Sr	521	99	180	280	85	105	270
Ba	267	-	22	145	24	51	115
V	-	-	130	160	120	140	105
Sc	-	-	44	52	52	49	40
Co	-	-	51	35	35	44	34

Table 3. (continued)

Plot No.	22	23	24	25	26	27	28
Reg. No.	85-0112	85-0113	85-0114	85-0115	85-0116	85-0117	85-0118
SiO_2	48.21	48.52	48.30	42.90	48.90	47.90	50.78
TiO_2	0.11	0.08	0.08	0.05	0.60	0.47	0.20
Al_2O_3	15.82	16.99	13.10	15.10	15.70	10.30	12.12
Fe_2O_3	1.09	0.68	0.95	3.90	0.67	1.50	0.57
FeO	6.08	4.92	5.60	1.40	8.70	7.80	4.75
MnO	0.18	0.12	0.13	0.21	0.22	0.18	0.40
MgO	11.26	11.02	11.50	7.40	8.40	13.30	12.24
CaO	13.02	14.19	17.00	27.50	10.10	13.30	10.96
Na_2O	0.98	0.92	0.43	0.16	1.30	1.30	0.15
K_2O	0.13	0.39	0.05	0.08	1.30	0.44	2.80
P_2O_5	0.03	0.05	0.01	0.05	0.06	0.05	0.11
CO_2	0.16	0.07	0.15	0.27	0.18	0.13	0.20
H_2O^+	2.59	1.66	1.70	1.00	2.50	2.50	3.89
H_2O^-	0.14	0.08	0.16	0.15	0.27	0.38	0.30
Total	100.52	99.69	99.16	100.17	98.60	99.55	99.47
Cr	600	320	718	341	538	1250	447
Ni	150	165	261	135	201	293	286
Zr	4	2	<4	28	21	20	111
Y	2	2	4	21	<4	10	15
Nb	<3	<3	<4	<4	<4	<4	<4
Rb	34	32	<4	55	5	15	258
Sr	160	51	24	214	79	232	48
Ba	59	85	-	-	-	-	227
V	100	95	-	-	-	-	-
Sc	38	40	-	-	-	-	-
Co	42	36	-	-	-	-	39

Table 3. (continued)

Plot No.	29	30	31	32	33	34	35
Reg. No.	85-0119	85-0120	85-0121	85-0122	85-0123	85-0124	85-0125
SiO_2	46.45	45.47	48.33	51.36	47.72	50.79	56.43
TiO_2	0.14	0.13	0.99	1.85	0.42	1.53	1.54
Al_2O_3	11.74	9.81	16.73	12.56	18.80	14.24	17.39
Fe_2O_3	1.53	1.43	2.60	3.00	2.07	5.24	2.90
FeO	6.58	6.88	8.02	9.24	4.53	8.65	7.97
MnO	0.83	1.66	0.25	0.35	0.10	0.25	0.14
MgO	12.26	14.10	7.98	6.77	6.42	4.85	3.89
CaO	15.65	15.59	4.43	5.60	11.01	5.76	1.17
Na_2O	0.31	0.32	1.76	2.79	2.20	3.39	4.00
K_2O	0.06	0.03	1.42	0.62	2.02	1.25	0.36
P_2O_5	0.10	0.10	0.08	0.16	0.07	0.20	0.17
CO_2	0.30	0.26	0.35	0.32	0.06	0.13	0.08
H_2O^+	3.95	4.02	5.06	3.30	3.72	2.75	4.09
H_2O^-	0.40	0.51	0.47	0.63	0.08	0.16	0.32
Total	100.30	100.31	98.47	98.55	99.22	99.19	100.45
Cr	626	698	371	292	330	270	340
Ni	111	100	117	80	185	280	220
Zr	13	5	48	107	30	105	89
Y	<4	<4	16	35	13	35	48
Nb	<4	<4	<4	7	<3	<3	<3
Rb	<4	<4	48	27	64	34	17
Sr	27	13	145	106	320	290	220
Ba	49	33	529	653	560	590	185
V	-	-	-	-	145	380	200
Sc	-	-	-	-	27	29	28
Co	57	65	42	41	31	33	32

Table 4. CHEMICAL ANALYSES (OXIDE WEIGHT %) AND STRUCTURAL FORMULAE OF CLINOPYROXENE (O=6) AND PLAGIOCLASE (O=8) FROM GROUP 1 AND GROUP 3 GABBRO SAMPLES

	Group 1			Group 3		
Plot No.	1	2	3	4	5	6
Reg. No.	85-0098	85-0101	85-0102	85-0121	85-0123	85-0124
	CPX	CPX	CPX	CPX	CPX	CPX
SiO_2	53.09	52.86	52.52	52.19	52.40	49.23
TiO_2	0.34	0.28	0.23	0.20	0.28	0.86
Al_2O_3	2.04	2.38	2.83	2.69	2.64	4.32
Cr_2O_3	0.31	0.44	0.59	0.50	0.33	0.21
FeO	7.52	7.51	5.90	6.09	5.51	11.77
MnO	0.24	0.28	-	-	-	0.25
MgO	16.52	16.85	17.26	17.49	16.57	13.90
CaO	20.08	19.66	20.24	20.18	22.03	19.07
Na_2O	-	-	-	-	-	0.27
K_2O	-	-	-	-	-	-
Total	100.14	100.26	99.57	99.34	99.76	99.88
Si	1.9507	1.9390	1.9281	1.9233	1.9266	1.8565
Ti	0.0094	0.0077	0.0064	0.0055	0.0077	0.0244
Al	0.0884	0.1029	0.1225	0.1169	0.1144	0.1921
Cr	0.0090	0.0128	0.0171	0.0146	0.0096	0.0063
Fe	0.2311	0.2304	0.1811	0.1877	0.1694	0.3712
Mn	0.0075	0.0087	-	-	-	0.0080
Mg	0.9046	0.9212	0.9443	0.9606	0.9080	0.7812
Ca	0.7906	0.7727	0.7962	0.7969	0.8679	0.7706
Na	-	-	-	-	-	0.0197
K	-	-	-	-	-	-
Total	3.9912	3.9954	3.9957	4.0054	4.0036	4.0299
Mg*	79.7	80.0	83.9	83.7	84.3	67.8
Ca	41.0	40.2	41.4	41.0	44.6	40.1
Mg	47.0	47.9	49.1	49.4	46.7	40.6
Fe	12.0	12.0	9.4	9.6	8.7	19.3

Table 4. (continued)

	Group 3		Group 1	
Plot No.	7	8	9	10
Reg. No.	85-0118	85-0118	85-0101	85-0102
	Amphibole	Amphibole	Plagioclase	Plagioclase
SiO_2	53.51	57.15	52.62	57.01
TiO_2	0.83	-	-	-
Al_2O_3	3.18	0.61	28.14	24.81
Cr_2O_3	0.19	-	-	-
FeO	7.63	11.71	3.36	2.05
MnO	0.47	0.43	-	-
MgO	20.21	24.81	1.30	1.36
CaO	10.51	2.47	7.25	7.05
Na_2O	-		3.32	5.58
K_2O	-		3.03	1.34
Total	96.53	97.18	99.01	99.20
Si	7.5841	7.9587	2.4380	2.5994
Ti	0.0885	-	-	-
Al	0.5314	0.1001	1.5371	1.3336
Cr	0.0213	-	-	-
Fe	0.9044	1.3638	0.1302	0.0782
Mn	0.0564	0.0507	-	-
Mg	4.2689	5.1492	0.0898	0.0924
Ca	1.5961	0.3686	0.3599	0.3444
Na			0.2983	0.4933
K			0.1785	0.0779
Total	15.0511	14.9912	5.0318	5.0194
Mg*	82.5	79.1		
Ca	23.6	5.4	Ca 43.0	37.6
Mg	63.1	78.8	Na 35.6	53.9
Fe	13.4	19.8	K 21.3	8.5

Table 5. CHEMICAL ANALYSES (OXIDE WEIGHT %) AND STRUCTURAL FORMULAE OF PYROXENE (O=6) AND PLAGIOCLASE (O=8) FROM GROUP 2 GABBRO

Plot No.	1	2	3	4	5	6
Reg. No.	85-0107	85-0126	85-0127	85-0107	85-0126	85-0127
	Low Ca Pyroxene			High Ca Pyroxene		
SiO_2	53.39	52.98	52.76	52.87	52.84	52.76
TiO_2	-	-	-	-	-	-
Al_2O_3	1.13	0.90	1.20	0.68	1.19	1.09
Cr_2O_3	0.14	-	-	0.25	-	0.26
FeO	19.35	18.54	19.55	8.36	7.68	7.44
MnO	0.28	0.31	0.30	0.18	-	-
MgO	23.40	24.92	24.53	14.49	15.66	15.36
CaO	2.38	1.80	1.79	22.60	22.32	22.74
Na_2O	-	-	-	-	-	
K_2O	-	-	-	-	-	
Total	100.07	99.45	100.13	99.43	99.69	99.65
Si	1.9678	1.9575	1.9454	1.9802	1.9636	1.9633
Ti	-	-	-	-	-	-
Al	0.0491	0.0392	0.0522	0.0300	0.0521	0.0478
Cr	0.0041	-	-	0.0074	-	0.0076
Fe	0.5965	0.5729	0.6029	0.2619	0.2387	0.2315
Mn	0.0087	0.0097	0.0094	0.0057	-	-
Mg	1.2854	1.3722	1.3480	0.8088	0.8673	0.8519
Ca	0.0940	0.0713	0.0707	0.9070	0.8887	0.9067
Na	-	-	-	-	-	-
K	-	-	-	-	-	-
Total	4.0056	4.0229	4.0285	4.0011	4.0104	4.0089
Mg*	68.3	70.5	69.1	75.5	78.4	78.6
Ca	4.8	3.5	3.5	45.9	44.6	45.6
Mg	65.1	68.1	66.7	40.9	43.5	42.8
Fe	30.2	28.4	29.8	13.2	12.0	11.6

Table 5. (continued)

Plot No.	7	8	9
Reg. No.	85-0107	85-0126	85-0127
		Plagioclase	
SiO_2	44.71	44.25	46.91
TiO_2	-	-	-
Al_2O_3	33.62	32.08	33.76
Cr_2O_3	-	-	-
FeO	1.02	1.67	0.41
MnO	-	-	-
MgO	0.19	-	-
CaO	19.37	19.90	17.31
Na_2O	0.93	1.45	1.44
K_2O	0.09	0.28	-
Total	99.93	99.63	99.83
Si	2.0829	2.0881	2.1592
Ti	1.84	-	-
Al	1.8465	1.7847	1.8319
Cr	-	-	-
Fe	0.0397	0.0659	0.0158
Mn	-	-	-
Mg	0.0132	-	-
Ca	0.9669	1.0062	0.8537
Na	0.0840	0.1327	0.1285
K	0.0053	0.0169	-
Total	5.0368	5.0944	4.9891
Ca	91.5	87.1	86.9
Na	8.0	11.5	13.1
K	0.5	1.5	0.0

Table 6. CHEMICAL ANALYSES (OXIDE WEIGHT %) AND STRUCTURAL FORMULAE OF PYROXENE (O=6) FROM THE CRIMSON CREEK FORMATION THOLEIITE BASALTS

Plot No.	1	2	3	4	5	6
Reg. No.	85-0001	85-0004	85-0005	85-0007	85-0008	85-0009
SiO_2	51.32	51.52	51.57	53.81	50.56	51.04
TiO_2	0.55	0.47	0.52	0.29	0.55	0.72
Al_2O_3	2.71	2.67	3.09	1.12	1.31	1.60
Cr_2O_3	0.26	0.37	0.32	0.42	0.26	-
FeO	10.74	10.01	10.35	4.33	14.65	16.18
MnO	0.25	0.19	0.17	0.35	0.33	0.56
MgO	15.95	16.32	16.12	16.46	11.10	11.26
CaO	18.17	18.49	17.70	23.16	21.31	18.60
Na_2O	-	-	-	0.26	-	-
Total	99.95	100.04	99.84	100.20	100.07	99.96
Si	1.9125	1.9132	1.9153	1.9680	1.9386	1.9542
Ti	0.0154	0.0131	0.0145	0.0080	0.0159	0.0207
Al	0.1191	0.1169	0.1353	0.0483	0.0592	0.0722
Cr	0.0077	0.0109	0.0094	0.0121	0.0079	-
Fe	0.3347	0.3109	0.3215	0.1324	0.4698	0.5181
Mn	0.0079	0.0060	0.0053	0.0108	0.0107	0.0182
Mg	0.8859	0.9032	0.8922	0.8972	0.6343	0.6425
Ca	0.7256	0.7357	0.7044	0.9076	0.8755	0.7631
Na_2O	-	-	-	0.0184	-	-
Total	4.0087	4.0098	3.9979	4.0030	4.0119	3.9890
Mg*	72.6	74.4	73.5	87.1	57.5	55.4
Ca	37.3	37.7	36.7	46.9	44.2	39.7
Mg	45.5	46.3	46.5	46.3	32.0	33.4
Fe	17.2	15.9	16.8	6.8	23.7	26.9

Table 6. (continued)

Plot No.	7	8	9	10
Reg. No.	85-0011	85-0012	85-0013	85-0051
SiO_2	51.84	51.32	52.06	51.48
TiO_2	0.38	0.45	0.38	0.72
Al_2O_3	3.08	3.62	2.89	3.25
Cr_2O_3	1.00	0.86	0.54	-
FeO	6.05	6.74	6.20	7.96
MnO	-	-	-	-
MgO	16.51	16.27	16.75	16.28
CaO	21.13	20.65	20.99	19.94
Na_2O				
Total	99.99	99.91	99.81	99.63
Si	1.9060	1.8920	1.9154	1.9058
Ti	0.0105	0.0125	0.0105	0.0200
Al	0.1335	0.1573	0.1254	0.1418
Cr	0.0291	0.0251	0.0157	-
Fe	0.1860	0.2078	0.1908	0.2464
Mn	-	-	-	-
Mg	0.9047	0.8939	0.9184	0.8982
Ca	0.8324	0.8157	0.8275	0.7910
Na_2O	-	-	-	-
Total	4.0022	4.0043	4.0036	4.0033
Mg*	82.9	81.1	82.8	78.5
Ca	43.3	42.5	42.7	40.9
Mg	47.0	46.6	47.4	46.4
Fe	9.7	10.8	9.9	12.7

Table 7a. CHEMICAL ANALYSES (OXIDE WEIGHT %) AND STRUCTURAL FORMULAE OF CHROME SPINEL (O=32) FROM HIGH-MAGNESIAN ANDESITE SAMPLES

Plot No.	1	2	3	4	5	6	7	8	9	10	11	12
Reg. No.	85-0085	85-0086	85-0087	85-0088	85-0089	85-0026	85-0027	85-0028	85-0023	85-0028	85-0029	85-0030
TiO_2	0.22	0.25	-	0.21	0.25	-	-	-	-	0.22	-	0.25
Al_2O_3	4.86	3.66	3.48	5.00	4.30	3.48	3.72	4.26	7.00	6.80	5.98	6.89
Cr_2O_3	63.39	64.28	66.74	63.14	63.83	66.11	64.62	64.77	61.10	59.20	63.19	58.96
FeO	16.34	17.40	13.90	16.70	18.50	15.58	16.72	16.61	19.69	19.48	17.20	18.98
MnO	0.42	0.48	0.36	0.38	0.38	0.38	0.46	0.39	-	0.43	-	0.44
MgO	14.48	13.23	15.24	14.38	12.45	14.16	13.76	13.56	11.80	13.76	13.08	14.04
CaO	0.24	0.34	0.31	0.32	0.30	-	-	-	-	-	-	-
NiO	-	-	-	-	-	-	-	-	-	-	-	-
Total	99.95	99.64	100.03	100.13	100.01	99.71	99.28	99.59	99.59	99.89	99.45	99.56
Ti	0.0432	0.0499	-	0.0412	0.0499	-	-	-	-	0.0431	-	0.0490
Al	1.4968	1.1461	1.0721	1.5372	1.3460	1.0842	1.1650	1.3296	2.1859	2.0880	1.8617	2.1169
Cr	13.0920	13.4972	13.7880	13.0172	13.3985	13.8109	13.5699	13.5555	12.7943	12.1896	13.1919	12.1472
Fe^{+3}	1.3680	1.3068	1.1398	1.4044	1.2056	1.1049	1.2652	1.1149	1.0198	1.6793	0.9464	1.6869
Fe^{+2}	2.2022	2.5583	1.8981	2.2378	2.9026	2.3383	2.4492	2.5626	3.3419	2.5640	2.8523	2.4499
Mn	0.0929	0.1080	0.0797	0.0839	0.0855	0.0851	0.1035	0.0875	-	0.0949	-	0.0971
Mg	5.6377	5.2369	5.9354	5.5888	4.9266	5.5766	5.4473	5.3500	4.6581	5.3412	5.1477	5.4530
Ca	0.0672	0.0968	0.0868	0.0894	0.0854	-	-	-	-	-	-	-
Ni	-	-	-	-	-	-	-	-	-	-	-	-
Mg^+	71.9	67.2	75.8	71.4	62.9	70.5	69.0	67.6	58.2	67.6	64.3	69.0
Cr*	89.7	92.2	92.8	89.4	90.9	92.7	92.1	91.1	85.4	85.4	87.6	85.2

Table 7a. (continued)

Plot No.	13	14	15	16	17	18	19	20	21	22	23
Reg. No.	85-0055	85-0056	85-0090	85-0057	85-0058	85-0061	85-0063	85-0064	85-0075	85-0076	85-0077
TiO_2	-	-	-	-	-	0.48	-	-	-	0.28	0.24
Al_2O_3	6.67	7.52	9.95	4.39	5.23	7.54	6.04	6.13	6.87	10.99	13.66
Cr_2O_3	61.36	60.96	43.05	57.78	59.07	41.13	58.81	59.23	55.05	36.58	38.84
FeO	20.12	17.62	43.67	33.42	32.32	49.03	30.72	29.21	35.89	45.87	41.68
MnO	-	-	2.13	0.70	-	0.65	-	0.52	0.69	-	0.48
MgO	11.23	13.08	0.52	3.22	2.80	1.44	3.81	4.47	1.14	5.38	6.46
CaO	-	-	-	-	-	-	-	-	-	-	-
NiO	-	-	-	-	-	-	-	-	-	-	-
Total	99.38	99.18	99.32	99.51	99.42	100.27	99.38	99.56	99.64	99.10	99.36
Ti	-	-	-	-	-	0.1014	-	-	-	0.0571	0.480
Al	2.0984	2.3308	3.3174	1.4753	1.7603	2.4961	2.0110	2.0266	2.3163	3.5150	4.2801
Cr	12.9449	12.6700	9.6247	13.0206	13.3317	9.1306	13.1299	13.1310	12.4464	7.8453	7.7405
Fe^{+3}	0.9567	0.9992	3.0580	1.5041	0.9080	4.2718	0.8592	0.8423	1.2373	4.5826	3.9314
Fe^{+2}	3.5337	2.8750	7.2706	6.4631	6.8087	7.2428	6.3964	6.0083	7.3470	5.8248	5.3332
Mn	-	-	0.5102	0.1690	-	0.1546	-	0.1235	0.1672	-	0.1081
Mg	4.4663	5.1250	0.2192	1.3679	1.1913	0.6026	1.6036	1.8682	0.4859	2.1752	2.5588
Ca	-	-	-	-	-	-	-	-	-	-	-
Ni	-	-	-	-	-	-	-	-	-	-	-
Mg^+	55.8	64.1	2.9	17.5	14.9	7.7	20.0	23.7	6.2	27.2	32.4
Cr*	86.1	84.5	74.4	89.8	88.3	78.5	86.7	86.6	84.3	69.1	64.4

Total iron reported as FeO. Structural formulae calculated assuming the general formula $R^{2+}R^{3+}O_4$ and apportioning total iron as Fe^{2+} and Fe^{3+} so that $2(Mg+Mn+Ca+Fe^{2+})=(Cr+Al+Ti+Fe^{3+})$.

Table 7b. CHEMICAL ANALYSES (OXIDE WEIGHT %) AND STRUCTURAL FORMULAE OF AMPHIBOLE (O=23) REPLACEMENT OF HIGH-MAGNESIUM ANDESITE PHENOCRYSTS AND GROUNDMASS

Plot No.	1	2	3	4
Reg. No.	85-0026	85-0027	85-0023	85-0028
SiO_2	56.21	41.34	50.16	54.31
TiO_2	-	-	-	-
Al_2O_3	0.86	8.21	3.44	2.75
Cr_2O_3	-	0.34	0.33	0.30
FeO	7.24	10.14	9.69	9.16
MnO	0.28	0.27	0.27	0.26
MgO	23.55	24.32	17.59	18.86
CaO	3.99	1.64	11.27	10.99
Na_2O	-	-	0.54	0.39
Total	92.13	86.35	93.29	97.02
Si	8.1002	6.5837	7.4943	7.7116
Ti	-	-	-	-
Al	0.1461	1.5415	0.6059	0.4603
Cr	-	0.0541	0.0390	0.0337
Fe	0.8726	1.3506	1.2108	1.0878
Mn	0.0342	0.0364	0.0342	0.0313
Mg	5.0577	5.7723	3.9167	3.9910
Ca	0.6161	0.2799	1.8042	1.6721
Na	-	-	0.1564	0.1074
Total	14.8268	15.6185	15.2615	15.0951
Mg*	85.3	81.0	76.4	78.6
Ca	9.4	3.8	26.0	24.8
Mg	77.3	78.0	56.5	59.1
Fe	13.3	18.2	17.5	16.1

Table 8. ANALYSES OF BASALT AND DERIVED TUFFACEOUS GREYWACKE SAMPLES FROM WITHIN THE CRIMSON CREEK FORMATION (Ecc, Eccb) IN THE MT LINDSAY-PIEMAN RIVER-MT RAMSAY AREA

Plot No.	1	2	3	4	5	6	7	8	9	10	11	12
Reg. No.	85-0001	85-0002	85-0003	85-0004	85-0005	85-0006	85-0007	85-0008	85-0009	85-0010	85-0011	85-0012
SiO_2	47.50	45.60	48.83	45.88	46.94	48.21	48.35	47.94	48.47	48.04	47.83	48.01
TiO_2	2.00	2.40	2.79	2.09	2.03	2.86	2.91	2.87	4.74	2.65	1.52	1.63
Al_2O_3	12.70	12.20	15.74	13.28	12.87	13.58	13.46	13.22	12.30	12.99	14.21	14.21
Fe_2O_3	4.70	1.70	3.00	5.49	5.38	3.32	2.90	3.08	3.43	4.10	2.46	2.15
FeO	9.40	11.50	11.68	9.31	9.31	10.80	10.80	10.80	12.35	13.57	10.35	10.25
MnO	0.25	0.24	0.15	0.32	0.26	0.22	0.21	0.24	0.25	0.67	0.28	0.25
MgO	5.30	8.50	5.78	6.03	5.57	5.47	5.36	5.53	3.67	3.69	7.11	7.26
CaO	8.90	10.90	2.74	9.73	9.08	7.19	8.49	8.07	6.55	5.49	10.07	10.00
Na_2O	3.50	1.00	2.50	3.17	3.45	2.52	2.61	2.33	2.69	2.56	3.04	3.02
K_2O	0.07	0.67	0.71	0.08	0.07	0.75	0.79	0.74	0.76	0.67	0.32	0.33
P_2O_5	0.23	0.26	0.30	0.24	0.26	0.29	0.29	0.29	0.35	0.20	0.22	0.25
CO_2	0.12	0.10	0.07	0.28	0.36	0.33	0.15	0.47	0.56	0.19	0.10	0.07
H_2O^+	3.60	3.20	3.72	3.61	3.57	3.90	2.77	3.82	3.45	3.57	1.51	1.67
H_2O^-	0.60	0.40	0.81	0.55	0.43	0.39	0.28	0.31	0.31	0.68	0.06	0.07
Total	98.87	98.67	98.82	100.06	99.58	99.83	99.37	99.71	99.88	99.07	99.08	99.17
Mg No.	50	57	47	54	52	47	47	48	35	33	55	56
Cr	94	439	162	70	60	111	117	118	31	39	180	180
Ni	72	192	102	65	59	86	80	78	20	38	70	73
Zr	127	210	230	128	125	164	164	166	219	127	105	115
Y	31	31	36	30	29	28	27	29	36	53	31	32
Nb	11	28	26	11	-	10	12	13	18	8	6	7
Rb	7	24	30	<4	<4	24	20	27	40	15	12	12
Sr	60	295	151	61	59	326	310	332	331	115	185	230
Ba	196	287	299	118	235	714	788	600	868	740	180	120
V	410	250	250	420	410				-	-	320	330
Sc	43	30	35	39	34				-	-	45	48
Co	51	41	49	53	50	45	48	47	41	56	45	45

Table 8. (continued)

Plot No.	13	14	15	16	17	18	19	20	21	22
Reg. No.	85-0013	85-0014	85-0015	85-0016	85-0017	85-0018	85-0019	85-0020	85-0021	85-0022
SiO_2	48.02	49.01	45.62	47.26	52.62	51.37	46.6	47.44	50.0	47.80
TiO_2	1.65	3.36	2.49	3.08	2.36	2.32	1.7	3.38	1.0	1.95
Al_2O_3	14.34	14.52	15.38	12.83	12.47	13.37	14.2	12.31	13.3	13.26
Fe_2O_3	1.73	1.22	3.48	6.36	4.47	3.74	3.3	4.67	2.5	3.09
FeO	10.91	12.27	8.01	8.32	7.64	8.93	9.2	9.15	8.0	9.68
MnO	0.30	0.27	0.23	0.33	0.14	0.15	0.22	0.27	0.19	0.18
MgO	7.45	5.24	6.94	5.03	6.45	6.61	7.5	5.54	8.2	6.34
CaO	9.58	7.84	9.25	5.68	4.13	2.39	9.7	7.89	9.1	8.83
Na_2O	2.71	3.12	2.14	3.23	1.99	1.54	2.8	3.39	2.2	3.33
K_2O	0.41	0.19	1.59	0.81	0.78	1.38	1.0	0.86	0.53	0.22
P_2O_5	0.22	0.52	0.42	0.27	0.26	0.27	0.07	0.36	0.16	0.21
CO_2	0.12	0.06	0.34	1.13	0.64	0.65		0.13		0.26
H_2O^+	2.04	1.48	3.80	3.19	4.57	5.53	4.06#	3.16	4.80#	3.54
H_2O^-	0.10	0.10	0.21	0.60	0.82	0.85		0.38		0.30
Total	99.58	99.20	99.90	98.12	99.32	99.10	100.42	98.93	99.98	98.99
Mg No.	55	43	61	-	-	-	52	43	59	
Cr	190	130	120	236	342	368	171	146	289	153
Ni	76	44	37	108	118	144	103	79	106	92
Zr	115	260	200	200	240	229	111	216	80	111
Y	32	59	30	35	34	39	22	33	25	20
Nb	16	5	5	-	-	24	-	-	-	-
Rb	18	10	54	37	26	46	20	8	12	4
Sr	230	200	330	212	99	116	484	288	147	222
Ba	200	125	220	334	235	791	-	-	-	-
V	330	440	260	-	-	-	-	-	-	-
Sc	49	54	34	-	-	-	-	-	-	-
Co	44	38	32	50	43	45	-	-	-	-

Table 8. (continued)

Basalt samples: 1-5 Mt Lindsay area
6-10 Pieman River - Renison Bell area
11-14 Mt Ramsay area

Tuffaceous greywacke samples: 16 Crimson Creek
17 Mt Lindsay
18 Pieman River - Ring River

Samples 19-22: Analyses of basalt and tuffaceous greywacke samples from Wandle River area (Williams and Brown, 1983, Table 1) -
Samples 19-21 basalt
Sample 22 tuffaceous greywacke

Analyses by Department of Mines Analytical Laboratory -
Analysts J. Furst, M. Firth, M. Pickering and R. Roby

Dash = Not determined

= Loss on ignition

Sample numbers are registered numbers in the Department of Mines collection.

Table 9. WHOLE ROCK MAJOR AND TRACE ELEMENT ANALYSES OF SAMPLES OF HIGH-MAGNESIAN ANDESITE

Plot No.	1	2	3	4	5	6	7	8
Reg. No.	85-0023	+38876	+60951	85-0024	85-0025	85-0026	85-0027	85-0028
SiO_2	51.20	50.96	53.57	56.93	53.40	50.39	53.13	51.13
TiO_2	0.07	0.18	0.07	0.15	0.09	0.03	0.08	0.04
Al_2O_3	8.40	7.56	7.20	4.14	10.30	6.43	10.43	4.56
Fe_2O_3	2.40	1.38	2.86	1.17	1.90	1.95	1.32	2.68
FeO	6.80	7.62	6.81	6.08	6.80	7.03	6.95	7.09
MnO	0.17	0.16	0.17	0.34	0.24	0.20	0.25	0.33
MgO	17.10	17.78	18.04	18.21	10.70	21.73	10.11	17.65
CaO	4.60	6.92	5.73	7.94	3.40	2.49	3.53	9.69
Na_2O	0.36	0.60	-	1.37	0.05	0.03	0.03	0.21
K_2O	0.06	0.00	-	0.01	0.77	0.02	0.95	0.19
P_2O_5	0.01	0.00	0.03	0.02	0.04	0.02	0.03	0.12
CO_2	0.49	-	-	0.14	6.00	0.91	6.21	-
H_2O^+	6.60	6.24	6.18	2.46	5.40	6.93	6.15	5.10
H_2O^-	1.20	-	-	0.20	0.99	1.22	0.12	0.00
Total	99.46	100.01	100.66	99.16	100.08	99.38	99.29	98.79
Mg No.	77	78	77	79	69	82	69	77
Cr	860	3190	-	3500	814	2454	875	2900
Ni	687	1080	-	490	161	601	165	570
Zr	6	<20	9	10	16	12	20	5
Y	7	<6	3	10	5	<4	<4	5
Nb	<4	-	1	<3	<4	<4	<4	<3
Rb	<4	<6	1	5	47	<4	54	13
Sr	10	15	14	4	39	11	41	32
Ba	39	-	-	<11	47	15	52	49
V	97	-	-	160	110	95	130	98
Sc	26	-	-	20	25	23	25	21
Co	-	-	-	34	-	-	-	74

Table 9. (continued)

Plot No.	9	10	11	12	13
Reg. No.	85-0029	85-0030	85-0031	85-0053	85-0054
SiO_2	51.25	51.93	52.26	48.19	53.15
TiO_2	0.12	0.10	0.10	0.08	0.13
Al_2O_3	5.52	4.81	4.92	5.46	6.27
Fe_2O_3	1.65	1.86	1.91	1.44	0.91
FeO	8.29	8.13	7.95	7.59	8.91
MnO	0.28	0.28	0.27	0.15	0.20
MgO	18.91	18.35	17.64	26.72	20.41
CaO	9.19	9.57	9.50	2.55	3.84
Na_2O	0.30	0.19	0.26	0.09	0.62
K_2O	0.28	0.27	0.37	0.08	0.37
P_2O_5	0.02	0.03	0.02	0.01	0.03
CO_2	0.14	0.13	0.14	0.15	0.14
H_2O^+	3.89	3.87	3.67	6.60	4.50
H_2O^-	0.37	0.32	0.31	0.43	0.21
Total	100.21	99.84	99.32	99.54	99.69
Mg No.	78	77	76	84	79
Cr	2600	2700	2900	3100	1650
Ni	570	570	580	800	370
Zr	5	5	3	3	9
Y	5	4	3	2	5
Nb	<3	<3	<3	<3	<3
Rb	16	15	21	8	14
Sr	28	26	30	6	15
Ba	57	51	58	14	37
V	115	105	105	55	98
Sc	26	23	24	16	32
Co	68	64	62	75	64

Samples: €ba - 1-4 Heazlewood
5-7 Magnet
8-11 Stonehenge

€bap - 12-13 Heazlewood

Dash = not determined

\+ = University of Tasmania registered sample number:

38876 from Rubenach (1973)
60951 from Creenaune (1980)

Other analyses by Department of Mines Laboratories, Launceston.
Analysts - J. Furst, M. Firth, M. Pickering and R. Roby.

Table 10. WHOLE ROCK MAJOR AND TRACE ELEMENT ANALYSES OF SAMPLES OF LOW-TITANIUM BASALT FROM THE BLACK HILL AREA

Plot No.	1	2	3	4	5	6	7	8	9
Reg. No.	85-0032	85-0033	85-0034	85-0035	85-0036	85-0052	85-0037	85-0038	85-0039
SiO_2	57.10	52.20	57.30	44.60	53.52	56.94	52.69	49.55	50.97
TiO_2	0.28	0.57	0.42	0.44	0.28	0.21	0.55	0.39	0.25
Al_2O_3	12.90	17.40	12.90	13.50	14.75	14.52	13.26	14.15	13.56
Fe_2O_3	5.00	2.00	2.10	2.30	3.15	0.75	5.54	3.78	3.55
FeO	7.50	6.90	6.40	9.90	8.78	5.94	7.41	7.10	7.41
MnO	0.13	0.09	0.14	0.18	0.20	0.14	0.19	0.18	0.18
MgO	4.40	3.90	4.60	6.10	5.22	6.35	5.00	7.55	6.79
CaO	7.60	3.30	4.40	7.10	8.54	3.43	6.34	8.65	10.27
Na_2O	1.60	1.40	2.90	2.00	1.74	4.37	5.18	2.82	3.83
K_2O	0.19	2.70	0.19	0.31	0.14	0.02	0.17	0.21	0.34
P_2O_5	0.04	0.06	0.05	0.05	0.05	0.07	0.07	0.06	0.05
CO_2	0.05	3.60	3.70	7.90	0.19	2.54	-	-	-
H_2O^+	2.40	4.60	4.00	4.60	2.80	3.69	2.65#	4.77#	3.37#
H_2O^-	0.35	0.37	0.36	0.45	0.25	0.15	-	-	-
Total	99.54	99.09	99.46	99.43	99.61	99.13	99.05	99.21	100.57
Mg No.	40	44	50	48	44	63	42	56	55
Cr	24	185	139	153	55	175	81	295	81
Ni	58	81	70	81	55	100	63	104	73
Zr	8	16	14	15	8	18	22	17	9
Y	8	11	9	14	9	7	18	14	8
Nb	<4	<4	<4	<4	<4	<3	-	-	-
Rb	6	78	6	15	<4	7	<4	5	10
Sr	49	40	64	64	68	27	210	171	107
Ba	41	439	44	53	60	18	140	130	950
V	260	490	230	280	390	115	370	290	420
Sc	47	57	44	52	67	19	54	56	33
CO	29	36	23	39	47	27	-	-	-

Samples 1-5 from Black Hill
6 from Magnet
7-9 from Wandle Road area (from Williams and Brown, 1983)

Dash = not determined

= loss on ignition

Analyses by Department of Mines Analytical Laboratory -
Analysts J. Furst, M. Frith, M. Pickering and R. Roby.

Table 11. WHOLE ROCK MAJOR AND TRACE ELEMENT ANALYSES OF LOW TITANIUM BASALT FROM THE HEAZLEWOOD RIVER AREA

Plot No.	1	2	3	4	5	6	7	8	9	10
Reg. No.	60896	60898	60894	60897	60895	60901	60892	60919	60900	60903
SiO_2	49.09	51.94	47.98	52.20	51.46	52.68	53.47	49.56	51.72	48.88
TiO_2	0.20	0.20	0.22	0.23	0.24	0.24	0.31	0.25	0.25	0.13
Al_2O_3	13.28	14.47	15.56	14.02	16.10	14.56	13.70	14.73	14.69	14.41
Fe_2O_3	3.29	3.04	3.35	2.97	3.34	3.52	4.11	3.17	3.59	2.90
FeO	7.20	6.07	6.98	6.53	8.36	7.62	6.84	6.68	6.67	5.89
MnO	0.09	0.17	0.19	0.18	0.13	0.18	0.23	0.18	0.18	0.22
MgO	11.66	9.08	11.31	9.14	2.13	7.58	8.07	10.49	8.91	9.99
CaO	12.76	12.10	10.52	12.78	15.96	8.36	9.06	11.72	9.73	13.48
Na_2O	0.00	1.95	2.52	0.98	0.00	0.63	3.49	1.44	2.24	1.70
K_2O	0.07	0.13	0.17	0.11	0.01	0.63	0.14	0.56	0.61	0.80
P_2O_5	0.15	0.05	0.04	0.05	0.08	0.02	0.04	0.04	0.03	0.01
LOI	1.37	1.52	2.27	0.98	2.54	2.04	2.80	1.71	1.64	2.00
Total	99.16	100.72	101.11	100.17	100.35	98.06	102.26	100.53	100.26	100.41
Mg No.	67	65	67	64	25	56	58	66	63	67
Cr	-	-	-	-	-	-	-	-	-	-
Ni	-	122	128	105	38	87	67	172	83	105
Zr	11	10	13	11	17	11	11	15	11	7
Y	16	12	11	9	16	12	18	14	16	7
Nb	1			2	3			2		1
Rb	1	1			1	12	1	7	7	19
Sr	38	39	35	52	208	89	50	36	91	49
Ba	-	-	-	-	-	-	-	-	-	-
V	390	217	281	230	466	263	261	214	262	167
Sc	-	-	-	-	-	-	-	-	-	-
Co	-	-	-	-	-	-	-	-	-	-

Analyses from Creenaune (1980). Samples 1-8 basalt, sample 9 coarse-grained basalt, sample 10 very coarse-grained basalt.
Registered numbers are University of Tasmania collection
Dash = not determined

Table 12. WHOLE ROCK MAJOR AND TRACE ELEMENT ANALYSES OF SAMPLES OF PRECAMBRIAN ALKALI BASALT

Plot No.	1	2	3	4	5
Reg. No.	85-0128	85-0129	85-0130	85-0131	85-0132
SiO_2	28.47	42.10	36.50	39.36	46.72
TiO_2	3.08	2.60	2.65	3.68	3.07
Al_2O_3	15.43	15.22	15.35	15.65	16.49
Fe_2O_3	1.71	1.12	0.71	1.22	1.05
FeO	17.24	9.78	14.00	23.06	9.35
MnO	0.52	0.26	1.60	0.20	0.07
MgO	6.89	7.56	6.18	5.72	7.41
CaO	6.87	4.55	1.45	1.22	2.41
Na_2O	0.10	0.14	0.10	0.16	4.61
K_2O	2.64	3.64	3.89	0.56	0.40
P_2O_5	1.17	0.98	0.91	0.68	0.73
CO_2	8.05	4.89	11.78	0.31	2.05
H_2O^-	5.56	5.92	3.63	8.02	5.07
H_2O^+	0.38	0.34	0.14	0.02	0.19
Total	98.21*	99.10	98.90	99.86	99.40
Cr	330	270	340	280	290
Ni	130	110	115	160	220
Zr	290	260	290	450	360
Y	42	23	26	37	30
Nb	130	110	115	79	150
Rb	200	310	370	95	30
Sr	85	68	66	56	300
Ba	530	1100	1500	80	200
V	280	210	260	-	-
Sc	31	25	28	28	25
Co	46	35	36	16	39

* This sample also contains 1.25 wt% SO_3.

Analyses by Department of Mines Analytical Laboratory -
Analysts J. Furst, M. Frith, M. Pickering and R. Roby.

Table 12. (continued).

Plot No.	6	7	8
Reg. No.	85-0133	85-0134	Anhydrous Average of 5-7
SiO_2	46.62	45.35	50.61
TiO_2	2.97	2.98	3.29
Al_2O_3	16.49	16.24	17.96
Fe_2O_3	1.08	0.98	1.14
FeO	8.36	7.43	9.17
MnO	0.07	0.09	0.09
MgO	9.22	8.80	9.29
CaO	2.77	3.85	3.30
Na_2O	2.61	2.06	3.37
K_2O	0.55	1.78	1.00
P_2O_5	0.70	0.73	0.79
CO_2	2.10	3.94	-
H_2O^-	5.55	5.24	-
H_2O^+	0.17	0.18	-
Total	99.26	99.65	-
Cr	290	290	
Ni	240	220	
Zr	340	340	
Y	31	39	
Nb	145	145	
Rb	40	105	
Sr	510	390	
Ba	280	420	
V	-	-	
Sc	24	22	
Co	33	44	

Table 13. LAYER RHYTHMS IN LPD SUCCESSION AT RILEY KNOB

Rock type	A	B	C	
	olc	ol + opxc	opxc	
Layer thickness				
≦ 5 mm	30	32	39	
6 ≦ 20 mm	30	17	54	
21 ≦ 50 mm	18	4	18	
51 ≦ 100 mm	6	2	4	
101 ≦ 200 mm	3	-	2	
Total	87	55	117	= 259
Total thickness	1926 mm	564 mm	2017 mm	= 4510 mm

Rhythms:-

ACAC	-	45.38%
ACBC	-	24.37%
ACAB	-	8.08%
ABCA	-	7.44%
ACBA	-	6.80%
ABCB	-	4.34%
ABAC	-	2.79%
ABAB	-	0.80%

olc = olivine cumulate

ol + opxc = olivine + orthopyroxene cumulate

opxc = orthopyroxene cumulate

Table 14. WHOLE ROCK MAJOR AND TRACE ELEMENT ANALYSES OF SAMPLES OF DUNITE, METADUNITE AND SERPENTINITE FROM THE LDH AND LPD SUCCESSION

Plot No.	1	2	3	4	5	6	7	8	9	10
Reg. No.	85-0135	85-0136	85-0137	85-0138	85-0139	85-0140	85-0141	85-0142	85-0143	85-0144
SiO_2	38.60	38.60	36.90	37.40	38.60	35.77	39.00	41.90	40.70	40.70
TiO_2	0.01	0.01	0.01	0.01	0.01	0.02	0.02	0.01	0.01	0.01
Al_2O_3	0.10	0.09	0.18	0.15	0.08	0.08	0.19	0.09	0.09	0.14
Fe_2O_3	5.00	4.80	2.90	3.60	3.30	5.49	3.10	2.00	1.90	3.60
FeO	1.30	1.70	3.60	2.30	3.40	0.72	3.80	3.80	4.70	3.60
MnO	0.11	0.09	0.09	0.08	0.09	0.08	0.15	0.10	0.10	0.12
MgO	39.40	40.50	44.70	41.70	45.70	41.53	44.90	48.20	49.50	47.20
CaO	0.70	0.03	0.03	0.11	0.02	0.02	0.16	0.01	0.06	0.03
Na_2O	0.01	0.01	0.01	0.01	0.01	0.03	0.01	0.01	0.01	0.01
K_2O	0.01	0.01	0.01	0.01	0.01	0.01	0.03	0.01	0.01	0.02
P_2O_5	0.01	0.01	0.01	0.01	0.01	0.01	0.01	0.01	0.01	0.01
CO_2	0.92	0.57	1.00	0.72	1.00	1.15	1.10	0.25	0.42	0.32
H_2O^+	12.40	11.70	8.10	12.00	6.70	13.16	6.00	2.70	2.10	1.80
H_2O^-	1.20	1.60	1.00	1.00	0.72	1.49	0.96	0.50	0.28	0.39
Total	99.77	99.72	98.54	99.10	99.65	99.56	99.43	99.59	99.89	97.95
Mg number	92.30	91.89	92.77	93.06	93.24	92.90	92.39	93.88	93.06	92.48
Cr	2010	2030	6860	1780	1940	1758	2180	2610	2630	13530
Ni	2470	2450	2280	2440	2660	2521	2580	2900	3090	2940
Zr	<4	<4	<4	<4	<4	<4	<4	<4	<4	<4
Y	<4	<4	<4	<4	<4	<4	<4	<4	<4	<4
Nb	<4	<4	<4	<4	<4	<4	<4	<4	<4	<4
Rb	<4	<4	<4	<4	<4	<4	<4	<4	<4	<4
Sr	<4	<4	<4	<4	<4	<4	<4	<4	<4	<4

Table 14. (continued)

Plot No.	11	12	13	14	15
Reg. No.	85-0145	85-0146	85-0147	85-0148	85-0149
SiO_2	34.90	36.80	38.89	36.10	40.30
TiO_2	0.01	0.02	0.02	0.11	0.02
Al_2O_3	0.11	0.11	0.56	7.14	0.54
Fe_2O_3	4.90	5.20	5.52	3.08	4.81
FeO	1.60	1.50	0.87	5.06	2.17
MnO	0.09	0.09	0.26	0.05	0.04
MgO	40.70	39.50	36.42	33.27	37.24
CaO	0.03	0.03	0.13	0.20	0.12
Na_2O	0.01	0.01	0.03	0.03	0.03
K_2O	0.01	0.01	0.02	0.02	0.04
P_2O_5	0.01	0.01	0.01	0.01	0.01
CO_2	1.40	1.10	0.37	0.51	0.79
H_2O^+	15.10	14.20	12.78	13.23	11.91
H_2O^-	1.20	1.10	1.65	0.89	0.46
Total	100.07	99.68	97.53	99.70	98.48
Cr	1670	2070	10857	2247	7698
Ni	2330	2100	2822	975	2072
Zr	<4	<4	<4	<4	<4
Y	<4	<4	<4	<4	<4
Nb	<4	<4	<4	<4	<4
Rb	<4	<4	<4	<4	<4
Sr	<4	<4	5	5	<4

Analyses 1-6 - Dunite samples from LDH succession
7-10 - Metadunite samples from LDH succession
11-13 - Serpentinite samples from LDH succession
14-15 - Serpentinite samples from LPD succession
Analyses by Department of Mines Analytical Laboratory -
Analysts J. Furst, M. Frith, M. Pickering and R. Roby

Table 15. WHOLE ROCK MAJOR AND TRACE ELEMENT ANALYSES OF SAMPLES OF PYROXENITE FROM THE LDH AND LPD SUCCESSIONS

Plot No.	1	2	3	4	5	6	7	8	9	10	11
Reg. No.	85-0150	85-0151	85-0152	85-0153	85-0154	85-0155	85-0156	85-0157	85-0158	85-0159	85-0160
SiO_2	51.60	52.90	51.85	53.85	54.67	50.48	52.38	51.57	55.55	54.96	54.19
TiO_2	0.01	0.01	0.02	0.02	0.01	0.02	0.02	0.02	0.02	0.02	0.02
Al_2O_3	0.21	0.21	0.41	1.29	1.04	2.98	1.13	1.90	1.01	1.12	1.12
Fe_2O_3	2.50	1.50	1.48	1.12	0.81	1.40	1.52	0.38	2.80	1.01	1.84
FeO	2.10	3.90	4.37	4.90	6.12	5.74	5.36	7.03	3.92	5.66	5.59
MnO	0.10	0.12	0.13	0.17	0.17	0.16	0.17	0.20	0.15	0.16	0.19
MgO	34.00	35.60	32.42	32.84	33.17	30.76	32.44	30.48	33.34	32.39	31.37
CaO	0.91	0.05	2.31	1.32	1.72	2.91	1.92	3.41	1.18	1.25	1.33
Na_2O	0.02	0.02	0.03	0.11	0.05	0.03	0.03	0.03	0.03	0.04	0.09
K_2O	0.01	0.02	0.02	0.01	0.01	0.02	0.01	0.01	0.01	0.01	0.03
P_2O_5	0.01	0.01	0.01	0.01	0.01	0.01	0.01	0.01	0.01	0.01	0.01
CO_2	0.07	0.15	0.35	0.27	0.19	0.21	0.19	0.15	0.18	0.16	0.17
H_2O^+	6.70	4.00	4.63	2.25	1.49	3.23	3.80	3.80	0.82	1.70	3.36
H_2O^-	1.20	0.63	0.56	0.39	0.23	0.46	0.29	0.40	0.39	0.35	0.57
Total	99.44	99.12	98.59	98.55	99.69	98.41	99.27	99.39	99.41	98.84	99.88
Cr	3150	5770	5246	5270	4862	4605	5340	4812	4492	5273	3402
Ni	772	903	429	743	626	724	678	671	483	430	398
Zr	<4	<4	<4	<4	<4	<4	<4	<4	<4	<4	<4
Y	<4	<4	<4	<4	<4	<4	<4	<4	<4	<4	<4
Nb	<4	<4	<4	-	<4	<4	<4	<4	<4	<4	<4
Rb	<4	<4	<4	<4	<4	<4	<4	<4	<4	<4	<4
Sr	<4	<4	9	<4	<4	4	<4	<4	<4	<4	6
Ba	-	-	19	-	<15	<15	<15	<15	<15	<15	<15
V	-	-	-	-	-	-	-	-	-	-	-
Sc	-	-	-	-	-	-	-	-	-	-	-
Co	-	-	77	-	79	81	76	64	85	79	75

Analyses by Department of Mines Analytical Laboratory - Analysts J. Furst, M. Frith, M. Pickering and R. Roby.

Table 15. (continued)

Plot No.	12	13	14	15	16	17	18	19
Reg. No.	85-0161	85-0162	85-0163	85-0164	85-0165	85-0166	85-0167	85-0168
SiO_2	49.24	50.40	51.40	52.80	52.40	44.90	52.67	53.06
TiO_2	0.02	0.02	0.02	0.01	0.02	0.01	0.02	0.02
Al_2O_3	1.18	1.90	1.80	1.30	2.10	0.87	2.11	1.97
Fe_2O_3	1.54	2.20	3.10	1.70	1.40	2.60	1.86	0.95
FeO	4.68	3.90	3.80	5.70	6.40	4.40	5.51	3.76
MnO	0.26	0.17	0.17	0.18	0.17	0.30	0.17	0.14
MgO	29.97	29.40	28.70	29.70	29.80	34.50	29.26	20.98
CaO	5.15	2.50	2.50	0.78	1.80	0.56	3.05	14.92
Na_2O	0.03	0.04	0.04	0.04	0.03	0.02	0.03	0.05
K_2O	0.02	0.01	0.01	0.02	0.02	0.01	0.01	0.05
P_2O_5	0.02	0.01	0.01	0.01	0.01	0.01	0.01	0.07
CO_2	0.30	0.34	0.27	0.20	0.03	0.02	0.15	0.18
H_2O^+	5.25	6.70	6.40	5.90	5.20	9.70	4.12	3.09
H_2O^-	0.63	1.10	0.60	0.81	0.39	1.00	0.57	0.57
Total	98.29	98.69	98.82	99.15	99.77	98.90	99.54	99.81
Cr	4836	5130	4500	4090	4240	3440	4325	4662
Ni	540	652	552	479	540	812	422	400
Zr	<4	<4	<4	<4	<4	<4	<4	<4
Y	<4	<4	<4	<4	<4	<4	<4	<4
Nb	<4	<4	<4	<4	<4	<4	<4	<4
Rb	<4	<4	4	4	<4	7	<4	<4
Sr	<4	4	<4	4	4	13	<4	<4
Ba	<15	-	-	-	-	-	<15	<15
V	-	-	-	-	-	-	-	-
Sc	-	-	-	-	-	-	-	-
Co	76	-	-	-	-	-	78	61

Analyses 1-3 LDH succession
4-8 LPD succession - Riley Knob
9-11 - Lynch Hill

Analyses 12 LPD succession - Huskisson River
13-14 - Ring River
15-17 - Dundas
18-19 - Colebrook Hill

Table 16. CHEMICAL ANALYSES (OXIDE WEIGHT %) AND STRUCTURAL FORMULAE (O=4) OF OLIVINES FROM THE LDH SUCCESSION

Plot No.	1	2	3	4	5	6	7	8	9	10
Reg. No.	85-0169	85-0135	85-0170	85-0171	85-0137	85-0172	85-0173	85-0174	85-0175	85-0176
SiO_2	41.00	41.35	42.41	40.88	41.69	41.11	41.48	41.56	41.51	41.45
FeO	6.60	7.03	6.44	6.57	7.01	6.76	6.47	6.67	6.40	6.36
MgO	52.34	51.34	50.86	50.05	51.97	52.05	51.85	51.60	51.42	51.82
NiO	-	-	-	-	-	-	0.35	0.32	-	-
Total	99.94	99.72	99.71	99.50	100.67	99.92	100.15	100.15	99.33	99.63
Si	0.9908	1.0019	1.0219	0.9921	1.0004	0.9939	1.0000	1.0023	1.0063	1.0021
Fe	0.1334	0.1425	0.1298	0.1333	0.1407	0.1367	0.1304	0.1345	0.1298	0.1286
Mg	1.8850	1.8538	1.8264	1.8825	1.8585	1.8755	1.8628	1.8546	1.8577	1.8671
Ni	-	-	-	-	-	-	0.0068	0.0062	-	-
Total	3.0092	2.9981	2.9781	3.0079	2.9996	3.0061	3.0000	2.9977	2.9937	2.9979
Mg*	93.4	92.9	93.4	9.34	93.0	93.2	93.5	93.2	93.5	93.6

Table 16. (continued)

Plot No.	11	12	13	14	15	16	17	18	19	20
Reg. No.	85-0177	85-0140	85-0178	85-0179	85-0181	85-0182	85-0183	39576+	85-0184	39595+
SiO_2	41.41	41.35	41.26	41.77	41.67	41.61	41.75	41.38	39.72	40.38
FeO	6.20	7.03	7.13	7.27	7.03	7.17	7.27	6.96	13.14	11.13
MgO	51.69	51.34	50.92	51.55	51.85	51.57	51.55	51.93	46.99	48.07
NiO	0.22	-	-	-	0.36	0.41	-	-	-	-
Total	99.52	99.72	99.31	100.59	100.91	100.76	100.57	100.27	99.85	99.58
Si	1.0026	1.0019	1.0041	1.0038	0.9994	1.0002	1.0036	0.9973	0.9902	0.9988
Fe	0.1255	0.1425	0.1451	0.1461	0.1410	0.1441	0.1462	0.1403	0.2739	0.2302
Mg	1.8651	1.8538	1.8467	1.8463	1.8533	1.8475	1.8467	1.8652	1.7457	1.7721
Ni	0.0043	-	-	-	0.0069	0.0079	-	-	-	
Total	2.9974	2.9981	2.9959	2.9962	3.0006	2.9998	2.9964	3.0027	3.0098	3.0012
Mg*	93.7	92.9	92.7	92.7	92.9	92.8	92.7	93.00	86.4	88.5

Analyses 1-12 - Harman River area - Dunite and pyroxene-bearing dunite samples.
13-14 - Mt Stewart area - Dunite and pyroxene-bearing dunite samples.
15-18 - Adamsfield area - Dunite and pyroxene-bearing dunite samples.
19 - Mt Stewart area - Coarse-grained orthopyroxenite sample.
20 - Adamsfield area - Coarse-grained orthopyroxenite sample.

\+ = University of Tasmania Registered Number.

Samples 18, 20: from Varne and Brown (1978).

Table 17. CHEMICAL ANALYSES (OXIDE WEIGHT %) AND STRUCTURAL FORMULAE (O=6) OF ORTHOPYROXENE FROM THE LDH SUCCESSION

Plot No.	1	2	3	4	5	6	7	8	9
Reg. No.	85-0172	85-0173	85-0174	39576+	85-0150	85-0151	85-0184	85-0152	39595+
SiO_2	58.32	58.29	58.49	57.94	57.75	57.90	57.96	58.56	57.43
Al_2O_3	0.45	0.30	0.28	-	0.31	-	-	0.24	-
Cr_2O_3	0.24	-	-	0.23	-	-	-	0.22	-
FeO	4.27	4.39	4.53	4.29	4.38	4.61	5.68	5.78	7.47
MgO	36.81	36.56	36.51	36.94	36.72	37.25	35.69	35.40	34.52
CaO	0.25	-	-	-	0.22	-	-	0.21	-
Total	100.34	99.54	99.81	99.40	99.38	99.76	99.33	100.41	99.42
Si	1.9835	1.9955	1.9977	1.9889	1.9837	1.9832	2.0002	2.007	1.9969
Al	0.0180	0.0121	0.0113	-	0.0126	-	-	0.0097	-
Cr	0.0065	-	-	0.0062	-	-	-	0.0059	-
Fe	0.1215	0.1257	0.1294	0.1232	0.1258	0.1321	0.1639	0.1651	0.2172
Mg	1.8658	1.8652	1.8584	1.8898	1.8798	1.9015	1.8356	1.8024	1.7889
Ca	0.0091	-	-	-	0.0081	-	-	0.0077	-
Total	4.0043	3.9985	3.9967	4.0080	4.0100	4.0168	3.9998	3.9915	4.0031
Mg*	93.9	93.7	93.5	93.9	93.7	93.5	91.8	91.6	89.2
Ca	0.5	0.0	0.0	0.0	0.4	0.0	0.0	0.4	0.0
Mg	93.5	93.7	93.5	93.9	93.3	93.5	91.8	91.2	89.2
Fe	6.1	6.3	6.5	6.1	6.2	6.5	8.2	8.4	10.8

Mg* = 100 Mg/Mg+Fe

Samples 1-4 - Harman River area. Pyroxene-bearing dunite samples.
5-6 - Harman River area. Coarse-grained orthopyroxenite samples.
7 - Mt Stewart area. Coarse-grained orthopyroxenite sample.
8 - Huskisson River area. Coarse-grained orthopyroxenite sample
9 - Adamsfield area. Coarse-grained orthopyroxenite sample.

\+ = University of Tasmania Registered Number.

Analysis 9 from Varne and Brown (1978).

Table 18. CHEMICAL ANALYSES (OXIDE WEIGHT %) AND STRUCTURAL FORMULAE (O=32) OF CHROME SPINEL FROM THE LDH SUCCESSION

Plot No.	1	2	3	4	5	6	7	8	9	10	11	12
Reg. No.	85-0169	85-0135	85-0170	85-0171	85-0185	85-0186	85-0172	85-0173	85-0174	85-0187	85-0175	85-0176
TiO_2	-	-	-	-	-	-	-	-	-	-	-	-
Al_2O_3	5.18	4.60	3.39	3.44	5.82	4.03	5.09	4.63	4.61	3.53	3.21	6.81
Cr_2O_3	65.82	66.52	66.93	67.32	61.88	67.01	64.03	65.87	64.61	68.71	68.88	64.77
FeO	18.83	19.90	18.81	20.53	24.57	18.95	20.36	20.45	19.92	18.40	19.20	17.60
MnO	-	-	-	-	0.65	-	-	-	0.38	0.64	-	-
MgO	9.54	8.79	10.58	9.50	8.03	9.53	10.30	9.57	10.39	9.65	8.96	10.57
CaO	-	-	-	-	-	-	-	-	-	-	-	-
Total	99.37	99.81	99.71	100.79	100.95	99.52	99.78	100.52	99.91	100.93	100.25	99.75
Ti												
Al	1.6635	1.4832	1.0850	1.0985	1.8534	1.2990	1.6182	1.4736	1.4659	1.1249	1.0362	2.1480
Cr	14.1739	14.3824	14.3640	14.4157	13.2144	14.4844	13.6505	14.0586	13.7771	14.6820	14.9105	13.6994
Fe^{3+}	0.1626	0.1345	0.5510	0.4858	0.9321	0.2166	0.7313	0.4678	0.7570	0.1931	0.0533	0.1526
Fe^{2+}	4.1271	4.4172	3.7195	4.1650	4.6186	4.1167	3.8605	4.1495	3.7366	3.9662	4.3436	3.7854
Mn	-	-	-	-	0.1487	-	-	-	0.0868	0.1465	-	-
Mg	3.8729	3.5828	4.2805	3.8350	3.2327	3.8833	4.1395	3.8508	4.1766	3.8873	3.6564	4.2146
Ca	-		-	-	-	-	-					
Mg^+	48.4	44.8	53.5	47.9	41.2	48.5	51.7	48.1	52.8	49.5	45.7	52.7
Cr*	89.5	90.7	93.0	92.9	87.7	91.8	89.4	90.5	90.4	92.9	93.5	86.4

Table 18. (continued)

Plot No.	13	14	15	16	17	18	19	20	21	22	23	24
Reg. No.	85-0177	85-0189	85-0188	85-0190	85-0191	85-0192	85-0193	85-0178	85-0179	85-0194	85-0195	85-0196
TiO_2	-	-	-	-	-	-	-	-	-	-	-	-
Al_2O_3	6.49	3.87	7.81	2.52	2.28	1.82	3.22	5.46	4.07	2.91	3.44	3.55
Cr_2O_3	66.16	64.91	62.43	67.10	71.00	71.09	69.50	65.56	66.90	66.95	67.37	66.80
FeO	17.05	19.15	19.11	20.39	16.30	15.75	15.98	19.51	19.62	21.57	19.75	20.62
MnO	-	-	-	0.50	-	0.56	-	0.69	-	0.62	0.61	0.63
MgO	10.74	11.50	10.38	9.98	10.83	10.98	11.05	8.89	8.70	7.18	8.61	8.01
CaO	-	-	-	-	-	-	-	-	-	-	-	-
Total	100.44	99.43	99.73	100.49	100.41	100.20	99.75	100.11	99.29	99.23	99.78	99.61
Ti		-			-	-	-	-	-	-	-	-
Al	2.0354	1.2299	2.4549	0.8069	0.7282	0.5825	1.0286	1.7471	1.3227	0.9616	1.1164	1.1584
Cr	13.9135	13.8328	13.1592	14.4071	15.2061	15.2656	14.8878	14.0686	14.5796	14.8354	14.6618	14.6167
Fe^{3+}	0.0511	0.9373	0.3859	0.7860	0.0657	0.1516	0.0836	0.1841	0.0977	0.2030	0.2217	0.2250
Fe^{2+}	3.7421	3.3800	3.8754	3.8454	3.6274	3.4263	3.5377	4.2450	4.4257	4.8535	4.3253	4.5482
Mn	-	-	-	0.1150	-	0.1288	-	0.1587	-	0.1472	0.1422	0.1477
Mg	4.2579	4.6200	4.1246	4.0396	4.3726	4.4449	4.4623	3.5964	3.5743	2.9993	3.5324	3.3041
Ca		-			-	-	-	-	-	-	-	-
Mg^+	53.2	57.8	51.6	51.2	54.7	56.5	55.8	45.9	44.7	38.2	45.0	42.1
Cr*	87.2	91.8	84.3	94.7	95.4	96.3	93.5	89.0	91.7	93.9	92.9	92.7

Table 18. (continued)

Plot No.	25	26	27	28	29	30	31	32	33	34
Reg. No.	85-0197	85-0181	85-0182	85-0183	+39575	85-0150	85-0151	85-0184	85-0152	+39595
TiO_2	-	-	-	-	0.15	-	-	-	0.29	-
Al_2O_3	6.01	2.00	2.89	4.01	2.53	3.29	3.69	5.21	5.79	2.03
Cr_2O_3	63.69	69.32	69.62	68.16	68.83	68.17	67.59	63.23	61.52	63.39
FeO	20.17	20.10	18.58	18.74	19.28	18.73	19.14	23.66	23.00	29.17
MnO	-	0.59	-	-	-	-	-	-	0.57	0.27
MgO	10.52	8.39	9.56	9.58	8.36	9.12	9.31	7.00	8.25	4.36
CaO	-	-	-	-	0.24	-	-	-		0.08
Total	100.39	100.40	100.65	100.49	99.39	99.31	99.73	99.10	99.42	99.30
Ti	-	-	-	-	0.0314	-	-	-	0.0597	-
Al	1.8898	0.6506	0.9268	1.2811	0.8290	1.0696	1.1910	1.7058	1.8682	0.6861
Cr	13.4294	15.1223	14.9710	14.6025	15.1237	14.8622	14.6283	13.9018	13.3106	14.3669
Fe^{3+}	0.6809	0.2271	0.1022	0.1164	0.0159	0.0682	0.1807	0.3925	0.7616	0.9470
Fe^{2+}	3.8184	4.4117	4.1245	4.1309	4.4656	4.2517	4.2015	5.1028	4.5029	6.0470
Mn	-	0.1379	-	-	-	-	-	-	0.1321	0.0656
Mg	4.1817	3.4504	3.8755	3.8691	3.4629	3.7483	3.7985	2.8972	3.3650	1.8629
Ca	-	-	-	-	0.0715	-	-	-	-	0.0246
Mg^+	52.3	43.9	48.4	48.4	43.7	46.9	47.5	36.2	42.8	23.6
Cr*	87.7	95.9	94.2	91.9	94.8	93.3	92.5	89.1	87.7	95.4

$Mg^+ = 100\ Mg/Mg+Fe^{2+}$ Cr* = 100 Cr/Cr+Al

Total iron reported as FeO. Structural formulae calculated assuming the general formula $R^{2+}R^{3+}O_4$ and apportioning total iron as Fe^{2+} and Fe^{3+} so that $2(Mg+Mn+Ca+Fe^{2+})=(Cr+Al+Ti+Fe^{3+})$.

Analyses of dunite and pyroxenite-bearing dunite samples from:

1-13 Harman River area
14-19 Serpentine Ridge
20-24 Mt Stewart area
25 Upper Huskisson River area
26-39 Adamsfield area

Analyses of coarse-grained orthopyroxenite samples from:

30-31 Harman River area
32 Mt Stewart area
33 Huskisson River area
34 Adamsfield area

+ = University of Tasmania registered sample number

Analyses 29, 34 from Varne and Brown (1978).

Table 19. CHEMICAL ANALYSES (OXIDE WEIGHT %) AND STRUCTURAL FORMULAE (O=4) OF OLIVINE FROM METADUNITE SAMPLES FROM THE LDH SUCCESSION

Plot No.	1	2	3	4	5	6	7	8	9	10
Reg. No.	85-0143	85-0144	85-0198	85-0199	85-0200	85-0201	85-0202	85-0203	85-0138	85-0180
SiO_2	41.47	42.40	40.85	41.78	41.82	41.28	41.75	42.58	41.38	41.55
FeO	5.99	3.65	6.51	3.86	4.53	5.02	5.13	6.28	6.37	7.09
MgO	51.86	53.69	52.44	54.14	54.37	53.14	52.17	50.87	51.67	51.97
NiO	-	-	-	-	-	-	-	-	0.22	-
Total	93.32	99.74	99.80	99.78	100.72	99.44	99.05	99.73	99.64	100.61
Si	1.0039	1.0103	0.9885	0.9979	0.9930	0.9950	1.0088	1.0246	1.0015	0.9983
Fe	0.1213	0.0727	0.1318	0.0771	0.0900	0.1012	0.1037	0.1264	0.1289	0.1425
Mg	1.8710	1.9066	1.8912	1.9271	1.9240	1.9089	1.8787	1.8243	1.8637	1.8609
Ni	-	-	-	-	-	-	-	-	0.0043	-
Total	2.9961	2.9897	3.0115	3.0021	3.0070	3.0050	2.9912	2.9754	2.9985	3.0017
Mg*	93.9	96.3	93.5	96.2	95.5	95.0	94.8	93.5	93.5	92.9

Analyses 1-9 = Harman River area

10 = Mt Stewart area

Table 20. CHEMICAL ANALYSES (OXIDE WEIGHT %) AND STRUCTURAL FORMULAE (O=32) OF CHROME SPINEL FROM METADUNITE SAMPLES FROM THE LDH SUCCESSION

Plot No.	1	2	3	4	5	6	7	8	9	10
Reg. No.	85-0143	85-0144	85-0198	85-0199	85-0200	85-0201	85-0202	85-0203	85-0138	85-0180
TiO_2									-	
Cr_2O_3	4.09	4.12	4.23	2.68	5.15	3.22	3.20	2.25	1.82	4.49
Fe_2O_3	67.34	68.02	65.23	68.15	65.64	66.93	61.81	62.79	70.07	65.41
FeO	21.82	18.46	23.91	21.08	22.21	21.49	28.87	27.70	21.43	22.86
Mn	-	0.51	-	-	-	-	0.49	0.83	-	0.93
MgO	7.66	9.10	6.12	7.69	7.41	7.40	5.27	6.06	7.43	6.71
Total	100.91	100.21	99.49	99.60	100.41	99.04	99.64	99.63	100.75	100.40
Al	1.3192	1.3237	1.3970	0.8804	1.6638	1.0630	1.0698	0.7473	0.5951	1.4618
Cr	14.5649	14.6550	14.4461	15.0132	14.2200	14.8162	13.8564	13.9841	15.3632	14.2797
Fe^{+3}	0.1159	0.0213	0.1569	0.1063	0.1163	0.1208	1.0739	1.2687	0.0417	0.2586
Fe^{+2}	4.8767	4.1862	5.4449	4.8064	4.9738	4.9118	5.7728	5.2576	4.9289	5.0209
Mn	-	0.1177	-	-	-	-	-	0.1981	-	0.2175
Mg	3.1233	3.6961	2.5551	3.1936	3.0262	3.0882	2.2272	2.5443	3.0711	2.7615
Mg*	39.0	46.9	31.9	39.9	37.8	38.6	27.8	32.6	38.4	35.5
Cr*	91.7	91.7	91.2	94.5	89.5	93.3	92.8	94.9	96.3	90.7

Analyses 1-9 - Harman River area
10 - Mt Stewart area

Total iron reported as FeO. Structural formulae calculated assuming the general formula $R^{2+}R^{3+}O_4$ and apportioning total iron as Fe^{2+} so that $2(Mg+Mn+Ca+Fe^{2+})=(Cr+Al+Ti+Fe^{3+})$.

Table 21. CHEMICAL ANALYSES (OXIDE WEIGHT %) AND STRUCTURAL FORMULAE (O=4) OF OLIVINE FROM THE LPD SUCCESSION

Plot No.	1	2	3	4	5	6
Reg. No.	85-0204	85-0205	85-0153	85-0207	85-0208	85-0209
SiO_2	40.83	40.10	39.71	40.17	39.92	40.33
FeO	10.13	11.98	12.76	12.69	12.26	13.22
MgO	48.57	47.47	47.36	47.73	47.64	47.30
Total	99.53	99.55	99.83	100.59	99.82	100.85
Si	1.0049	0.9965	0.9886	0.9913	0.9912	0.9945
Fe	0.2085	0.2490	0.2657	0.2619	0.2546	0.2726
Mg	1.7816	1.7580	1.7572	1.7554	1.7629	1.7383
Total	2.9951	3.0035	3.0114	3.0087	3.0088	3.0055
Mg*	89.5	87.6	86.9	87.0	87.4	86.4

Analyses 1-3 - Riley Knob area

4 - Dundas area

5-6 - Adamsfield area

Table 22. CHEMICAL ANALYSES (OXIDE WEIGHT %) AND STRUCTURAL FORMULAE (O=4) FOR ORTHOPYROXENE FROM THE LPD SUCCESSION

Plot No.	1	2	3	4	5	6	7	8	9	10	11	12
Reg. No.	85-0204	85-0154	85-0155	85-0205	85-0156	85-0157	85-0206	85-0210	85-0211	85-0153	85-0161	85-0158
SiO_2	57.25	57.30	56.90	56.31	57.06	56.23	54.01	55.14	55.29	55.81	56.92	57.27
Al_2O_3	0.95	0.96	1.89	1.89	1.15	1.82	0.16	1.31	1.33	1.93	1.25	0.87
Cr_2O_3	0.40	0.34	0.62	0.54	0.47	0.61	-	0.27	0.27	0.40	0.53	0.39
FeO	6.64	6.79	6.34	7.68	6.80	7.54	11.12	11.20	11.41	7.68	6.76	6.37
MnO	0.24	0.22	-	-	0.21	-	0.13	-	-	-	-	-
MgO	33.82	33.91	33.51	32.88	33.32	32.11	34.08	30.56	30.30	32.63	32.94	33.73
CaO	0.89	0.59	0.81	0.89	1.10	1.64	0.31	1.21	1.20	0.95	0.92	0.92
Total	100.19	100.11	100.07	100.19	100.11	99.95	99.81	99.69	99.80	99.40	99.32	99.55
Si	1.9768	1.9789	1.9622	1.9532	1.9743	1.9579	1.9194	1.9562	1.9602	1.9517	1.9809	1.9848
Al	0.0387	0.0391	0.0768	0.0773	0.0469	0.0747	0.0067	0.0548	0.0556	0.0796	0.0513	0.0355
Cr	0.0109	0.0093	0.0169	0.0148	0.0129	0.0168	-	0.0076	0.0076	0.0111	0.0146	0.0107
Fe	0.1917	0.1961	0.1829	0.2228	0.1968	0.2196	0.3305	0.3323	0.3383	0.2246	0.1967	0.1846
Mn	0.0070	0.0064	-	-	0.0062	-	0.0039	-	-	-	-	-
Mg	1.7404	1.7453	1.7222	1.6997	1.7181	1.6662	1.8050	1.6158	1.6010	1.7005	1.7084	1.7422
Ca	0.0329	0.0218	0.0299	0.0331	0.0408	0.0612	0.0118	0.0460	0.0456	0.0356	0.0343	0.0342
Total	3.9984	3.9969	3.9909	4.0008	3.9959	3.9964	4.0773	4.0126	4.0082	4.0030	3.9862	3.9921
Mg*	90.1	89.9	90.4	88.4	89.7	88.4	84.5	82.9	82.6	88.3	89.7	90.4
Cr*	22.0	19.2	18.0	16.1	21.5	18.4	-	12.1	12.0	12.2	22.1	23.1
Ca	1.7	1.1	1.5	1.7	2.1	3.1	0.5	2.3	2.3	1.8	1.8	1.7
Mg	88.6	88.9	89.0	86.9	87.9	85.6	84.1	81.0	80.7	86.7	88.1	88.8
Fe	9.8	10.0	9.4	11.4	10.1	11.3	15.4	16.7	17.0	11.5	10.1	9.4

Analyses 1-6 - Riley Knob area
7-9 - Harman River area
10 - Serpentine Ridge area
11 - Huskisson River area

Table 22. (continued)

Plot No.	13	14	15	16	17	18	19	20	21	22	23	24
Reg. No.	85-0159	85-0160	85-0212	85-0213	85-0167	85-0168	85-0164	85-0214	85-0207	85-0166	85-0208	85-0209
SiO_2	56.92	57.10	56.48	56.29	56.81	55.85	55.60	56.36	55.28	56.94	55.99	56.26
Al_2O_3	0.93	0.78	0.77	0.84	1.60	3.43	1.23	1.55	1.78	1.10	1.42	1.33
Cr_2O_3	0.41	0.31	0.28	0.22	0.56	1.07	0.59	0.40	0.67	0.51	0.34	0.35
FeO	6.48	6.70	7.94	8.82	7.45	7.01	7.50	8.01	8.13	5.86	7.75	8.32
MnO	0.27	0.21	-	0.17	0.22	-	-	-	-	-	-	-
MgO	33.50	33.25	33.53	32.26	32.22	30.11	33.06	33.11	33.00	34.94	32.99	32.90
CaO	0.91	0.88	0.53	0.86	1.86	1.97	1.28	0.69	1.34	1.21	0.98	1.01
Total	99.42	99.23	99.53	99.46	100.72	99.44	99.26	100.12	100.20	100.56	99.47	100.17
Si	1.9796	1.9893	1.9722	1.9769	1.9641	1.9496	1.9510	1.9579	1.9293	1.9556	1.9578	1.9585
Al	0.0381	0.0320	0.0317	0.0348	0.0652	0.1412	0.0509	0.0635	0.0732	0.0445	0.0585	0.0546
Cr	0.0113	0.0085	0.0077	0.0061	0.0153	0.0295	0.0164	0.0110	0.0185	0.0138	0.0094	0.0096
Fe	0.1885	0.1952	0.2319	0.2591	0.2154	0.2047	0.2201	0.2327	0.2373	0.1683	0.2266	0.2422
Mn	0.0080	0.0062		0.0051	0.0064	-	-	-	-	-	-	-
Mg	1.7364	1.7264	1.7449	1.6885	1.6602	1.5664	1.7289	1.7142	1.7164	1.7884	1.7192	1.7068
Ca	0.0339	0.0328	0.0198	0.0324	0.0689	0.0737	0.0481	0.0257	0.0501	0.0445	0.0367	0.0377
Total	3.9957	3.9904	4.0081	4.0027	3.9956	3.9651	4.0154	4.0049	4.0249	4.0152	4.0082	4.0094
Mg*	90.2	89.8	88.3	86.7	88.5	88.4	88.7	88.0	87.9	91.4	88.4	87.6
Cr*	22.8	21.0	19.6	14.9	19.0	17.3	24.3	14.8	20.2	23.7	13.8	15.0
Ca	1.7	1.7	1.0	1.6	3.5	4.0	2.4	1.3	2.5	2.2	1.9	1.9
Mg	88.6	88.3	87.4	85.3	85.4	84.9	86.6	86.9	85.7	89.4	86.7	85.9
Fe	9.6	10.0	11.6	13.1	11.1	11.1	11.0	11.8	11.8	8.4	11.4	12.2

Analyses 12-14 - Lynch Hill area
15 - 14 km quarry, Lower Pieman Dam Road
16 - South Pieman track
17-18 - Colebrook Hill
19-22 - Dundas
23-24 - Adamsfield area

Table 23. CHEMICAL ANALYSES (OXIDE WEIGHT %) AND STRUCTURAL FORMULAE (O=6) FOR CLINOPYROXENE FROM THE LPD SUCCESSION

Plot No.	1	2	3	4	5	6	7	8
Reg. No.	85-0204	85-0154	85-0205	85-0156	85-0157	85-0153	85-0161	85-0158
SiO_2	54.63	54.30	53.28	53.79	93.67	52.90	54.53	54.77
TiO_2	-	-	-	-	-	-	-	-
Al_2O_3	1.07	1.71	1.75	1.70	2.26	2.20	0.97	0.91
Cr_2O_3	0.76	0.78	1.02	1.07	1.15	1.10	0.69	0.72
FeO	2.01	2.10	2.80	2.42	2.70	2.78	2.08	2.08
MnO	-	-	-	-	-	-	-	-
MgO	17.58	17.72	17.76	17.48	16.69	16.88	17.85	17.55
CaO	23.92	23.45	22.91	23.17	23.74	23.79	23.44	23.88
Total	99.97	100.06	99.52	99.63	100.21	99.65	99.56	99.61
Si	1.9798	1.9645	1.9466	1.9589	1.9485	1.9357	1.9823	1.9858
Ti	-	-	-	-	-	-	-	-
Al	0.0457	0.0729	0.0754	0.0730	0.0967	0.0949	0.0416	0.0389
Cr	0.0218	0.0223	0.0295	0.0308	0.0330	0.0318	0.0198	0.0206
Fe	0.0609	0.0635	0.0856	0.0737	0.0820	0.0851	0.0632	0.0631
Mn	-	-	-	-	-	-	-	-
Mg	0.9495	0.9554	0.9670	0.9487	0.9030	0.9205	0.9671	0.9483
Ca	0.9288	0.9091	0.8969	0.9041	0.9235	0.9328	0.9130	0.9277
Total	3.9865	3.9878	4.0009	3.9892	3.9867	4.0009	3.9870	3.9844
Mg*	94.0	93.8	91.8	92.8	91.7	91.5	93.9	93.8
Cr*	32.3	23.4	28.1	29.7	25.4	25.1	32.3	34.7
Ca	47.9	47.1	46.0	46.9	48.4	48.1	47.0	47.8
Mg	49.0	49.6	49.6	49.2	47.3	47.5	49.8	48.9
Fe	3.1	3.3	4.4	3.8	4.3	4.4	3.3	3.3

Analyses:
1-5 Riley Knob area
6 Serpentine Ridge area
7 Huskisson River area
8 Lynch Hill area

Table 23. (continued)

Plot No.	9	10	11	12	13	14	15
Reg. No.	85-0213	85-0167	85-0168	85-0215	85-0214	85-0208	85-0209
SiO_2	53.80	53.53	53.41	53.98	53.19	52.48	52.90
TiO_2	-	-	-	0.28	-	-	-
Al_2O_3	1.22	2.36	1.91	1.17	2.02	1.73	1.72
Cr_2O_3	0.58	1.06	0.75	0.41	1.32	0.81	0.89
FeO	3.78	2.87	3.30	4.28	2.89	3.21	3.25
MnO	-	-	-	0.37	-	-	-
MgO	17.23	16.81	16.86	16.48	16.95	18.18	17.91
CaO	23.21	23.19	23.35	23.16	23.08	22.64	23.05
Total	99.82	99.82	99.58	100.13	99.45	99.05	99.72
Si	1.9664	1.9490	1.9541	1.9724	1.9469	1.9316	1.9353
Ti	-	-	-	0.0077	-	-	-
Al	0.0526	0.1013	0.0824	0.0504	0.0872	0.0751	0.0742
Cr	0.0168	0.0305	0.0217	0.0118	0.0382	0.0236	0.0257
Fe	0.1155	0.0874	0.1010	0.1308	0.0885	0.0988	0.0994
Mn	-	-	-	0.0115	-	-	-
Mg	0.9386	0.9122	0.9193	0.8974	0.9246	0.9972	0.9765
Ca	0.9090	0.9047	0.9154	0.9068	0.9052	0.8929	0.9036
Total	3.9989	3.9851	3.9939	3.9888	3.9905	4.0191	4.0147
Mg*	89.0	91.3	90.1	87.3	91.5	91.0	90.8
Cr*	24.2	23.1	20.8	19.0	30.5	23.9	25.8
Ca	46.3	47.5	47.3	46.9	47.2	44.9	45.6
Mg	47.8	47.9	47.5	46.4	48.2	50.1	49.3
Fe	5.9	4.6	5.2	6.8	4.6	5.0	5.0

Analyses: 9 South Pieman Track
10-12 Colebrook Hill
13 Dundas
14-15 Adamsfield area

$Mg^* = 100\ Mg/Mg+Fe^+$

$Cr^* = 100\ Cr/Cr+Al$

Table 24. CHEMICAL ANALYSES (OXIDE WEIGHT %) AND STRUCTURAL FORMULAE (O=32) FOR CHROME SPINEL FROM THE LPD SUCCESSION

Plot No.	1	2	3	4	5	6	7	8	9	10	11	12
Reg. No.	85-0204	85-0154	85-0155	85-0205	85-0156	85-0216	85-0217	85-0218	85-0153	85-0206	85-0210	85-0211
TiO_2	-	-	-	-	-	-	-	-	-	0.36	0.40	0.45
Al_2O_3	16.09	16.67	23.69	22.81	16.78	21.49	13.85	15.4	30.30	13.60	18.19	18.45
Cr_2O_3	50.05	50.20	41.81	42.88	49.79	44.58	52.78	52.94	36.46	37.79	43.39	43.82
FeO	22.09	21.21	22.62	24.10	21.50	22.32	24.44	22.26	20.66	43.17	31.21	31.38
MnO	0.60	0.54	0.34	0.29	0.47	-	-	0.57	-	0.41	-	-
MgO	10.55	10.79	10.83	9.43	10.93	11.40	8.35	9.32	12.66	4.27	5.94	6.10
Total	99.38	99.41	99.29	99.51	99.47	99.79	99.42	100.49	100.08	99.60	99.13	100.20
Ti	-	-	-	-	-	-	-	-	-	0.0730	0.0793	0.0882
Al	4.8825	5.0384	6.9584	6.7761	5.0609	6.3184	4.3093	4.6855	8.5143	4.3239	5.6556	5.6701
Cr	10.1844	10.1742	8.2351	8.5419	10.0699	8.7892	11.0121	10.8009	6.8702	8.0567	9.0465	9.0305
Fe^{+3}	0.9331	0.7874	0.8064	0.6820	0.8692	0.8924	0.6787	0.5137	0.6155	3.5464	1.2185	1.2111
Fe^{+2}	3.8222	3.7602	3.9069	4.3968	3.7308	3.7629	4.7158	4.2908	3.5029	6.1902	5.6653	5.6302
Mn	0.1308	0.1173	0.0718	0.0619	0.1018	-	-	0.1246	-	0.0937	-	-
Mg	4.0470	4.1226	4.0213	3.5413	4.1673	4.2371	3.2842	3.5846	4.4971	1.7162	2.3347	2.3698
Mg*	51.4	52.3	50.7	44.6	52.8	53.0	41.1	45.5	56.2	21.7	29.2	29.6
Cr*	67.6	66.9	54.2	55.8	66.6	58.2	71.9	69.7	44.7	65.1	61.5	61.4

Total iron reported as FeO. Structural formulae calculated assuming the general formula $R^{2+}R^{3+}O_4$ and apportioning total iron as Fe^{2+} and Fe^{3+} so that $2(Mg+Mn+Ca+Fe^{2+}) = (Cr+Al+Ti+Fe^{3+})$.

Location of chrome spinel samples from the LPD succession - 1-8 - Riley Knob area
9 - Serpentine Ridge area
10-12 - Harman River area

Table 24. (continued)

Plot No.	13	14	15	16	17	18	19	20	21	22	23
Reg. No.	85-0161	85-0158	85-0159	85-0160	85-0212	85-0213	85-0167	85-0164	85-0166	85-0208	85-0209
TiO_2	-	0.22	-	-	0.25	0.78	-	-	-	-	-
Al_2O_3	18.68	12.68	14.54	14.87	10.88	11.65	24.72	16.39	16.83	20.87	18.58
Cr_2O_3	48.42	51.28	50.19	51.00	53.82	49.59	38.52	51.57	51.37	44.30	45.32
FeO	19.95	25.32	25.60	24.31	28.79	33.95	23.94	21.66	20.59	24.94	27.71
MnO	0.35	0.33	0.47	0.30	0.57	0.62	0.47	-	-	0.48	-
MgO	11.93	9.44	9.55	9.40	5.94	5.65	11.69	10.17	10.84	10.12	8.96
Total	99.33	99.27	100.35	99.88	100.25	99.24	99.34	99.79	99.63	100.71	100.57
Ti	-	0.0436	-	-	0.0507	0.1591	-	-	-	-	-
Al	5.5599	3.9349	4.4303	4.5513	3.4598	3.7250	7.1783	4.9671	5.0752	6.1528	5.5772
Cr	9.6641	10.6709	10.2549	10.4674	11.4767	9.9892	7.5008	10.4801	10.3878	8.7579	9.1223
Fe^{+3}	0.7760	1.3507	1.3148	0.9813	1.0128	2.1267	1.3209	0.5528	0.5370	1.0893	1.3005
Fe^{+2}	3.4364	4.2232	4.2186	4.2970	5.4819	5.5739	3.6107	4.1038	3.8677	4.1267	4.6001
Mn	0.0748	0.0736	0.1029	0.0660	0.1302	0.1424	0.0981	-	-	0.1017	-
Mg	4.4888	3.7032	3.6785	3.6370	2.3879	2.2837	4.2913	3.8962	4.1323	3.7716	3.3999
Mg*	56.6	46.7	46.6	45.8	30.3	29.1	54.3	48.7	51.7	47.8	42.5
Cr*	63.5	73.1	69.8	69.7	76.8	72.8	51.1	67.8	67.2	58.7	62.1

Location of chrome spinel samples from the LPD succession - 13 - Huskisson River area
14-16 - Lynch Hill area
17 - 14 km quarry, Lower Pieman Dam Road
18 - South Pieman track
19 - Colebrook Hill
20-21 - Dundas
22-23 - Adamsfield

Table 25. CHEMICAL ANALYSES (OXIDE WEIGHT %) AND STRUCTURAL FORMULAE FOR PYROXENE (O=6) AND AMPHIBOLE (O=23) FROM THE LPG SUCCESSION

	OPX (6 oxygens)			CPX (6 oxygens)			Amphibole inclusions in spinel grains (23 oxygens)			
Plot No.	1	2	3	5	6	7	8	9	10	11
Reg. No.	85-0065	85-0222	85-0223	85-0065	85-0222	85-0223	85-0219	85-0220	85-0221	85-0223
SiO_2	56.01	55.85	56.04	52.79	53.10	53.78	55.47	53.35	54.10	53.69
TiO_2	-	-	-	-	-	-	-	-	-	-
Al_2O_3	1.60	1.60	1.79	1.81	2.05	1.51	2.43	3.81	3.82	3.95
Cr_2O_3	0.42	0.45	0.58	0.91	1.03	0.84	1.27	1.48	1.80	1.76
FeO	7.62	7.60	6.99	2.86	2.55	2.24	2.33	4.39	2.46	2.97
MnO	-	-	-	-	-	-	-	-	-	-
MgO	32.93	33.03	33.19	17.31	17.20	17.70	24.18	24.33	22.88	22.36
CaO	1.17	0.81	1.39	23.49	23.59	24.27	11.37	9.56	11.76	11.84
Na_2O							0.45	0.57	0.59	0.65
Total	99.75	99.34	99.98	99.17	99.52	100.34	97.50	97.49	97.41	97.22
Si	1.9533	1.9538	1.9466	1.9406	1.9416	1.9499	7.6237	7.3954	7.4769	7.4580
Ti	-	-	-	-	-	-	-	-	-	-
Al	0.0658	0.0660	0.0733	0.0784	0.0884	0.0645	0.3937	0.6226	0.6224	0.6469
Cr	0.0116	0.0124	0.0159	0.0264	0.0298	0.0241	0.1380	0.1623	0.1967	0.1933
Fe	0.2222	0.2224	0.2031	0.0879	0.0780	0.0679	0.2678	0.5089	0.2843	0.3450
Mn	-	-	-	-	-	-	-	-	-	-
Mg	1.7115	1.7220	1.7182	0.9483	0.9373	0.9564	4.9528	5.0264	4.7126	4.6289
Ca	0.0437	0.0304	0.0517	0.9252	0.9243	0.9429	1.6744	1.4200	1.7415	1.7623
Na	-	-	-	-	-	-	0.1199	0.1532	0.1581	0.1751
Total	4.0081	4.0070	4.0088	4.0070	3.9993	4.0058	15.1704	15.2888	15.1926	15.2095
Mg*	88.5	88.6	89.4	91.5	92.3	93.4	94.9	90.8	94.3	93.1
Ca	2.2	1.5	2.6	47.2	47.7	47.9	24.3	20.4	25.8	26.1
Mg	86.6	87.2	87.1	48.3	48.3	48.6	71.8	72.3	69.9	68.3
Fe	11.2	11.3	10.3	4.5	4.0	3.5	3.9	7.3	4.2	5.1

Table 26. CHEMICAL ANALYSES (OXIDE WEIGHT %) AND STRUCTURAL FOMRULAE (O=32) FOR CHROME SPINEL FROM THE LPG SUCCESSION

Plot No.	1	2	3	4	5	6	7	8	9	10	11	12
Reg. No.	85-0067	85-0224	85-0222	85-0223	85-0066	85-0225	85-0226	85-0227	85-0219	85-0220	85-0221	85-0228
TiO_2	-	-	-	-	0.15	-	-	-	-	-	-	-
Al_2O_3	22.14	19.98	19.09	14.83	16.65	22.30	23.71	19.40	14.55	14.82	14.83	15.64
Cr_2O_3	43.79	44.23	47.68	49.09	45.60	42.69	41.77	45.89	49.82	46.86	50.26	50.36
FeO	23.74	25.59	22.19	27.40	28.35	23.16	23.25	23.10	26.45	31.50	26.37	24.90
MnO	-	-	-	-	-	-	-	-	0.55	-	-	0.30
MgO	10.29	9.80	11.10	8.29	8.85	11.43	11.58	11.36	8.98	6.68	8.36	9.19
Total	99.96	99.60	100.06	99.61	99.60	99.58	100.31	99.75	100.35	99.86	99.82	100.39
Ti	-	-	-	-	0.0292	-	-	-	-	-	-	-
Al	6.5315	5.9805	5.6678	4.5827	5.0825	6.5424	6.8682	5.7538	4.4502	4.6172	4.5744	4.7570
Cr	8.6627	8.8777	9.4926	10.1723	9.3341	8.3985	8.1137	9.1268	10.2180	9.7899	10.3957	10.2713
Fe^{3+}	0.8057	1.1419	0.8396	1.2449	1.5542	1.0592	1.0182	1.1194	1.3318	1.5929	1.0299	0.9717
Fe^{2+}	4.1625	4.2918	3.8340	4.7616	4.5849	3.7609	3.7596	3.7408	4.4071	5.3691	4.7402	4.4009
Mn	-	-	-	-	-	-	-	-	0.1209	-	-	0.0656
Mg	3.8375	3.7082	4.1660	3.2384	3.4151	4.2391	4.2404	4.2592	3.4721	2.6309	3.2598	3.5335
Mg*	48.0	46.4	52.1	40.5	42.7	53.0	53.0	53.2	44.1	32.9	40.7	44.5
Cr*	57.0	59.7	62.6	68.9	64.7	56.4	54.2	61.3	69.7	68.0	69.4	68.3

Samples: 1-4 Orthopyroxene-rich sequence
5-8 Olivine-rich sequence
9-12 Chrome-spinel rich zone.

For location of samples see Brown *et al.* (in prep.)

Total iron reported as FeO. Structural formulae calculated assuming the general formula $R^{2+}R^{3+}O_4$ and apportioning total iron as Fe^{2+} and Fe^{3+} so that $2(Mg+Mn+Ca+Fe^{2+})=(Cr+Al+Ti+Fe^{3+})$.

Table 27. WHOLE ROCK MAJOR AND TRACE ELEMENT ANALYSES OF SAMPLES OF AMPHIBOLITE AND AMPHIBOLITISED PYROXENITE

Plot No.	1	2	3	4	5	6	7	8	9	10
Reg. No.	85-0229	85-0230	85-0231	85-0232	85-0206	85-0233	85-0234	85-0235	85-0236	85-0215
SiO_2	43.00	44.03	43.20	53.70	51.70	54.80	50.40	45.50	44.61	41.98
TiO_2	0.31	0.93	<0.01	0.01	0.03	0.03	0.01	0.03	0.07	0.10
Al_2O_3	10.80	15.00	6.81	0.47	2.10	1.60	1.80	8.37	6.67	11.14
Fe_2O_3	3.00	2.45	3.10	1.60	2.80	1.30	2.40	2.02	1.40	1.52
FeO	6.30	8.86	4.90	2.70	9.30	12.60	4.50	3.69	5.44	7.03
MnO	0.15	0.17	0.20	0.14	0.20	0.25	0.15	0.44	0.56	0.93
MgO	21.00	14.65	20.30	19.40	26.00	25.50	22.80	20.56	23.46	17.99
CaO	8.50	5.32	13.40	19.20	3.50	0.94	14.00	13.21	9.69	13.43
Na_2O	0.65	1.24	0.17	0.15	0.12	0.20	0.06	0.08	0.07	0.06
K_2O	0.06	0.69	0.11	0.04	0.05	0.02	0.01	0.09	0.04	0.12
P_2O_5	0.03	0.05	0.02	0.02	0.02	0.01	0.01	0.05	0.04	0.04
CO_2	0.24	0.29	3.10	0.24	0.15	0.01	0.13	0.29	0.16	0.18
H_2O^+	4.70	5.85	4.10	2.10	3.10	2.10	2.20	5.33	7.00	6.28
H_2O^-	0.40	0.49	0.81	0.37	0.44	0.17	0.30	0.44	0.50	0.49
Total	99.14	100.02	100.23	100.14	99.51	99.53	98.77	100.10	99.71	101.29
Cr	2840	1059	9110	3030	2690	4300	4900	2128	2465	1164
Ni	921	351	526	507	667	632	447	471	582	279
Zr	7	34	<4	<4	<4	<4	<4	<4	<4	<4
Y	12	20	41	23	<4	<4	<4	<4	<4	4
Nb	<4	<4	<4	<4	<4	<4	<4	<4	<4	<4
Rb	<4	32	4	<4	<4	<4	<4	4	<4	8
Sr	21	147	22	<4	8	<4	<4	71	19	9
Ba	-	330	-	-	-	-	-	71	21	90
V	-	-	-	-	-	-	-	-	-	-
Sc	-	-	-	-	-	-	-	-	-	-
Co	-	61	-	-	-	-	-	51	59	86

Analyses by Department of Mines Analytical Laboratory - Analysts J. Furst, M. Frith, M. Pickering and R. Roby.

Table 28. CHEMICAL ANALYSES (OXIDE WEIGHT %) AND STRUCTURAL FORMULAE FOR: (a) AMPHIBOLE (O=23); (b) PYROXENE (O=6); AND (c) CHROME SPINEL (O=32) FROM AMPHIBOLITE AND AMPHIBOLITISED PYROXENITE SAMPLES

	Amphiboles							
Plot No.	1	2	3	4	5	6	7	8
Reg. No.	85-0206	85-0206	85-0206	85-0235	82-0236	85-0229	82-0229	R-38850+
Mineral	Actinolite	Tremolite	Anthophyl-lite	Tremolite	Tremolite	Magnesio-Hornblende	Magnesio-Hornblende	Magnesio-Hornblende
SiO_2	54.99	56.52	54.99	53.11	55.05	46.43	46.74	45.81
TiO_2	-	-	-	-	-	0.31	1.11	0.45
Al_2O_3	3.54	1.23	0.91	2.77	1.88	11.65	10.81	11.84
Cr_2O_3	0.32	-	-	0.24	0.38	0.24	-	0.24
FeO	5.28	4.50	10.47	4.18	2.94	6.73	11.96	7.28
MnO	-	-	-	-	-	-	0.29	0.19
MgO	21.83	23.94	31.39	21.19	21.46	17.40	15.01	17.57
CaO	11.31	10.45	0.22	11.98	14.73	11.36	10.82	12.28
Na_2O	-	-	-	-	-	1.13	1.82	1.29
K_2O	-	-	-	-	-	-	-	0.05
Total	97.27	96.64	97.98	93.47	96.44	95.25	98.56	97.00
Si	7.6334	7.8380	7.5571	7.6674	7.7157	6.7146	6.7087	6.5690
Ti	-	-	-	-	-	0.0337	0.1198	0.0485
Al	0.5793	0.2011	0.1474	0.4715	0.3106	1.9862	1.8292	2.0016
Cr	0.0351	-	-	0.0274	0.0421	0.0274	-	0.0272
Fe	0.6130	0.5219	1.2033	0.5047	0.3446	0.8140	1.4357	0.8731
Mn	-	-	-	-	-	-	0.0353	0.0231
Mg	4.5162	4.9477	6.4290	4.5591	4.4826	3.7502	3.2108	3.7548
Ca	1.6823	1.5528	0.0324	1.8532	2.2122	1.7603	1.6641	1.8868
Na	-	-	-	-	-	0.3169	0.5065	0.3587
K	-	-	-	-	-	-		0.0091
Total	15.0593	15.0615	15.3692	15.0832	15.1079	15.4033	15.5101	15.5520
Mg*	88.0	90.5	84.2	90.0	92.9	82.2	69.1	81.1
Ca	24.7	22.1	0.4	26.8	31.4	27.8	26.4	29.0
Fe	9.0	7.4	15.7	7.3	4.9	12.9	22.8	13.4
Mg	66.3	70.5	83.9	65.9	63.7	59.3	50.9	57.6

Table 28. (continued)

	Pyroxenes				Chrome Spinels			
Plot No.	1	2	3	4	1	2	3	4
Reg. No.	85-0235	85-0235	85-0236	85-0236	85-0206	85-0229	85-0235	85-0236
Mineral Species	OPX	CPX	OPX	CPX				
SiO_2	56.25	53.90	56.60	53.55				
TiO_2	-		-	-	0.36	0.21	0.63	1.24
Al_2O_3	0.82	0.90	0.86	1.33	13.60	22.31	11.02	13.98
Cr_2O_3	-	0.53	0.22	0.61	37.79	39.78	49.05	40.65
FeO	9.08	3.02	8.41	3.97	43.17	30.76	33.37	36.92
MnO	-	-	0.18	-	0.41	0.39		0.61
MgO	32.53	17.54	31.94	17.05	4.27	6.11	5.48	6.35
CaO	0.59	23.75	1.20	23.01				
Na_2O								
K_2O								
Total	99.27	99.64	99.41	99.52	99.60	99.56	99.55	99.75
Si	1.9777	1.9703	1.9853	1.9644				
Ti	-	-	-	-	0.3552	0.2098	0.6273	1.2256
Al	0.0340	0.0388	0.0356	0.0575	13.4187	22.2853	10.9724	13.8173
Cr	-	0.0153	0.0061	0.0177	37.2863	39.7359	48.8383	40.1769
Fe	0.2670	0.0923	0.2467	0.1218	Fe^{3+} 17.2419	5.4943	8.7802	14.0815
					Fe^{2+} 27.0802	25.7831	25.3255	23.8196
Mn	-	-	0.0053	-	0.4045	0.3896		0.6029
Mg	1.7045	0.9556	1.6697	0.9321	4.2131	6.1032	5.4563	6.2761
Ca	0.0222	0.9303	0.0451	0.9044				
Total	4.0053	4.0026	3.99	3.9980				
Mg*	86.5	91.2	87.1	88.4	Mg^+ 21.7	29.7	27.7	32.0
Ca	1.1	47.0	2.3	46.2	Cr* 65.1	54.5	74.9	66.1
Mg	85.5	48.3	85.1	47.6				
Fe	13.4	4.7	12.6	6.2				

Total iron reported as FeO. Structural formulae calculated assuming the general formula $R^{2+}R^{3+}O_4$ and apportioning total iron as Fe^{2+} and Fe^{3+} so that $2(Mg+Mn+Ca+Fe^{2+})=(Cr+Al+Ti+Fe^{3+})$.

Table 29. MEAN NOMINAL EQUILIBRATION TEMPERATURES FOR OLIVINE-SPINEL PAIRS USING THE GEOTHERMOMETERS OF:- (a) JACKSON (1969), (b) ROEDER et al. (1979)

	Registered No.	Temperature (a)	Temperature (b)
1	85-0135	1204	621
2	85-0141	1260	644
3	85-0169	1227	635
4	85-0170	1416	717
5	85-0172	1330	687
6	85-0173	1222	631
7	85-0174	1377	707
8	85-0175	1210	617
9	85-0176	1270	664
10	85-0177	1284	669
11	85-0178	1224	635
12	85-0179	1233	633
13	85-0181	1253	633
14	85-0182	1356	685
15	85-0183	1331	679
16	85-0186	1302	666
17	85-0190	1433	722
18	85-0184	1298	1018
19	85-0138	1090	552
20	85-0143	1015	524
21	85-0144	936	482
22	85-0180	1007	523
23	85-0198	912	471
24	85-0199	868	442
25	85-0200	850	442
26	85-0201	940	482
27	85-0202	762	390
28	85-0203	938	481
29	85-0153	1265	820
30	85-0204	1327	754
31	85-0205	1067	652
32	85-0208	1225	733
33	85-0209	1190	701

LDH Succession

1-17: Dunite and pyroxene-bearing dunite samples.

18: Coarse-grained orthopyroxenite sample.

19-28: Metadunite samples.

LPD Succession

29-33: Peridotite samples.

Table 30. EQUILIBRATION TEMPERATURES FOR COEXISTING OPX-CPX PAIRS FOR SAMPLES FROM THE LPD AND LPG SUCCESSIONS USING THE GEOTHERMOMETERS OF:- (a) WOOD AND BANNO (1973); (b) WELLS (1979).

	Registered No.	Temperature (a)	Temperature (b)
1	85-0154	1127	1054
2	"	1030	932
3	"	998	889
4	85-0155	1045	944
5	"	1095	1003
6	"	1070	974
7	85-0156	1064	974
8	85-0157	950	851
9	"	1038	955
10	"	1016	927
11	85-0204	1011	906
12	"	1011	910
13	"	1037	935
14	"	1037	938
15	"	1025	924
16	85-0205	1126	1064
17	"	1030	947
18	"	1078	1005
19	"	1024	937
20	"	1068	990
21	85-0161	1058	964
22	"	1059	968
23	85-0236	1021	947
24	85-0158	1039	942
25	"	1016	911
26	"	1030	962
27	85-0167	1031	943
28	"	1056	975
29	"	1037	953
30	"	1053	970
31	85-0214	1044	956
32	"	1018	932
33	"	1051	972
34		1039	958
35	85-0208	1068	992
36	"	1022	942
37	85-0065	985	889
38	"	988	893
39	"	957	857
40	"	992	894
41	"	1012	921
42	85-0223	1013	922
43	85-0224	988	886
44	85-0107	893	903
45	85-0126	937	953
46	85-0127	910	922

LPD Succession

1-20: Riley Knob area

21-22: Huskisson River

23: South Pieman Track

24-26: Lynch Hill area

27-30: Colebrook Hill

31-34: Dundas

35-36: Adamsfield

LPG Succession

37-43: Peridotite sequences

44-46: Two-pyroxene gabbro samples